Probabilistic analysis of radionuclide transport for radioactive waste disposal systems in soil and fractured rocks

A THESIS SUBMITTED FOR THE DEGREE OF

DOCTOR OF PHILOSOPHY

IN THE FACULTY OF ENGINEERING

BY

K GEETHA MANJARI

DEPARTMENT OF CIVIL ENGINEERING
INDIAN INSTITUTE OF SCIENCE
BANGALORE-560012, INDIA

NOVEMBER 2019

Dedicated to my parents

Acknowledgements

Abstract

The safe management of radioactive waste disposal facilities is increasingly becoming a necessary condition for the future development of nuclear industry. To ensure long-term safety of these disposal facilities, performance assessment models need to be developed that can quantitatively estimate the potential impact of disposal on biosphere. These models facilitate in envisioning the extent of safety achieved due to the isolation of waste and estimate the amount of risk caused because of the failure of disposal systems by considering various scenarios of release and pathways of intrusion to the geosphere. They also treat the uncertainties associated with input characteristics and quantify them using probabilistic techniques. In this thesis, efficient performance assessment models are developed focusing mainly on understanding the migration process of low and intermediate level radioactive wastes through the geological medium into the biosphere by predictive radionuclide transport models. These models are developed for different geological environments which include soil and fractured rocks. As an intrinsic part of performance assessment, the aleatory (spatial variability due to inherent randomness in soil properties) and epistemic uncertainties (due to parameter and model uncertainties) in the geological and transport properties of the medium and radionuclides are quantified using various probabilistic methods. These methods have been implemented to estimate the limits above which the eventual release of radioactive wastes from disposal facility will pose un-

acceptably high risks. Also, the critical parameters affecting the radionuclide migration are evaluated using various sensitivity methods. Several algorithms are developed and implemented in PYTHON and MATLAB to add new features that introduce complexity in the numerical models and also, interface the deterministic and probabilistic analyses.

Chapter 1 presents a general introduction on one of the global burning issues, the waste management, especially radioactive waste management and the challenges faced in handling and disposing radioactive waste. The significance of developing predictive performance assessment models that help in gauging the extent of risk possible due to barrier system failure is mentioned. The need to conduct the study and objectives of the study are highlighted in this chapter. A brief overview of the organization of the thesis is also presented.

Chapter 2 presents an overview of the various studies carried out in developing performance assessment models to monitor the safety of radioactive waste disposal facilities. As one of the critical components of the performance assessment involves modelling geosphere transport, the analytical and numerical models that have been developed so far to predict the contaminant transport behaviour in different geological media are discussed. Studies on estimating the uncertainties and incorporating their influence on the overall performance of radioactive waste disposal facilities are discussed in detail. Keeping in view the gaps identified from the literature, the objectives, and scope of the thesis are presented.

Chapter 3 presents the guidelines formulated by AERB (2006) for probabilistic safety assessment of near surface disposal facilities (NSDFs). The deterministic and probabilistic components of performance assessment model are presented in this chapter. The deterministic components that include analytical and numerical models adopted to describe

the process of radionuclide transport in geosphere are presented. Also, various probabilistic techniques used to handle the probabilistic component of performance assessment model are presented. They include analytical and simulation methods for reliability analysis, followed by the variance reduction techniques. A brief overview of meta-modelling techniques that propagate the uncertainties and improve the computational efficiency of the model; discretizing techniques developed to model a spatially varying random field and; sensitivity methods that evaluate the critical parameters affecting the performance of radioactive waste disposal systems are discussed.

In **Chapter 4**, a probabilistic performance assessment model is developed to estimate the risk and reliability of near surface disposal facilities. The radiation reaching the biosphere due to the release of radioactivity from the barriers is modelled analytically. The annual release rate, radiation dose and the risk due to radiation from seven radionuclides (^{3}H, ^{14}C, ^{59}Ni, ^{99}Tc, ^{129}I, ^{237}Np and ^{239}Pu) at the end-point of interest are evaluated using the model. Meta-models are developed by implementing collocation-based stochastic response surface method (CSRSM) to propagate the effect of input parameter uncertainties on the radiation dose from the radionuclides. These uncertainties are quantified using reliability analysis and the computational efficiency of meta-models over the analytical model is demonstrated. Also, the critical parameters affecting the safety of disposal systems are estimated by employing global sensitivity analysis.

In **Chapter 5**, probabilistic performance assessment models that can predict the risk and radiation dose due to radionuclide transport in soils (from NSDFs) are developed. The effect of uncertainties due to lack of knowledge (epistemic) and due to inherent randomness in soil medium (aleatory) on the radionuclide transport are examined and also quantified using probabilistic techniques. A three-dimensional groundwater radionuclide

transport model with a decaying mass source is developed. The concentration of radionuclides evolving over spatial and temporal scales is computed from the model. This numerical model handles more complexities in the system than the analytical model studied in previous chapter. To propagate the parametric uncertainty, CSRSM is adopted and surrogate models are developed. Further, the probability of radiation dose exceeding permissible value is estimated by implementing subset simulation (SS) method as Brute-force Monte-Carlo method is computationally expensive (with the increase in the number of uncertain parameters). The computational efficiency of meta-model over the numerical model in estimating the probability of failure (P_f) is also demonstrated. The critical parameters affecting the radionuclide transport are identified using two methods (post processing CSRSM and SS).

The spatial variability inherent in the soil medium (aleatory uncertainty) is characterized by modelling hydraulic conductivity as a random field and the radionuclide transport through this field is analysed through a two-dimensional numerical model. The random field is discretized (i.e., transformed into a set of random variables) by employing Karhunen-Loeve (K-L) series expansion. The correlated random variables are transformed into uncorrelated space using eigen decomposition. The random field is generated for an exponential covariance function and, the number of random variables to be truncated to achieve the least error in generating the random field is also computed. The probability of radiation dose exceeding the permissible value (P_f) in spatially variable soil medium is computed by using subset simulation method. This chapter is mainly focussed on modelling a complex geological environment numerically and examining the influence of different uncertainties in assessing the safety of NSDFs.

In **Chapter 6**, a probabilistic performance assessment model is developed to predict

the safety of disposal facilities near sedimentary rock formations. To predict the flow and transport behaviour of a contaminant through fractured rock, a new hybrid model that integrates a stochastic fracture pattern generation algorithm, and a numerical contaminant transport model is proposed. Also, a new feature that handles the effect of local aperture variation along the fracture is integrated into the hybrid model. The analysis is carried out for a non-reactive contaminant and also a reactive contaminant. The finite element mesh generated numerically could accommodate fracture sets with four fracture orientations $(0°, 45°, 90°, 135°)$ and combinations of these orientations. A parametric study is carried out to investigate the effect of number of fracture sets, local variation in aperture sizes, matrix diffusion and dispersion and also fracture diffusion on the transport behaviour for both the contaminants. From the deterministic analysis, the radiation dose and risk due to radionuclide transport through fractured rock (for different fracture sets and local aperture variations) are evaluated. As the algorithm for fracture generation is stochastic in nature, this effect is quantified by carrying out reliability analysis for fracture set combination $45°$ - $90°$. Similarly, the parametric uncertainties in geological and transport properties of fracture and rock are quantified from reliability analysis. The critical parameters affecting the radiation dose for both non-reactive and reactive contaminant are estimated using sensitivity analysis. The model developed in this chapter could successfully integrate the complexities involved in transport through fractured network and also the probabilistic techniques that quantify the effect of uncertainties involved in such a medium.

Chapter 7 summarises the conclusions from various studies carried out in the thesis. Appendices, list of references and the scope for future work are provided at the end of the thesis.

Contents

List of Figures

List of Tables

Nomenclature

$\Gamma_{.,.}$ multivariate Hermite polynomial

∇h change in hydraulic head

Ψ_κ Order of the term in PCE

$\tilde{v}$ average linear velocity

D_f diffusion coefficient

$K_{d'}$ distribution coefficient of rock matrix

$\frac{\partial C}{\partial t}$ rate of change in concentration

$\tilde{\varphi}$ the approximate solution

C' solute concentration in the rock matrix

$S_p(t)$ inventory post dumping period

α phase of the system (solid, liquid, gaseous)

α_L longitudinal dispersivity

β Reliability Index

χ Buoyancy coefficient

δ input random variable

$\delta = (\delta_{i_1}, \delta_{i_2} \cdots, \delta_{i_{nn}})$ the vector of independent standard normal random variables

δ_{ij} Kronecker delta function

ε porosity

$\frac{\partial h}{\partial t}$ rate of change in hydraulic head

$\frac{dC}{dX}$ concentration gradient

Γ individual polynomial of the basis

$\Gamma_p(\delta_{i_1}, \delta_{i_2} \cdots, \delta_{i_{nn}})$ multi-dimensional hermite polynomial of degree p

λ_f conditional failure rate

λ_i, ϕ_i eigen values and eigen vectors of the auto-correlation function

λ_p decay constant of the radionuclide

$\lambda_{ab}(\xi)$ the density of fractures from set b intersecting the set a

μ_g, σ_g mean and standard deviation of g

μ_{ln} mean of underlying normal field

ν infiltration rate of water from the disposal facility

$\Phi(.)$ probability distribution function of standard normal random variable

ψ transport quantity

ρ_b bulk density

ρ_s specific density

ρ_{UV} correlation coefficient

σ_{ln} standard deviation of underlying normal field

θ_g effective porosity

θ_a fracture orientation

φ_j unknown coefficients

φ_j^l set of unknown coefficients

ξ, ζ growing tip of fractures 1 and 2 respectively

A cross sectional area of aquifer

a half of the fracture width

a_i, b_i coefficients obtained by the least squares method

a_r parameter vector

A_v vector of unknown coefficients

$a_{i_1 \cdots i_n}$ coefficients to be evaluated

B width of the disposal facility

B_t aperture/thickness

C solute concentration

c reciprocal of auto-correlation length

$C(t)$ activity of the radionuclide at time t

$C(X,t)$ maximum concentration within the time period t computed from the numerical model.

$C(x_1,x_2)$ covariance kernal

C_0 permissible concentration

c_r concentration in ground water

C_{max} maximum concentration for the reference level

$COV(P_f)$ coefficient of variation of failure probability

D'_{yy} diffusion coefficient in the rock matrix

$D(X)$ function of uncertain input parameters

D_d mechanical dispersion

D_r maximum permissible radiation dose in the drinking water pathway

D_x retarded longitudinal dispersion coefficient

D'_x, D'_y, D'_z retarded longitudinal; lateral and vertical dispersivity

D_y retarded lateral dispersion coefficient

d_{in} drinking water intake

D_{xx} diffusion coefficient in the fracture

do_{in} ingestion dose coefficient

F output vector

F_m mass flux

$f_s(t)$ exponential failure probability density of the barrier system

f_t failure distribution of barrier

$F_{ab}(x)$ tracelength distribution of fracture sets a and b

$g(X)$ limit state function

H height of the disposal facility

h hydraulic head

$H(x,\theta)$ Random field

H_g aquifer thickness

i hydraulic gradient

I_f indicator function

I_i set of indices

K hydraulic conductivity

K_d distribution coefficient

K_f hydraulic conductivity of fracture

K'_f distribution coefficient in fracture

K_l leach rate or fractional release rate of the nuclide

K_m hydraulic conductivity of rock matrix

L length of the disposal facility

l auto-correlation length

l_e the length of element in the FE mesh respectively

l_f length of fracture

m number of random variables

M_{in} inventory of the radionuclide corresponding to 50 GWe.y energy production

N number of collocation points used to estimate the PCE coefficients

n_F samples belonging to failure event

N_j set of basis functions

$N_j^l(x^l)$ C_0 continuous basis function

N_p maximum number segments in each fracture

n_T total number of samples

N_{ss} Number of samples per subset

nn number of independent inputs

p order of polynomial

$P(F)$ unconditional probability density function

$P(f_i)$ probability of intermediate failure events

p_a probability that fracture will continue or terminate when it meets the other fracture

$p_a(X)$ joint probability distribution of load

$p_b(X)$ joint probability distributions of resistance

P_f probability of failure

P_n number of unknown coefficients

p_r vector of random inputs

Q specific mass supply

q Darcy velocity

Q^α phase internal supply of mass

Q^I, Q^T, Q^B interfacial, top and bottom exchange terms

q_d Darcy velocity field

q_r vector of outputs/output metrics

Q_{ex}^α phase change of mass respectively

R retardation factor in fracture

r particle radius

R' retardation factor in rock matrix

$R(x)$ explicit function of the random variables

R_d retardation factor

RD radiation dose

S source/sink term

$S_d(T)$ inventory during dumping period

S_r surface area of the disposal facility

t time elapsed after disposal

t_o operation time of the barrier

u_a speed of propagation

U_x retarded groundwater velocity

U'_x, U'_y, U'_z retarded longitudinal, lateral and vertical advective velocity

V volume of the disposal facility

var variance

X matrix of dimension $N \times P$

x, r displacements of fracture 1 and fracture 2 from their respective seed points (O and T)

$X - X_1, X_2...X_9$ set of random variables

$x^{(1)}, \ldots x^{(N)}$ sequence of independent and identically distributed samples

x_i random variables

$xi_n(\theta)$ coordinates of realization of random field corresponding to the deterministic function $\phi_n(x)$

$Z(X_i)$ value of the property Z at location X_i

M   number of terms for truncation

Chapter 1

Introduction

1.1 General Introduction

Waste management is one of the crucial challenges faced by the global community today due to its alarming effects on the environment. The generation of waste has increased multi-fold over the past three decades due to ever-growing population, economic growth, urbanization and industrialization. To tackle this issue, a number of waste management methods have been developed which include waste minimization, recycling (helps in energy recovery), treatment, processing and disposal. But, the waste management technique to be implemented relies most importantly on the type of waste (hazardous / non-hazardous). For instance, any issue in handling and managing non-hazardous waste might cause very less or no impact on the environment, while, a disastrous consequence is inevitable in the case of hazardous waste like nuclear waste. Radioactive waste is considered as one of the most destructive forms of waste in the history due to the presence of radioactivity that lasts for hundreds of thousands of years. The reason for the rise of nuclear industry was to meet the global energy demand for developing a sustainable form of energy. So, it emerged in 1950s as a viable source of energy with low carbon emissions over fossil fuels. Since then, nuclear power plants began functioning and at present the

nuclear industry provides almost 11% of the world's electricity (World Nuclear Association, 2015). However, this industrial activity resulted in accumulation of a humongous amount of waste over the past five decades from different sources which include mining and milling, nuclear power plant operations and decommissioning, reprocessing and recycling facilities, research reactors, medical and industrial sources, nuclear weapon programs and accidental releases. The global volume of waste from spent fuel was 2,76,000 tonnes of heavy metal (tHM) by the year 2006, and projected to increase to 4,45,000 tHM by 2020 (ie., growth by approximately 12,000 tonnes annually, IAEA 2006). In India, nuclear industry is the fifth largest source of electricity providing almost 3.22% electricity nationally (IAEA, 2018). The amount of radioactive waste generated is around 4 tonnes per GW-year of electricity generation (DAE, 2014). This statistic is similar to the amount of waste generated in other countries. The rate of radioactive waste is likely to increase further with the emerging nuclear reactors and nuclear power plants in the near future. This appalling trend is a major concern globally and nationally, hence, there is a need to resolve this problem by developing efficient radioactive waste management practices.

The International Atomic Energy Agency stated that " The main objective of radioactive waste management is to deal with radioactive waste in a manner that protects human health and the environment now and in the future, without imposing undue burden on future generations" (IAEA, 1995a). To contain radioactive waste from reaching the geosphere, waste disposal facilities are designed with a set of engineered barriers and natural barriers. The performance of these facilities mainly depends on the physico-chemical properties of radioactive waste planned for disposal, geological properties of containment material used for construction, and, the geo-hydrological conditions of the natural formations (soils or rocks) around the facility. Radioactive waste disposal facilities have been in

existence for past few decades. However, their efficiency reduces over long time periods due to degradation of barriers. In the event of failure of disposal facility, the radionuclides can release into the geosphere and pollute the medium creating a serious damage to the environment and human health. Therefore, to ensure the long term safety of disposal facilities, efficient performance assessment models need to be developed that can quantitatively estimate the potential impact of disposal as it reaches the biosphere.

The general requirements of these models are to predict the extent of safety achieved due to isolation of wastes and, to estimate the risk caused due the failure of these systems by taking into account various scenarios of release of radioactivity through different pathways of intrusion. In the process of formulating a conceptual model that provides the basis for mathematical models, it is necessary to incorporate the effect of all the components involved in the system. However, due to assumptions and simplifications, the real systems are abstracted. So, to bring a sense of realism, the process of radionuclide transport in different geological media (soil and fractured rocks) with complex geometry (ie., dimensionality of problem) and boundary conditions (decaying source term) needs to be addressed in the model. Moreover, the large spatial and temporal scales involved in these models emphasize the need to develop realistic radionuclide transport models that can improve their predictive ability. During the post-closure phase of disposal facility, the temporal scales involved may lead to temperature variations, seasonal fluctuations that can potentially affect the system leading to variabilities in the properties of the system and also the surrounding geological environment. So, ignoring these effects leads to either an underestimation or overestimation of disposal system performance. So, as an integral part of the performance assessment, it is necessary to treat the uncertainties due to inherent randomness in the geological medium, the lack of knowledge in estimating the

transport parameters of the radionuclides and quantify their effect. Using probabilistic analysis, it is possible to estimate the probability of failure by calculating probability of radiation dose exceeding the permissible limit. It is a unique value which delineates the measure of the overall safety in various engineering disciplines (Ang and Tang, 1975). This value is an indication of compliance with set regulatory criteria. Thus, a framework for performance assessment model that integrates the effect of uncertainties in the system helps in providing a basis for a protected and safe environment.

1.2 Need for the study

As mentioned earlier, radioactive wastes have caused more public concern than any other type of waste. So, the systems developed to contain radioactive waste requires more attention due to the high risk (release of radioactivity) caused by any unforeseen incident. An effective radioactive waste disposal system aims for safe containment and isolation of waste from the surrounding environment. According to World Nuclear Association (WNA), out of the total radioactive waste generated around the world, almost 97% of the volume is low and intermediate level waste (LILW), which is volumetrically the most substantial form of radioactive waste and the remaining 3% of volume belongs to high level waste (HLW). To dispose these wastes, containment systems called near surface disposal facilities (NSDF) are designed for LILW (few tens of meters below the ground surface) and, deep geological repositories for the disposal of HLW (few hundreds of meters below the surface). Construction of deep geological repositories has been a debatable subject and they have not been operational anywhere in the in the world so far. On the other hand, NSDFs have been functional in many countries including India from past few decades.

The rising public awareness on the concerns of radioactive waste disposal in NSDFs has impelled the need for an acceptable and trustworthy radioactive waste management program. So, it has become increasingly important to address the issues involved in NSDFs by timely monitoring of the disposal facilities and predicting the possible radiological impact on the environment.

The national and international agencies have provided guidelines for evaluating the performance of the disposal facilities. Safety assessment standards provided by IAEA emphasized the need for the development of integrated performance approach to ensure long-term safety of NSDFs by providing a basis for safety assessment strategies right from the commencement of the construction of disposal facility (pre-operational and operational phases) till the post closure phase period (IAEA, 2011). In the first two phases, safety objective is to site, design, construct, operate and close a disposal facility so that protection after its closure is optimized. The timeline for the safety assessment during these phases last for few years whereas, in the post-closure phase, the time scales become very large ranging to few thousands of years. Therefore, the primary objective after the closure of facility is not just to evaluate the performance and radiological impact of the disposal facility, but also to discern the behaviour of the system and the surrounding geological environment evolving over time. In India, any radioactive waste generated during the treatment processes of reprocessing is disposed following the Atomic Energy (Safe Disposal if Radioactive) Rules 1987, published under the Atomic Energy Act, 1962. So, the safe management of nuclear waste has been given utmost priority from the inception of the Indian nuclear energy programme. Atomic Energy Regulatory Board (AERB), provided the regulations for the safety assessment by taking into account the waste inventory, features of engineered and geological barriers, time frame for the analysis (AERB, 2006).

Failure to acknowledge and represent this uncertainty can result in serious criticism of a performance assessment. So, the significance of considering probabilistic aspects in performance assessment was recognised and the influence of uncertainties have been reviewed (Gallegos and Bonano,1993; Helton, 2003). Also in India, the safety standards and regulations that integrate the effect of uncertainty in the parameters in the overall performance assessment have been laid (AERB, 2006). In this thesis, the critical stage of performance assessment (i.e., post-closure safety) is investigated as the complexity, uncertainties and time scales associated with the stage are very high and they are not completely explored.

Although, the predictive models developed so far take into account the factors mentioned above, they lack in incorporating complex geosphere transport models (like radionuclide transport in a fractured rock medium) in the performance assessment. A typical fractured rock deposit consists of a complex heterogeneous network of fractures with unique physical and chemical properties for fracture and rock matrix. To predict the radionuclide transport in such medium, the geometry of fractures and their network needs to be modelled. Also, the effect of geological properties of the fracture and intact rock matrix and geochemical properties of the radionuclide in both fracture and rock matrix should be considered. Ignoring any of these effects leads to impractical results. In India, some potential sites have been proposed for radioactive waste disposal near sedimentary rock deposits which includes Kudankulam (Chennai), Gogi (Karnataka) and Tummalapalle area (Andhra Pradesh) (Elango et. al., 2012; Makolil and Nagar, 2015) which reinforces the need to develop safety assessment model that entails geosphere transport near fractured geological media. As an integral part of performance assessment, the effect of uncertainties have been unified in these models, but most of these methods are con-

servative. So, advanced probabilistic techniques needs to be adopted to treat all forms of uncertainties that include epistemic (due to lack of knowledge) and aleatory (due to inherent randomness in the system). However, it becomes computationally intensive to include both complex geosphere models and the effect of different forms of uncertainties in the performance assessment. So, in this thesis, integrated performance assessment models have been developed for radioactive waste disposal facilities by implementing methodologies that improve the computational efficiency of the models. A schematic view of key areas in the performance assessment of low and intermediate level radioactive waste disposal systems is presented in Figure 1.1.
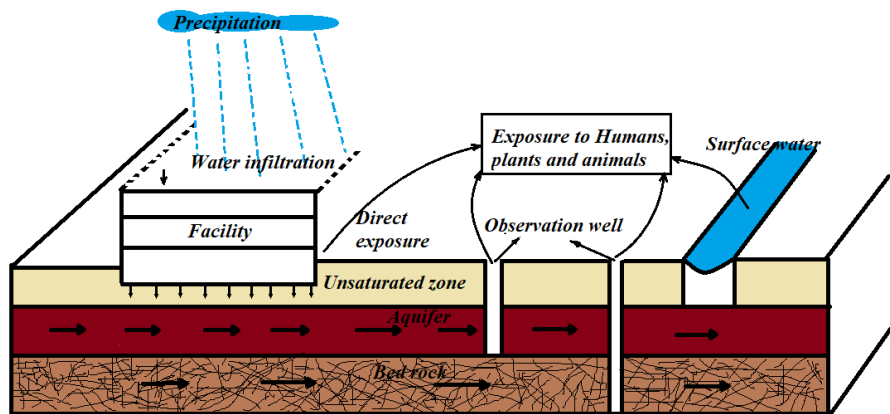
Figure 1.1: Schematic diagram of various components in performance assessment model

The figure presents various physical processes involved in transport of radionuclides from the disposal facility into different geological media including soil and rocks and the possible areas of exposure. This thesis addresses all the above issues and presents an advanced, more detailed, and systematic approach of developing conceptual radionuclide transport models in different geological environment for the performance assessment of radioactive waste disposal facilities. The uncertainties of various forms are addressed to generate realistic results in the prediction of their performance. The algorithms for handling the complexities in radionuclide transport models and integrating the probabilis-

tic techniques are coded using MATLAB and PYTHON and simulations are automated. Also, the thesis intends to bring out the advantages of this approach over traditional methods that can help further in improving the quality of risk and radiological impact assessment for the practitioners. Overall, this thesis presents safe, economically optimal and acceptable solution strategies for radioactive waste management.

1.3 Objectives of the thesis

Ensuring long-term safety of radioactive waste disposal facilities requires development of models that can predict the risk and radiological impact caused due to release of radioactivity from the facilities to biosphere. This involves modelling complex radionuclide transport process and quantifying the effect of various uncertainties on their performance. Such models help in decision making, enhancing the long-term performance and implementing cost-effective, competent design for radioactive waste containment systems and most importantly achieving a protected environment. Keeping all the above factors in the viewpoint, the objectives of the thesis are presented below.

1. To develop computationally efficient performance assessment models for NSDFs that can estimate the critical radionuclides causing maximum radiological impact on the environment and also quantify the influence of input parameter uncertainties in the model.

2. To develop a radionuclide transport model that can incorporate the complexities in the domain and boundary conditions and also, propagate the effect of epistemic and aleatory uncertainties in the system by efficient probabilistic techniques. To develop algorithms that can integrate the deterministic and probabilistic components

of performance assessment models.

3. To develop numerical model that can predict the radionuclide transport through fractured rock and treat the uncertainties involved in geological and transport properties of radionuclide. To develop new add-in features that can create stochastic fracture patterns, local aperture variations along the fracture and finally integrate these features into numerical model.

4. To identify the critical parameters that leads to failure of disposal systems by performing sensitivity analysis and also measure the probable chance of failure through probabilistic simulation techniques. These measures give a reasonable assurance of safety of structures.

1.4 Organisation of thesis

The thesis is organized into seven chapters including the current chapter (Introduction). A brief overview of each chapter is given below.

Chapter 1 presents a general introduction on the global concerns involved in radioactive waste management and also, the waste management practices that have been implemented so far to ensure a protected environment. The need to develop models that can assess the performance of disposal facilities is emphasized. Also, the need to integrate the effect of various uncertainties in these performance assessment models for a better safety estimate is highlighted in this chapter. The objectives of the thesis and the order in which this thesis is organized are also presented in this chapter.

Chapter 2 gives a detailed review on various performance assessment models presented in the literature so far. The geological transport of radionuclides constitutes the

9

crucial part of integrated performance assessment. So, an overview of various contaminant transport models through various geological media (soil and fractured rocks) are presented. Also, various probabilistic techniques developed by the researchers to take into account, the effect of uncertainties and employ them in various engineering problems are also discussed in detail. The need to integrate these methods into performance assessment framework is also highlighted in this chapter. This chapter provides the scope of the thesis by identifying the areas that received little attention in literature.

Chapter 3 provides an overview of the deterministic and probabilistic components of performance assessment model for radioactive waste disposal facilities. The analytical and numerical formulations involved in source term, repository failure, geological transport and radiological models are presented. Various probabilistic techniques adopted to propagate and quantify the effect of uncertainties on the performance of disposal facilities are discussed. These methods include simulation methods like Monte Carlo simulation and subset simulation for reliability analysis. The random field modelling to discretize a spatially varying medium is discussed briefly. Also, meta-modelling techniques adopted to improve the computational efficiency and sensitivity methods to estimate the critical parameters affecting the response of the system are discussed.

In **Chapter 4**, probabilistic performance assessment model is developed for NSDFs. The risk and radiation dose due to release of a radionuclides from the facility to the human habitat is evaluated from an analytical model. The computational issues involved in propagating parametric uncertainties using analytical model are overcome by adopting efficient meta-modelling technique (Collocation based Stochastic Response Surface Method). Further, the parameters that critically affect the safety of the system are identified by adopting global sensitivity analysis.

In **Chapter 5**, a three-dimensional radionuclide transport model through soil that accounts for complexity in domain and boundary conditions is developed. The effect of epistemic and aleatory uncertainties on the performance of disposal facilities is explored. To integrate and quantify the effect of epistemic uncertainties, computationally effective meta-modelling technique is adopted. The inherent heterogeneity in the soil medium and its stochastic nature is modelled as a random field. The effect of such spatially varying environment on the flow and transport of radionuclide is assessed. This uncertainty is also quantified by subset simulation method. A new improved numerical model is developed with additional features like the complexity in the geological medium and their variabilities. The model results give a broader perspective on the important aspects of probabilistic performance assessment model for NSDFs.

In **Chapter 6**, the effect of a fractured rock medium on the safety of disposal facilities is explored. A new hybrid model that predicts the flow and transport behaviour of contaminant through fractured sedimentary rock is proposed. The effect of local aperture variation along the fracture (developed as an add-in feature) is also investigated. The overall performance assessment of the disposal facility is estimated using this numerical model. The analysis is carried out for both non-reactive contaminant (brine) and reactive contaminant (radionuclide). The parametric uncertainties in the geological properties of the fractured medium and the transport properties of the contaminant are treated and quantified by adopting efficient probabilistic methods. Also, the critical parameters affecting the radiation dose and risk are identified by adopting sensitivity methods.

Chapter 7 presents the major conclusions from the various studies carried out in the thesis. Appendices, references and scope for future work are presented at the end of thesis.

Chapter 2

Literature review

2.1 Introduction

The safe management of radioactive waste plays a key role in the nuclear power industry. It involves development of disposal facilities that can isolate the radioactive waste and also provide long-term protection to human health and environment. The functionality of a disposal facility is hinged on confirming the radiation dose and risk levels to be as low as attainable during operational, closure and post-closure phases of disposal (which lasts for few thousands of years). So, it becomes crucial to quantitatively predict the radiological impact (dose, risk) due to the failure of radioactive waste repository by means of performance (or safety) assessment models (Campbell and Cranwell, 1988). The safety is sought over large spatial and temporal scales which indicates the potential impact of variations in climate and surrounding geosphere on overall performance. In such a complex environment, there is a definite effect of uncertainties from various sources (like parameter uncertainties, inherent randomness in the system, design life of barriers etc) on the performance of the disposal system and, ignoring these uncertainties leads to limitations like underestimation or overestimation of results. So, uncertainty analysis becomes an intrinsic part of performance assessment modelling. To increase the

confidence that the predictive model results are adequate, the primary goal is to systematically implement techniques for identification, propagation, quantification and reduction of uncertainty. To deal with these aspects, reliability and sensitivity analyses need to be performed by implementing efficient probabilistic methodologies. By advocating these techniques, reasonable assurance can be achieved on the overall performance results and eventual decision making.

In this chapter, a review of the safety assessment modelling procedures developed to predict the radiological impact due to the release of radionuclides from the waste disposal systems into the biosphere are presented. Before discussing the modelling studies, a brief outline of the radioactive waste management practices adopted in India and the designs of near surface disposal facilities (NSDFs) (to contain low and intermediate level wastes) developed so far and implemented in disposal sites are presented. Though the conceptual modelling aspects involved in predicting the safety of the disposal system remains the same (i.e., source term, geosphere transport etc), there has been an advancement in mathematical and numerical modelling techniques over the past few decades to model the contaminant transport in the geosphere. The evolution of these techniques and their impact on the post-closure safety assessment of radioactive waste disposal systems are also discussed. In the process of contaminant transport modelling, the geological medium of transport also affects the flow path of contaminant, and hence, the studies carried out on contaminant transport in different geological media are also presented. The mathematical models developed so far succeeded in accounting for complexity in the system to an extent, but, they lack in eliminating the uncertainty in the predicted results for risk and radiation dose. So, different sources of uncertainties dealt by the researchers in the past and the techniques used to handle and quantify the uncertainties are reviewed in the chapter.

Also, a brief review of studies that incorporate the reliability and sensitivity methods in the safety assessment models and, the scope of the present study are presented.

2.2 Radioactive waste management

Nuclear power is one of the reliable and efficient sources of energy despite its controversial reputation. It is economically feasible, environmentally friendly and provides more than 11% of the global electricity. For instance, the green house gas emissions from a nuclear power plant are by two orders of magnitude lower than those of fossil-fuelled power plants (Abu-Khader, 2009). Moreover, to meet the increasing energy demands and reduce green house gas emissions, it becomes necessary to expand nuclear industry worldwide. The international energy forecast predicts large growth in nuclear power generation over the next 30-50 years. Needless to say, any industrial activity involves generation of waste and, nuclear industry is no exception. A large amount of radioactive waste has been accumulating over the last five decades and the expansion of commercial nuclear power production further will result in increased radioactive waste generation. It is critical to manage this waste effectively and this became the primary consideration for future nuclear fuel cycles around the world. The International Atomic Energy Agency (IAEA) stated that fundamental principle of radioactive waste management is to handle the waste such that it protects the human health, environment and does not impose unreasonable burden on future generations (IAEA, 1995). Keeping this in the viewpoint, radioactive waste management practices were developed. The desirable sequence of waste management practices include waste minimization, recycling (which can recovery energy), treatment and processing, and disposal. Though the most preferred practice is to prevent waste

generation, it becomes inevitable to stop the process. So after undergoing segregation, conditioning, treatment and processing, the waste is disposed in proper disposal facilities. A great deal of work has been carried out in this area in various countries, especially in UK, USA, Czech Republic, Finland, France, Japan, Netherlands, Spain, Sweden, Korea, and Lithuania. To assign proper management system, firstly, the radioactive waste need to be classified. Internationally, the waste classes include: exempt waste, low-level waste, intermediate-level waste, high-level waste and transuranic waste. This classification is based on the level of activity in the waste in the order of least to highest activity. Once the wastes are classified, they are treated and disposed. Overall, the main functions involved in radioactive waste management can be broadly categorized into two phases (Grill, 2005; Abu-Khader, 2009). They are:

1. Short-term management: This phase involves an immediate treatment of waste. For example, treating the waste such that it attains a stable form (by some chemical process like vitrification, ion-exchange etc) (Sobolev et. al., 2005; Raj, et. al., 2006).

2. Long-term management: After proper treatment, in this phase, the waste can moved to storage facilities. Further, depending on the level of activity, they are disposed in geological formations. Also, transmutation (transformation of the waste into an inert non-hazardous form), reuse and space disposal are other long-term waste management options. (Rice et al., 1982; Duncan, 2003; Hoffman and Stacey, 2004; Crow, 2007)

Although, disposal systems are designed to contain radioactive wastes from the surrounding environment, it is necessary to ensure long-term performance of the disposal system.

Even in the case of the unforeseen accidents, consequences of radioactivity releasing should be within the safe regulatory limits. In this context, a performance assessment model is developed which is quantitative evaluation of potential releases of radioactivity from a disposal facility into the environment, and assessment of the resultant radiological doses. The term performance assessment can refer to the process, model, or collection of models used to estimate future doses to human receptors (NRC, 2000). Generally, performance assessment is conducted to demonstrate whether a disposal facility has met its safety objectives. So, this chapter discusses the literature on various performance assessment models that were developed to meet the design and safety objectives of radioactive waste disposal systems in various countries.

2.2.1 Radioactive waste management in India

In India, nuclear power has become the fifth largest source of electricity after the thermal and hydel sources of power. Since 2017, almost 3.22% of electricity is supplied from the seven operational nuclear power plants. A few more plants are upcoming and under construction which are shown in Figure 2.1. It is inevitable to eliminate the process of waste generation from industrial activities. Moreover, with the ever increasing energy demand and advancement in field of nuclear technology, there is an absolute need to develop strategies for radioactive waste management. In India, radioactive waste management facilities have been operating for almost three decades. So, the Indian nuclear energy programme aims to establish radiation protection goals that accounts for the environment concerns right from its inception. Atomic Energy Regulatory Board (AERB) and BARC (Bhaba Atomic Research Center) Safety Council (BSC), are the regulatory bodies constituted in the years 1983 and 2000 respectively under the Atomic Energy Act, 1962.

NPP Operating and Under Construction in India

Figure 2.1: Operating and planned nuclear power plants in India, (WNA, 2019)

They are entrusted with the responsibility of protecting workers, public and the environment against harmful effect of ionising radiation.While BSC regulates safety of BARC facilities, AERB regulates nuclear and radiological facilities in public domain (Jayarajan, 2017). They develop guidelines for management of radioactive waste in India. So, the various stages of radioactive waste management includes six main processes namely characterization, treatment, conditioning, storage, disposal and monitoring of waste (Raj et. al., 2006; Wattal, 2013). The mechanisms involved in each of these processes are presented in Figure 2.2. It is essential to understand the classification (or characterization) of radioactive waste to set up proper management system.
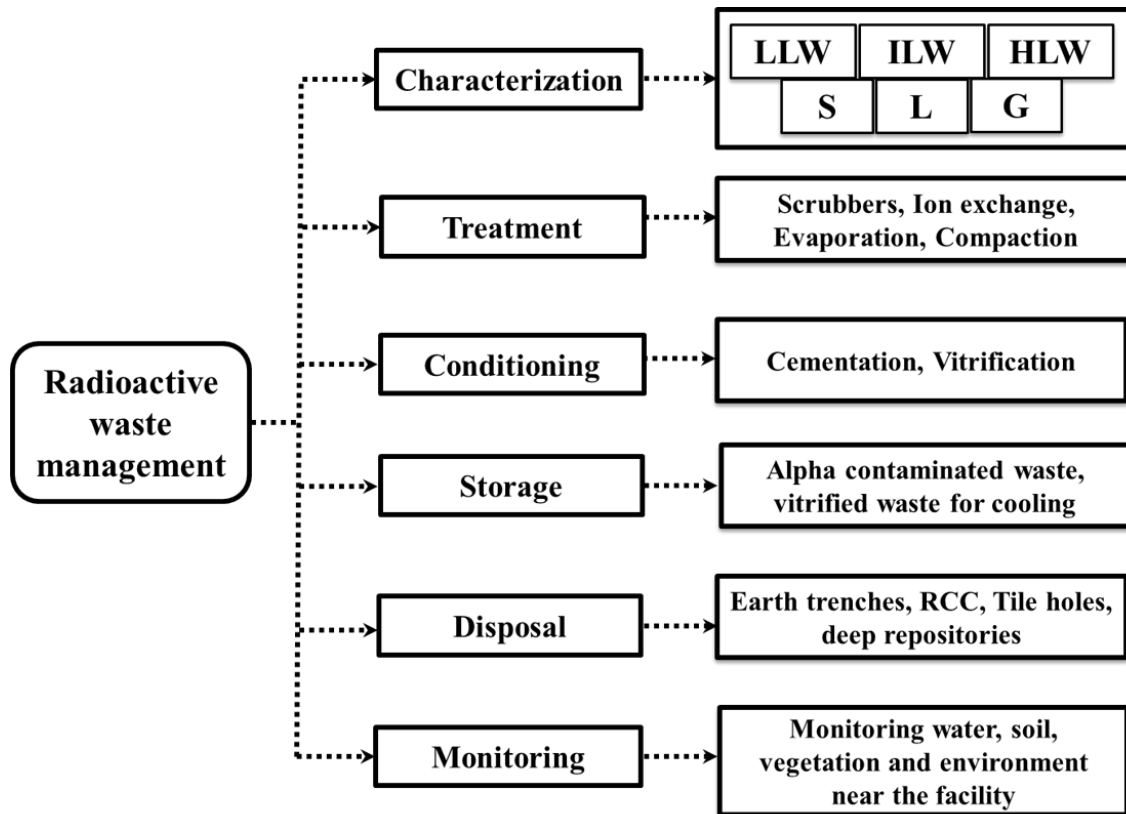
Figure 2.2: Different steps involved in radioactive waste management

So firstly, the waste is characterized both qualitatively (source and nature of waste) and quantitatively (type and amount of radioactivity) (AERB, 2011) to determine its physical, chemical and radiological properties. By characterizing the waste, it can be segregated for re-use and disposal. Further, based on the waste charaterization i.e., physical state of radioactive waste (solid (S), liquid (L) and gas (G)) and the level of activity (low-level, intermediate level, high level), they are treated and conditioned. The treatment process is employed to reduce the activity concentration to a level that can allow its discharge to the environment (as per national regulations). The treated waste is immobilized by implementing conditioning techniques like cementation and vitrification. In the final stage, the waste is stored and disposed in proper disposal systems.

2.2.1.1 Waste disposal systems

The waste generated from different locations during the operation of : nuclear facilities, fuel fabrication, research reactors, fuel processing, isotope production and research laboratories are collected and disposed in the site (Kumar et. al., 2013). Based on the type of waste disposed, the geological characteristics of the site, different waste disposal facilities are designed and the design specifications and regulations are provided by AERB. For example, low and intermediate level wastes (LILW) are disposed in systems that are within 50 m from the surface and over three decades, the designs of these systems have been refined and improvised. On the other hand, high level radioactive wastes (HLW) are disposed in deep geological repositories located few hundreds of meters below the surface. Some potential geological sites have been identified for high and long-lived radioactive wastes repositories, however, they are not operational anywhere in the world so far.

2.2.1.1.1 Near Surface Disposal Facilities

Near Surface Disposal Facilities (NSDFs) are designed to contain low and intermediate level radioactive wastes. In India, they are located near the seven nuclear power plants. The disposal modules include (Raj et. al., 2006):

1. **Stone-lined earth trenches**: These systems are developed to contain radioactive wastes with surface dose rate less than 2 mGy/h. The soil is excavated at a depth of 1 m - 4 m with stone lining. The lining provides stability to the system. A typical stone line trench is shown in Figure 2.3 (i).

2. **Reinforced concrete trenches**: The wastes with surface dose rate between 2 - 500 mGy/h are disposed in these systems. A typical RCC trench is 4.8 m deep, 2.5

m wide and 15 m long as shown in Figure 2.3 (ii). The outer containment wall thickness varies from 350 mm at the top to 750 mm at the bottom. Adequate water-proofing is provided all around to prevent ingress of groundwater.

3. **Tile holes**: The wastes with surface contact dose above 500 mGy/h due to beta, gamma activity are stored in tile holes. These are circular vaults, nearly 4 m below ground level having an average inside diameter of 710 mm. These are made of 6 mm thick carbon steel shell with 25 mm thick concrete lining on both sides and provided with adequate waterproofing. The schematic of a tile hole is presented in Figure 2.3 (iii).

The low and intermediate level wastes (i.e., beta gamma activity belonging to Category I, II, and III) are disposed in earth / stone lined trenches, RCC trenches and tile holes depending on the activity content and the waste form. High level waste, which belongs to Category III and IV are generally stored in high integrity containers and / or tile holes. Further, the wastes with high alpha specific activity are shifted for storage and further transported to deep geological repositories. Kumar et. al., (2013) discussed various options for disposal of solid waste based on the above categories. After the storage and disposal of radioactive waste, provisions are made to monitor the design of the disposal facility. They include bore holes, site-specific soil samples, groundwater samples to check the uptake of radioactivity in the surrounding geological medium. Although the technologies adopted currently for the design of disposal systems are sufficient, there is still a scope for improving these technologies to enhance their performance and meet the future challenges.
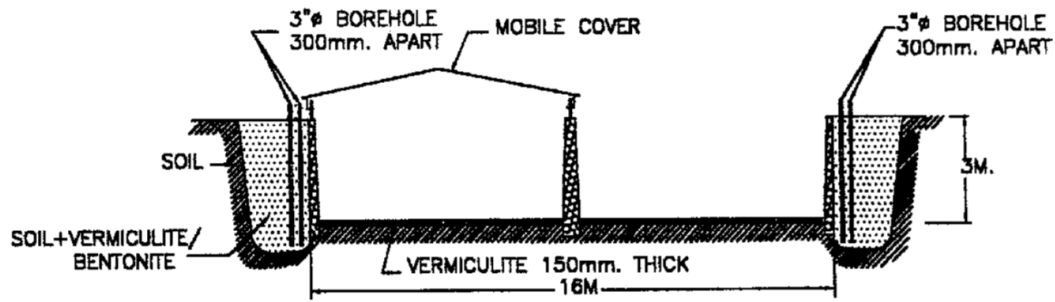
(i) Stone line trench
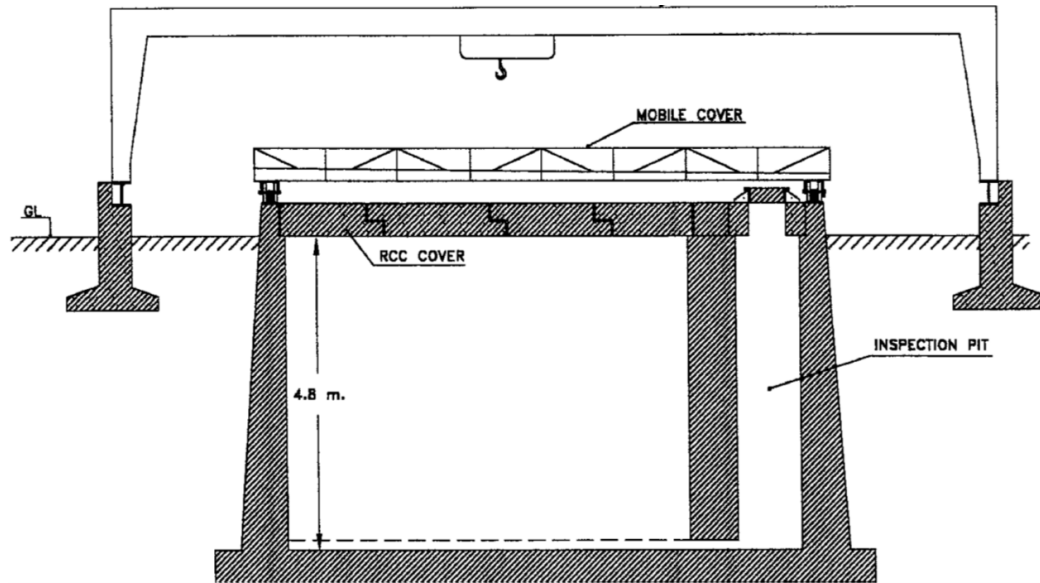
(ii) RCC trench
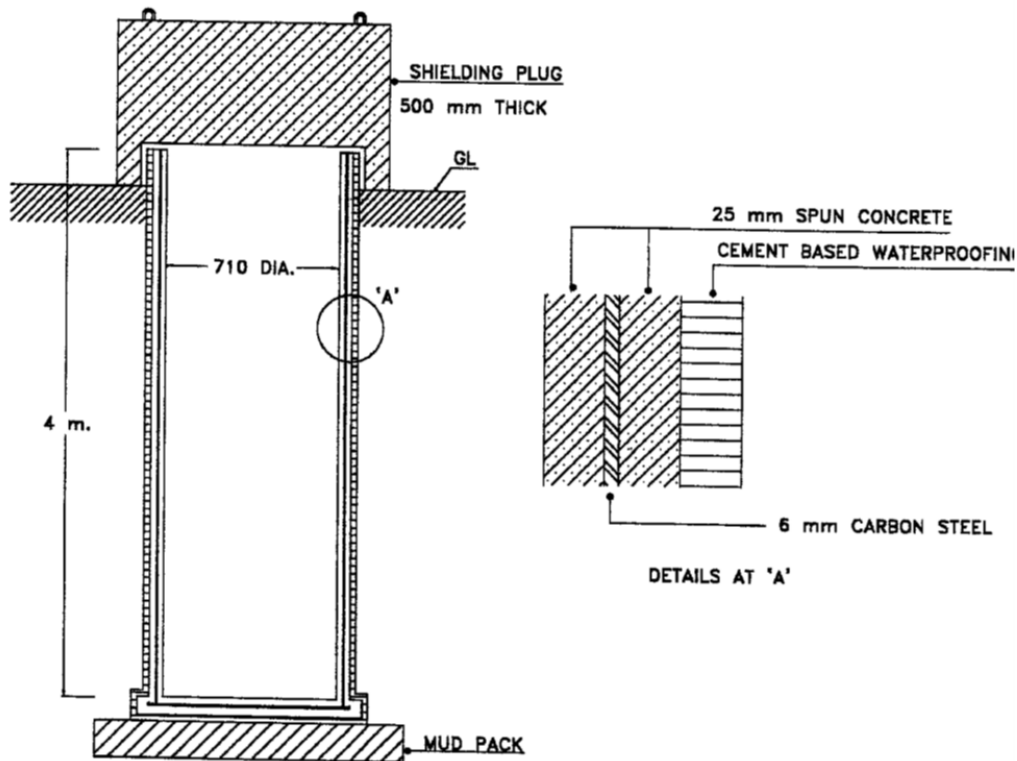
(iii) Tile holes

Figure 2.3: Types of NSDFs (Rakesh et. al., 2005)

21

To achieve this safety objective, there is a need to carry out performance assessment of the disposal systems by developing predictive models. In the next section, various studies that were carried out in developing performance assessment models are presented.

2.3 Performance assessment model for radioactive waste disposal facilities

To assess the long-term safety of radioactive waste disposal facilities, performance assessment models are developed. This approach has been widely accepted in estimating the long-term performance of radioactive waste repositories in various countries (Hoffman and Miller, 1983; Apostolakis, 1990; Helton, 1993; IAEA, 1995; Neretnieks, 1999; NRC,2000; Ramsøy et. al., 2004; AERB, 2006). Although, over the past three decades, many improvements have been suggested in the guidelines, the basis for developing the performance assessment model remains the same. It takes into account the nature of the facility, radioactive inventory, geo-hydrological and geo-chemical behaviour of the site, pathways and possible scenarios for release and transport of radioactivity and translate them into mathematical models based on the input characteristics. Further, these models are used to calculate the radiological dose estimates. These values may not necessarily predict the exact behaviour of the disposal system over time, but they provide a sufficient quantification to demonstrate safety through compliance with the standards set by regulatory authorities. Since the waste considered for the analysis is radioactive in nature, the spatial and temporal scales of analysis are quite large. So, it is important to note that the time scale considered in the safety assessment must be comparable with the duration for which the waste potentially remains hazardous to man.

2.3.1 Theoretical framework and reports for developing performance assessment models in soil and fractured rocks

Campbell and Cranwell, (1988) presented one of the earliest works to assess performance of a geologic radioactive waste repository in the form of a theoretical framework. The primary concept of this methodology is to generate scenarios and evaluate its consequence. The releases of radionuclide was estimated by accounting for all significant processes and events that could affect a repository, examining the effect of these processes and events on the performance of a repository and demonstrate compliance or non-compliance with the standards as well as with other EPA (US Environmental Protection Agency) and NRC (US Nuclear Regulatory Commision) regulations.

The reports by regulatory body International Atomic Energy Agency (IAEA) (IAEA, 1995; IAEA, 1999; IAEA, 2004; IAEA, 2014) presented safety guidelines for classification of radioactive waste, design of near surface disposal facilities for radioactive waste and safety assessment for near surface disposal of radioactive waste which encompasses a complete set of regulatory procedures to be followed for safe disposal of radioactive wastes. The safety procedures are developed right from the inception of radioactive disposal which involves site characterization, design, construction, operation and closure of disposal facility so that protection after its closure is optimized. The social and economic factors are also taken into account to attain a reasonable assurance that doses and risks to members of the public in the long term do not exceed the dose constraints or risk constraints that were used as design criteria.

To provide the national safety codes, guidelines and manuals for classification and management of radioactive waste in India, the reports AERB (2006), AERB (2007) and AERB

(2011) have been developed. They are formulated on the basis of nationally and internationally accepted safety criteria for design, construction and operation of specific equipment, structures, systems and components of nuclear and radiation facilities. The report by AERB (2006) provides guidelines for near surface disposal of radioactive solid waste. It also provides a guidance on siting, design, construction and operation of near surface disposal facility (NSDF) to facilitate safe disposal of low and intermediate level radioactive solid waste. The salient responsibilities of the waste generator / manager for safe disposal of radioactive waste are also mentioned in this report. It also describes various types of near surface repositories, available options, acceptance criteria, safety assessment, radiation protection and site remediation activities in case of incidental / accidental radioactive contamination. To evaluate the performance of disposal facility and its components individually and also, estimate the radiological impact on public and the environment, safety assessment is carried out by developing predictive models. It provides reasonable assurance of safety of the NSDF in terms of radiation dose or risk to members of the public. The sequence of steps followed in safety assessment modelling given by AERB (2006) are presented in Figure 2.4. This framework is followed in the present thesis to develop the safety assessment model for near surface disposal facilities. Each of these components are discussed elaborately in the next chapter.

These reports give a general overview of the safety procedures to be adopted for safe disposal of radioactive waste. There were many performance assessment models developed worldwide by adopting these safety procedures. Since the geosphere surrounding the disposal facility also plays a critical role in estimating the performance, various models developed near soil and fractured rock are discussed in the following section.
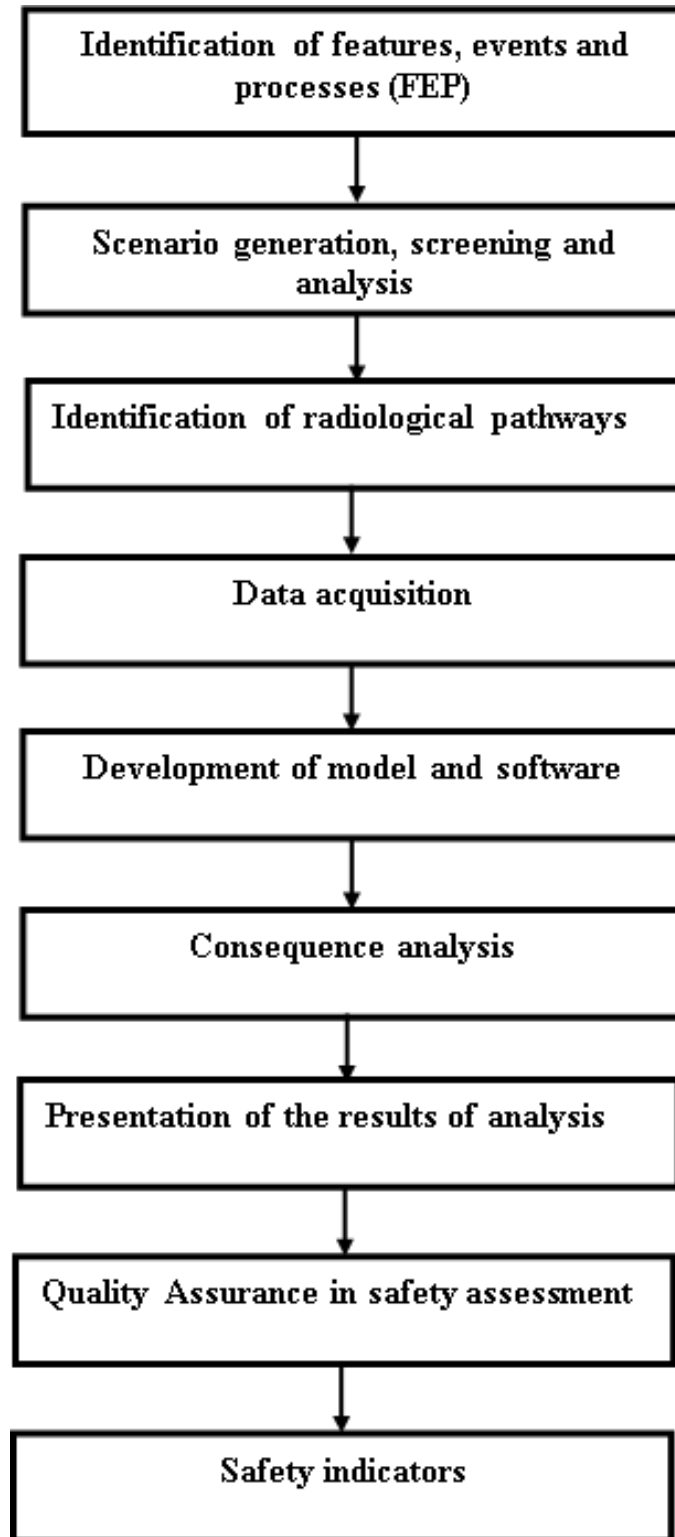
Figure 2.4: Steps followed in safety assessment modelling

2.3.2 Performance assessment models for radioactive waste disposal systems near soil and fractured rocks

2.3.2.1 Soils

Kim et. al., (1993) developed a simplified mathematical model for risk assessment of shallow land burial, designed to dispose low level radioactive waste. The composite model formulated mathematical equations for source term, repository failure model, geosphere model, biosphere model, and finally, a dose-and-health-effects model. The results suggested that the highest value of the total annual dose appeared at about 100 years after disposal, and the dominant nuclides were ^{63}Ni and ^{13}Cs. The analytical model developed in this work provided a basis for decision making regarding management of waste repository system.

Krishnamoorthy et. al., (1997) presented a comprehensive analysis of estimating the activity concentrations and dose limits of 26 radionuclides that migrated from shallow land burial facilities at Trombay in Mumbai (India) using different release scenarios. The exposure pathways considered for the analysis are well water drinking pathway, marine food consumption pathway and exposure to workers. The results showed that short-lived radionuclides ^{54}Mn, ^{55}Fe, ^{65}Zn, ^{60}Co and $^{103/106}$Ru were restricted within the disposal system due to high distribution coefficients and short half-lives. On the other hand, long-lived radionuclides ^{14}C, ^{99}Tc and ^{129}I could easily migrate from the repository and reach the environment due to low distribution coefficient and long half-lives. By quantifying dose limits and activity limits, this study helped in providing insights on the critical radionuclides that could potentially affect the performance of shallow land burial facilities

at a typical coastal site.

Nair and Krishnamoorthy (1999) developed probabilistic safety assessment model for NS-DFs. The end-points of assessment are expressed as radioactivity release rate, radionuclide concentration in ground water, radiation dose to a member of the critical group through drinking water pathway and total risk to critical group due to disposal practice. The results indicated that amongst different long-lived and short-lived radionuclides, ^{129}I was the critical radionuclide delivering maximum dose in most cases though it constituted a low percentage in the low-level radioactive waste inventory. The aspects of uncertainty and sensitivity analyses were also presented. The mathematical model was coded in FORTRAN-90 for the ease of adaptability in different computational environments.

Rakesh et. al., (2005) carried out radiological impact studies at Radioactive waste Storage and Management Site (RSMS) which is close to a near surface disposal facility (NSDF) situated at Bhabha Atomic Research Centre, Trombay. The post-closure safety and uncertainty analysis of RSMS, Trombay site was performed using site-specific data (i.e., geo-hydrological and geo-chemical parameters). The important pathways considered were drinking water pathway, marine water pathway and human intrusion pathway for the calculation of expected radiological dose to critical group. The radioactivity in spent resin and sludge cakes was roughly 90% ^{137}Cs and 10% ^{90}Sr, while, the radioactivity in spent sources was 100% ^{60}Co. The radiation dose results showed that there was no contribution from any of these radionuclides due to their high values of distribution coefficient. The predicted maximum possible dose that a critical group member got due to radioactive waste disposal from RSMS site was by marine exposure pathway (2.55×10^{-7} Sv/y), which was less than the dose specified by the regulatory body. This analysis confirmed the overall efficiency of NSDF located near Trombay.

Nair et. al., (2006) developed generic method to evaluate the reasonable upper-bound (RUB) dose from the seven near-surface radioactive waste disposal facilities (located in India) through drinking water pathway. The concentrations and effective radiation dose rates due to different radionuclides were evaluated at different distances from the disposal facilities. The RUB effective dose rates for sites with ground water velocity greater than 10 cm/day at 1, 2, and 3 km were ;0.03, 0.02, and 0.01 mSv/yr, respectively, for a nuclear power level of 1 GW (electric). These dose rates were reduced by a factor of 2 for disposal sites with ground water velocity less than 10 cm/day. This method was found useful for screening analysis of proposed low-level radioactive waste disposal sites as the RUB effective dose rates could be estimated as a function of distance and nuclear power capacity for different categories of sites.

The performance assessment models presented so far were developed by translating the conceptual model to mathematical models (or analytical models). So, the components of the model (i.e., source term, repository failure, geological transport and radiological models) were developed using mathematical equations. However, with the increase in complexity of domain / geological media, it becomes difficult to develop analytical closed form solutions. In such cases, modelling is carried out using numerical methods which include finite element methods, finite difference methods etc. Some of the past studies that developed numerical models for performance assessment are presented below.

Jakimavičiūte-Maseliene et. al., (2006) presented model studies to evaluate the activity of long-lived radioactive wastes disposed in deep geological formations in Lithuania. The migration of ^{129}I through tectonically fractured domain was modelled using FEFLOW (numerical software) and the results showed that that doses reaching human habitat did not exceed the existing dose restrictions. Predicted volumetric activity of ^{129}I at 363 m

distance from repository in groundwater was of the order 10^{-3} Bq/l. The results from this study indicated repository built in crystalline basement could contain long-lived and high-level radioactive wastes.

Nair et. al., (2010) and Chopra et. al., (2013) developed numerical models that predict the contaminant transport due to the decay of radionuclides from uranium tailings pond. These studies were similar to radionuclide transport from the waste repositories into geosphere except that the radionuclides (in uranium tailings pond) are different in these cases. Nair et. al., (2010) developed a three-dimensional numerical groundwater contaminant transport model that can handle heterogeneity for decay chain transport in groundwater from uranium tailings ponds. In this study, it was shown that exclusion of the decay chain transport underestimates the radiological impact of uranium tailings ponds by a factor of 100. The necessity to monitor short-lived progeny radionuclides also, apart from their long-lived ones, in the groundwater in the vicinity of uranium tailings ponds during their institutional control period is demonstrated. Chopra et. al., (2013) modelled the groundwater flow and contaminant transport model for uranium tailings pond site using FEFLOW. The radiological impact of the tailings pond at Turamdih, Jharkhand, India, to the public was estimated. The dose rates due to ^{238}U and its progeny through drinking water pathway were found to be 0.068 and 0.026 mSv/year at distances of 500 and 600 m from the tailings pond centre along the direction of groundwater flow and these values were found to be within the regulatory threshold.

2.3.2.2 Fractured rocks

Neretnieks (1990) reported solute transport modelling through fissured rocks and applied to radioactive waste repositories. The strong influence of flow rate and flow distribution

at repository depth on radionuclides, the influence of the flow paths and velocities on the travel time, were studied in this report. The investigations aimed at assessing the long term safety of nuclear waste repositories where the time scales involved ranged from hundreds of years to many millions of years because of the very long half-lives of several of the radionuclides. The influence of each transport process along fractures and rock matrix were quantitatively illustrated in the form of tracer tests. The influence of sorption and other geochemical reactions were found to influence the movement of radionuclides along fractures (only for sorbing radionuclides). Also diffusivities through the rocks of different genesis were determined for Iodide. The peak arrival times, the residence time distribution and the spatial distribution of the tracers were presented in the report. The simulations indicated that only a few percent of the fractures were open to flow and for reacting solutes they had a very large impact because they would see much less rock to react with. These results presented baseline for the important factors that affect the transport of radionuclides in crystalline rocks.

Krishnamoorthy et. al., (1992) developed a radionuclide transport model to predict the movement of radionuclides in the fracture of a host rock matrix. The mathematical formulations consisted of one-dimensional coupled equations for fracture and rock matrix. The transport mechanisms included advection, diffusion, dispersion, radioactive decay and adsorption. However, advection was assumed to be the predominant transport mechanism in fracture, while, diffusion in rock matrix. From the analysis, the spatial and temporal extent of concentration and flux at the outlet of fracture were estimated for radionuclides typically encounted in high-level radioactive waste repositories. The concentration values reduced with the increase in distance along the fracture due to sorption and decay. But, the results for ^{129}I did not not exhibit any variation due to different fracture length for

varied fracture apertures. Also, the transport process showed retention of a significant fraction of radioactivity in the micro-fissures of the host rock, with only a small fraction finding its way into the fracture water.

Yim and Simson (2000) reviewed performance assessment models and their application to civilian LLW disposal facilities in the U.S.A. Near field models were developed which accounted for water infiltration into the concrete vaults, waste containers and release into the geosphere. Further, the model for groundwater flow and transport of contaminants to biosphere were also modelled. From the analysis, it was found that conceptual performance assessments with overly conservative assumptions resulted in conceptual non-compliance with regulatory requirements. The approaches that were taken to remedy this included, better characterization and modelling in areas identified by the performance assessments as the most important places to estimate dose to humans. In this way, they suggested that performance assessment can be continued for both refinement of the analyses and, as a tool to demonstrate the compliance of a particular site to the regulatory requirements.

Blum et. al., (2005) presented a methodology for upscaling hydro-mechanical (HM) processes from the small scale (metre scale) to the large scale (kilometre scale), to assess the performance of deep waste disposal systems. The results showed strong sensitivity of the hydraulic apertures to the mechanical properties of the rock mass and the fractures. The results from HM analysis indicated that, in the small and large-scale analyses, mechanical properties and their spatial variations; uncertainty in the fracture density and the spatial distribution of the fracture density were critical factors in performance assessment of deep waste disposal.

Jakimavičiūte-Maseliene et. al., (2006) presented a numerical model to simulate the migration of radionuclides from crystalline basement near Lithuania. The lithology of do-

main included limestone, sandstone, weathered rocks and crystalline rocks underlying sandy loam. FEFLOW software was used to model various geological environments in the system. The results indicated that concentration of ^{129}I was within the limits and the site functioned well for deep waste disposal.

Kautsky et. al., (2016) discussed the challenges associated with the development of models that simulate surface ecosystems over such long time scales. The assessment was carried out for repository (with disposal chambers situated in rock at 60 m depth beneath the present-day sea floor) that contains low and intermediate level nuclear waste in Forsmark, Sweden. The surface ecosystem which consisted of landscape, climatic factors, rock outcrops etc were modelled and fully linked. The external conditions along transport pathways were subject to coordinated spatial and temporal changes. The release of radionuclides, their transport and radiation dose results indicated that calculated risk for humans did not exceed the risk criteria or the screening dose rate for non-human biota, indicating that the repository design was sufficient to protect future populations and the environment. It was also found that, diversity of food and water pathways need to be maintained, as key pathways for radionuclide accumulation and exposure partly worked in parallel.

Overall, from the above literature, it is clear that, most of the models developed for quantitative assessments of near surface disposal systems, especially in India were all analytical. But, to understand the influence of dimensionality of the domain, the complexities in boundary conditions (hydraulic and transport) and also heterogeneity in the geological medium on the radiation doses, efficient numerical methods must be developed. The numerical modelling techniques include, finite element method (FEM), finite difference method (FDM), finite volume method (FVM) and so on. Also, not many stud-

ies have focussed on understanding the behaviour of radioactive waste in fractured rock medium. So, in the Indian context, performance assessment models need to be developed for ensuring the long-term safety of disposal facilities near fractured rock medium.

2.3.3 Geosphere transport models

From the previous section, it is clear that the type of geological environment affects the transport of radionuclides moving through the medium. Hence, the component, geosphere transport, plays a critical role in performance assessment modelling as the radionuclide concentrations (radiation dose) are affected along the path that leads to the end-point. This indicates the need to understand various processes involved in modelling the transport of contaminant. In any geological medium, the main transport mechanisms that describe the movement of contaminant are advection, hydrodynamic dispersion (i.e., combination of molecular diffusion and mechanical dispersion), adsorption and radioactive decay. The mechanics of transport involved in each phenomenon is presented in Figure 2.5.

There can also be an influence of other chemical reactions like acid-base reactions, solution-precipitation reactions, oxidation-reduction reactions, ion pairing or complexation, and biological reactions like microbial cell synthesis barring from the previous transport mechanisms, depending on the reactive nature of contaminant. But, in this thesis, these effects are not considered in modelling the contaminant transport .

2.3.3.1 Soils

It is important to note that besides the transport mechanisms mentioned above, a contaminant transport model also needs to account for factors such as type of soil, the reactive nature of solute / contaminant, type of investigation, process of modelling the transport

and the dimensionality of the problem which are presented in Figure 2.6.
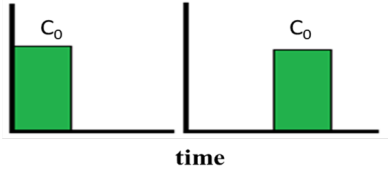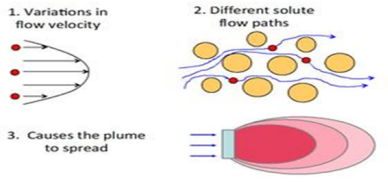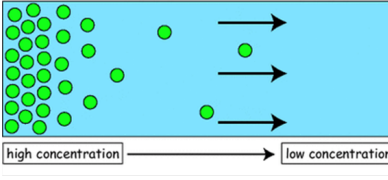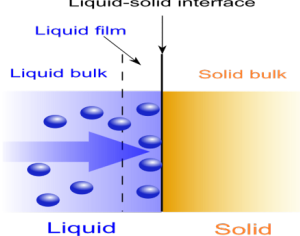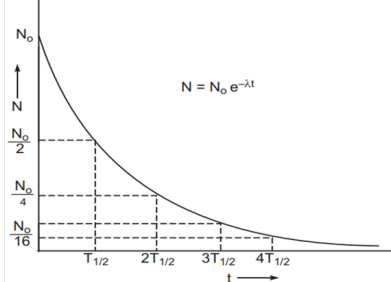
Transport process	Definition	
Advection	Bulk movement of solute due to flowing groundwater	
Dispersion	Spreading of solute due to different velocities along the pore channels, difference in pore sizes along flow paths	
Diffusion	Movement of solute under the influence of concentration gradient	
Adsorption	Solute gets sorbed onto the solid mass due to chemical adsorption leading to change in concentration	
Radioactive decay	Radioactive contaminant are influenced by radioactive decay	

Figure 2.5: Various transport mechanisms in geosphere: Dispersion (ITRC, 2011), Diffusion (Rohit, 2017), Adsorption (Daniele Pugliesi, 2012) and Radioactive decay (Sanjaydas, 2018)

From Figure 2.6, it is evident that a broad spectrum of models can be developed by choosing a factor from each category and combining them. However, it becomes extremely difficult to encompass all these aspects in the present thesis. Some of the significant studies carried out on contaminant transport through soil are presented.
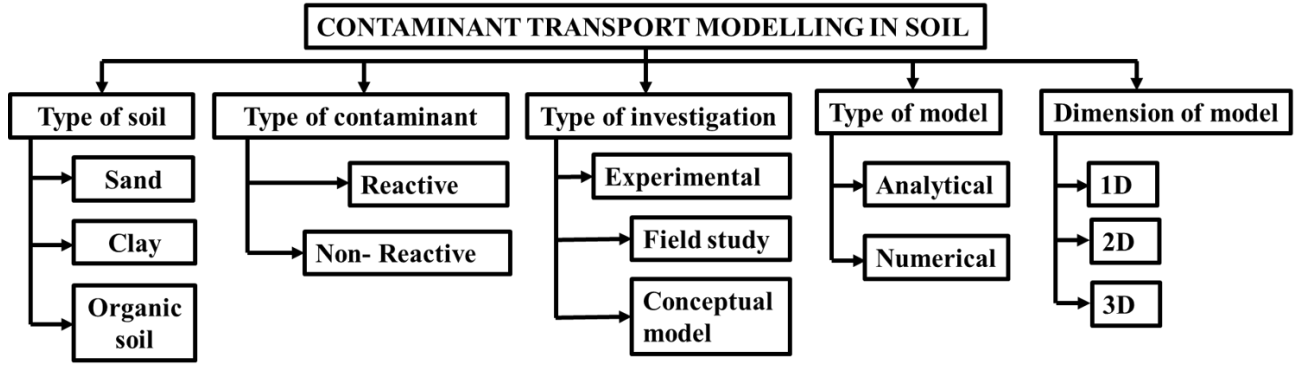
Figure 2.6: Important factors that decide the contaminant transport through soil

One of the earliest works on contaminant transport modelling in porous medium can be traced back to 1960s where, Ogata and Banks (1961) derived the solution for longitudinal dispersion in porous media. The governing differential equation is given by:

$$\frac{\partial C}{\partial t} = D\frac{\partial^2 C}{\partial x^2} - q\frac{\partial C}{\partial x} \tag{2.1}$$

In equation (2.1), the advection ($q\frac{\partial C}{\partial x}$), hydrodynamic dispersion ($D\frac{\partial^2 C}{\partial x^2}$) components of transport are taken into account.The initial and boundary conditions are

$$C(x,0) = 0 \quad \text{where} \quad x > 0$$

$$C(0,t) = C_0 \quad \text{where} \quad t > 0 \tag{2.2}$$

$$C(\infty,t) = 0 \quad \text{where} \quad t > 0$$

By solving the equation using Laplace transform, the solution for concentration is given by

$$C = \frac{C_0}{2}\left[\text{erfc}\left(\frac{x-qt}{2\sqrt{Dt}}\right) + \exp\left(\frac{qx}{D}\right)\text{erfc}\left(\frac{x+qt}{2\sqrt{Dt}}\right)\right] \tag{2.3}$$

Since the contaminant considered in thesis are radionuclides, their reactive nature needs to be taken into account in the form of adsorption and radioactive decay to solve the contam-

35

inant transport equation. Van Genuchten and Wierenga (1976) developed analytical models by accounting for the effect of sorption on mass transport through porous media. Later, Higashi and Pigford (1980) considered the effect of both sorption and radioactive decay in their mathematical model. They developed analytical models for one-dimensional migration of radionuclides in geologic sorbing media. For two and three member decay-chains, the solutions for step-release and impulse-release sources were proposed. In these models, the effect of nuclides specific leach rates and the effect of decrease in the release rates of radionuclides with decrease in their amounts in the repository (i.e., decaying source concentration) were taken into account. The efficiency of this model in predicting hydrogeological transport of high-level waste decay chain $^{238}Pu \rightarrow \,^{234}U \rightarrow \,^{230}Th \rightarrow \,^{238}Ra$ was demonstrated.

Nair and Krishnamoorthy (1997) developed one-dimensional and two-dimensional analytical models for all the possible scenarios associated with shallow land burial of low level radioactive waste. The general mathematical model incorporating the advection, diffusion, disperion, sorption and radioactive decay processes was based on mass conservation and control volume approach. Since the model was applied to shallow land burial of radioactive waste, the environment was assumed to be a saturated porous medium. The concentration of radionuclides in the pore water of the medium were computed as a function of space and time. These models were integrated into the perfromance assessment modelling framework for shallow land burial sites to evaluate the radiation dose and risk values and check their complaince with the safety standards.

Thiessen et. al., (1999) presented the different applications and types of mathematical models used to represent the distribution and transport of radionuclides in different environments, integrated global models for selected radionuclides and special issues in the

fields of solid radioactive waste disposal and dose reconstruction. A comprehensive study on the important factors involved in modelling radionuclide movement in different environments were carried out which include atmospheric deposition and the terrestrial environment; soil-to-plant transfer processes and near-surface hydrology; and aquatic environment.

Park and Zhan (2001) developed analytical solutions of contaminant transport from one-, two-, and three-dimensional sources in a finite-thickness aquifer. The types of sources included : point source, line source and area source. Solutions were derived for all the above source configurations. The results indicated the contaminant concentration in the near field was found to be sensitive to the source geometry and anisotropy of the dispersion coefficients. One the other hand, for far field scenario, the contaminant concentration was found to be less sensitive to the source geometry.

Bossew and Kirchner (2004) developed an alternative procedure for solving the equations that model vertical distribution of radionuclides in soil. The convection-dispersion (CDE) model was focussed on predicting the migration results of radionuclide being available for plant uptake, and rise of external doses over time. Using site specific soil transport parameters from 528 measured radionuclide soil profiles, the radionuclide migration process was analysed. The model results showed that the mobilities of radionuclides in soils increased in the sequence ^{137}Cs (weapons fallout) $< ^{134}$Cs (Chernobyl) $< ^{106}$Ru $\approx ^{125}$Sb. The differing mobilities of the two Cs (different origin) was attributed to the inadequacy of CDE model and assumptions used in simulations.

The geosphere transport models for radionuclide migration were also solved analytically using techniques like Green's function and Laplace transform methods in Rakesh et. al., (2005) and Mayya (2015). Further, the application of these techniques to real problems

in hydrological dispersion and aerosol transport was demonstrated.

Numerical models can model more realistic problems with complex boundary conditions, groundwater flow and transport of solutes, and geochemical reactions between solid and aqueous phases. Some of the previous studies that adopted numerical techniques to solve the radionuclide transport through the geological medium are presented below. Butler et. al., (1999) developed a model that could predict the upward migration of radionuclides from a contaminated water table into arable and pasture crops. The models were developed based on site-specific data for rainfall and potential evaporation rates; soil physical and hydraulic properties; crop growth measurements and; lower boundary concentrations for the radionuclides ^{22}Na, ^{36}Cl, ^{99}Tc and ^{137}Cs to assess the accuracy of the tested models and identify major errors associated with model structure and its parameters. Finite difference numerical models were developed to simulate the radionuclide transport through soils. The results showed that characterising the soil hydrology is very important in modelling the upward movement of radionuclides in the vadose zone. This model also highlighted the influence of the above models in risk (safety) assessment of radionuclide migration in the biosphere.

Geiser (2001) developed a numerical model for the decay and sorption of radionuclides and their transport in a double porosity media. By implementing an operation splitting method the transport and reaction components of the model were decoupled. With this information, the reaction equations was solved exactly. The transport equation was discretized by adopting a finite volume (FV) scheme and the efficiency model results was demonstrated with a simple problem. However, the influence of sorption was not considered in this model.

Trefry and Muffels (2007) presented an overview of FEFLOW, an advanced Finite-Element

subsurface FLOW and transport modeling system with an extensive list of functionalities, including variably saturated flow, variable fluid density mass and heat transport, and multispecies reactive transport. The efficiency of the software was demonstrated by comparing the results with benchmark problems.

Miller et. al., (2010) reviewed the challenges involved in upscaling sorption / desorption processes in reactive transport models to describe metal / radionuclide transport. The inclusion of smaller scale processes in a numerical solver need not always lead to better descriptions of larger scale behaviour because of unknown conceptual model errors, discrepancy in the scale of model discretization relative to the scale of the chemical / physical process, and omnipresent chemical and physical heterogeneities. The significance of developing a Representative Elemental Volume (REV) in fluid flow and mass transport, and; the influence of chemical reactions and the inability to discern cause and effect relating to transport were found to be some of the critical aspects in modelling reactive transport. To bridge the bench and field data (i.e., upscale the behaviour), it was found that a new set of experiments were needed at the intermediate scale where, the physical and chemical heterogeneities can be controlled and quantified.

Nair et. al., (2010) developed a three-dimensional numerical model using finite difference scheme that handled inhomogeneity and anisotropy for the decay chain transport in groundwater from uranium tailings ponds. The source term of the system was modelled as a decaying mass boundary condition (function of infiltration and radioactive decay). The results from the numerical model showed that the effective dose to members of the public through the groundwater drinking pathway with the decay chain transport are about 100 times higher than that without the decay chain transport. So, this study highlighted the sigficance of modelling a decay chain transport for radionuclide migration.

Simunek et. al., (2013) discussed the process of modelling contaminant transport using HYDRUS software and its specialized modules. The overview of various components developed in the software which involves different types of mathematical models that describe the transport of agricultural chemicals in both the vadose zone and groundwater were presented. The numerical software demonstrated efficiency in modelling the first order decay chains of radionuclides ^{238}U, ^{234}U, ^{230}Th, ^{226}Ra, and ^{210}Pb. Also some special modules developed in this software package to handle geochemical process in the radionuclide transport were discussed.

Piquè et. al., (2013) developed conceptual and numerical reactive transport model to understand and assess the retention capacity of soils for selected radionuclides at a geological repository site planned at Forsmark, Sweden. The computed results showed the heterogeneity of distribution coefficient (K_d) in space. The effective K_d values were estimated from modelled breakthrough curves at the discharge area of the model. The numerical predictions, suggested that the repository-derived nuclides that exhibited maximum retention were Th, Ni, and Cs, mainly through sorption onto clays and further U, C, Sr, and Ra, were retained due to sorption and/or incorporation into mineral phases.

Many researchers modelled the groundwater flow and radionuclide transport in geological medium using FEFLOW, a finite element modelling software (Jakimavičiūte-Maseliene et. al.,, 2006; Ashraf and Ahmad, 2008; Elango et. al., 2012; Chopra et. al., 2013). This software could model site-specific hydro-geological conditions and also boundary conditions efficiently covering large study area to predict radionuclide migration process. The radionuclides considered for the analysis were ^{238}U,^{230}Th , ^{226}Ra and ^{129}I. Eventually, the radiological impact (radiation dose and risk) from these radionuclides were computed from the model results.

Adinarayana et. al., (2017) developed a two-dimensional numerical model of NSDF using CFD (computational fluid dynamics) software PORFLOW. The influence of soil layers and external environmental factors on the radonuclide release from the facility was studied. The water ingress from top soil layer and infiltration into the concrete vault was modelled with appropriate details of the facility, radionuclide inventory, properties of the soil layers and the boundary conditions assigned to the model. The simulations were carried out for a period of 104 yrs and the results showed that the radionuclides ^{55}Fe, ^{58}Co, ^{60}Co and ^{144}Ce decayed within the vault for the given time scale.

So far, various models that described the radionuclide transport in soil medium have been discussed. However, the geological medium is also composed of rocks. More so, many radioactive waste repositories, specially the high-level wastes consider deep geological formations (i.e., bed rocks) as potential sites for disposal. Hence, as an integral component of performance assessment for radioactive waste disposal systems, there is a need to understand various aspects involved in radionuclide transport through rocks.

2.3.3.2 Fractured rocks

Unlike soils, it is more demanding to model the behaviour of contaminant (or radionuclide) in rocky medium. It involves modelling two interacting subsystems namely fractures and the intact rock matrix. As mentioned in section 2.3.3, the various transport mechanisms describing the contaminant movement remains the same in fractured rock also. However, the dominant transport mechanisms in a fracture and rock matrix may vary.
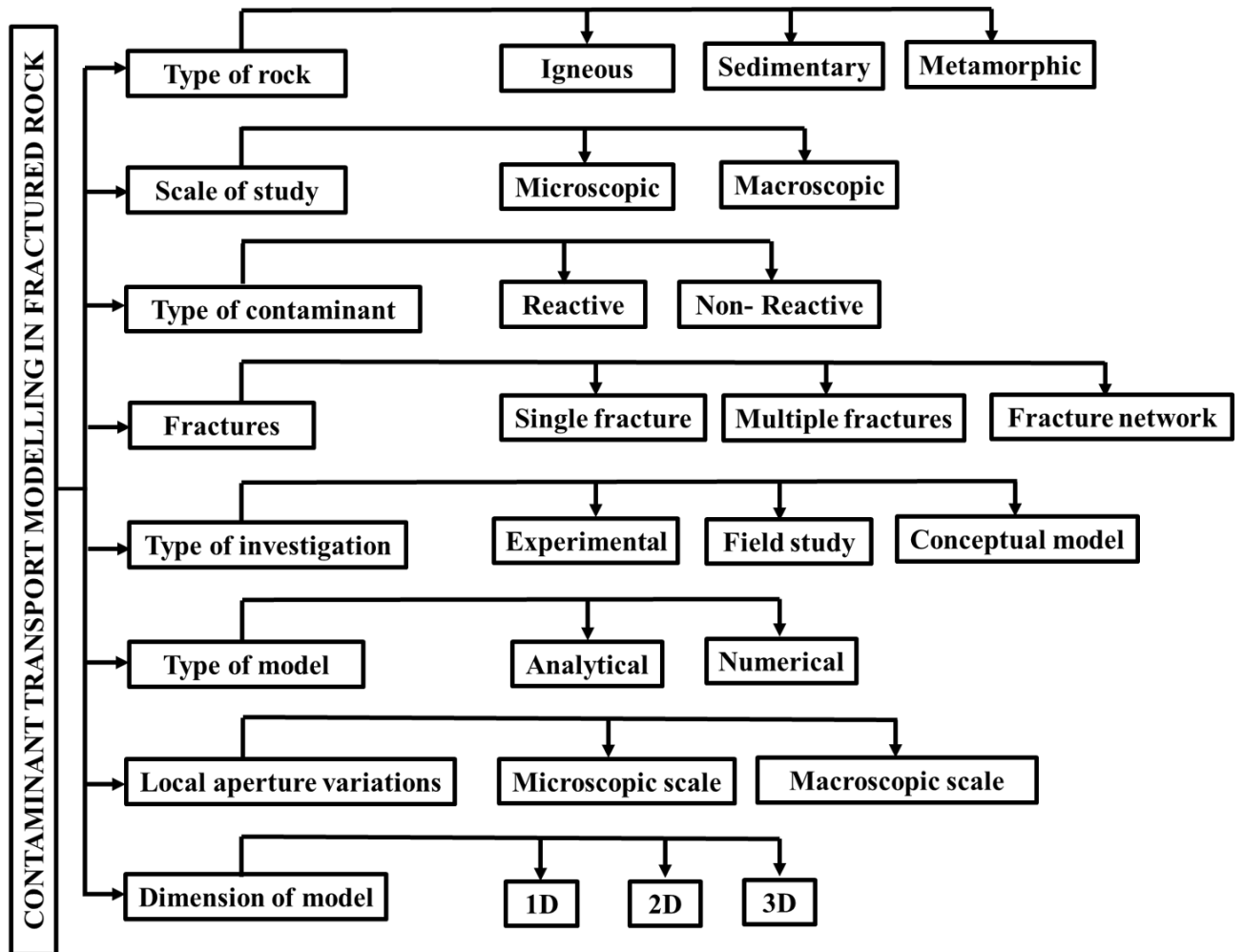
Figure 2.7: Important factors that decide the contaminant transport through fractured rock

In addition to these mechanisms, there are some important components of rock mass and contaminant that decide the contaminant transport processes through fractured rock. Figure 2.7 presents a broad overview of eight different categories which include: type of rock, scale of the study, type of contaminant, fractures, type of investigation, type of model, local aperture variations and dimension of model that can influence the type of radionuclide transport model. By combining one component from each category, a new radionuclide transport model can be developed.

Fractures are ubiquitous natural discontinuities formed in rocks of any genesis. The role of fractures in flow and transport through fractured rock masses are manifold. Insights

in this area help in many engineering applications like, exploitation of petroleum, gas and geothermal reservoirs, fluid pressure studies in deforming the rock, seepage process in mining and dams, isolation of contaminant in the geo-sphere (especially in radioactive waste disposal sites). So, in the recent years there is an increased attention on developing models that can predict the flow and transport behaviour of contaminant through fractured networks. The flow characteristics of a fluid in a fractured rock mass are highly influenced by the fracture morphology, fracture geometry (orientation, aperture, length), interconnectivity of void spaces, roughness, fluid pressure and confining pressure around the fractures (Bear et. al., 1993; Huenges and Zimmerman, 1999; Singh et. al., 2015; Lei et. al., 2017). Also, the spatial complexity of fracture patterns, the variations in aperture sizes and the pathways of propagation, the hydro-geological and transport properties of the media affect the transport of contaminant through the rock mass (Smith and Schwartz, 1984; Schmelling and Ross, 1989; Bear et. al., 1993; Worman et. al., 2004; Faybishenko et. al., 2005). One of the governing factors that influences contaminant migration through fractured rocks, is the 'scale' of the problem, that can vary from few centimetres (single fracture) to few kilometres (fractured rock site) (Berkowitz, 2002; Neumann, 2005). In the microscopic scale studies, the flow and contaminant transport needs to be modelled through a single fracture or a set of randomly oriented fractures. However, when the scale of study increases to field scale (or macroscopic scale), it becomes imperative to model the fracture network to discern the behaviour of contaminant in the system. So, to represent natural fracture network, discrete fracture network (DFN) models are developed and these models require geometrical properties of each fracture in the network. To generate a DFN model, three distinct modelling approaches have been developed. They are geological mapping approach, geomechanical approach and stochastic approach. The un-

derlying concept involved in developing fracture patterns and various models developed under each category are presented below.

1. **Geological mapping :** In this approach, the fracture patterns are created by mapping the exposed rock out-crops or man-made excavations. This information is used in various areas of research that deal with understanding their behaviour during the formation and estimating the statistics of fracture populations in a rock. These discrete fracture patterns can also be simulated numerically to study the connectivity, solute transport and hydro mechanical behaviour of fractured systems belonging to that region. Such studies were carried out in the past (NRC, 1996; Josnin et. al., 2002; Geiger et. al., 2010; Lei et. al., 2017). Although, the natural fracture patterns can be preserved in this approach, the analysis is constrained to 2D because of the increasing complexities and computational limitations in the fractured network generated from this approach.

2. **Geomechanical approach :** According to fracture mechanics, the growth of fracture in a system is governed by the stress / strain conditions and it propagates further based on physical laws. The increased knowledge in this area leads to the development of geomechanics based fracture patterns (Pollard, 1987). This method can link the geometric and topological features to the physics of fracture growth. Many numerical models have been developed to generate geomechanically grown fractures (Renshaw and Pollard, 1994; Paluszny and Matthai 2009; Paluszny and Zimmerman, 2013; Lei and Wang, 2016). But, the simulators based upon the mechanics of fracture propagation remain computationally expensive for large-scale problems.

3. **Stochastic approach :** The fracture networks are modelled stochastically due to

limited data availability and also the challenges involved in acquiring complete details of in-situ fracture system. It is the most popular method among the three approaches. The stochastic fracture network considers all the geometric features of a fracture to be random variables with underlying probability distributions. Stochastic algorithms are developed to model the fracture patterns of rocks from different origin (Snow, 1970; Hudson and Priest, 1983; Bonnet et. al., 2001; Riley, 2004; Davy et. al., 2013). The probability distributions of various fracture features considered in the literature are presented in Table 2.1.

Table 2.1: Geometrical properties of fracture and their distributions (Lei et. al., 2017)

Geometric property	Distribution
Fracture orientation	Uniform / Normal / Fisher
Fracture apertures	Lognormal / Power law
Fracture spacing	Negative exponential / Lognormal / Normal
Fracture size	Negative exponential / Lognormal / Gamma / Power law

To understand the flow and transport behaviour of contaminant in fractured rock, various analytical and numerical models were developed over the last five decades. These investigations encompassed the influence of each of factors mentioned in Figure 2.7. However, in the thesis only some of the significant studies carried out in this area are presented. Many deterministic models that describe the flow and transport of contaminant through fractured rock were developed over last five decades. Tang (1981) developed an analytical solution for contaminant transport along a discrete fracture in a porous rock matrix. The solution accounted for advective transport in the fracture, longitudinal mechanical dispersion in the fracture, molecular diffusion in the fracture fluid along the fracture axis, molecular diffusion from the fracture into the matrix, adsorption onto the face of the

matrix, adsorption within the matrix, and radioactive decay. The solution was obtained by solving the governing partial differential equation using Laplace transform and Gauss quadrature methods. Under the conditions of large diffusive loss, the analytical and numerical solutions matched well. This solution was able to determine the ultimate penetration of a contaminant along a single fracture and the time taken to reach this penetration efficiently.

Sudicky and Frind (1982) developed an exact analytical solution for the problem of transient contaminant transport in discrete parallel fractures situated in a porous rock matrix. This analytical model was an extension to the model developed by Tang (1981). The properties and transport mechanisms considered for the mathematical formulation of flow and transport in fracture and rock matrix also remained the same. In the model, a two-dimensional system is reduced to two one-dimensional problems that were much more amenable to solve by analytical techniques. From the model illustrations it was found that penetration distances along fractures were substantially larger through multiple, closely spaced fractures than through a single fracture because of the limited capability of the finite matrix to store solute. The results also showed that spacing between the fractures had a significant effect on the advance rate and ultimate penetration of a contaminant in the system.

Lowell (1987) developed analytical models for contaminant transport in a single, planar fracture. The models that were derived considered the effects of a fracture skin that inhibits the diffusion of contaminant into the porous rock matrix. Also, the phenomenon of radial transport of contaminant away from an injection well was considered. The steady-state results showed that contaminant could be transported several kilometres downstream from the well, particularly in narrow fractures. Also, the influence of radioactive decay in

the fracture was observed to control the downstream penetration rather than diffusion in the rock matrix. These models provided useful insights for interpreting laboratory or field experiments of contaminant transport in fractured rock.

Krishnamoorthy and Nair (1992) developed an analytical model with two coupled one-dimensional equations, one for the fracture and the other for the porous rock matrix to predict the migration of radionuclides from a granite repository. The transport processes considered were advection, dispersion, radioactive decay and adsorption in the fracture, and; diffusion, radioactive decay and adsorption in the micro fissures of the host rock. The concentration of radionuclides ^{90}Sr, ^{239}Pu, ^{129}I and ^{237}Np were evaluated from the model. The influence of sorption of radionuclide on the fracture surface affecting the transport was quantified from the analysis.

Some studies focussed on understanding the effect of aperture variations in fracture network on the contaminant transport along them. Oron and Berkowitz (1998) investigated the validity of applying the "local cubic law" (LCL) to flow in a fracture bounded by impermeable rock surfaces. Modelling studies resulted in generating three conditions for the applicability of LCL flow, as a leading-order approximation in a local fracture segment with parallel or non-parallel walls. The complexity of local flow behaviour was demonstrated and the results also indicated that applying global cubic law was incorrect for every fracture (i.e., applying cosine law for non parallel-walled pathways).

Suresh Kumar and Sekhar (2005) analysed the spatial moments for transport of non-reactive solutes in a single fracture-matrix system. The temporal behaviour of solute velocity, macrodispersion coefficient, and dispersivity were found to follow two broad regimes which are pre-asymptotic and asymptotic regions. The properties: effective solute velocity and effective macrodispersion coefficient in the preasymptotic stage were

functions of matrix diffusion coefficient, matrix porosity, fracture spacing, local fracture dispersivity, and injected solute velocity in the fracture. However, in the asymptotic stage the effective solute velocity was dependent only on matrix porosity, fracture spacing, and injected solute velocity. This study was conducted to characterize the solute mobility and solute spread in fractured formations.

Mahmoudzadeh et. al., (2014), developed an analytical model that described the solute transport and retention in fractured rock. This model accounted for advection along the fracture, molecular diffusion from the fracture to the rock matrix composed of several geological layers, adsorption on the fracture surface, adsorption in the rock matrix layers and radioactive decay-chains. The analytical solution could be applied in a fracture network model or a channel network model to predict radionuclide transport through channels in heterogeneous fractured media consisting of an arbitrary number of rock units with piecewise constant properties. The results from the model showed that different mechanisms operate collaboratively to retard nuclide transport in fractured rocks. The results showed that, when the rock matrix consisted of several layers with different properties, an additional space for diffusion and sorption in the intact wall rock was provided for radionuclides. This lead to a significant change in the concentration ie., there was a decrease the peak value and also increase peak arrival time.

Suresh Kumar (2014) presented an improved mathematical model that can predict groundwater flow and solute transport in saturated fractured rock. The model described fluid flow through a coupled fracture-matrix system using a dual-porosity approach. It was suggested that mathematical model needs to account for fluid flow through a single fracture, and a transient fluid exchange term at fracture-matrix interface along with matrix flow equation. Also, to enhance the model, it was suggested to use the Langmuir and

Freundlich sorption isotherms in the fracture and rock matrix, respectively, than the usage of the same isotherms both in the fracture and rock matrix.

Though the analytical models predicted the flow and transport efficiently, achieving a closed form solution for geometrically complex domain (like fracture network) becomes computationally demanding. So numerical models have been developed to overcome this problem. One of the earliest works of investigating the flow through fractures was carried out by Wilson and Witherspoon (1974). They developed two numerical models using finite element method and calculated the flow characteristics of rigid networks in planar fracture. A two-dimensional flow model was developed to predict the water flow through fractured rock of arbitrary orientation and aperture distribution. Further, numerical models were developed to investigate the influence of fracture geometry and transport properties of fracture on mass transport in fractured medium (Grisak and Pickens, 1980; Bibby,1981; Smith and Schwartz, 1984).

Rasmuson and Neretnieks (1986) investigated the process of radionuclide transport in isolated flow channels in fissured crystalline rocks. They used finite difference method to estimate radionuclide movement for the case of flow and dispersion in a cylindrical channel coupled to diffusion and sorption in the matrix. Diffusional transport in the matrix was assumed to be one-dimensional instead of two-dimensional for numerical simplification. The results showed that dispersion in individual channels as well as in networks of channels had a strong impact on overall transport of the species. Also the sorption of species was affected by the wetted surface of fracture. Some examples illustrated in the paper showed the applicability of model in parallel and uniform fractured systems.

Long et. al., (1989) emphasized the need to consider the numerical modelling of fractures exclusively, confirming the significance of fracture geometry on the hydrological

behaviour of the rocks at field scale. This study investigated only the hydraulic flow behaviour through fracture. Further, the contaminant transport modelling through fracture network and the influence of the fracture geometry was studied by Odling and Roden (1997). The results showed some non-intuitive effects that were captured well with the help of the model. It was found that fracture connectivity played a secondary role to fracture orientation and density and; in the case of connected fracture systems break-through curves of contaminants were smoother whereas the contaminant plume was spatially highly heterogeneous.

Nordqvist et. al., (1992) developed a three-dimensional variable aperture fracture network model for flow and transport in fractured rocks. The model generated both the network of fractures and the variable aperture distribution of individual fractures in the network. The spatially varying aperture field within an individual fracture plane was constructed by geostatistical methods. The results from breakthrough curves of the variable aperture fracture network model had more than one peak. They showed that variable apertures govern not only the transmissivity of the fractures but also the smaller-scale dispersion that originates from the multitude of different pathways in each and every fracture.

Schoniger et. al., (1997) carried out modelling studies to understand the flow and transport process in fractured rock on a small basin scale. For conceptual modelling numerical softwares ROCKFLOW and FEFLOW were used. For site specific investigation, a study basin near Groβe Schacht, northern Germany was chosen and the geo-hydrological data was acquired from the experiments. By assigning these input parameters and appropriate boundary conditions, the velocity fields, the concentration fields, groundwater levels, discharge and transit times were computed. The long-term geochemical behaviour of tritium (^{3}H) and oxygen (^{18}O) isotopes and; groundwater transit time under the given conditions

were evaluated. This study demonstrated the efficiency of the model in predicting the flow and transport behaviour with respect to the site specific conditions.

Poteri (1997) developed fracture network model of groundwater flow in the Romuvaara site, Finland. Using site specific borehole data an intact rock with the fracture network of volume of $16 \times 16 \times 16$ m^3 was developed. The hydraulic conductivity tensor was estimated from the simulations. Numerous computer packages were used to create the fracture network and model the flow through the network. They included FEFLOW which was used to compute the hydraulic head, pressure, temperature and concentration of a flow field under consideration. The results showed that, as the distance from the repository to the nearest fracture zone was more than 10 m, the greatest flow rates were significantly reduced. Also, flow distribution along homogeneous and heterogeneous fractures were compared. The simulations showed that, in the case of homogeneous fractures a single flow path was developed, but the variations in the flow rate in the fracture plane were smooth. In the case of heterogeneous fractures, several separate channels were developed and the results showed that fluctuations in the flow rate in the fracture plane were higher than those observed in the homogeneous case.

Cvetkovic et. al., (2004) studied the migration of sorbing tracers through crystalline rock by combining relatively simple transport measures with particle tracking in a discrete fracture network. The radionuclides considered for the study were ^{97}Tc (strongly sorbing) and ^{90}Sr (weakly sorbing). The transport measures were conditioned on two random variables namely: the water residence time (τ) and a parameter which quantifies the hydrodynamic control of retention (β). The results showed that any DFN model assumption which affects the distribution of β was likely to be significant for transport predictions. On the other hand, the choice of the hydraulic law had a significant impact on τ but no

impact on β. So, the need for further studies on upscaling of τ, β distributions as well as estimating effective parameters for hydraulic control of retention was established from this study.

Sarkar et. al., (2004) studied fluid flow in fractures using numerical simulation and addressed the challenging issue of characterizing hydraulic property in fractures. The models were developed to analyse flow in single fractures, series and parallel combination of fractures, inclined fractures, intersecting fractures, mixed networks, in real (rough-surface) fractures, uniform and variable aperture fracture models. The flow through the system was assumed to follow cubic law and equivalent aperture sizes were estimated to characterize the fractures. It was observed that for fractures connected in series, the equivalent hydraulic aperture was a weighted harmonic mean of cubed apertures of all fractures; for fractures connected in parallel, the equivalent flow was simply the sum of all flows through individual fractures; for fracture inclined with respect to the axis of pressure gradient, the amount of flow was reduced by a factor of cosine of the inclination angle. Also, the results for a network of randomly intersecting fractures were similar to the case where the network was replaced by a single fracture to give flow equivalence. This study illustrated the effect of all important combinations of aperture variations encountered in modelling.

Dong (2011) developed a hybrid mixed finite element (MFE) method to predict the velocities field for both the fractures and matrix which are crucial to the convection part of the transport equation. The effect of fracture thickness, dispersion, distribution coefficient on concentration plume for randomly oriented fractures was discussed. But, these studies were mostly based on modelling single fracture or few randomly oriented fractures at a microscopic scale.

Parker et. al., (2012) developed discrete fracture network model for investigating contaminated sites with chlorinated solvents on fractured sedimentary rocks. The analysis was carried out for eight study sites to understand the transport behaviour in fractured rock. The average linear groundwater velocities in fractured sedimentary rock were relatively large, however, matrix diffusion was the main transport mechanism that led to the contaminant plumes at the eight sites. This strong plume front retardation in the rock was primarily due to matrix diffusion, causing contaminant transfer from groundwater flowing through fractures to the low permeability rock matrix, as well as contaminant storage in the matrix due to sorption. Also, it was observed that the transverse spreading of contaminants and their degradation resulted in attenuated contaminant plumes.

Robinson et. al., (2012) presented studies on radionuclide transport in large-scale unsaturated zone below the repository at the Yucca Mountain, Nevada. It was shown that for many radionuclides, including most strongly sorbing species, the unsaturated zone was found to reduce the rate of movement of radionuclides substantially to the accessible environment. The influence of quantity of recharge and deep percolation of water, flow partitioning between fractures and rock matrix, diffusion of radionuclides from water flowing in fractures into the pores of the rock matrix, sorption of radionuclides onto rock or mineral surfaces, and colloid filtration were studied.

Wei et. al., (2017) implemented probability distribution method to assess the uncertainty of DFN models that simulated the high-level radioactive waste disposal reservoir site in Beishan, China. Particle tracking modelling was employed using the random walk method to simulate the radionuclide transport and the probability distribution method was implemented with multi-realization of fracture network. The results showed that areas near the contaminant release point were more concentrated than the farther areas. The efficiency

of DFN model in predicting the contaminated areas was demonstrated.

In most of the performance assessment methodologies, deterministic and probabilistic calculations are seen as complementary, and, both approaches are applied. So far, the literature relevant to the deterministic part of performance assessment modelling have been discussed thoroughly. In the following sections, literature on the different forms of uncertainty and techniques employed to quantify these uncertainties are presented.

2.4 Sources of Uncertainty

Regulatory bodies like International Atomic Energy Agency (IAEA), Nuclear Regulatory Commission (NRC), Atomic Energy Regulatory Board (AERB) etc recognized the significance of uncertainty in estimating the performance of radioactive waste repositories. The role of uncertainties embarks right from the inception of the repository design, construction, operation, closure and extends upto the post-closure phases of the disposal system. Therefore, uncertainty analysis is considered as an inherent component of the performance assessment (for low and intermediate level radioactive wastes) in the safety guidelines and safety codes developed by the regulatory agencies (AERB, 2006; IAEA, 2014). Uncertainty analysis has the important goal of extending understanding and quantifying the effect of variabilities in the parameters and, achieve a reasonable assurance associated with the safety of the system. This led to the incorporation of the concepts of reliability in the performance assessment methodology. Some of the previous studies that significantly contributed in understanding the effect of various uncertainties are mentioned below.

Hoffman and Miller (1983) reported the significance of different forms of uncertainties in

the safety assessment modelling. Since, the environmental radiological assessments rely on mathematical models, the predictions from such models are inherently uncertain. This is due to the fact that models are approximate representations of actual systems. So they implemented stochastic procedures to assess the effect of model and parameter uncertainties on the safety indicators of the model.

Apostolakis (1990) discussed a theoretical framework for the probabilistic assessment of risks from technological systems like nuclear power plants, chemical process facilities, and hazardous waste repositories. Bayesian theory of probability was proposed as the appropriate methodology in the quantification process. It involved both experimental results and statistical observations to produce quantitative measures of the risks from these systems. Also, the information of the past and future relative frequencies, the issues associated with the elicitation and use of expert opinions were discussed.

Gallegos and Bonano (1993) emphasized the need to consider uncertainties in evaluating the performance assessment of radioactive waste disposal systems. They classified uncertainty into three broad cases which include

1. Uncertainty in the future state of the disposal system. Due to the large spatial and temporal scales involved in estimating the results, the impact of climatic factors may change the properties of different components of the facility and surrounding medium.

2. Uncertainty in models. This includes the uncertainty in conceptual models, mathematical models, and computer codes. Since the mathematical models are abstract versions of the actual system, uncertainties are inevitable.

3. Uncertainty in data and parameters. The parameters exhibit uncertainties due to

lack of sufficient information and also due the inherent randomness in the system that cannot be reduced.

They advocated probabilistic performance assessment modelling to represent the above uncertainties in the model predictions and provided a systematic way to arrive at a decision regarding the safety of a radioactive waste disposal facility.

Winkler (1996) discussed the importance of treating different forms of uncertainties in performance assessment of complex systems. This led to an increased attention in distinguishing types of uncertainty in such assessments and in risk analysis more generally. Distinguishing uncertainty by 'types of uncertainties' was questioned at basic level. However, it was suggested that a closer look at such distinctions indicated that they were driven by important modelling issues related to model structuring, probability assessment, information gathering, and sensitivity analysis. So, the issues involved in distinguishing and treating the uncertainties of complex systems were addressed in this study.

Helton (2003) developed design methodologies of performance assessment for radioactive waste disposal in the form of mathematical and numerical approaches to deal with uncertainties. The two components of uncertainty: (i) stochastic or aleatory uncertainty, which arises because the system under study can potentially behave in many ways, and (ii) subjective or epistemic uncertainty, which arises from a lack of knowledge about quantities that were assumed to have fixed values within the computational implementation of the performance assessment model. The incorporation of these uncertainties into performance assessment was essentially a multi-dimensional integration problem which can place significant computational burdens on the analysis. So it was suggested to adopt good numerical procedures and appropriate computational strategies. Also, the advantages of implementing a probabilistic performance assessment was highlighted in this study.

El-Ghonemy and Fowler (2005) developed a methodology to perform quantitative risk assessments in the contaminated land industry in the UK by treating the uncertainties. The features, events and processes that need to be addressed during the development of conceptual models were presented. The different types of uncertainties considered for the analysis were scenario uncertainty, conceptual model uncertainty and parameter uncertainty. This approach developed conceptual models and addressed uncertainties when undertaking contaminated land risk assessments. To illustrate this method, it was applied to a low-level radioactive waste disposal site at Drigg in Cumbria. The advantages of this approach in the contaminated land industry were also emphasized.

Lee and Lee (2006) proposed a general approach of integrating the Bayesian network concept to the nuclear risk assessment. Also, the proposed method was illustrated by considering a problem with delay time, retardation coefficient, infiltration rate and dilution volume as random variables. Based on the consequences for risk assessment, different evolution scenarios called the altered evolution scenarios were developed. By adopting uncertainty analysis under Bayesian framework, scenarios that caused contamination were estimated.

From the above studies, it is evident that knowing various sources of uncertainties associated with model is a pre-requisite to assess the performance of complex technological systems like radioactive waste disposal facilities. So, the literature related to various forms of uncertainties considered in performance assessment modelling are presented in the following sections.

2.4.1 Uncertainties in design parameters

In the process of developing an efficient performance assessment model, the input parameters involved in different phases of the model exhibit substantial variability. The lack of reliable data and complexity of the natural environmental systems results in predictions that are subjected to large uncertainties. For reliable decision-making, predictive models are required to explicitly consider uncertainties associated with the input parameters. So,the uncertainty in various input parameters from the literature are assembled and presented below.

2.4.1.1 Repository failure rate

To evaluate the release rate of radionuclides from the multi-barrier system into groundwater, repository failure model is developed. It is a component of performance assessment model which is function of failure rate of each (natural and engineered) barrier of the multi-barrier system. Many researchers represented the failure distribution of the barriers to be exponentially distributed (Kim et. al., 1993; Nair and Krishnamoorthy, 1999; Cadini et. al., 2012) and the variability in failure rate of each barrier from the literature are summarized in Table 2.2.

2.4.1.2 Geological and transport parameters of the medium

The geological medium and its properties play a critical role in the contaminant transport behaviour. This further influences the performance of disposal system. Geological medium consists of both soils and fractured rocks. These natural formations are inherently random and the uncertainties in their properties are inevitable. So, assuming that

the geological properties of medium are constant leads to unrealistic modelling. They are assumed as random variables following certain distribution.

Table 2.2: Variabilities in barrier failure rate

Property	Distribution	5th percentile of λ_i	95th percentile of λ_i	Reference
Top cover (y^{-1})	Lognormal	1/50	1/10	
Waste container (y^{-1})	Lognormal	1/25	1/5	
Waste form (y^{-1})	Lognormal	1/4000	1/300	
Backfill (y^{-1})	Lognormal	1/55	1/12	Cadni et. al., 2012
Bottom cover (y^{-1})	Lognormal	1/26	1/6	
Unsaturated zone (y^{-1})	Lognormal	1/85000	1/25000	
Property	**Distribution**	**Mean (λ_i)**		**Reference**
Top cover (y^{-1})	Exponential	0.06		
Waste container (y^{-1})	Exponential	0.12		
Waste form (y^{-1})	Exponential	0.0018		Sujitha and Sivakumar Babu (2017)
Backfill (y^{-1})	Exponential	0.051		
Bottom cover (y^{-1})	Exponential	0.103		

Smith and Schwartz (1981) performed experimental and field studies to demonstrate the need to characterize uncertainty in the geological properties (i.e., hydraulic conductivity). Further, various studies were carried out to investigate the uncertainties in geological properties of soil based on the type of soil (i.e., soil or sand). Typical set of coefficient of variation (COV) in geological properties: hydraulic conductivity, porosity and groundwater velocity are summarized in Table 2.3.

Deb and Shukla (2012) reviewed the experimental and field studies addressing the measurements and variability of hydraulic conductivity. The COV in hydraulic conductivity will have a considerable effect on transport process and with large variations in hydraulic conductivity, the advective component of transport is affected. The transport

parameters of soil depends on the type of soil and the type of contaminant considered for the study. Most of the analysis carried out in the thesis is focussed on radionuclide transport in clayey soils. Hence, the literature pertaining to transport process of radionuclides in clayey medium have been considered. Rakesh et. al., (2005) documented the range of values for groundwater velocity (0.1-1.5) m/day, distribution coefficient (140-300) ml/g and thickness of aquifer (2-8) m. Sujitha and Sivakumar Babu (2017) indicated that the groundwater velocity follows Weibull distribution with scale and shape parameters (1.21×10^4, 2.78). The transport parameters groundwater velocity, distribution coefficient, diffusion, dispersivity, thickness of aquifer and their variability in soil are summarized in Table 2.4.

Table 2.3: Variability in geological properties of soil

Property	Distribution	COV (%)	Reference
Hydraulic conductivity	-	44 -83	Gupta et. al., 1993
	-	60 - 90	Duncan, 2000
	Lognormal	40 - 87	Gupta et. al., 2006
	Lognormal	60 - 90	Srivastava et. al., 2010
	Uniform	57	Datta and Kushwaha, 2011
	Lognormal	46 - 224	Deb and Shukla, 2012
Porosity	-	20 - 60	Hassan et. al., 1998
	Normal	5	Guedes et. al., 2010
	Truncated normal	6	Johari and Amjadi, 2017

The radionuclides react chemically with the surrounding medium and adsorbs onto its surface. So, the distribution coefficient is unique to each radionuclide and in Table 2.4, typical range of uncertainty in distribution coefficient observed in previous studies are presented. The transport parameters distribution coefficient, dispersivity and aquifer

thickness were observed to follow Weibull distribution with scale and shape parameters
(843.89, 8.23), (278.52, 1.46) and (558, 3.23) respectively in Sujitha ans Sivakumar Babu
(2017).

Table 2.4: Variability in transport properties of soil

Property	Distribution	COV (%)	Reference
Groundwater velocity	-	28 - 100	Smith and Schwartz, 1981
	Lognormal	4	Nair et. al., 2006
Distribution coefficient	Uniform	30	Nair et. al., 2006
	Uniform	53	Datta and Kushwaha, 2011
	Lognormal	0.00024 - 0.00822	Chopra et. al., 2013
	Uniform	30	Ciriello et. al., 2013
Dispersivity	Uniform	0.08 - 43	Garcia et. al., 2005
	Lognormal	0.03	Nair et. al., 2006
	Uniform	47	Chopra et. al., 2013
	Uniform	10	Ciriello et. al., 2013
Thickness of aquifer	Lognormal	0.5	Nair et. al., 2006

In the case of fracture rock, the geological and transport properties of rock mass and
fractures are presented in Table 2.5 and Table 2.6. Aladejare and Wang (2017) evaluated
the rock property variabilities based on the genesis of rock (i.e., igneous , sedimentary and
metamorphic) and their properties and also documented the COVs. In Table 2.5, the COV
values of porosity for sedimentary rocks are presented. Similarly, the COV of hydraulic
conductivity of typical fractured rock mass are presented in Table 2.5. However, in the
thesis a fractured rock mass is modelled as two interacting subsystems, intact rock matrix
and fractures. The hydraulic conductivity of intact rock is governed by the porosity of the
rock. In the case of porous rocks like limestone, sandstone, the hydraulic conductivity is
relatively higher than rocks like granite (due to less porosity). The hydraulic conductivity

of an intact sedimentary rock matrix varies from 10^{-12} to 10^{-8} m/s (Zhao, 1998; Graf and Therrien, 2005). Based on the variations presented in the literature, the conductivity and porosity of intact rock matrix are assumed to follow log-normal distribution in the thesis. To demonstrate the influence of COV of these properties on the overall transport behaviour, COV values of 10%, 15%, 20%, 30% and 40% were considered in the thesis. The probability distribution of geometric properties of fracture are mentioned in Table 2.1 and the COV of fracture transport properties are presented in Table 2.6.

Table 2.5: Variability in rock mass properties

Property	Distribution	COV (%)	Reference
Conductivity	-	4 - 32	Yao et. al., 2015
	-	33 - 100	Piscopo et. al., 2017
Porosity	-	1 - 181	Aladejare and Wang 2017
	-	1.51-141.48	Aladejare et. al., 2018

Table 2.6: Variability in fracture properties

Property	Distribution	COV (%)	Reference
Fracture aperture	Lognormal	18 - 130	Hakami, 1995
	Lognormal	25 - 200	Zhou et. al., 1995
	Lognormal	4 - 80	Zheng et. al., 2009
	Power law	176 - 200	Miranda et. al., 2018
Fracture orientation	Truncated normal	-	Riley, 2004
	Fisher	20-100	Gutierrez et. al., 2015
Fracture spacing	-	28 - 90	Benaafi at. al., 2018
Fracture dispersivity	-	0 - 48	Kumar et. al., 2006
	-	0 - 64	Kumar et. al., 2008
	Normal	4 - 120	Zheng et. al., 2009
Fracture diffusion	Lognormal	5 - 20	Sharma et. al., 2013

2.4.2 Model uncertainty

In the field of performance assessment modelling, model uncertainty is one of the main sources of uncertainty. In the process of translating the conceptual model (that represents the actual system) to mathematical models, uncertainties are inevitable in the form of approximations and possible alternative interpretations to various phenomenon within the system. In light of the information acquired about the system, these uncertainties are characterized. Some of the studies that addressed the model uncertainty in performance assesment modelling are presented in this section.

Hoffman and Miller (1983) presented the implications of the various uncertainties in environmental radiological assessment models. In the absence of extensive testing (model validation) conducted over a range of conditions, it becomes difficult to handle model uncertainties. The sources of model uncertainties considered for the analysis were attributed to the translated effect of parameter uncertainties; to distribution of model results and; through modal validation studies under certain conditions. The results showed that, compared to regulatory limits the implications of model uncertainties for human health protection was greatest at high dose rates, whereas, at low dose rates their effect became almost negligible.

Zio and Apostolakis (1996) addressed the problem of model uncertainty both from theoretical and practical point of view and presented two mathematical approaches to treat the model uncertainty and help in formulation of judgements. The first approach was called alternate-hypotheses formulation, which amounts to constructing a suitable set of plausible hypotheses and evaluating their validity. The second approach was called adjustment-factor formulation where it was necessary to identify a reference model and its predictions

be directly modified through an adjustment factor that accounts for the uncertainty in the models. These theoretical frameworks allowed additional forms of structural uncertainty to enter the probabilistic calculations quantitatively. This greater acknowledgement of model uncertainty led to widening of the uncertainty bands in pursuit of better calibration. To illustrate these methods a case study of model uncertainty regarding alternative models for the description of groundwater flow and contaminant transport in unsaturated, fractured tuff was presented.

Yim and Simson (2000) presented a review of performance assessment models in the U.S.A for low-level radioactive waste disposal. They highlighted the need to characterize, quantify and reduce uncertainties by developing sophisticated models and more realistic parameter ranges in performance estimate. Uncertainties in performance assessment include model uncertainty and parameter uncertainty. Model uncertainty refers to the uncertainty regarding abstracting a real system and its evolution into a form that can be mathematically modelled. It includes uncertainty about the interpretation and use of data and assumptions about heterogeneity, system dimensionality, isotropy, and initial boundary conditions. Various mathematical formulations were proposed to address model uncertainty. These formulations were categorized as model-focused or prediction-focused depending upon whether the attention was directed towards the plausibility of the model hypotheses or to the accuracy of its predictions. It was suggested to address model uncertainty using a logic tree approach and reduce model uncertainty by validation (i.e., the process by which assurance is obtained that conceptual and mathematical models, as employed in the computer model, are an accurate representation of the process or the system for which the models are intended). It was also mentioned that performance assessment relies heavily on the use of computer models and model uncertainty remains a major por-

tion of uncertainty in any performance assessment.

Linkov and Burmistrov (2003) carried out a study on addressing model uncertainty in practical applications of risk assessment. The use of several alternative models to derive a range of model outputs or risks is one of the few available techniques. This article addressed difference in problem formulation, model implementation, and parameter selection (i.e., modeller uncertainty) originating from subjective interpretation of the problem at hand. The results of the study showed that even for a relatively simple ecosystem and well-controlled deposition scenarios, the differences in model predictions may be quite high. In this exercise, the differences among models were as high as seven orders of magnitude for short-term predictions following the acute radionuclide deposition. It was also found that the differences among models (i.e., model uncertainty) seemed to be much higher than parameter uncertainties for a given model. Probabilistic models calibrated using Bayesian techniques were suggested as they perform well (specially in cases when the prior information helps in improving the predictions of the model).

2.4.3 Spatial variability

The material properties, geometry of the problem and the conditions that characterize the problem on hand are often described under probabilistic framework as single random variables. In such cases, it is assumed that the value remains constant over the entire domain (i.e., a homogeneous medium). However, such assumption cannot simulate a realistic model. So, to model the radionuclide transport through a geological medium be it soil or rock, an important aspect of uncertainty to be considered is the heterogeneity in the geological properties. Further, in the case of contaminant transport modelling through geological medium, the anisotropy and heterogeneity in geological properties and transport

parameters need to be modelled as random field to illustrate their efficacy in obtaining meaningful estimates of contaminant for long spatial and temporal scales. This section addresses some of the factors that contribute to the spatial variability in geosphere which affects the contaminant (radionuclide) transport and also, performance assessment as reported in literature.

Smith and Schwartz (1981) presented one of the earliest works on the influence of spatial variability of hydraulic conductivity on the mass transport patterns through the aquifer systems. A stochastic analysis of mass transport was carried out to investigate various relationships between the number of hydraulic conductivity measurements available to characterize that heterogeneity and the resulting uncertainty in transport prediction. From the analysis, a complex dependence was observed between the uncertainty in the velocity field and the hydraulic conductivity measurements. The predictions of contaminant movement were sensitive to the arrangement of the heterogeneities inferred from the dataset. So, the results suggested that for a given set of data points, the unknown patterns of spatial variation in hydraulic conductivity were more important source of uncertainty than errors in estimating the mean statistical parameters of hydraulic conductivity distribution.

Ghanem and Dham (1998) developed a two-dimensional multiphase model that simulates the movement of non-aqueous phase liquid compounds (NAPL) in heterogeneous aquifers. Heterogeneity in intrinsic permeability of the porous medium was modelled as a stochastic process. The implementation of various expansions into the multiphase flow equations resulted in the formulation of discretized stochastic differential equations that was solved for the deterministic coefficients appearing in the expansions representing the unknowns. This method allowed the computation of the probability distribution functions of the unknowns for any point in the spatial domain of the problem at any time instant.

Krupka et. al., (1999) documented the variation of partition coefficient values and its influence on contaminant transport (Environmental Protection Agency report). It described the conceptualization, measurement, and use of the partition (or distribution) coefficient (K_d), the geochemical aqueous solution and sorbent properties that are most important in controlling adsorption/retardation behavior of selected contaminants. It also discussed the influence of coupled hydraulic and chemical heterogeneity (i.e., spatial variability in hydraulic conductivity and sorption). Since spatial variability provides additional complexity to understanding and modelling contaminant retention to subsurface soils, a single K_d value was considered insufficient for an entire study site. The study also illustrated the effect of spatially varying K_d by analytical and numerical models.

Simmons et. al., (2001) presented some approaches to model the variable density groundwater flow and solute transport through heterogeneous geological media. The heterogeneity was modelled in various forms which included: sinusoidal, stochastic permeability distributions and discretely fractured geological media. The results suggested that growth and decay of convective instabilities were related to the structure and variability of permeability field. The responses for cases (1) long and vertical high permeability regions with intermediate low permeability regions (2) stochastic distributions (3) realistic non-uniform distributions exhibited varying results. While some controlling factors were apparent, an overall generalization on the impact of heterogeneity could not be made because each case exhibited different styles growth and decay.

Vrankar et. al., (2004) presented a relatively new approach to model radionuclide migration through the geosphere using radial basis function method. They also determined the average and sample variance of radionuclide concentration with regard to spatial variability of hydraulic conductivity modelled by a geostatistical approach. A conceptual model

was developed to describe the radionuclide migration where the fluid velocities were estimated in the first step and the advection-dispersion equation was solved for concentration of contaminant in the second step. The results showed that, different types of conductivity, variogram input parameters and different types of kriging were necessary to find an appropriate shape parameter which can give us results comparable to the test method. This study also explored the residual errors and their influence on optimal shape parameters.

Huysmans and Dassargues (2006) performed stochastic analysis to understand the influence of the spatial variability of diffusion parameters on radionuclide transport. So, effective diffusion coefficient and the diffusion accessible porosity with geo-statistical techniques were simulated and their heterogeneity was also incorporated in the low permeability transport model. It was observed that the diffusion coefficient showed a strong correlation with all secondary variables (porosity, grain size, conductivity etc.). The output fluxes of this model were compared with a homogeneous model and with a model with a heterogeneous hydraulic conductivity distribution. From the results it was found that, although hydraulic conductivity had a much larger relative spatial variability than the diffusion coefficient and the diffusion accessible porosity, the heterogeneity of the diffusion parameters had a much larger effect on the output fluxes than the heterogeneity of hydraulic conductivity. The reason for such behaviour was because the transport process was controlled by diffusion in low permeability media. So, the solute concentrations and fluxes were much more sensitive to changes in diffusion parameters than to changes in hydraulic conductivity.

Srivatsava et. al., (2010) and Cho (2012) highlighted the influence of spatial variability of permeability property on steady state seepage flow and slope stability analysis,.

These studies modelled permeability as a random field following log-normal distribution. The results from seepage studies in spatially variable soil showed that at very high auto-correlation length seepage discharge becomes independent of variance in permeability and tends to attain a value close to the theoretical discharge for uniform soil. Also, the results showed that the probabilistic framework can be used to efficiently consider the various flow patterns caused by the spatial variability of hydraulic conductivity in seepage assessment of geological structures.

Ciriello et. al., (2013) developed a model for radionuclide migration in a randomly heterogeneous aquifer. In this study, the aquifer hydraulic conductivity was modelled as a stationary stochastic process in space. The influence of uncertain parameters: in the first two (ensemble) moments of the peak concentration, as a consequence of incomplete knowledge of the parameters characterizing the variogram of hydraulic conductivity, the partition coefficient associated with the migrating radionuclide, and dispersivity parameters at the scale of interest were investigated. Global sensitivity analysis was carried out using polynomial chaos expansion to estimate the critical parameters affecting the transport. Although, the partition coefficient exhibited highest sensitivity, the log-conductivity correlation scale was the most influential factor affecting the uncertainty of the standard deviation of the peak concentration.

2.5 Reliability analysis of performance assessment models

The need to incorporate the concept of reliability analysis in the design of radioactive waste disposal has been recognised in the recent years and there have been efforts put

forth in this area to quantify and reduce the uncertainties in the system. So, studies on reliability analysis, development of probabilistic design procedures, by implementing various techniques for ensuring the safety and achieving the design objective of the system were carried out. In the context of disposal system performance, reliability is defined as the probability that system sustains the surrounding geological and environmental conditions (i.e., radiation dose or risk at the end-point of assessment fall within the permissible limits) within the design life of the system. This indicates that the performance of the system is dependent on the design life of each barrier in the disposal system, geological, transport properties of the geosphere which makes the process augmented and unpredictable. So, by employing reliability analysis, a rational framework for addressing uncertainties and evaluating the predicted performance of an engineering structure can be developed. A review of the literature on reliability analysis in performance assessment modelling has been divided into three categories namely probabilistic analysis of performance assessment models, sensitivity analysis studies in performance assessment modelling, and studies on the influence of spatial variability in performance assessment.

2.5.1 Probabilistic analysis for performance assessment models

There has been an increased awareness on the existence of uncertainties in the input parameters of performance assessment models which necessitated implementing probabilistic approach to the design procedures of these models. The disposal system should be designed for a specific level of reliability instead of a deterministic value for long-term safety of the system. This approach helps practitioners in decision making on the extent of safety achieved. Apostolakis (1990) discussed a rational probabilistic framework for the assessment of the risks from technological systems (like waste repositories). The basis for

this framework was that the performance (or safety) assessment of nuclear waste repositories required the inspection of the occurrence and consequences of rare events where the rare events indicated the release and transport of radionuclides into biosphere due to the failure of the repository. It was suggested to incorporate the concept of Bayesian theory within which expert opinions, experimental results and statistical observations were combined to produce quantitative measures of the risks from these system.

Deering and Kozak (1990) summarized the NRC's (Nuclear Regulatory Commission) approach for conducting evaluations for low-level radioactive waste facilities. They suggested the use bounding analysis to deal with different forms of uncertainties in performance assessment where the scenarios, models, and parameters are conservative to enable a more simplistic assessment.

Song and Lee (1992) evaluated the system performance of radioactive waste repository using First Order Reliability Method (FORM). The stochastic analysis was performed by treating the parameter uncertainties of the predictive model as random variables. Since the uncertainties in radionuclide transport parameters and random nature of container failures impact the estimation of release rates at the waste package system boundary, the failure probability of a single container, diffusional release from the failed container, releases from multiple container failures over time and geosphere transport to the accessible environment were modelled. For instance, the failure of barriers led to release of radionuclides into geosphere and their concentration values exceeded acceptable limits. So, C_a (i.e., permissible concentration) exceeds C_i (estimated concentration from the model) and the reliability (R) was defined mathematically as the probability that C_a will exceed C_i which is given as

$$R = P(C_i < C_a) \tag{2.4}$$

So, the performance function (or the safety margin) was given by $g = C_a - C_i$. The probability of failure which implies the samples with $g < 0$ was determined in terms of the reliability index, β as given below.

$$P_f = \Phi(-\beta) \qquad (2.5)$$

where $\Phi(.)$ is probability distribution function of standard normal random variable and β = $\frac{\mu_g}{\sigma_g}$. In this formula, μ_g and σ_g are mean and standard deviation of g respectively. This analysis was carried out for radionuclides[14]C and [79]Se. For reliability analysis, concentration of radionuclides, ground water velocity, porosity and dispersivity were assumed to follow normal distribution and retardation coefficient was assumed to be uniformly distributed. The results showed that for permissible concentration values 0.1 Ci/MTU and 0.01 Ci/MTU, the probability of failure estimated were 1 and 2.8×10^{-4} respectively. These values quantified the effect of individual and public health effects in probabilistic terms.

Gallegos and Bonano (1993) addressed the need to incorporate uncertainty analysis in performance assessment modelling. The source and treatment of various uncertainties were discussed and a flowchart for performance assessment model under probabilistic framework is given in Figure 2.8. In the figure, the various sources of uncertainties are identified and once the important uncertainties are characterised, their effect is allowed to propagate and quantified in a systematic fashion. In order for the uncertainty in the performance measures to be directly correlated to uncertainty in the input to the assessment, they are propagated by implementing appropriate probabilistic techniques. They suggested Bayesian modelling approach to quantify the uncertainties and Monte Carlo

simulation method to be efficient in uncertainty propagation. This methodology was tailored to the assessment of compliance with risk-based regulatory criteria. They advocated that the assesment needs to be probabilistic and, the regulatory criteria governing the disposal should be probabilistic to remove, or at least, minimize the ambiguity associated with a deterministic measure for risk-based methods.

Crowe et. al., (2002) presented probabilistic performance assessment model for optimization of maintenance studies in low-level radioactive waste disposal sites at the Nevada test site. Under the maintenance program by US Department of Energy (DOE), the probabilistic performance assessment modelling was carried out. The test site, Area 5 Radioactive Waste Management Site (RWMS) was located in north central Frenchman Flat in the southeast part of the NTS approximately 100 km north-west of Las Vegas. A comparative study on the results from conservative deterministic estimations of radiological releases from the facility and performance objectives of DOE was performed. Also, the difference between deterministic and probabilistic performance assessment and the impact of conservatism on long-term management of a low-level waste disposal facility were examined. GoldSim probabilistic simulation software was selected for use in the performance assessment maintenance program. Based on the results from both the analyses, maintenance strategy for area 5 and area 3 facilities were proposed.

Durga Rao et. al., (2009) developed probabilistic safety assessment (PSA) for nuclear power plants based on a probability bounds (PB) approach. This approach was effective in addressing uncertainty over the distribution of the component characteristics. PB analysis combines probability theory and interval arithmetic to produce probability boxes (p-boxes), structures that allow the comprehensive propagation of both aleatory uncertainty and epistemic uncertainty through calculations in a rigorous way.
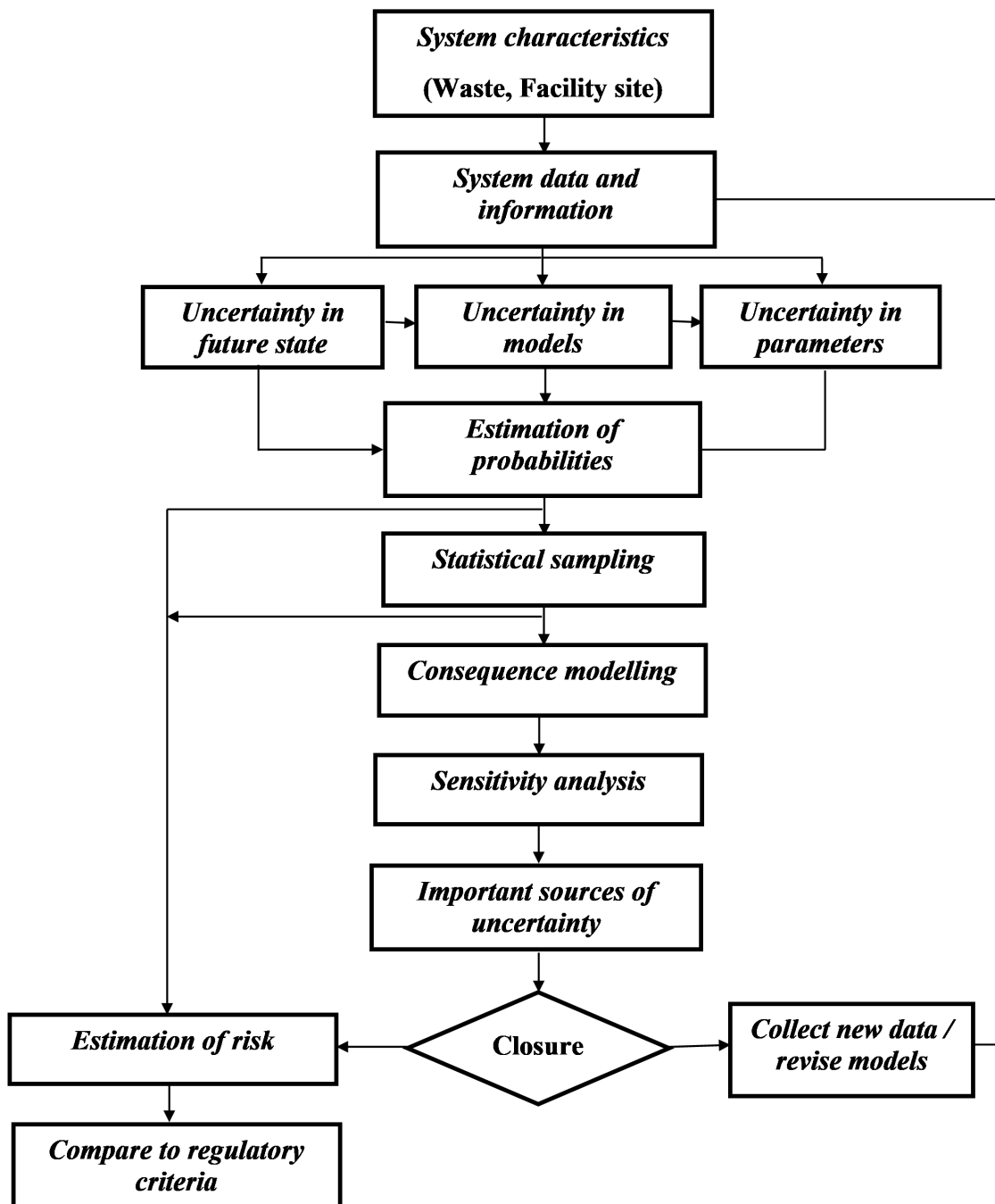
Figure 2.8: Generic probabilistic performance assessment modelling framework (Gallegos and Bonano (1993)

Using this approach, p-box for component characteristics was defined and it was found to be effective in separating uncertainty and variability in the parameters. Also, it was efficient when parameter values for input distributions, precise probability distributions

(shape), and dependencies between input parameters were not specified. The model characteristics were quantified from this study. A practical case study (power supply system of nuclear power plant) was also carried out with the developed code, based on the PB approach and compared with the two-phase Monte Carlo simulation results.

Nair et. al., (2006) developed a generic method to evaluate the reasonable upper-bound dose from near-surface radioactive waste disposal facilities through drinking water pathway. The results from deterministic analysis were discussed in section 2.3.2.1. They also discussed the influence of uncertainty as it becomes critical for the full characterization of risk to evaluate the implications and limitations of the risk assessment. However, to evaluate point estimates for regulatory requirements rather than a range of estimates, the uncertainties were handled by providing a prudently conservative upper bound of safety in terms of a safety factor. This safety factor was estimated by the uncertainty analysis of the safety assessment model using Stochastic Response Surface Method (SRSM). The distribution coefficient, fractional release rate, groundwater velocity, longitudinal dispersivity, and thickness of the aquifer were considered as uncertain parameters. The probability distribution of peak effective dose rates at 0.5 km, with 5% and 95% confidence limits were estimated as 1.61×10^{-4} and 6.91×10^{-3} mSv/yr per GW(electric).yr, respectively and the 90% confidence interval of the distribution was between these limits. Thus, the uncertainty analysis quantified the response (i.e., radiation dose) of the system.

Helton et. al., (2011) illustrated the quantification of margins and uncertainties in the analysis of complex systems. Three sites were considered for the probabilistic risk assessment which included (i) Surry Nuclear Power Station, (ii) Waste Isolation Pilot Plant (iii) high-level radioactive waste repository at Yucca Mountain, Nevada. The US NRC (Nuclear Regulatory Commission) considered two safety goals for individual fatality risk

and three quantitative risk goals for accident frequency. Once the probability space was defined, it was necessary to sample from this space in order to propagate epistemic uncertainty and thus obtain the 'margins and uncertainty'. Also, the complementary cumulative probability was estimated in each case. All the three sites used Latin hypercube sampling to generate the needed sample as this technique supported both uncertainty analysis and sensitivity analysis (as recommended in the NAS / NRC report).

Datta and Kushwaha (2011) quantified the uncertainties associated with the input parameters of a groundwater contaminant transport model by employing stochastic response surface method (SRSM). As the geosphere transport is a component of performance assessment of radioactive waste disposal facilities, this study helps in knowing the role of various hydro geologic parameters in the uncertainty assessment of the contaminant concentration. Hydraulic conductivity and distribution coefficient were assumed to be uncertain and their uncertainties were propagated using SRSM. The results showed that the cumulative probability of the concentration (of trichloroethylene) being zero was an indicator of the failure probability and the cumulative response surface of the solute concentration also provided the knowledge on the reliability of the model adopted for study.

Cadini et. al., (2012) estimated the performance of radioactive waste repository using subset simulation technique. The logic of the protective barriers of the repository was represented by a reliability model. So, the mean time to failure of each barrier was assumed to be log-normally distributed. The failure event was defined as the case when, the dose at a reference location x downstream from the disposal site is larger than the threshold of acceptability d^* which was given by $F = d(x,t) - d^*$. The repository containment failure probability was estimated by $P_f = \frac{n_F}{n_T}$ where n_F - samples belonging to failure event and n_T - total number of samples. The P_f value was estimated by imple-

menting subset simulation. It allowed improving the efficiency of the random sampling for estimating the repository containment failure probability.

Chopra et. al., (2013) used response surface method (RSM) coupled with first order reliability method (FORM) and estimated the probability that the dose rate value through drinking water pathway at a location around the tailings pond exceeds the WHO guidelines for drinking water. The radionuclide transport was modelled for Turamdih study (in Jharkand state, India) area using FEFLOW software (with all the initial and boundary conditions) and flow pattern of contaminant was estimated. The five parameters including longitudinal and transverse dispersivities, and distribution coefficients of uranium, thorium and radium were considered uncertain and propagated through the model. Using RSM, the equation for radiation dose as a function of the five uncertain parameters were obtained. Finally, using FORM, the P_f values were estimated and the results showed that it decreased as the distance from the tailings pond increased. The importance of quantifying uncertainties (in input parameters) in case of actual field problems was highlighted in this study.

Cadini et. al., (2015) developed meta-modelling based importance sampling algorithm for estimating the performance of radioactive waste repositories. The design life of each barrier of the repository was considered as random variable following lognormal distribution. In these systems, the estimation of probability of failure (P_f) is quite challenging due to their very low values and applying classical methods like Monte Carlo Simulation to evaluate P_f becomes impractical. So, an algorithm that makes use of an estimated optimal importance density and a surrogate, kriging-based meta-model approximating the system response was developed. Further, using the accurate analytic analysis of the algorithm, a modification was proposed which allowed further reduction in the computational efforts

by a more effective training of the meta-model.

Sujitha and Sivakumar Babu (2017) developed a reliability-based design procedure that accounts for the uncertainties associated with the barrier system. This methodology evaluated both component and system reliabilities. In the case of component reliability, it was found that amongst the barriers of disposal facility (top cover, waste container, waste form and bottom cover), the top cover contributed more to the failure of the barrier system. The study also advocated optimisation techniques to evaluate the probability of failure. The probability of simultaneous occurrence of all the failures was estimated as 0.022, which was very close to the probabilities of the individual components. This study highlighted the importance of system reliability in radioactive waste disposal systems.

2.5.2 Sensitivity analysis studies for performance assessment models

As per the safety guidelines formulated by the regulatory bodies (AERB, 2006; IAEA, 2014), sensitivity analysis is one of the important components of probabilistic safety assessment model for radioactive waste disposal systems. So, a number of studies have conducted sensitivity analysis for these models to investigate the influence of variability in key input parameters. Sensitivity analyses are recommended to identify factors that are significant to safety and to group them according to their significance in the system response. From the design point of view, this knowledge would allow the designer in directing attention more towards the determination of those variables that have maximum effect on the results.

Hoffman and Miller (1983) reported a theoretical structure to develop performance assessment models. They stressed on the need to carry out uncertainty and sensitivity analyses to understand the long-term behaviour of environmental radiological assessment

models and their implications. They suggested that various approaches must be considered for addressing model uncertainties. These approaches included the use of screening procedures to identify potentially important radionuclides and exposure pathways, sensitivity analyses to identify important groups of model parameters, stochastic analysis to determine the effect of parameter uncertainty on model predictions, and comparisons among the predictions of different models. They also emphasized the need to investigate each of these approaches and discussed different procedures of performing sensitivity analysis.

Helton (1993) presented a review of uncertainty and sensitivity analyses techniques for use in performance assessments for radioactive waste disposal. The methodologies discussed for these analyses included differential analysis, Monte Carlo analysis, response surface methodology, and Fourier amplitude sensitivity test. The algorithm for implementing each of these techniques for both uncertainty and sensitivity analyses were presented and the advantages and limitations of each techniques were discussed. Also, an illustrative study was carried out using Monte Carlo analysis performed as part of a preliminary performance assessment for the Waste Isolation Pilot Plant (USA).

Kim et al., (1993) developed a composite risk assessment model for the shallow-land burial of low-level radioactive waste. Sensitivity analysis was carried out as an integral part of probabilistic risk assessment to determine the parameters that were most significant in contributing to the overall uncertainty. The amount of variation in the model output due to an arbitrary variation in the model input parameters was quantitatively estimated with the sensitivity analysis. The results indicated that the uncertainty associated with the public risk was strongly sensitive to the volume flow rate, irrigation rate of surface water and the retardation coefficient of geological structure.

Toran et. al., (1995) performed sensitivity analysis using a numerical model for fractured porous media to find out how porous media and fracture parameters affect solute transport. A two-dimensional, saturated fracture flow and transport code FRACTRAN was used to conduct the simulations. Seven parameters were considered for the analysis and they were matrix hydraulic conductivity, matrix porosity, retardation of the matrix, gradient of the flow field, fracture retardation, fracture aperture, and fracture probability (which incorporates fracture spacing and fracture length). A Latin-hypercube design was used to select a matrix of parameter values that minimized correlations among the design parameters.The greatest influence was exhibited by matrix parameters, in particular hydraulic conductivity and porosity. Also, fracture probability was nearly equivalent in importance. The results indicated that field characterization in fractured porous media should emphasize on fracture location, which strongly influences directions of contaminant transport, and also matrix properties, which have a major influence on contaminant residence times and breakthrough concentration.

Nair and Krishnamoorthy (1999) developed probabilistic safety assessment model for near surface disposal facilities. The uncertain input parameters considered were distribution coefficient of radionuclides, seepage velocity in the unsaturated zone between the facility and the water table, dispersivity in ground water and thickness of the unsaturated zone. Sensitivity analysis was carried out to identify the critical parameters, which have maximum effect on the concentration of ^{129}I in groundwater located 1.6 km from the facility. The sensitivity index for the change of a candidate parameter was defined as

$$SI = \frac{1 - \frac{C_{max}}{C_{par}}}{P_i} \qquad (2.6)$$

where C_{max} represented the maximum concentration for the reference level and C_{par} is the maximum concentration computed using the candidate parameter P whose impact needs to be evaluated. The index P_i was defined as $[1 - (P/P_r)]$ for a decrease of the candidate parameter in relation to the reference parameter P_r and as $[1 - (P_r/P)]$ for an increase of the candidate parameter. From the sensitivity analysis it was found that distribution coefficient was the most sensitive parameter followed by seepage velocity, dispersivity and thickness of unsaturated zone.

Volkova et. al., (2008) described the methods of uncertainty propagation and global sensitivity analysis that were applied to a numerical model of radionuclide migration in a sandy aquifer in the area of the RRC "Kurchatov Institute radwaste disposal site" in Moscow, Russia. The global sensitivity analysis algorithm involved uncertainty propagation, correlation analysis of obtained data and non-linear sensitivity analysis. In the final step, the Sobol sensitivity indices based on complete variance decomposition were estimated. The input parameters considered for sensitivity analysis were hydraulic conductivity, longitudinal dispersivity, transverse dispersivity, volumetric distribution coefficient and infiltration for different model layers. Sensitivity analysis was conducted for the radionuclide ^{90}Sr and the results showed that concentration values predicted by the model for the end of the year 2010 were mostly influenced by uncertainty in the values of distribution coefficient of the first and second model layers and infiltration intensity in the zones of pipe leakage on the site. On the other hand, longitudinal and transverse dispersivities as well as model porosity values had practically no influence as compared to the other inputs. From this study, the knowledge of the most influential parameters were acquired which lead to reduction in prediction uncertainty of the model.

Cadini et. al., (2012) carried out reliability analysis for a radioactive waste repository

as a part of performance assessment. The analysis was carried out using subset simulation method. The set-partitioning scheme of the subset simulation method was exploited for sensitivity analysis of the importance of the uncertain model parameters based on the conditional sample distributions at different failure probability levels. For the analysis six input random variables were considered which included failure rate of top cover, waste container, waste form, backfill, bottom cover and unsaturated zone. From the sensitivity analysis it was observed that the performance of barrier system was strongly sensitive to the parameter, near field (natural barrier) failure rate and waste form failure rate.

Ciriello et. al., (2013) proposed an approach for performing global sensitivity analysis (GSA) of a high-complexity theoretical and numerical model descriptive of the potential release of radionuclides from a near surface radioactive waste repository and their subsequent migration in the groundwater system. The uncertainty was considered due to incomplete knowledge of the variogram and transport parameters (i.e., the auto-correlation length of the variogram of log-conductivity, the partition coefficient associated with the migrating radionuclide and the dispersivity at the scale of interest) and from the random nature of the hydraulic conductivity field. GSA was performed through the polynomial chaos expansion technique (PCE) technique. Sobol indices for radionuclide ^{239}Pu revealed that the (ensemble) mean of the peak concentration was strongly influenced by the uncertainty in the partition coefficient and the longitudinal dispersivity, and the effects of these parameters shadowed the impact of the spatial coherence of the log-conductivity field at the scale analysed.

Shahkarami et. al., (2015) developed an analytical model to describe radionuclide chain transport in fractured rocks. The model considered processes of diffusion into stagnant water zones, radioactive ingrowth and hydrodynamic dispersion during transport of an

arbitrary-length decay chain through a single fracture. The model also takes advection, matrix diffusion and sorption into account and the analysis was carried out for radionuclides ^{239}Pu and ^{243}Am. By applying variance-based global sensitivity analyses, sensitivity of the results to parameter uncertainties was observed. The sequence of uncertain parameters according to their priorities from GSA were N (ratio between the diffusion rate into the stagnant water zone and the mass flow rate through the channel), MPG$_s$ (material property group of the rock matrix adjacent to the stagnant water zone), F$_s$ (ratio of the stagnant-water-wetted surface to the diffusion conductance of the stagnant water zone), F$_f$ (ratio of the flow-wetted surface of the flowing channel to the volumetric water flow rate) and MPG$_f$ (material property group of the rock matrix adjacent tothe stagnant water zone), however, all of the variables continuously influenced the model output. Also, it was found that for time periods greater than a few thousand years, the uncertainty of the model output is more sensitive to the values of the individual parameters than to the interaction between them.

2.5.3 Influence of spatial variability in performance assessment modelling

The geological formations are natural and inherently random, which reflects on the geological and transport properties of the medium. Fenton (1997) mentioned that uncertainty is a fact of life in geotechnical and geo-environmental engineering practice. This led to a rise in implementing the randomness in diverse disciplines to model heterogeneous patterns of variation and correlation using random fields. Random fields have been applied to many real-world problems for assessing the reliability of structural components with geometrical or material variability. In the field of performance assessment modelling, the

influence of heterogeneity in geological medium on the radiation dose and risk needs to be examined. A few studies that have highlighted the need for spatial variability in the design and analysis of radionuclide migration from the repository to geosphere are discussed here.

Bonano and Cranwell (1988) discussed various regulations involved in disposal of high-level radioactive wastes in deep geological repositories. The long regulatory period involved and the complex nature of the events and processes of interest, mandates the inclusion of uncertainties in the prediction of the performance of the disposal system. They mentioned that the uncertainty associated with values of parameters include measurement error, paucity of data, misinterpretation of data, spatial variation of parameters, and assumptions regarding behaviour of the system. The strategies of treating and quantifying these uncertainties were discussed.

Gutjahr and Bras (1993) reviewed the influence of spatial variability on subsurface flow and transport. Stochastic models of spatial variation in saturated and unsaturated flow and transport problems were examined. Both modelling and data interpretive geostatistical approaches were reviewed and an integrated discussion combining the two approaches were given. The methodologies included continuous stochastic models, kriging method, model based geostatistical studies and spectral methods. The probabilistic content was of special interest for reliability and risk calculations for waste management and groundwater pollution studies.

Wörman et. al., (2003), investigated the radionuclide transport by groundwater motion in fractured bedrock for performance assessment purposes. A three-dimensional flow model and a one-dimensional mass transfer model was developed and integrated for risk assessments and performance assessments. Using this model, they demonstrated the combined

effect of uncertainty due to spatial variability of water flow and solute mass transfer. The analyses (of geological data from ÄspöHard Rock Laboratory, Sweden) indicated that the the influence of spatial variability in regional / global variation of fracture probably dominates over the local variation due to the longer auto-correlation lengths. Also, the heterogeneity of the rock properties (physical and geochemical) in single fractures contributed in increasing significantly both the variance and the skewness of the residence time probability density function for a pulse travelling in a fracture.

Huysmans and Dassargues (2006) presented a stochastic analysis by incorporating spatial variability of the effective diffusion coefficient and the diffusion accessible porosity (i.e., the proportion of the total volume of a porous material that is available for diffusion) with geostatistical techniques and incorporated their heterogeneity in the transport model of a low permeability formation. Boom clay (Belgium), a candidate host rock for the deep geological disposal of high-level radioactive waste was considered for the study. The calculated output radionuclide fluxes of this model were compared with the fluxes calculated with a homogeneous model and a model with a heterogeneous hydraulic conductivity distribution. The results from the analysis showed that, the heterogeneity of the diffusion parameters has a much larger effect on the calculated output radionuclide fluxes than the heterogeneity of hydraulic conductivity in the low permeability medium under study.

2.6 Concluding remarks

In this chapter, some of the important studies reported in the literature related to performance assessment models of radioactive waste disposal systems and also the probabilistic considerations that have gained importance in the recent past have been documented. The

design procedures formalized by the regulatory bodies nationally and internationally were also presented to get an overview of various aspects involved in the process of developing performance assessment models. One of the important components of performance assessment is the geosphere transport (i.e., the type of geological medium) which plays a critical role in the radionuclide migration. So, the studies that were carried out exclusively on radionuclide transport behaviour in soil and also in fractured rocks have been summarized. The complexities involved in the flow and contaminant transport through soil and fractured rock with respect to the dimensionality of problem, the geological and transport properties of the medium are identified from the literature. The literature on uncertainty and sensitivity analyses which form an integral part of performance assessment are also presented. The research in the area of performance assessment models have some significant findings, however, they lack in integrating various uncertainties that influence the transport both locally and globally in different geological media and also quantify the effect of these uncertainties by performing reliability analysis using efficient probabilistic techniques. The other aspects that require due consideration in the probabilistic performance assessment of radioactive waste disposal systems are summarized through the scope of the study.

2.6.1 Scope of the study

From the review of literature, it is clear that significant research has been directed towards understanding the process of radionuclide transport using performance assessment models. However, the conceptual models developed for performance assessment of radioactive waste disposal systems in different geological media needs to be improved further to model a more realistic geological medium, quantify the local and global uncertainties

using reliability analysis. A review of the uncertainty and sensitivity studies that have been carried out to treat the uncertainties also highlights the need to employ computationally efficient probabilistic techniques for uncertainty propagation and quantification. The scope of the present study is sorted through the following objectives and the performance assessment modelling strategies followed to achieve these objectives are presented in Figure 2.9. The objectives are stated as:

1. To develop comprehensive predictive models (analytical and numerical models) that assess the performance of radioactive waste disposal system by integrating the source term, repository failure, geosphere transport and radiological models and quantitatively assess the risk experienced at the end-point (near human habitat). Also, estimate the critical radionuclides causing maximum radiological impact (section 4.3 of chapter 4 and section 5.3 in chapter 5).

2. To address the computational issues involved in employing reliability techniques using analytical and numerical modelling approaches for performance assessment by constructing of meta (surrogate) models, for efficient uncertainty propagation. (section 4.5 in chapter 4 and section 5.3.1.5 in chapter 5)

3. To develop systematic and detailed approach for reliability analysis by taking into account of the uncertainties in input parameters (epistemic uncertainty) and estimate the probability of failure of the system (section 4.5.2 in chapter 4 and section 5.3.1.3.2 in chapter 5).

4. To identify the critical parameters that affect the radioactive waste repository performance (due to release of activity from disposal system) when the uncertain input parameters that influence the critical responses are propagated through the system,

through global sensitivity techniques (section 4.5.3 chapter 4 and 5.3.1.3.3 in chapter 5).

5. To develop a probabilistic performance assessment framework and analyse the effect of spatial variability in the hydraulic conductivity of soil medium (aleatory uncertainty) on the radiation doses at the end-point, and justify the need for incorporating spatial variability in the reliability analysis of performance assessment models (section 5.4 in chapter 5).

6. To propose new hybrid model that captures the features of fracture geometry, variation in aperture sizes along the fracture and their influence on contaminant migration including the radionuclide transport and systematically investigate their effect (section 6.5 and section 6.6 in chapter 6).

7. To develop an efficient probabilistic performance assessment framework by integrating geosphere transport model (hybrid model) for fractured rock into the performance assessment model. Also, to investigate the influence of stochastic nature of fracture generation algorithm, uncertainties in the geological and transport properties of fractures and intact rock; and estimate the most influential parameters in the model through uncertainty propagation and quantification techniques; and sensitivity analysis (section 6.6.5 and section 6.7.5.1 chapter 6).
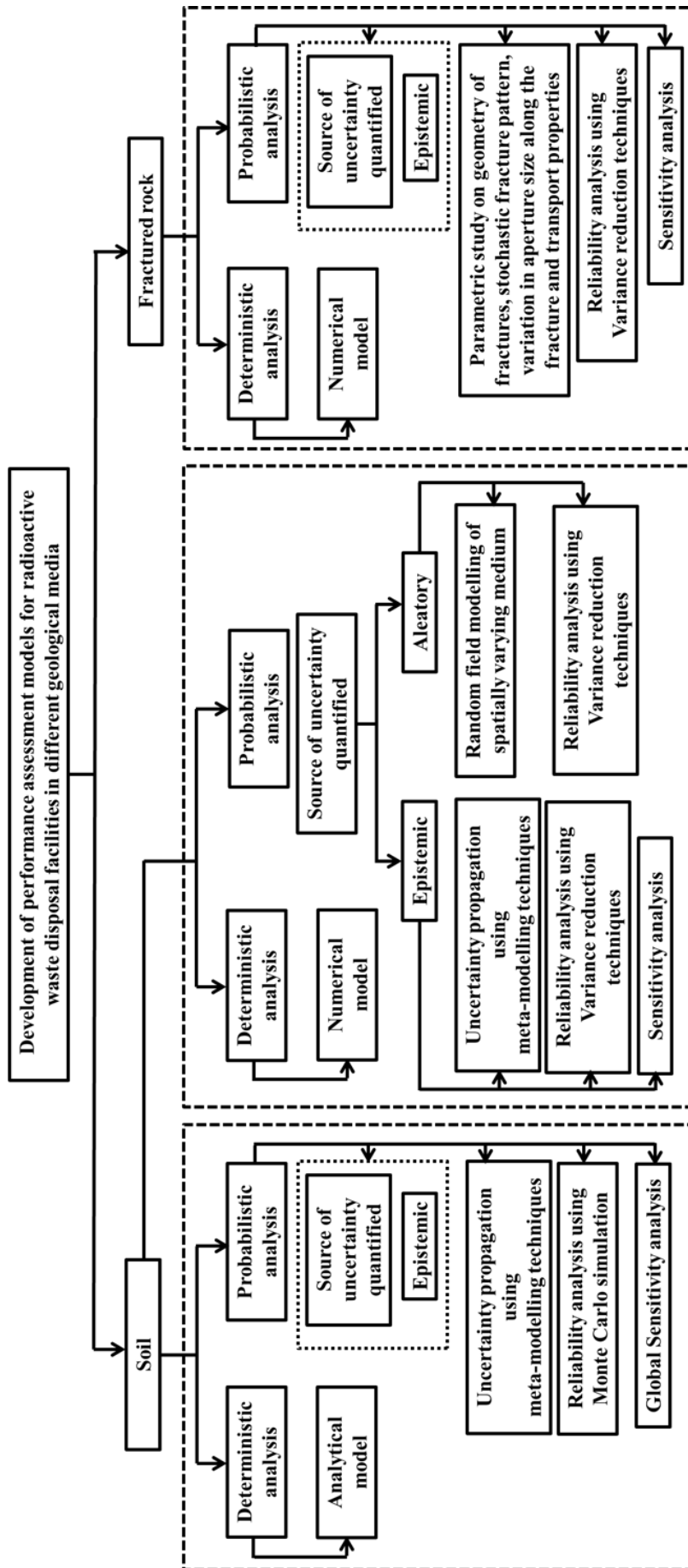
Figure 2.9: Overview of different techniques adopted to develop performance assessment models in soils and fractured rocks

Chapter 3

Methods of analysis

3.1   Introduction

The long-term safety of radioactive waste disposal systems are ensured by developing efficient performance assessment models (Campbell and Cranwell, 1988). The fundamental part of a performance assessment lies in the application of mathematical models. These models are used to estimate the dose-equivalents and health risks to humans resulting from release of radioactivity in biosphere by means of external and internal exposure pathways. So, a detailed overview of various mathematical models (analytical and numerical) involved in the performance assessment of radioactive waste disposal facility are discussed in detail in the first part of the chapter. The critical component of the performance assessment is the transport of radionuclide in geosphere. To study this behaviour in complex geological environment like fractured rocks, initially, models for fracture pattern generation are presented and later, various modelling approaches that predict the transport behaviour through fractured media are discussed. Since all the models at their very best are only inexact representations of real systems, emphasis is being placed on increasing the realism of model predictions, by incorporating different forms of uncertainties in the system. Moreover, deterministic models lack in accommodating the spatial and temporal

variations in geological properties of the medium, uncertainties in the model parameters etc that can lead to inaccurate prediction of results. So, in the later part of chapter, sources and characterization of different uncertainties for risk and reliability assessment of radioactive waste disposal facilities are discussed. Random field modelling has been adopted to capture the uncertainty due to spatial variability of soil and the underlying concepts of these methods are presented. Also, the reliability techniques that can handle these uncertainties and quantify their effect are presented. These techniques include the analytical and the numerical simulation methods that have been developed for reliability analysis. The computational effort involved in single numerical simulation of performance assessment models is very high, hence, variance reduction and meta-modelling techniques have been implemented to address this issue. Finally, different methods of sensitivity analysis are presented to specify the relative effect of changes in the values of model parameters on the predicted quantity.

3.2 Performance assessment model for radioactive waste disposal

In general, the low and intermediate level radioactive wastes (LILW) from various sources of nuclear industry are disposed in near surface disposal facilities (NSDFs) (IAEA 1999, AERB 2006). It is of utmost importance to create a protected environment by ensuring long-term containment of these systems from any unforeseen incident. To achieve this safety objective, guidelines are developed right from site characterization, design development, construction, operation to closure and post-closure of the facility. Based on the timeline involved in these stages, they are broadly divided into three phases namely

pre-operational, operational and post-closure period as shown in Figure 3.1.
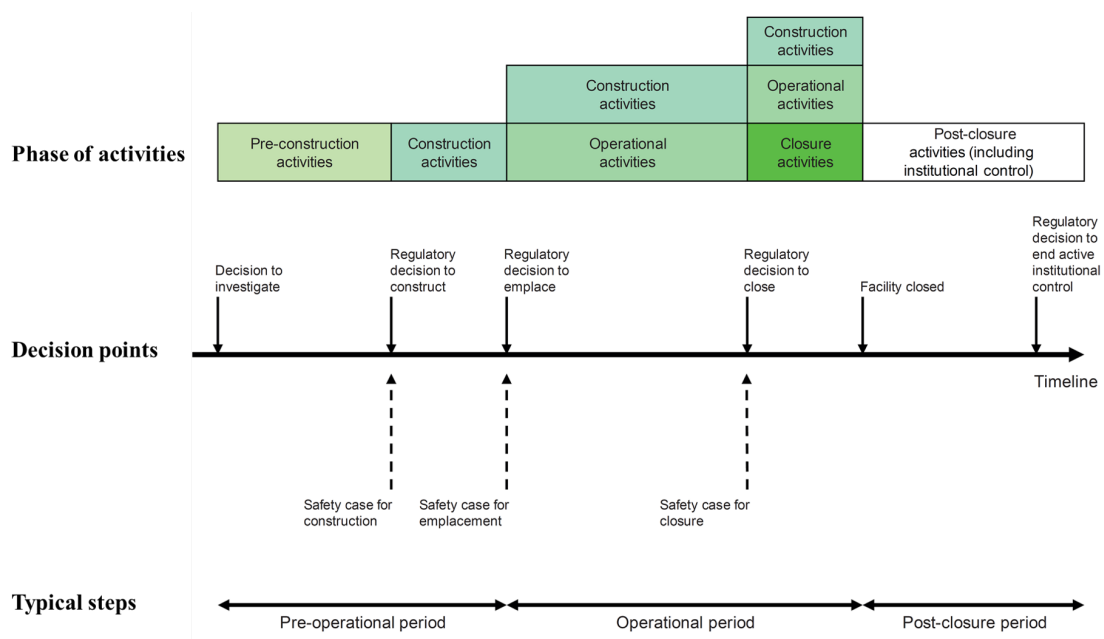
Figure 3.1: Timeline to illustrate development, operation and closure of NSDF (IAEA, 2014)

In the Figure 3.1, the activities involved in different phases (i.e., development, operation and closure) of NSDF are presented and also, the points where regulatory decisions are taken are mentioned. The first two phases handle the safety in site characterization, design, construction, operation and closure of disposal facility so that protection after closure is optimized. The time frame for the safety assessment during post-closure phase becomes very large ranging in few thousands of years when compared to time frame for safety assessment in first two phases together (operational time of facility may be around 50-70 years). Further, the post-closure safety of facility is not just focussed on evaluating the performance and radiological impact of the disposal facility, but also, to discern the behaviour of the system and the surrounding geological environment evolving in time. Assessing the safety of NSDF during the operational and post-closure phases provides a reasonable assurance that the NSDF meets the design objective, intended performance

and the regulatory requirements. This is possible by developing predictive performance assessment models which provide a basis for rational and viable decisions in establishing waste repositories.

The performance (or safety) assessment modelling methodology followed in this thesis has been adopted from AERB (2006), which provides the safety guidelines for the NSDFs designed for low and intermediate level waste disposal in India. The safety assessment methodology considers the disposal facility and its environment as a system. The first step involved in the development of the performance assessment model is to identify the features, events and processes (FEPs) which might affect the isolation of waste in the long run and results in radionuclide migration.

3.2.1 Identification of features, events and processes (FEPs)

The features, events and processes (FEPs) should be examined thoroughly for the factors that might influence the long-term safety of a repository. These aspects will help in constructing scenarios and pathways for radionuclide release. Typical FEPs for NSDFs are presented in the Figure 3.2. By studying the potential FEPs from Figure 3.2, the scenarios that can appropriately lead to release of radionuclide from the NSDF can be considered. It is important to develop a scenario that encompasses the operational, closure and post-closure safety aspects of the NSDF. In the thesis, the scenario of barrier failure is assumed to occur due to rainfall (event) leading to infiltration of water into the barrier system (features), radionuclide release into geosphere and migration of these radionuclides ultimately to the biosphere (process). Based on the type of radionuclide (short-lived or long-lived) considered for the analysis, both the near-field and far-field scenarios are investigated .
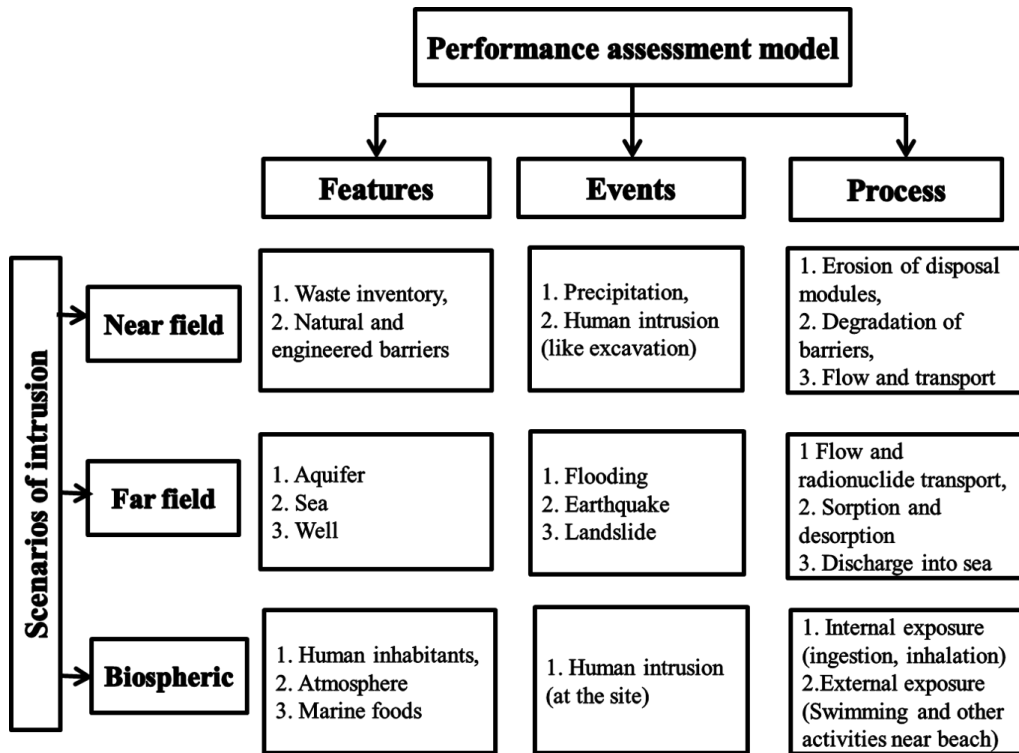
Figure 3.2: Features, Events and Processes for various scenarios

Once the scenarios are identified, a conceptual model that provides an overall idea of the performance of disposal system over a period of time needs to be developed. This model has to account for waste inventory, features of engineered and geological barriers, time frame and uncertainty in the parameters. The conceptual model is then translated into mathematical model which is represented by a system of equations. The general procedures used to develop such models are well accepted, and these predictive mathematical models have to be effective both in the level of detail and complexity. They should be used to describe individual processes, subsystems and overall system performance. A brief overview of the mathematical formulations (Nair and Krishnamoorthy, 1999; Nair et. al., 2010) considered in the thesis are discussed in a sequential order in the following sections.

3.2.2 Source term model

There is a need to identify and characterize waste in terms of inventory, wasteform and package. This information should be sufficiently extensive to allow adequate modelling of radionuclide releases. Source term evaluates the inventory of radioactive waste in the disposal facility. A basic model for source-term can be evaluated using the equation

$$S = M_{in} exp[-\lambda_p t] \tag{3.1}$$

where M_{in} - inventory (Bq) of a radionuclide in the total waste; λ_p - radioactive decay constant (y^{-1}); t - time elapsed after disposal (y).

Equation 3.1 can be refined further by developing a conceptual model with more information on the waste and the disposal system. For example, the source term is essentially a function of the mode of disposal (single dump mode, multiple dump mode) and radioactive decay and in some cases, a function of infiltration velocity and the volume of the facility. These conceptual models are discussed in section 4.3.1.2 in chapter 4 and section 5.3.1.1 in chapter 5.

3.2.3 Repository failure model

Radioactive waste disposed in NSDF can be engineered vaults or stone / RCC trenches or tile holes constructed at varying depths- from a few metres to a few tens of metres. They are made up of a system of engineered and natural barriers. In order to develop an adequate understanding of the behaviour of the disposal facility, there is a need to characterize and assess the system components in terms of their initial performance. In fact, the

extent to which the barriers (engineered and natural) contribute to the overall containment can differ widely for different types of NSDFs (i.e., stone line trenches, tileholes, RCC trenches). This factor should be taken into account as it contributes to the overall performance. The concept of repository failure due to degradation of each barrier is considered in the thesis to develop the mathematical model. The equation to estimate the failure of each barrier is given by

$$f_t = \lambda_f exp(-\lambda_f t) \tag{3.2}$$

where f_t - failure distribution of barrier; λ_f - the reciprocal of mean time-to-failure of the barrier (failure rate, y^{-1}); t - time elapsed after disposal (y). The repository failure distribution model is used to evaluate the radioactivity release rate into ground water through the multi-barrier system and discussed in section 4.3.1.2 of Chapter 4. The consequence of source leaching from the barrier system by taking into account the source term and repository failure models results in the evaluation of radioactivity release rate.

3.2.4 Geosphere transport model

To translate the radioactivity release rate into radionuclide concentration in ground water, a geosphere transport model is developed. The geosphere transport involves evolution of environment in the vicinity of radioactivity releases and radionuclide transfer through the evolving environment mathematically. The primary focus of this model is to understand the fate and transport of radionuclides, to estimate the concentrations evolving over spatial and temporal scales in the subsurface environment and also the time of arrival of peak concentration. The underlying transport mechanisms involved in radionuclide migration include advection, diffusion and dispersion, chemical reactions like sorption and radioac-

tive decay. The mathematical equations for representing each of these mechanisms are presented in Table 3.1. These mechanisms are considered to describe the contaminant transport in the geosphere, and they are translated to differential equation which is given by

$$\frac{\partial C}{\partial t} = D\frac{\partial^2 C}{\partial x^2} - v\frac{\partial C}{\partial x} + \frac{\gamma}{n}\frac{\partial S}{\partial t} + \lambda C \tag{3.3}$$

In equation (3.3), the advection ($v\frac{\partial C}{\partial x}$), hydrodynamic dispersion ($D\frac{\partial^2 C}{\partial x^2}$), sorption ($\frac{\gamma}{n}\frac{\partial S}{\partial t}$) and radioactive decay (λC) components are taken into account to understand the rate of change in concentration over time at distance x from the source. This partial differential equation is solved for given initial and boundary conditions through analytical and numerical modelling techniques.

3.2.4.1 Contaminant transport modelling in different geological media

The geological environment surrounding the disposal system is critical in governing the movement of radionuclide reaching the human habitat. In this thesis, the transport of radionuclides is considered in different geological media. The medium of transport (which mainly consists of soils or rocks) and their properties play an important role in transport process. So, in this section, the formulation of radionuclide transport models for soils are discussed followed by transport modelling in fractured rocks.

3.2.4.2 Soils

Soils are natural geological formations originated by weathering of rocks. The studies on contaminant transport through soils can be traced back to 1960 (Ogata and Banks, 1961). Since then many analytical models have been developed to understand the transport behaviour. The models that have been adopted in the thesis are presented below. The

Table 3.1: Various transport processes in the geosphere (for a radioactive contaminant)

SNo	Transport mechanism	Definition	Formula
1	Advection	It is attributed to bulk movement of solute due to flowing groundwater. Here, $\tilde{v}$ is the average linear velocity, q - Darcy velocity (where $q = Ki$, K - hydraulic conductivity, i - hydraulic gradient), ε is porosity	$\tilde{v} = q/\theta$
2	Mechanical dispersion	Spreading of solute due to different velocities along the pore channels, difference in pore sizes along flow paths (dispersion can be longitudinal or transverse). Here, D_d - mechanical dispersion, α_L - longitudinal dispersivity, $\tilde{v}$ is the average linear velocity	$D_d = \alpha_L \tilde{v}$
3	Molecular diffusion	Movement of solute under the influence of concentration gradient. Here, F_m - mass flux, D_f - diffusion coefficient, $\frac{dC}{dX}$ - concentration gradient (Note: Hydrodynamic dispersion (D) is the sum of mechanical dispersion (D_d) and molecular diffusion (D_f))	$F = -D_f \frac{dC}{dX}$
4	Sorption	Solute gets adsorbed onto the solid mass due to chemical adsorption leading to change in concentration (slower movement). Here, S - mass of the solute species adsorbed, C - solute concentration, K_d - distribution coefficient	$\frac{dS}{dC} = K_d$
5	Radioactive decay	The spontaneous transformation of an unstable atomic nucleus into a lighter one, in which radiation is released in the form of alpha particles, beta particles, gamma rays, and other particles. Here, C - solute concentration, λ_p - radioactive decay constant, t - elapsed time	$C = Ce^{-\lambda t}$

governing differential equation for radionuclide transport is

$$\frac{\partial C}{\partial t} = D'_x \frac{\partial^2 C}{\partial x^2} + D'_y \frac{\partial^2 C}{\partial y^2} + \frac{\partial^2 C}{\partial z^2} + D'_z \frac{\partial^2 C}{\partial z^2} - U'_x \frac{\partial C}{\partial x} - U'_y \frac{\partial C}{\partial y} - -U'_z \frac{\partial C}{\partial z} - \lambda_p C + S \quad (3.4)$$

where C - concentration of radionuclide (Bq/l), x, y, z - longitudinal, lateral and vertical distances (m), D'_x, D'_y, D'_z - retarded longitudinal; lateral and vertical dispersivity (m^2/s); U'_x, U'_y, U'_z - retarded longitudinal, lateral and vertical advective velocity (m/s); λ_p - radioactive decay constant; K_d - distribution coefficient of radionuclide; R_d - retardation factor $(1 + \frac{K_d \rho_b}{\theta}$; ρ_b - bulk density; θ - porosity; S - source term.

3.2.4.2.1 Analytical models

The governing equations are solved for given initial and boundary conditions mathematically. There are many techniques like Fourier transforms, Laplace transforms, Green's function, perturbation methods, complex variable techniques that can be used to solve for exact solutions. Some of the analytical formulations developed by researchers in the past few decades have been adopted in the thesis. They include one-dimensional (1D), two-dimensional (2D) and three-dimensional (3D) solutions for different boundary conditions (mostly used for practical applications). Some of the closed form solutions considered for the analysis are mentioned below.

1. **Ogata and Banks (1961)**: The concentration of contaminant in a three-dimensional medium with an instantaneous source is

$$C = \frac{C_0}{2} \left[\text{erfc} \left(\frac{x - \tilde{v}t}{2\sqrt{Dt}} \right) + \exp \left(\frac{\tilde{v}x}{D} \right) \text{erfc} \left(\frac{x + \tilde{v}t}{2\sqrt{Dt}} \right) \right] \quad (3.5)$$

where C is concentration after elapsed time t, x is the end-point of interest.

2. **Nair and Krishnamoorthy (1999)**: The one-dimensional solution of concentration of radionuclide in groundwater for the instantaneous release of unit activity from a line source is given by

$$C_g(x,t) = \frac{exp(-\lambda_p t)exp(-(x-U_x t)^2/4D_x t)}{2\pi A R_g \theta_g \sqrt{D_x t}} \qquad (3.6)$$

where D_x is the retarded longitudinal dispersion coefficient (cm^2/y), U_x is the retarded groundwater velocity (cm/y), A is the cross sectional area of aquifer (cm^2), R_g is the retardation factor which is $1 + \frac{K_d \rho_b}{\theta_g}$ where K_d is the distribution coefficient (ml/g), ρ_b is the bulk density (g/cc), θ_g is the effective porosity. Similarly a two-dimensional solution is also developed which is presented in section 4.3.1.3 of chapter 4.

3. **Park and Zhen (2001)**: The contaminant transport through a three-dimensional aquifer system is modelled and the solution is obtained using Green's function method. The concentration of contaminant for an instantaneous point source is given by the equation

$$C(x,y,z,t) = \frac{1}{4d\pi\sqrt{D_x D_y}} \int_0^t q_p(t-\tau)\exp(-\lambda\tau)exp\left[-\frac{(x-v\tau)^2}{4D_x\tau}\right] \times exp\left[-\frac{y^2}{4D_y\tau}\right]$$

$$\times \left[1 + 2\sum_{n=1}^{\infty} cos\frac{n\pi z_0}{d}cos\frac{n\pi z}{d}exp\left[-\frac{D_z n^2 \pi^2}{d^2}\tau\right]\right]\frac{d\tau}{\tau} \quad (3.7)$$

In the process of transition from conceptual models to mathematical models, errors may be introduced owing to the simplifications, approximations, or modelling assumptions. Further, problems involving irregular geometry, materials with variation in properties, nonlinear relationships and/or complex boundary conditions cannot be handled by ana-

lytical methods. In such cases, numerical models are adopted in the form of finite difference method, finite element method, finite volume method, meshless method, boundary element method and so on. However, in this thesis, finite element model (FEM) has been implemented to solve the radionuclide transport problems and to help in the numerical formulation of the problem FEFLOW software version 6.2x is used.

3.2.4.2.2 Numerical models

As mentioned above, numerical methods are used to achieve an approximate solution for the complex differential equations by spatial and temporal discretization. After discretizing space and time, at every point, approximate values are estimated by transforming partial differential equations into a set of linear algebraic functions. As the results are approximate, numerical errors are bound to occur. So effort is put forth to attain least possible error for the given problem. The numerical software is designed to handle the flow, mass and heat transport through porous and fractured media. To model the flow and transport through soil, it is treated as a porous medium. The concept of representative elemental volume (REV) is applied, which allows for macroscopization (that implies continuum in all the three phases - solid (s), liquid (l) and gaseous (g)) of the properties in the porous medium. Also, it follows the fundamental assumption of soil mechanics which states that the average properties have to be independent of size of REV region dV. A typical case of soil property (porosity) with microscopic variations, continuum and macroscopic variations are shown in Figure 3.3.
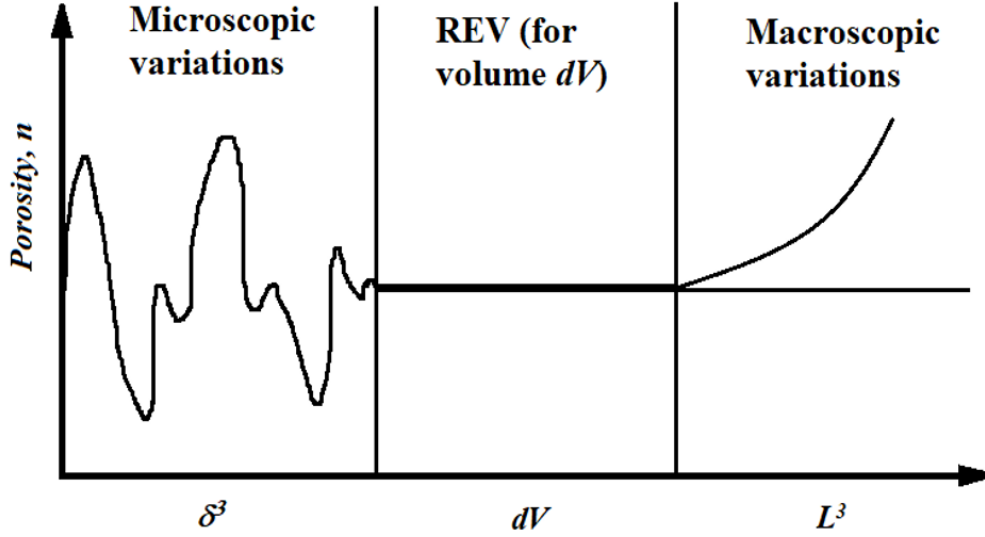
Figure 3.3: Variations in average volume as a function of porosity

The mathematical models are developed based on four balance laws. They are mass balance, momentum balance, total energy balance and entropy balance. The formulations for all the balance laws are presented by Diersch (2014). For instance the conservation of mass is given by equation,

$$\frac{\partial}{\partial t}(\varepsilon_\alpha \rho^\alpha) + \triangledown.(\varepsilon_\alpha \rho^\alpha v^\alpha) = \varepsilon_\alpha \rho^\alpha (Q^\alpha + Q_{ex}^\alpha) \tag{3.8}$$

where $\alpha = s, f \in (l, g)$, ε - fraction of volume dV occupied by α phase, ρ - is intrinsic mass density, v^α - velocity in α phase and $(Q^\alpha, Q_{ex}^\alpha)$ are (phase internal supply of mass, phase change of mass) respectively. Further, the strain tensor and the relative velocity in α phase are evaluated. The transfer of fluid into different phases is considered based on constitutive equations. Using all the above laws, the governing equations for fluid flow and mass transport are given by:

1. **Fluid flow**: In a fully saturated medium, the equation for law of conservation of

102

momentum in the liquid phase (l) is given by

$$q = -Kf_\mu(\nabla h + \chi e) \tag{3.9}$$

where q - Darcy velocity, K - Hydraulic conductivity, f_μ - viscosity function, ∇h - change in hydraulic head, χ - Buoyancy coefficient. Similarly, governing equation for conservation of mass is given by

$$S_0 \frac{\partial h}{\partial t} + \nabla.q = Q \tag{3.10}$$

where S_0 - specific storage coefficient (the volume of water that a unit volume of aquifer releases from storage under a unit decline in hydraulic head), h - hydraulic head (sum of pressure head and elevation head), $\frac{\partial h}{\partial t}$ - rate of change in hydraulic head, q - Darcy velocity and Q - specific mass supply. In steady state conditions, the rate of change in hydraulic head is zero, while, in the transient state conditions it is a non-zero quantity (i.e.,the magnitude or direction of the flow velocity at any point varies with time). Substituting equation (3.9) in the equation (3.10) we get

$$S_0 \frac{\partial h}{\partial t} + \nabla.[-Kf_\mu(\nabla h + \chi e)] = Q \tag{3.11}$$

These equations describe the governing equations for fluid flow.

2. **Mass transport**: The governing equation for mass transport is given by

$$\theta R_d \frac{\partial C}{\partial t} + q.\nabla C + \nabla.j + \varepsilon R_d \nu C = S \tag{3.12}$$

where ε - porosity, R_d - retardation factor, $\frac{\partial C}{\partial t}$ - rate of change in concentration, q - Darcy velocity, S - source / sink term

Similarly, equations for energy and entropy balance are also developed in FEFLOW. But in the thesis only flow and transport aspects are studied. Once the governing equations are derived mathematically, the equations can be solved by assigning initial conditions (IC) and boundary conditions (BC). The boundary conditions mainly include:

(i) Dirichlet-type conditions (1st type BC) - it specifies the values that a solution $[(h,t)$ -(head, concentration)] needs to take along the boundary of the domain.

(ii) Neumann-type conditions (2nd type BC) - it specifies the values in which the derivative of a solution $[(\frac{dh}{dx}, \frac{dC}{dx})$ - (head gradient, concentration gradient)] is applied within the boundary of the domain

(iii) Cauchy-type conditions (3rd type BC) - it specifies both the function value (h,t) and normal derivative $(\frac{dh}{dx}, \frac{dC}{dx})$ on the boundary of the domain.

The approximate solution is expressed in a functional form given by

$$\varphi(x,t) \approx \tilde{\varphi}(x,t) = \sum_j N_j(x)\varphi_j(t) \tag{3.13}$$

In the equation (3.13), the $\tilde{\varphi}$ - the approximate solution, N_j - set of basis functions, φ_j - unknown coefficients. It can be observed that the the spatial and temporal components are separated. The semi-discrete method is adopted in numerical modelling which discretizes the space first and then the time (time marching procedure).

Spatial discretization:

The basis functions (N_j) are polynomials like Chebyshev, Lagrangian, Hermite etc. The approximate solution is given by a series expansion, and, the difference between exact

and approximate solutions is defined by error $E = \varphi - \tilde{\varphi}$. (in the FE mesh the error is estimated at discrete set of points or nodes).

By implementing the method of weighted residuals the approximate solution for equation (3.13) is obtained. A weighting function should be chosen such that $\int_{\omega} w(x,t) R d\omega = 0$, where $w(x,t)$ is the weighting function. This method of approximation is adopted to the flow and transport PDE (equation (3.11) and (3.12)). Since the domain is divided into an FE mesh with a set of non-overlapping elements, the solution $\tilde{\varphi}(x,t)$ is considered as a union of element-wise continuous approximation which is given by

$$\tilde{\varphi}^l(x^l,t) = \sum_{j=1}^{N} N_j(x^l)\varphi_j^l(t) \tag{3.14}$$

where φ_j^l are set of unknown coefficients (corresponds to concentration C in a mass transport problem) at nodes j belonging to element l. $N_j^l(x^l)$ is the C_0 continuous basis function (or shape functions) related to element l and node j. These shape functions are nothing but polynomial of certain degree. The types of shape functions and the transformation of shape functions from local to global co-ordinate system (through Boolean matrices (Δ_{Kj}^e)) are discussed in detail in Diersch (2014). By discretising domain ω and its boundary B by finite elements and introduce basis functions, the approximate solution is given by

$$\tilde{\varphi}(x,t) = \sum_{j=1}^{N_p} \sum_{K=1}^{N_T} NK^e(\eta)\Delta_{Kj}^e\varphi_j(t) \tag{3.15}$$

Equation (3.13) is solved using Galerkin method (where weighing function is equal to the basis function). The assembled global matrix system of equations is used to solve for unknown coefficients φ.

Temporal discretization:

By implementing the Galerkin approximation of the governing partial differential equation (PDE) it gets transformed to a system of ordinary differential equations (ODE) given by

$$O \cdot \dot{\varphi} + L \cdot \varphi = F \qquad (3.16)$$

where $\dot{\varphi}$ - derivative of state variable , O - mass matrix, L - matrix corresponding to advection, dispersion, sorption and decay and, F - source / sink term. By assigning the initial condition $t = t_0$, we get $\varphi(t_0) = \varphi_0$. The general solution for ODE is in the form of homogeneous part and particular integral. This solution is not easily obtained from analytical methods. Several numerical schemes including time marching recurrence schemes, implicit and semi-implicit schemes should be implemented to solve the equations. So, the general outline for achieving solution for flow and mass transport of a system numerically is presented elaborately in this section. The same sequence of steps are followed for saturated / unsaturated and variable density of flow and mass transport in 2D and 3D medium. Also in this numerical model, error minimization in geometry is implemented through adaptive mesh refinement schemes. Hence, by using FEFLOW 6.2, numerical models for radionuclide transport modelling with different initial and decaying source boundary conditions are developed and implemented in the present study.

3.2.4.3 Fractured rocks

As mentioned earlier, the geosphere is mainly composed of soils and rocks. So far, the different formulations that are considered in the thesis for radionuclide transport through soils have been discussed. In this section, the modelling techniques for radionuclide transport through fractured rock mass are presented in detail. Rock is a natural solid mass formed by physical, chemical and biological process of geosphere. Depending on the

source of origin, rocks are classified as igneous, sedimentary and metamorphic. In most of the rocks, the existence of fractures is ubiquitous (due to stress imbalances). Modelling contaminant flow and transport through a fractured rock mass is a complex process as it involves characterization of two subsystems: fractures and intact rock matrix. The fracture patterns are generated based on geological mapping, geomechanical approach and stochastic approach. Many models were developed by adopting these approaches and they are discussed in section 2.3.3.2 of chapter 2. In the thesis, an attempt has been made to develop a numerical model that can create fracture pattern stochastically and simulate the radionuclide transport through the system. In stochastic approach, the fractured network is described under probabilistic framework and the real network is assumed to be one among the realizations (simulated from the model). Also, the randomness in the geological system is captured in the stochastic fracture generation models which makes it the most popular approach among discrete fracture network models (Herbert, 1996). Due to the robustness and efficiency in generation of fracture patterns, a stochastic fracture generating algorithm developed by Michael Riley (2004) is implemented in this thesis. The details of this methodology are discussed in the next section.

3.2.4.3.1   Algorithm for fracture generation

This method is designed to simulate the style of fracturing seen in the Lincolnshire Limestone in United Kingdom and similar layered sedimentary rocks. The growth algorithm constitutes of a special case where the fracture density within a set is homogeneous, all fractures in a set are parallel, the speed of propagation is constant and the same for each fracture in a set, and all fractures are initiated simultaneously. The fractures are generated based on the assumptions that:

1. The crack propagates at the point of weakness of the rock.

2. The domain consists of seed points through which the fractures propagate and they are inclined in the direction based on the distribution of fracture sets.

3. The density of fractures sets are assumed to be the same as that observed typically in the field. The orientation of the fractures in the fracture sets are associated with the orientation distribution.

4. Each fracture is allowed to propagate in both the directions from the seed point at speed,u_a until they meet the other fracture. Further, they continue or terminate based a fixed probability, p_a.

To illustrate the efficiency of the algorithm, a typical rock outcrop observed in limestone and the fracture pattern generated from the algorithm are presented in Figure 3.4 (a) an Figure 3.4 (b) respectively. This parallel fracture model is a function of four parameters which include: fracture density (λ_{ab}), fracture orientation (θ_{ab}), speed of propagation (u_a) and the probability that that fracture will continue or terminate when it meets the other fracture (p_a). The parameters λ_{ab} and θ_{ab} can be determined from the field data and reproduced automatically, while, the parameters u_a and p_a are used to match the field data with the statistical distributions of fracture trace lengths obtained from the method. The fracture trace length distribution of rock mass is developed by implementing this algorithm. So, the following steps present the methodology and their mathematical formulations to evaluate the fracture trace length distribution as a function of the four parameters.

1. The distance from the seed point of a fracture (from a particular fracture set) to one of its ends is considered as a random variable X_a (where $'a'$ is the fracture set) with a probability distribution function (PDF), $F_a(x)$. The total trace length of a fracture

can then be considered as the sum of two independently drawn samples from $F_a(x)$

(since the fracture densities are homogeneous).

(a)   (b)
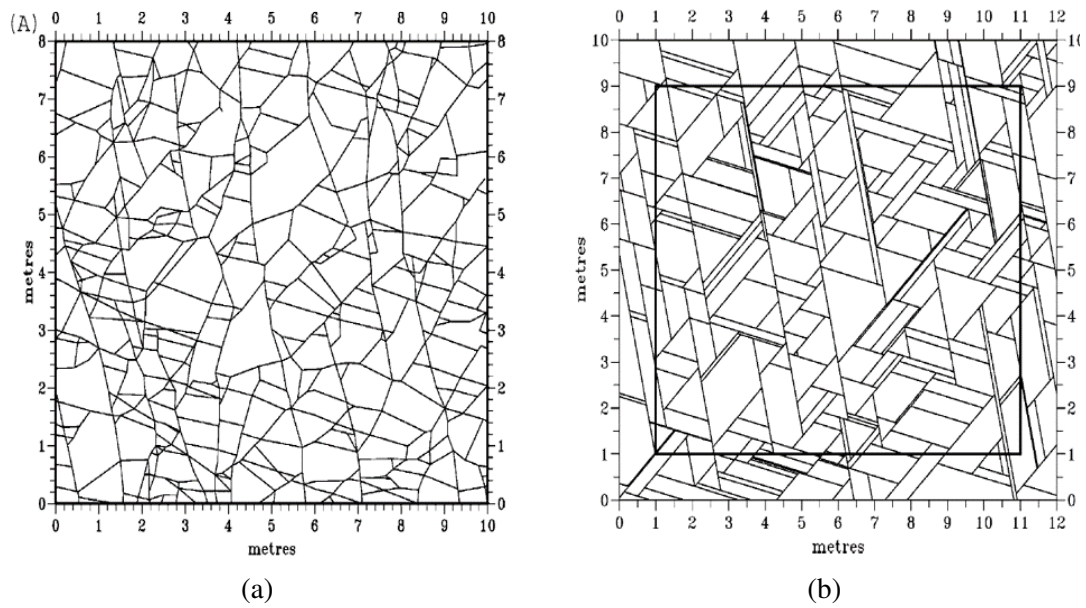
Figure 3.4: (a) Typical fractured rock pattern of limestone observed in United Kingdom
(b) Typical fractured rock pattern generated from the algorithm (Riley, 2004)
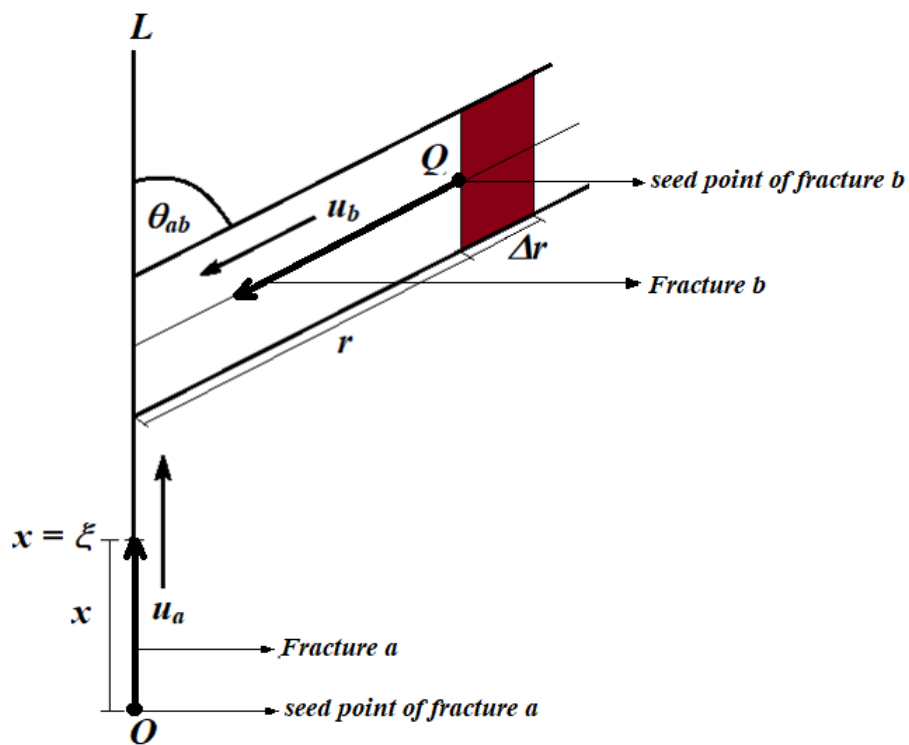
Figure 3.5: Schematic of fracture from set a intersecting another fracture from set b (Riley 2004)

2. In Figure 3.5, it can be observed that a fracture from set a growing from the seed point O in the direction OL with a speed u_a. $x = \xi$ is the growing tip of the fracture at any time and θ_{ab} is the angle between the fracture sets a and b. So, the objective is to estimate the fracture trace length distribution of two fracture sets, $F_{ab}(x)$. So, it is necessary to know the number of intersections occurred with pre-existing fractures, on average, within a given time t. This is again a function of $F_{ba}(r)$ the PDF of the distance from the point at which a fracture from set b is seeded to its end. An implicit expression for $F_{ab}(x)$ is developed by deriving $F_{ba}(r)$ in terms of $F_{ab}(x)$.

$$
\begin{aligned}
F_{ab}(x) &= P(X_a \leq x) \\
&= \sum_{n=1}^{\infty} [P(X_a(n) \leq x) \cap P(N = n)]
\end{aligned}
\tag{3.17}
$$

where X_a is the distance from the origin of the fracture to its end, $X_a(n)$ is the distance from O to the nth encounter, N is the number of encounters from O to the end of the fracture, x - displacement from O along OL.

(i)**Estimation of $P(X_a(n) \leq x)$**

The number of intersections is modelled as a Poisson process with non homogeneous mean, $g_{ab}(x)$. Thus, if $X_a(n)$ is the distance from O to the nth encounter, then the probability that this distance is less than x is given by

$$
P(X_a(n) \leq x) = 1 - exp[-g_{ab}(x)] \sum_{m=1}^{n-1} \frac{[g_{ab}(l)]^k}{k!}
\tag{3.18}
$$

where $g_{ab}(x) = \int_0^l \lambda_{ab}(\xi) d\xi$ and $\lambda_{ab}(\xi)$ is the density of fractures from set b intersecting set a at a distance of 'ξ'.

(ii)**Estimation of $P(N = n)$**

110

The probability that the growing fracture terminates at the nth encounter is given by

$$P(N = n) = p_a^{n-1}(1 - p_i) \tag{3.19}$$

where p_a - constant probability that a fracture from set a continues after encountering another fracture. By substituting equations (3.18) and (3.19) in equation (3.17) we get

$$F_{ab}(l) = 1 - exp[-(1 - p_a)g_{ab}(x)] \tag{3.20}$$

3. The density of fracture from set b is estimated as $2\rho_b sin\theta_{ab}\Delta r$ which is nothing but the length on either side of OL. Here, ρ_b is the density of fractures from set b. Now, the probability, $\pi_{ba}(r)$, that an individual fracture from set b seeded at a distance r from OL intersects the fracture from set a, is given by

$$\pi_{ba}(r) = \begin{cases} 1 - F_{ba}(r), & t_{ba} < t_{ab}, \\ \\ 0, & \text{otherwise} \end{cases}$$

where t_{ab} is the time taken by the fracture from set a to reach the point of potential intersection with the fracture belonging to set b. To calculate the time to intersection, it is necessary to account for the velocities at which fractures propagate. Assuming that the velocities of propagation of fractures belonging to sets a and b are $u_a(x,t)$ and $u_b(x,t)$, respectively. They are independent and the initial value

problems are solved to determine t_{ab} and t_{ba}.

$$\frac{d}{dt}[x(t)] = u_a(x,t) \quad x(t_0) = 0$$
$$\frac{d}{dt}[r(t)] = u_b(r,t) \quad r(t_0) = 0 \tag{3.21}$$

u_a and u_b, are constant for each fracture set, and all fractures are assumed to grow simultaneously at $t_{ab} = \frac{\xi}{u_a}$ and $t_{ba} = \frac{r}{u_b}$

4. By substituting the estimates from the previous equations, the equation for fracture trace length distribution in the case of two fracture sets is given by

$$F_{ab}(x) = 1 - exp\left(-2(1 - p_a)\rho_b sin\theta_{ab} \int_0^{x \frac{u_b}{u_a}\xi} \int_0^{\xi} exp\left[-2(1-p_a)\rho_b sin\theta_{ab} \int_0^{r \frac{u_b}{u_a}\zeta} \int_0^{\zeta} 1 - F_{ab}(x)dxd\zeta \right] drd\xi \right) \tag{3.22}$$

Similarly for multiple fracture sets, it is

$$F_a(x) = 1 - exp\left(-2(1 - p_a) \sum_{b=1,b\neq a}^{n} \rho_b sin\theta_{ab} \int_0^{x \frac{u_b}{u_a}\xi} \int_0^{\xi} exp\left[-2(1-p_a) \sum_{c=1,c\neq b}^{n} \rho_c sin\theta_{bc} \int_0^{r \frac{u_c}{u_b}\zeta} \int_0^{\zeta} 1 - F_{ab}(x)dxd\zeta \right] drd\xi \right) \tag{3.23}$$

The equations (3.22) and (3.23) are used as an iterative scheme for simultaneously calculating $F_a(x)$ for $i = 1, ..., n$. A code is developed using the above mathematical equations and the fracture trace length distributions are evaluated and this algorithm is implemented in the thesis. The details of input parameters in fracture generation algorithm are presented in chapter 6.

After modelling the fracture network, the radionuclide transport through the fractured rock mass is described using analytical and numerical models.

3.2.4.3.2 Analytical models

It is important to note that in the presence of fractures in a rock mass, the contaminant transport takes place either through fractures or intact rock matrix or both. A typical fractured rock mass is presented in Figure 3.6. If K_f is the conductivity of fracture and K_m is the conductivity of rock matrix, then, there are four possible combinations of fracture-rock conductivities namely, (1) $K_f > 0, K_m = 0$, (2) $K_f >> K_m$, (3) $K_f > K_m$ and (4) $K_f < K_m$ (Robinson et. al., 1998). In most cases, fractures act as conductive flow channels that allow the contaminant to migrate and the transport process in intact rock matrix is due to diffusion. So, it becomes imperative to formulate mathematical models that can translate the process of transport through fracture and intact rock matrix individually. Further, initial and boundary conditions are applied separately for fractures and rock matrix.
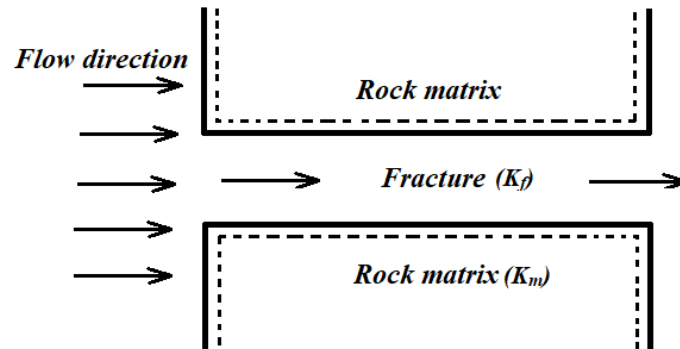
Figure 3.6: Schematic of fractured rock mass

1. **Tang et. al., (1981)**: A simple analytical model for movement of contaminant through fracture - matrix system is developed by applying Laplace transforms. It includes, (1) advective transport along the fracture, (2) longitudinal dispersivity in the fracture, (3) molecular diffusion within the fracture, in the direction of the

fracture axis, (4) molecular diffusion from the fracture into the matrix, in the y-direction perpendicular to the fracture axis, (5) linear adsorption onto the face of the matrix, (6) linear adsorption within the matrix and (7) radioactive decay. The general solution of the equation is evaluated using Gauss quadrature method and the concentration variation is evaluated spatially and temporally. The transient solution by neglecting dispersivity is given by equation

In fracture

$$
\frac{C}{C_D} = \frac{1}{2}\exp\left(-\frac{\vartheta Rx}{v}\right)\left[\exp\left(-\frac{\varepsilon\sqrt{\vartheta R'D'}}{av}x\right)\right.
$$
$$
\mathrm{erfc}\left(\frac{\varepsilon\sqrt{R'D'}}{2avR\sqrt{t-xR'/v}}x - \sqrt{\vartheta}\sqrt{t-xR'/v}\right)\right] +
$$
$$
\exp\left(-\frac{\varepsilon\sqrt{\vartheta R'D'}}{av}x\right)\mathrm{erfc}\left(\frac{\varepsilon\sqrt{R'D'}}{2avR\sqrt{t-xR'/v}}x + \sqrt{\vartheta}\sqrt{t-xR'/v}\right) \quad (3.24)
$$

The above equation holds good for the condition $(t-xR/v) > 0$

In rock matrix

$$
\frac{C}{C_D} = \frac{1}{2}\exp\left(-\frac{\vartheta Rx}{v}\right) \times \left[\exp\left(-\frac{\varepsilon\sqrt{\vartheta R'D'}}{av}x - \sqrt{\vartheta}A(y)\right)\right.
$$
$$
\mathrm{erfc}\left(\frac{\varepsilon\sqrt{R'D'}}{2avR\sqrt{t-xR'/v}}x + \frac{A(y)}{2\sqrt{t-xR/v}} - \sqrt{\vartheta}\sqrt{t-xR'/v}\right)\right] +
$$
$$
\left[\exp\left(-\frac{\varepsilon\sqrt{\vartheta R'D'}}{av}x + \sqrt{\vartheta}A(y)\right)\right.
$$
$$
\mathrm{erfc}\left(\frac{\varepsilon\sqrt{R'D'}}{2avR\sqrt{t-xR'/v}}x + \frac{A(y)}{2\sqrt{t-xR/v}} + \sqrt{\vartheta}\sqrt{t-xR'/v}\right)\right] \quad (3.25)
$$

where $A(y) = \sqrt{\frac{R'}{D'}}(y-a)$

Some more notable analytical solutions are developed for a system of parallel fractures

(Sudicky and Frind, 1982; Barker, 1982) which were discussed in Chapter 2. But, it becomes complex to solve a system with random network of fractures. In this thesis, the fracture patterns are generated stochastically and, in such cases, closed form solution cannot be achieved. So radionuclide transport through fractured network is modelled numerically using FEFLOW 6.2.

3.2.4.3.3 Numerical model

To solve the fluid flow and contaminant transport problem in fractured media, firstly the concept of REV needs to be developed. The REV for fractured medium is based on the concept of discrete feature approach as shown in Figure 3.7. When the fractures and the porous media don't have an overlapping continuum, they must be solved on separate scale and coupled through macroscopic interface conditions. This can be done using discrete feature approach. This scenario happens when fractures have large apertures and voids in porous medium is small.
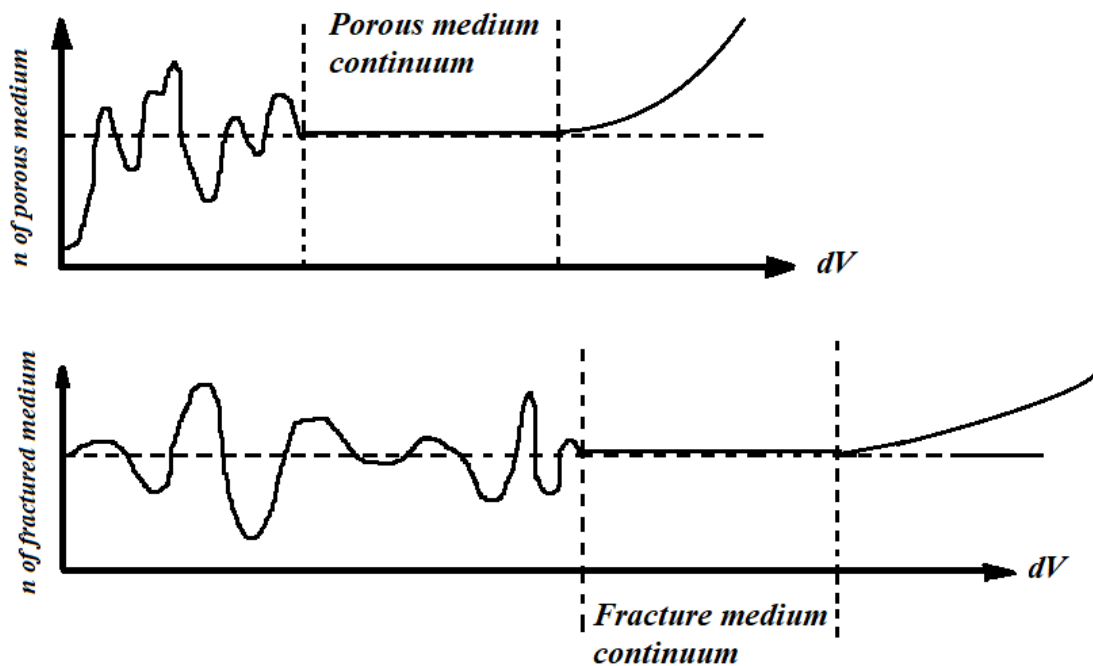
Figure 3.7: REV for fractures without overlapping continuum

So, the fluid flow and contaminant migration through fractures are modelled by introducing a new feature called the 'discrete element' (Diersch, 2014). This feature acts as a link between complex geometries for subsurface and surface systems, porous and fractured media and also incorporates structures in modelling flow and mass transport. In general, it geometrically represents a lower dimension that has notable fluid conductance than the porous medium. For instance, in a two-dimensional (2D) porous medium, fractures are represented by one-dimensional (1D) elements. As the mathematical formulations discussed in section 3.2.4.2.2 are generalized, they are also valid for discrete features just by reducing the dimensions and phases. In a fractured media, there are two systems one is the intact rock matrix and the other is the fractures. Some of the salient features involved in the numerical modelling for fractured medium are given below.

1. **Intact rock matrix**: The flow and transport in the intact rock matrix is same as that of porous medium. So the equations in section 3.2.4.2.2 are valid.

2. **Fractures**: The flow through fractures is modelled as flow between two parallel plates. This flow law is termed as Hagen-Poiseuille law (also known as cubic law). The equation for conductivity is given by

$$K = \frac{r^2 \rho_0 g}{a \mu_0} \delta \qquad (3.26)$$

where r - is the hydraulic radius (m), ρ_0 - density of water (kg/m^3), g - gravity(m/s^2), μ_0 - viscosity (Pa-s), δ - friction factor (=1 mostly). The balance laws for conservation of mass, momentum, energy and entropy remains the same except four additional terms that account for (1) thickness; exchange terms at (2) interface (3) top and (4) bottom boundaries of the system. The mass conservation equation given in

equation (3.8) for porous medium transforms to

$$\frac{\partial}{\partial t}(B_t \varepsilon s \rho) + \nabla \cdot (B_t \varepsilon s \rho v) = B_t \varepsilon s \rho Q + B_t Q^I + Q^T - Q^B \qquad (3.27)$$

where Q^I, Q^T, Q^B corresponds to interfacial, top and bottom exchange terms and B is the aperture / thickness. These new terms account for the interaction between the fracture and porous medium.

The equation for fluid flow and mass transport are given by

$$S\frac{\partial h}{\partial t} - \Delta.(Kf_\mu B_t.(\Delta h + \Phi e)) - Q = 0 \qquad (3.28)$$

$$S\frac{\partial C}{\partial t} + q.\nabla C - \nabla.(B_t \varepsilon D.\nabla C) + \Phi C - Q = 0 \qquad (3.29)$$

Both the equations are similar to the ones for porous medium except the term B.

3. **Interface systems**: Discrete features (i.e, fractures) and the porous medium, the two interacting sub-systems are treated as a monolithic feature, where all components are integrated into the solution domain consisting of the joint porous-medium domain Φ_P and a number of non-overlapping discrete feature domains Φ_F.

$$\Phi = \Phi_p \cup \sum_F \Phi_F \qquad (3.30)$$

They are governed by different balance equations solvable through common state variable $\omega = \omega(x,t)$(where h is for flow, C_k is for concentration and T is for transport). To solve for any quantity in variably saturated flow, variable-density flow, species mass, and heat transport, the global contributions from porous medium and

the corresponding fracture systems are assembled with respect to the state variables as mentioned above.

As the discrete feature elements share the same nodal points as that of the porous medium, the result of the combined process is obtained by exchanging (advective and dispersive) fluxes between the porous medium and discrete features. If K_m and K_f represent the conductivities of the porous medium and discrete feature, at the same node, then, the exchanging flux between the porous medium and discrete feature is affected by its effective conductivity $K = K_m + K_f$. If $K_f \gg K_m$, then the flux will be dominated by the discrete feature property. However, the effect from DFE disappears for $K_F \rightarrow 0$ and the exchanging flux is determined by the porous medium property alone. The procedure to assemble global matrix for flow and transport is determined by adding the contribution from fractures and porous media. The remaining steps followed to discretize the FE mesh and obtain the approximate solution to the problem remains the same as discussed in the previous section.

Radionuclide transport modelling in geosphere gives us an understanding on the movement of radionuclide in the medium extending over spatial and temporal scales, their concentration front and also the time of arrival of maximum concentration. Further the radiological impact is estimated using a radiological model.

3.2.5 Radiological model

The radiological hazard due to radioactive waste will reduce with time because of radioactive decay. However, the time scales over which the hazard remains significant can extend to over thousands of years, depending on the radionuclides involved. The expo-

sure pathways leading to radionuclide transport to the biosphere can be modelled through drinking water pathway or marine pathway or human intrusion pathway. The quantitative measure of radiological hazard, that is, the consequence of radionuclide migration to human habitat is estimated by radiation dose. This quantity is a function of the pathway of exposure, ingestion of radiation etc. In the thesis, the radiological model is used to evaluate radiation dose to a member of the critical group due to consumption of ground water for drinking. It is mathematically expressed as

$$RD = c_r \times d_{in} \times do_{in} \tag{3.31}$$

where RD - is the radiation dose (mSv/y); c_r - concentration in ground water (Bq/l); d_{in} - drinking water intake (l/day); do_{in} - ingestion dose coefficient (Sv/Bq). Further, the risk to a member of the critical group due to the waste disposal practice is also estimated. The doses and risks to members of the public for different radionuclides are computed from the radiological model. These values are estimated in Chapter 4, 5 and 6 for different geological environment and compared with the threshold dose or risk values used as design criteria.

3.2.6 Uncertainty analysis

As mentioned earlier, an integrated safety assessment model takes into account the effect of uncertainties. Failure to acknowledge and represent uncertainty can result in serious criticism of performance assessment. The probabilistic analysis should include computation of risk measures, sensitivity studies besides uncertainty analysis to develop confidence in analysis results. The main sources of uncertainties and variance reduction

techniques employed to handle these uncertainties are discussed elaborately in sections 3.3 to 3.7.

3.2.7 Safety indicator

The overall outcome of performance (or safety) assessment models is primarily focussed on establishing safety indicators which provide a prior indication of radionuclide contamination in the environment due to any release of radionuclide from NSDFs. They are mainly:

1. Concentration of radionuclide and their trends in air, surface water, groundwater, soil and vegetation forms an important indicator to monitor NSDFs.

2. Dose and risk to the individual and to the critical group form the primary indicators which play an important role in the safety assessment.

Also as mentioned in Section 3.2.6, the effect of uncertainty in input parameters of the system, the probability that the quantities exceed the design threshold can be quantified. The probability of exceedence (or failure) is one of the most important safety indicators which quantifies the effect of uncertainties in the safety assessment model for NSDFs. By implementing sensitivity analysis, the critical parameters influencing the performance of the system can be estimated. In the thesis, all the above safety indicators are estimated.

3.3 Sources of uncertainties

In the design of geo-environmental systems, uncertainties are quite pervasive and unavoidable from various sources that include properties of geologic environment (geologi-

cal and transport properties), boundary conditions of the system, design life of the struc-

tures and climatic factors such as temperature and rainfall. So, it becomes imperative

to consider the main sources of uncertainty that influence the system response and also

quantify their effect to attain a level of safety on the performance of the system. The un-

certainties are broadly branched into aleatory and epistemic (Baecher and Christian, 2003,

Der Kiureghian and Ditlevsen, 2009). The uncertainties due to inherent randomness in

some of the properties of the system is categorized as aleatory, while, the uncertainties

due to lack of sufficient information (knowledge or data) is characterized as epistemic.

They are categorized further and presented in Figure 3.8.
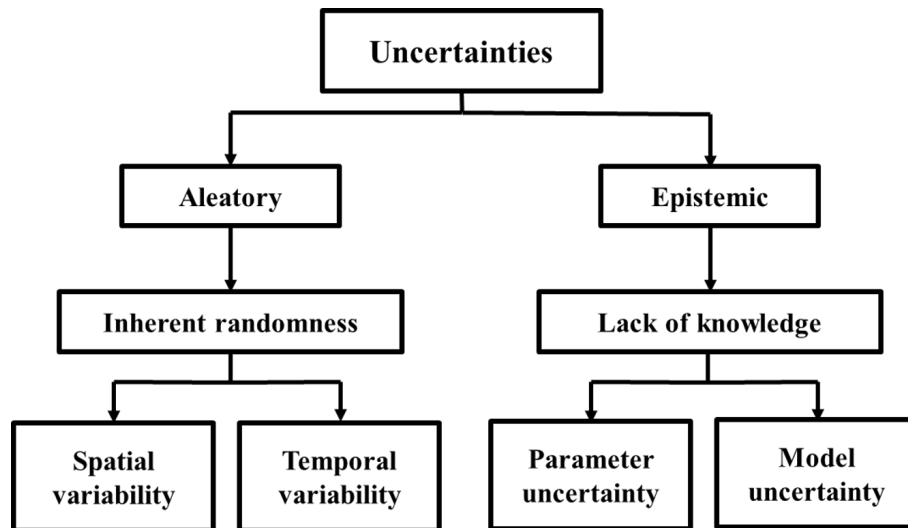
Figure 3.8: Types of uncertainties

The intrinsic nature of aleatory uncertainty makes it irreducible. They are further di-

vided into spatial and temporal variabilities (refer Figure 3.8). The variation in soil prop-

erties along longitudinal and lateral directions can be characterized as spatially variability

and the groundwater and soil contamination due to failure of containment system falls

under temporal variability. On the other hand, epistemic uncertainty occurs due to lack

of data, or inability to model the underlying mathematical phenomenon. The epistemic

uncertainties are classified further into parameter and model uncertainties. Parameter uncertainty emerges due to inaccuracy in field or laboratory measurements and limited sampling. Model uncertainty occurs due to inability of a capture the actual phenomenon involved in the system and represent it as a mathematical model. There is a possibility to reduce them by gathering more data or by refining the models.

In modelling the radiological safety assessment models also, the significance of uncertainties has been long recognised (Hoffman and Miller, 1983; Helton 1993; Gallegos and Bonano, 1993; Nair and Krishnamoorthy, 1999; Dutta and Khuswaha, 2011). These multifaceted models are a combination of engineered systems and natural geological medium where many uncertainties arise in the form of material properties, construction procedures involved in barriers, design life of the barriers, fluctuations of groundwater table of the aquifer, boundary conditions of the model, transport properties of the medium, inherent variability in the soil/ rock properties and influence of climatic factors like rainfall and temperature. This thesis focusses on addressing the effects of some of the important aleatory and epistemic uncertainties involved in these models. They include: aleatory uncertainty due to spatial variability in soils and epistemic uncertainties in geological properties of the medium (lie hydraulic conductivity, porosity etc), transport properties of the medium (advection, diffusion and dispersion components of transport) and also geochemical properties of the radionuclide (distribution coefficient i.e, adsorption component). Additionally the stochastic nature of fractures in fractured network belonging to sedimentary rock genesis is also addressed. All these uncertainties are treated in the performance assessment models and their effect has been quantified.

3.4 Random field modelling

The properties of natural materials like soils show a complex paradigm of variation in space and time (Vanmarcke (1977)). To model the inherent randomness in the systems extending over space, random field theory has emerged. Let Ω be a set R^n describing the system geometry such that $x \in \Omega$, then $H(x, \theta)$ is defined as random field, which is nothing but a collection of random variables indexed by the parameter x. From Figure 3.9 we can observe that, for a given x_0, $H(x_0, \theta)$ is a random variable. On the other hand, for a given outcome θ_0, $H(x, \theta_0)$ is a realization of the field.
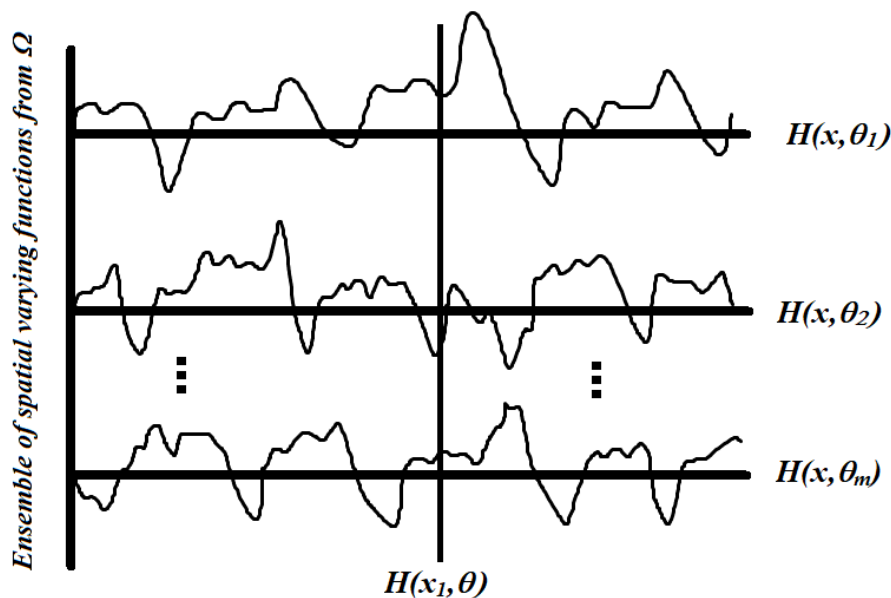
Figure 3.9: Realizations of a random field

The statistical descriptors of a random field are (i) mean (ii) standard deviation and (iii) auto correlation function. It can be noted that, in addition to mean and standard deviation, a measure of distance over which the values of the soil parameter exhibit strong correlation is also considered to describe random field. The factor that, the values at adjacent locations are more related than those separated by some distance is taken into

account (Vanmarcke 1983). To estimate the correlation coefficient between two arbitrary points, auto correlation function (ACF) needs to be estimated. It is given by the equation

$$\rho_{(dh)} = \frac{C[Z(X_i), Z(X_{i+dh})]}{\sigma_z^2} = \frac{1}{\sigma_z^2} E\left\{[Z(X_i) - \mu_z][Z(X_{i+dh}) - \mu_z]\right\} \tag{3.32}$$

where X is the vector which represents the location. It is given by $X = (x)$ in the case of a one-dimensional random field $X = (x,y)$ in the case of a two-dimensional (2D) random field and $X = (x,y,z)$ in the case of a three-dimensional (3D) random field. On the other hand, $Z(X_i)$ is the value of the property Z at location X_i, $Z(X_{i+dh})$ is the value of the property Z at location, X_{i+dh}, dh is the separation distance between the data pairs, $E[]$ is the expected value, C is the covariance and μ_Z and σ_Z^2 are respectively the mean and standard deviation of the property Z. The ACF is often used to determine the distance over which a property exhibits strong correlation. Further, the autocorrelation distance (l) can be evaluated. The autocorrelation distance (l) is defined as the distance required for the autocorrelation function to decay from 1 to e^{-1} (0.3679). On the other hand, the scale of fluctuation is defined as the area under the ACF (Fenton, 1999). There are several types of autocorrelation functions which include white noise, linear, exponential, squared exponential, and power autocorrelation functions (Baecher and Christian, 2003). To demonstrate the effect of auto-correlation length, hydraulic conductivity in aquifer system is identified as a spatially varying property and modelled as a random field. From the Figure 3.10 (i), it can be noticed that for a auto-correlation length of 0.5 m, the random field is rough. This is because, as $l \to 0$, all points in the field become uncorrelated with one another and the field becomes infinitely rough. This is physically unrealisable, however, as the auto-correlation length increases, the field becomes smoother (Griffiths

and Fenton, 2006). As the auto-correlation length increases they become smoother (Figure 3.10(ii)). Here, as $l \to \infty$, all points in the field become completely correlated (for finite-scale correlation functions). If the field is stationary, this means that the random field becomes completely uniform (i.e, each realization is composed of a single random variable (traditional soil model).

(i)

(ii)
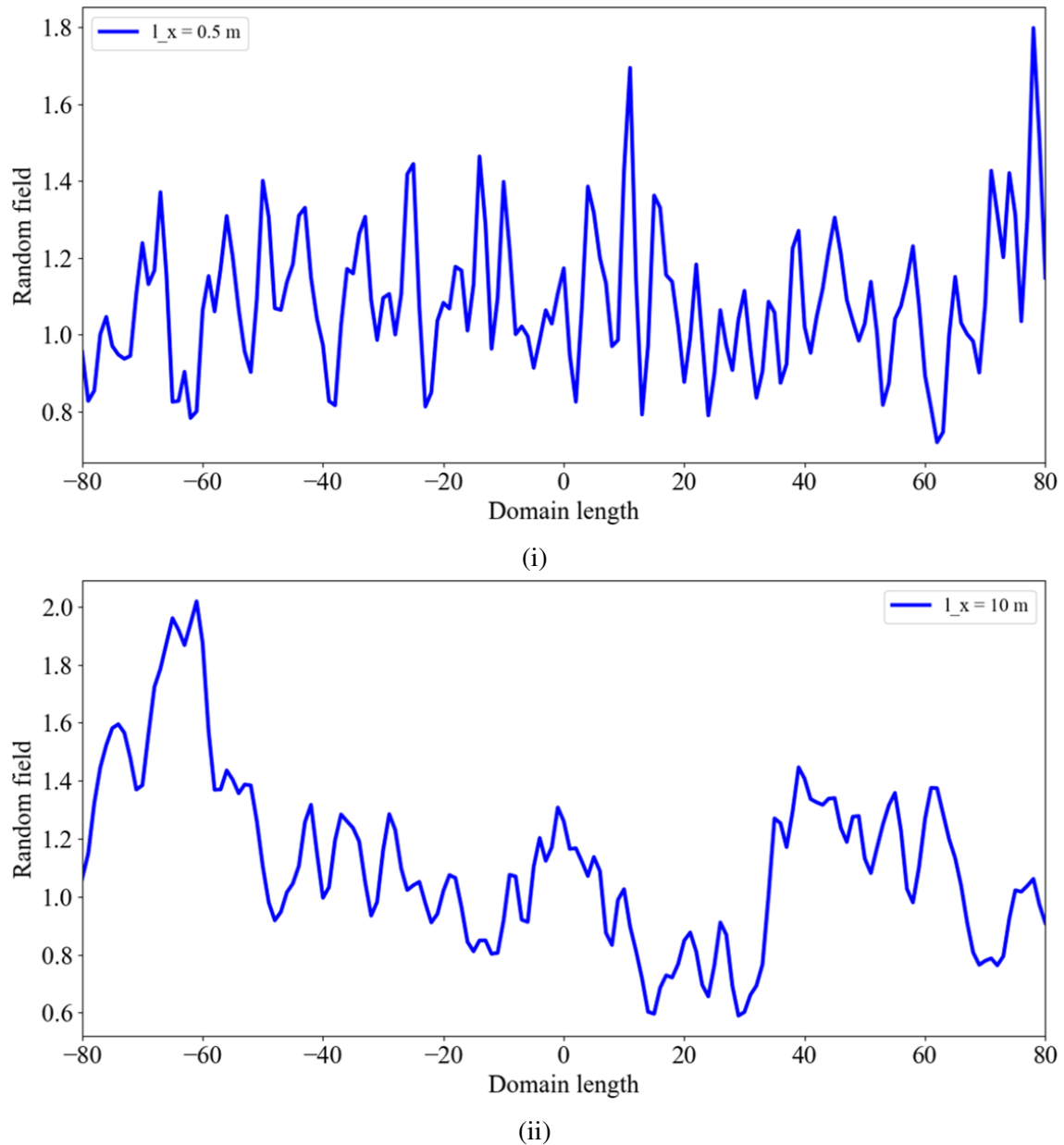
Figure 3.10: Realization of random field (i) Rough field (ii) Smooth field

3.4.1 Random field discretization

The random field Z (represented as an infinite set of random variables) has to be discretized in order to generate a finite set of random variables that can be allocated to the discrete points. If the finite element / finite difference method is the method used in the mechanical analysis, it is convenient to evaluate the random field values in the same way as the finite element / finite difference model (i.e. at the nodes of the deterministic mesh or at the element mid points of this deterministic mesh). The discretization methods can be divided into three main groups (Sudret and Der Kiureghian, 2000). They are mainly categorized into three groups (Al-Bittar, 2012). They are

1. Point discretization methods: In this category, the random variables χ_j are selected values of Z at some given points X_j. The methods under this category include mid point method, shape function method and integral point method.

2. Average discretization methods: In this category, the random field in each element of the finite element / finite difference mesh is approximated by a constant computed as the average of the original field over that element. The methods under this category include spatial average method and weighted residual method.

3. Series expansion methods: In this category the random field is approximated by an expansion that involves deterministic and stochastic functions. The realization of random field $H(x, \theta_0)$ over a complete set of deterministic functions are expanded and discretized further by truncating the series into finite number of terms. The methods under this category include Karhunen-Loeve (K-L) series expansion method, Orthogonal series expansion (OSE) method and Expansion optimal linear

estimation (EOLE) method.

The first two categories of methods lack in achieving an optimal solution as the number of random variables needed to discretize the random fields using these methods are mesh dependent. Conversely, the series expansion methods provide the optimal number of random variables needed to accurately discretize the random field. So, in this thesis, K-L expansion method is used for the discretization of random field. This method is explained in the following section.

3.4.1.1 Karhunen-Loeve series expansion

This method is based on spectral decomposition of auto covariance function $C_{hh}(x_1, x_2)) = \sigma(x)\sigma(x^1)\rho(x_1, x_2)$. The deterministic function over which the random field $H(x, \theta_0)$ is expanded is defined by an eigen value problem.

$$\sigma^2 \int_{-a}^{a} \exp\left[-\frac{|x_1 - x_2|}{l_x}\right] \phi(x_1)dx_1 = \lambda \phi(x_2) \tag{3.33}$$

The covariance kernel is bounded, symmetric and positive definite and due to this property the eigenfunctions are orthogonal and form a complete set. Any realization of $H(.,.)$ can be expanded over this basis which is given by

$$H(x, \theta) = \mu_x + \sum_{n=1}^{\infty} \sqrt{\lambda_n}\xi_n(\theta)\phi_n(x) \tag{3.34}$$

where $\xi_n(\theta)$ denotes the coordinates of realization of random field corresponding to the deterministic function $\phi_n(x)$. Further, ξ_n becomes a numerable set of random variables by taking into account all the possible realizations of the field. In the process of solving the the covariance matrix the expectation of random variables is given by $E[\xi_i, \xi_j] =$

δ_{ij}, where δ_{ij} is Kronecker delta function. This implies that the random variables are orthonormal. By truncating the series given in equation (3.34) upto mth term gives the approximated random field as

$$H(x,\theta) = \mu_x + \sum_{n=1}^{m} \sqrt{\lambda_n} \xi_n(\theta) \phi_n(x) \tag{3.35}$$

Equation (3.35) can be solved analytically only for few auto covariance functions and domain geometries. In this method, estimation of the random variables in the series becomes easier due to the orthonormality of eigen function, the mean square error of covariance function can be minimized making it simpler to achieve optimal solution, the eigen values are not gathered around non-zero values which makes it easier for truncation of the series (Sudret and Der Kiureghian, 2000). Close form solutions are developed for triangular and exponential covariance functions for one-dimensional homogeneous fields for a domain $[-a,a]$ (Spanos and Ghanem, 1989; Ghanem and Spanos, 1991). One of these solutions for a one-dimensional random field with an exponential covariance $C(x_1,x_2)$ kernel is briefly presented below. The integral equation to solve the for eigen values and eigen functions is given by

$$\int_{-a}^{a} e^{-b|x_1-x_2|} f(x_2) dx_2 = \lambda f(x_1) \tag{3.36}$$

$$\int_{-a}^{x} e^{-b|x_1-x_2|} f(x_2) dx_2 + \int_{x}^{a} e^{-b|x_1-x_2|} f(x_2) dx_2 = \lambda f(x_1) \tag{3.37}$$

By double differentiating equation (3.37) with respect to x_1, it becomes

$$\lambda f''(x) = (-2c + c^2\lambda) f(x) \tag{3.38}$$

where c is the reciprocal of auto-correlation length. By introducing a new variable, $\omega = \frac{2c - c^2\lambda}{\lambda}$, the above equation becomes,

$$f''(x) + \omega^2 f(x) = 0 \quad -a \leq x \leq a \tag{3.39}$$

By substituting boundary conditions $cf(a) + f'(a) = 0$ and $cf(-a) - f(a) = 0$ in ordinary differential equation given in equation (3.39), the following transcendental equations are obtained given by

$$a_1(c - \omega tan(\omega a) + a_2(\omega + ctan(\omega a)) = 0 \tag{3.40}$$

$$a_1(c - \omega tan(\omega a) - a_2(\omega + ctan(\omega a)) = 0 \tag{3.41}$$

By assigning determinant of homogeneous system of equations (3.40) and (3.41) to zero, transcendental equations are obtained and they are given as

$$c - \omega_i tan(\omega_i a_x) = 0 \qquad \text{for i odd}$$
$$\omega_i + ctan(\omega_i a_x) = 0 \qquad \text{for i even} \tag{3.42}$$

The transcendental equations (3.42) are solved for eigen values and eigen functions. They are presented below.

Eigen value

$$\lambda_i = \frac{2c\sigma^2}{\omega_i^2 + c^2} \tag{3.43}$$

Eigen vector

$$\phi_i = \frac{cos(\omega_i x)}{\sqrt{a_x + \frac{sin(2\omega_i a_x)}{2\omega_i}}} \qquad \text{for i odd}$$

$$\phi_i = \frac{sin(\omega_i x)}{\sqrt{a_x - \frac{sin(2\omega_i a_x)}{2\omega_i}}} \qquad \text{for i even}$$

(3.44)

Equations (3.43) and (3.44) are the eigen values and eigen functions respectively. The quality of the representation calculated from equation (3.35) is decided based on the truncation order. It is necessary to define analytically the accuracy of such approximation. The discretization is assumed to be accurate if, for a given truncation order, the error with reference to the relevant properties of the random process is less than a proper target accuracy. In the case of a gaussian random field, the error estimate of the K-L expansion with m terms can be calculated as follows (Sudret and Berveiller, 2008).

$$\varepsilon = 1 - \frac{\sum\limits_{i=1}^{m} \sqrt{\lambda_i}\phi_i(x)\xi_i(\theta)}{\sigma^2}$$

(3.45)

To demonstrate the functionality of K-L expansion for an exponential covariance function the the following example is considered. A one-dimensional horizontal Gaussian random field with auto-correlation length of 1 m, is generated in the interval [-0.5 m, 0.5 m] using the above set of equations. The covariance function is presented in Figure 3.11. The roots of the transcendental equations are evaluated and presented in the Figure 3.12. The odd and even roots are substituted in equations (3.43) and (3.44). The eigen values and eigen functions are estimated and plotted in Figures 3.13 and 3.14. By substituting the eigen values and eigen functions in equation (3.35), the error versus number of terms to be truncated is determined.
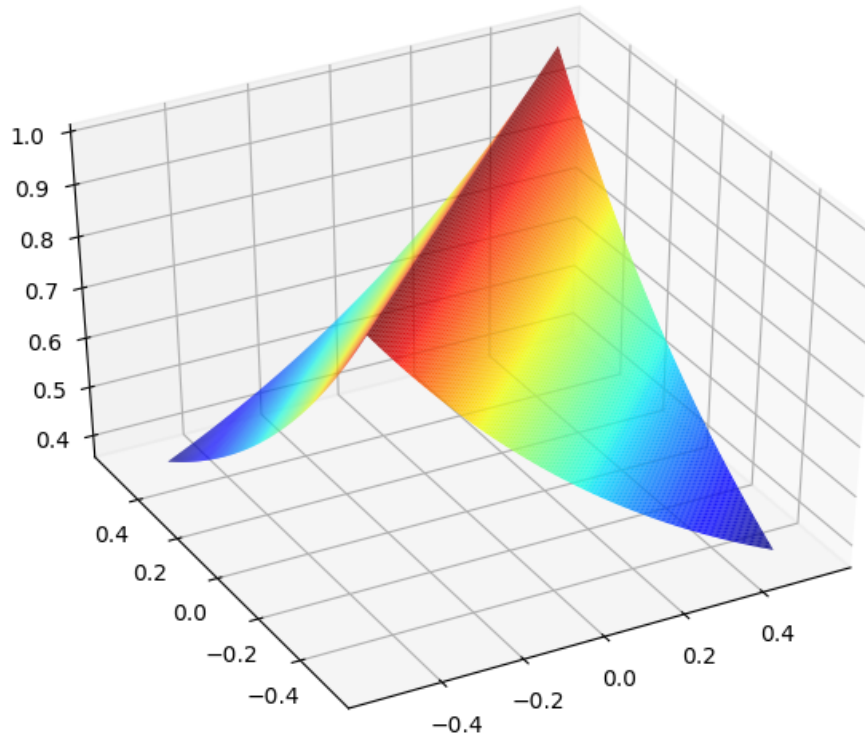
Figure 3.11: Exponential covariance function
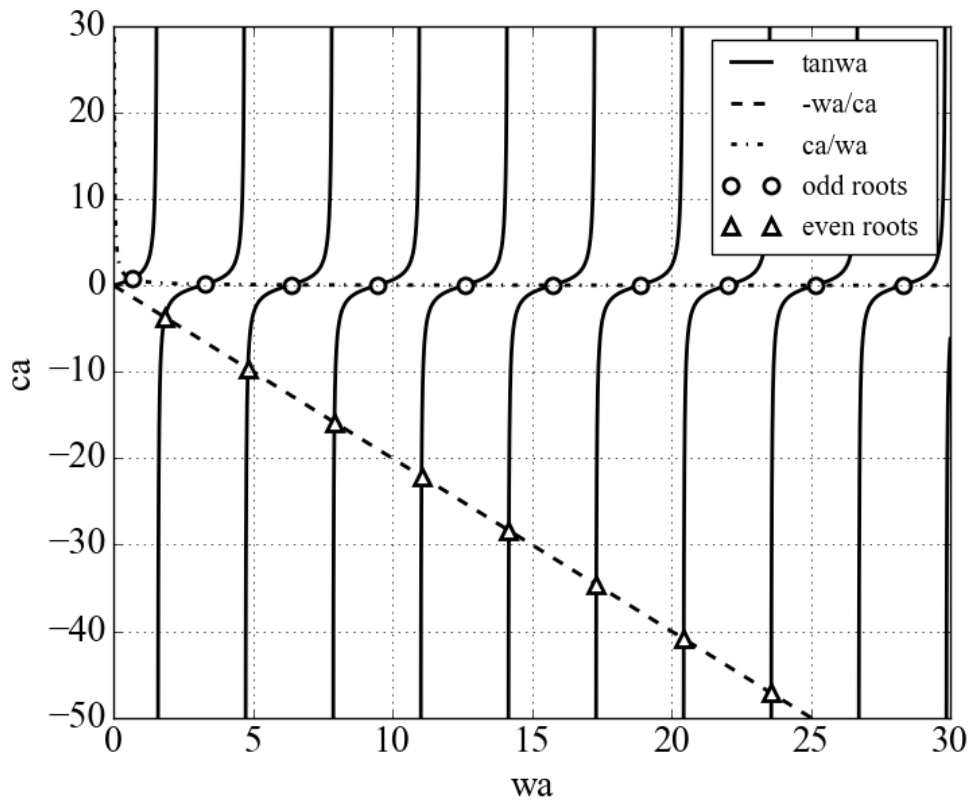
Figure 3.12: Roots of the transcendental equations
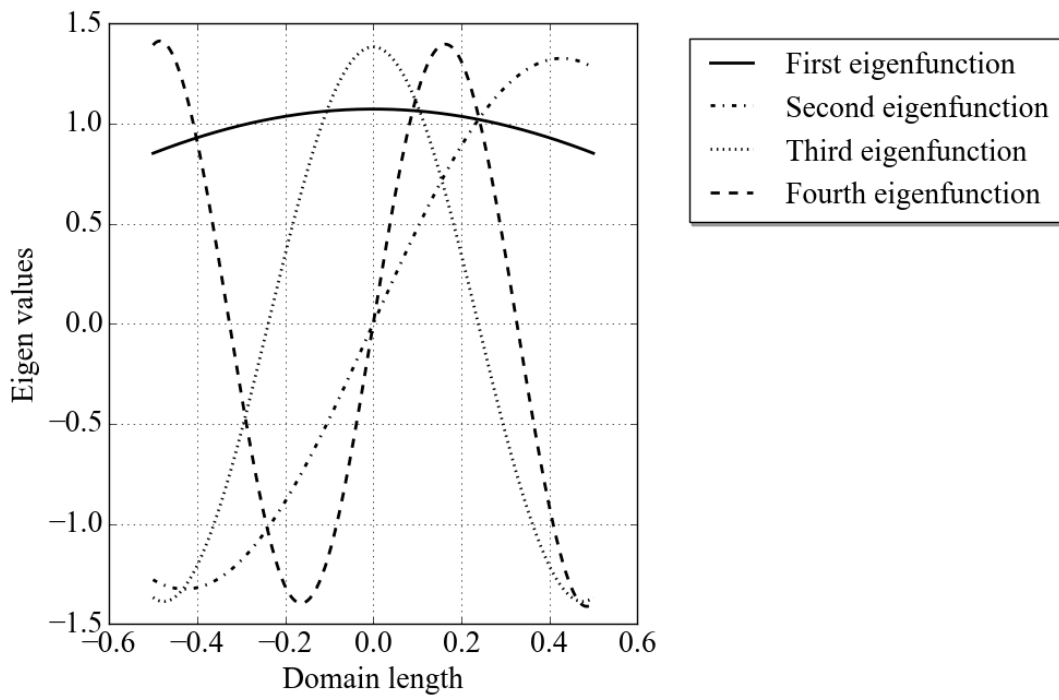
Figure 3.13: Eigen functions ϕ
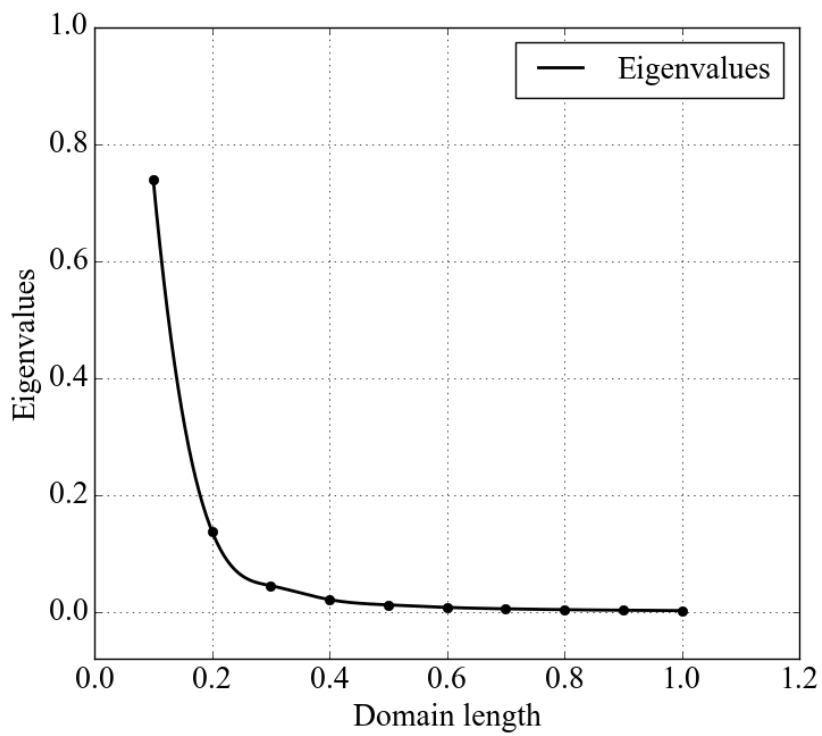
Figure 3.14: Eigen values λ

132
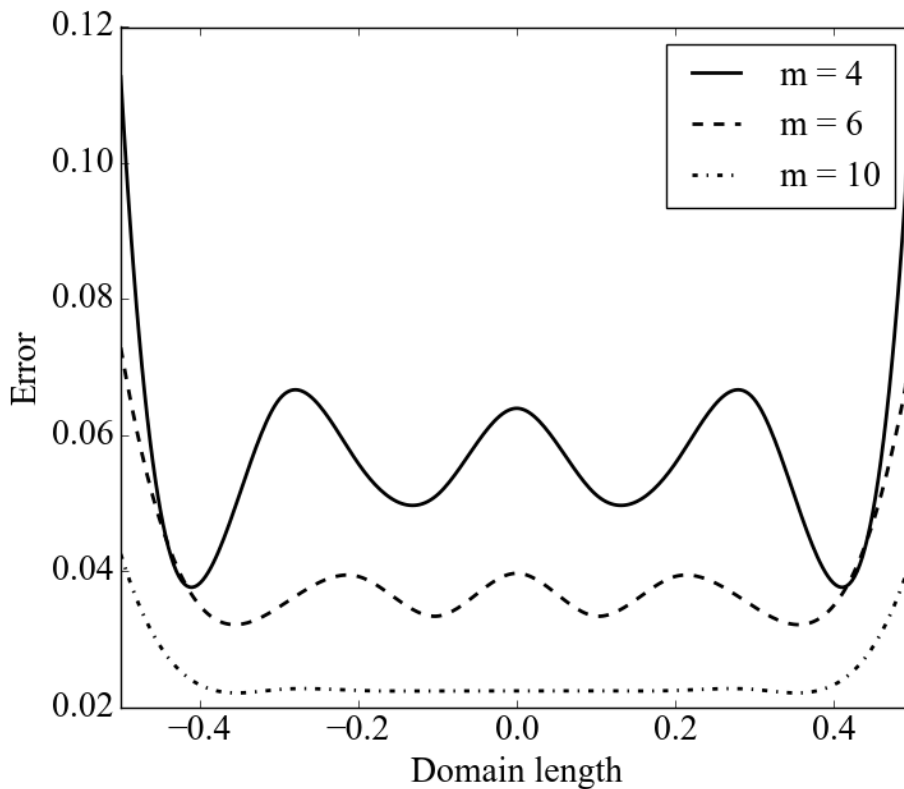
Figure 3.15: Error estimate versus different orders of expansion (exponential function)

From Figure 3.15, it can be noticed that when the number of terms increased from four to ten, the error estimate reduced from 0.11 to 0.04. The ease of computing all the components of random field using K-Lexpansion is presented in this example and the same equations are used in the present thesis.

3.5 Meta-modelling techniques

The design of complex geo-environmental systems is a daunting task as they involve description of the underlying physical and chemical processes in the form of mathematical equations and most importantly, the randomness that entails the input parameters in the form of computationally intensive mathematical / numerical models. Meta-modelling techniques are introduced to handle such systems. The meta-models approximate the

original model response with a cheaper surrogate version. The advantage of using a surrogate modelling technique is that, the uncertainty quantification methods that need a large number of simulations of the model, such as Monte Carlo methods, can be employed. However, the construction of an accurate surrogate model can be difficult. Some of the interesting meta-modelling techniques available in the literature include, the Response Surface Methodology (RSM) (Box et. al., 1978; Montgomery and Myers, 1995) which is one of the popular methods for constructing simple approximation of complex numerical model using polynomial regression, kriging method (Sacks et. al., 1989; Booker et. al., 1999) which is based on interpolation and finally the Polynomial Chaos Expansion (PCE) (Spanos and Ghanem, 1989; Isukapalli et. al., 1998; Xiu and Karniadakis, 2002; Sudret and Berveiller, 2008; Huang et. al., 2009; Blatman and Sudret, 2010), which in essence provides a rigorous approximation of complex numerical models with decent computation effort. In the next section, the process of employing RSM is briefly discussed, followed by a detailed presentation of the PCE methodology which is the meta modelling technique (also called stochastic response surface method) applied in this thesis.

3.5.1 Response surface method

Response surface methodology (RSM) is a collection of statistical and mathematical techniques used for developing, improving and optimizing process (Box and Draper, 1987; Myers et. al., 2009). In this method, a functional relationship is established between the response of interest and its associated input variables. The functional relationship is developed based on regression analysis. The choice of the design of experiments (selection of points where the response has to be evaluated) affects the accuracy of design and computational cost of constructing a response surface. Hence, different methodologies are

developed for an optimal design. The formulation of response surface equation hinges on the interactions of input variables for a set of combinations (design of experiments). The system response $R(x)$ can be approximated by an explicit function of the random variables. The most popular form of this function is a second order polynomial model, which can be expressed as:

$$R(x) = a_0 + \sum_{i=1}^{m} a_i x_i + \sum_{i=1}^{m} b_i x_i^2 \tag{3.46}$$

where x_i are the random variables, m is the number of random variables; a_i, b_i are coefficients obtained by the least squares method. In this method, the sum of the squares between the predicted values $R_{RSM}(x^{(i)})$ and model values $R = \left\{ R(x^{(1)}), ..., R(x^{(p)}) \right\}$ (where p is the number of sample points) is minimized. It should be emphasized that, second order polynomial used in the RSM method cannot provide good approximation for highly non-linear models. In such cases, higher-order polynomial response surfaces have to be generated to approximate the behaviour, nonetheless, instabilities may arise (Barton 1992). Additionally, they require large number of sample points and the computational time increases enormously leading to an ineffective result from RSM.

3.5.2 Stochastic Response surface method

The stochastic response surface method (SRSM), an extension of the traditional response surface method has been successively applied in many areas of research (Li et. al., 2011). Isukapalli (Isukapalli 1999) introduced SRSM for uncertainty propagation analysis in environmental and biological systems. The basic concept of uncertainty propagation in this method is to represent the model response as a function of the input parameters (in standard normal space) using polynomial chaos expansion. The three steps followed in SRSM

are (1) representation of inputs of the model (2) representation of output of the model and (3) estimating the coefficients of output polynomial. Further the statistical properties of the output are estimated. SRSM replaces the complex numerical model with an approximated less-expensive surrogate model. Let us consider a model $q_r = F(p_r)$, where p_r is the vector of random inputs and q_r is the vector of outputs / output metrics. The output vector q_r is represented as a function of $p_r = h(\delta)$(random variables (rvs) transformed to independent identically distributed (iids) sequence of standard normal random variables (srvs),δ). The functional representation of the output is $q_r = f(\delta, a)$, where 'a_r' is the parameter vector. Based on the complexity of the model, the parameters / unknown coefficients ('a_r') are estimated in various methods (Galerkin projection method, Monte Carlo method, regression methods etc). Probabilistic collocation method (PCM) approximates the unknown output vector by a set of random variables (Tatang, 1995; Webster et. al., 1996; Huang and Kou, 2007). This method is conditioned on an assumption that the estimates of outputs are exact at a set of collocation points, thus making the residuals at the points to zero. Many researchers (Huang et. al, 2007; Mao et. al., 2012; Jiang et. al., 2014) used probabilistic collocation method to model the systems and characteristize the response of these systems. Sudret (2008) and Mao et. al., (2012) highlighted the method of choosing the collocation points by the invertibility of information matrix. This is done by arranging the collocation points into a list with the points closer to the origin placed on the top. It reduces the computational effort further by reducing the number of collocation points needed to build the polynomial. Datta and Kushwaha (Datta and Kushwaha, 2011) carried out uncertainty modelling for a one-dimensional contaminant transport problem through groundwater and the quantified the uncertainties in input parameters using SRSM by Galerkin projection method. The polynomial chaos theory assigns the type of poly-

nomial associated with the distribution (Hermite polynomials for Gaussian distribution, Legendre polynomials for uniform distribution, Jacobi polynomials for beta distribution and Laguerre polynomials for Gamma distribution) (Wiener, 1938; Isukapalli, 1999; Karniadakis, 2002; Ghanem and Spanos, 2003). All the input uncertainties are transformed to iids in standard normal space and the output vector is represented as an expansion of truncated set of Hermite polynomials with unknown coefficients.

The iid sequence of standard random variables are represented as $\{\delta\}_{i=1}^{n} n$ where nn is the number of independent inputs, and each δ_i has zero mean and unit variance. The expressions of the one-dimensional Hermite polynomials are given in Appendix A. The output vector represented as a multidimensional Hermite polynomials is given by the equation

$$F(\delta) = a_0 + \sum_{i_1=1}^{nn} a_{i_1} \Gamma_1 \delta_{i_1} + \sum_{i_1=1}^{nn} \sum_{i_2=1}^{i_1} a_{i_1 i_2} \Gamma_2(\delta_{i_1} \delta_{i_2}) + \sum_{i_1=1}^{nn} \sum_{i_2=1}^{i_1} \sum_{i_3=1}^{i_2} a_{i_1 i_2 i_3} \Gamma_3(\delta_{i_1} \delta_{i_2} \delta_{i_3}) \cdots$$

(3.47)

where F - the output vector , $a_{i_1 \cdots i_{nn}}$- coefficients to be evaluated, Γ- individual polynomial of the basis, $\delta = (\delta_{i_1}, \delta_{i_2} \cdots, \delta_{i_{nn}})$ - the vector of independent standard normal random variables and $\Gamma_p(\delta_{i_1}, \delta_{i_2} \cdots, \delta_{i_{nn}})$- multi-dimensional hermite polynomial of degree p given by

$$\Gamma_p(\delta_{i_1}, \delta_{i_2} \cdots, \delta_{i_{nn}}) = (-1)^p e^{\frac{1}{2}\delta^T \delta} \frac{\partial^p}{\partial \delta_{i_1} \partial \delta_{i_2} \cdots \partial \delta_{i_p}} e^{-\frac{1}{2}\delta^T \delta}$$

(3.48)

The number of unknown coefficients for the polynomial of order p is given by

$$P_n = \frac{(nn+p)!}{nn! p!}$$

(3.49)

Based on the order of PCE, the collocation points are chosen at the regions of highest probability, thereby reducing the number of evaluations. In this method, the deterministic response evaluation and stochastic analysis are de-coupled (Huang et. al., 2009; Liu, 2013; Jiang et. al., 2014). The coefficients are determined by regression method (Isukapalli 1999). Based on the regression method, the sets of collocation points 'N'' are chosen and the outputs of the model at these points are estimated $Y = [Y_1, Y_2, \cdots, Y_N]^T$ by the deterministic evaluations. A system of linear equations are constructed as

$$XA_v = Y \tag{3.50}$$

where A_v is the vector of unknown coefficients and X is the matrix of dimension $N \times P$ consisting of Hermite polynomial at the collocation points (Hermite polynomial information matrix)and given by

$$X = \begin{bmatrix} \Gamma_0(\delta_1) & \Gamma_1(\delta_1) & \cdots & \Gamma_{P-1}(\delta_1) \\ \Gamma_0(\delta_2) & \Gamma_1(\delta_2) & \cdots & \Gamma_{P-1}(\delta_2) \\ \vdots & \vdots & \ddots & \vdots \\ \Gamma_0(\delta_N) & \Gamma_1(\delta_N) & \cdots & \Gamma_{P-1}(\delta_N) \end{bmatrix} \tag{3.51}$$

The unknown coefficients are determined by solving the equation (3.50). Further, the regression based SRSM can be represented as $X^T X A = X^T Y$ and finally the coefficient vector is given by single value decomposition as $A = (X^T X)^{-1} X^T Y$. Once the unknown coefficients in the Hermite PCE are estimated, the response can be represented as a function of input random variables by an analytical PCE. The statistical properties of the output response which include probability density functions (pdf), various order statistical

moments, and correlations between an output and an input, or between two outputs can be evaluated by post processing the results.

3.5.2.1 Determination of collocation points

The number of collocation points depends on the order of polynomial and the number of uncertain inputs. The collocation points are placed at the roots of the next higher order Hermite polynomials (Tatang, 1995; Webster et. al., 1996). For example, for a second-order expansion, the roots of the third-order Hermite polynomial are 0 and $\pm\sqrt{3}$. This way of selecting collocation points would capture points from regions of high probability (Tatang et. al., 1997) resulting in less function evaluation with high accuracy. As the order of PCE and number of inputs increases, the number of collocation points, $'N'$ increases. For an odd order of the polynomial the number of collocation points are increased since origin is not included (Mao et al., 2012). The total number of collocation points is given by the combinations of these roots. The number of collocation points of PCE of order p with nn uncertain inputs is given as

$$N = (p+1)^{nn} \tag{3.52}$$

Equation (3.52) generates a system of linear equations where number of equations N is greater than the number p of unknowns. Suppose, a second order polynomial with five uncertain inputs is considered, it gives $(2+1)^5 = 243$ collocation points.

3.5.2.2 Validation of PCE

The order of PCE decides the quality of output approximation (Mao et. al., 2012; Ahmed and Soubra 2012). The goodness of fit of a model is determined by its coefficient of

determination R^2 (to obtain an optimal order of PCE). When $R^2 = 1$, it indicates a perfect fit of the true model response, whereas, $R^2 = 0$ indicates a non linear relationship between the true model Y and the PCE model Y_{app}. The coefficient of determination is estimated as

$$R^2 = 1 - \frac{\frac{1}{N} \sum\limits_{i=1}^{n} [Y(\delta^{(i)}) - Y_{app}(\delta^{(i)})]^2}{var(Y)} \tag{3.53}$$

where N is the number of collocation points used to estimate the PCE coefficients. The order of the PCE is successively increased until a sufficiently large value of R^2 is obtained. Further, the convergence property of the PCE order is satisfied when the PCE coefficient corresponding to a given multivariate polynomial tends to a constant value when the PCE order increases.

3.6 Methods of reliability analysis

In estimating the performance of any structural system, it is imperative to consider various uncertainties involved in the process and quantify their effect. Reliability is defined as the probabilistic measure of the assurance achieved on the performance of a system for a specified period of time under specified conditions and it is expressed as "reliability index (β)". The probabilistic measure of its complementary event is called the probability of failure denoted by P_f. The main purpose of reliability analysis is to evaluate P_f or β which gauges the adequacy of the system over its lifetime. A typical civil engineering problem can be formulated primarily as a problem of load (demand) versus resistance (supply). The condition for a safe system is to ensure that there is enough resistance in the system to withstand the maximum load applied in its lifespan. Let U and V denote the load and resistance respectively of a system. The effect of uncertainty is taken into

account by representing U and V as random variables. In mathematical terms, the event that represents a reliable system is (V > U) and thus the reliability is given as P(V > U). In other words, probability of failure is,

$$P_f = P(V < U) = \sum_{\forall u} P(V < U | U = u) P(U = u) \qquad (3.54)$$

The continuous random variables U and V are described by their probability distribution functions $P_U(u)$ and $P_V(v)$ and their density functions are given by $p_U(u)$ and $p_V(v)$ respectively. Assuming that the random variables are statistically independent, the probability of failure is given by the equation

$$P_f = \int_{-\infty}^{\infty} P_V(u) p_U(u) du \qquad (3.55)$$
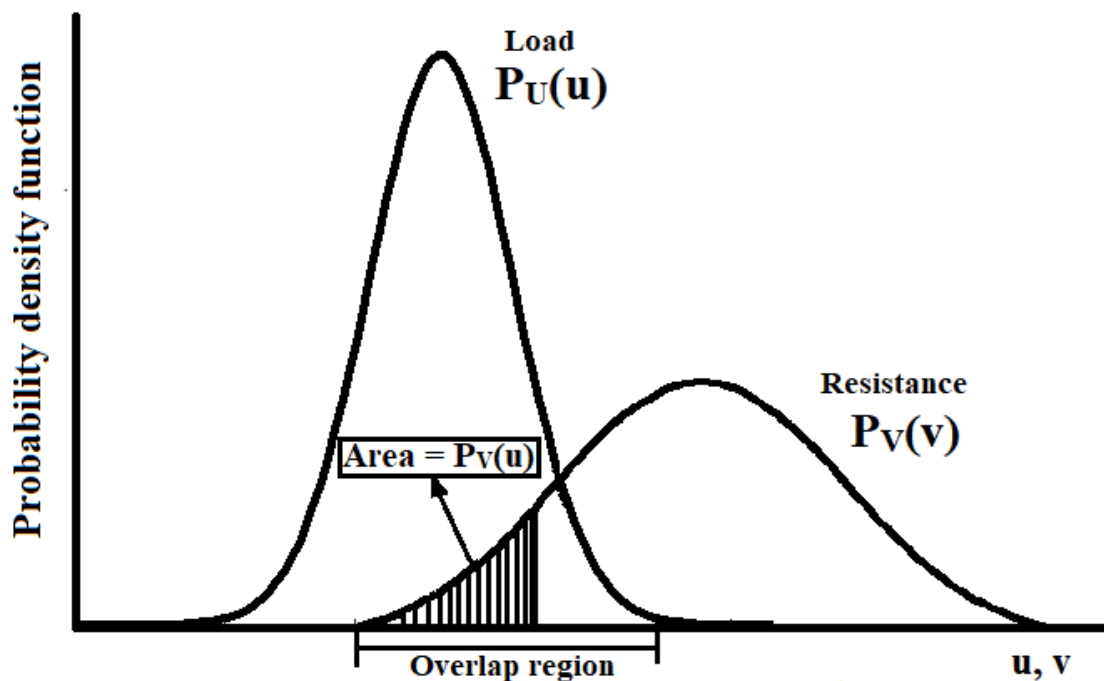
Figure 3.16: Probability density functions of random variables load and resistance

141

The probability density functions, their overlap region and the P_f are shown in Figure 3.16. With this it is evident that, the form of random variables, the extent of dispersion and their descriptors (i.e, their moments) are very important in estimating the region of failure. These random variables are seldom independent and in such cases there exists a correlation between them described by correlation coefficient. For such cases the probability of failure is estimated by joint probability density functions given by the equation

$$P_f = \int\limits_{-\infty}^{\infty} \left[\int\limits_{-\infty}^{u} p_{uv}(u,v)dv \right] du \tag{3.56}$$

So far the event of failure is given by $(V < U)$ and this event in other terms can be expressed as $(V - U < 0)$. This means that $(M = V - U)$ specifies the margin of safety of the system. M is also a random variable and the descriptors of random variable irrespective of the distributions of U and V are: mean $\mu_M = \mu_U - \mu_V$ and standard deviation $\sigma_M = \sqrt{\sigma_U^2 + \sigma_V^2 - 2\rho_{UV}\sigma_U\sigma_V}$ where ρ_{UV} is correlation coefficient. The failure probability can be represented as $P(M < 0)$ which is given by equation

$$P_f = \int\limits_{-\infty}^{0} p_M(m) \tag{3.57}$$

The safe and the unsafe regions on either sides of the safety margin is presented in Figure 3.17. If random variable M is standard normal, the probability of failure is given by the equation

$$P_f = F_M(0) = \Phi\left(\frac{0 - \mu_M}{\sigma_M}\right) = 1 - \Phi\left(\frac{\mu_M}{\sigma_M}\right) \tag{3.58}$$
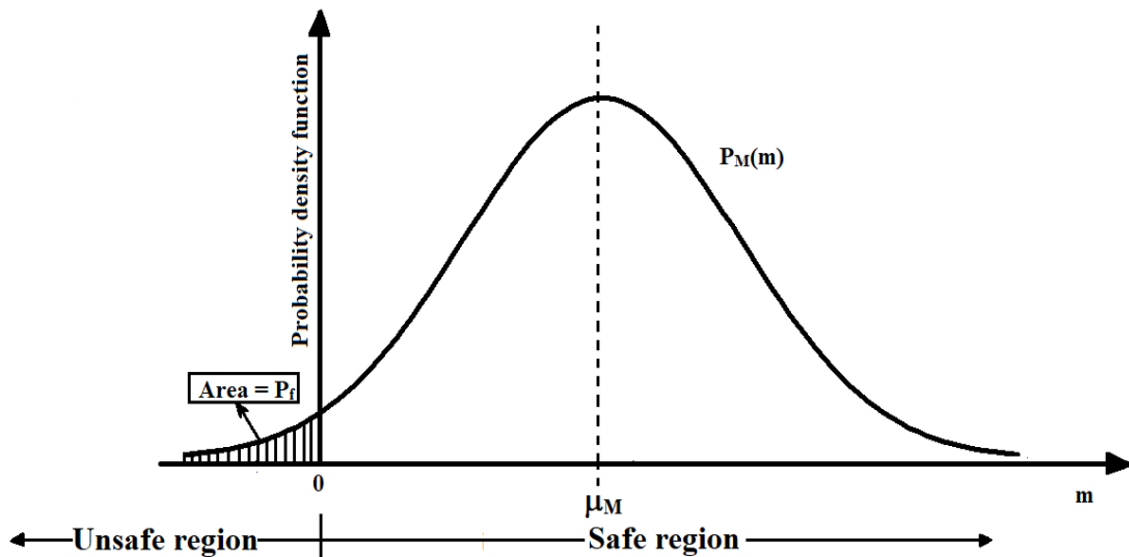
Figure 3.17: Probability density function of M

This implies $\beta = \Phi\left(\frac{\mu_M}{\sigma_M}\right)$. When the load and resistance components of a system are a function of many factors, then their reliability will involve a vector of random variables $(X = [X_1, X_2, X_3 \ldots])$. The performance / limit state function is generalized into $g(X) = p_a(X) - p_b(X)$ where $p_a(X)$ and $p_b(X)$ are joint distributions of load and resistance respectively. So $g(X) = 0$ represents an n-dimensional surface called the limit surface and the safe $(g(X) > 0))$ and unsafe $(g(X) < 0))$ states are similar to the observations made in Figure 3.17. The probability of failure of this system is given by

$$P_f = \int_{(g(X)<0)} \cdots \int p_{X_1,X_2,X_3\ldots,X_n}(x_1,x_2,x_3,\ldots,x_n) \tag{3.59}$$

When the system is statically independent as mentioned in the earlier cases, the joint pdf of the multi dimensional integral can be expressed as a product of individual pdfs. It is nearly impossible to obtain the joint pdf of a correlated system. So alternative methods have been developed to solve the integral and estimate the reliability of engineering system over the past few decades. They are broadly categorized into three forms namely:

1. **Analytical methods:** The integral can solved analytically based on the concept of Taylor series expansion. These methods include first order reliability method (FORM) (Hasofer and Lind, 1974; Ang and Tang , 1975) , second order reliability method (SORM) (Melchers, 1999) etc.

2. **Surrogate methods**: As the dimensionality of the problem increases, analytical techniques might fail. In such cases, they can be solved using surrogate modelling techniques like response surface method which closely approximates the performance function (Faravelli, 1989; Melchers, 1999).

3. **Simulation methods:** To meet the computational demands of the complex performance functions, another class of numerical approximation are developed called the Monte Carlo simulation methods. They include importance sampling (Engelund and Rackwitz, 1993), Latin Hypercube sampling (McKay et. al., 1979), subset simulation method (Au and Beck, 2001) and so on.

In the thesis, surrogate methods of modelling have been discussed in the previous section and the same concept is implemented for estimating the performance function. Methods of estimating reliability using simulation based techniques are discussed in the next section.

3.6.1 Simulation methods

Let X be a vector of input variables of dimension d and performance function $g(X) = x_p - f(x)$, then the failure domain (in input space) is defined by

$$F = \{x : g(X) < 0\} \quad = \{x : x_p < f(x)\} \tag{3.60}$$

In the performance function x_p represents the critical threshold. When the engineering system is complex, then the probability of failure (over the failure domain) is given by

$$P_f = P(x \to F) = \int_F p_X(x)dx \qquad (3.61)$$

In these systems the integral cannot be solved analytically as the failure domain is not explicitly known. Also, since it is not known in advance whether a given point is a failure point or not (the failure domain F is not known explicitly), the failure criterion must be checked for all x. In such cases, simulation techniques can be adopted using the equation

$$P_f = \int_{x \to F} I_f(x)p_X(x)dx \qquad (3.62)$$

where I_f stands for indicator function that takes value of 1 if $x \to F$ and 0 otherwise.

3.6.1.1 Direct Monte Carlo simulation

One of the oldest and powerful forms of simulation based methods for estimating the probability of failure is the Monte Carlo simulation. This statistical sampling technique was originally developed by Stan Ulam in late 1940s. It is based on the concept of "law of large numbers" where the empirical average of an iid sequence from a pdf $p(x)$, ie., $\frac{1}{n}\sum_{i=1}^{n} s(x^{(i)})$ converges to its true average i.e., $E[s(x)]$ as $n \to \infty$. In simple terms, this method estimates the expectation of a function $s : \Xi \to R$ with respect to the pdf $p(x)$. The expected value is given by $E[p(x)] = \int_\Xi s(x)p(x)dx$. In the case of reliability problem, the probability of failure is nothing but the expectation of the indicator function

$$P_f = \frac{1}{n}\sum_{i=1}^{n} I(x^{(i)}) \qquad (3.63)$$

where $x^{(1)},....x^{(N)}$ are sequence of iid samples from $p(x)$. The key advantage of direct Monte Carlo simulation (DMC) over numerical integration is that the precision in results does not depend on the dimension d of the input space. Also, it can handle non-linear performance functions, the complexities that cannot be handled when using analytical techniques like FORM / SORM can be easily overcome in DMC. However, in most of the simulation methods, including DMC, the input variables x are assumed to be independent and normally distributed. But such cases seldom occur in an engineering system. So, if the variables are non-normal and correlated they can be transformed to independent normal space through different methods of transformation. When the joint pdf $P_X(x)$ is known, then Rosenblatt transformation (Rosenblatt, 1952) can be applied while, Nataf transformation (Nataf, 1962) can be applied when the marginal pdfs and their correlation structure is specified.

3.6.1.1.1 Accuracy of MCS

It is necessary to know the error underlying an estimated probability (probability of failure). The number of simulations that leads to a certain accuracy is dependent on the coefficient of variation of failure probability ($COV(P_f)$). This is given by

$$COV(P_f) = \sqrt{\frac{(1-P_f)P_f}{n_s P_f}} \tag{3.64}$$

For low values of P_f, the above equation is approximately $\frac{1}{\sqrt{n_s P_f}}$. This implies to achieve a $COV(P_F)$ around 10% for a problem with P_f value 10^{-7}, almost 10^9 samples are required. One of the limitations of DMC is that, it becomes computationally expensive when the system becomes complex. In order to improve the efficiency of Monte Carlo methods, variance reduction techniques have been implemented widely. These techniques improve

the precision of the estimates that can be obtained for a lesser number of iterations, i.e., a smaller value of $COV(P_f)$ can be attained without increasing n_s. One such techniques that received special attention is the subset simulation method. This method was developed by Au and Beck (2001) with a simple concept of representing an event with small failure probability as a product of events of large failure probabilities. This technique helps in estimating the P_f with lesser number of samples and without compromising on the accuracy of the estimate.

3.6.1.2 Subset simulation method

Estimating the probability of failure of a rare event is challenging as they have very small failure probabilities. It becomes unreliable to opt for conventional techniques like Monte Carlo simulation , FORM / SORM etc as they not only become computationally demanding but also leads to questionable results in achieving a convergence towards the actual solution. An alternative and efficient technique called subset simulation is developed to estimate the P_f for such rare events (Au and Beck, 2001). The underlying idea in subset simulation is to break down a rare event into a sequence of frequently occurring events. Let the failure event be F, be a sequence of intermediate events such that $F_1 \supset F_2 \supset \ldots \supset F_r = F$. Thus, the failure event is nothing but the intersection of all the intermediate events (in Figure 3.18) $F_j = \bigcap_{i=1}^{j} F_i \ \ j = 1, 2, \ldots r$. By conditioning the event F_i sequentially, the failure probability $P(F)$ is

$$P(F) = P(F_r) = P(F_1)P\left(\frac{F_2}{F_1}\right)P\left(\frac{F_3}{F_2}\right)\ldots P\left(\frac{F_r}{F_{r-1}}\right)$$

$$= P(F_1)P(F_2|F_1)P(F_2|F_1)\ldots P(F_r|F_{r-1}) \tag{3.65}$$

$$= P(F_1)\prod_{i=1}^{r-1} P(F_{i+1}|F_i)$$

From equation (3.65), it can be noticed that the small failure event is divided into r intermediate events and one of the critical steps in this method is the proper sequencing of events. It is handled in subset simulation suitably as algorithm proceeds. In this method the input random variables are considered to be independent and normally distributed. If they are not in independent and identically distributed (iid) sequence of normal random variables, they are transformed into iid space by applying any of the transformations mentioned in the previous section. Contrary to DMC, where sampling the input space becomes demanding, SS method explores the input space adaptively. To determine $P(F_1)$ standard Monte Carlo (MC) simulation method is used and the conditional probabilities are estimated by employing Markov Chain Monte Carlo (MCMC) simulation.

Step 1. Estimation of $P(F_1)$:

In the first step, a few iid samples (assume n) are simulated $x_0^{(1)}, x_0^{(2)}, \ldots x_0^{(n)}$ and the corresponding responses (values of performance function) are given by $g(x_0^{(1)}), g(x_0^{(2)}), \ldots g(x_0^{(n)})$ are estimated. The subscript 0 represents the 0th stage of algorithm. As the event being modelled is rare, these 'n' samples are not good enough to estimate $P(F)$ but, the information taken from the samples help in moving towards the failure region. So, 'n' samples are arranged in descending order such that the sample closest to failure is given by $x_0^{(1)}$ and the safest sample corresponds to $x_0^{(n)}$. Let $p \in (0, 1)$ be any number such that np is integer and the first intermediate failure domain is given by $F_1 = x : g(x) > g_1(x)^*$. As a result, F_1 is estimated using Direct Monte Carlo based is equal to p,

$$P(F_1) \approx \frac{1}{n} \sum_{i=1}^{n} I_{F_1}(x_0^{(i)}) = p \tag{3.66}$$
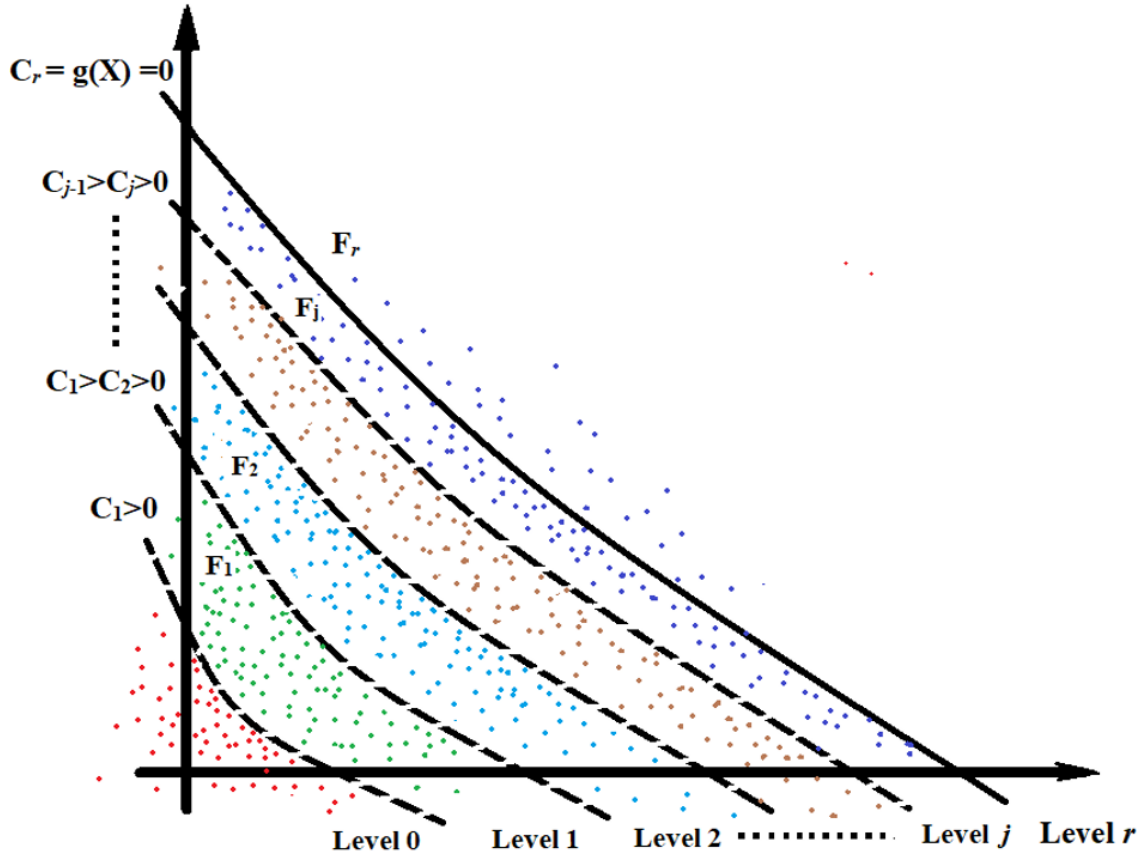
Figure 3.18: Typical sequence of limit surfaces in subset simulation

A value of $p = 0.1$ is used in the previous studies and also make F_1 a relatively frequent event. The steps followed in Monte Carlo simulation is discussed already in Section 3.6.1.1. In this step the first failure domain is populated to proceed to the next step.

Step 2. Estimation of conditional events $P(F_r|F_{r-1})$:

In the equation $P(F) = P(F_1)P(F|F_1)$, $P(F_1)$ is already known and the remaining conditional probability $P(F|F_1)$ needs to be estimated. Using the samples from the previous step, the samples for the pdf of conditional distribution $p(x|F_1)$ are obtained. The conditional pdf is given by the equation

$$p(x|F_1) = \frac{p(x)I_{F_1}(x)}{P(F_1)} = \frac{I_{F_1}(x)}{P(F_1)} \prod_{s=1}^{t} \gamma(x_s) \tag{3.67}$$

Modified Metropolis algorithm (MMA) is used to sample these conditional distributions. MMA belongs to the category of Markov chain Monte Carlo (MCMC) algorithms which are helpful in sampling from complex pdfs (as above) that cannot be sampled directly.

3.6.1.2.1 Modified Metropolis Hastings algorithm

Let $x \approx p(.|F_1)$ be conditional sample drawn from conditional distribution $p(.|F_1)$. To generate more samples from $p(.|F_1)$ MMA is used. The sequence of steps followed in the algorithm are presented below

1. Generate a candidate sample ψ. For each coordinate $s = 1, ..., t$.

    (a) A proposal distribution defined by $q_s(.|x_s)$ is considered and samples $\delta_s \approx q_s(.|x_s)$ are drawn from the distribution. It is a univariate PDF obeying symmetric property which can either follow Gaussian $N(x_s, \sigma_s^2)$ or uniform distribution $U(x_s - \alpha, x_s + \alpha)$.

    (b) Compute the acceptance ratio $r_s = \frac{\gamma(\eta_s)}{\gamma(x_s)}$

    (c) Define the sth coordinate of the candidate sample by accepting r rejecting η_s

$$
\psi_s = \begin{cases} \eta_s, & \text{with probability } min\{1, r_s\}, \\ \\ x_s, & \text{with probability } 1 - min\{1, r_s\} \end{cases}
$$

    (d) Accept or reject the candidate sample ψ by setting

$$
\tilde{x} = \begin{cases} \psi, & \text{if } \psi \in F_1, \\ \\ x, & \text{if } \psi \notin F_1 \end{cases}
$$

From MMA, the sample $\tilde{x}$ is generated and it follows $p(.|F_1)$. When the sample is accepted, then the new $\tilde{x}$ value is moved to ψ, while it remains at x only when the sample is rejected. The transition pdf after the candidate samples are generated for the first conditional level is given by the equation

$$t(\tilde{x}_s|x_s) = q(\tilde{x}_s|x_s)min\left\{1, \frac{\psi(\tilde{x}_s)}{\psi(x)_s}\right\} \tag{3.68}$$

The condition for detailed balance is also verified. In this way the samples from conditional distribution are obtained using Modified Metropolis algorithm.

Step 3: Sampling at higher conditional levels

Among the n samples the first np MCMC samples are sampled from the conditional distribution using MMA. The sequence of first $\frac{1}{p}$ samples is Markov chain with stationary distribution $p(.|F_1)$. These conditional samples are schematically shown in Figure 3.8. The MCMC samples $(x_1^{(1)}, ..., x_1^{(n)})$ can be used in the similar way as the Monte Carlo samples $x_0^{(1)}, ..., x_0^{(n)}$ were used. By using equation 3.66, the conditional probability $P(F_2|F_1)$ is estimated.

Step 4: Stopping criterion

Let $n_F(l)$ denote the number of samples in the failure region at l^{th} level i.e., $n_F(l) = \sum_{k=1}^{n} I_F(x_l^{(k)})$. The adaptive scheme of generating the P_f is given by

$$P_f = p^l P(F|F_l) \tag{3.69}$$

As 'l' is the last conditional level, the conditional probability is estimated by the equation $P(F|F_l) \approx \sum_{j=1}^{n} I_F(x_l^{(i)}) = \frac{n_F(l)}{n}$. Also assumption of an estimate for the level probability and proposal pdf plays an important role in achieving faster pace of convergence which

are discussed in (Au and Beck, 2001; Zuev, 2015; Papaioannou et. al., 2014). Thus the steps followed will help in estimating the probability of failure of a rare event.

3.6.1.2.2 Accuracy of SS

To verify the accuracy of failure probability estimated from subset simulation, a set of 25 to around 50 independent simulations are run (Au and Beck, 2001; Ahmed and Soubra, 2012). The results for $COV(P_f)$ versus N_{ss} and P_f versus N_{ss} are plotted to observe the level of convergence obtained in each case. The typical trends in these cases are presented in Figure 3.19. The number of samples per subset that results in low values of $COV(P_f)$ and unchanged value P_f will be considered as the simulation with least error for the corresponding N_{ss} .

3.7   Methods of sensitivity analysis

Sensitivity analysis measures the impact of input uncertainties on the response of the system. Uncertainty analysis studied so far, focuses only on quantifying uncertainty in the model output, whereas, the sensitivity analysis attributes the uncertainty in the output to different sources of input variables and uses the extent of contribution of an input to characterize its importance. The uncertainties are identified and ranked in order of their importance (with respect to their impact on the uncertainty of the performance measures). This ranking becomes the basis for prioritizing data collection and model improvement, so that, these activities are focused only on those uncertainties that have maximum influence. It results in the reduction of the most significant sources of uncertainty which will most likely lead to change the results of the performance assessment (Gallegos and Bonano 1993). Sensitivity analysis can assist modellers in a number of ways, such as detecting

modelling errors, controlling model uncertainty, and reducing model complexity (Liu, 2013).

(a) (b)
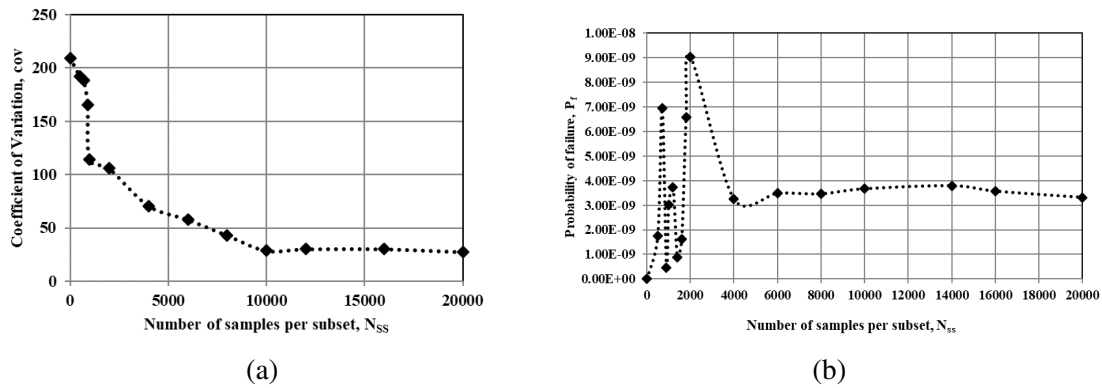
Figure 3.19: (a) Coefficient of variation of probability of failure for different number of samples per subset (b) Probability of failure for different number of samples per subset

The objectives of a sensitivity analysis are (1) to check whether a given dataset has adequate details; to determine a parameter given uncertainty of other parameters, (2) to determine how to allocate limited resources to estimate each parameter as a part of analysis, and (3) to reduce the number of parameters to be varied or estimated and hence to reduce computational burden in parameter estimation and uncertainty analysis.

Sensitivity methods can either be local or global. Different methods of local and global sensitivity analysis were compared in the previous studies (Wainwright et al 2014). Local sensitivity analysis is usually described by the partial derivatives of the output with respect to the input parameters. It estimates the value of output by taking into account, the impact of varying single input variable around a certain value while, the other inputs are kept constant at their nominal values. Suppose $y = f(x_i), \{i = 1, 2...n\}$, then the local sensitivity index for parameter i is defined as the scaled partial derivative of y with respect to x_i (Cacuci, 2003). Conversely, global sensitivity analysis considers variations of all input parameters at the same time. This method is described in the next section.

3.7.1 Global Sensitivity Analysis

Global Sensitivity Analysis (GSA) essentially involves quantification of effects of uncertainty in the output of a model (numerical or otherwise) with respect to different sources of uncertainty in the model input (in terms of their variances). Some of the early works estimated the sensitive parameters by finding the sensitivity of reliability index β (from FORM, SORM) to equal changes in uncertain parameters (Jang et. al., 1994). Homma and Saltelli (1996) presented a method of GSA where the Sobol indices are estimated by decomposing the response variance as sum of contribution of input variance. So, by assuming an independent set of input random variables δ_i; $\{i = 1, 2...n\}$, the variance of output variable y_1 is given by

$$\sigma(y_1) = \sum_{i=1}^{n} \sigma_i + \sum_{1 \leq i < j \leq n} \sigma_{i,j} + \ldots + \sigma_{1,2,...n} \tag{3.70}$$

In the equation (3.70), the first order terms σ_i represent the partial variance in the output due to the individual effect of a random variable x_i, the higher order terms show the interaction effects between two or more random variables. The effect of terms associated with only one random variable and the terms with both individual effect of a random variable as well as its interaction with other random variables are presented. Further, a more convenient approach developed by Saltelli et al., (2000) and Sobol (2001) to estimate the first order Sobol index is give by the equation

$$S(\delta_i) = \frac{var[E(y|\delta_i)]}{var[Y]} \tag{3.71}$$

154

where y is the system response, $E(y|\delta_i)$ is the expectation of y conditional on a fixed value of δ_i, and *var* denotes the variance. Sudret (2008) presented a method of Global Sensitivity Analysis by Polynomial chaos expansion (PCE) and calculated the Sobol indices. The coefficients of polynomial from CSRSM are post-processed to obtain Sobol indices. As discussed in the previous section, the response variable is represented as a series of orthogonal polynomials given in equation (3.47). The mean and variance of the PCE are

$$Y = E[f(\delta)] = a_0 \qquad D_{PC} = var[\sum_{j=0}^{p-1} a_j \Gamma_j(\delta)] = \sum_{j=0}^{p-1} E[\Gamma_j^2(\delta)] \qquad (3.72)$$

The multi-variate polynomials are represented as multi-index $\alpha = (\alpha_1, \alpha_2, \ldots, \alpha_n)$ and the Sobol decomposition of the polynomial is given by the equation

$$F(\delta) = f_0 + \sum_{i=1}^{n} \sum_{\alpha \varepsilon I_i} f_\alpha \Gamma_\alpha(\delta_i) + \ldots\ldots + \sum_{\alpha \varepsilon I_{1,2,\ldots n}} f_\alpha \Gamma_\alpha(\delta_1, \delta_2, \ldots, \delta_n) \qquad (3.73)$$

So, the system response is represented by a PCE. Thus, by replacing y in the equation with the PCE expression, one obtains the Sobol index formula as a function of the different terms of the PCE .

$$S(\delta_i) = \frac{\sum\limits_{\beta \varepsilon I_i} \alpha_\beta^2 E(\Gamma_\beta^2)}{D_{PC}} \qquad (3.74)$$

where I_i denotes the set of indices κ for which the corresponding terms Γ_β are only functions of the random variable δ_i and $E(\Gamma_\kappa^2) = \prod\limits_{i=1}^{n} \alpha_i!$. The construction of a PCE and the derivation of the equations providing Sobol indices are illustrated with an example of a PCE of order p=3 using only M=2 random variables in Appendix A.

3.7.2 Post processing the results from subset simulation

Sensitivity measures can be estimated by processing the conditional levels in subset simulation (Cadini et. al., 2012). The empirical probability density function (pdf) is estimated at each conditional level, and compared with the unconditional probability density function. The underlying concept followed in this method is Bayes theorem, which gives an indication of how critical the uncertain parameter is in affecting the system failure.

$$P(F|x_p) = \frac{q(x_p|F)}{q(x_p)} P(F) \ \ x_p = 1, 2, ...n \tag{3.75}$$

In the equation (3.75), it can be observed that, when the conditional pdf $P(F|x_p)$ is similar to the unconditional pdf $P(F)$, then that parameter is insensitive to the system failure. The change in the sample distributions at different conditional levels with respect to the unconditional distribution of the parameter represents its influence on the response of the system. So, the empirical pdf that exhibits maximum shift from the unconditional pdf represents the most sensitive parameter.

3.8 Concluding remarks

In this chapter, various methodologies adopted in the thesis are discussed in detail. The framework to develop performance (or safety) assessment model and predict the safety design of a radioactive waste disposal system are presented elaborately. The different components of a performance assessment model and detailed set of mathematical formulations for each component (using analytical and numerical methods) that are implemented in the thesis are presented. As an integral part of performance assessment model,

different forms of uncertainties that need to be considered are presented. The impact of these uncertainties can be estimated by implementing various uncertainty modelling, propagating and quantifying methods. The concepts of random field modelling to handle the spatial variability in geological medium and the meta-modelling technique adopted for propagating uncertainties have been discussed thoroughly. The methods of reliability analysis which include Monte Carlo simulation, variance reduction techniques like subset simulation (which help in estimating safety indicators of performance assessment model) and the different sensitivity methods used to recognise the critical parameters among the various uncertain parameters are also discussed.

Chapter 4

Risk and reliability analysis for near surface radioactive waste disposal facilities

4.1 Introduction

The main objective of the radioactive waste management is to adopt efficient strategies that can isolate radioactive waste from the surrounding environment. Near Surface Disposal facilities (NSDFs) are designed to contain low and intermediate level radioactive wastes, while, high level wastes are disposed in deep geological repositories. The safety of a disposal facility depends on how effectively it is designed against release and eventual migration into the geosphere. The transport behaviour of radionuclides is a complex process involving physical and chemical interactions with the surrounding media (in the form of advection, diffusion, dispersion, adsorption etc). The movement of contaminants through relatively impermeable soil is quite slow; however, it is conceivable that significant contamination might occur in the long term. So, it becomes important to design the disposal sites such that they prevent the possible contamination of the groundwater system in both short-term and long-term (Rowe and Booker, 1985). During the post-closure phase of near surface disposal facilities, one of the major safety issue is the possibility of

radiation exposure and environmental impacts over time periods far into the future. Some effects may be assumed to occur, for example, owing to gradual leaching of radionuclides into groundwater and subsequent migration through environmental media and transfer to humans. As a whole, the behaviour of the site and disposal facility may need to be projected for time periods of the order of hundreds or even thousands of years. Number of models have been developed in the past to predict the safety assessment of radioactive waste disposal facilities (Cho et. al., 1992; Kim et. al., 1993; IAEA, 1995; Nair and Krishnamoorthy, 1999; Rakesh et. al., 2005). In most of these studies, the complexity in the transport problem is limited to a simple contaminant transport model and the mechanism of radionuclide release from the facility is mainly diffusion controlled. Moreover, mathematical modelling implies many assumptions and estimations, which increase the uncertainty of the output of radionuclide migration.

For a predictive model that produces reliable results, input data should be accurate and representative of the real situation in the field (Baalousha and Kongeter, 2006). Further, the existence of uncertainty, such as data and model uncertainty greatly affects the predictive ability of these models. Error in accommodation of physical parameter uncertainty in contaminant transport models casts serious doubts on the ability to accurately delineate the contamination at a given site (Baalousha, 2003). So, an integral part of the predictive modelling is uncertainty analysis, due to the inherent uncertainty of the physical parameters in subsurface contaminant transport problems. This is manifested in the basic heterogeneity of the geological formations and the uncertainty related to the chemical, physical and biological properties of the contaminant being released and transported (Hamed, 1996). Further, the long time scales considered in geological disposal repository are a key feature making treatment of uncertainties more challenging. Therefore, the

safety assessment of waste disposal using a deterministic approach could result in either an underestimation or overestimation of the repository performance. As the transport occurs in extremely complex geological environments, the predictive modelling can be a complicated task. In such a complicated structural system, the problem of deterministic analysis by a mathematical model (Kim et al., 1993; Nair and Krishnamoorthy, 1999) can be overcome by adopting probabilistic methodologies (Kim and Na, 1997; Das and Zheng, 2000; Huang et. al., 2009; Cadini et. al., 2012).

Stochastic methods have been established as viable tools for analysing contaminant transport in porous media. These tools can be used to assess the behaviour of radionuclide transport in heterogeneous porous and fractured geological media, and to obtain the estimates of uncertainty associated with predicting radionuclide transport in the subsurface (Harter 2000). So, an integrated performance assessment model takes into account these uncertainties and quantifies their effect on the overall performance of the system (IAEA). The most common method to handle uncertainty problem is the classic Monte Carlo simulation method (MCS). Monte Carlo simulations are perhaps the most intuitive, and for many site-specific studies, statistically the most accurate approach to uncertainty or risk analysis of contaminant transport in the subsurface (Harter 2000). As the number of simulations increases, the convergence to the actual solution is ensured. However, if the probability of failure is small or the number of random variables are large, MCS becomes time consuming and computationally intensive. Recently many probabilistic methodologies / variance reduction techniques have been adopted for reliability analysis which include response surface methods (RSM). An improvement over the basic RSM methodologies were are developed by vector projection of sampling points (Kim and Na, 1997), constructed response surface in a cumulative manner and used in reliability analy-

sis of plate structures (Das and Zheng, 2000). Duborg et. al., (2013) adopted meta-model based importance sampling technique in determining the reliability of structural systems. Further, sensitivity analysis can be performed to identify the critical parameters affecting the response of the system (Sudret 2008; Volkova et. al., 2008; Liu, 2013). By integrating these stochastic methods into the performance assessment model, the model becomes more realistic and efficient in computation. However, the previous studies have lacked in exploring these aspects and also the computational effort involved analysing the performance of NSDFs was very high. So, there is need to develop a framework for an efficient probabilistic performance assessment of NSDFs that systematically analyses the radionuclide transport process from the disposal facility to biosphere and, resolves the computational issues by integrating effective techniques in the model.

4.2   Objectives

Keeping the above aspects in the viewpoint, a probabilistic framework for performance assessment of NSDFs has been developed in this chapter and the objectives of study are:

1. To determine release rate, concentration and radiation dose of radionuclides from the disposal facility to biosphere through drinking water pathway. To investigate the influence of the mode of disposal (i.e., single dump and multiple dump) and the dimensionality (ie., one-dimensional and two-dimensional) of contaminant transport model on the results.

2. To develop meta-models by employing collocation based stochastic response surface method (CSRSM) method and determine the statistical properties of response (dose rate of radionuclide).

3. To perform reliability analysis using Monte Carlo simulation method and test the computational efficiency of the mathematical model and meta-model.

4. To employ global sensitivity techniques using PCE-based Sobol indices to identify the critical parameters contributing to the failure in NSDF's performance.

4.3   Development of performance assessment model

To understand the functionality of a disposal facility, it is necessary to develop methods that can predict the possible risk it causes to the human health and the environment due to exposure to radiation. The international nuclear regulatory bodies like International Atomic Energy Agency (IAEA), Nuclear Regulatory Commission (NRC) and the national regulatory bodies in India including Atomic Energy Regulatory Board (AERB) and Bhaba Atomic Research Center (BARC) have developed various strategies to quantitatively assess the performance of radioactive waste disposal facilities. A performance assessment model predicts the future behaviour of a disposal facility. These models entail identification of scenarios that affect the performance of the disposal facility, quantification of the consequence of events and the treatment of associated uncertainties (i.e., radionuclide migration to biosphere via geological medium), and comparison of results (risk, radiation dose etc) with the permissible limits set by the regulatory bodies. So, the main components of a performance assessment model are (1) Source term model (2) Repository failure model (3) Geosphere transport model and (4) Radiological model.
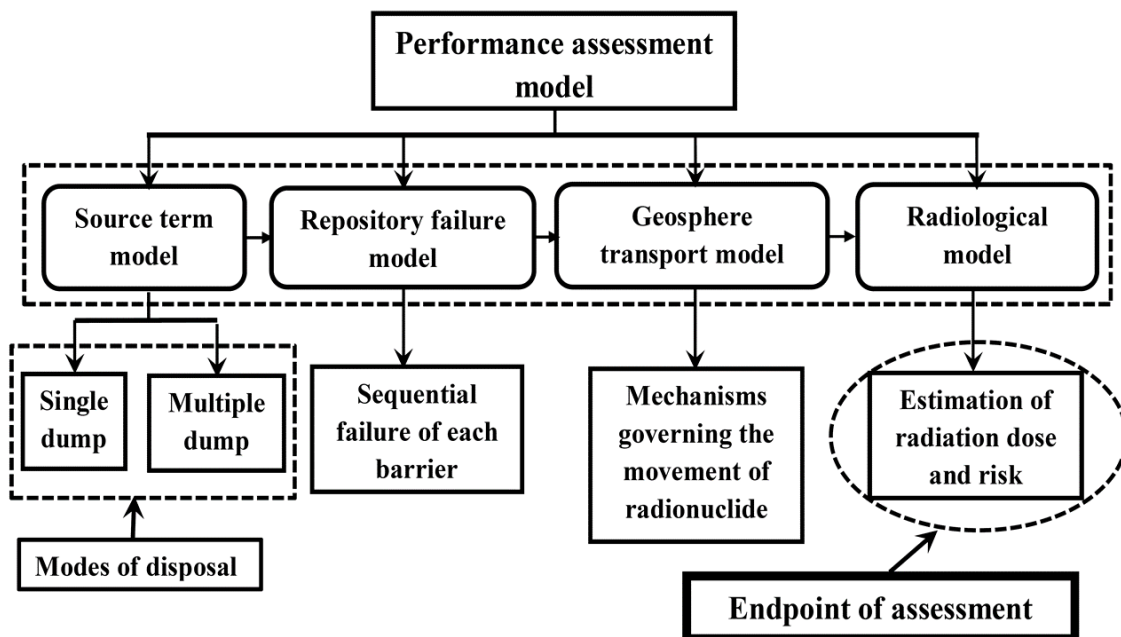
Figure 4.1: Main components of a performance assessment model

Figure 4.1 presents the key components of performance assessment model. In the figure, it can be noticed that the source term can be evaluated for two cases: single dump and multiple dump modes. They refer to the modes of disposal practised in different countries. In single dump mode, the dumping operation in NSDF will be over within 10 to 20 years. In multiple dump mode, the disposal operation of low-level radioactive waste starts from the inception of nuclear power plants and continues for a long period till their permanent closure. In countries like Spain and France, single dump mode of disposal is practised, while, in countries like India, multiple dump mode of disposal is adopted. The influence of both the modes are explored in this study. After evaluating the source term, it is required to develop a scenario for barrier system failure followed by release of radionuclides into geosphere. Once the radionuclides enter the geosphere, it reaches the human habitat and, the radiation dose and risk values are evaluated at the end-point. As disposal facility is made of many engineered and natural barriers, a multi-barrier system is considered to model the safety assessment scenario. The details are presented in the

next section.

4.3.1 Model for multi-barrier system

The sequence of components in multi-barrier system are top cover, waste container, waste form, backfill material, bottom cover and the near field geosphere. After proper conditioning, the radioactive waste in the solidified form (waste form) is packed in steel drums (waste container) and buried in the facility. The top concrete cover ensures a long term protection from infiltration due to rainfall. The waste containers are disposed over a backfill made of soil mixed with clay and the bottom concrete cover which enhances the isolation capacity. The final release of the radioactive waste to the groundwater is retarded by near field geosphere (unsaturated zone). The model for multi-barrier system is presented in Figure 4.2.
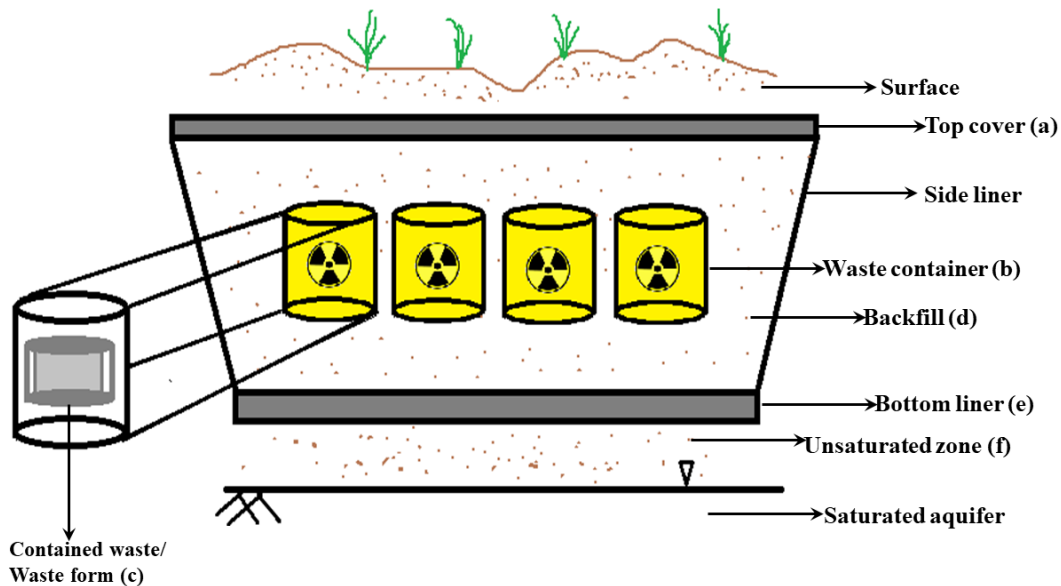
Figure 4.2: Components of a barrier system

4.3.1.1   Sequence of failure of barrier system

Though the barrier system is designed for safe environment, a failure scenario may be encountered due to infiltration. The radionuclide release to the groundwater is estimated by considering the sequential failure of the barrier system due to ingress of rain water into the facility. This infiltration leads to failure of top cover (Barrier a), and then, the water gets in contact with the waste container (Barrier b) leading to corrosion of mild steel. As the corrosion proceeds, water interacts with the solidified waste (Barrier c) resulting in leaching of radionuclides from the waste form. The leached radioactivity begins to migrate through the backfill (Barrier d) and after the failure of the bottom cover (Barrier e) reaches the geosphere (Barrier f). If the system is assumed to operate without any repair and the failure is random, the probability density function $f(t)$ is expressed as (Kim et al.,1993).

$$f(t) = \lambda exp(-\lambda t) \tag{4.1}$$

where, λ is the conditional failure rate (i.e., reciprocal of mean time to failure) and t is the operation time of the barrier (y). Equation (4.1) represents an exponential probability distribution for single barrier. So, the failure probability density of the disposal system can be determined analytically as,

$$f_s(t) = \left(\prod_{i=a}^{f} \lambda_i \right) \left(\sum_{i=a}^{f} \frac{e^{-\lambda_i t}}{\prod_{\substack{j\neq i}} (\lambda_j - \lambda_i)} \right) \tag{4.2}$$

where $f_s(t)$ is the exponential failure probability density of the barrier system (y^{-1}).

4.3.1.2 Radioactive release rate for different modes of disposal

The release rate of the radionuclide into groundwater for single dump mode is calculated as,

$$R_s(t) = S_s(t)f_s(t) \tag{4.3}$$

where is the source term (Bq) $S_s(t) = Mexp(-\lambda_p t)$, M is the inventory (Bq) of the radionuclide corresponding to 50 GWe.y energy production, λ_p is the decay constant of the radionuclide (y^{-1}) and t is the time elapsed after disposal (y). In the case of multiple dump mode, the source term needs to be evaluated in two phases: during the dumping period and after termination of disposal (post dumping period). Since, the source term affects the other components of performance assessment, two stages of modelling is done for multiple dump mode. So, the release rate during dumping period is,

$$R_d(T) = S_d(T)f_s(T) \tag{4.4}$$

where $S_d(T) = (Q/\lambda_p)(1 - exp(-\lambda_p T))$ is the inventory (Bq) during dumping period T (50 years), Q is the annual disposal rate (Bq/y) of the radionuclide. The release rate for post dumping period is evaluated as,

$$R_p(t) = S_p(t)f_s(t+T) \tag{4.5}$$

where $S_p(t) = S_d(T)exp(\lambda_p t)$ is the inventory (Bq) of the radionuclide after time t in years from closure of the disposal facility ie., post dumping period. Once the radionuclides release into geosphere, the transport process of radonuclides in geosphere needs to be modelled to evaluate the concentration of radionuclides.

4.3.1.3 Concentration reaching the groundwater in single and multiple dump modes

of disposal

As mentioned earlier, the analytical solutions developed for one-dimensional and two-dimensional contaminant transport are considered for the analysis (Nair and Krishnamoorthy, 1997). The governing differential equation of transport include, advection and hydrodynamic dispersion (i.e., dispersion due to mechanical mixing and molecular diffusion) is given in equation (3.4) (chapter 3). For a given set of initial and boundary conditions, the one-dimensional solution for concentration of radionuclide in groundwater is given by

$$C_g(x,t) = \frac{exp(-\lambda_p t)exp(-(x-U_x t)^2/4D_x t)}{2\pi A R_g \theta_g \sqrt{D_x t}} \tag{4.6}$$

The two-dimensional solution of contaminant transport model with an instantaneous release of unit activity from a line source is given by

$$C_g(x,y,t) = \frac{exp(-\lambda_p t)exp(-(x-U_x t)^2/4D_x t)exp(-y^2/4D_y t)}{4\pi H_g R_g \theta_g \sqrt{D_x D_y t^2}} \tag{4.7}$$

where D_x is the retarded longitudinal dispersion coefficient (cm^2/y), D_y is the retarded lateral dispersion coefficient ((cm^2/y), U_x is the retarded groundwater velocity (cm/y), A is the cross sectional area of aquifer (cm^2), R_g is the retardation factor which is $1 + \frac{K_d \rho_b}{\theta_g}$ where K_d is the distribution coefficient (ml/g), ρ_b is the bulk density (g/cc), H_g is the aquifer thickness (cm) and θ_g is the effective porosity.

The time dependent concentration of the radionuclide in the groundwater for single dump

mode is evaluated as a convolution integral,

$$C_{gs}(x,t) = \int_0^t R_s(t-\tau)C_g(x,\tau)d\tau \tag{4.8}$$

$$C_{gs}(x,y,t) = \int_0^t R_s(t-\tau)C_g(x,y,\tau)d\tau \tag{4.9}$$

where, t is the time elapsed after disposal and x is the longitudinal distance parallel to the flow and y is the lateral distance normal to the flow. The equation (4.8) corresponds to one-dimensional flow and equation (4.9) corresponds to two-dimensional flow. The time dependent concentration of the radionuclide in the groundwater for multiple dump mode during dumping period can be evaluated as a convolution integral,

$$C_{gs}(x,t) = \int_0^t R_s(t-\tau)C_g(x,\tau)d\tau \tag{4.10}$$

$$C_{gs}(x,y,t) = \int_0^t R_s(t-\tau)C_g(x,y,\tau)d\tau \tag{4.11}$$

Similarly the concentration after the post closure period can be evaluated as

$$C_{gp}(x,t) = \int_0^T R_d(t-\tau)C_g(x,t+\tau)d\tau + \int_0^t R_p(t-\tau)C_g(x,\tau)d\tau \tag{4.12}$$

$$C_{gp}(x,y,t) = \int_0^T R_s(t-\tau)C_g(x,y,t+\tau)d\tau + \int_0^t R_s(t-\tau)C_g(x,y,\tau)d\tau \tag{4.13}$$

In the above equations (4.10) and (4.12) represents one-dimensional transport model and equations (4.11) and (4.13) represents the convolution integral for two-dimensional transport model.

4.3.1.3.1 Input data considered for the study

The low and intermediate level radioactive waste is composed of both short-lived and long-lived radionuclides. Radionuclides which have half-lives shorter than 30 years are called short-lived and, the ones with half-lives longer than 30 years are called long-lived radionuclides. The input data of radionuclides which include the inventory value, half-life, distribution coefficient and ingestion dose coefficient are presented in Table 4.1. The barriers of disposal facility and their mean-time to failure are presented in Table 4.2. Further, the geochemical and hydrological data for the model obtained at the solid waste management facility at Trombay in Mumbai (Narayan, 1998; Nair and Krishnamoorthy, 1999) are considered for the analysis. They are presented in Table 4.3.

Table 4.1: Input parameters for different radionuclides considered in the model

Radionuclide	Half-life (yrs)	Radioactive waste inventory (Bq/GWe.y)	Distribution coefficient (ml/g)	Ingestion dose coefficient (Sv/Bq)
^{3}H	12.3	7.4×10^{10}	0	1.8×10^{-11}
^{14}C	5730	4.81×10^{12}	20	6.2×10^{-12}
^{59}Ni	75000	6.29×10^{11}	100	6.3×10^{-11}
^{99}Tc	212000	5.55×10^{8}	10	6.4×10^{-10}
^{129}I	1.7×10^7	1.11×10^8	1	1.10×10^{-7}
^{237}Np	2.14×10^6	5.18×10^5	700	1.10×10^{-7}
^{239}Pu	24400	1.59×10^{10}	2000	2.5×10^{-7}

Table 4.2: Different barriers and their mean time to failure (MTTF)

Notation	Barrier	MTTF(years)
A	Top cover	25
B	Waste container	12.5
C	Waste form	300
D	Backfill	30
E	Bottom cover	15
F	Near field geo-sphere	$R_d T_r$

4.3.1.4 Radiological model

The radiation dose due to the consumption of groundwater and also the risk due to radiation are evaluated from the radiological model. The radiation dose due to the radionuclide through the drinking water pathway is calculated as the product of concentration of radionuclide in the ground water, drinking water intake and the ingestion dose coefficient. For the analysis, the dose limit estimated from the model is compared with the dose limit recommended by the International Commission of Radiological Protection (ICRP, 1990). Further, the risk to a member of the critical group from the disposal practice is evaluated by considering the effect of risk factor and ingestion dose coefficient. The total risk factor to the public as recommended by International Commission of Radiation Protection (ICRP) is 7.3×10^{-5} mSv^{-1}. This risk factor includes risk due to fatal cancer, non-fatal cancer and severe hereditary effects. The product of the risk factor and the dose received gives the risk to the critical individual. The estimated risk is compared with the normal risk in a modern society. The results from radiological model quantifies the performance

of radioacive waste disposal facility.

Table 4.3: Geohydrological and transport properties considered for the study

Parameter	Unit	Value
Bulk density (ρ_b)	g/cc	1.7
Porosity (θ_g)	-	0.3
Longitudinal distance parallel to the flow (x)	m	300
Groundwater velocity	cm/s	1.16×10^{-4}
Dispersivity (α)	cm	100
Thickness of unsaturated zone	cm	200
Water intake	l/day	2.2
Risk factor	mSv^{-1}	7.3×10^{-5}
Aquifer thickness (H)	cm	600
Aquifer cross sectional area (A)	cm^2	1.0×10^6
Seepage velocity of unsaturated zone (U_z)	cm/s	1.16×10^{-8}

4.4 Results and discussion

The domain considered for the analysis is presented in the Figure 4.3. As indicated earlier, the failure of barrier system leads to release of radionuclides into geosphere. In the Figure 4.3, it can be observed that, the radionuclides reach the aquifer system and migrates towards the nearby biosphere. The end-point of assessment is located at a distance of 1.6 km from the facility (Nair and Krishnamoorthy, 1999). To perform the analysis, the four components of performance assessment model are programmed in MATLAB and the program accounts for all the scenarios: single dump - 1D transport model, single dump - 2D

transport model, multiple dump - 1D transport model and multiple dump - 2D transport

model. By running the program for each case, the results for radioactive release rate, con-

centration of radionuclide in the groundwater, radioactive dose to the critical individual

through groundwater are estimated.
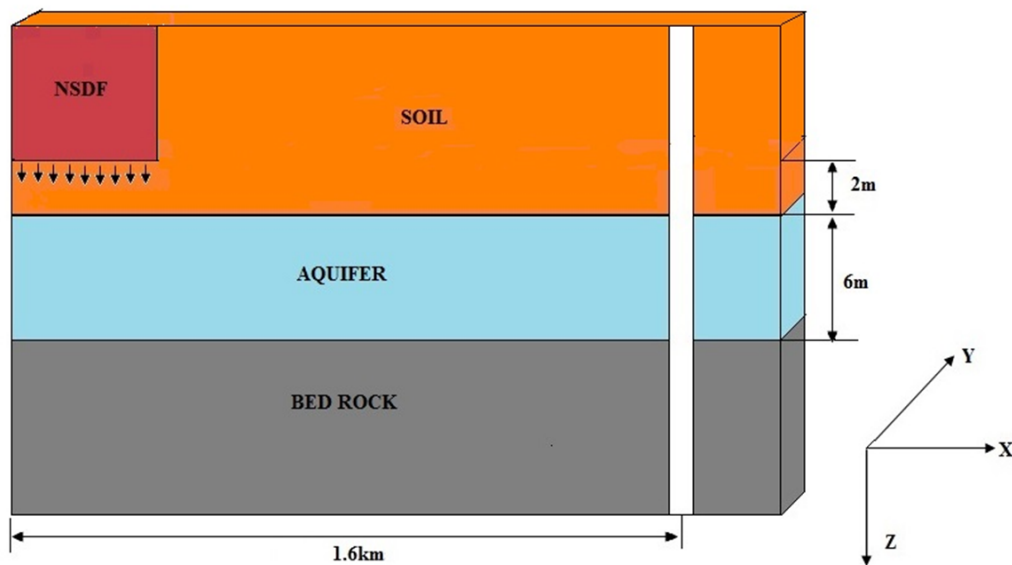
Figure 4.3: Domain considered for the present study

4.4.1 Singele dump mode

The radioactivity release rate of seven radionuclides into the groundwater are computed

using equation (4.3). The evolution of release rate over time is shown in Figure 4.4. From

the figure, it can be noted that the highest release rate is delivered by ^{14}C due to its low

retardation factor and high inventory value. The lowest release rate is delivered by ^{239}Pu

as the retardation factor is high and inventory is low. Except for ^{3}H which is a short-lived

radionuclide, the other radionuclides continue to release their activity for long periods

depending on their half-lives. The total annual release rate of all the radionuclides attain

a maximum of 4×10^9 Bq/GWe.y at 10^3 years and declines further to lower levels.
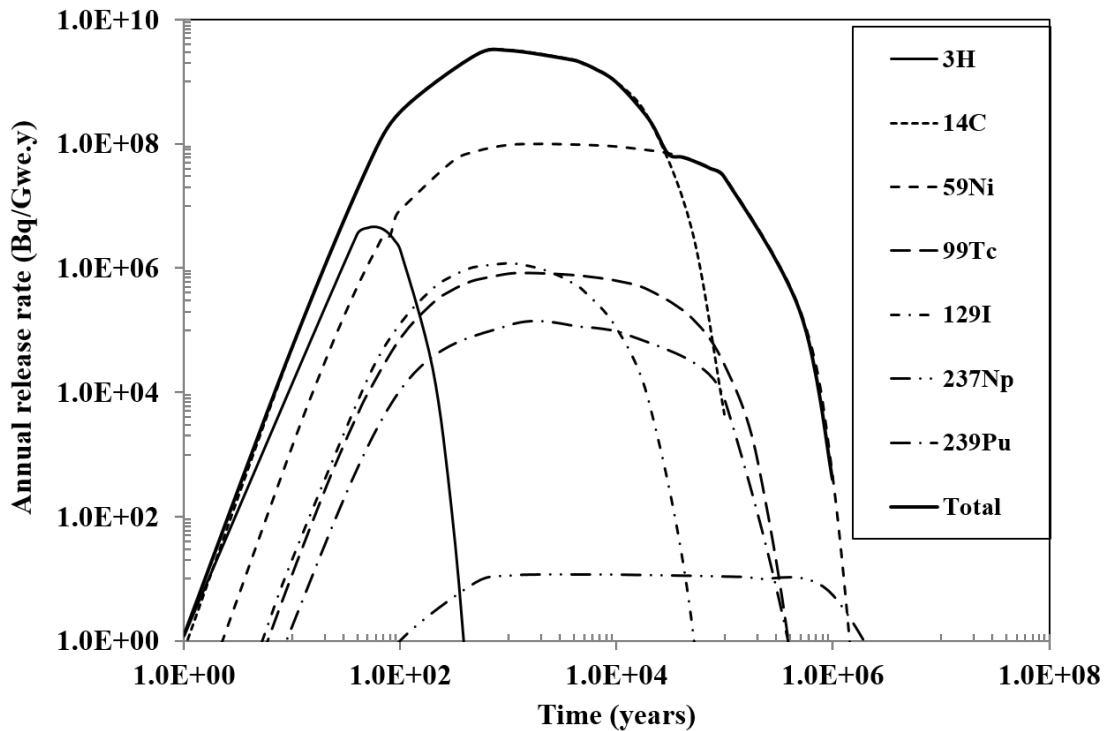
Figure 4.4: Time history of radioactivity release rate into groundwater for single dump mode

From two-dimensional dispersion model given in equation.4.7, the radionuclide concentrations are computed. The evolution of radionuclide concentration over time at the end-point shown in Figure 4.5. The results show that the concentration of radionuclide at any distance depends on radionuclide inventory, half-life, sorption capacity and transit period to reach that end-point. Since most of the radionuclides considered for the analysis are long-lived, they reach 1.6 km distance with significant concentrations. The highest concentration is delivered by ^{14}C (1.85^{-1} Bq/ml) followed by ^{59}Ni (8.3×10^{-3} Bq/ml), ^{129}I (1.3×10^{-4} Bq/ml), ^{99}Tc (8.89×10^{-5} Bq/ml) and ^{3}H (4.13×10^{-5} Bq/ml). The maximum concentrations of these radionuclides occur between 1×10^{2} and 2.8×10^{4} years. All these four radionuclides are less sorbing. The concentration of the long-lived and high sorbing radionuclides such as ^{237}Np and ^{239}Pu are 1.18×10^{-9} Bq/ml and 5.21×10^{-12} Bq/ml respectively which are quite low in comparison to other radionuclide concentra-

tions.
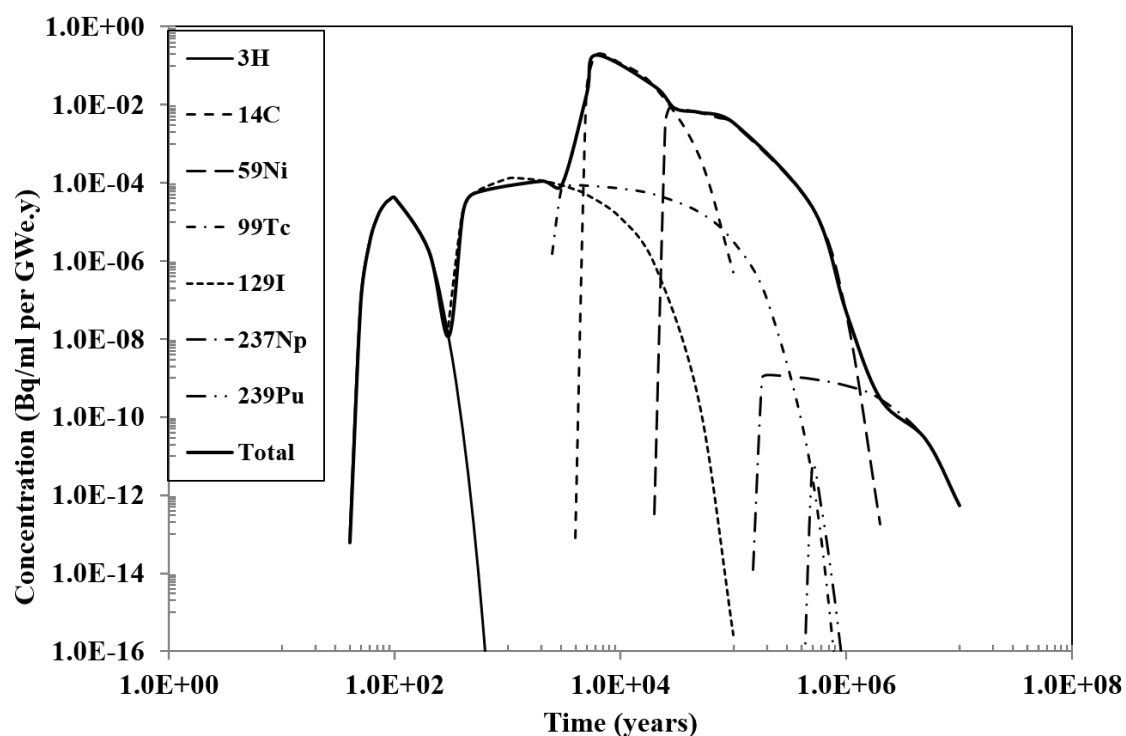
Figure 4.5: Time history of radionuclide concentration into groundwater at 1.6 km parallel to flow for single dump mode

During the later periods when the concentration of 14^C starts decreasing, the contribution from ^{59}Ni becomes significant. The time-history of annual effective dose in groundwater at 1.6 km away from the facility is shown in Figure 4.6. The maximum concentration and maximum dose rate values for single dump mode for ^{3}H, ^{14}C, ^{59}Ni, ^{99}Tc, ^{129}I, ^{237}Np and ^{239}Pu are given in Table 4.4. It is observed that the maximum annual dose is contributed by ^{129}I (1.15×10^{-2} mSv) at 1.2×10^3 years after disposal, followed by ^{14}C, ^{59}Ni and ^{99}Tc. The doses delivered by ^{3}H, ^{237}Np and ^{239}Pu are low owing to low ingestion dose coefficient (in case of ^{3}H) and low inventory and high K_d value (in case of ^{237}Np and ^{239}Pu). The dose during the first 150 years is dominated by ^{3}H, between 50 and 1.5×10^4 years by ^{129}I and beyond 1.5×10^4 years by ^{59}Ni.

174

Table 4.4: Maximum concentration and maximum dose for single dump mode

Radionuclide	Maximum concentration(Bq/ml)	Maximum Dose(mSv/y)	Arrival time of maximum(y)
Singledump mode- 1D dispersion transport model			
^{3}H	4.9×10^{-5}	7.14×10^{-7}	1.0×10^2
^{14}C	2.24×10^{-1}	1.12×10^{-3}	6.0×10^3
^{59}Ni	1.01×10^{-2}	5.09×10^{-4}	2.8×10^4
^{99}Tc	1.07×10^{-4}	5.56×10^{-5}	4.0×10^3
^{129}I	1.54×10^{-4}	1.39×10^{-2}	1.3×10^3
^{237}Np	1.46×10^{-9}	1.27×10^{-7}	2.0×10^5
^{239}Pu	6.63×10^{-12}	1.34×10^{-9}	5.0×10^5
Singledump mode- 2D dispersion transport model			
^{3}H	4.19×10^{-5}	6.05×10^{-7}	1.0×10^2
^{14}C	1.85×10^{-1}	9.29×10^{-4}	6.0×10^3
^{59}Ni	8.3×10^{-3}	4.15×10^{-4}	2.8×10^4
^{99}Tc	8.89×10^{-5}	4.57×10^{-5}	4.0×10^3
^{129}I	1.3×10^{-4}	1.14×10^{-2}	1.3×10^3
^{237} Np	1.18×10^{-9}	1.05×10^{-7}	2.0×10^5
^{239}Pu	5.21×10^{-12}	1.05×10^{-9}	5.0×10^5

4.4.2 Multiple dump mode

The radioactivity release rate of seven radionuclides into the groundwater is computed using equation (4.4) and equation (4.5). The trends of release rate evolving over time is shown in Figure 4.7. The results indicate that, ^{14}C delivers the maximum release rate and ^{237}Np delivers the lowest release rate in the case of multiple dump mode. The same trend was observed in single dump mode of disposal. The total annual release rate of all the radionuclides attain a maximum of 4×10^9Bq/Gwe.y at 10^3 years and then declines

to lower levels (see Figure 4.7). The maximum concentration and maximum dose rate values for multiple dump mode of the seven radionuclides are given in Table 4.5.
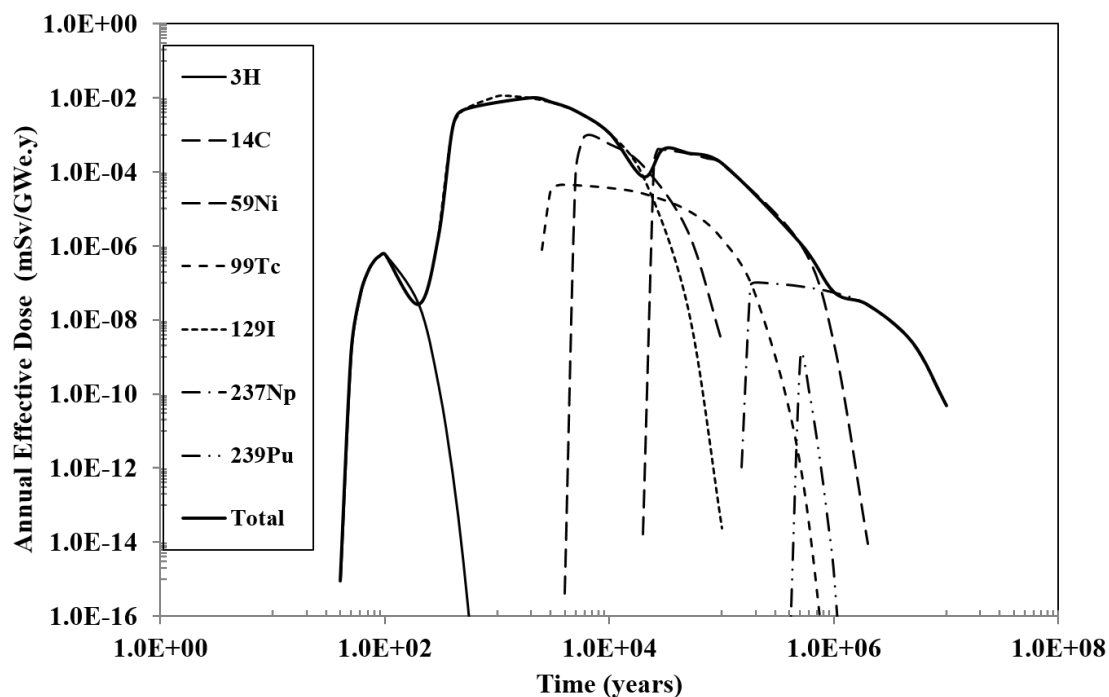
Figure 4.6: Time history of annual effective dose into groundwater at 1.6 km parallel to flow for single dump mode

Using the equations (4.6) and (4.7) (i.e., one-dimensional and two-dimensional dispersion models), the concentration of radionuclides in groundwater is computed. However, unlike single dump mode, the concentration and annual radiation dose are computed in two phases ie., during dumping period and post closure period. Using equation (4.10) and (4.12), the results of contaminant transport in one-dimensional dispersion model are calculated. Similarly, by solving the convolution integral in equation (4.11) and (4.13), the results of contaminant transport in one-dimensional dispersion model is calculated. From the analysis, it can be observed that, the highest concentration is delivered by ^{14}C (2.28×10^{-1} Bq/ml) followed by ^{59}Ni (8.28×10^{-3} Bq/ml), ^{129}I (1.3×10^{-4} Bq/ml), ^{99}Tc (8.89×10^{-5} Bq/ml) and ^{3}H (2.28×10^{-4} Bq/ml). The maximum concentrations of these

176

radionuclides occur between 6×10^1 and 6.0×10^5 years. The maximum annual dose is contributed by ^{129}I (1.17×10^{-2} mSv) at 1.4×10^3 years after disposal followed by ^{14}C , ^{59}Ni and ^{99}Tc.
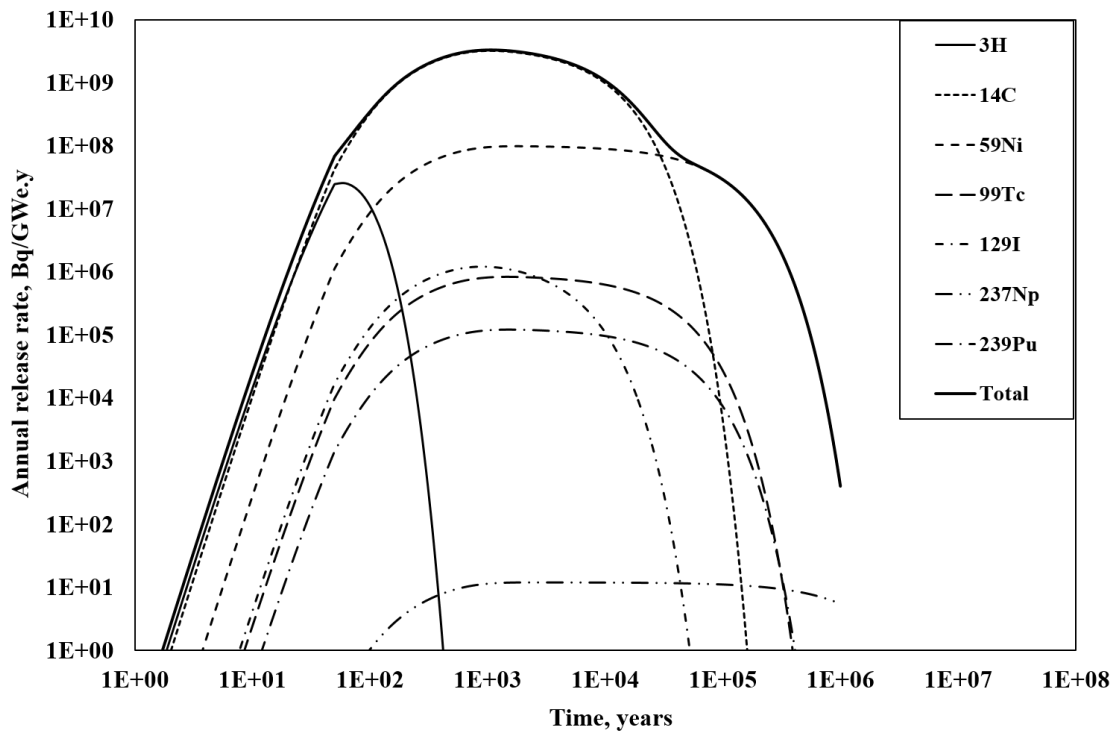
Figure 4.7: Time history of radionuclide release rate into groundwater at 1.6 km parallel to flow for multiple dump mode

From Table 4.4 and 4.5, it can be noted that, the maximum concentration values of long-lived radionuclides remains same and unaffected by the mode of disposal. However, small variations in the values are expected only for short-lived radionuclides like ^{3}H and for short distances from the facility. The dimensionality of transport process has a marginal effect on the overall concentrations. The concentrations computed from 1D model are slightly higher (around 16%) than the concentrations computed from 2D model. The reduction in concentration for 2D model could be because of the dispersion of radionuclide in both the direction. Also, the effect of uncertainty in evaluation of the cross-sectional area of aquifer and the assumption of uniform lateral mixing in the ana-

lytical case affect the results to some extent.

Table 4.5: Maximum concentration and maximum dose for multiple dump mode

Radionuclide	Maximum concentration(Bq/ml)	Maximum Dose(mSv/y)	Arrival time of maximum(y)
Multipledump mode- 1D dispersion transport model			
^{3}H	2.74×10^{-4}	3.9×10^{-6}	1.0×10^2
^{14}C	2.28×10^{-1}	1.15×10^{-3}	6.05×10^3
^{59}Ni	1.1×10^{-2}	5.09×10^{-4}	2.8×10^4
^{99}Tc	1.05×10^{-4}	5.56×10^{-5}	4.0×10^3
^{129}I	1.58×10^{-4}	1.39×10^{-2}	1.27×10^3
^{237}Np	1.45×10^{-9}	1.28×10^{-7}	2.0×10^5
^{239}Pu	6.03×10^{-12}	1.23×10^{-9}	6.0×10^5
Multipledump mode- 2D dispersion transport model			
^{3}H	2.28×10^{-4}	3.4×10^{-6}	1.0×10^2
^{14}C	1.87×10^{-1}	1.57×10^{-5}	6.05×10^3
^{59}Ni	8.28×10^{-3}	4.3×10^{-4}	2.8×10^4
^{99}Tc	8.89×10^{-5}	4.6×10^{-5}	4.0×10^3
^{129}I	1.3×10^{-4}	1.17×10^{-2}	1.27×10^3
^{237}Np	1.18×10^{-9}	1.06×10^{-7}	2.0×10^5
^{239}Pu	5.21×10^{-12}	1.06×10^{-9}	6.0×10^5

From the deterministic analysis, it is evident that ^{14}C is one of the critical radionu-clides that exhibits the maximum concentration in the groundwater. the risk to a member of critical group is computed as mentioned in section 4.3.1.4. The risk estimated from the analysis is low in comparison to the risk due to natural catastrophes which falls in range 10^{-3} - 10^{-4} y^{-1}. The average annual dose due to natural background radiation is estimated to be 2.4 mSv world-wide. The corresponding risk due to natural back-

ground radiation can be estimated using the ICRP total risk factor (7.3×10^{-5} mSv^{-1}) as $1.8 \times 10{-4}$ y^{-1}. However, there is a need to incorporate the effect of uncertainty in modelling the performance of complex systems. The reason being, the impact of these uncertainties are particularly important in the assessment of several potential regulatory options. The uncertainty greatly affects the predictive ability of groundwater flow and contaminant transport models (Chopra, et. al., 2013). So, by accounting for physical parameter uncertainty in transport models the contaminant plume can be delineated and the time frames for remediation scheme can be estimated. So, ^{14}C is considered for probabilistic analysis and the various methods implemented for handling the uncertainties in the system are presented in the following sections.

4.5 Probabilistic analysis

Probabilistic analysis forms an integral of performance assessment model. So, in this study, the uncertainties in the geological and transport parameters of the medium is characterized propagated and quantified by employing efficient probabilistic techniques. An overview of the steps followed for the probabilistic analysis is presented in Figure 4.8. From the Figure 4.8, it can be noted that the random input parameters are propagated through the system and new surrogate models (meta-models) are constructed based on collocation based stochastic response surface method (CSRSM). Further, reliability analysis is employed to quantify the uncertainties and estimate the reliability index for the NS-DFs.The uncertainties are characterized, propagated and quantified using efficient probabilistic techniques in the next section.
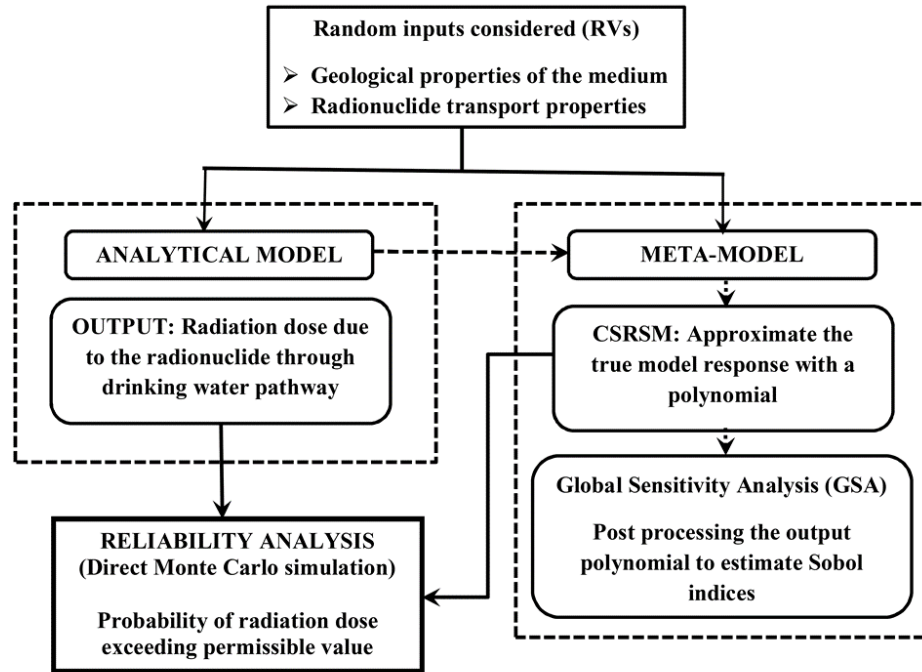
Figure 4.8: Sequence of steps followed in probabilistic analysis

In this chapter, only parametric uncertainty has been dealt and four critical parameters have been identified. They are groundwater velocity, distribution coefficient, longitudinal dispersivity and thickness of unsaturated zone and their variability. The input data of the type of distribution and ranges of values for the random variables considered are provided in Table 4.6. In the Table 4.6, a^x indicates minimum for uniform distribution; geometric mean for lognormal distribution; mean for normal distribution. b^y indicates maximum for uniform distribution and geometric standard deviation for lognormal distribution; standard deviation for normal distribution.

4.5.1 Collocation based Stochastic Response Surface Method

To propagate and quantify the uncertainties, collocation based stochastic response surface method is implemented. The steps followed in this method is discussed in section 3.5.2 of chapter 3. In this method, the complex analytical model is replaced by surrogate model

which is a function of uncertain input parameters. Based on the order of polynomial and number of uncertain parameters, the number of terms in the polynomial (surrogate model) is estimated. For example,the total number of terms in a function with four random variables and a third order polynomial, is obtained from equation (3.49) as 35.

Table 4.6: Statistical properties of the input parameters considered for the study

Parameter	Range	a^x	b^y	COV (%)	Distribution
Distribution coefficient (ml/g) K_d	10-50	10	30	-	Uniform
Groundwater velocity (cm/s) g_w	10^{-6}-10^{-3}	0.0005	0.00025	50	Lognormal
Longitudinal dispersivity (cm) α_L	10-500	255	122.5	48	Lognormal
Thickness of unsaturated zone (cm) z	100-400	250	75	30	Normal

The annual dose rates of radionuclide are approximated by second and third order polynomials where each of the four input random variables influencing the response are transformed to the standard space and take the values of the roots of the univariate Hermite polynomials of the higher order. The total number of collocation points decides the number of simulations required to generated the polynomial. It is calculated from the equation (3.52). In this study, all the collocation points are used to obtain the coefficients. To check the accuracy of the surrogate model (approximated polynomial) with the actual model, coefficient of determination is estimated (from equation (3.53)). The results for all the four cases are presented in Table 4.7.

Table 4.7: R^2 values for different polynomials

S.No	Order of polynomial	R^2			
		Single dump 1D	Multiple dump 1D	Single dump 2D	Multiple dump 2D
1	2nd order polynomial	0.95	0.95	0.95	0.96
2	3rd order polynomial	0.99	0.99	0.99	0.99

From the Table 4.7 it can be noted that, third order polynomial provided the best possible output response with an R^2 of 0.99. The computation is extended till 4th order polynomial (70 coefficients) which gave approximately the same R^2 value as 3rd order. But owing to more computational effort, the analysis was restricted to 3rd order polynomial. To check the accuracy of the polynomial functions, direct simulation (using equation (4.12) and (4.13) from analytical model) is carried out by using Monte Carlo simulation (10000 runs). Using CSRSM, only 81 and 625 collocation points were sufficient to generate the second and third order polynomials respectively. Comparisons of second and third order polynomials with direct simulation for all the four cases are presented in the form of cumulative distribution function (CDF) of dose rate of radionuclide (^{14}C) in Figures 4.9 - 4.12.

For one-dimensional case
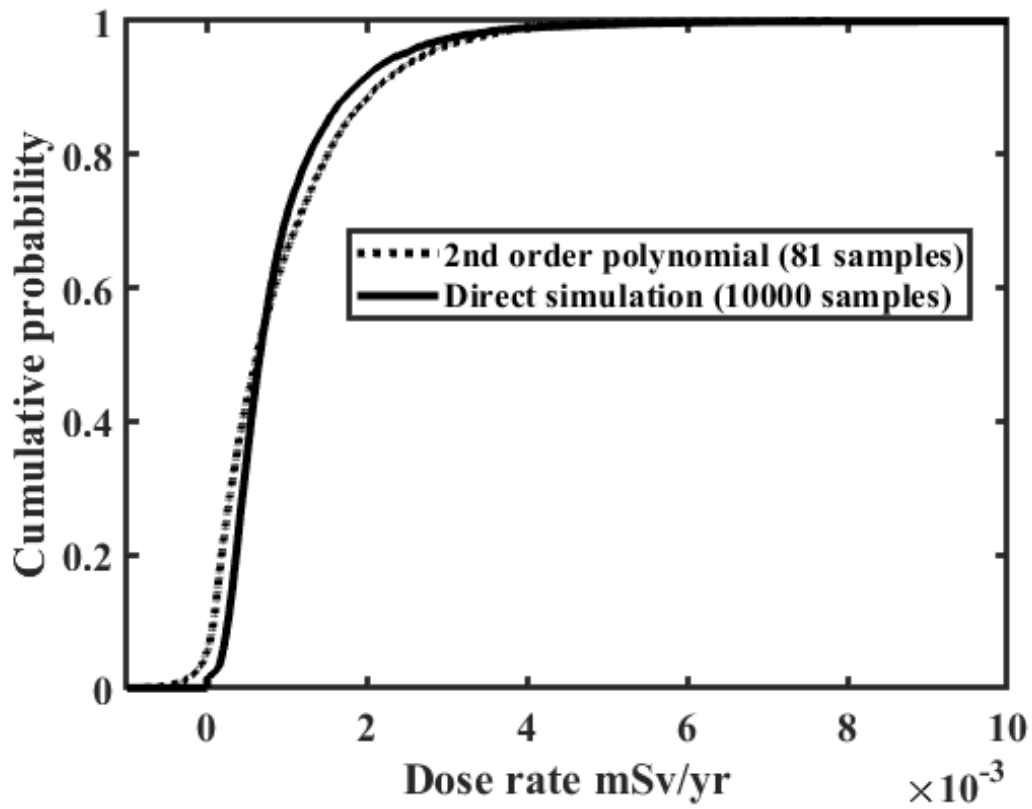
(i) 2nd order polynomial
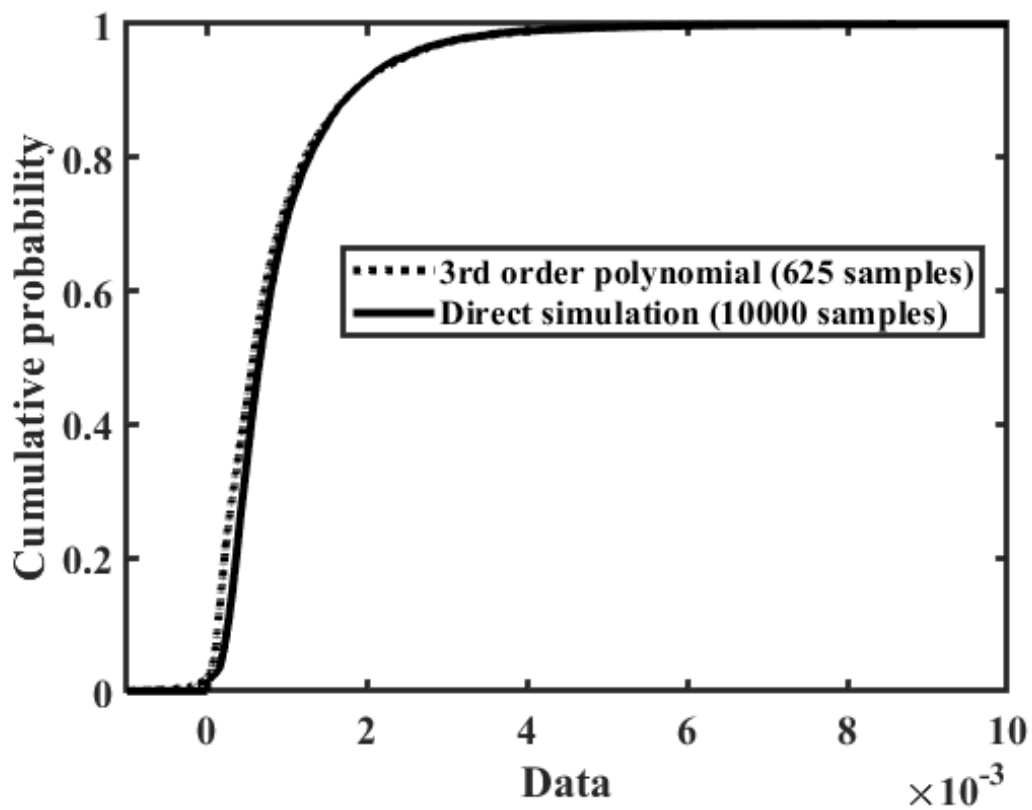
(ii) 3rd order polynomial

Figure 4.9: Comparison of Direct simulation with CSRSM for single dump 1D mode of disposal

183
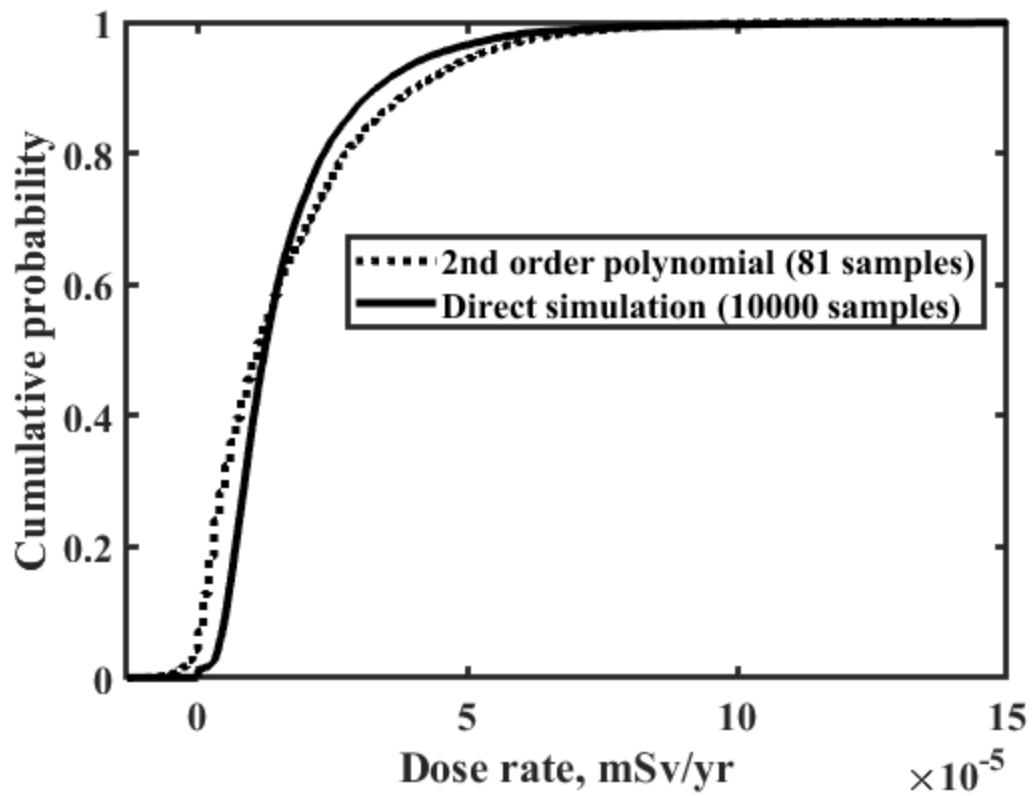
(i) 2nd order polynomial

(ii) 3rd order polynomial

Figure 4.10: Comparison of Direct simulation with CSRSM for multiple dump 1D mode of disposal

For two-dimensional case
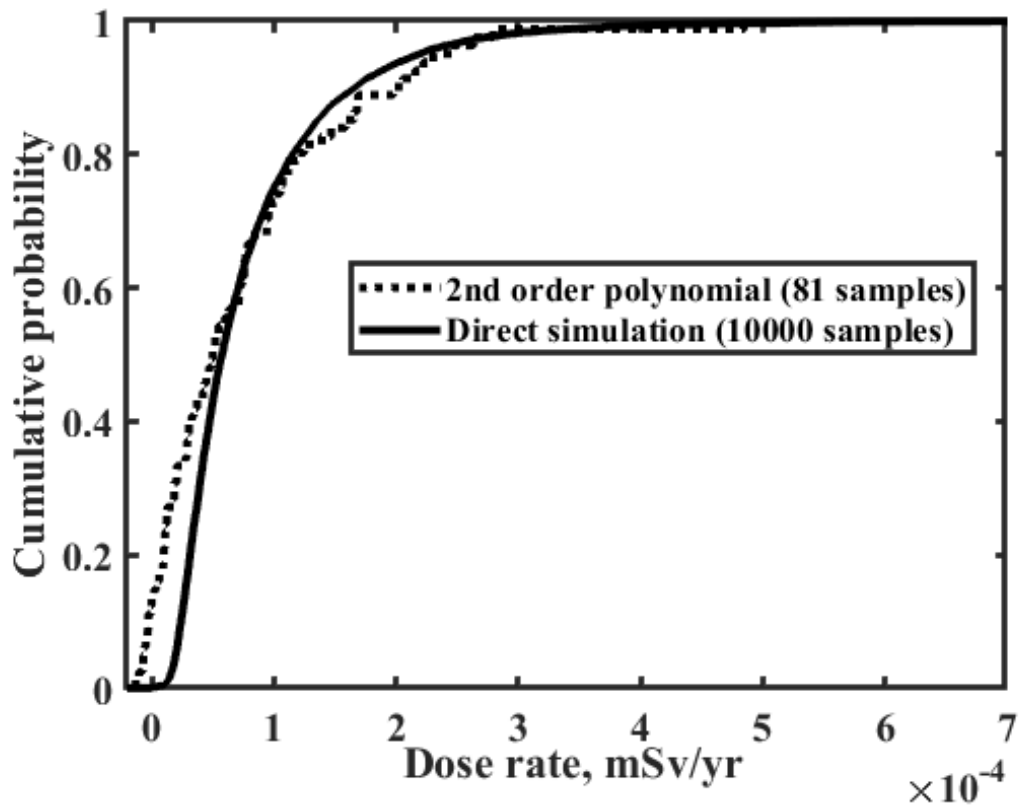
(i) 2nd order polynomial
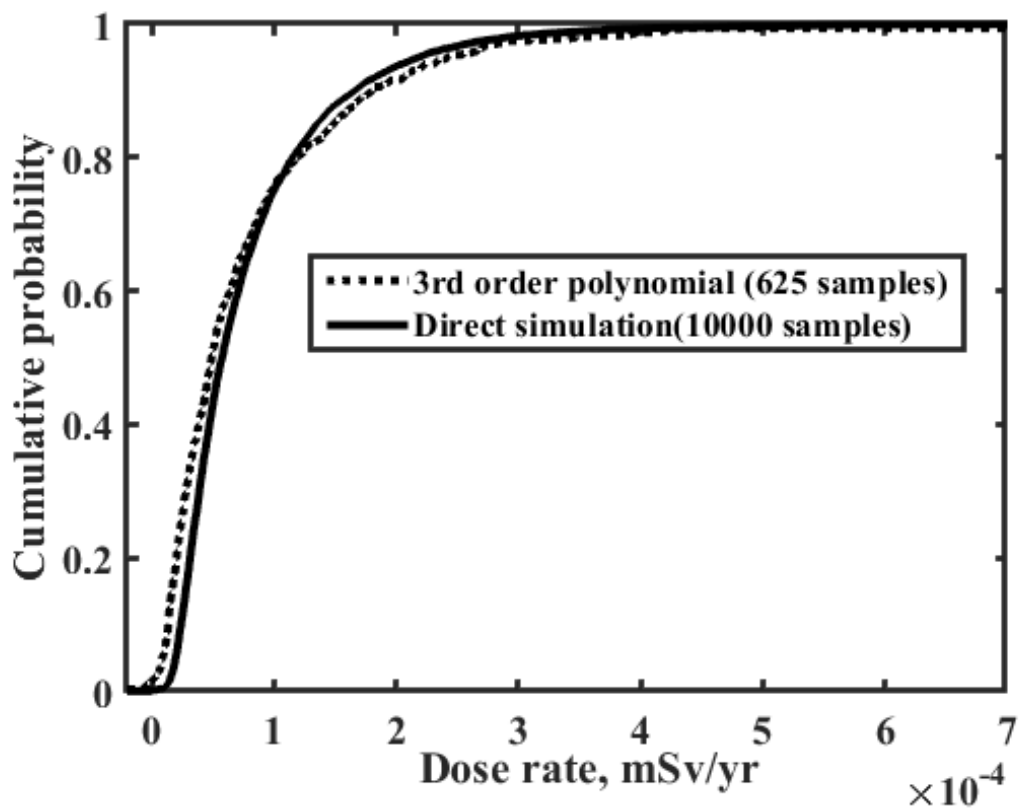
(ii) 3rd order polynomial

Figure 4.11: Comparison of Direct simulation with CSRSM for single dump 2D mode of disposal
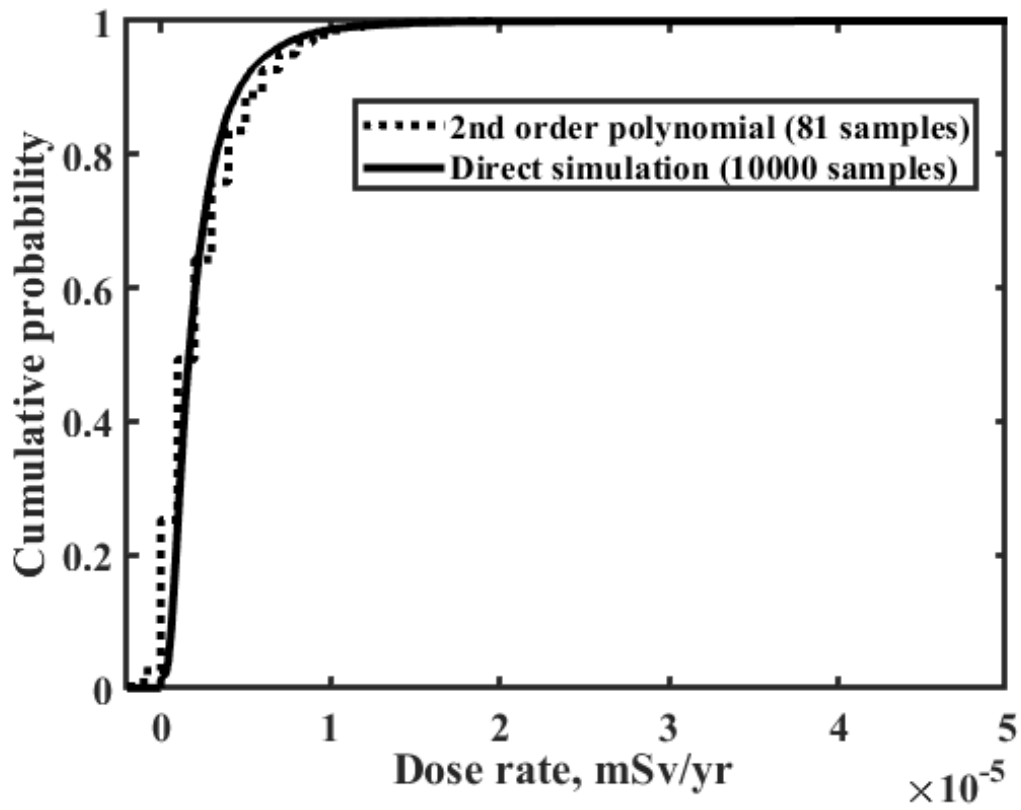
(i) 2nd order polynomial
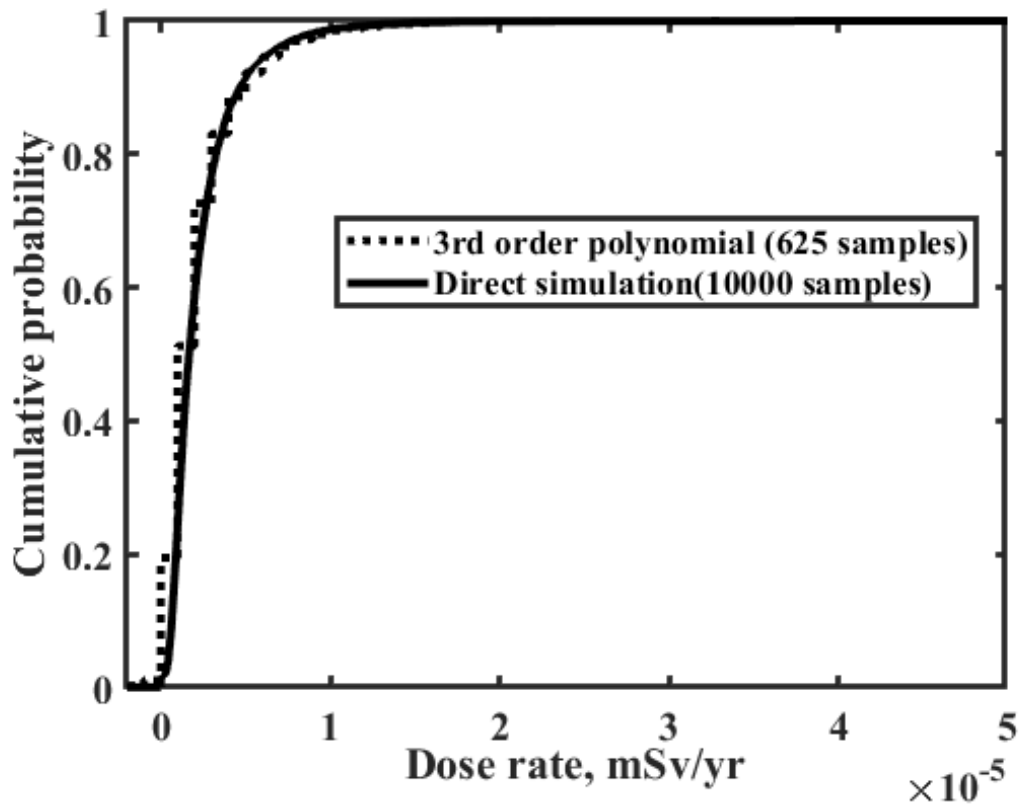
(ii) 3rd order polynomial

Figure 4.12: Comparison of Direct simulation with CSRSM for multiple dump 2D mode of disposal

The dashed lined in these Figures represents the CDF of annual dose rate estimated from CSRSM and, the solid line represents CDF of annual dose rate estimated from actual model (i.e., analytical model). From the plots, it is evident that CDF from third order polynomial matches well with the actual response. Also, it is observed that, CSRSM simulated the output distribution (expressed as a function of four variables) from less number of simulations when compared to direct simulation through Monte Carlo method. This study demonstrates the computational efficiency of CSRSM.

4.5.2 Reliability Analysis

In a complex structural system like a near surface disposal facility, the amount of radionuclide released into the groundwater through drinking water pathway is a major concern for their post closure safety. To estimate the effect of migration, it is worthwhile to know the probability of the radiation dose in the drinking water pathway of a particular radionuclide reaching an expected value as the parameters for the estimation of dose are random variables. The expected concentration released into groundwater is also a random variable and it is useful in assessing the risk to human society. Reliability of a system is defined as probability of safety of the system under given environment and loading conditions. The limit state function, $g(X)$ is defined in terms of the basic random variables $X_i = [X_1, X_2, X_3, X4]$, and the functional relationship among them. The failure condition is defined as

$$g(X) = [D_r - D(X)] < 0 \tag{4.14}$$

where D_r is maximum permissible radiation dose in the drinking water pathway (the maximum effective annual radiation dose possible over time) and $D(X)$ is the function

187

of the four uncertain input parameters. Monte-Carlo simulations are run to estimate the probability of failure (P_f) .

For the reliability analysis radioactive carbon (^{14}C) is considered it delivers the maximum concentration in the groundwater. The permissible values of radiation dose considered in this study for different modes of disposal is assumed as a factored value of the typical regulatory threshold 1mSv/yr (IAEA, 2011). To get a good estimate of probability of failure through this method, 10,000 simulations are run. The P_f for all the cases are of the order of 10^{-3}. Most importantly, the computational time taken to estimate the P_f from the analytical solution is very high when compared to that of CSRSM equation. The efficiency of the probabilistic methodology (CSRSM) in reducing the computational time is manifested from these values. The P_f values estimated for all the four cases are provided in Table 4.8.

Table 4.8: Comparison of probability of failure for different cases

Dumping mode	Number of simulations	Permissible value of radiation dose (mSv/GWe.y)	Probabilitiy of failure	Reliability index	Time for computation using mathematical equation(s)	Time for computation using CSRSM equation(s)
Single dump 1D	10000	0.004	0.0075	3.43	2182.4	1.06
Single dump 2D	10000	9.2215×10^{-4}	0.0083	3.39	2357.5	1.07
Multiple dump 1D	10000	7.5553×10^{-5}	0.0085	3.38	2863.5	1.06
Multiple dump 2D	10000	1.5747×10^{-5}	0.0025	3.807	3332.9	1.10

The values of P_f are used to gauge if a reasonable level of assurance (reliability of system) is achieved in the design. It can be observed that the simulation time taken to determine the reliability of the system from the analytical solution varies from 2182 - 3332 seconds (nearly 40 minutes). However, when analytical model is replaced with 3rd order polynomial (from CSRSM), the computation time taken is just one second. So, in

this chapter, an improved performance assessment model is developed which requires the

computational effort and time over the complex mathematical model. Since the reliability

index is high, the barrier system is designed efficiently and the radiological impact due to

leaching of radionuclide (^{14}C) through drinking water pathway is almost negligible.

4.5.3   Global Sensitivity Analysis

In a contaminant transport process there are many parameters that influence the concentration of contaminant and some of them are critical in affecting its behaviour. Sensitivity

analysis is performed to identify and rank in order of importance the uncertainties with

respect to their impact on the uncertainty of the performance measures of interest. One

of the early works by Cawlfield et. al., (1993) presented a probabilistic sensitivity analysis for a 1D and 2D reactive solute transport in porous media. Sudret (2008) presented a

method of Global Sensitivity Analysis (GSA) by Polynomial Chaos Expansion and calculated the Sobol indices. In this method, the sobol indices are estimated by post-processing

the polynomial computed from CSRSM. Using GSA (i.e., by post processing the results

obtained from CSRSM), the critical parameters affecting the system are obtained.

Using equation (3.71) in chapter 3, the sobol indices are calculated for all the four

cases. From Figure 4.13, the parameter that has maximum effect in influencing radiation

dose is the distribution coefficient and its sobol index lies in the range 0.38 - 0.42 (for all

the scenarios). The sobol index for thickness of unsaturated zone lies in the range of 0.16-

0.17 suggesting a slight effect of this parameter as well on the radiation dose. The values

becomes slightly lesser for groundwater velocity and almost negligible for longitudinal

dispersivity indicating that these parameters are insignificant in affecting the radiation

dose.
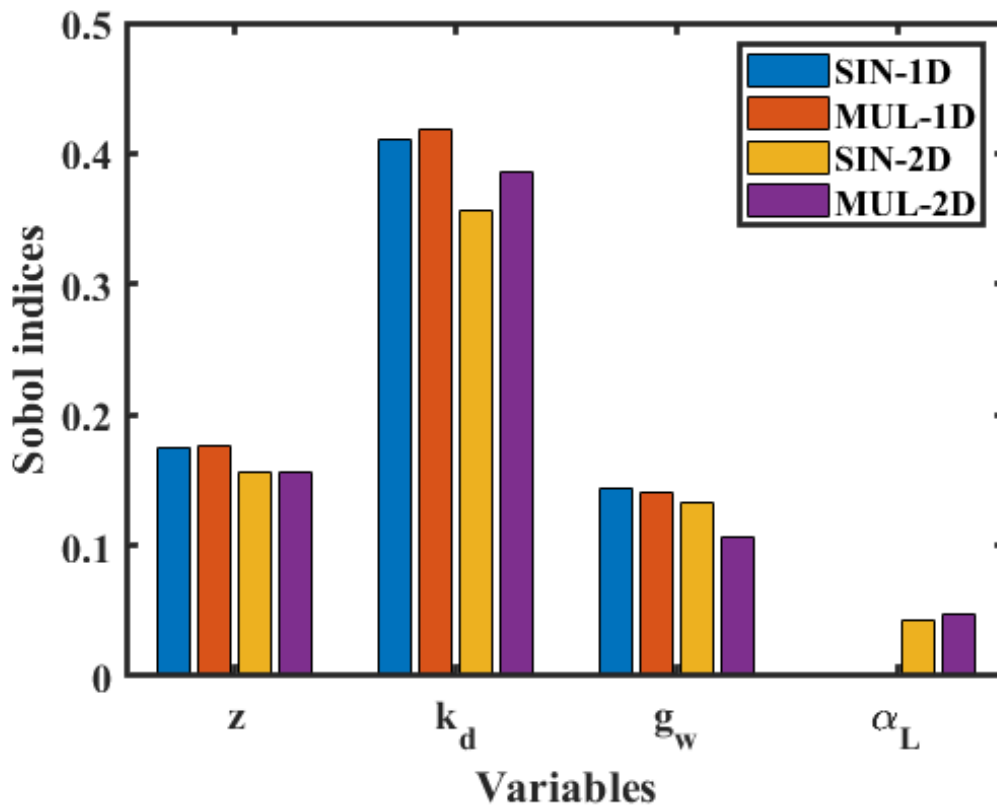
Figure 4.13: Sobol indices for different modes of disposal

4.6 Concluding remarks

In this chapter, a framework for an efficient probabilistic performance assessment of near surface disposal facilities is developed. The components of performance assessment model are programmed in MATLAB to estimate the radionuclide release, radionuclide concentration, dose rate of radionuclides in groundwater. The mathematical formulations in this model accounted for the influence of mode of disposal and the dimension of radionuclide dispersion model to generate four scenarios of modelling. They are single dump - 1D, single dump - 2D, multiple dump - 1D and multiple dump - 2D models. Further, uncertainty and sensitivity analyses are carried out to quantify the effect of uncertainties in the geological and transport parameters of geosphere.

1. The maximum concentration/release rate in ground water is delivered by radioactive carbon (^{14}C) and and maximum effective dose is observed in radioactive iodine ^{129}I in all the four scenarios due to their low distribution coefficient and high half-life values.

2. Risk evaluated for far field scenario (for seven radionuclides) is compared with the risk due to industrial failures / catastrophes and it was observed the values are within safe limits.

3. The uncertainties associated with input parameters (distribution coefficient, dispersivity, groundwater velocity and thickness of unsaturated zone) are characterized and surrogate models are developed using CSRSM for radiation dose as a function of the input parameters in all the four scenarios. Third order polynomial gave the best fit for the deterministic model and R^2 is 0.99.

4. The probability of radiation dose exceeding the permissible value is estimated as 10^{-3} for all the cases from reliability analysis. The computational time taken to estimate the probability of failure was reduced significantly when the analytical model was replaced with CSRSM. So, a computationally efficient model is developed in this chapter to analyse the system's performance. Since the P$_f$ value is low, it can be assured that the barrier system is designed efficiently and the effect of leaching of radionuclide (^{14}C) through drinking water pathway is negligible.

5. By performing global sensitivity analysis, the sobol indices for the four random variables are estimated. In all the four cases, the critical parameter affecting the model response is determined as distribution coefficient.

Chapter 5

Probabilistic analysis of radionuclide transport for radioactive waste disposal facilities in soil

5.1 Introduction

In many countries around the world, disposal of radioactive waste in containment systems is the benchmark solution for radioactive waste management. The safety standards report for NSDFs (IAEA, 2004) mandates the development of safety assessment models to protect people and environment. The extent of safety achieved from these model results decides the approval of the radioactive waste disposal practice. In the previous chapter, an analytical model was considered to estimate the risk and radiological impact due to intrusion of radionuclide into geological medium (soil). The parametric uncertainties were propagated through the model using meta-modelling techniques and computationally efficient surrogate models were developed. Also, reliability analysis and sensitivity analysis were carried out to quantify the probability of failure and estimate the critical parameters affecting the safety of barrier system respectively. As mentioned in Section 3.2, each component of performance assessment model (i.e., source term, repository failure, geosphere transport etc) is a combination of various processes. So, it becomes important to

identify the critical ones amongst these components that can influence the dose rates of radionuclides. This can be decided based on the sensitivity of each component to the overall response. For example, let us examine the sensitivity of *source term* and the *geosphere transport*. Generally, the source term is used to express the inventory value of the radioactive waste at any given time after disposal. This is conceptually simple when compared to geosphere transport which requires detailed characterization of the geological medium, transport parameter values for accurate prediction of the process. In particular, insufficient characterization of subsurface hydrological and chemical properties of the system often complicates the development of conceptual models, simulation strategies, and domain and boundary conditions. Further, the transport process is affected even more due to heterogeneity in the soil medium. So, in this chapter performance assessment models have been developed focussing primarily on simulating the migration process of low and intermediate level radioactive wastes through a complex, heterogeneous soil medium following the radioactive release from Near Surface Disposal Facilities (NSDFs). Also, this model aims at quantifying the effect of uncertainties in the form of parameter uncertainty and spatial variability by adopting advanced probabilistic techniques.

In chapter 4, the geosphere transport modelling through soil was solved analytically for one-dimensional and two-dimensional domain. However, with the increase in the dimensionality of the problem, heterogeneity in the medium, fractures in the rocks, seasonal variations in rainfall leading to fluctuations in groundwater table, development of analytical closed form solutions becomes challenging. So, numerical models have been developed to address these issues. They provide reliable quantitative evaluations for safety assessment of disposal systems (Nair et. al., 2010). Also, from section 2.3 of chapter 2, it is evident that the groundwater flow and radionuclide transport system can be modelled

efficiently using Finite element and subsurface flow systems (FEFLOW) to predict the concentration of radionuclide at the end-point of interest in the recent past (Jakimavičiūte-Maseliene et. al.,, 2006; Chopra et. al., 2013). So, in this chapter, a numerical model for three-dimensional radionuclide transport in geosphere is developed using FEFLOW.

Uncertainty analysis is an intrinsic part of performance assessment model as they affect the predictive ability of the models. Therefore, it becomes imperative to consider uncertainty in the geological medium to quantitatively estimate the potential impacts of radioactive disposal and also judge with what probability the radiation dose exceeds the permissible limits. There are many sources of uncertainties in existence and, they are broadly categorized as (1) epistemic and (2) aleatory uncertainties (Baecher and Christian, 2003; Der Kiureghian and Ditlevsen, 2008). They are discussed in detail in Section 3.3 of chapter 3. The epistemic uncertainty corresponds to uncertainty due to lack of knowledge in determining the actual model behaviour while the aleatory uncertainty corresponds to inherent randomness in the system that cannot be reduced. To address these uncertainties in the radionuclide transport model, and treat them by implementing appropriate probabilistic methods, the analysis carried out in this chapter is broadly divided into two subdivisions. The first part of the analysis handles parametric uncertainty and the second part handles spatial variability which is shown in Figure 5.1. In a geological medium like soil, most of the real world modelling scenarios represent the uncertainty in the geological and transport parameters due to lack of adequate data which is a classic example of parametric uncertainty. Failure to accommodate parameter uncertainty in contaminant transport models causes serious doubts on the capability to delineate the contaminant front. Studies have been carried out in the past where the parametric uncertainty was considered in the radionuclide transport models (Hoffman and Miller, 1983;

Chopra et. al., 2013). On the other hand, the very nature of origin of soil leads to spatially variable geological properties. Most of the previous studies simplify the flow and solute transport models by assuming the properties to be homogeneous and uniform resulting in conservative concept of modelling. Some of the recent studies focussed on stochastic modelling of spatial varying transport properties on the radionuclide transport (Vrankar et. al., 2004; Huysmans and Dassargues, 2006). But, these studies have not explored the effect of the heterogeneity in geological medium under the framework of performance assessment modelling for NSDFs. Also, the quantification of the influence of both parametric uncertainty and spatially varying random field on the reliability of these systems should be studied.
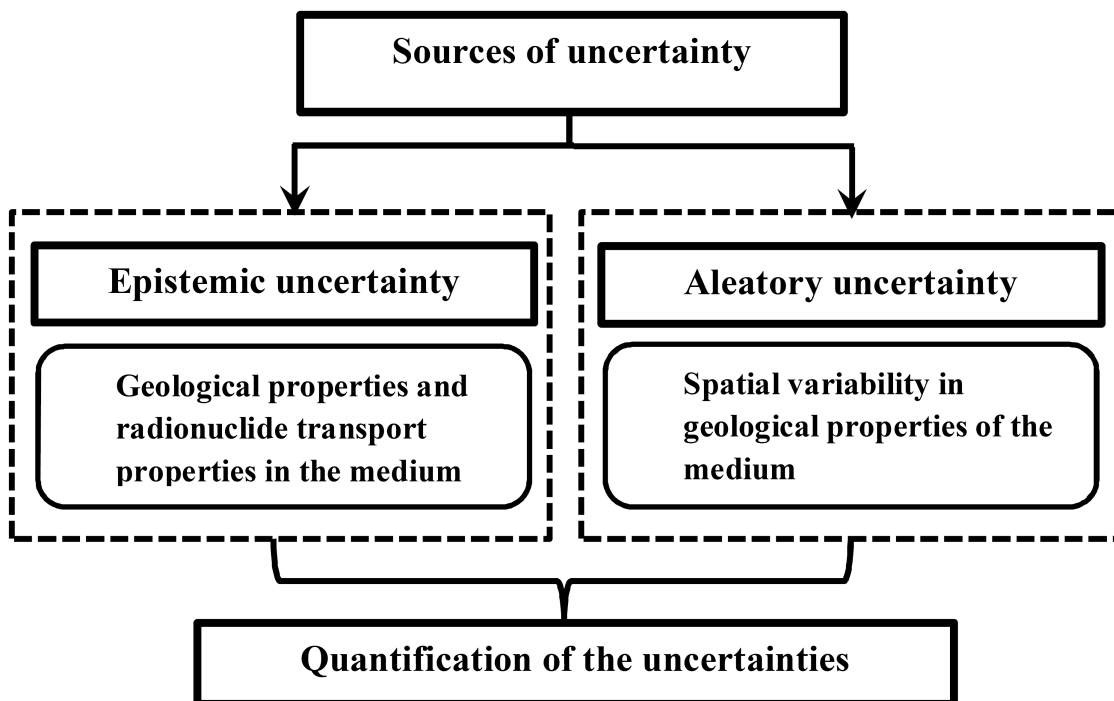
Figure 5.1: An overview of the uncertainties quantified in this study

Once the uncertainties involved in the system are recognised, it becomes useful to comprehend how the uncertainty (either aleatory or epistemic) can propagate, through model representation and, estimate their impact on the model outputs. These models can

be represented in the form of algebraic equations, integral equations, differential equations or a combination of all of them. The choice of method of uncertainty propagation depends on the computational time taken to run each simulation in the model. They can be computed using methods like Monte Carlo simulation, response surface methods etc (Chopra et. al., 2013). Further, a mathematical description of how the computational results are likely to possess certain values or to lie in a certain range of values, in the presence of model uncertainty sources can be carried out through uncertainty quantification methods. For instance, the probability of radiation dose exceeding permissible limit can by computed by adopting techniques like First Order Reliability Method (FORM) / Second Order Reliability Method (SORM), and variance reduction techniques like importance sampling, subset simulation method (Au and Beck, 2001; Cadini et. al., 2012). Furthermore, if uncertainty in a given parameter has a minimal impact on the results, the value of including it in the Monte Carlo process is outweighed by the additional computational effort. So, sensitivity analysis needs to be performed to identify the key parameters influencing the radionuclide transport and also gain a level of confidence in model results (Saltelli et. al., 2000). In this chapter, all the above mentioned aspects involved in probabilistic analysis have been integrated to quantify the uncertainties and, enable in the development of a framework for an efficient performance assessment model.

5.2 Objectives

The general framework of performance assessment for near surface disposal facilities is developed where, the geosphere transport component is modelled numerically. Uncertainty analysis is carried out using different probabilistic methods and the influence of

epistemic and aleatory uncertainties are illustrated as two subdivisions in this chapter. In the first subdivision, the framework for performance assessment of NSDF by treating the parameter uncertainties is developed and in the second subdivision, the framework for performance assessment of NSDF under the influence of spatial variability is developed. The main objectives of this study are:

1. To model the the fate and movement of radionuclides numerically and estimate the spatial and temporal variations of concentration and radiation dose of radionuclides using:

   (a) A three-dimensional radionuclide transport model that discerns the behaviour of short-lived (Strontium (^{90}Sr), Caesium(^{137}Cs)) and long-lived radionuclides (Carbon(^{14}C) and Iodine(^{129}I).

   (b) A two-dimensional numerical model to predict the radionuclide transport of Iodine ^{129}I in spatially variable medium and estimate its radiological impact.

2. To investigate the effect of (i) parametric uncertainties in the transport parameters due to radionuclide release into the geosphere and (ii) spatially varying soil properties on the radionuclide transport and their impact on the response of the system.

3. To quantify the effect of both the uncertainties and evaluate the safety limits by carrying out reliability analysis.

4. To identify the critical parameters amongst the uncertain input parameters that can cause maximum effect on the performance of the disposal system through sensitivity analysis.

5.3 Effect of parameter uncertainty on performance assessment model

Radiological impact assessments depend strongly on mathematical models. The predictions from these models are inherently uncertain due to lack reliable information about the parameters which will eventually lead to approximation (inexact representation) of real systems. Proper parameter estimation is difficult because relevant data is seldom available and these models generally employ a data base of 'default values' recommended for use in the absence of site-specific or population-specific data. However, these conservative values cannot be applied in all the cases. So, by employing stochastic methods, the parameter uncertainties can be translated into uncertainties in model predictions by treating the uncertain parameters as random variables from which a distribution of values of model output is produced. They overcome the limitations of deterministic modelling and also permit the importance of model parameters on the overall predicted uncertainty. This indicates that, the inclusion of uncertainty in parameters reflects on the risk and radiation dose values of performance assessment model (Hoffman and Miller, 1983; Nair et. al., 2006; Chopra et. al., 2013). The sequence of steps followed to investigate the effect of parametric uncertainties on the radiation dose are presented Figure 5.2. From the figure, it can be noted that the uncertainties in geological and transport parameters are propagated through the numerical model, then, CSRSM, GSA and reliability analysis are employed systematically to compute the combined effects of these uncertainties.
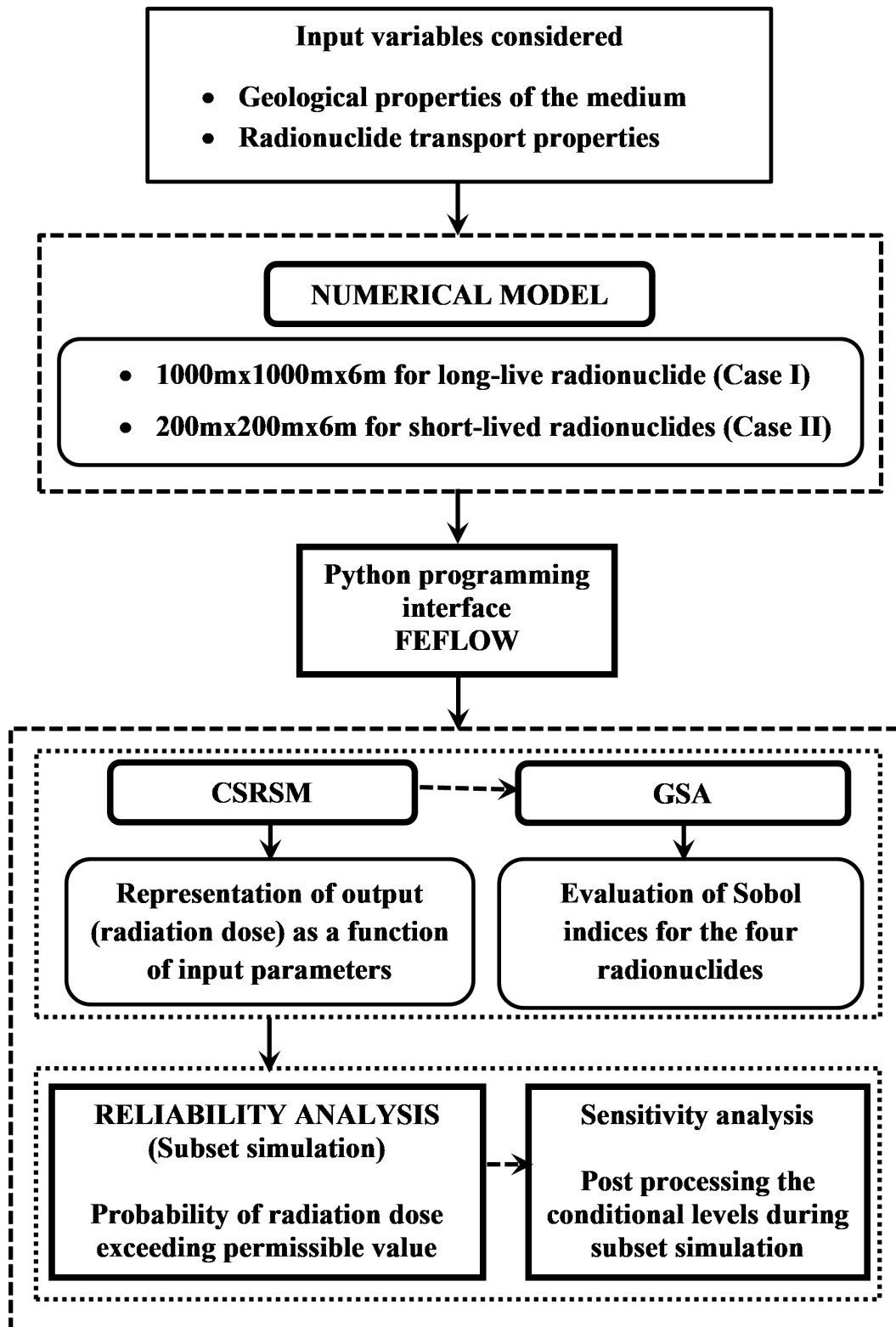
Figure 5.2: Framework for performance assessment of NSDF with parametric uncertainty

By developing python and matlab programs, the stochastic analysis to generate random realizations of geological and radionuclide transport parameters and; to estimate the probability of failure using subset simulation are automated. Before dealing with the probabilistic part of the analysis, a deterministic performance assessment model needs to be developed for a three-dimensional radionuclide transport system.

5.3.1 Development of performance assessment model

As mentioned in chapter 4, in any performance assessment model, initially, the pathway leading to the failure of the radioactive waste disposal system should be identified. Here, it is assumed that the disposal facility failed due to infiltration of water into the system that resulted in radionuclide release and transport in geosphere. Once the failure scenario is recognised, the source term and geosphere transport modelling are carried out. Typically, the critical processes involved in performance assessment are judged based on sensitivity of the process. In this chapter, the focus is mainly on discerning the behaviour of radionuclides in the geosphere and its impact on the radiation dose. So, a simple source term model is considered followed by, three-dimensional radionuclide transport modelling. Further, the influence of this model and various uncertainties on the overall response of the system are investigated.

5.3.1.1 Source term model

The source term refers to the inventory of radioactivity (i.e., waste dumped) within the facility at any given time. The concentration of the radionuclide at the source area can be

computed using the following equations (Nair et al., 2010)

$$C(t) = \frac{C(t)}{\theta V R_f} exp[-(\lambda_p + K_l)t] \qquad (5.1)$$

$$K_l = \frac{v S_r}{\varepsilon V R_f} \qquad (5.2)$$

$$\frac{dc}{dt} = -(\lambda_p + K_l)C \qquad (5.3)$$

with the initial condition $C(t = 0) = C_0$ where C is the inventory of the nuclide (Bq) at time t; K_l is the leach rate or fractional release rate of the nuclide; λ_p is the radioactive decay constant; t is the time (T); L is the length, B is the width and H is the height (m) of the disposal facility; v is the infiltration rate of water from the disposal facility (m/s); S_r is the surface area of the disposal facility (L^2); V is the volume of the disposal facility (L^3); ε is the porosity of the soil; $C_0(t)$ is the concentration of the nuclide at the source area (Bq); $C(t)$ is the activity of the radionuclide at time t (Bq); and C_0 is the initial concentration of radionuclides in the disposal facility.

As the source term is modelled numerically in this chapter, this mathematical formulation is assigned as a decaying mass boundary condition (due to combined effect of radioactive decay and leach rate).

5.3.1.2 Geosphere transport model

The radionuclides released in the geosphere get dissolved in the groundwater and migrate through the medium. Estimation of the spatial and temporal behaviour of radionuclides in a three-dimensional medium is more complex as it includes advective dispersive, sorption and decay components of transport. Numerical models allow the consideration of

more realistic problems with complex boundary conditions, coupled groundwater flow, transport of solutes, and geochemical reactions between solid and aqueous phases. So, in the present study, a numerical model that can translate the conceptualized model based on these processes is considered. The geosphere transport is modelled numerically using FEFLOW, a numerical modelling software developed by Diersch (2014). It can handle multi-dimensional (1D, 2D and 3D) problems with variability in flow (unsaturated/saturated conditions), variable fluid density, coupled /decoupled mechanisms of flow and transport, reactive species transport and heat transfer problems. The theoretical formulations are based on physical conservation principles for mass, chemical species, linear momentum and energy in a transient multi-dimensional space and these concepts are discussed in detail in section 3.2.4.2.2 of chapter 3. The groundwater and contaminant transport from a radioactive waste disposal facility in a 3D space is analysed. The general governing equation of groundwater and contaminant transport is given by

$$\frac{\partial}{\partial t}(R_d \psi) + \bigtriangledown .(q_d \psi) - \bigtriangledown .(D. \bigtriangledown \psi) - \lambda_p \psi = S \qquad (5.4)$$

where ψ = transport quantity (i.e., concentration); R_f = Retardation factor; q_d = Darcy velocity field; D = dispersion tensor; λ_p = decay constant; S= source/sink term.

5.3.1.2.1   Validation with an analytical model

To check the efficiency of the numerical model and the extent of convergence achieved from the FE mesh refinement, the results from numerical model are compared with an analytical solution. Park and Zhan (2001) developed a closed form solution for contaminant transport from a point, line and an area source in a finite aquifer system. The governing

differential equation is given by:

$$\frac{\partial C}{\partial t} - D_x \frac{\partial^2 C}{\partial x^2} - D_y \frac{\partial^2 C}{\partial y^2} - D_z \frac{\partial^2 C}{\partial z^2} + v \frac{\partial C}{\partial x} + \lambda C = q_v(x,y,z,t) \tag{5.5}$$

Boundary conditions considered are

$$C(x,y,z,0) = 0 \quad -\infty < x < \infty \quad -\infty < y < \infty \quad 0 < z < d$$

$$C(\pm\infty,y,z,t) = 0 \quad\quad -\infty < y < \infty \quad 0 < z < d \quad t > 0$$

$$C(x,\pm\infty,z,t) = 0 \quad\quad -\infty < y < \infty \quad 0 < z < d \quad t > 0 \tag{5.6}$$

$$\frac{\partial}{\partial z}C(x,y,0,t) = \frac{\partial}{\partial z}C(x,y,d,t) = 0 \quad -\infty < x < \infty \quad -\infty < y < \infty \quad t > 0$$

Let q_v be a three-dimensional finite source, assumed to be a Heaviside step function

$$q_v(x,y,z,t) = \begin{cases} q_0 f(t), & \text{if } 0 < x < x_0, -y_0 < y < y_0, z_0 < z < z_1, t > 0 \\ \\ 0, & \text{otherwise} \end{cases} \tag{5.7}$$

Equation (5.5) is solved using Green's function method for the given initial and boundary conditions (equation (5.6)). The steps followed to achieve the solutions are presented by Park and Zhan (2001). Thus, the concentration of contaminant for an instantaneous point source is given by the equation

$$C(x,y,z,t) = \frac{1}{4d\pi\sqrt{D_x D_y}} \int_0^t q_p(t-\tau)\exp(-\lambda\tau)exp\left[-\frac{(x-v\tau)^2}{4D_x\tau}\right] \times exp\left[-\frac{y^2}{4D_y\tau}\right]$$

$$\times \left[1 + 2\sum_{n=1}^{\infty} cos\frac{n\pi z_0}{d}cos\frac{n\pi z}{d}exp\left[-\frac{D_z n^2 \pi^2}{d^2}\tau\right]\right]\frac{d\tau}{\tau} \tag{5.8}$$

The input parameters considered for the study are presented in the Table 5.1.

Table 5.1: Model input parameters

S.No	Property	Value
1	Groundwater velocity (m/day)	0.1
2	Dispersion (m^2/day)	0.1
3	Source strength function (g/day)	0.09
4	Time scale (days)	600

By assigning the input values (from Table 5.1) to the model, the movement of contaminant over time is computed at a distance of 10 m and 20 m from the source. The results obtained from equation (5.8) are compared with the results computed from the numerical model.
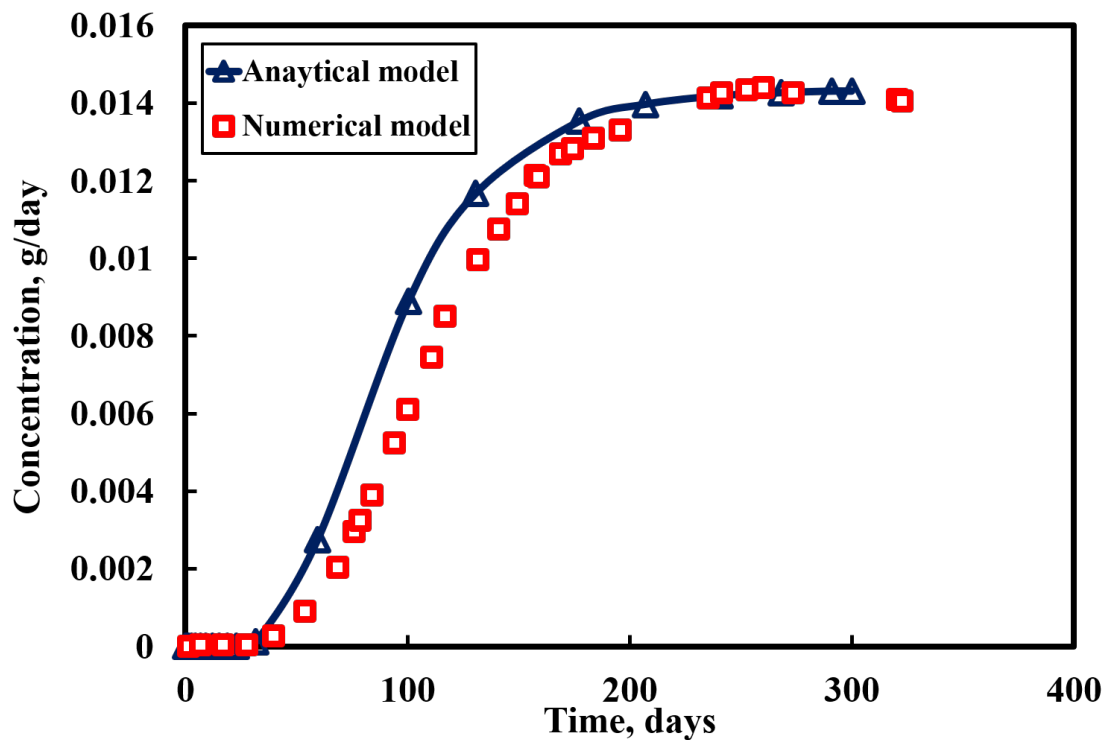
(a)
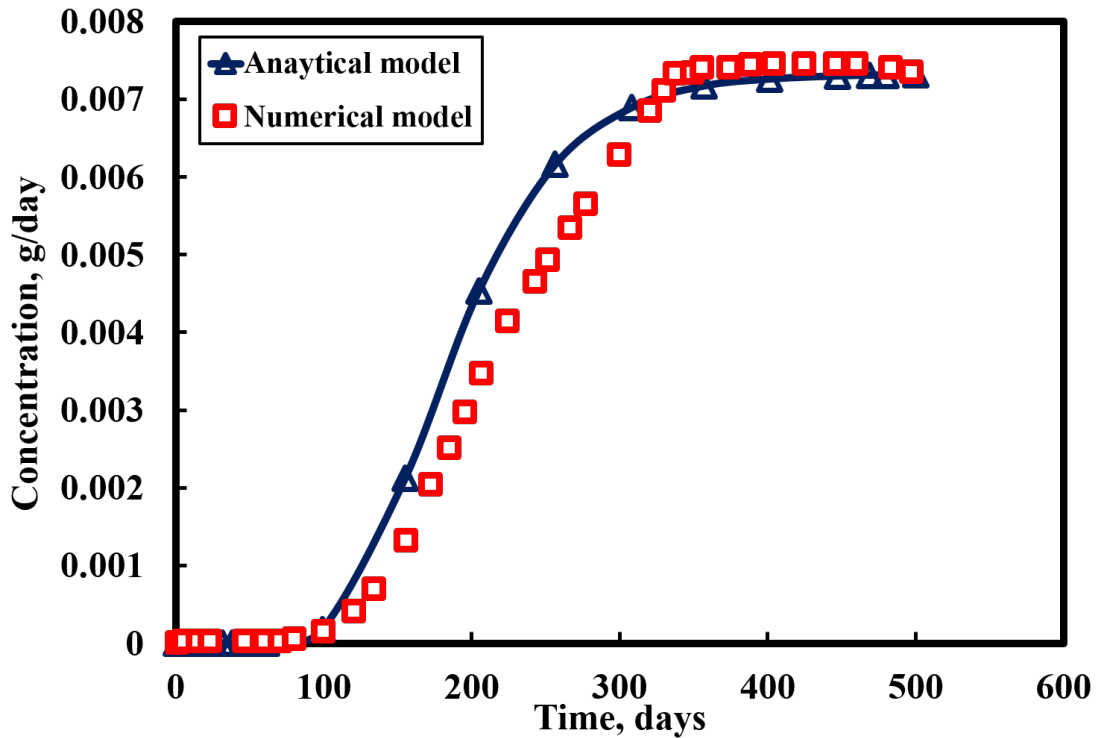
(ii)

Figure 5.3: Concentration versus time at a distance of (a) 10 m and (b) 20 m from the source

The concentration versus time plots are presented in the Figure 5.3. Figure 5.3 (a) and (b) presents the concentration trends at observation points located 10 m and 20 m from the source. It can be observed that the results from the numerical model match well with the analytical solution.

5.3.1.2.2 Input data considered for the analysis

The radionuclides considered for the performance assessment modelling analysis are Strontium (^{90}Sr) and Caesium (^{137}Cs) (short-lived) ; Carbon (^{14}C) and Iodine (^{129}I) (long-lived). The two long-lived radionuclide deliver very high concentration values (observed in chapter 4). Hence, they become critical for the analysis involving far field scenarios. On the other hand, the two short-lived nuclides considered for the study are predominant in low level radioactive waste and, therefore, their impact needs to be examined for near

field scenarios. To reduce the high computational time of the model, the inventory values are reduced to around 100 times the actual inventory value (in Table 5.2). The input properties of these radionuclides are presented in Table 5.2 and Table 5.3.

Table 5.2: Decaying source concentration and other properties of the four radionuclides (Nair and Krishnamoorthy, 1999; Rakesh et. al., 2005)

S.No	Type of radionuclide	Radionuclide	Inventory (Bq)	Half-life (yrs)	Distribution coefficient (ml/g)	Ingestion dose coefficient (Sv/Bq)
1	Short-lived	Strontium	1.4×10^{12}	28.8	220	2.8×10^{-8}
2		Caesium	1.6×10^{10}	30.2	800	1.3×10^{-8}
3	Long-lived	Carbon	4.8×10^{8}	5.73×10^{3}	20	6.12×10^{-12}
4		Iodine	1.11×10^{6}	1.7×10^{7}	1	1.1×10^{-7}

Table 5.3: Input parameters to estimate the decaying source concentration

S.No	Property	Value
1	Infiltration velocity (m/s)	1×10^{-8}
2	Volume of barrier (L $\times$ B $\times$ H) m^3	15 $\times$ 2.5$\times$4.8
3	Porosity	0.3
4	Hydraulic conductivity (m/day)	5
5	Drinking waste intake (l/day)	2.2

Figure 5.4 presents the plan and sectional view of the domain and the location of the point source. The size of the domain considered for short-lived and long-lived radionuclides are 200 m $\times$ 200 m $\times$ 6 m and 1000 m $\times$1000 m$\times$ 6 m respectively. In both the cases, the domain size is selected based on the criteria that the boundary effects do not interfere with the transport process (i.e., domain size is greater than the zone of influence due to advection (vt where v - linear velocity, t - typical time period of interest) and dis-

person ($\sqrt{Dt}$ where $D = \alpha v + D^*$, D^* - diffusion coefficient, α - dispersivity and v - linear velocity).
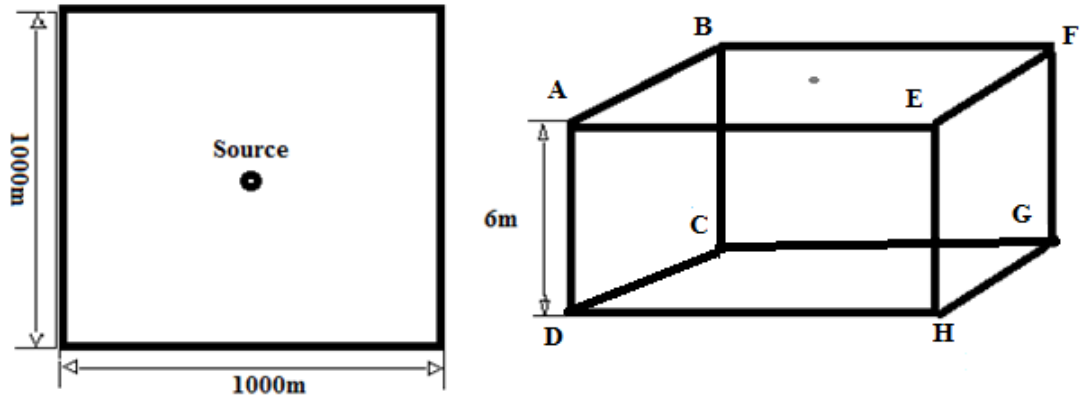
Figure 5.4: Plan and Sectional view of the domain
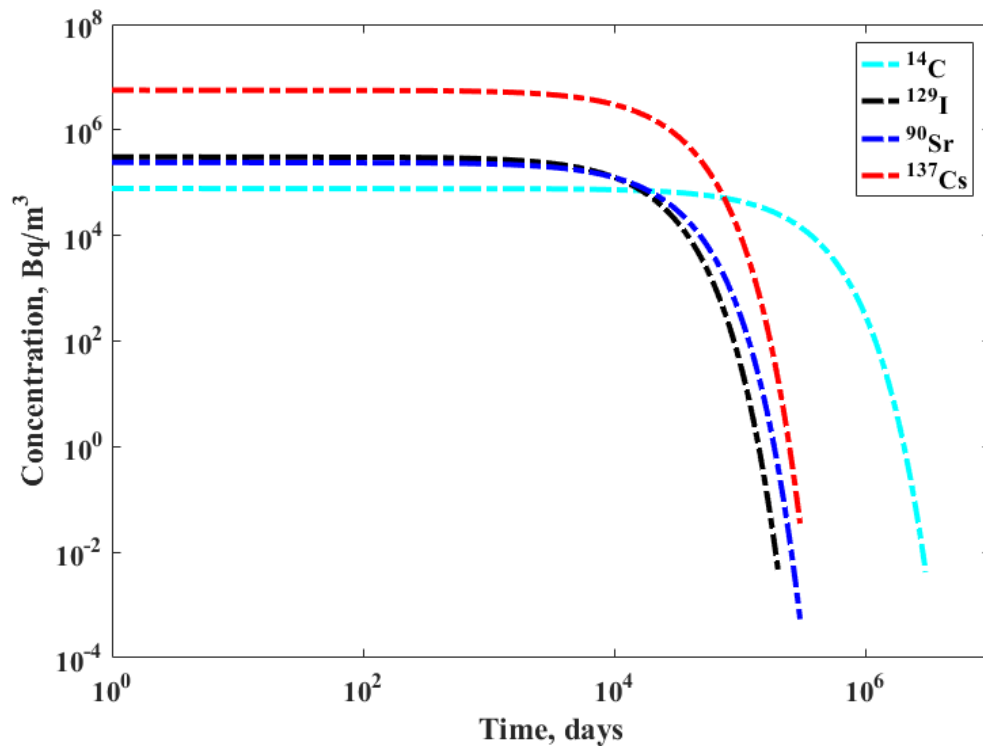
Figure 5.5: Source concentration versus time

Figure 5.5 shows the decaying concentration trends with time for Iodine, Carbon, Caesium and Strontium evaluated from equation (5.1). It can be observed that, the concentration of radionuclides reach innocuous levels between 10^4 and 10^6 years. The max-

imum time taken to decay is observed in Carbon due to its high half-life value and low distribution coefficient.

5.3.1.2.3 Initial and boundary conditions

A triangular finite element mesh is generated with 55,496 nodes for Case I and 55,489 nodes for Case II. Th discretized mesh obeys Delaunay criterion (which relies on the property that no other point is contained within the circumcircle formed by the nodes of the triangle). In the model, the fluid flow and mass transport conditions are assigned separately. Initially the model is run for steady state hydraulic head conditions (to stabilize the steady state hydraulic head values) and then it is run for the transient conditions of mass transport. In order to simulate the effect of leaching from the disposal facility to the aquifer in the numerical model, the node corresponding to the source is treated as an injection well. The other initial and boundary conditions for flow and radionuclide transport are given in Table 5.4 and equation (5.9).

Fluid flow

Table 5.4: Boundary conditions for fluid flow

Section	Type	Value	Comment
A-E-H-D	-	-	-
A-B-C-D	Dirichlet	H=150 m	Pervious boundary (Inflow)
E-F-G-H	Dirichlet	H = 130 m	Pervious boundary (Outflow)
B-E-G-C	-	-	-

Mass transport

$$C(x,y,z,0) = 0 \quad -\infty < x < \infty \quad -\infty < y < \infty \quad 0 < z < d$$

$$C(\pm\infty, y, z, t) = 0 \qquad -\infty < y < \infty \quad 0 < z < d \quad t > 0$$

$$C(x, \pm\infty, z, t) = 0 \qquad -\infty < y < \infty \quad 0 < z < d \quad t > 0$$

$$\frac{\partial}{\partial z}C(x,y,0,t) = \frac{\partial}{\partial z}C(x,y,d,t) = 0 \quad -\infty < x < \infty \quad -\infty < y < \infty \quad t > 0$$

(5.9)
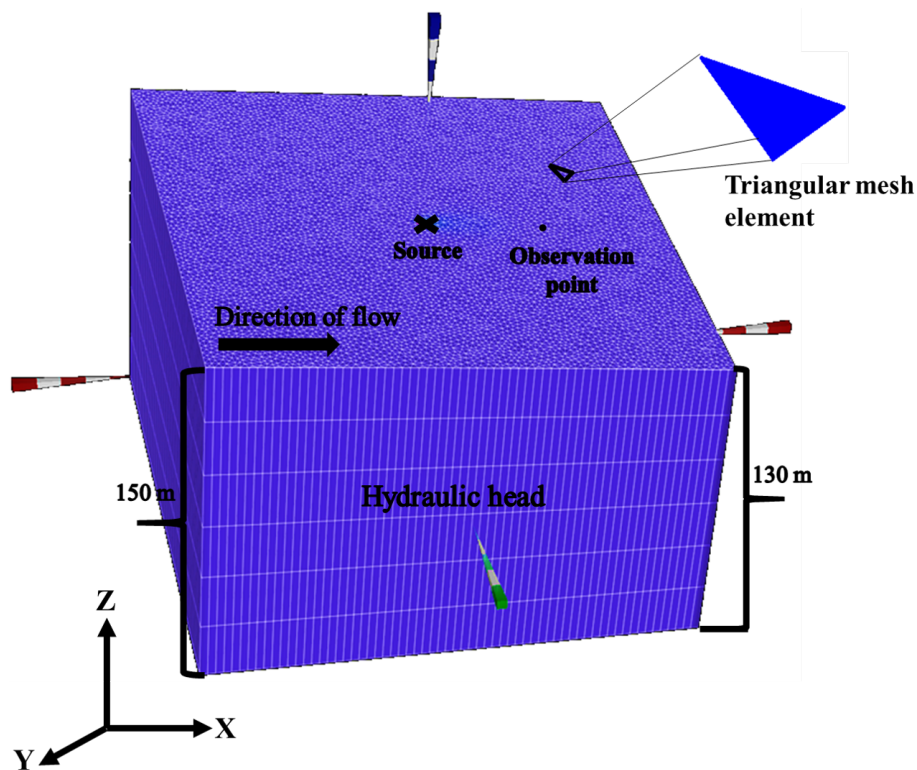
Figure 5.6: Three-dimensional view of the mesh developed from the numerical model

A schematic of the finite element mesh generated to model the radionuclide transport and, the input conditions of the model are presented in Figure 5.6. Now, the calibrated numerical model is used to predict radionuclide transport within groundwater and compute its potential effect on the environment. To discern the effect of distance on the transport behaviour of radionuclides, their concentration is estimated at different points

(located away from the source) beyond which their effect becomes negligible. The results obtained from deterministic analysis are discussed in Section 5.3.2.

5.3.1.3 Probabilistic analysis

The input properties of the transport process in the geosphere i.e., soil medium are treated as random variables following lognormal distribution. The deterministic transport parameters are considered as mean values (underlying normal distribution) and presented in Table 5.5. Stochastic methods are used to characterize and quantify the estimates of radiation dose for long time scales. The statistical properties of these parameters for four radionuclides are presented in the Table 5.5. To investigate the effect of these parameters on the radionuclide concentration, the coefficient of variation (COV) and probability distribution reported in literature have been considered (referred from section 2.4.1 of chapter 2).

5.3.1.3.1 Collocation based stochastic response surface method (CSRSM)

The uncertainty propagation and quantification are performed using collocation based stochastic response surface method (CSRSM). The main reason for using CSRSM is to reduce the computation effort involved in running large number of simulations for traditional probabilistic methods (Monte Carlo simulation, Latin Hyper cube sampling). In this method, the response of the system is approximated by a polynomial which is a function of the input parameters. To represent the radiation dose as a function of the five transport parameters, a second order approximation is made. The details of procedure is presented in section 3.5.2. The input parameters are transformed to standard normal space and assumed to take the values of roots of Hermite polynomials of higher order. The number of

terms for a five parameter second order polynomial is estimated as 21 from the equation (3.49). A typical five parameter second order polynomial is given by

$$Y = x_1 + x_2 u_1 + x_3 u_2 + x_4 u_3 + x_5 u_4 + x_6 u_5 + x_7(u_1^2 - 1) + x_8(u_2^2 - 1) + x_9(u_3^2 - 1)$$

$$+ x_{10}(u_4^2 - 1) + x_{11}(u_5^2 - 1) + x_{12}(u_1 u_2) + x_{13}(u_1 u_3) + x_{14}(u_1 u_4) + x_{15}(u_1 u_5)$$

$$+ x_{16}(u_2 u_3) + x_{17}(u_2 u_4) + x_{18}(u_2 u_5) + x_{19}(u_3 u_4) + x_{20}(u_3 u_5) + x_{21}(u_4 u_5) \quad (5.10)$$

where $x_1, x_2...$ are the coefficients of the polynomial and u_1, u_2, u_3, u_4, u_5 are the input parameters in standard normal space. The results of the meta-model are discussed in section 5.3.2.

Table 5.5: Statistical properties of parameters

S.No	Property	Caesium		Stontium		Carbon		Iodine		Distribution
		Mean	COV	Mean	COV	Mean	COV	Mean	COV	
1	Longitudinal dispersivity (m)	3	0.09	3	0.09	3	0.09	3	0.09	Lognormal
2	Transverse dispersivity (m)	0.3	0.09	0.3	0.09	0.3	0.09	0.3	0.09	Lognormal
3	Porosity	0.3	0.09	0.3	0.09	0.3	0.09	0.3	0.09	Lognormal
4	Distribution coefficient (ml/g)	800	0.1	220	0.1	20	0.1	1	0.1	Lognormal
5	Diffusion coefficient (m^2/s)	5×10^{-10}	0.08	1.11×10^{-12}	0.1	5×10^{-8}	0.08	5×10^{-8}	0.08	Lognormal

5.3.1.3.2 Reliability analysis

To check the probability of radiation dose exceeding the permissible limit, reliability analysis is carried out for short-lived and long-lived radionuclides. Since the radiation dose of the radionuclides estimated are very low, subset simulation method is used to find the probability of failure (Au and Beck, 2003; Cadini et. al., 2012). The main idea of subset

simulation (SS) method is to represent small failure (rare events) probabilities as a product of large failure (frequent events) probabilities. The failure probability (P_f) is estimated from the equation

$$P_f = P(f_1)P(F_1)\prod_{i=1}^{r-1}P(f_{i+1}f_i)$$

(5.11)

where $P(f_i)$ - probability of intermediate failure events. During the simulation, the conditional samples are generated by means of a Markov chain designed so that the limiting stationary distribution is the target conditional distribution of some adaptively chosen intermediate event. By doing so, the conditional samples gradually populate the successive intermediate regions up to the target (rare) failure region. The mathematical formulation of this method is discussed in section 3.6.1.2. These simulations are run to estimate the probability of radiation dose exceeding the permissible limit and illustrated in the next section for two cases (short-lived and long-lived radionuclides). The limit state function, $g(X)$ is defined in terms of the basic random variables $X_i(X_1, X_2, X_3, X_4, X_5)$, and the functional relationship among them. The failure condition is defined as

$$g(X) = D_r - D(X_i)$$

(5.12)

where D_r is maximum permissible radiation dose in the drinking water pathway and $D(X)$ is the function of the uncertain input parameters. The permissible radiation dose values used for the analysis are given in Table 5.6. These threshold values are lower than that representative of the best practices in other countries. For the simulation the conditional probability is constantly maintained as $P(F_1) = 0.1$. An algorithm is written and coded in matlab to run the subset simulation.

5.3.1.3.3 Sensitivity Analysis

Sensitivity analysis is performed to identify and rank in order of importance the uncertainties with respect to their impact on the uncertainty of the performance measures of interest. This ranking is then the basis for prioritizing data collection and model improvement, so that these activities are focused on those uncertainties, the reduction of which is most likely to change the results of the performance assessment (Gallegos and Bonano 1993). Sudret (2008) presented a method of Global Sensitivity Analysis (GSA) by Polynomial chaos expansion to compute the Sobol indices. The coefficients of polynomial from CSRSM are post-processed to obtain Sobol indices. To reiterate the results obtained from this method, sensitivity analysis is carried out by processing the conditional levels in subset simulation. The procedure followed to evaluate the sensitive measures from both the methods are presented in section 3.7 of chapter 3. The SS method confirms the capability of examining the range of variability (including regions of rare occurrence) of each uncertain parameter using MCMC method that gradually populates intermediate conditional levels (Au and Beck 2003). So, the sensitive parameters estimated from both the methods are discussed in section 5.3.2.

5.3.2 Results and Discussion

The radionuclide transport from an NSDF to geosphere is modelled numerically and the simulation time periods for the model are varied upto 2,00,000 days (approximately 548 years) for short-lived radionuclides to 30,00,000 days (approximately 8200 years) for long-lived radionuclides. The time-scale is chosen such that the concentration became negligible beyond these time periods. The spatial and temporal variations in concentra-

tions and the annual effective dose rate are computed from the model. The radiation dose is estimated as the product of concentration of radionuclide, drinking water intake and ingestion dose coefficient. So, the deterministic analysis results showed that the concentration of radionuclides are highly dependent on the inventory value, their distribution coefficient and half-lives. Amongst the radionuclides considered in the chapter, Iodine delivered the highest concentration and radiation dose because of its high inventory value and ingestion dose coefficient over other radionuclides. Since the source concentration decays after few years, the concentration at any point reaches a maximum value and then reduces to zero. The radionuclides Caesium and Strontium decay to innocuous levels beyond 50 m (from the source) due to their high distribution coefficients and short half-lives. When the distribution coefficient value is high, it retards the mobility of the contaminant. So, the transit times become longer and, the concentration reduces further due to decay. The variation of concentration over distance is computed upto 200 m and 50 m for long-lived and short-lived radionuclides. They are shown in Figure 5.7(a) and 5.7(b) (for long-lived) and, Figure 5.8(a) and 5.8(b) (for short-lived). To understand the pre-peak concentration behaviour of radionuclides, the trends are plotted for time periods before the arrival of maximum concentration. It can be observed that the concentration values decrease with the increase in the distance from the source. This can be attributed to sorption which occurs in the process of contaminant movement. The radionuclides get sorbed to the neighbouring porous media resulting in lesser concentrations.
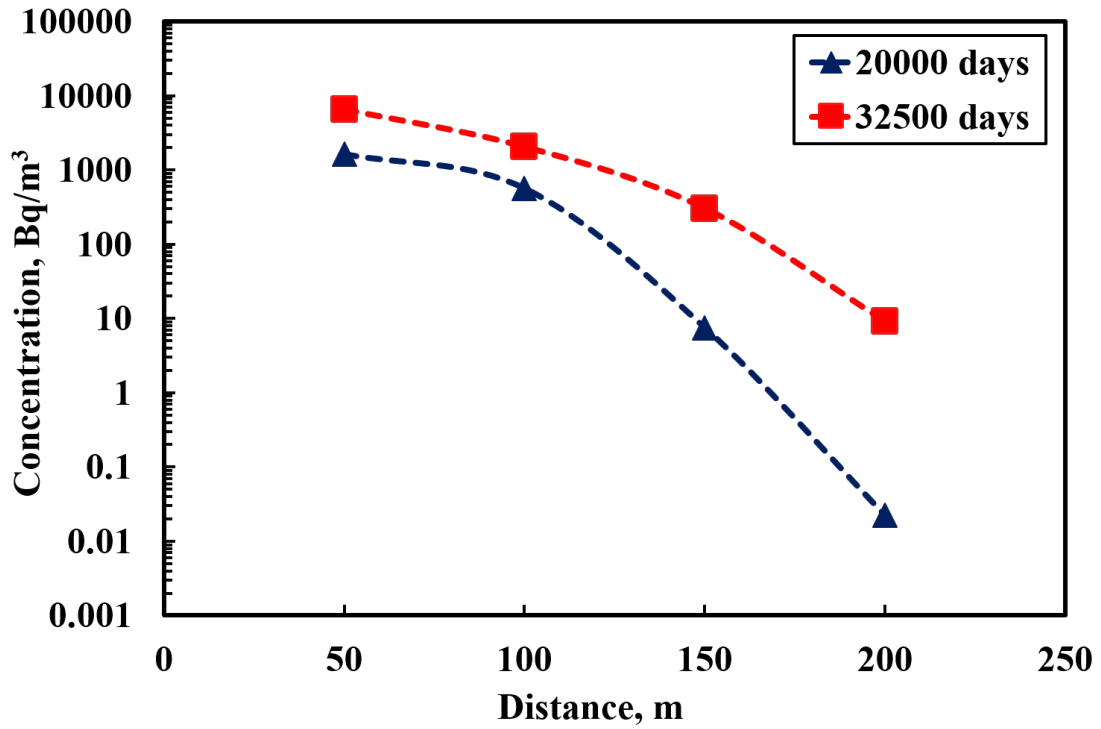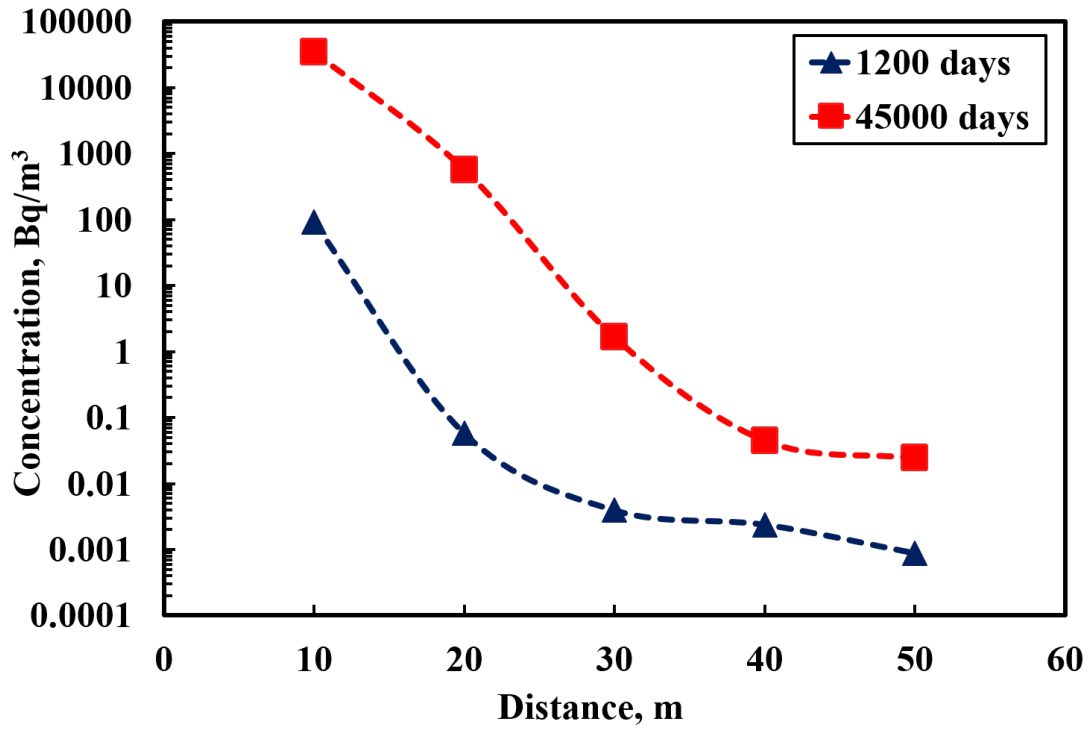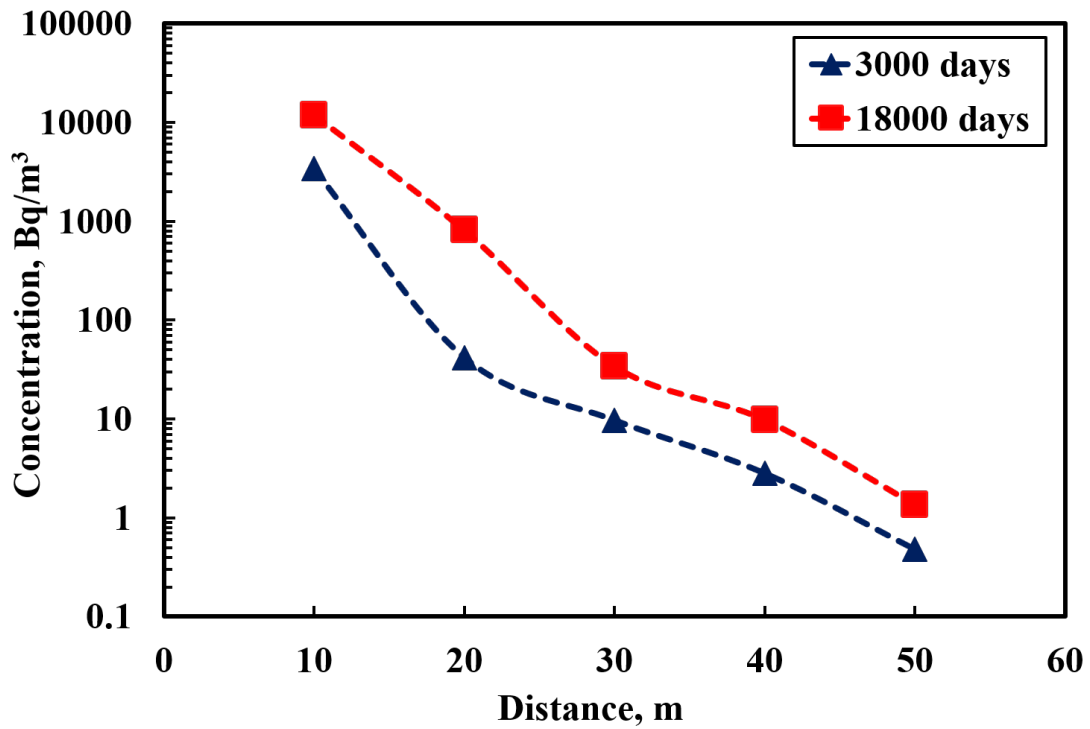
(a)
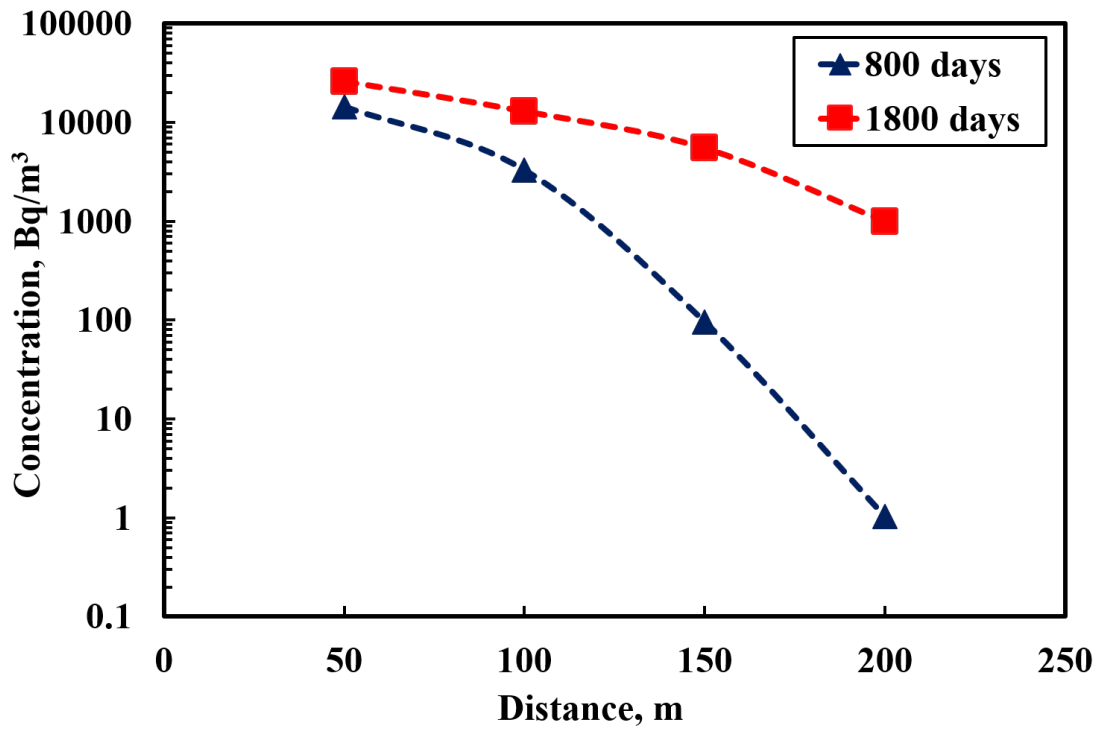
(b)

Figure 5.7: Concentration versus distance time periods (Pre-peak: Before the arrival of maximum concentration) (a) Carbon (b) Iodine

215

(a)

(b)

Figure 5.8: Concentration versus distance time periods (Pre-peak: Before the arrival of maximum concentration) (a) Caesium (b) Strontium

The risk factor due to radiation to a member of public (including risk due to fatal cancer, non-fatal cancer and severe hereditary effects) recommended by ICRP is $7.3 \times 10^{-5} \mathrm{mSv}^{-1}$ (Nair and Krishnamoorthy 1999). The maximum risk values evaluated from the radiological model are lower than the risk observed from industrial accidents and natural catastrophes $(1 \times 10^{-3}$ -$1 \times 10^{-4})\mathrm{y}^{-1}$. Similar trend is observed for all the radionuclides.

For the time scale considered in the problem, it is necessary to account for the effect of uncertainties on the concentration of radionuclides. The results from probabilistic analysis are evaluated by adopting two methodologies. The sequence of steps followed for uncertainty propagation, quantification and sensitivity analysis using both the methods are presented in Figure 5.9. They are :

1. In Method 1, the uncertainties are propagated through the numerical model and a new computationally efficient meta-model is developed that replaces the complex numerical model. This process is carried out using CSRSM and then the probability of failure is also estimated by substituting $D(X_i)$ with the surrogate model in the limit state function. Finally global sensitivity analysis is carried out by post processing CSRSM results to identify the critical parameters affecting the response.

2. In Method 2, the uncertainties are propagated through the complex numerical model and the limit state function to estimate P_f is formulated by using $D(X_i)$ as the numerical model. Finally, sensitivity analysis is carried out by post processing subset simulation results.
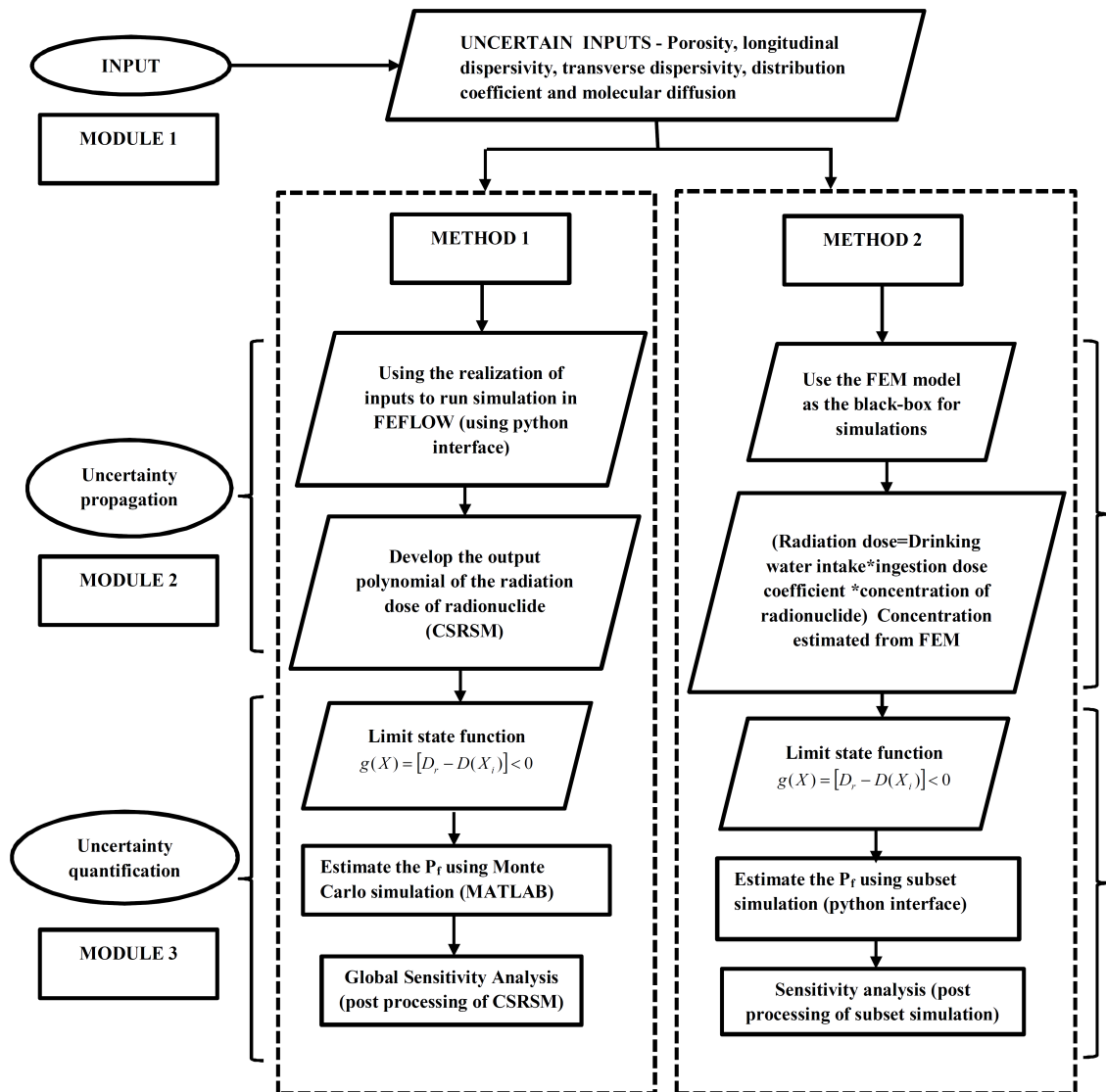
Figure 5.9: Algorithm for performance assessment using Method 1 and Method 2

Both the methodologies are helpful in performance assessment of disposal systems. It becomes easier to follow Method 1 when there are lesser number of uncertain parameters. It enables in building surrogate models that reduce the computational difficulties. Conversely, it becomes computationally challenging to use CSRSM when the uncertain parameters are more in number(>5). In such cases, Method 2 is efficient.

The results from both the methods are presented subsequently. The parameter un-

certainty and the model uncertainty (for abstracting the real response of the system) are propagated using non-intrusive CSRSM to build the surrogate model and represent radiation dose as a function of uncertain parameters.

From the numerical model, for short-lived and long-lived radionuclides, the realizations of concentration versus time at distances 10 m, 20 m, 30 m and 40 m away from the source and 50 m, 100 m, 150 m and 200 m away from the source respectively are obtained and presented in Figures 5.10(a) and 5.10(b); 5.11(a) and 5.11(b). These plots re-iterate the effect of distribution coefficient on the concentration of radionuclides. As the distribution coefficient is lower for the long-lived radionuclides, the spread of concentration over time for these radionuclides (seen in Figure 5.10) is not so wide when compared to the short-lived radionuclides as seen in Figure 5.10. This effect leads to faster arrival of peak concentration in the case of long-lived radionuclides than the short-lived ones. A second order polynomial approximated the response of the system and the R^2 value estimated from equation (3.53) is 0.99 for all the radionuclides. This method helps in quantifying the model response by describing the probability density function (pdf). Figure 5.12(a) to 5.12(p) shows different distributions (pdf). The pdf of concentration and radiation dose is observed to follow 'Weibull distribution' in Case I (Figure 5.12(a) to 5.12(h)) and 'Lognormal distribution' in Case II (Figure 5.12(i) to 5.12(p)). The knowledge of the type of distribution followed by the concentration of radionuclides will reduce the uncertainties involved in the output and help in improving the efficiency of the performance assessment model.
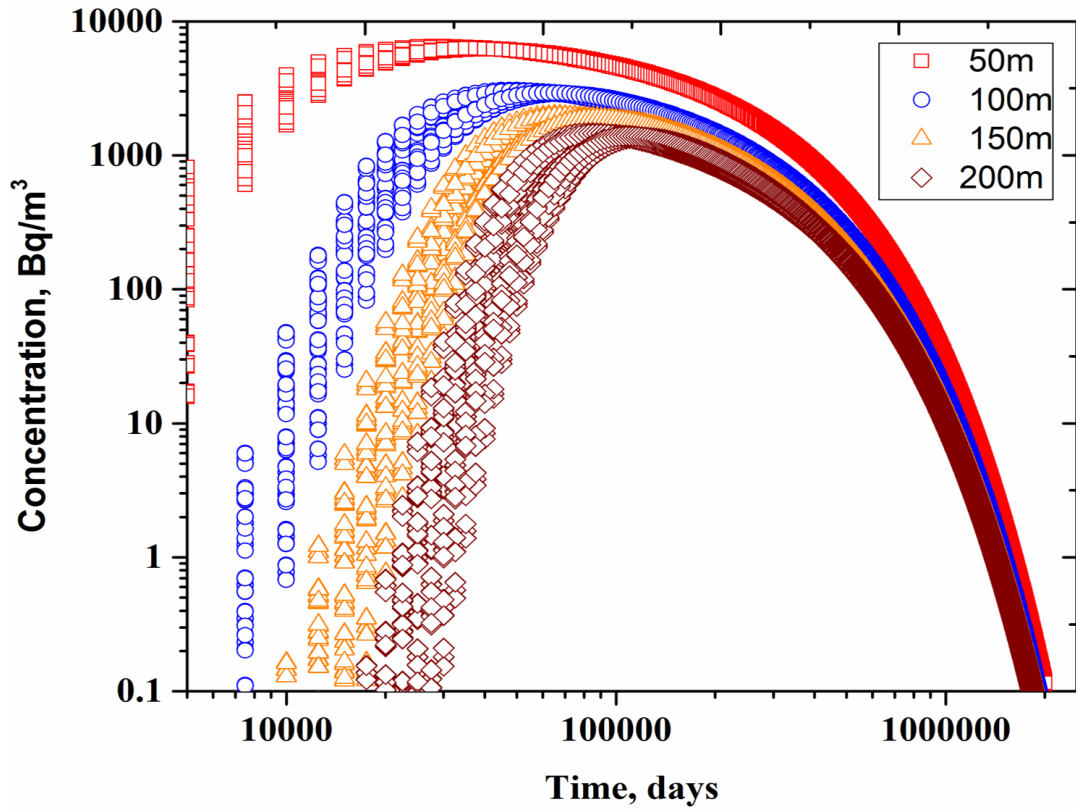
(a)
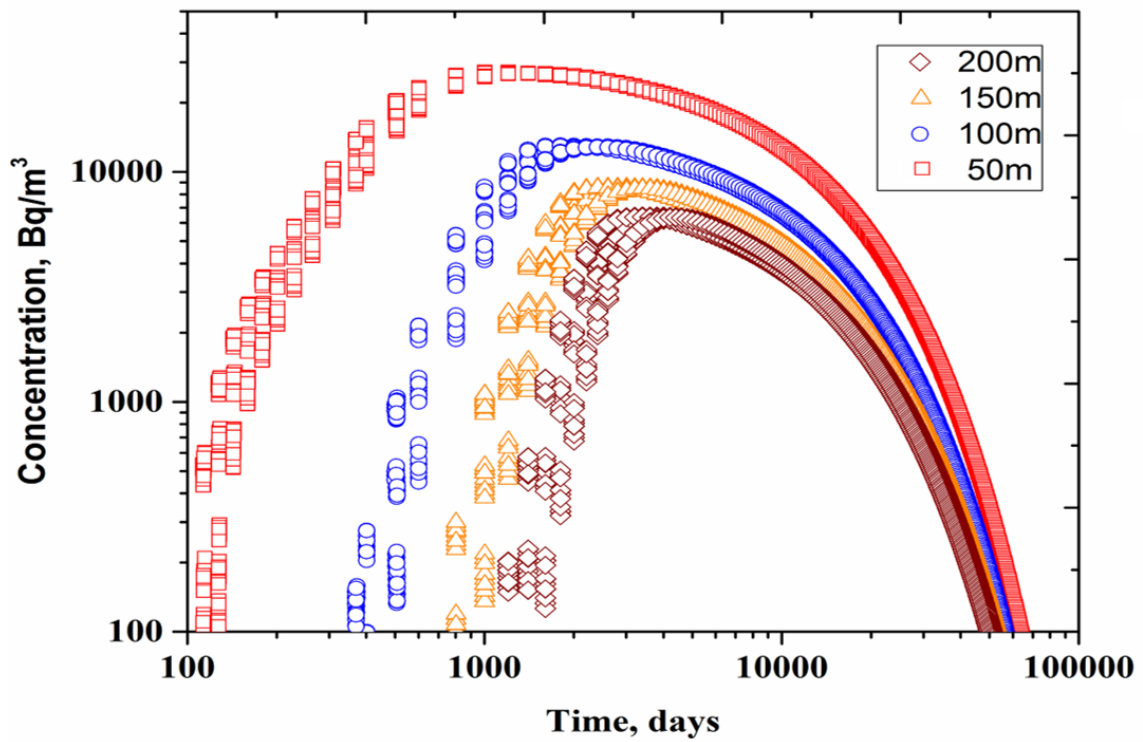
(b)

Figure 5.10: Concentration versus time trends at 50m, 100m, 150m and 200m away from the source for (a) Carbon (b) Iodine

(i)

(ii)
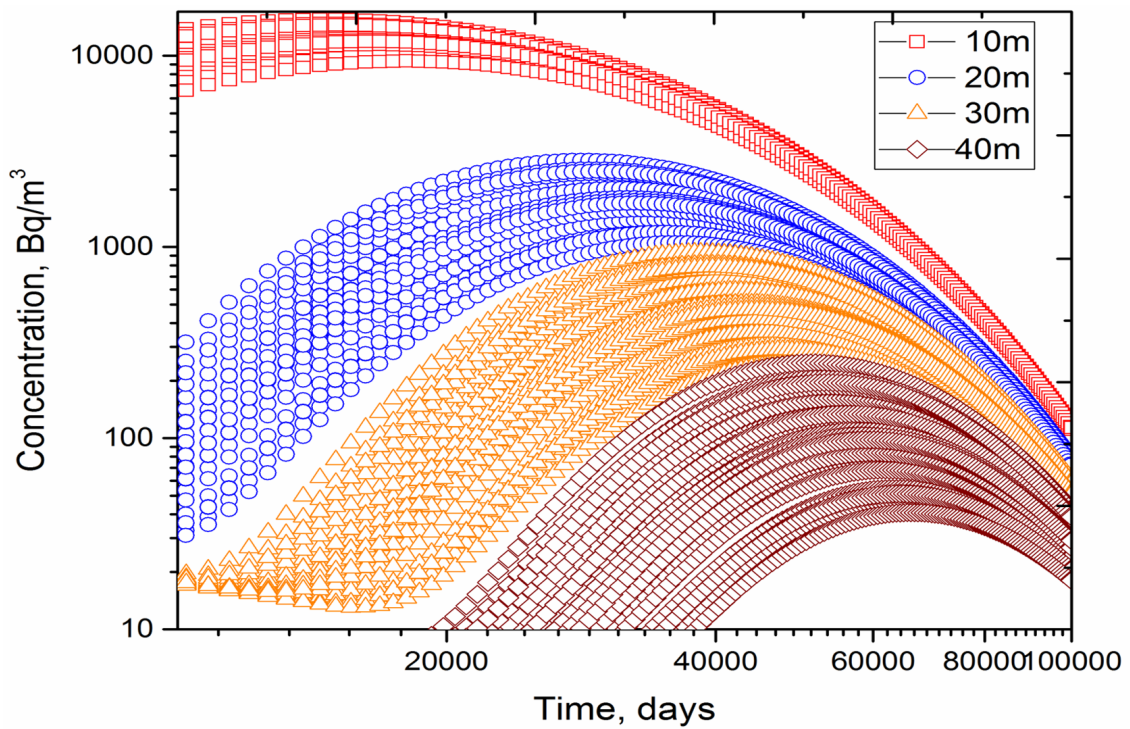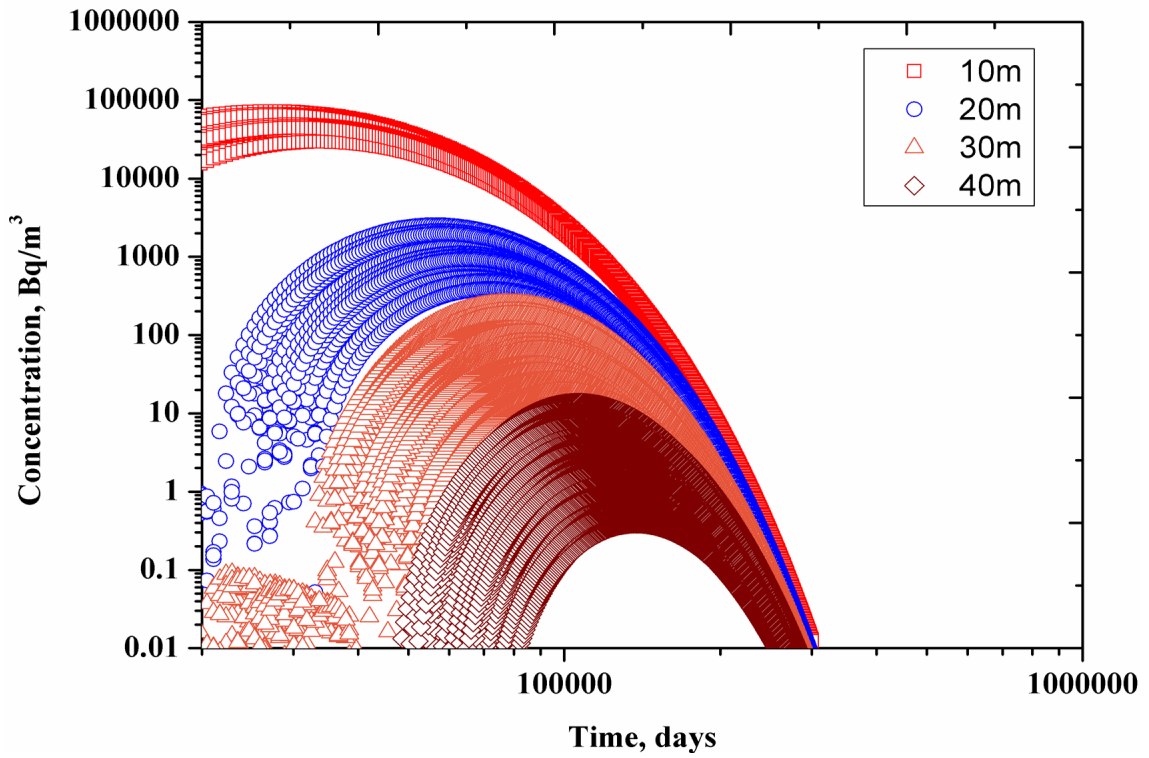
Figure 5.11: Concentration versus time trends at 10m, 20m, 30m and 40m away from the source for (a) Caesium (b)Strontium
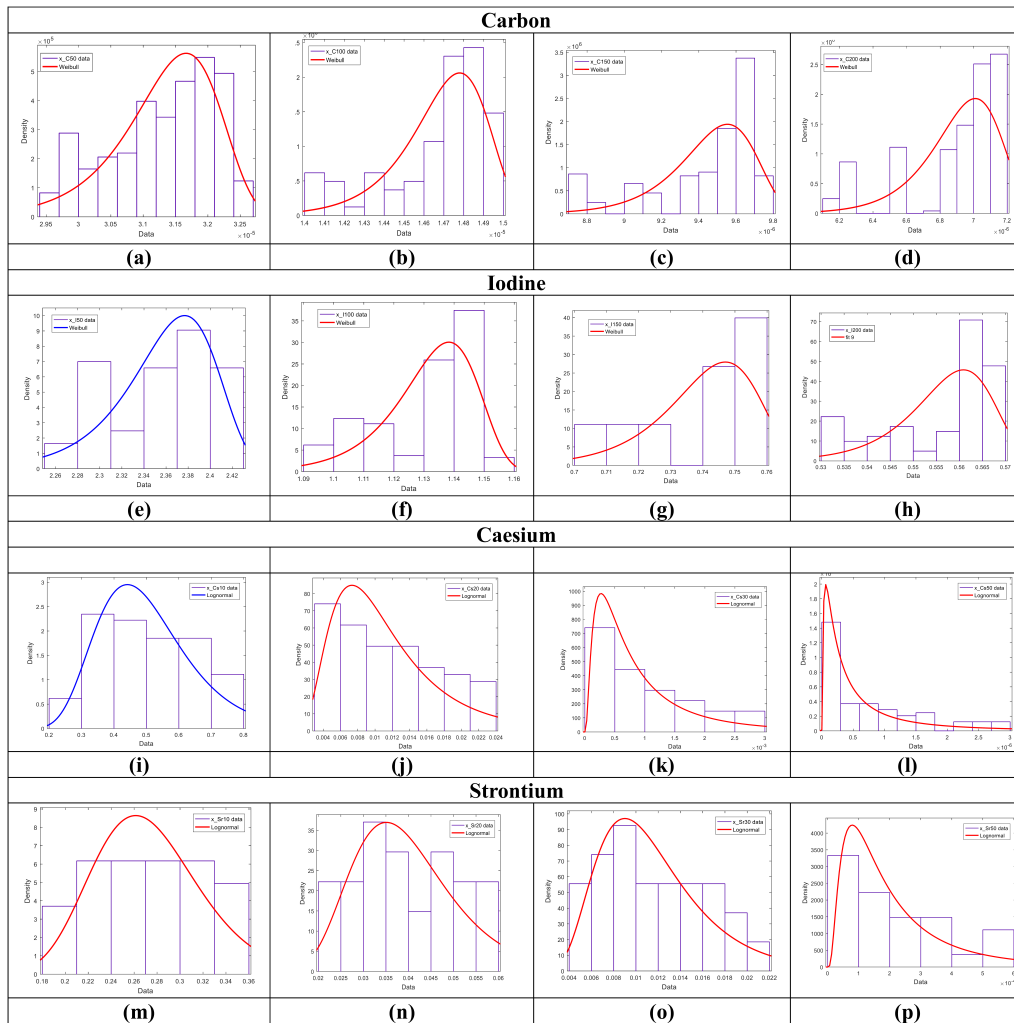
Figure 5.12: The output distributions of radionuclides at different distances (a) Carbon at 50m (b) Carbon at 100m (c) Carbon at 150m (d) Carbon at 200m (e) Iodine at 50m (f) Iodine at 100m (g) Iodine at 150m (h) Iodine at 200m (i) Caesium at 10m (j) Caesium at 20m (k)Caesium at 30m (l)Caesium at 50m (m) Strontium at 10m (n) Strontium at 20m (o) Strontium at 30m (p) Strontium at 50m

Reliability analysis is carried out to estimate probability of failure (P_f) i.e, the probability of radiation dose exceeding permissible limit. In equation (5.12), D_r corresponds to the threshold value; $D(X_i)$ corresponds to surrogate model and numerical model for Method 1 and Method 2 respectively. It is important to note that, the peak radiation dose value is critical in estimating P_f. So, the analysis is carried out such that $D(X_i)$ computed from each simulation corresponds to peak radiation dose (for a given time period). The results from both the cases are presented in Table 5.6. The probability of failure esti-

mated from both the methods are same. The P_f values in Table 5.6 indicate that there is a very low radiological effect to the human habitat due to the release of radioactivity. The computational time taken to evaluate the results from Method 1 and Method 2 are also presented in Table 5.6. Since the number of uncertain parameters considered for the analysis are five, Method 1 is more efficient and the same is illustrated for both long-lived and short-lived radionuclides. To check the variability of estimates, the sample coefficient of variation (COV) of failure probability over 25 independent subset simulation runs are plotted.

Table 5.6: Probability of failure estimated from subset simulation

SNo	Radionuclide	Permissible limit(mSv/yr)	Probability of failure	Computational time (sec)	
				CSRSM Method 1	Numerical model Method 2
1	Caesium	0.85	4.5×10^{-8}	12	121422 ($\approx$ 33 hrs)
2	Iodine	0.77	3.5×10^{-9}	10	260398 ($\approx$ 72 hrs)

(a)

223
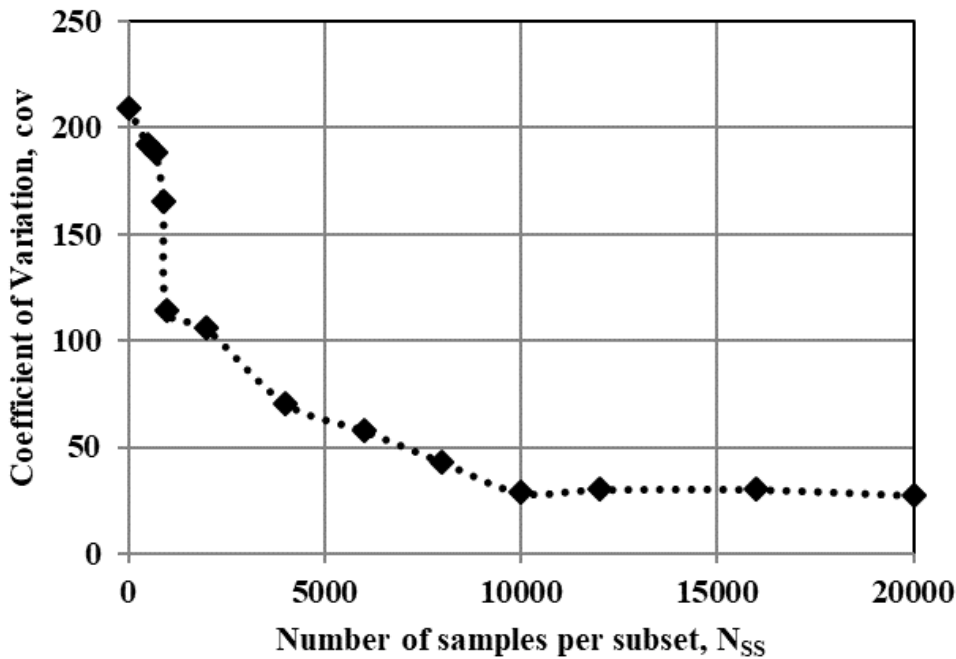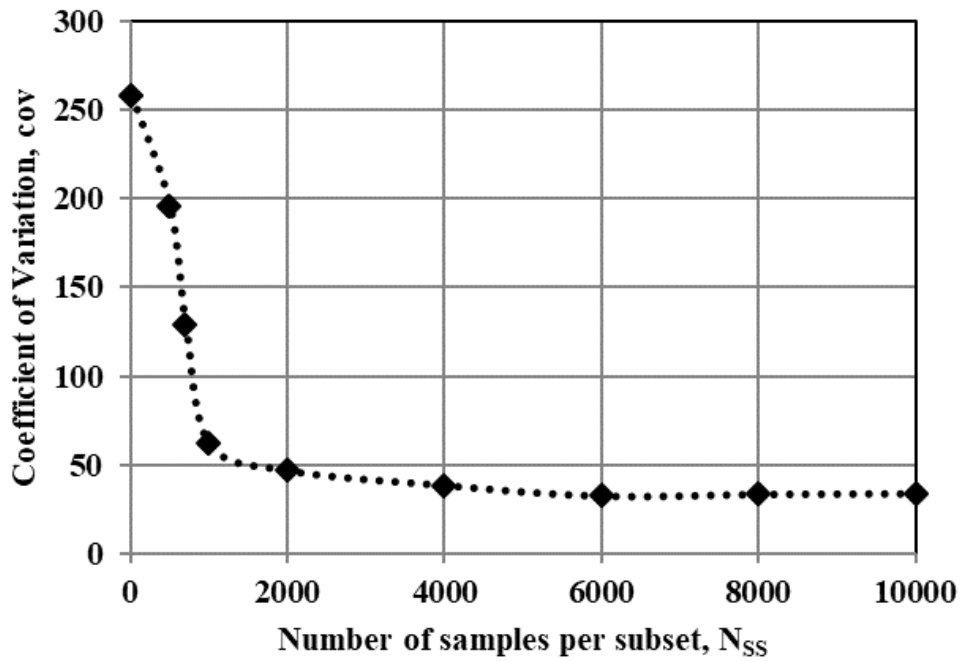
(b)

Figure 5.13: Coefficient of variation of probability of failure for different number of samples per subset (a) Iodine (b) Caesium

(a)

(b)
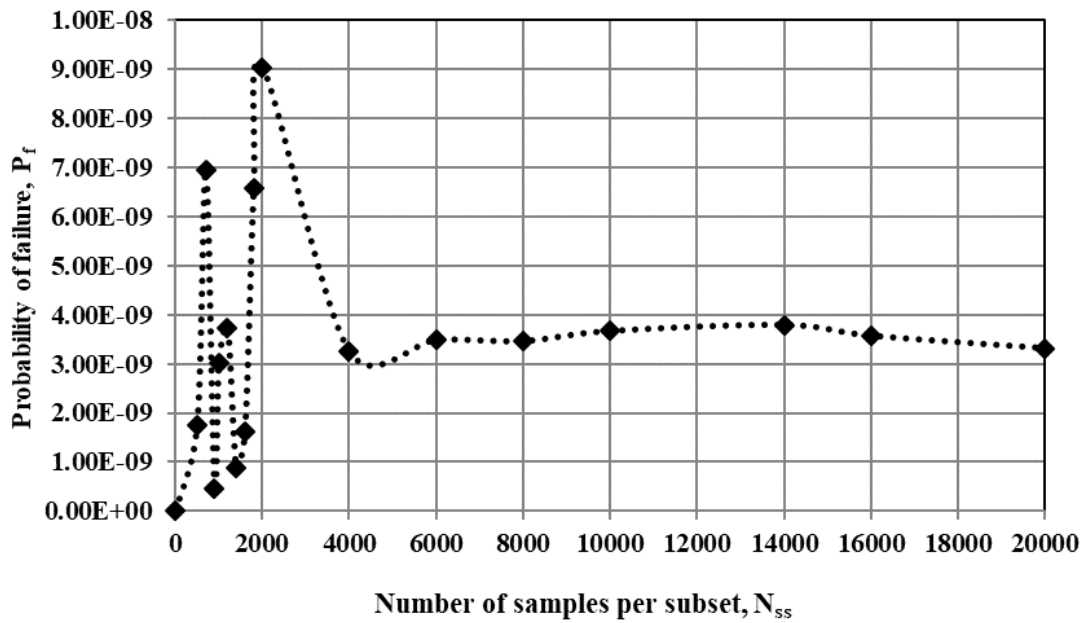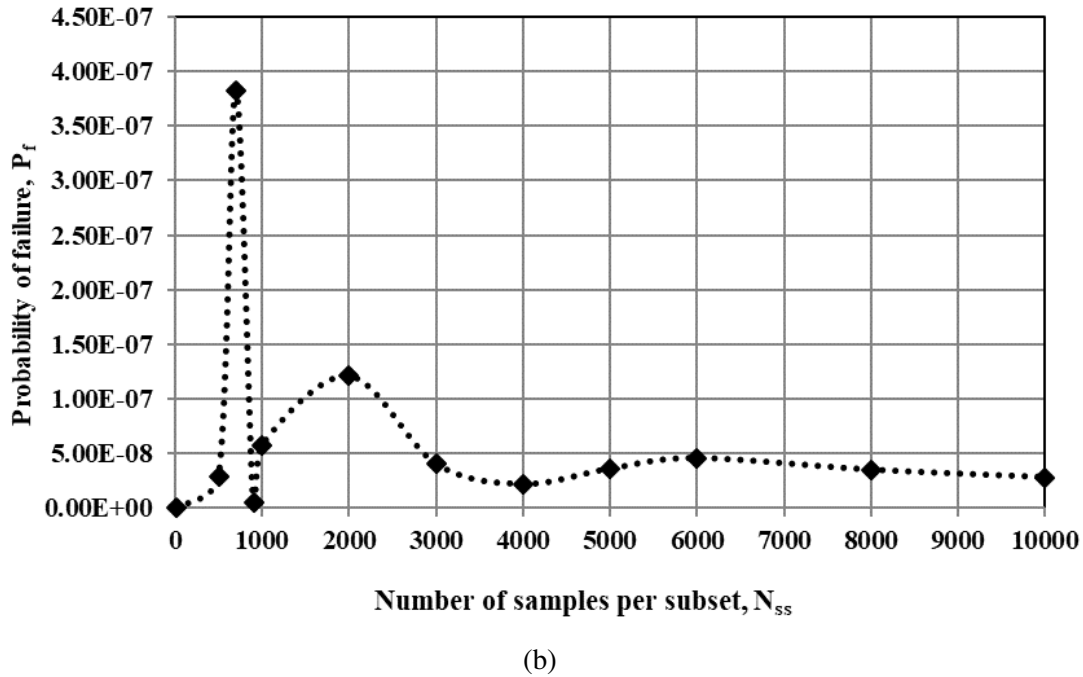
Figure 5.14: Probability of failure for different number of samples per subset (a) Iodine (b) Caesium

A comparison is made between the coefficient of variation and number of samples per subset and the results are presented in Figure 5.13. Also, the effect of number of samples per subset and probability of failure are presented in Figure 5.14. From the Figures 5.13 and 5.14 it can be observed that in the case of Iodine, 20,000 samples per subset and 10,000 samples per subset for Caesium enable to obtain a convergent solution (with a 24% COV). Further, sensitivity analysis is carried out to quantify the effect of the input parameters in influencing the variance of the response. The advantage of sensitivity analysis using polynomial chaos based approaches is that the full randomness of the response is represented in the set of the coefficients. From the analysis, the sensitive parameter affecting the concentration trends is distribution coefficient and its sobol index lies in the range 0.814 - 0.93 (for all the cases) in the case of both short-lived and long-lived radionuclides. It can also be noted that, there is very slight effect of porosity which lies in the range 0.1 - 0.2 also on the overall response of the system.

(a)

(b)
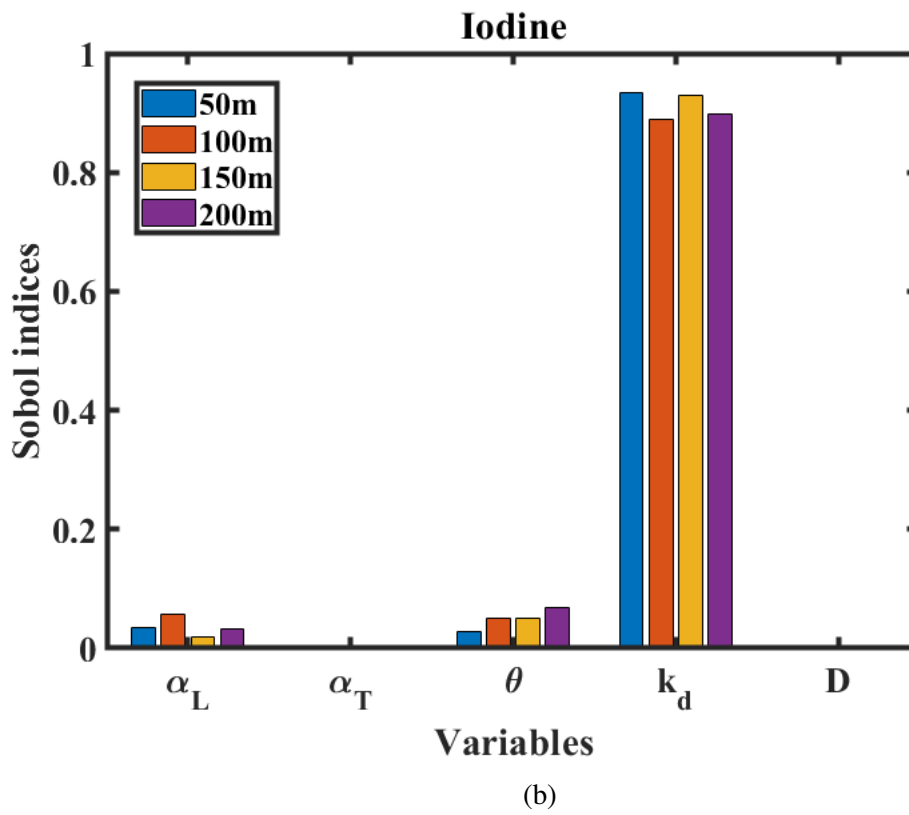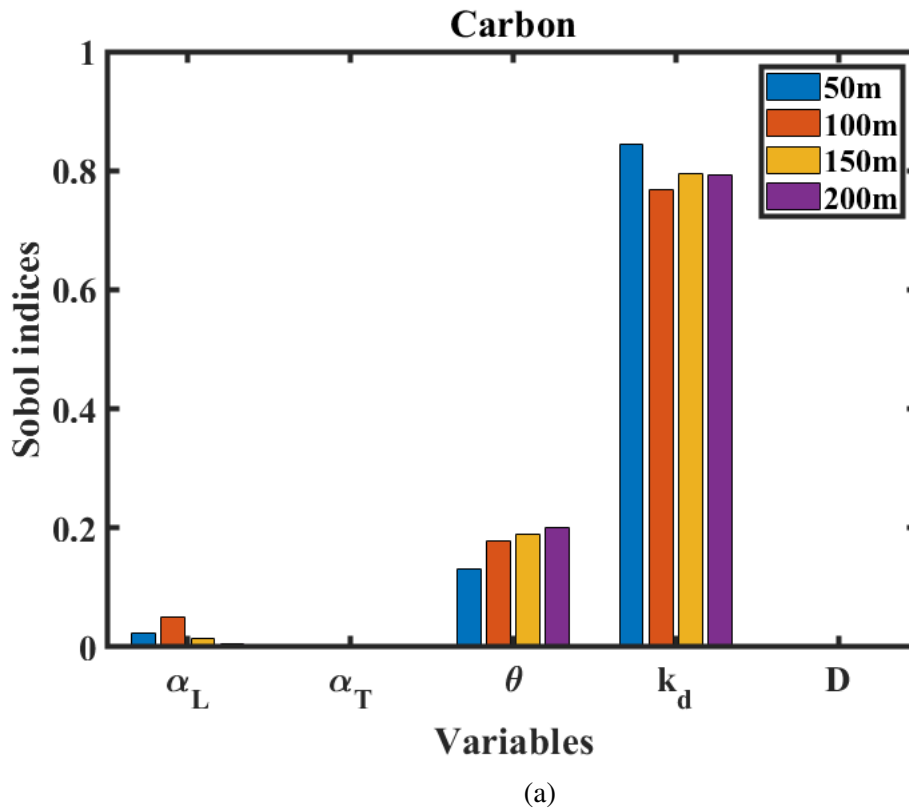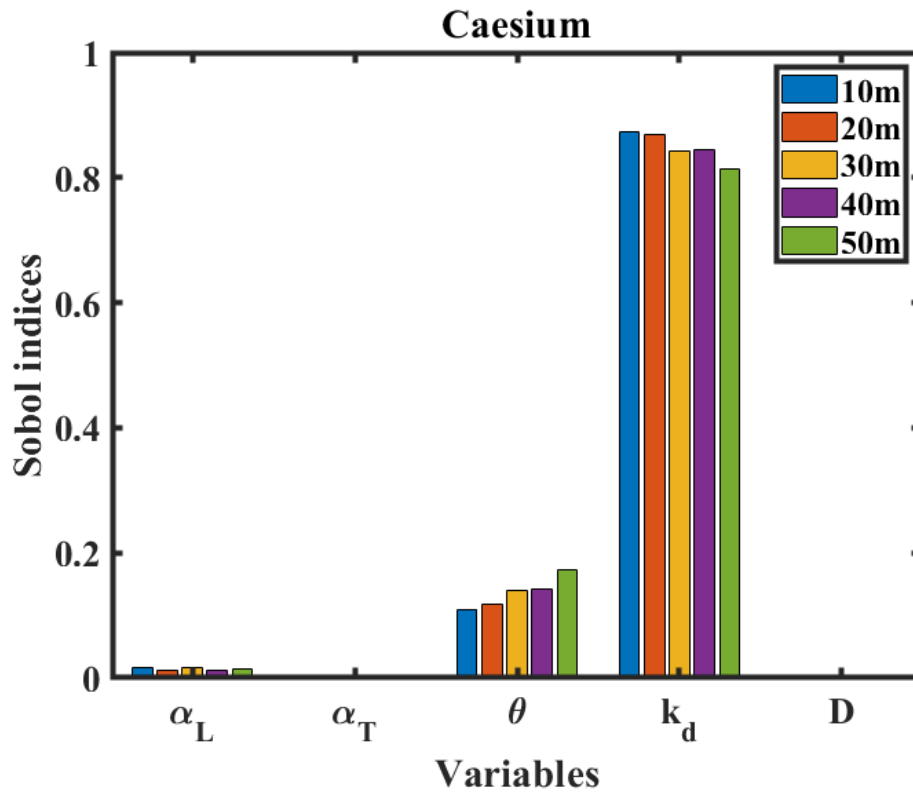
(c)
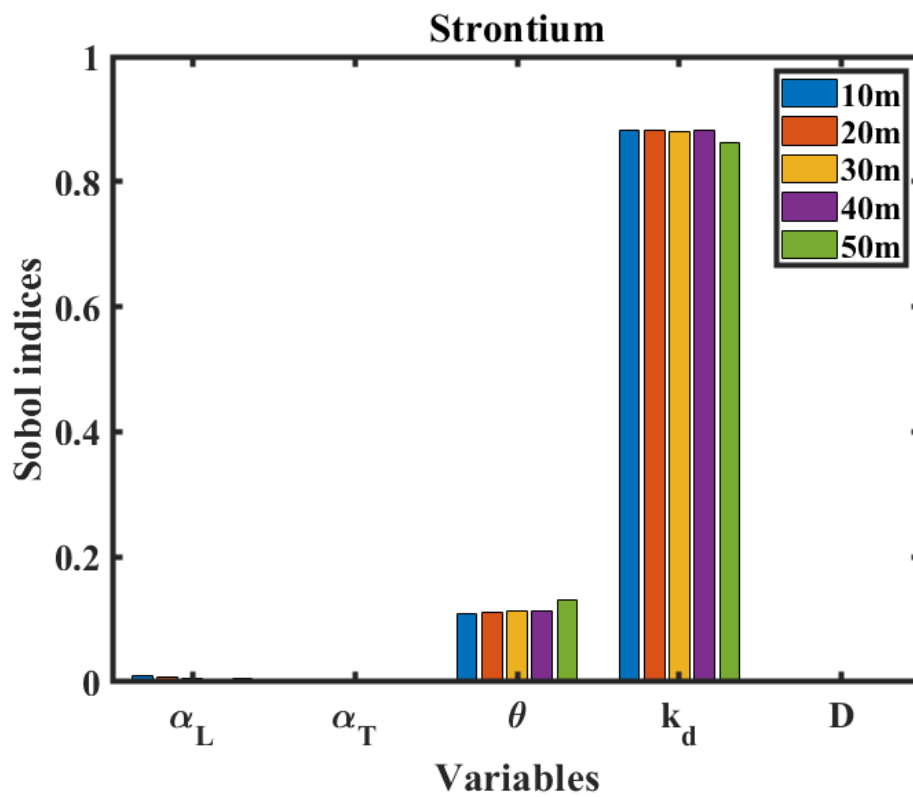
(d)

Figure 5.15: Sobol indices for all the radionuclides

From Figure 5.15, it can be observed that as the distance from the source increased, the Sobol index of porosity increased slightly and there is a decrease in the values of distribution coefficient. This implies that, with the increase in the distance from the source, the porosity of the medium (i.e., groundwater velocity= Darcy velocity / porosity) becomes critical. The sensitive parameters are also estimated by post processing the conditional levels during subset simulation. Figures 5.16 - 5.20 represent the histograms of conditional levels for the five uncertain parameters.

(i) 1st conditional level (ii) 2nd conditional level
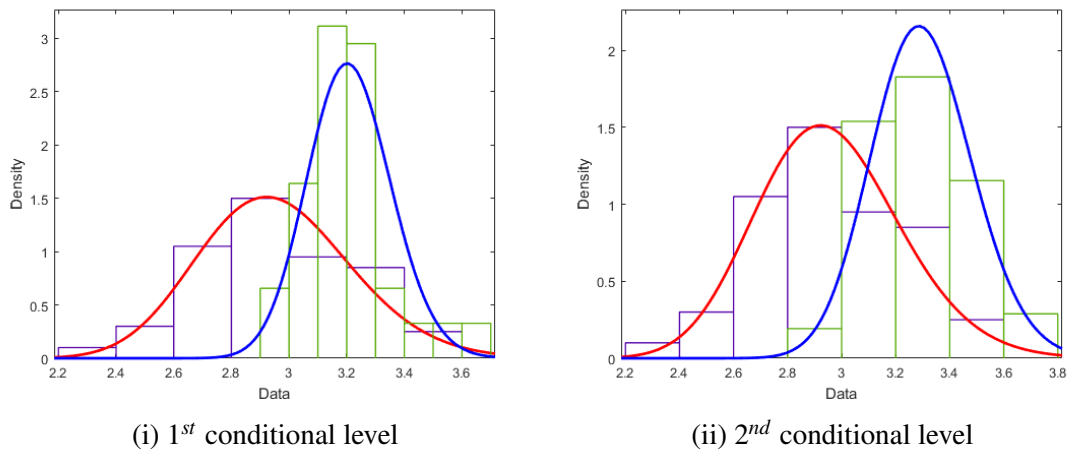
Figure 5.16: Shift in the distribution over two conditional levels for longitudinal dispersivity

(i) 1st conditional level (ii) 2nd conditional level
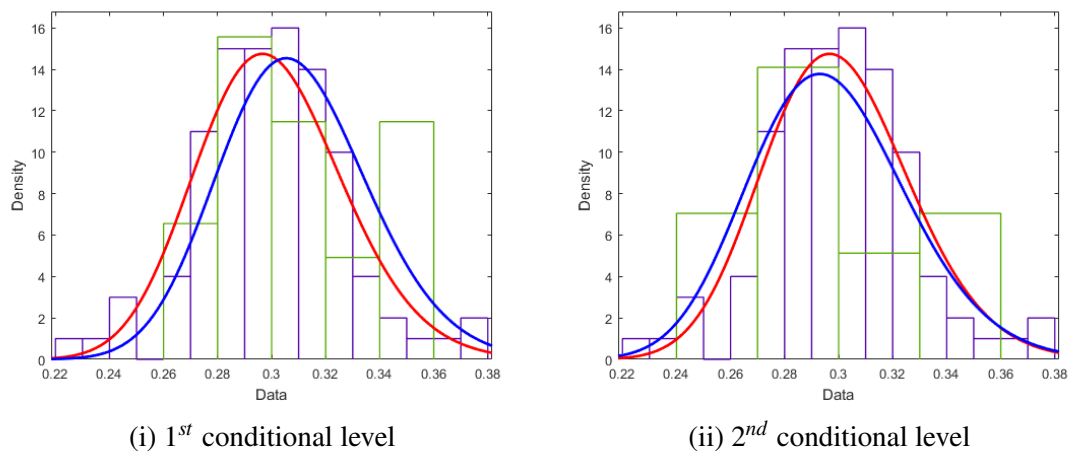
Figure 5.17: Shift in the distribution over two conditional levels for transverse dispersivity

(i) 1st conditional level

(ii) 2nd conditional level
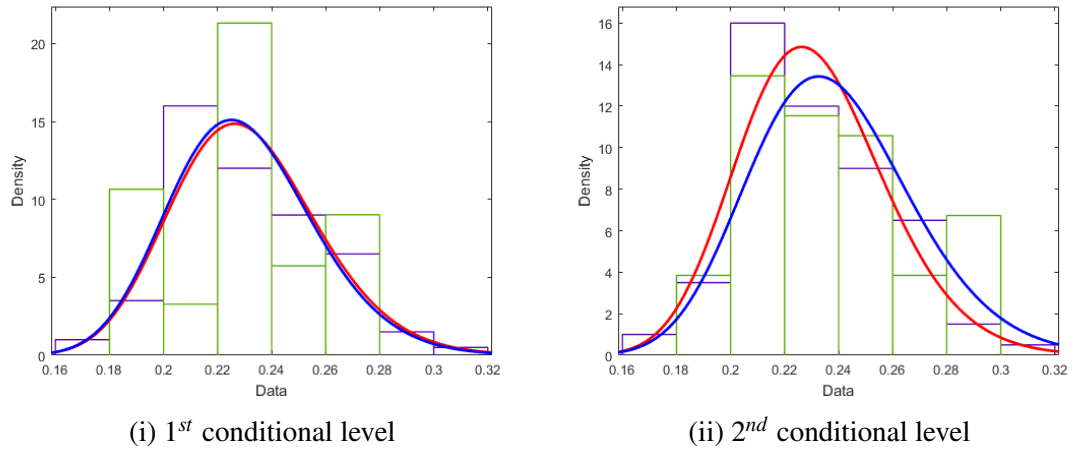
Figure 5.18: Shift in the distribution over two conditional levels for porosity

(i) 1st conditional level

(ii) 2nd conditional level
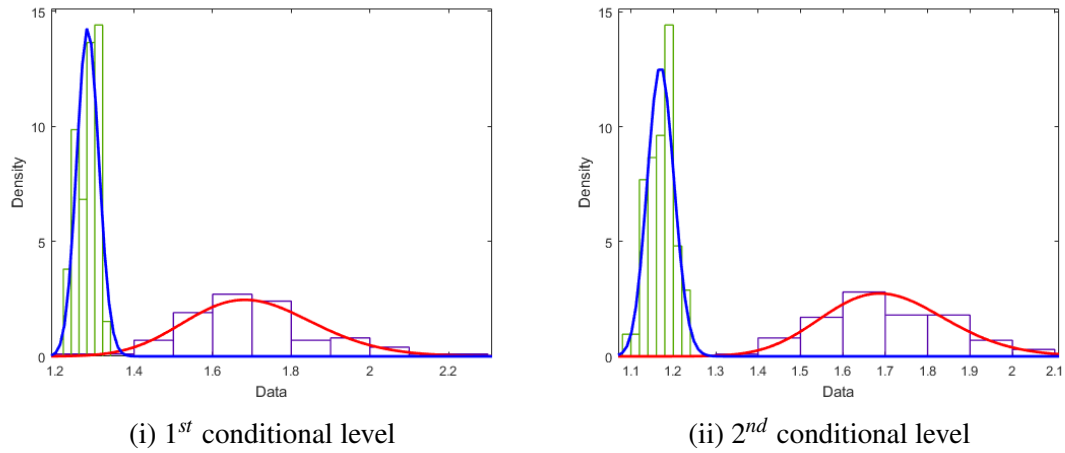
Figure 5.19: Shift in the distribution over two conditional levels for distribution coefficient

(i) 1st conditional level

(ii) 2nd conditional level
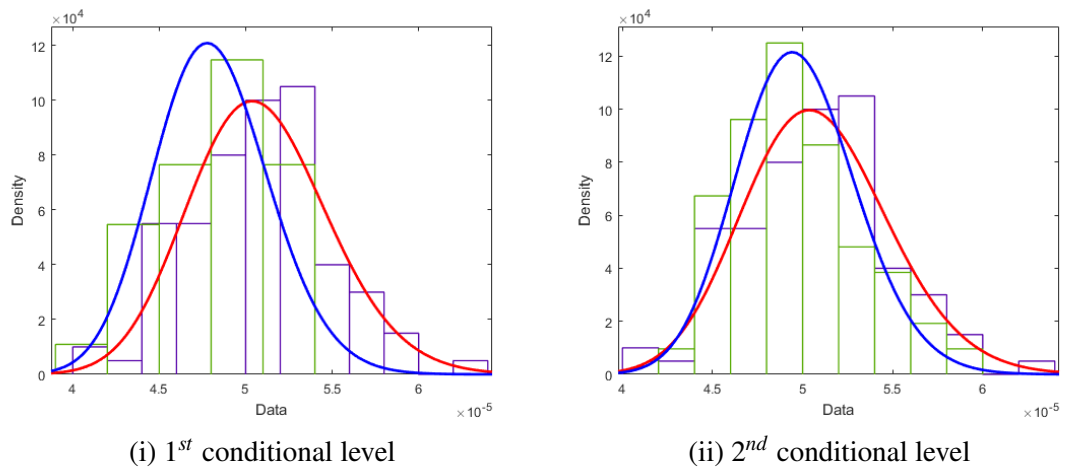
Figure 5.20: Shift in the distribution over two conditional levels for molecular diffusion

229

The red trend line refers to actual distribution and the blue trend line refers to empirical distribution (from conditional samples). From the results it can be indicated that, amongst the five input parameters, distribution coefficient showed maximum shift (leftward) with respect to the actual distribution while moving from conditional level one to conditional level two (within one SS run). Also, the gap between the actual and empirical distribution increased towards the final conditional level. This suggests that distribution coefficient displays maximum sensitivity. The inferences made from this analysis are consistent with the observations made in the previous studies (Nair and Krishnamoorthy, 1999; Volkova et. al., 2008). So far, a integrated performance assessment model that quantifies the effect of parameter uncertainty is developed. Its safety indicators (radionuclide concentration, radiation dose, risk and P_f) are estimated which suggest that there is a very low radiological impact due to the radionuclide release in biosphere.

5.4 Effect of spatial variability on performance assessment model

Geosphere is seldom homogeneous or isotropic system. For instance, the formation of soil is a natural process and due to the surrounding environmental conditions, their properties also vary from place to place at a given time and, this variability cannot be reduced as it is a natural phenomenon. The sources of heterogeneity in soil can also exist due to different depositional conditions and loading histories. However, this variability is rarely taken into account directly in traditional geotechnical analysis. In the field of contaminant transport studies, hydrologic properties of aquifers were estimated using homogeneity assumption because of mathematical challenges associated with the heterogeneity of aquifers. Also,

spatial averaging of the properties to determine the effective parameters led to inaccurate representation of soil. In the last two decades, the geotechnical community recognised these issues and began to use probabilistic methods to take spatial uncertainties directly into account. The importance of modelling spatial variability has been demonstrated in the literature (Vanmarcke, 1983; Phoon and Kulhaway, 1998; Phoon and Ching, 2014; Griffiths et. al., 2015). Also in the field of contaminant transport studies the influence of spatially varying transport has been recognised (Simmons et. al., 2001). Characterizing this form of uncertainty impacts the response of the system indicating that there is a need to understand this impact on performance assessment of radioactive waste disposal system. So, in this subdivision a predictive model is developed that can compute the radiation dose in a spatially varying medium and quantify the uncertainties associated with it. The sequence of steps followed for the analysis are presented in Figure 5.21.
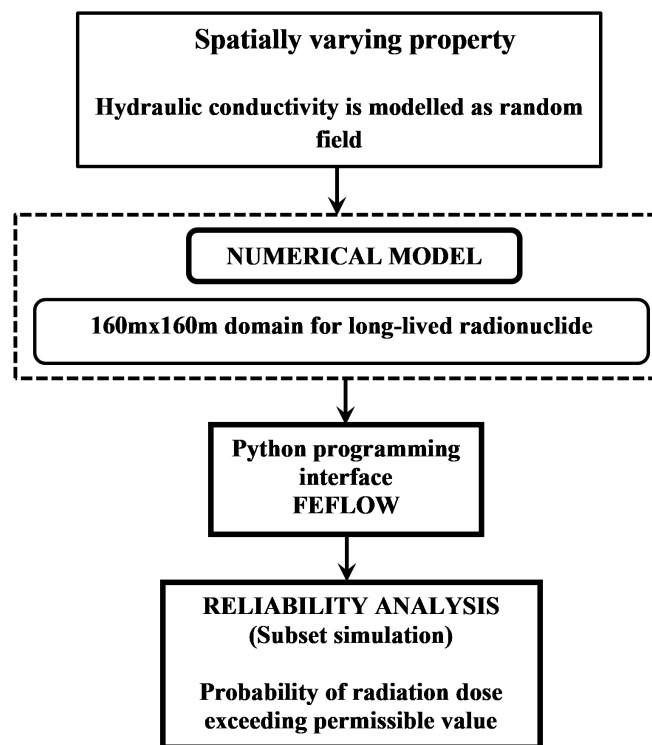
Figure 5.21: Framework for performance assessment of NSDF with spatial variability

From Figure 5.21, it can be noted that the spatially varying parameter is input to the numerical model and radiological impact experienced due to spatial variability of soil is estimated. Further, using python-interface program, the probabilistic methods used to estimate the failure probability is automated. A detailed discussion of the procedures involved in each step are presented in following sections.

5.4.1 Random field modelling

The concept of random field can be illustrated by a simple example. When a soil property, say permeability P is measured at a position x, time t, the property P can be modelled as $P(x,t) = d(x,t) + e(x,t)$, where $d(x,t)$ is some deterministic function and $e(x,t)$ corresponds to some measurement error that can fluctuate randomly. The random fluctuations at each point can be modelled by a set of random variables called the random process. A random process that is indexed by a spatial variable is called a random field. In other words, random field is nothing but an indexed set of random variables (Adler, 1981; Vanmarcke, 1983). In the assessment of random fields the data needs to be conditioned and sense of stationarity (weak stationarity or statistical homogeneity) and ergodicity must be achieved. The stationarity of random field means that the observations have a constant mean and an autocovariance which is a function of separation distance (irrespective of the location points). It can be achieved by trend removal, differencing, and /or variance transformation (Stuedlein et. al., 2012). The ergodic nature of random field indicates that the ensemble and spatial averages converge.

To describe a random field, the joint distribution of the random variables $\{R(x_1), \ldots, R(x_n)\}$ for any n and, the location points $\{x_1, x_2, \ldots, x_n\}$ must be specified. When the field is Gaussian, the random variables are defined by multivariate normal distribution (with

statistical parameters mean and covariance). However, for non-gaussian field which is specified by marginal probability density function and its correlation structure, a non-linear transformation with an underlying Gaussian distribution needs to be performed (Papaioannou and Straub, 2012). It is also known as Nataf transformation and the joint distribution is called Nataf multivariate distribution. To describe Gaussian random field completely, one-point statistical parameters like mean μ and variance σ^2 and their correlation structure ρ needs to be specified. Here, the autocorrelation distance is defined as the spatial extent within which soil properties show a strong correlation. It is also represented as the distance up to which the autocorrelation function decays to $1/e$. Beyond this distance, they can be treated as independent random variables. The exponential autocorrelation function $\rho(x, x')$ is given by

$$\rho(x, x') = exp\left(-\frac{|x - x'|}{l}\right) \tag{5.13}$$

In the equation (5.13), l is the auto-correlation length which is expressed as the separation distance within which two random values (spatially varying property) are significantly correlated. When the 'l' value is small, it indicates a strong correlation and viceversa. This implies that for a homogeneous material l is a large value, while, it is low when the material exhibits strong variation over small distances. These aspects are discussed in detail in section 3.4 of chapter 3. In this chapter, the spatial variability of hydraulic conductivity is modelled as a one-dimensional isotropic and heterogeneous random field. The heterogeneity is modelled in the system to investigate the radionuclide movement through the medium. A schematic of random field realizations along a 160 m domain is presented in Figure 5.22.
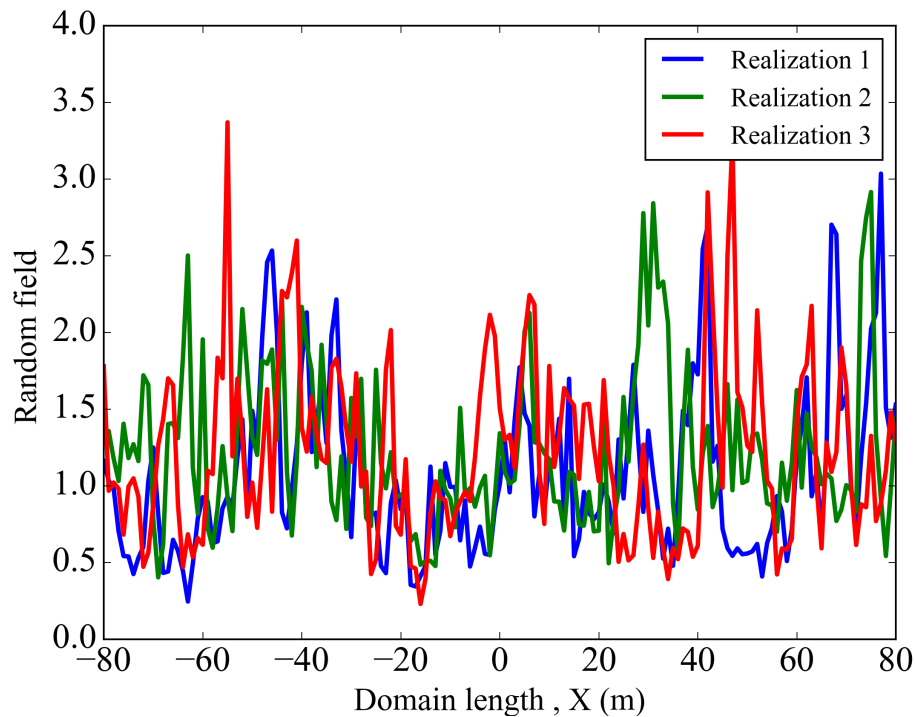
Figure 5.22: Typical set of realizations in spatially variable soil

5.4.1.1 Discretization of random fields

To approximate the mechanics of response of the system in finite element method, spatial discretization methods were developed (Der Kiureghian and Ke, 1988). The discretization aims to replace a continuous random process by a finite set of random variables. They are categorized into point discretization methods, average discretization methods and series expansion methods which have been discussed in detail in section 3.4 of chapter 3. Some of these methods are relatively inefficient in the sense that a large number of random variables are required to achieve a good approximation of the field. However, series expansion methods like Karhunen-Loeve (K-L) expansion and expansion optimal linear estimation (EOLE) methods have been developed to overcome the above constraints (Sudret and Der Kiureghian, 2002). In this chapter, the random field is discretized using K-L expansion. This method is based on the concept of spectral decomposition of its

autocorrelation function $\rho(x,x')$, which is bounded, symmetric, and positive definite. Let $H(x,\theta)$ be random field associated with spatial parameter $x \in \Lambda$. The set of deterministic functions over which any realization of the field $H(x,\theta_0)$ is expanded is defined by the eigenvalue problem given by

$$\int_\Lambda \rho(x,x')\phi_i(x')d\Lambda_{x'} = \lambda_i\phi_i(x) \tag{5.14}$$

where λ_i, ϕ_i are eigen values and eigen vectors of the auto-correlation function. The series expansion is given by the equation

$$H(x,\theta) = \left[\mu + \sum_{i=1}^{M} \sqrt{\lambda_i}\phi_i(x)\xi_i(\theta)\right] \tag{5.15}$$

In the case of an exponential autocorrelation function (equation (5.13)), for a one-dimensional case, the eigenvalue problem (equation (5.14)) can be solved analytically. The derivation is presented in section 3.4. In this chapter, the parameter is modelled as a log-normal random field. So the expansion becomes (Cho and Park, 2010)

$$H(x,\theta) \approx exp\left[\mu_{ln} + \sum_{i=1}^{M} \sqrt{\lambda_i}\phi_i(x)\xi_i(\theta)\right] \tag{5.16}$$

where μ_{ln} is the mean of underlying normal field. The statistical parameters of log-normal random field are given as

$$\sigma_{ln} = \sqrt{ln(1+(\sigma/\mu)^2)}$$
$$\mu_{ln} = ln\mu - 0.5\sigma^2 \tag{5.17}$$

By solving the eigen problem analytically, mathematical expressions for eigen value and eigen vectors are estimated. Before estimation of these values, the roots of transcendental equations are estimated. All the mathematical equations are coded in python program and the stochastic analysis to generate the random field of soil property is automated. For a domain of 160 m with an interval [-80 m, 80 m] and auto-correlation length of 2 m, a log-normal random field is discretized using K-L expansion and results are presented in Figure 5.23 - 5.25. In Figure 5.23, the roots of transcendental equations are estimated at the points of intersection of curve 1, curve 2 and curve 3 (from section 3.4). The monotony of decay observed in Figure 5.24 (eigen values) is ensured by the symmetry of the covariance function, and the rate of the decay is related to the auto-correlation length of the process being expanded. In Figure 5.25, the first eight eigen functions are plotted. These functions are orthogonal and complete.
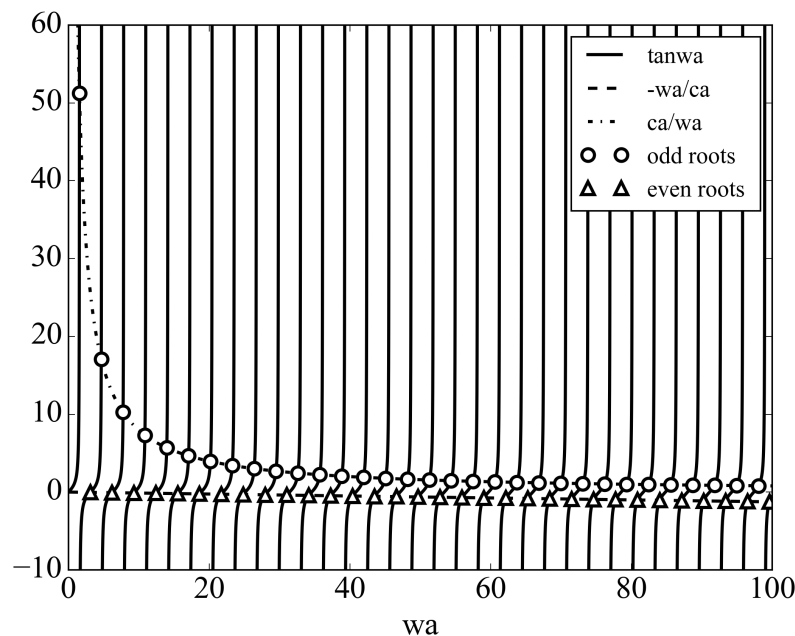
Figure 5.23: Roots of transcendental equations represented graphically
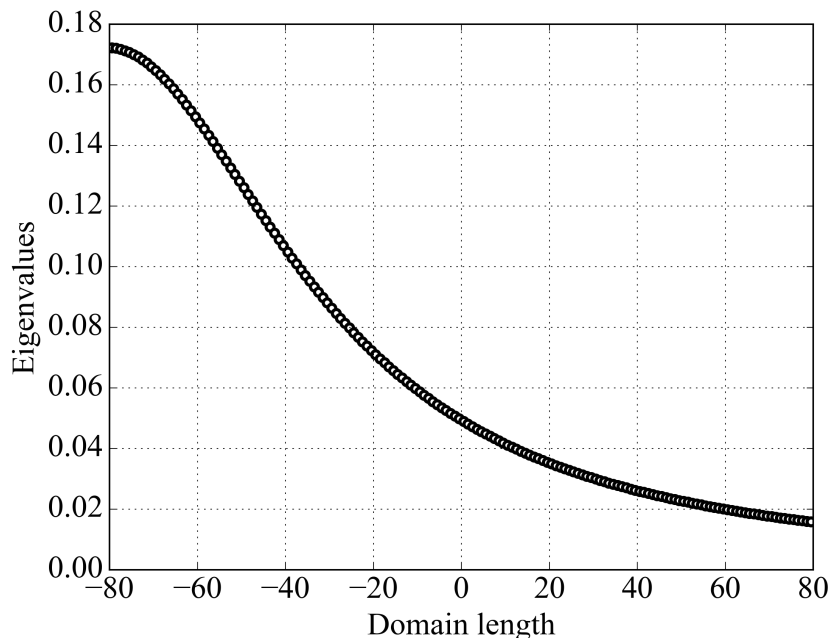
Figure 5.24: Eigenvalues λ_n for the exponential kernel and auto-correlation length ($l_x = 2$)
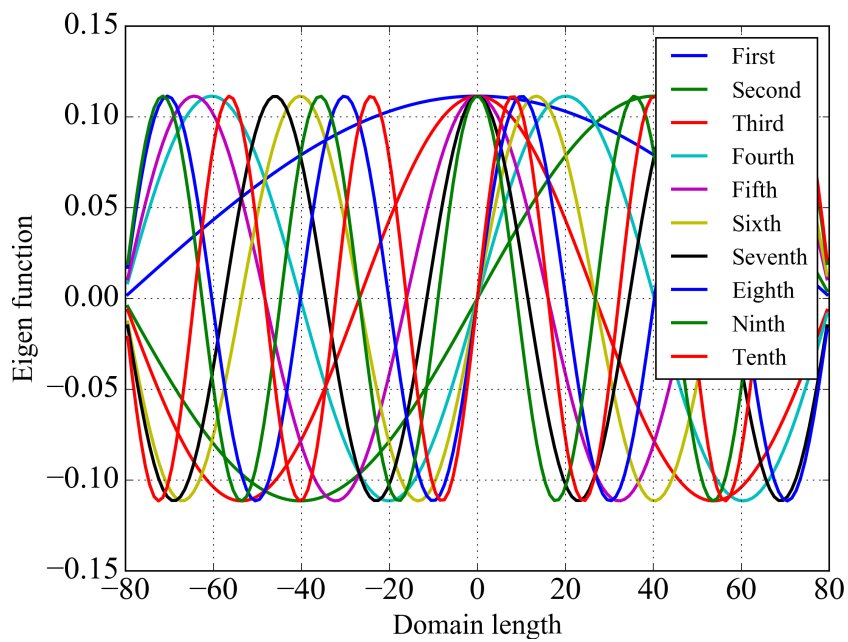
Figure 5.25: Eigenfunctions for the domain $-80 \leq x \leq 80$

The realization of random field for the given auto-correlation length using K-L expansion is presented in Figure 5.26. This kind of approximation should be performed

carefully, aiming to represent accurately the random process with the smallest number of random variables. The number of terms required to approximate random field with least error requires the truncation of terms. The error is estimated from the equation developed by Sudret and Bervellier (2008). Using equation (3.45) (in chapter 3), the evolution of error over the length of the domain is presented in Figure 5.27. Further, the error versus number of terms used for truncation is presented in Figure 5.28. From the results it can observed that, the error reduced from 85% to 11% with the increase in the number of terms from 10 to 300. So, for an auto-correlation length of 2 m, 300 terms are used to approximate the random field.
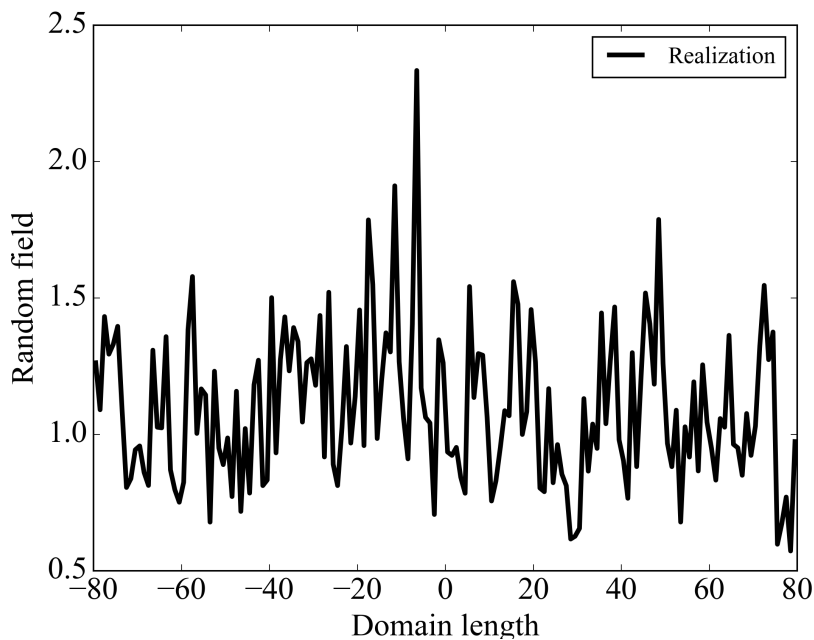
Figure 5.26: A typical random field realization obtained from K-L expansion

To understand the effect of auto-correlation length on the random field, five different auto-correlation lengths (2 m, 5 m, 10 m, 15 m and 20 m) are considered for the analysis. It was observed that the number of truncation terms required to approximate the random field reduced with the increase in auto-correlation length. The results for all the above

auto-correlation lengths are presented in the Table 5.7.

Table 5.7: Number of truncation terms for different auto-correlation lengths

SNo	Auto-correlation length (m)	Number of terms for truncation	Error (%)
1	2	300	11
2	5	250	9
3	10	100	8
4	15	60	8
5	20	30	8
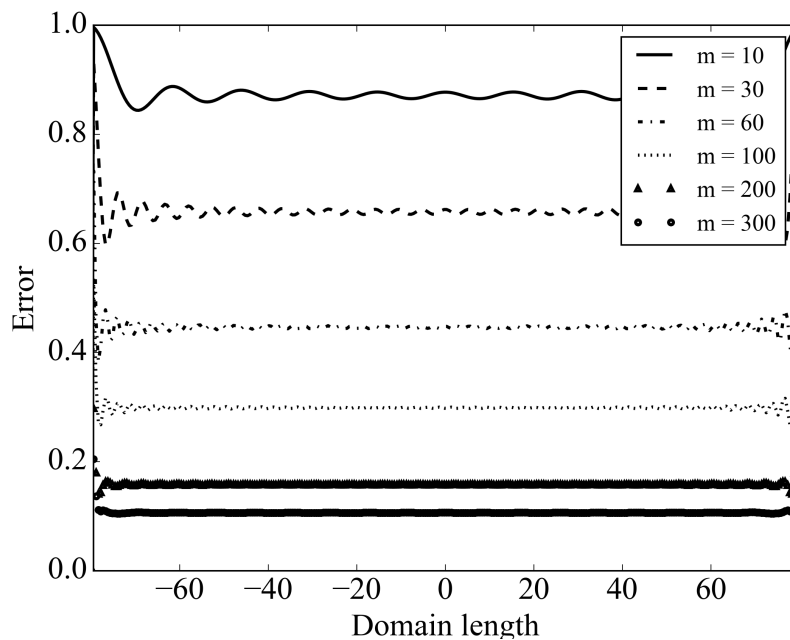
Figure 5.27: Error along the domain for different values of M

This observation indicates that the medium becomes homogeneous with the increase in auto-correlation length. By generating the random variables according to their truncation order, the random field is simulated numerically. In the next section, the modelling procedure followed to develop performance assessment model in a spatially variable ge-

ological environment is discussed in detail. This analysis quantifies the risk associated with the radionuclide doses in a spatially varying medium for long time scales by implementing efficient probabilistic tools.
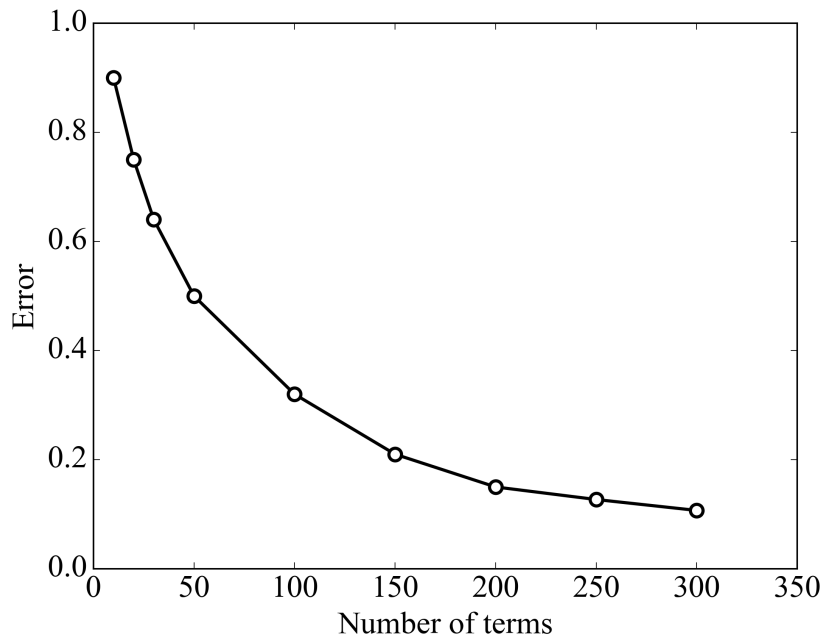
Figure 5.28: Error versus number of terms for series expansion

5.4.2 Development of performance assessment model

The source term component of performance assessment model remains the same as in the previous case (section 5.3.1.1). It is assigned as a decaying mass boundary condition. Also, the failure of disposal system is assumed to occur due to infiltration of water leading to consequent release of radionuclide into geosphere. Further, the geosphere transport and the radiological impact due to the radionuclides reaching the biosphere are estimated.

5.4.2.1 Geosphere transport model

To simulate a spatially varying medium and explore the effect of radionuclide transport through heterogeneous system, a two-dimensional numerical model is developed. The

governing equation of transport remains the same as mentioned in section 5.3.1.2 and, the numerical modelling process is described in detail in chapter 3.

5.4.2.1.1 Input data considered for the analysis

From the previous analysis, it is clear that among the four radionuclides, long-lived radionuclide Iodine (^{129}I) delivered the highest concentration. So, the critical one amongst all the radionuclides is considered in this study. Hydraulic conductivity of the domain is modelled as the spatially varying property. This geological property has been considered to model the heterogeneity in the previous studies as well (Sudicky, 1986; Cho, 2014). The input data considered for the study is presented in Table 5.8 and the source term decaying with time estimated from equations (5.1) - (5.3) is plotted in Figure 5.29. The boundary conditions and transport properties of the medium considered for the analysis are presented in Table 5.8.
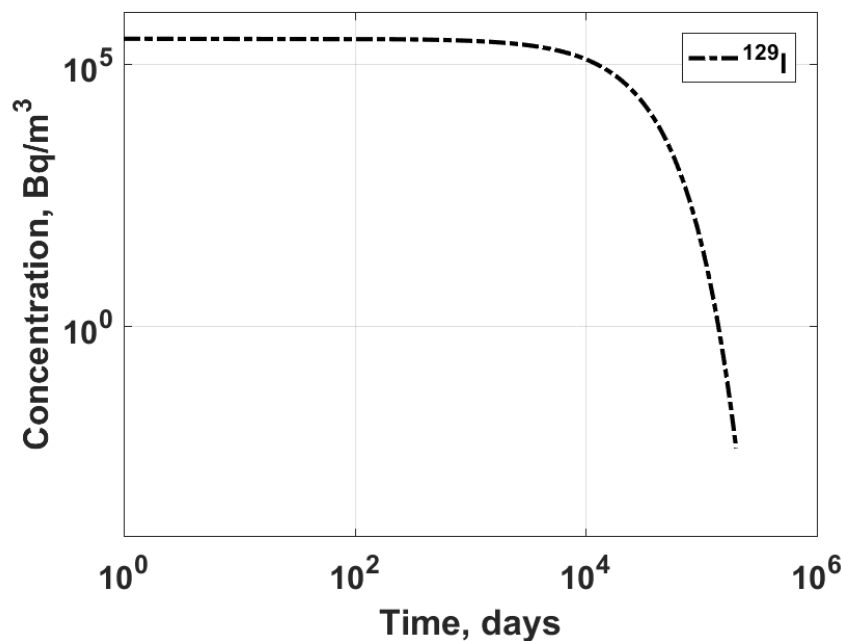
Figure 5.29: Source concentration versus time

Table 5.8: Input data considered for the analysis

Quantity	Value
Study domain	
Domain length (m)	160
Domain width (m)	160
Hydraulic conductivity (m/day)	0.05
Porosity	0.3
Molecular diffusion (m^2/s)	5×10^{-10}
Longitudinal Dispersivity (m)	1
Transverse Dispersivity (m)	0.1
Flow IC and BC's	
Dirichlet-type BC on upstream side ($-80 \leq x \leq 80, y = -80$) ($m$)	50
Dirichlet-type BC at downstream side ($-80 \leq x \leq 80, y = 80$) ($m$)	10

A domain of size 160 m $\times$ 160 m is modelled in FEFLOW. The sectional view of the two-dimensional FE mesh is presented in Figure 5.30.
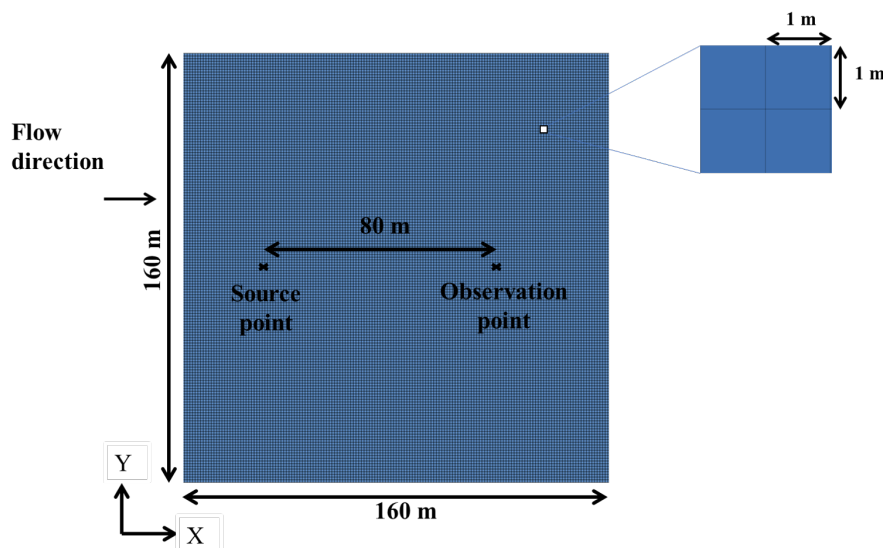
Figure 5.30: Domain considered in the present study

The finite element mesh is generated with 25,921 nodes. The fluid flow and mass

transport conditions are assigned separately. So, the contaminant transport process is simulated numerically as a coupled flow and mass transport. To model the effect of leaching from the barrier to the aquifer, the source is treated as an injection well. The concentration and radiation dose of the radionuclides are computed at a distance of 80 m from the source.

5.4.2.2 Probabilistic analysis

The random nature of hydraulic conductivity can have an impact on the radionuclide concentration, radiation dose and risk over spatial and temporal scales. In this analysis, the influence of spatial auto-correlation length, coefficient of variation and the time of arrival of maximum concentration are investigated. Also, to quantify the effect of spatial variability, reliability analysis is carried out to estimate probability of failure. In the following section, the process of integrating K-L expansion and subset simulation is presented.

5.4.2.3 Integrating the K-L expansion and subset simulation

To estimate the failure probability, subset simulation and K-L expansion are linked. This methodology is presented by Ahmed and Soubra (2018). The general algorithm of subset simulation remains the same as mentioned in section 3.6.1.2. Also two critical steps are introduced to integrate both the methods and they are presented below:

1. To substitute the vector $\xi_{i_{i=1,...,M}}$, generated in the first step of subset simulation, in K-L expansion. Then, assign these values at the centres of the different elements of the deterministic finite element mesh to simulate the random field.

2. By assigning these values to the mesh a new deterministic model (i.e., realization) is created each time and the corresponding system response is computed.

This process is repeated till the random field generated from the random variables belonging to the last failure region are estimated. The process of integrating both the methods is coded using python programming interface and automated.

5.4.3 Results and Discussion

To investigate the influence of spatially variable medium on the radionuclide transport, hydraulic conductivity is modelled as a log-normally distributed random field with an exponential autocorrelation function. The random field is discretized using K-L expansion and the results were presented in section 5.4.1.1. The numerical model corresponding to spatially varying medium with a auto-correlation length of 2 m is considered as deterministic case. The sectional view of heterogeneous domain are presented in Figure 5.31.
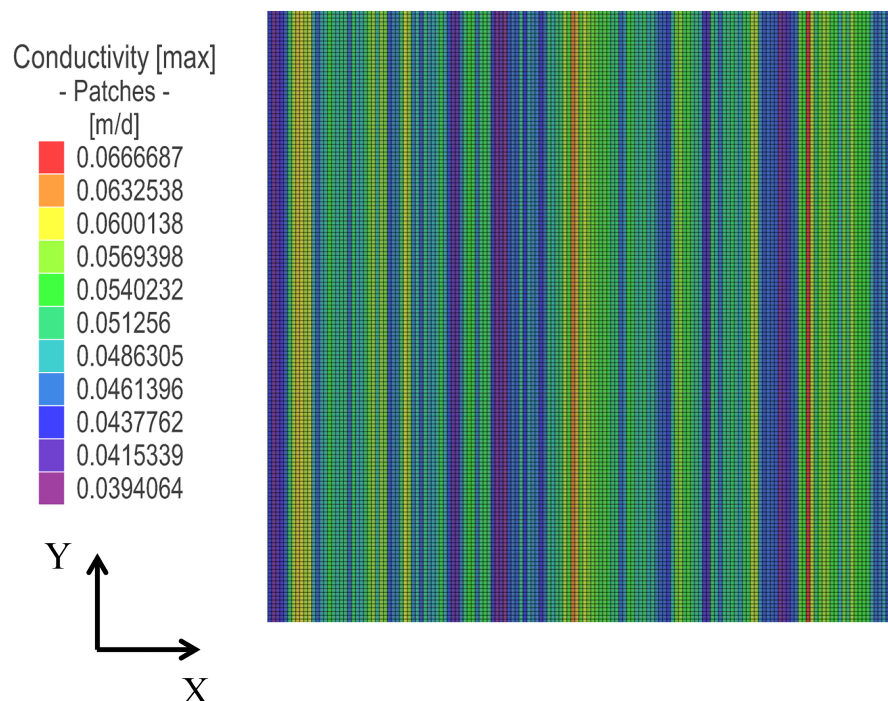
Figure 5.31: Spatially varying hydraulic conductivity along the domain

From the figure, it can be observed that there is varying hydraulic conductivity (indi-

cated by the colour spectrum). However, the hydraulic conductivity is same at a particular point in both x and y directions confirming the isotropic nature of the medium. So, it is a one-dimensional heterogeneous, isotropic system. The radionuclide concentration trend extending over space and time are plotted and the deterministic results are presented in Figure 5.32. The concentration trends are computed at 80 m, 100 m and, 200 m from the source. The results indicate that there is almost 15% decrease in peak concentration value with the increase in distance from the source. Also, the time of arrival of peak concentration increased with the increase in the distance from the source. The results present a strong influence of the heterogeneity in the medium on the resultant concentration. The radiation dose and risk computed from the formulation for radiological model are compared with the risk due to natural catastrophes and, it was observed that they were within the safe limits.
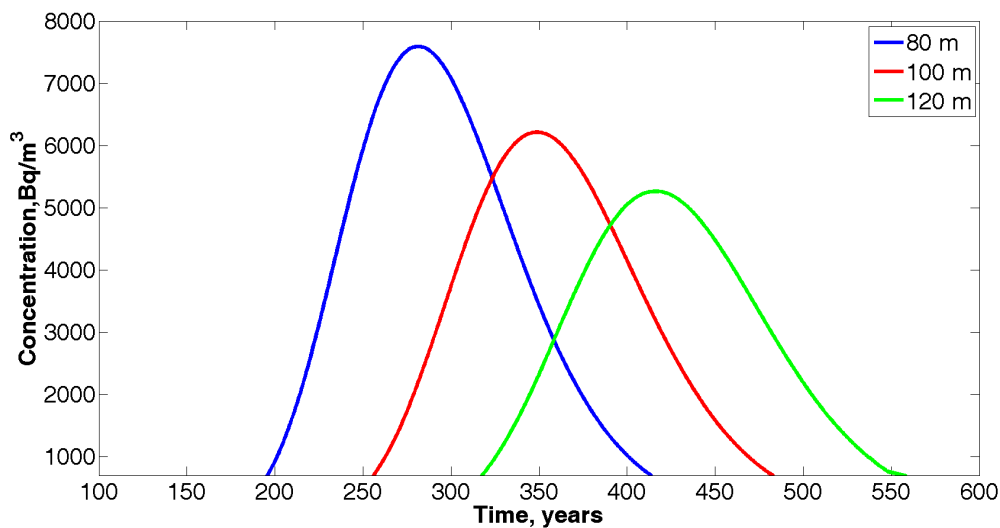
Figure 5.32: Concentration versus time for various distances

Since it is known that a deterministic design presents conservative results, attention is also drawn to understand the probabilistic behaviour corresponding to different values of the spatial auto-correlation length. To demonstrate the effect of variability on the resul-

tant concentration trends, a set of Monte Carlo simulations are run (for spatially varying medium (l_{lnx} = 5 m, COV = 50%)) and the realizations are presented in Figure 5.33. In the Figure 5.33, homogeneous case refers to constant hydraulic conductivity in the entire medium. As mentioned earlier, the figure shows that in the deterministic case (i.e., homogeneous and realization at mean), the results are within the safe limits. Further, among the deterministic cases it can be noticed that, the concentration value is lesser in homogeneous case (black line) than the spatially variable case (red line). Overall, in the spatially variable case, the fluctuations in radionuclide concentrations are very high. There is a variation of almost 50% when compared to deterministic case results.
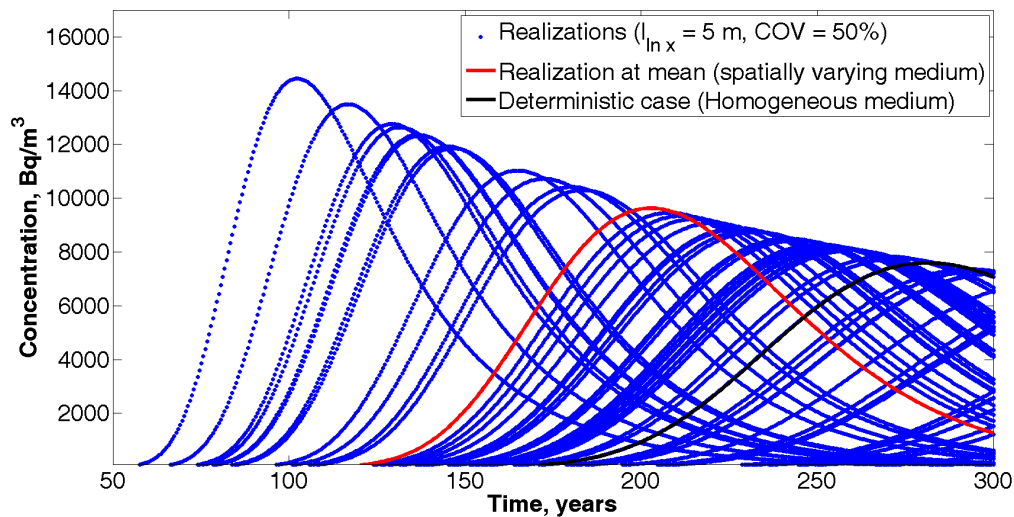
Figure 5.33: Concentration versus time for various cases

Further, the radionuclide concentration contours at the end of 200 years for a homogeneous and different spatially variable cases are compared and presented in Figure 5.34. The end-point is located at 80 m from the source and marked as '×' in the figure. The concentration contours for a homogeneous medium is presented in Figure 5.34 (a) and spatially varying medium in Figures 5.34 (b) - (d). The contours are more spread out in Figure 5.34 (a) indicating more dispersion and concentration at the end-point in this case

than the other cases (Figure 5.34 (b) -5.34 (d)). Also, a faster rate of movement of radionuclide can be noticed in the homogeneous medium than a spatially varying medium. This is because, the flow of radionuclide is mainly driven by advection, and, any factor promoting advective process influences the resultant concentration reaching the end-point of the domain. In fact, when the hydraulic conductivity is high, it indicates high seepage velocity which affects advection and mechanical dispersion. The fluctuations in conductivity are frequent in a spatially varying medium leading to a slower rate of flow and lower concentration. To illustrate this effect, the concentration spread along x and y directions for 2500 Bq/m^3 contour are measured and the results are presented in the Table 5.9.

Table 5.9: Dispersivity for a 2500 Bq/m^3 contour with varying a auto-correlation length and coefficient of variation

Case	Random field, SPV*	Dispersivity (m)	
		Longitudinal	Transverse
(a)	Homogeneous medium	57	14
(b)	SPV l_{lnx} = 5 m; COV = 50%	51	12
(c)	SPVl_{lnx} = 5 m; COV = 10%	49	11
(d)	SPVl_{lnx} = 2 m; COV = 50%	45	10

*SPV- Spatially varying field

In the case of homogeneous medium, the longitudinal dispersivity is 57 m (from Figure 5.34 (a)) and for different cases of spatially varying medium it is 45 m, 51 m and 49 m respectively (from Figures 5.34 (b), 5.34 (c), 5.34 (d)). The dispersion is highest for homogeneous case and reduces in spatially variable case. Amongst the heterogeneous cases considered, the dispersivity decreased with the decrease in auto-correlation length. The same trend is observed for both longitudinal and transverse dispersion. These obser-

vations reiterate the influence of spatially variability on the radionuclide transport.
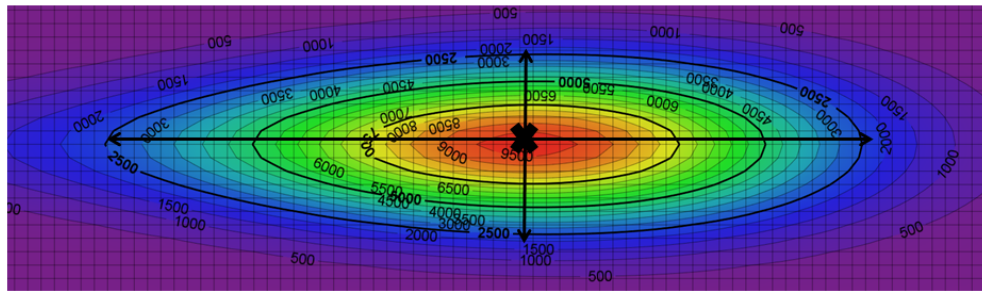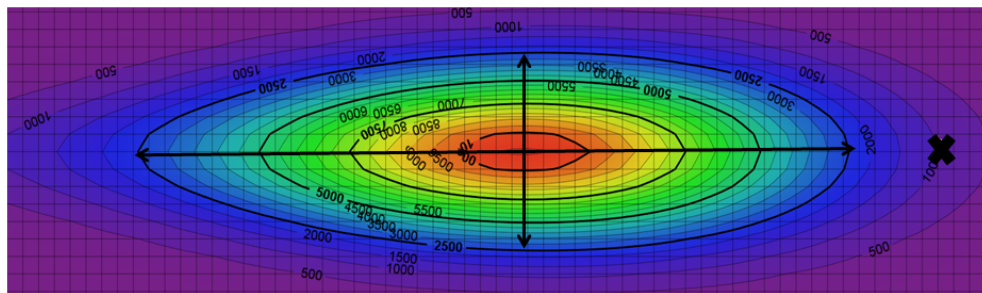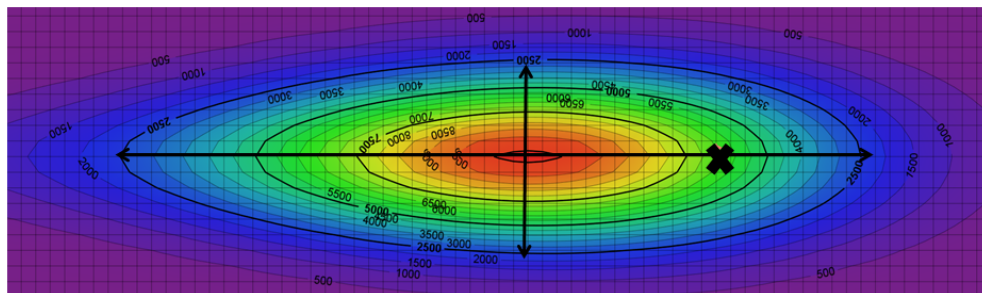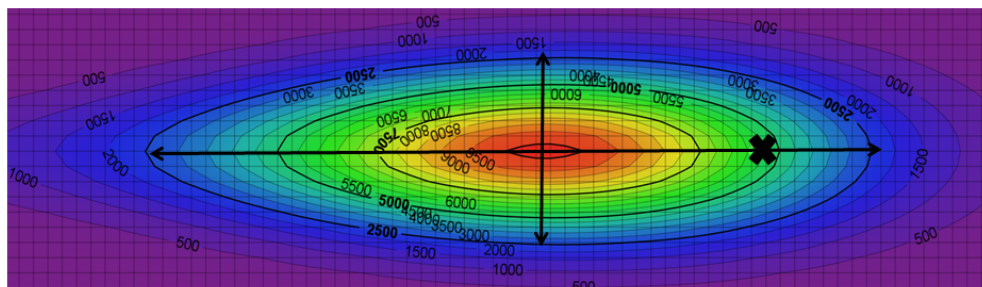
Figure 5.34: Concentration contours in (a) Homogeneous medium (b) Spatially varying medium (l_{lnx} = 2 m ; COV = 50%))(c) Spatially varying medium (l_{lnx} = 5 m ; COV = 50%) (d) Spatially varying medium (l_{lnx} = 5 m ; COV = 10%)))

5.4.3.1 Influence of auto-correlation distance and coefficient of variation on P_f

The influence of auto-correlation length and coefficient of variation (COV) on the radiation dose reaching a certain point of interest are also investigated. The probability of radiation dose exceeding its permissible value is determined using Monte Carlo simulation and subset simulation methods for different cases of auto-correlation length and COV values. Results are presented in Figure 5.35.
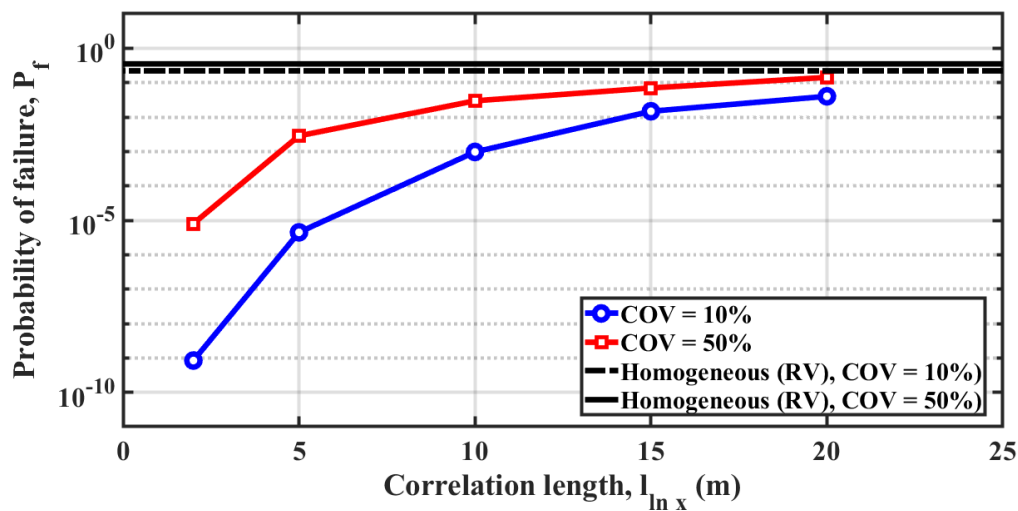
Figure 5.35: Probability of failure for different number of samples per subset

The range of P_f varied from 10^{-9} - 10^{-1}. The results show that, as the COV of the random field increased, the probability of failure of the system also increased. Similar observations were made in the previous studies (Fenton and Griffths, 2006; Haldar and Babu, 2008). From the Figure 5.35 it can be noted that, the probability of failure increased with the increase in correlation distance. In the figure, an increase in auto-correlation length from 2 m to 5 m, showed reduction in failure probability by a factor of 10^4. Further, with an increment of l_{lnx} from 5 m to 10 m and more, the P_f value is reduced by 10 times which is not very significant. So, the influence of the auto-correlation distance for the problem considered in the study is highest between 2 m - 5 m. When the medium is

quite erratic (i.e., small auto-correlation length), the scale of transition in the conductivity values become more often along the length and cause the radionuclide to travel slower. However, when the medium is smoother (i.e., large auto-correlation length), it becomes less heterogeneous, and thus, allows the radionuclide to move faster. The probability of failure (P_f) is estimated for a homogeneous soil and as mentioned earlier, it is higher than that of P_f for spatially varying soil. As the auto-auto-auto-auto-correlation length of the random field increases it becomes more homogeneous and leads to the same behaviour as homogeneous soil.

In spatially variable soil, radionuclide concentration becomes independent of variance at very high auto-correlation length and tries to attain a value close to the homogeneous case. The solid and the dashed black lines are for the homogeneous case. The studies carried out by Srivatsava et. al., (2009) support the observations presented in the present analysis. Also from the design point of view, it is necessary to model heterogeneity in soil in order to assess the risk associated with the radionuclide migration precisely. From the model results, it can be inferred that by assuming a medium to be homogeneous, a high P_f value is obtained, but, in reality (i.e., heterogeneous medium), the P_f is quite low. Since the extent of heterogeneity also influences the safety of the system, it is advisable to model a realistic spatially variable medium to understand the behaviour of radionuclide transport.

The extent of influence coefficient of variation has on P_f is estimated from the following analysis. The time taken for each simulation ranged from one hour (for high P_f values) to three days (for low P_f values) depending on the range of P_f computed from the simulation. The sample COV of failure probability over 25 independent subset simulation runs are plotted to observe the variability in P_f.

(i) COV Vs N_{ss}

(ii) P_f Vs N_{ss}
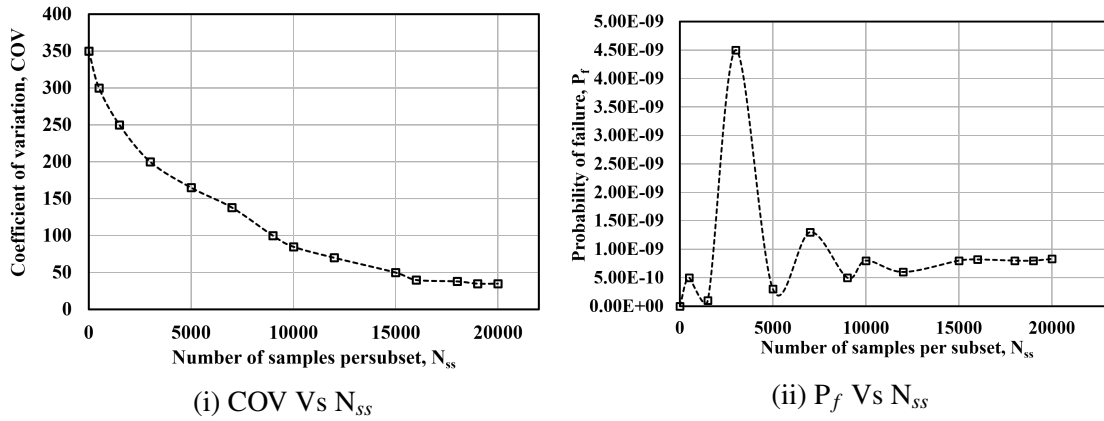
Figure 5.36: Trends of coefficient of variation and probability of failure for different number of samples per subset (auto-correlation length of 2 m and 10% COV)

(i) COV Vs N_{ss}

(ii) P_f Vs N_{ss}
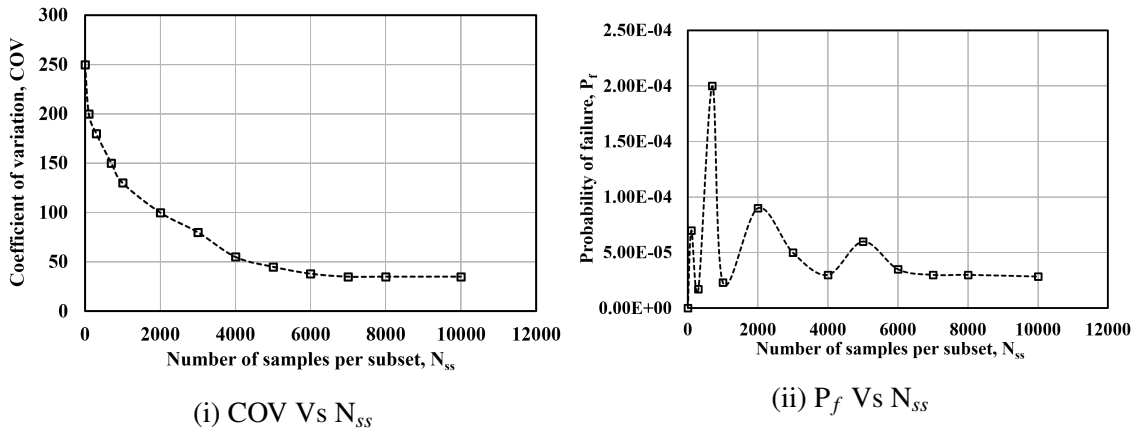
Figure 5.37: Trends of coefficient of variation and probability of failure for different number of samples per subset (auto-correlation length of 5 m and 10% COV)

(i) COV Vs N_{ss}

(ii) P_f Vs N_{ss}
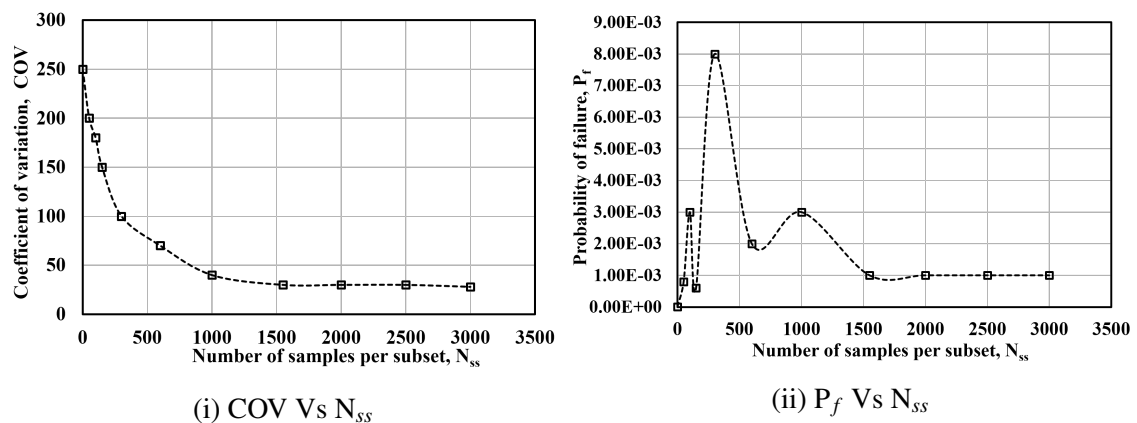
Figure 5.38: Trends of coefficient of variation and probability of failure for different number of samples per subset (auto-correlation length of 10 m and 10% COV)

(i) COV Vs N_{ss}

(ii) P_f Vs N_{ss}
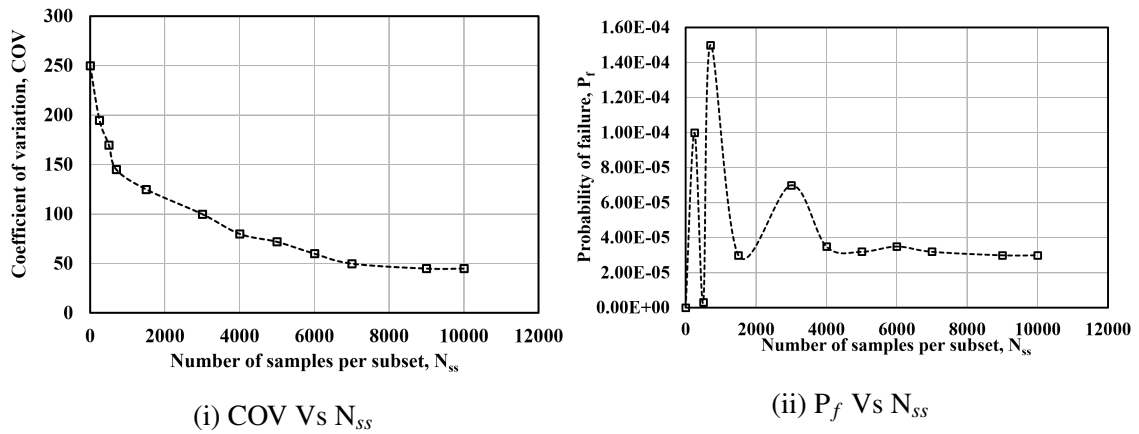
Figure 5.39: Trends of coefficient of variation and probability of failure for different number of samples per subset (auto-correlation length of 2 m and 50% COV)

(i) COV Vs N_{ss}

(ii) P_f Vs N_{ss}
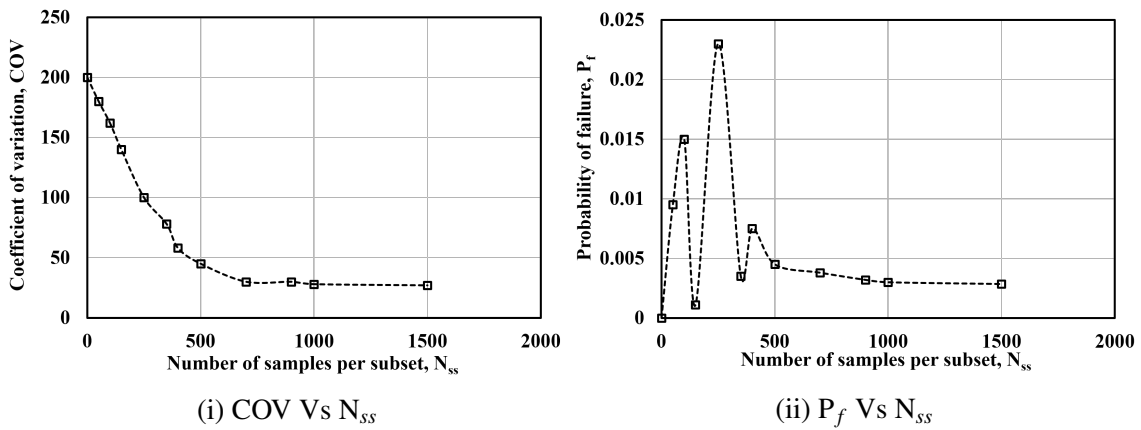
Figure 5.40: Trends of coefficient of variation and probability of failure for different number of samples per subset (auto-correlation length of 5 m and 50% COV)

(i) COV Vs N_{ss}

(ii) P_f Vs N_{ss}
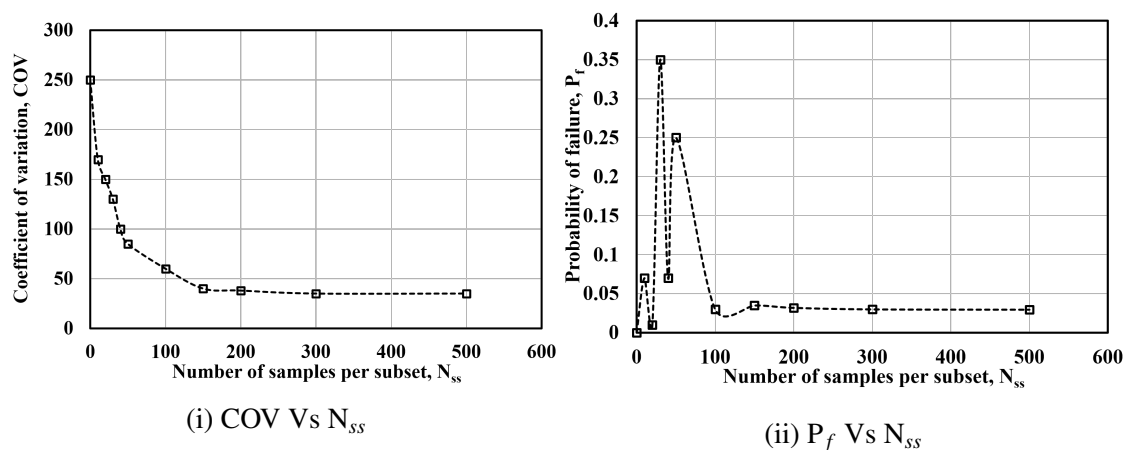
Figure 5.41: Trends of coefficient of variation and probability of failure for different number of samples per subset (auto-correlation length of 10 m and 50% COV)

To ensure the convergence of subset simulation results, the coefficient of variation

and number of samples per subset results are compared. The results from this analysis are presented in Figure 5.36 (i) - 5.41 (i). Also the effect of number of samples per subset and probability of failure are presented in Figure 5.36 (ii) - 5.41 (ii). The number of samples per subset, N_{ss} were varied from 500 to 20000 for the parameter COV of 15% to 40% to obtain a convergent solution (with around $20\% - 30\%$ COV). These results indicate that with the increase in number of realizations, the $COV(P_f)$ decreases. As the computational time required to run the simulations is quite high, the N_{ss} has been increased upto a maximum of 20000. But, to achieve a lower $COV(P_f)$,the N_{ss} needs to be increased further.

5.5 Concluding remarks

The safety of radioactive waste disposal facilities require efficient performance assessment models that can (i) predict the concentrations over extremely large spatial and temporal scales, (ii) take into account the uncertainties associated with the input characteristics of the problem and (iii) treat the uncertainties that include its propagation and quantification using robust techniques. In this chapter, a probabilistic safety assessment model that entails all the above aspects of analysis is presented. As mentioned earlier, the effect of epistemic and aleatory uncertainties on the radiological values (risk and radiation dose) are investigated in detail in two subdivisions. The main conclusions from the first subdivision are:

1. One of the critical components of the performance assessment model that handles the transport of radionuclide in geosphere is developed numerically. A three-dimensional domain with a decaying source concentration is modelled and the con-

centration is measured at distances upto 50 m and 200 m away from the source for short-lived (Strontium (^{90}Sr), Caesium(^{137}Cs)) and long-lived radionuclides (Carbon(^{14}C) and Iodine(^{129}I)) respectively.

2. The potential risk to a critical group through drinking water pathway are calculated for all the radionuclides. The computed maximum values are lower than the risk observed from industrial accidents and natural catastrophes (10^{-3} - 10^{-4} y^{-1}).

3. The influence of uncertain input parameters (epistemic uncertainty) on the overall performance of the model is estimated. The uncertainties are propagated using CSRSM based on polynomial chaos expansion (PCE). To integrate the deterministic numerical model and the random inputs from probabilistic model, run the simulations and make the model computationally efficient, codes are developed using the built-in python interface. The development of these codes bridged the deterministic FEM with the probabilistic analysis.

4. Reliability analysis is carried out to estimate the probability of radiation dose exceeding the permissible limit using subset simulation method. The values of probability of failure ranged between 10^{-8} - 10^{-9} which suggested that the system is safe from risk due to radiation through the drinking water pathway. The computational efficiency of Method 1 (using CSRSM) and Method 2 (using numerical model) in estimating the reliability of the system are also demonstrated.

5. Global sensitivity analysis based on PCE is carried out to estimate the Sobol indices. The results indicated that critical parameters influencing the response of the system (i.e., radiation dose) are mainly distribution coefficient and porosity, while, longitudinal dispersivity, transverse dispersivity and diffusion coefficient are non-

influential in radionuclide transport. These results are compared with the sensitivity measures acquired by post-processing conditional levels in subset simulation. It was observed that the results from both the methods were identical. These results indicated that the reactive nature (i.e., sorption effect) of radionuclides in soil plays a significant role in affecting the response of the system.

The main conclusions from the second subdivision are:

1. A two-dimensional numerical model is developed to understand the influence of spatial variability in soil (geosphere) on radionuclide transport. The effect of this geosphere transport model in assessing the long-term performance of radioactive waste disposal facilities is investigated.

2. The influence of spatial variability of hydraulic conductivity on radionuclide concentration is studied. The deterministic analysis results for a heterogeneous medium indicated that the radiation dose reaching the end-point and the risk values were all within the safe limits.

3. When the radionuclide movement was compared between homogeneous and spatially varying medium, it was observed that the rate of movement of radionuclide was faster in a homogeneous medium than a spatially varying medium. This can be attributed to the frequent fluctuations in conductivity in a spatially varying medium that led to a slower rate of flow (and contaminant movement) and lower concentration at the end-point of interest.

4. The probability of failure values are estimated using subset simulation for cases corresponding to low P_f and Direct Monte Carlo simulation for higher P_f cases. The range of P_f values observed between $10^{-9} - 10^{-1}$.

5. The P_f values increased monotonically with an increase in coefficient of variation and the spatial auto-correlation length.

6. The trends showed that with the increase in auto-correlation length, the results converge towards the results for homogeneous case. The reason being, random fields became smoother with the increase in auto-correlation length and get closer to homogeneous medium.

7. From the design point of view, radionuclide transport through homogeneous system results in high P_f. But in reality, the medium is heterogeneous and the estimated P_f values are quite low. This implies that the performance of system is underestimated by assuming the medium to be homogeneous. Hence, it is imperative to carryout geosphere transport modelling in a spatially varying medium to predict the performance accurately.

So, both the performance assessment models developed in this chapter systematically quantify different sources of uncertainty in the geological medium. Also, for the given environment, the safety indicators (radionuclide concentration, radiation dose and risk) estimated from the analysis and the reliability analysis results were compared with the design threshold values. The predicted results show a reasonable assurance that the radioactive waste disposal facility meets the design objective, intended performance and the regulatory requirements.

Chapter 6

Probabilistic analysis of contaminant transport in fractured rocks

6.1 Introduction

One of the design characteristics that decides a potential site for disposal facility is the geological environment around the system. Needless to say, geosphere is mainly composed of soil and rocks that are formed by complex inter-play of different physico-chemical and biological processes. The presence of a complex geological environment affects the geosphere transport of contaminant and this effect contributes to the overall performance assessment of radioactive waste disposal systems. The influence of this factor (with soil as the geological medium of transport) is explored thoroughly in chapters four and five. An extensive study on the various aspects involved in the development of efficient performance assessment models for radioactive waste barrier systems are presented in these chapters. The effect of heterogeneity in the soil medium and the variability in the geo-hydrological and transport properties on radionuclide transport are quantified both through analytical and numerical models. Also, different sources of uncertainties and their influence on the performance of the barrier systems are also explored. There is a need to extend these studies to rocky subsurface medium to understand the impact

of such environment on the contaminant transport. In fact, from the past two decades, there has been an increased attention to understand the flow and transport behaviour of contaminants in rocks. The reason being, many countries including India have planned radioactive waste repositories near rock formations owing to their high containment and attenuation properties (Zhao et. al., 2011; Makolil and Nagar, 2015). But, the presence of naturally occurring discontinuities often governs the flow and transport behaviour of contaminant through rocks. This entails development of models with complex heterogeneous network of fractures, channelized flow pathways and unique geo-hydrological and transport properties (in fracture and intact rock matrix).

A fractured rock mass is delineated by two interacting subsystems that are represented as (i) fractures and (ii) rock matrix as shown in Figure 6.1. In general, fractures act as the principal pathways of contaminant migration in a fractured rock mass. It implies that the advective component is predominant along the fracture, while, diffusion component is dominant in the adjacent rock matrix and the same trend can be observed in Figure 6.1. So, each subsystem of rock mass have unique flow and transport characteristics.
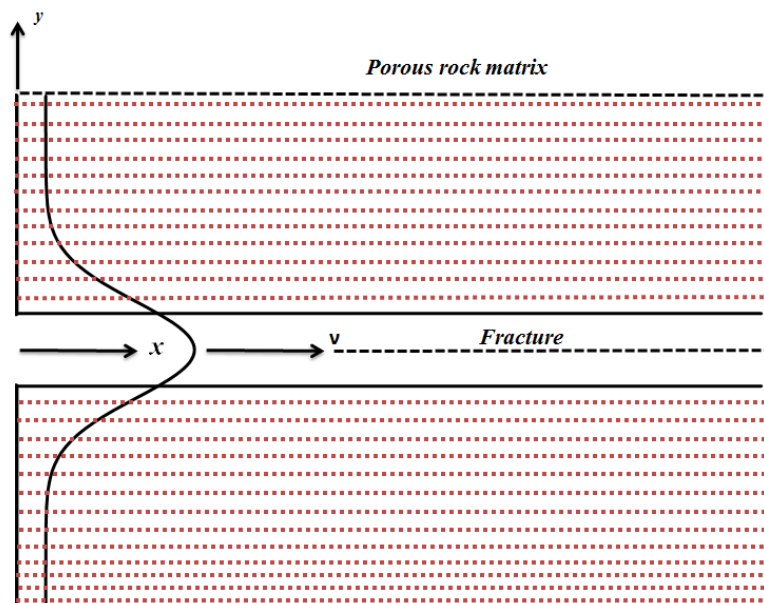
Figure 6.1: Schematic diagram of fracture-rock matrix system

One of the governing factors that influences the contaminant transport in fractured media is the 'scale' of the problem, that could vary from a few centimetres (single fracture) to few kilometres (fractured rock mass) (Berkowitz, 2002). So, to generate realistic results, it becomes imperative to study the phenomena of contaminant transport in fractured rock at a field scale. The heterogeneity of fracture network leads to variations in the paths of contaminant propagation through the rock mass. Also, examining the influence of fracture geometry, fracture orientation, density of fracture sets and other features of fractures are important as they can alter the flow paths of contaminant movement. Models were developed in the past to understand the small scale influence of local aperture variations along the fracture on the transport behaviour (Sarkar et. al., 2004). However, simulating the local aperture variations at a field scale encompasses the local and global factors that contribute to the contaminant transport through a fractured network. Different types of contaminants react differently with surrounding geological medium. For instance, when a reactive contaminant enters the medium, influence of chemical reactions which allows the dissolution and retardation of solute needs to be considered in addition to the advective and dispersive components of transport. So, the reactive nature of the contaminant also plays a significant role in transport behaviour. By conceptualizing the contribution from each of these factors and, the interactions of contaminant and medium over time, mathematical models (analytical or numerical) are formulated that describe the long-term behaviour of contaminant transport in a fractured medium. Once this model is developed for fractured rock medium, it can handle the geosphere transport component of the performance assessment model for radioactive waste repositories.

Besides modelling the contaminant transport in fractured rock medium (i.e., deterministic analysis), there is need to account for the uncertainties involved in the system to as-

sess the long-term safety performance of nuclear waste disposal facilities. Moreover, uncertainty analysis is an intrinsic part of performance assessment modelling (IAEA, 2004; AERB, 2006). It is a tool for assessing compliance with safety requirements in the face of uncertainty. Uncertainties can occur in the form heterogeneity in the medium (inherent randomness), the input parameters of the model (measurement uncertainties) and also due to the simplification of actual process (modelling uncertainties) (Helton, 1993). However, the stochasticity in the geohydrological properties of the fractures and intact rock and transport properties of the contaminant convolutes the problem into a more complicated system. In practice the repository is designed as a reliable system and any event of failure in the system is a considered to be rare. Also, the risk associated with these systems is a function of many input parameters which makes the traditional simulation based techniques like Monte Carlo simulation computationally expensive. In such cases, adopting probabilistic techniques which are effective in rare event modelling, like variance reduction methods facilitates in quantifying the response of the system with lesser computational effort. Although the the probabilistic modelling of these systems require a large number of input parameters, in most cases only a limited number of parameters happen to influence the overall response. Identifying these parameters reduces the variance of the system to a great extent and also helps in focussing on key areas that needs utmost importance in the analysis. This can be carried out by sensitivity analysis which ascertains existence of interaction effects within the model (IAEA, 1999). By integrating the above mentioned deterministic and probabilistic components in the performance assessment model, a probabilistic framework to assess the safety of disposal facilities designed near complex fractured geological system can be developed.

6.2   Need for the study

To meet the design objectives of radioactive waste repositories, performance assessment models must be developed. When the repositories are designed near rocky subsurface formations, geosphere transport becomes a critical component of performance assessment. In fact, the presence of such complex heterogeneous medium can potentially affect the concentration of contaminant and radiation dose reaching the end-point of assessment. Therefore, it is imperative to understand the plausible transport behaviour of the contaminant in fractured medium. Flow and transport through individual fractures, as well as fracture networks, has been studied extensively over the past years both experimentally and using simulations. Many analytical models have been developed in the past five decades to describe the flow and transport of contaminant through fractured rock. They were developed by translating the conceptual model into mathematical equations and solving them under given initial and boundary conditions (Berkowitz et. al., 1988; Bear, 1993; NRC, 1996; Pierre and Thovert, 1999; Neuman, 2005). Further, the geometrical complexities in the medium were handled by developing numerical models (using finite element methods, finite difference methods, finite volume methods etc). One of the earliest works by Wilson and Witherspoon (1974) presented a two-dimensional finite element model to predict the water flow through fractured rock. Freeze and Cherry (1979) drew attention to the importance of matrix diffusion involving discrete fractures in contaminant hydrogeology for fractured porous media including sedimentary rock and fractured clayey deposits. Further, the need to consider fractures exclusively was emphasized confirming the significance of fracture geometry on the hydrological behaviour of the rocks (Long et. al., 1989). This led to the development of discrete fracture network (DFN) models, where

each fracture is explicitly represented by its geometry (by their orientation, size, aperture etc) and the relation between fractures and fracture sets are also described. Many studies adopted DFN approach for contaminant transport modelling in fractured rock (Smith and Schwartz, 1984; Berkowitz and Scher, 1997; Alexander et. al., 2003; Dong, 2011; Parker et. al., 2012; Lei et. al., 2017). However, most of these works have been limited to non-reactive contaminant transport. Although understanding non-reactive transport is a prerequisite for quantifying reactive transport in fracture networks, reactive nature of contaminant adds further challenges for modelling which received comparatively less attention in the literature. When a reactive contaminant such as radionuclide is considered, there is an added effect of radioactive decay and retardation (and some more geochemical reactions depending on the type of rock) that can alter the contaminant concentrations. As mentioned in Chapter 2, developing a transport model for fractured rock is quite complex due to interplay of various factors (see Figure 2.7) that can strongly affect the movement of contaminant. Here, some of the important aspects that highlights the need for this study have been discussed. In a nutshell, a new contaminant transport model needs to be developed for a fractured rock that can encapsulate the effect of (1) fracture geometry (2) type of contaminant (3) local aperture variations (4) geological properties of the medium and (5) transport properties of the contaminant.

Since a complex geological medium is considered for performance assessment, the uncertainties involved in the system will also be higher. So, unlike chapters four and five, meta-modelling techniques cannot be implemented for uncertainty propagation due to curse of dimensionality in those methods. To quantify the probable risk associated with the system, reliability analysis has to be adopted. The probability of failure involved in designing a disposal system, especially for hazardous waste is very low. The probabilistic

analysis of such rare events can be handled by employing Markov Chain Monte Carlo (MCMC) algorithms such as subset simulation method. Further, sensitivity analysis can also be carried out by post processing the results from subset simulation to estimate the critical parameters affecting the safety of radioactive waste repository.

6.3 Objectives

This chapter aims at developing a probabilistic framework for performance assessment modelling in fractured rock medium. To gain an overall understanding of the transport behaviour in a complex fractured medium, geosphere transport modelling is carried out for a non-reactive contaminant (case I) and a reactive contaminant (case II). These two cases are studied as two major subdivisions in this chapter. In the first subdivision, performance assessment modelling is carried out for a non-reactive contaminant and in the second subdivision, performance assessment modelling is carried out for a reactive contaminant. The main objectives of this chapter are as follows:

1. To develop a new hybrid model that integrates a stochastic fracture pattern generating algorithm for sedimentary rocks and a numerical model that can model the flow and transport of contaminant.

    (a) Estimate the contaminant concentration reaching the end-point of interest (for case I).

    (b) Estimate the radiation dose and risk due to transport of radionuclides through fractured rock to the nearby human habitat (for case II).

2. To carry out a parametric study and understand the influence of (i) geometric properties of fracture (such as number of fracture sets, fracture orientation etc) on the

contaminant migration, (ii) transport properties of contaminant (i.e., diffusion and dispersion) in fractures and intact rock matrix on the contaminant migration (in both the cases).

3. To model the aperture variations along the fracture and address their impact on the contaminant concentration (for both the cases).

4. To quantify the effect of uncertainties using probabilistic analysis.

   (a) Estimate the probability of concentration of contaminant exceeding the permissible value (for case I)

   (b) Estimate the probability of radiation dose for radionuclide exceeding the permissible value (for case II)

5. To examine the effect of probability of failure for different values of coefficient of variation (COV) (for both the cases).

6. To carry out sensitivity analysis and estimate the critical parameters affecting the contaminant migration (in both the cases).

The sequences of steps followed to quantify the effect of uncertainties in the performance assessment model are presented in Figure 6.1. From the Figure, it can be observed that the uncertainties (or the random variables) in the system are propagated non-intrusively (i.e., without altering the model) through the numerical model and depending on the type of contaminant, the respective estimates are computed using reliability and sensitivity analyses.
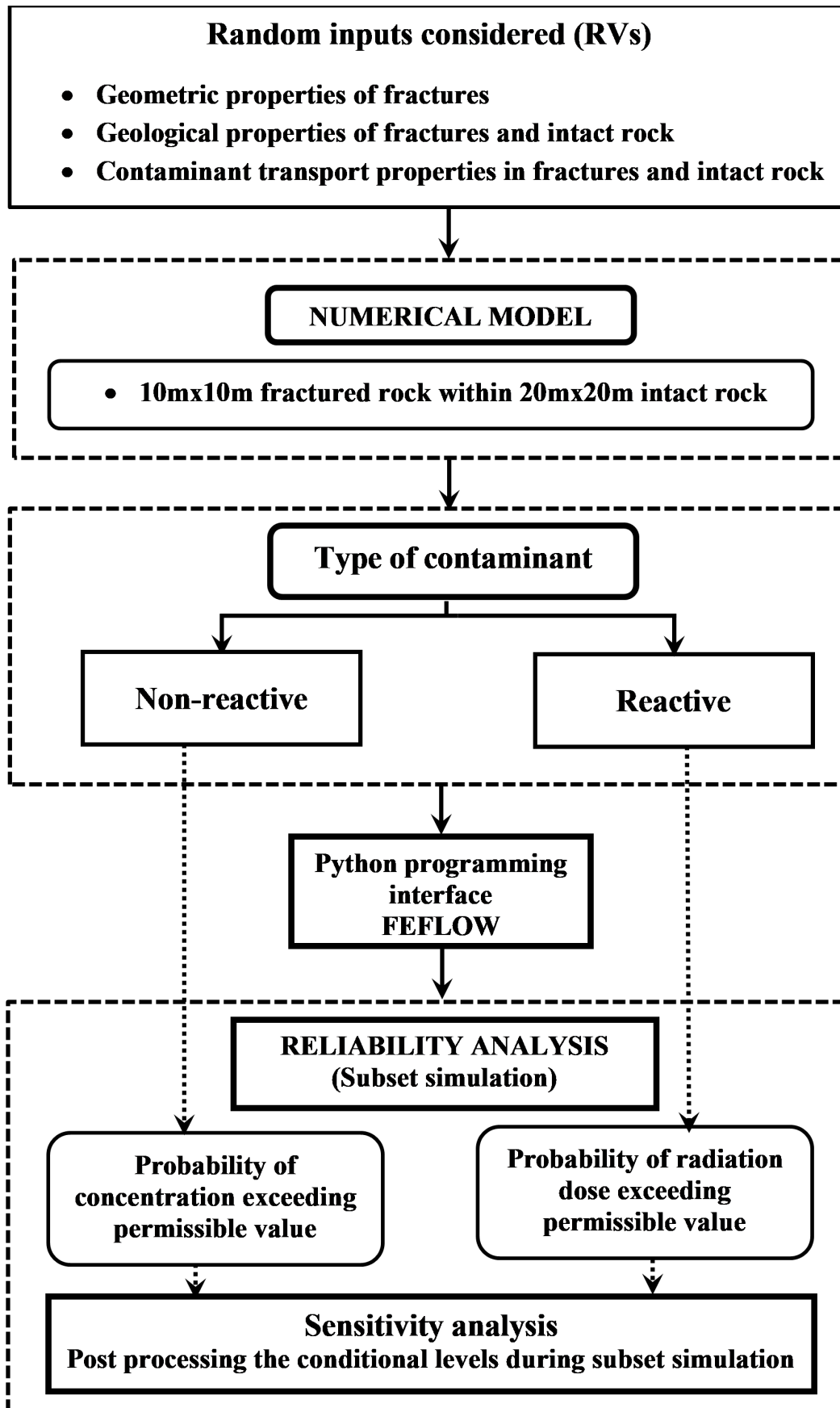
Figure 6.2: Sequence of steps followed in carrying out probabilistic analysis of contaminant transport through fractured rocks

The deterministic and probabilistic parts of the analysis are integrated by coding in python programming interface.With the help of these programs, the generation of random realizations for probabilistic analysis are automated.

6.4 Development of performance assessment model

Disposal systems are structures designed to contain and isolate any form of waste from the surrounding environment. The choice of disposal method to isolate the waste from the human habitat relies on the hazard and the longevity of the waste. To ensure the long-term safety of these disposal systems, performance (or safety) assessment models are developed. They aim to assess the performance of disposal facilities using predictive models and quantitatively estimate the potential impact of contaminant concentration (or radiation dose) on the environmental safety and public health. As the disposal systems are generally constructed below the ground surface, the geological environment surrounding the disposal facility has an important role in predicting the performance of the system. In this chapter, the geological site for disposal is considered to be fractured rock. Unlike soil medium, fractured rock needs much more attention in modelling the transport process. The heterogeneity in the medium (i.e., geological properties of discrete set of fractures and the intact rock matrix) and, the reactive nature of the contaminant can alter the flow path and transport process significantly. To acquire a thorough understanding of the different facets involved in modelling flow and contaminant transport through fractured rock, the following studies are carried out. Also, for an overall understanding of transport behaviour in fractured rock, both non-reactive and reactive contaminants are considered in the chapter. So, the other components of performance assessment model

namely the source term, the failure scenario leading to contaminant release (from the disposal facility) are evaluated accordingly in the corresponding sections.

6.5 Geosphere transport model

Fractured rock mass is a complex network of naturally occurring fractures (or discontinuities) and intact rock matrix. The two primary components involved in modelling contaminant transport in fractured rock are:

1. Geometric representation of fracture pattern by means of discrete fracture network model

2. Development of a numerical model that solves the flow and transport process along fractures and intact rock matrix

In this section, the second component i.e., numerical model used to compute the flow and transport process in fractures and rock matrix is discussed. This model introduces the concept of discrete elements which are used to create fractures in the finite element mesh (as a discrete feature). Once the process of generating and modelling transport along a single fracture is clear, it becomes straightforward to generate a network of fractures. So, the method used for fracture pattern generation is discussed in the subsequent sections.

6.5.1 Numerical model for fractured rock medium

To develop a numerical model, theoretical knowledge on different concepts of continuum and the representation of fractures and matrix in the system is essential. The conceptual model formulation requires information regarding the geology of rock formation and scale

of problem. The origin of rock can modify conductive nature of fracture and this further decides the pathway of contaminant movement. As noted earlier, the scale of the problem also influences the fractures and the transport pathways. These formulations are translated into mathematical equations under three broad categories of continuum namely (1) equivalent continuum models (2) discrete fracture models and (3) hybrid models (NRC, 1996). They differ in representing heterogeneity in the fractured medium. In the first category, the models for representing fractured media are of two general types, single and dual porosity. Single porosity models represent hydrology in terms of a single continuum where all porosity is assumed to reside in the fracture. Dual-porosity models are based on two overlapping continua the both fractures and matrix blocks are assigned a value of porosity greater than zero. Unlike the previous case, fractured mass consists of matrix blocks separated by discontinuities, and, therefore a possible approach to representing these systems can be through non-overlapping continuum models. So, fractures and porous media must be solved in a separate scale and have to be coupled via macroscopic interface conditions by using a discrete fracture approach. These type of models fall in second category and they are called discrete fracture network models. The final category of models works on discrete fracture models with continuum approximations .

In this chapter a two-dimensional finite element model with a fractured network generated based on discrete fracture network concept is developed. In simple terms, discrete network models are developed under the assumption that fluid flow behaviour can be predicted from knowledge of the fracture geometry and data on the hydraulic properties of individual fractures. This happens when fracture apertures are more conductive in comparison to voids in the porous blocks. The discrete fracture approach requires information (e.g., aperture, length, orientation, spacing etc) of every individual fracture.

The procedure for numerical modelling through discrete fractured network is discussed elaborately in sections 3.2.4.2.2 and 3.2.4.3.4 of Chapter 3. The fractures are created as a discrete element with a node-to-node connectivity in the finite element mesh (using arbitrary nodal path). The steps followed in modelling the fracture and efficacy of numerical model is demonstrated with a simple example that considered flow and transport of non-reactive contaminant through a single fracture (refer Appendix B). The concept of discrete fracture modelling mainly focuses on the highlighting the influence of fractures on the contaminant migration process. So, the porous media and the set of fractures are represented as two distinct interacting subsystems coupled through interfaces. Typical set of equations for fluid flow and mass transport are

Fluid flow

$$S_0 \frac{\partial h}{\partial t} + \nabla.[-Kf_\mu(\nabla h + \chi e)] = Q \tag{6.1}$$

Mass transport

$$\theta R_d \frac{\partial C}{\partial t} + q.\nabla C + \nabla.j + \varepsilon R_d vC = S \tag{6.2}$$

where ε - porosity, R_d - retardation factor, $\frac{\partial C}{\partial t}$ - rate of change in concentration, q - Darcy velocity, S - source / sink term Usually, the spatial dimension of fractures is lower than the domain (i.e., for a two-dimensional (2D) domain, the fractures are modelled as one-dimensional (1D) elements). The governing equations for fluid flow and contaminant transport are considered separately in porous medium (equations (6.1) and (6.2)) and the same equations are lowered by spatial dimension in the case of fractures. To solve for concentration of contaminant, the discrete features (fractures) and the porous medium are treated as a unitary feature, where all components are integrated into the solution domain consisting of the joint porous-medium domain O_P and a number of non-overlapping

discrete feature domains O_F.

$$O = O_p \cup \sum_F O_F \tag{6.3}$$

As the discrete feature elements share the same nodal points as that of the porous medium, the concentration of contaminant for combined process is obtained by exchanging (advective and dispersive) fluxes between the porous medium and discrete features. When the contributions from porous medium and the corresponding fracture are assembled, the overall concentration from both the systems are estimated.

These studies help in investigating the requirements for characterization of a fracture network, studying the scale dependence of the transport processes (specially dispersion), examining how network geometry influences spreading patterns, and evaluating issues related to the reliability of data on fracture position and orientation.

6.5.1.1 Validation of the model

The efficiency of numerical model is tested by comparing the numerical model results with an analytical solution. The analytical solution developed by Tang (1981) is used to predict the contaminant migration through a horizontal fracture. The solution accounts for advective transport, longitudinal mechanical dispersion, molecular diffusion in the fracture and also molecular diffusion from fracture to matrix, adsorption on the matrix and radioactive decay processes are considered. These processes are mathematically represented as partial differential equations for fracture and porous matrix. The equations are coupled, and the general solution for the fracture-matrix system is obtained. The mass

balance of contaminant in fracture is given by the equation below:

$$R\frac{\partial C}{\partial t} + v\frac{\partial C}{\partial x} - D_{xx}\frac{\partial^2 C}{\partial x^2} + R\vartheta C - \frac{\varepsilon D'_{yy}}{a}\frac{\partial C'}{\partial y}\bigg|_{y=a} = 0 \quad (0 \leq x \leq \infty, 0 \leq y \leq a) \qquad (6.4)$$

The initial and boundary conditions are given below

$$C(x,0) = 0, \ \ C(0,t) = C_D, \ \ C(\infty,t) = 0 \qquad (6.5)$$

The governing mass balance equation in the porous rock matrix is

$$R'\frac{\partial C'}{\partial t} - D'_{yy}\frac{\partial^2 C'}{\partial y^2} + R'\vartheta C' = 0 \qquad (6.6)$$

where

$R = 1 + \frac{K'_d}{a}$ and $R' = 1 + \frac{\rho_s K_d}{\varepsilon}$ are the the retardation factors in fracture and rock matrix

$D_{xx} = D + \alpha_L \lambda_p = D$ and $D'_{yy} = D'$ are the diffusion coefficients in the fracture and rock matrix

C and C' are the solute concentrations in the fracture and rock matrix

a is the half of the fracture width

K_d and $K_{d'}$ are the distribution coefficients of fracture and rock matrix

ε porosity of rock matrix

α_L is the longitudinal dispersivity

The general solution of the equation is evaluated using Gauss quadrature method and the concentration variation is evaluated spatially and temporally. The transient solution by neglecting dispersivity is given by equation

In fracture

$$
\frac{C}{C_D} = \frac{1}{2}\exp\left(-\frac{\vartheta Rx}{v}\right)\left[\exp\left(-\frac{\varepsilon\sqrt{\vartheta R'D'}}{av}x\right)\right.
$$

$$
\left.\text{erfc}\left(\frac{\varepsilon\sqrt{R'D'}}{2avR\sqrt{t-xR'/v}}x - \sqrt{\vartheta}\sqrt{t-xR'/v}\right)\right] +
$$

$$
\exp\left(-\frac{\varepsilon\sqrt{\vartheta R'D'}}{av}x\right)\text{erfc}\left(\frac{\varepsilon\sqrt{R'D'}}{2avR\sqrt{t-xR'/v}}x + \sqrt{\vartheta}\sqrt{t-xR'/v}\right) \quad (6.7)
$$

The above equation holds good for the condition $(t-xR/v) > 0$

In rock matrix

$$
\frac{C}{C_D} = \frac{1}{2}\exp\left(-\frac{\vartheta Rx}{v}\right) \times \left[\exp\left(-\frac{\varepsilon\sqrt{\vartheta R'D'}}{av}x - \sqrt{\vartheta}A(y)\right)\right.
$$

$$
\left.\text{erfc}\left(\frac{\varepsilon\sqrt{R'D'}}{2avR\sqrt{t-xR'/v}}x + \frac{A(y)}{2\sqrt{t-xR/v}} - \sqrt{\vartheta}\sqrt{t-xR'/v}\right)\right] +
$$

$$
\left[\exp\left(-\frac{\varepsilon\sqrt{\vartheta R'D'}}{av}x + \sqrt{\vartheta}A(y)\right)\right.
$$

$$
\left.\text{erfc}\left(\frac{\varepsilon\sqrt{R'D'}}{2avR\sqrt{t-xR'/v}}x + \frac{A(y)}{2\sqrt{t-xR/v}} + \sqrt{\vartheta}\sqrt{t-xR'/v}\right)\right] \quad (6.8)
$$

where $A(y) = \sqrt{\frac{R'}{D'}}(y-a)$

A two-dimensional finite element mesh is generated with 3288 nodes as shown in Figure 6.3. The fracture-rock matrix is discretized using quadrilateral mesh in the numerical model. L and $D-a$ are the dimensions of rock matrix along x and y direction respectively. The fracture is modelled as 1D discrete finite elements sharing the edges of rock matrix at $y = a$, $0 \leq x \leq L$ and they are assumed to follow Hagen-Poiseuille law of flow motion and the input properties for the fracture and rock matrix from Table 6.1 are assigned to the model. As the analytical solution is only valid for negligible dispersion, the dispersion

is set to zero in the numerical model. The flow and mass transport boundary conditions
(bc) are presented in Table 6.2. (Note: The dirichlet-type condition specifies the head or
concentration value at the boundary, Neumann-type condition specifies the derivative of
head or concentration value at the boundary)

Table 6.1: Input data considered for the study (Diersch, 2014)

Quantity	Value
Half domain	
Domain length, L (m)	3
Domain width, D (m)	5×10^{-03}
Half fracture width, a (m)	5×10^{-03}
Porous matrix	
Isotropic hydraulic conductivity (m/s)	10^{-22}
Porosity	0.35
Molecular diffusion (m^2/s)	$10^{-10} - 10^{12}$
Longitudinal Dispersivity (m)	0
Transverse Dispersivity (m)	0
Fracture	
Flow law	*Hagen Poiseuille*
Cross-sectional area (m^2)	6×10^{-5}
Hydraulic Aperture (m)	1.2×10^{-4}
Hydraulic radius (m)	6×10^{-5}
Longitudinal Dispersivity (m)	0
Molecular diffusion (m^2/s)	0
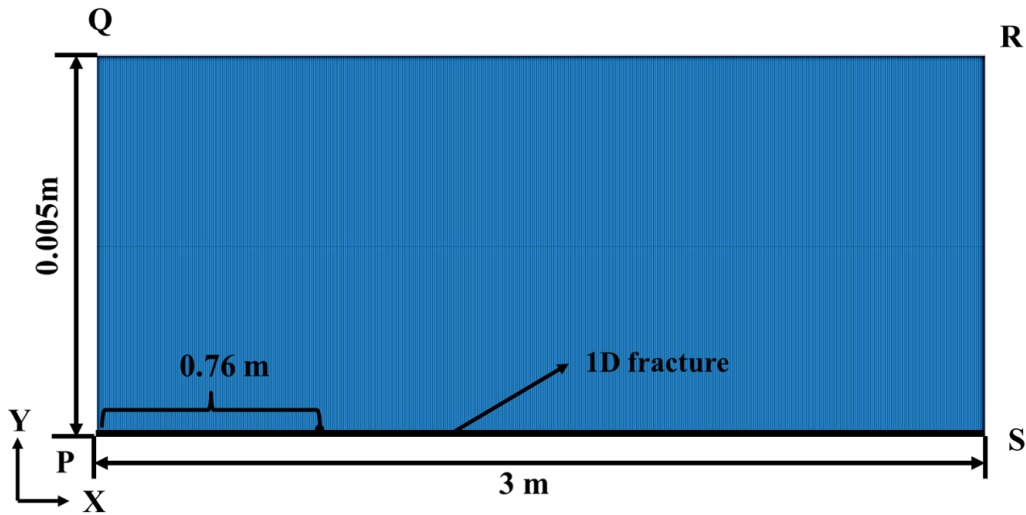
Figure 6.3: Finite element mesh of the half-space fracture matrix domain with 2D quadri-lateral porous matrix elements combined with 1D discrete fracture elements

Table 6.2: Initial and boundary conditions for fluid flow and mass transport (Diersch, 2014)

Location	Quantity	Value
Fluid flow		
P	Neumann-type bc at fracture inlet $(x = 0, y = a)$ (m/day)	-2
S	Dirichlet-type bc at fracture outlet $(x = L, y = a)$ (m)	0
Mass transport		
-	Initial condition of solute (mg/l)	0
P	Dirichlet-type bc on top at $(x = 0, y = a)$ (mg/l)	10

A typical non-reactive contaminant is considered for the analysis and hence the retardation factor is $R_d = 1$. The concentration of contaminant varying over time is estimated at a distance of 0.76 m from the source point. The snippets of contaminant front moving along the domain in four days is presented in Figure 6.4. The results obtained from analytical solutions through equation 6.7, are compared with that obtained from numerical model for different diffusion coefficients. It can be observed that results match well as

shown in Figure 6.5.

(a)

(b)

(c)

(d)
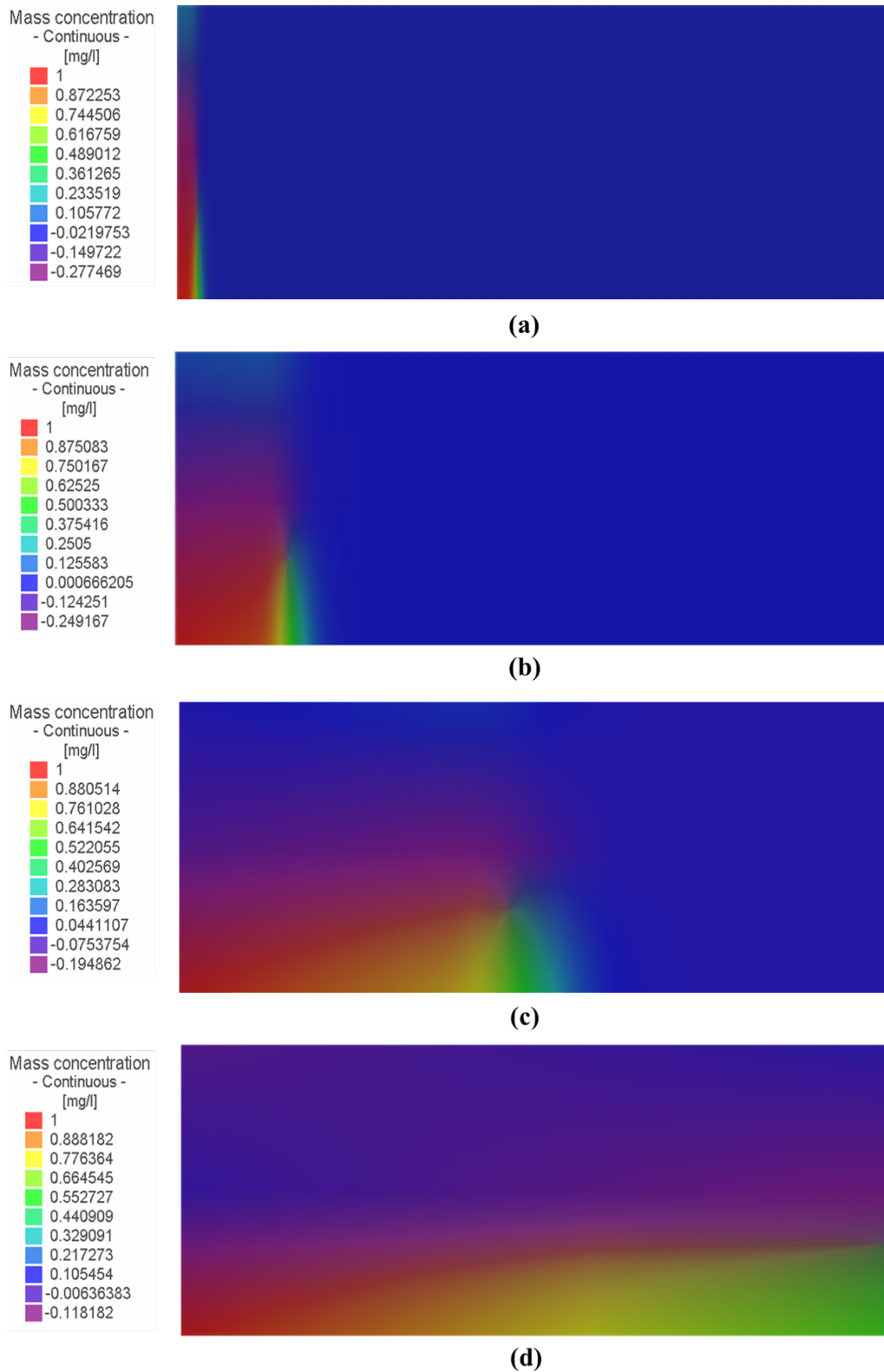
Figure 6.4: Concentration contours (a) After 3 hours (b) After 1 day (c) After 2 days (d) After 4 days
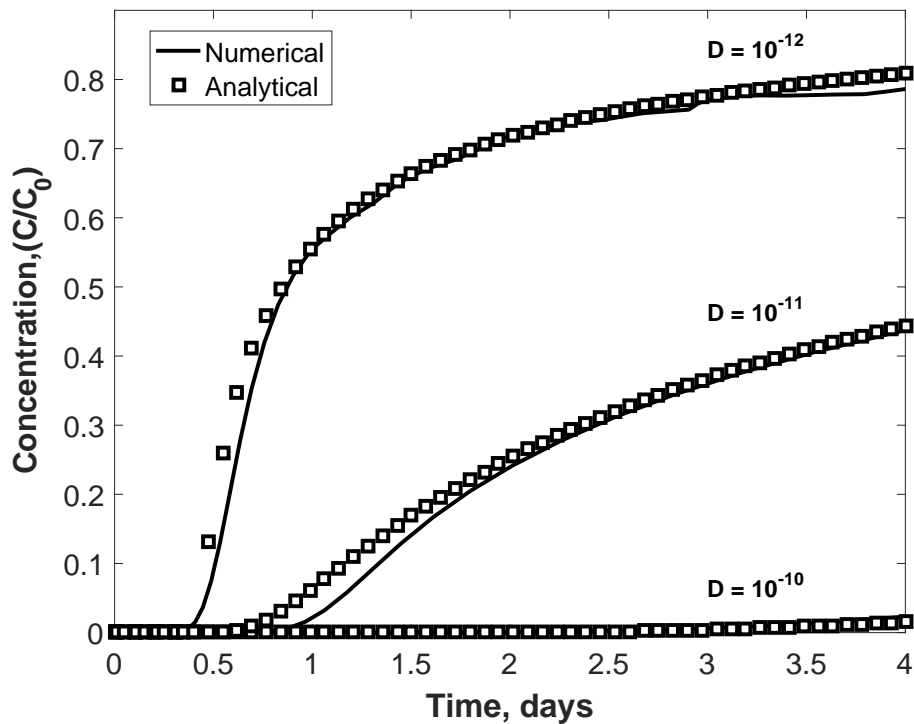
Figure 6.5: Comparison of relative concentration versus time for analytical and numerical models with different molecular diffusion values

From this analysis, it is evident that the movement of contaminant through fracture can be simulated efficiently using the numerical model. Here, the analysis is carried out for a single fracture. In the following sections, the transport behaviour of contaminant in a fracture network is modelled and the results are elaborately discussed.

6.5.2 Algorithm for fracture pattern generation

When the flow and transport of contaminant in fractured rock mass is governed by heterogeneous system of fractures, then it becomes necessary to simulate the natural fracture network explicitly with respect to their geometry. In the discrete network modelling framework, they are generated based on three approaches namely (1) geological mapping (fracture patterns are generated based on the exposed rock outcrops) (2) stochastic

276

approach (fracture patterns are generated based on stochastic modelling of fracture geometry) (3) geomechanical approach (fracture patterns are generated based on geological history and formation mechanism) (Renshaw and Pollard, 1994; Gringarten, 1998; Josnin et. al., 2002; Lei et. al., 2017). These approaches are discussed elaborately in chapter 2. However, discrete network models are closely linked with the concepts of stochastic simulation. Also, it is important to note that the method of fracture generation depends on the genesis of rock. For example, a crystalline rock has only few significant fractures whereas, layered rocks consists of dense interconnected set of fractures. So, modelling transport through layered sedimentary rock formations will be more challenging because (a) high fracture density often forms tortuous pathways for transport and (b) the reactive nature of sedimentary rocks leads to geochemical reactions between the rock and contaminant (dissolution, sorption etc). In this chapter, a stochastic algorithm developed by Riley (2004) is employed to generate fractures for a layered sedimentary rock.

In this method, the fracture trace length distributions and fracture spacing distributions are derived for a given fracture density and orientation distribution of layered rocks. The algorithm for fracture pattern generation are:

1. The crack is allowed to propagate at the point of weakness of the rock (underlying physical concept involved in crack propagation is not modelled explicitly).

2. For a given fracture set (k), the seed points (i.e., the points from which crack initiates) are placed within the model domain with density ρ_k (observed in the field).

3. At each point, an orientation (θ_k) is assigned by sampling from orientation distribution (acquired from field data with respect to the fracture set).

4. Each fracture is allowed to propagate from the seed point in both directions parallel

to that orientation at speed, u_k, until it meets other fractures whereupon it continues according to a fixed probability, p_k.

Also, to simplify the mathematical formulation of the model, it is assumed that all fractures are initiated simultaneously, the fracture density is homogeneous, all fractures with a fracture set are parallel and the speed of propagation is constant for all fractures within a set. Basically the model has four parameters for each fracture set. They are ρ_k, θ_k, u_k and p_k. The first two parameters (ρ_k, θ_k) are determined from field data. However, the other parameters (u_k, p_k) are used to match the statistical distributions of fracture trace lengths estimated from the method with those determined from field observations.
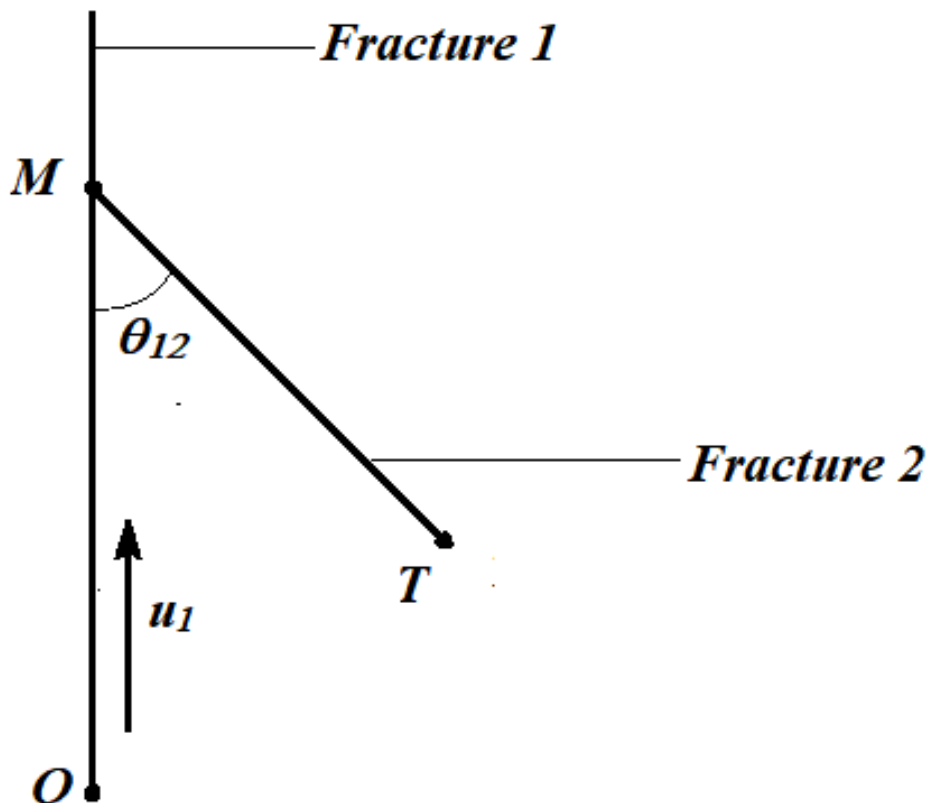
Figure 6.6: Schematic of fractures and their parameters

Figure 6.6 shows a schematic of two fractures belonging to fracture set 1 and fracture set 2 where points 'O' and 'T' represent the seed points from which the fracture originates.

u_1 is given by the speed of crack propagation from set 1 and θ_{12} represents the angle between fracture sets 1 and 2. At point M, the fracture from set 2 intersects with an already existing fracture from set 1. Now, the distance from the seed point of a fracture (from set 1) to one of its ends to be represented by the random variable, X_1 and probability distribution function $P_1(x)$. So, the total trace length of a fracture is nothing but the sum of two independently drawn samples from $P_1(x)$. The derivation of this term is presented in detail in Chapter 3. Poisson process is perhaps one of the most important stochastic processes used to define geometry of the fracture system. This random process is controlled by only one parameter that is the density parameter. In the algorithm, the number of fracture intersections are modelled as Poisson process. So, the distance from 'O' to 'n^{th}' encounter is given by random variable $X_1(n)$. Then, $P(X_1(n) \leq x) = 1 - exp[-g_{12}(x)] \sum_{i=0}^{n-1} \frac{[g_{12}(x)]^i}{i!}$ where $g_{12}(x)$ is the density of fractures. Further, the probability of growing fracture to terminate at n^{th} encounter is given by $P(N = n) = p_1^{n-1}(1 - p_1)$. By combing the above equations, the equation for fracture trace length is given by

$$P_{12}(x) = 1 - exp[-(1 - p_i)g_{12}(x)] \qquad (6.9)$$

So, the final equation for propagation of fracture given two fracture sets (set 1 and set 2) is given by

$$P_{12}(x) = 1 - exp\left(-2(1 - p_1)\rho_2 sin\theta_{12} \int_0^x \int_0^{\frac{u_2}{u_1}\xi} exp\left[-2(1 - p_1)\rho_2 sin\theta_{12} \int_0^r \int_0^{\frac{u_2}{u_1}\zeta} 1 - P_{12}(x)dxd\zeta \right] drd\xi \right)$$

$$(6.10)$$

where x, r are displacements of fracture 1 and fracture 2 from their respective seed points (O and T) and ξ, ζ are growing tip of fractures 1 and 2 respectively. The above equation can be implemented as an iterative scheme for simultaneously calculating $P_k(x)$. The fractures generated from these realizations become the conductive elements in a fracture network. This algorithm is used to not only regenerate the fracture patterns, but also investigate the effect of number of fracture sets, their orientation on contaminant transport.

6.5.2.1 Effect of fractures on contaminant transport

To demonstrate the extent of influence fractures can have on the contaminant transport, the following analysis is carried out. It is assumed that there is an accidental release of contaminant leading to its transport through a geological medium. Here, three scenarios of geological conditions are considered. They are (1) Intact rock (2) Rock with single fracture (3) Highly fractured rock (generated from the algorithm). To predict the contaminant transport behaviour, an intact rock of size 20 m $\times$ 20 m is modelled. The input parameters of the model are presented in Table 6.3. In the first case, the contaminant is allowed to migrate through the intact rock and the concentration contaminant is evaluated over time. In the second case, the contaminant transport is modelled in the same system, but with a horizontal fracture of 10 m length within the rock. In the third case, a series of horizontal parallel fractures are considered within the intact rock. For all the above cases, the concentration of contaminant is evaluated at four observation points.

A two-dimensional finite element mesh is generated in quadrilateral mode with 40401 nodes. Each quadrilateral element is divided further into four small triangular elements leading to 80401 nodes in the mesh. The flow motion along the fracture is assumed to follow Hagen-Poiseuille law.

Table 6.3: Geological properties of rock (Šperl and Trčková, 2008; Diersch, 2014; Piscopo et. al., 2017) and the contaminant transport properties (Graf and Therrien, 2005; Diersch, 2014)

Quantity	Value
Study domain	
Domain length (m)	20
Domain width (m)	20
Porous matrix	
Isotropic hydraulic conductivity (m/s)	10^{-9}
Porosity	0.13
Molecular diffusion (m^2/s)	5×10^{-10}
Longitudinal Dispersivity (m)	0.1
Transverse Dispersivity (m)	0.05
Fracture	
Flow law	*Hagen Poiseuille*
Fracture area (m^2)	6×10^{-5}
Hydraulic Aperture, b (m)	1.2×10^{-4}
Hydraulic radius (m)	6×10^{-5}
Longitudinal Dispersivity (m)	0.1
Molecular diffusion (m^2/s)	5×10^{-9}

(a)

(b)

(c)
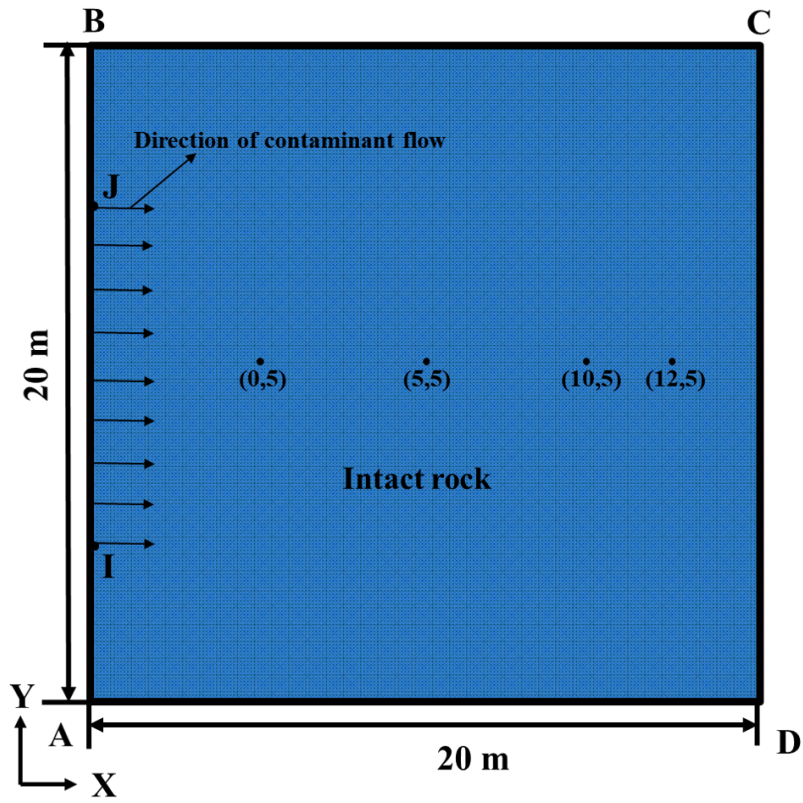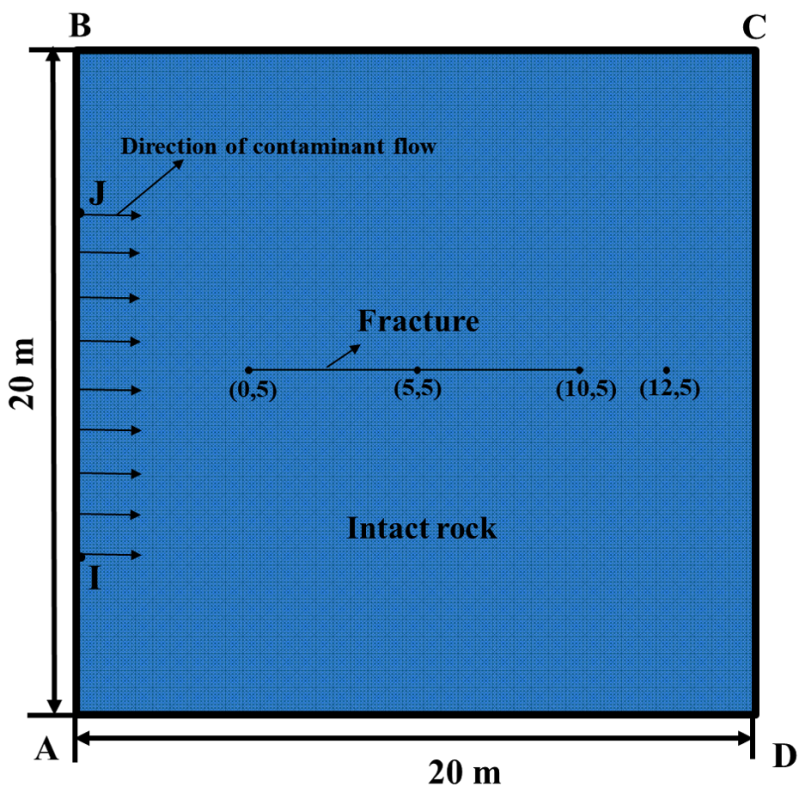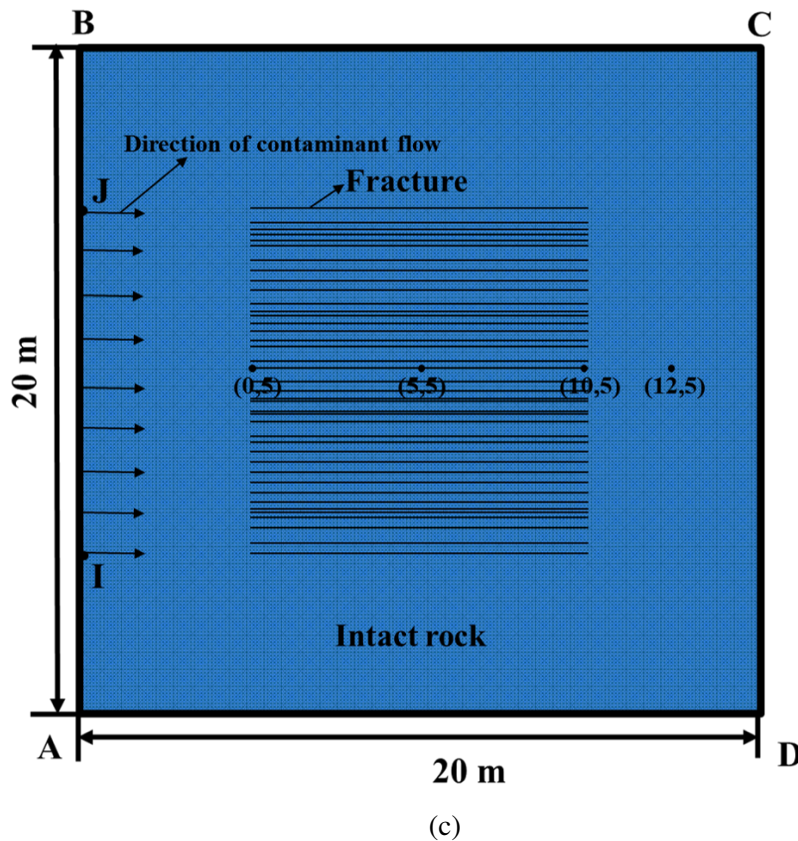
Figure 6.7: Finite element mesh (a) Intact rock (b)Rock with single fracture (c) Highly fractured rock

According to this law, the fracture walls are represented by two smooth, parallel plates, separated by an aperture 'b' and the flow takes place in the space between these parallel plates. For case (1), the properties of intact rock are assigned over the entire domain. In cases (2) and (3), transport properties of contaminant through fracture are assigned for discrete elements and the rest of the medium with the properties of porous intact rock matrix (as given in Table 6.3). The direction of flow of contaminant is considered along x direction. The initial and boundary conditions for fluid flow and contaminant transport are given in Table 6.4. Under these conditions, the results of contaminant migration with respect to time are estimated at points (x, y): (0 m, 5 m), (5 m, 5 m), (10 m, 5 m), (12 m, 5 m) and presented in Figure 6.8. From Figure 6.8, it can be observed that the (at observation point (0 m,5 m)), time taken for contaminant to reach its peak concentration

is least (around 27 years) in the case of highly fractured rock (case 3) and highest (around 54 years) in the case of intact rock (case 1). This indicates that case 1 takes almost double the time to reach the peak concentration than case 3. The concentration front of case 2 lies between the case 1 and case 3.

Table 6.4: Fluid flow and mass transport boundary conditions (Diersch, 2014)

Section	Quantity	Value
	Solute IC and BC's	
AB	Dirichlet-type BC at LHS ($-5 \leq y \leq 15, x = -5m$) (m)	10
DC	Dirichlet-type BC at RHS ($-5 \leq y \leq 15, x = 15m$) (m)	0
	Solute IC and BC's	
-	Initial condition (IC) of solute (mg/l)	0
IJ	Dirichlet-type BC at LHS ($0 \leq y \leq 10, x = -5m$) (mg/l)	1
AI	Dirichlet-type BC at LHS ($-5 \leq y \leq 0, x = -5m$) (mg/l)	0
JB	Dirichlet-type BC at LHS($0 \leq y \leq -15, x = -5m$) (mg/l)	0

Figure 6.8: Comparison of relative concentration versus time for intact rock and fractured rock

As the observation point moves away from the source, there is a significant increase in

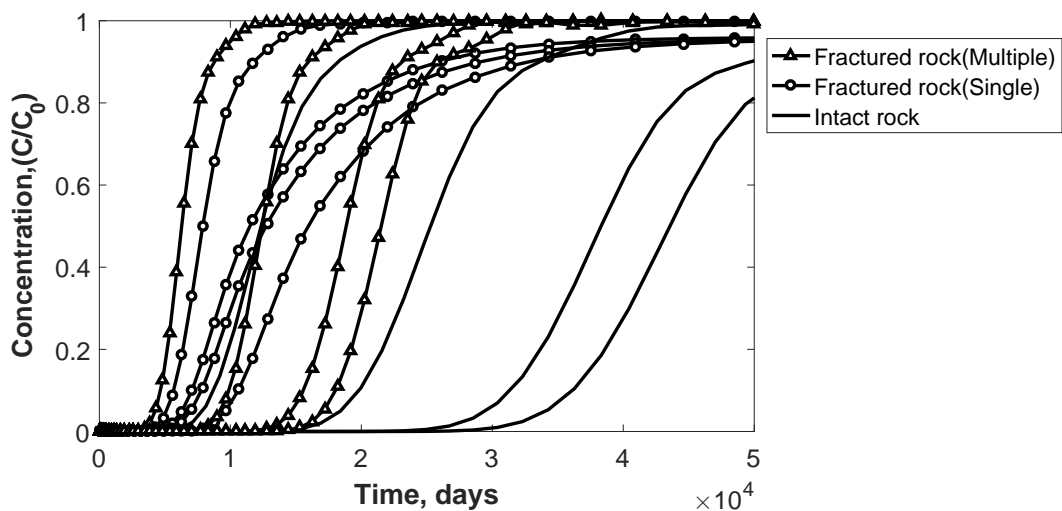the travel time of contaminant for case 1. But in case of fractured rock, there is not much of a difference in the travel time with respect to the distance from the source. These results highlight the fact that the presence of fractures leads to a higher conductance (dominant advective component) of contaminant. Also, the hydro-geological properties of fractures and rock matrix influence the contaminant migration especially the orientation of fractures. In further sections, the effect of the orientation of fracture on the contaminant migration is studied.

6.5.3 Modelling the aperture variations along the fracture

Fracture geometry plays an important role in modelling the flow and transport of contaminant through fractured rock. One of the important geometrical features of fracture is its 'aperture'. Fracture aperture is the perpendicular width between the walls of an open fracture. The role of apertures on fluid flow and solute transport have been attributed to both microscopic scale studies (Tsang and Witherspoon, 1983; Neretnieks, 2002; Briggs et. al., 2017) as well as large scale field studies (Tsang et. al., 1988; Oron and Berkowitz, 1998; Sarkar et. al., 2004) in the literature. Also, the variation in aperture along the fracture is also critical in predicting the flow along a fracture and several authors have studied on this effect (Wilson and Witherspoon, 1976; Bear et. al., 1993; Sarkar et al., 2004). A schematic of fracture and different approximations made in representing the aperture variations along the fracture is presented in Figure 6.9. Figure 6.9 (a), represents a natural fracture, with rough walls (i.e., lot of variations in aperture) along the length. It becomes an arduous task to model such complex pattern. To simplify this task, a model concept called the parallel plate concept is used. It can be applied globally as shown in Figure 6.9 (b) or locally as shown in Figure 6.9(c) (Oron and Berkowitz, 1998; Dietrich et. al.,

2010).

(a)

(b)

(c)
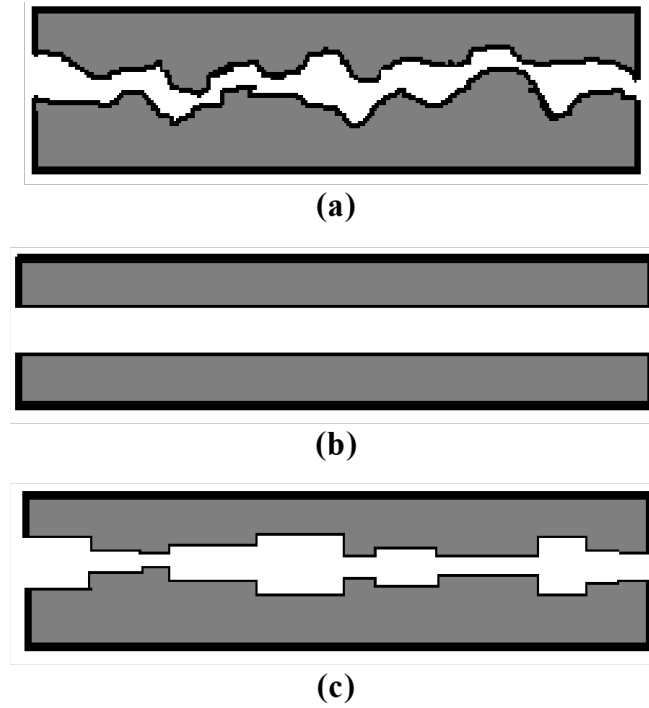
Figure 6.9: Schematic of fracture apertures patterns

In this study, the local parallel plate approximation has been used to simulate local aperture variations along the fracture. The underlying idea in developing this model is to approximate each fracture as a series of 'N_p' discrete segments with different aperture sizes. Each segment within the fracture is modelled as a parallel plate. The number of segments in each fracture is a function of the length of each element in finite element mesh, the length of fracture and also the extent of variations observed from in-situ/experimental investigations. By integrating the effect of all these factors, maximum number of segments in a fracture is given by

$$N_p = \frac{l_f}{l_e} \tag{6.11}$$

where N_p, l_f and l_e are the maximum number segments in each fracture, length of fracture and the length of element in the FE mesh respectively. For example, for a mesh element

of length 0.1 m and fracture of length 10 m , the 'maximum' number of segments along the fracture are (10/0.1 = 100). This implies that the number of segments cannot exceed length of mesh element. To avoid any errors, a finite element mesh that can account for the aperture variation needs to be generated. By adding this component to the geosphere transport model, the influence of local aperture variations on contaminant transport can also be investigated.

6.5.4 Python-interface

To examine various factors involved in contaminant transport modelling through fractured rock mass, a geosphere transport model has been developed that accounts for (1) generating fractures using stochastic algorithm, (2) generating a finite element mesh that can model fluid flow and contaminant transport process (i.e., advection, diffusion etc) in fractures and intact rock matrix and, (3) generating aperture variation along the fracture. These three components have been integrated by coding in python programming interface. The computational efficiency of the model increased by automating these components. The sequence of steps followed to generate the FE mesh with all the integrated components is presented in Figure 6.10.

6.5.4.1 Module 1: Generation of fractures using stochastic algorithm

This module considers the size of fracture domain, number of fracture sets, density of fractures in each set, their orientation etc to generate output. It can also handle uncertainties in the input data (like orientation distribution). The output from this module are coordinates of fractures and their respective sets. It has to be processed further and then integrated to FE mesh.

6.5.4.2 Module 2: Generation of FE mesh that can model fluid flow and contaminant transport process

In the second module, an FE mesh of the domain is generated. The boundary conditions and the properties of the intact rock are assigned to the mesh. Using the python API (application programming interface) functions and some of the GUI (graphical user interface) features in FEFLOW, these properties are assigned.

6.5.4.3 Module 3: Generation of local aperture variations along fracture

This module post processes the output from module 1, incorporates the effect of aperture variation along the fracture and finally integrates the fracture network on to FE mesh.

1. The results from module 1 gives the co-ordinates of fracture and the corresponding fracture set. But, these values cannot be directly imported into the software. So, a sub-routine is written such that, based on the highest and lowest values of co-ordinates within the fracture set, the angle of orientation of fracture is determined. Also, a sub-routine to create the fracture through node-to-node connectivity (as the co-ordinates obtained from the algorithm are random) is written.

2. Each fracture generated from module 1 are divided into m segments. So, module 3 requires the value of 'm'. A sub-routine is written such that the module divides the fractures into the required number of segments automatically, irrespective of the various lengths of fractures in the fracture network. (Note: 'm' cannot be less than node-to-node length of FE mesh (p), $m \not< p$)

With the help of these modules, the factors affecting the flow and transport through fractured rocks are thoroughly studied and discussed in Section 6.6.2.
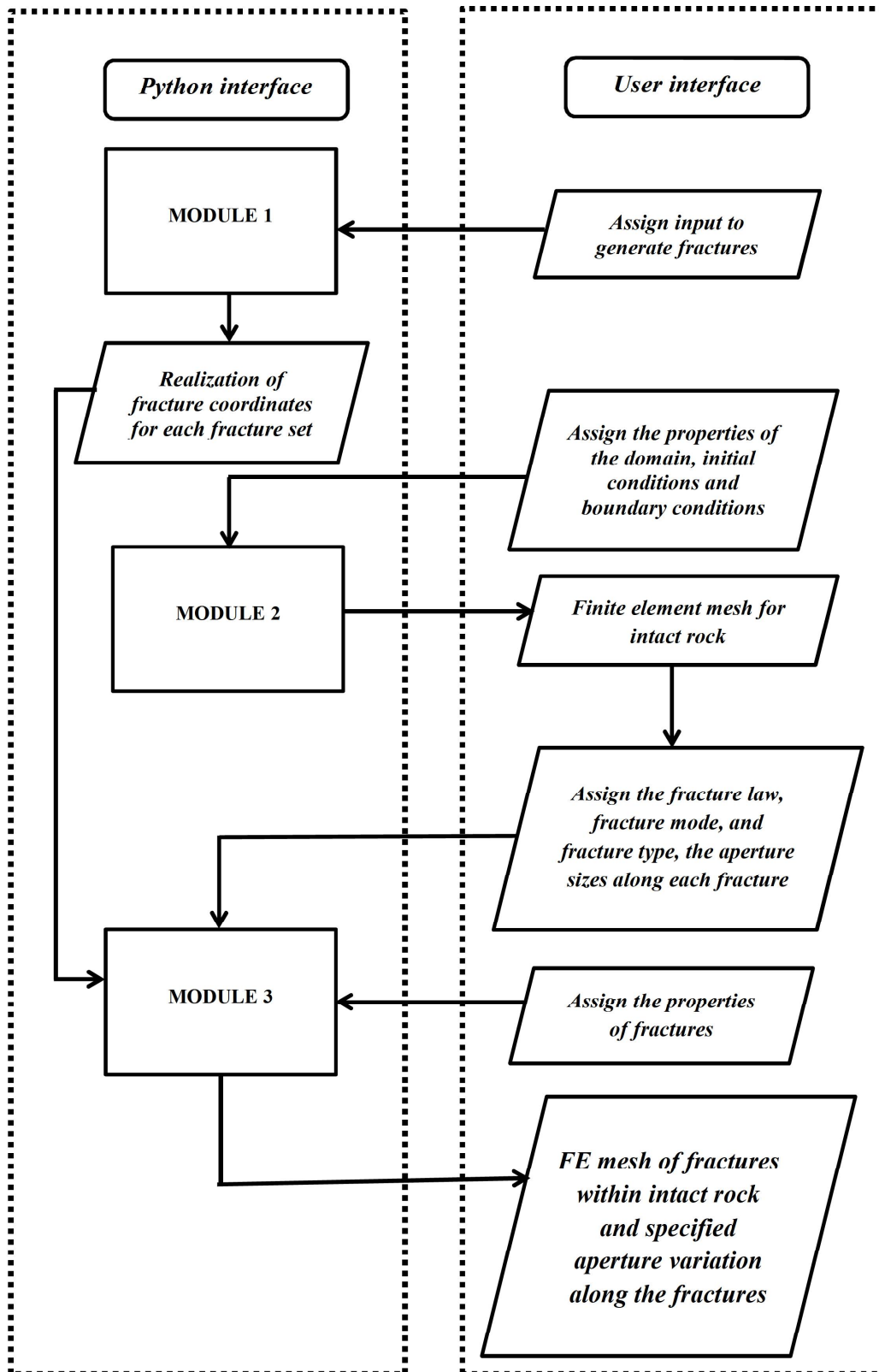
Figure 6.10: Sequence of steps followed in building the numerical model

6.6 Probabilistic safety assessment model for disposal system with non-reactive contaminant

In designing waste disposal systems such as landfills (or radioactive waste repositories), there are numerous problems of environmental concern which involve migration of contaminant plumes due to their leakage from the disposal systems. In general, salt solution is chosen as tracer instead of actual pollutant due to its non-reactive nature and also, to avoid problems associated with their handling and disposal (Asif, 2004; Peter et. al., 2009). There have also been investigations on the modelling variable-density groundwater flow and transport due to salt-water intrusion in exploited coastal aquifers, aquifers overlying salt formations, leakage from landfills, and disposal of radioactive or toxic wastes in salt rock formations (Shikaze et. al., 1998; Ackerer et. al., 1999; Graf and Therrien, 2005; Graf and Simmons, 2008). The density-driven advective, dispersive and diffusive characteristics of solute (salt) during the transport process in fractured geological media (containing single fracture or a simple network of parallel fractures) were examined already in section 6.5.2.1. In this study, flow and transport behaviour of non-reactive contaminant in a complex fracture network is investigated. This model is integrated to the performance assessment modelling framework to predict the risk due to failure of waste disposal systems.

6.6.1 Source term model

The first component of safety assessment modelling, is to identify the event for the failure of disposal system. Here, the failure scenario is assumed to be due to infiltration of water

into the system, leading to a repository failure and leaching of contaminant from the system. The inventory of contaminant released from the system is estimated from the source term. Since, the contaminant is non-reactive, the contaminant concentration released from the system has a relative concentration of $\frac{C}{C_0} = 1$, where C is the concentration at time t and C_0 is the initial concentration.

6.6.2 Input properties considered for the model

From the previous studies, it could be noted that the general range of fracture orientations observed from the field and modelling investigations was $0° - 130°$ (Bai and Pollard, 2000; Burg, 2012; Narr and Suppe, 1991; Yue et. al., 2017). Amongst the fracture orientations, the horizontal and vertical fractures are the most frequently occurring patterns. Apart from these orientations, $45°$ and $135°$ fracture sets (typical zones of failure due to stresses) are considered for the study. So fracture orientations (θ_k) considered for the study are $0°$, $45°$, $90°$ and $135°$. The other input parameters of the fracture generation algorithm are presented in Table 6.5.

Table 6.5: Input data considered for the fracture generation

Quantity	Value
Length of domain in x-direction (m)	10
Length of domain in y-direction (m)	10
Number of fracture sets	1, 2, 3
Density of fractures (λ_k) (m^{-1})	1, 2
Probability of continuation at fracture intersections (p_k)	0, 0.1, 0.2
Velocity of propagation (u_k)	2, 1
Inhibition distances for initial point simulation (m)	0.1

6.6.3 Geosphere transport model

A rock mass of size 20 m $\times$ 20 m is considered, with fracture network of dimension 10 m $\times$ 10 m modelled within the domain. The schematic of fractured rock mass is presented in Figure 6.11.
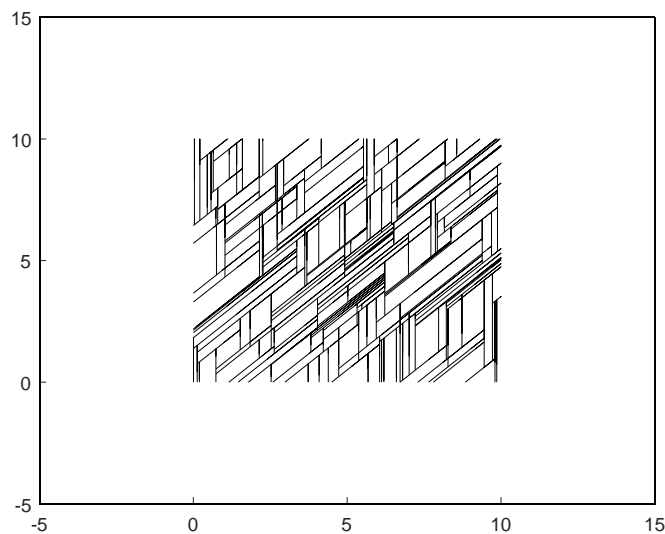
Figure 6.11: Schematic diagram of fracture-rock matrix system

The geological and transport parameters for the analysis are summarized in Table 6.3. This domain is discretized into a two-dimensional quadrilateral mesh with 40401 nodes and the fractures are modelled as 1D discrete elements. To model the inclined fractures in FE mesh, each quadrilateral element is divided further into four small triangular elements leading to 80401 nodes in the mesh. The spatially discretized FE mesh is shown in Figure 6.12. The contaminant flow is considered along x-direction and y-direction to examine the influence of heterogeneity in fractures.
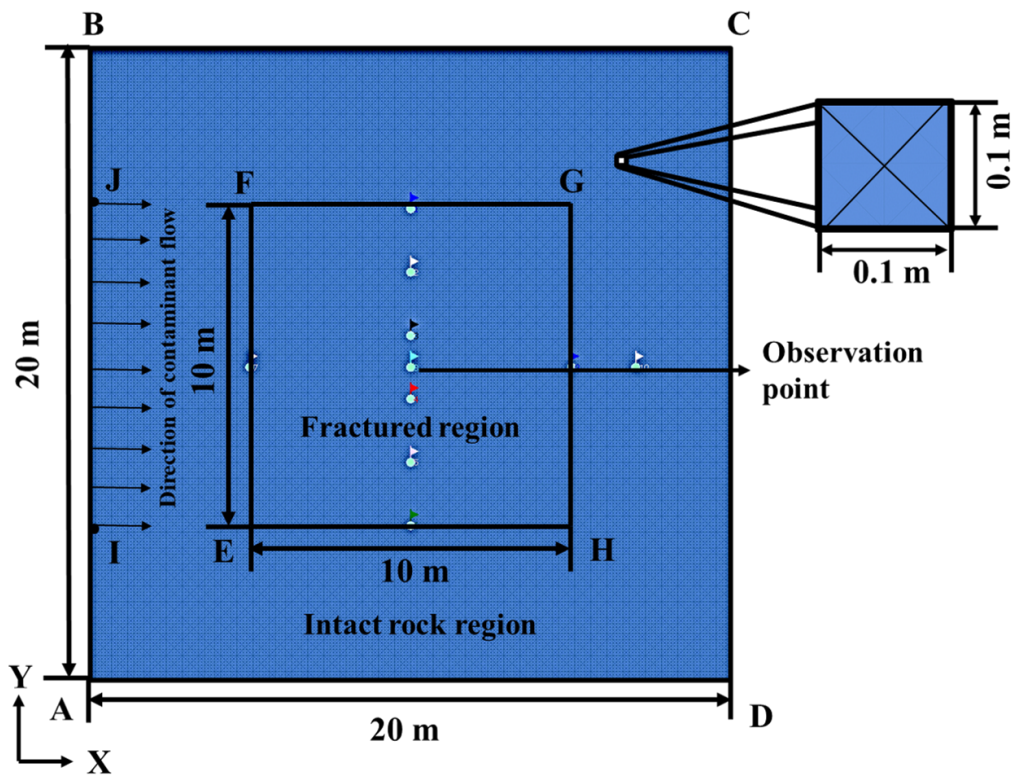
(a)
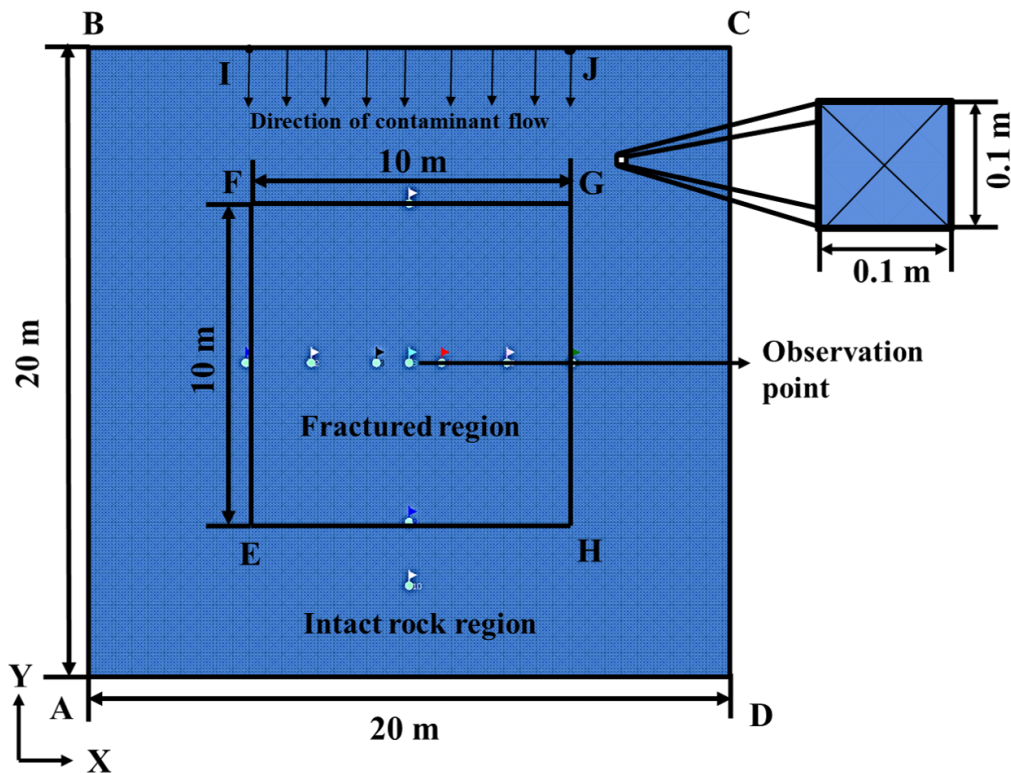
(b)

Figure 6.12: Finite element mesh geenerated for the problem (a) when flow is in x-direction (b) when flow is in y-direction

The initial conditions and the boundary conditions for fluid flow and mass transport are presented in Table 6.6. Since the direction of contaminant flow is varied in x and y directions, the boundary conditions (bc) are mentioned for both the cases.

Table 6.6: Fluid flow and mass boundary condition

Section	Quantity	Value
For the case of flow in horizontal direction		
Fluid Flow		
AB	Dirichlet-type bc at LHS $(-5 \leq y \leq 15, x = -5m)$ (m)	10
DC	Dirichlet-type bc at RHS $(-5 \leq y \leq 15, x = 15m)$ (m)	0
Mass transport		
-	Initial condition of solute (mg/l)	0
IJ	Dirichlet-type bc at LHS $(0 \leq y \leq 10, x = -5m)$ (mg/l)	1
AI	Dirichlet-type bc at LHS $(-5 \leq y \leq 0, x = -5m)$ (mg/l)	0
JB	Dirichlet-type bc at LHS$(0 \leq y \leq -15, x = -5m)$ (mg/l)	0
For the case of flow in vertical direction		
Fluid flow		
BC	Dirichlet-type bc at LHS $(-5 \leq x \leq 15, y = 15m)$ (m)	10
AD	Dirichlet-type bc at RHS $(-5 \leq x \leq 15, y = -5m)$ (m)	0
Mass transport		
-	Initial condition of solute (mg/l)	0
IJ	Dirichlet-type bc at LHS $(0 \leq x \leq 10, y = 15m)$ (mg/l)	1
BI	Dirichlet-type bc at LHS $(-5 \leq x \leq 0, y = 15m)$ (mg/l)	0
JC	Dirichlet-type bc at LHS$(0 \leq x \leq -15, y = 15m)$ (mg/l)	0

Using the above input data, the contaminant transport modelling is carried out and the results are presented in the following sections.

6.6.4 Deterministic analysis

In section 6.5.2.1, the extent of influence a set of fractures can create on the contaminant transport is investigated. Clearly, in discrete fracture network models, fractures and their geometry contribute to the overall contaminant movement. Also, it is important to note that, though fractures are primary pathways of contaminant migration, the effect of diffusive properties of rock matrix cannot be neglected. So, the influence of some of important properties of fractures and rock matrix are examined in this section. The parameters considered for the analysis are :

1. Effect of fracture geometry (fracture orientation and number of fracture sets) on the contaminant transport

2. Effect of aperture variations along the fracture on the contaminant transport

3. Effect of matrix diffusion and dispersion and also fracture diffusion on the contaminant transport

4. Effect of contaminant transport by applying the concept of equivalent porous medium

The influence of each parameter is studied systematically and their long-term effects are discussed. Due to large spatial extent of fractures (10 m × 10 m) and heterogeneity in the fracture network, it becomes difficult to decipher the pathway of contaminant movement through the system. So, some critical observation points are considered as shown in Figure 6.13. The evolution of contaminant concentrations over time are evaluated at these points.
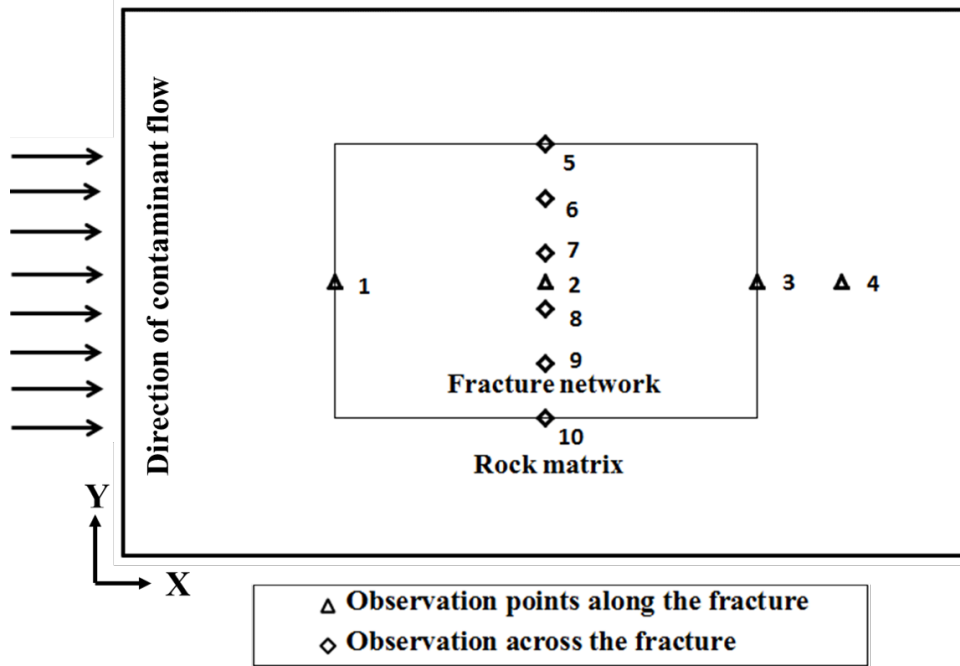
(a)
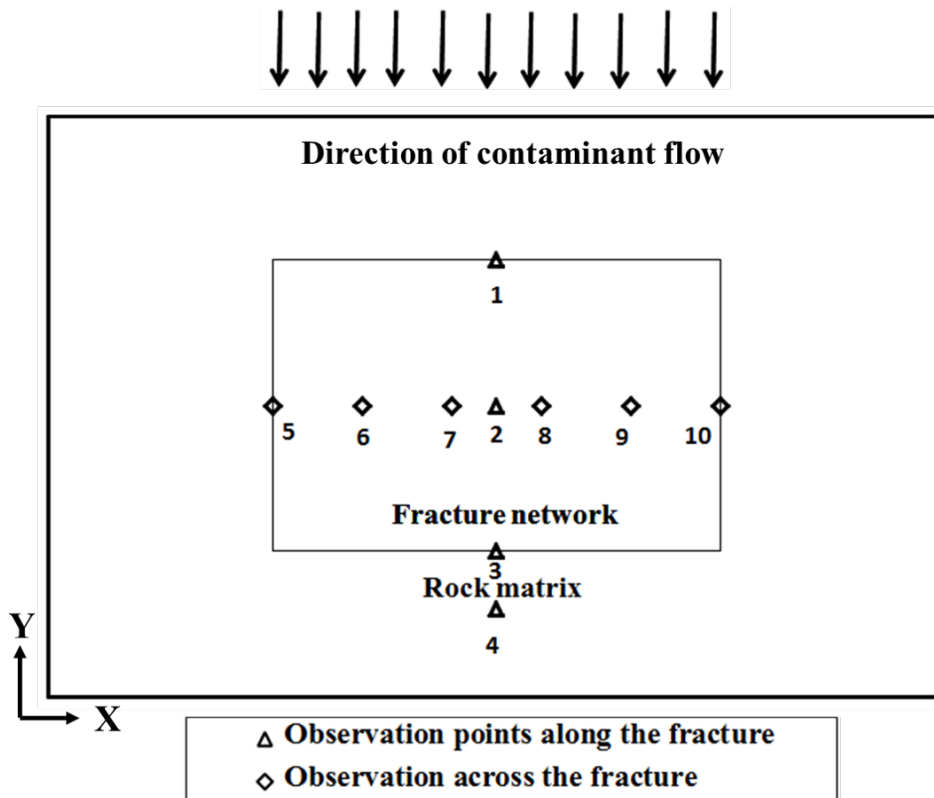
(b)
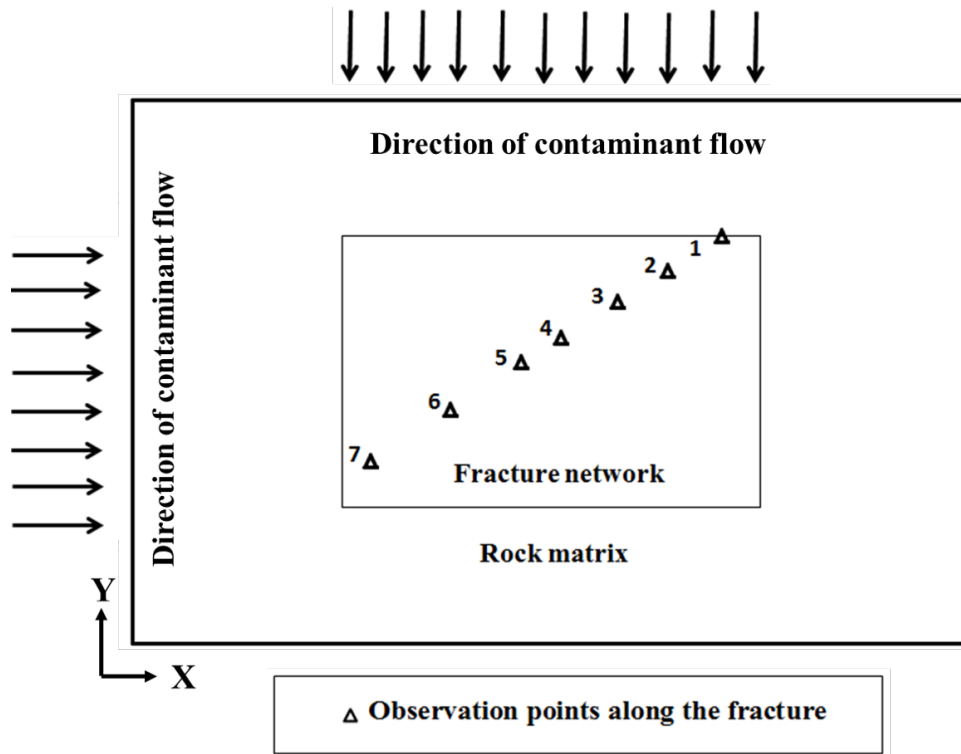
(c)
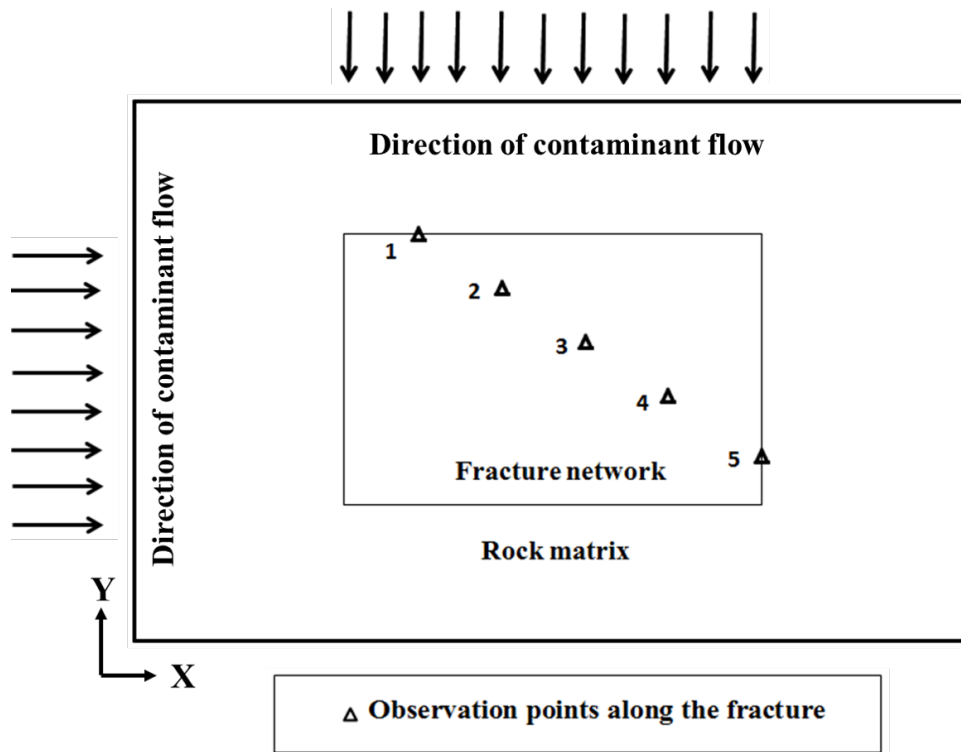
(d)

Figure 6.13: Observation points considered for the analysis

From Figure 6.13 (a) and 6.13 (b), it can be noted that observation points are ordered

along x-direction and y-direction. This indicates that, the observation points in Figure 6.13 (a) are considered when the direction of contaminant is along x-direction. Similarly, the observation points in Figure 6.13 (b) are considered when the direction of contaminant is along y-direction. In Figure 6.13 (c) and 6.13 (d), the observation points are arranged sequentially at an angle of 45° and 135° respectively. So, observation points Figure 6.13 (c) and 6.13 (d) are considered only for the case of series of parallel fractures oriented at 45° and 135° respectively. Thus, the observation points are chosen to reckon the influence of direction of contaminant flow and orientation of fracture considered for the analysis.

6.6.4.1 Effect of fracture orientation and number of fracture sets

To investigate the effect of network geometry, different combinations of fracture sets and fracture orientations are modelled. By running simulations through these networks, the contaminant concentration evolving with time are presented. So, the results at each observation point are denoted according to Figure 6.13. For example, when the contaminant flow is modelled along x direction, the concentration versus time trend corresponding to observation point '1' is denoted as 1(a) in the plot.

6.6.4.1.1 Single fracture set

As a preliminary study, fracture network is modelled with a single fracture set. The fracture generation algorithm assumes all the fractures within a fracture set to be parallel. So, for a domain size of 10 m, a series of 100 parallel fractures are generated. For each fracture orientation, the corresponding network of fractures are presented in Figure 6.14.

(i) 0° inclination

(ii) 90° inclination

(iii) 45° inclination
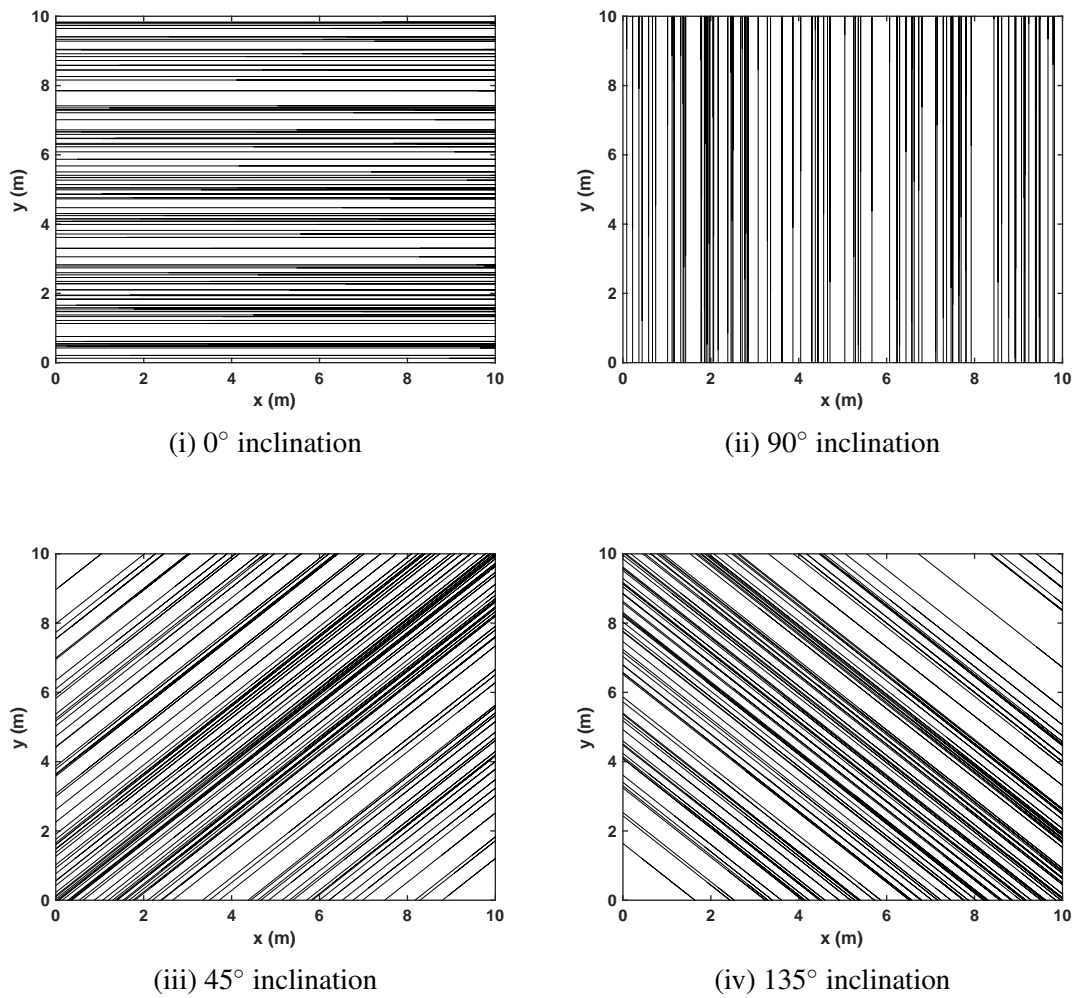
(iv) 135° inclination

Figure 6.14: Fractures with different inclinations

Each simulation is run for a time period of 70 years. The reason being, during the simulation the contaminant takes almost 30 years to travel through the intact rock region (due to its impermeable nature) and reach the fractured rock. Further, by observing the breakthrough trends, the movement of contaminant through the fractured medium (which is critical for the study) is analysed for an additional time period of 40 years. To investigate the effect of heterogeneity, the flow of contaminant is considered both in x-direction and y-direction. The results for horizontal and vertical fracture sets are presented in Figure 6.15 and Figure 6.16 respectively.
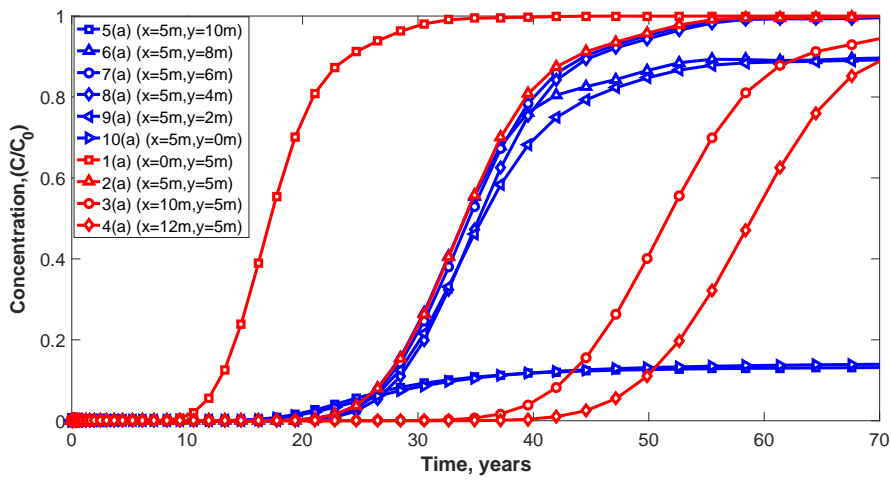
(i) Concentration versus time for flow along x direction
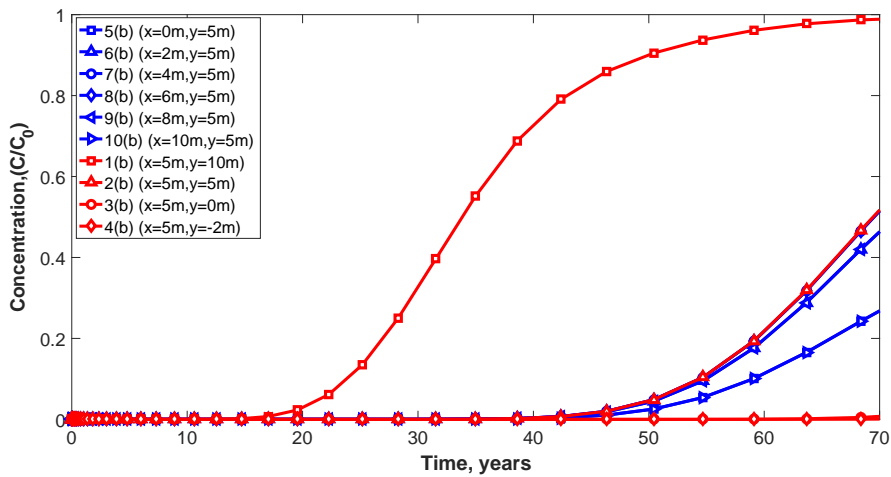
(ii) Concentration versus time for flow along y direction

Figure 6.15: Concentration versus time for different cases $0°$ fracture set

(i) Concentration versus time for flow along x direction
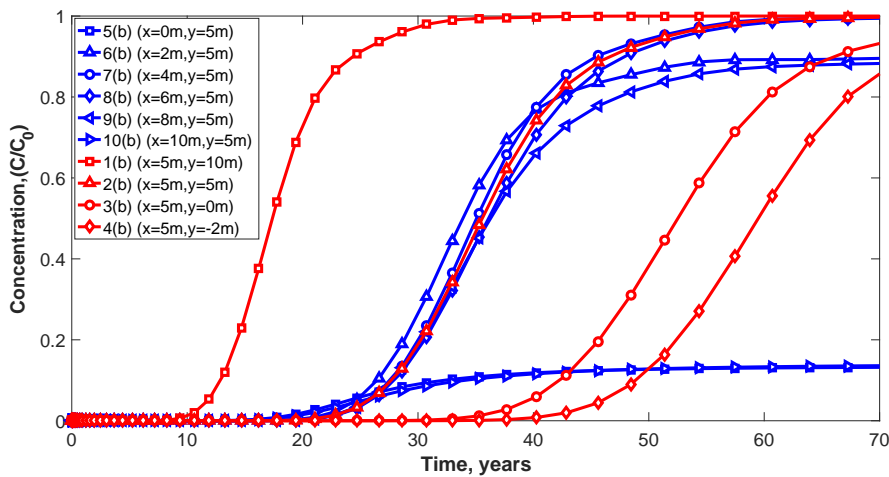
(ii) Concentration versus time for flow along y direction

Figure 6.16: Concentration versus time for different cases 90° fracture set

Figures 6.15 (i) shows the concentration profiles of the non-reactive contaminant migrating through 0° fracture network when the flow is along x-direction. In this plot, the red lines present the concentration trends at observation points along flow direction (i.e., 1(a), 2(a), 3(a), 4(a) from Figure 6.13(a)). From the results, it can be noticed that the time of arrival of peak concentration at observation point 1(a) is around 25 years while it is almost 50 years at point 2(a). It indicates that as the distance from the source increased, time taken for the arrival of peak concentration increased. In the same figure, blue lines present the concentration trends at observation points across the flow direction (i.e., 5(a), 6(a), 7(a), 8(a), 9(a), 10(a) from Figure 6.13 (a)). The concentration has not even reached 20% C_0 at observation points 5(a) and 10(a) whereas, the concentration reached peak value at observation points 6(a)-9(a). This indicates that the rate of movement of contaminant (or the contaminant plume) becomes slow in the regions transverse to the flow direction.

In Figure 6.15 (ii), the concentration trends of the non-reactive contaminant travelling through 0° fracture network when the flow is along y-direction is presented. In this case,

301

the direction of contaminant flow is opposite to the fracture orientation. The concentration reached maximum value within 70 years at observation point 1(b) (from Figure 6.13 (b)). However, none of the other points show concentration values more that $0.6 C_0$. This indicates that, since the rock fractures are opposite to the direction of flow of contaminant, there is very less movement of contaminant through the network. Through visual inspection of Figures 6.15 (i) and 6.15 (ii), it can be noted that, the contaminant plume will more spread out in the first case (6.15 (a)) since the concentration has reached peak value at all the observation points. On the other hand, there is not much of contaminant movement in 6.15 (ii) indicating a small contaminant plume. This analysis demonstrates the influence of heterogeneity in fractures. Figure 6.16 presents the results for non-reactive contaminant migrating through $90°$ fracture network. Figure 6.16 (i) and 6.16 (ii) presents the results for flow along x-direction and y-direction respectively. The observations from these plots are very similar to that of the observations made in Figure 6.15. The plots 6.15 (i) and 6.16 (ii); and plots 6.15(i) and 6.16(ii) are almost same. This is because the orientation of fractures changed from $0°$ to $90°$ while the other input conditions remain unchanged. So, the contaminant is more spread out when the flow direction and the direction of fracture orientation are same and viceversa.

The concentration profiles for fracture set $45°$ and $135°$ are presented in the figures 6.17 and 6.18 respectively. Also, the contaminant flow directions are considered along x-direction and y-direction in each case. The concentration values of contaminant in Figure 6.17 (i) and (ii) look very similar. However, the contaminant flow is in x-direction for 6.17 (i) and y-direction in Figure 6.17 (ii).
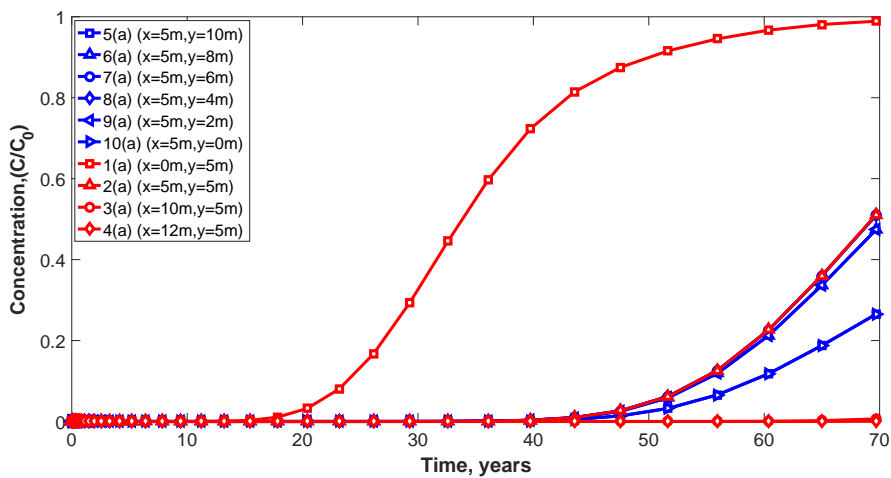
(i) Concentration versus time for flow along x direction
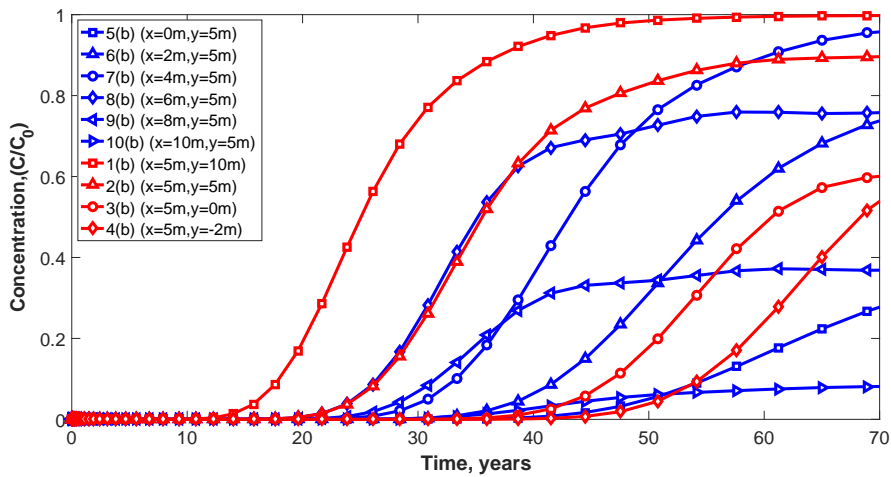
(ii) Concentration versus time for flow along y direction
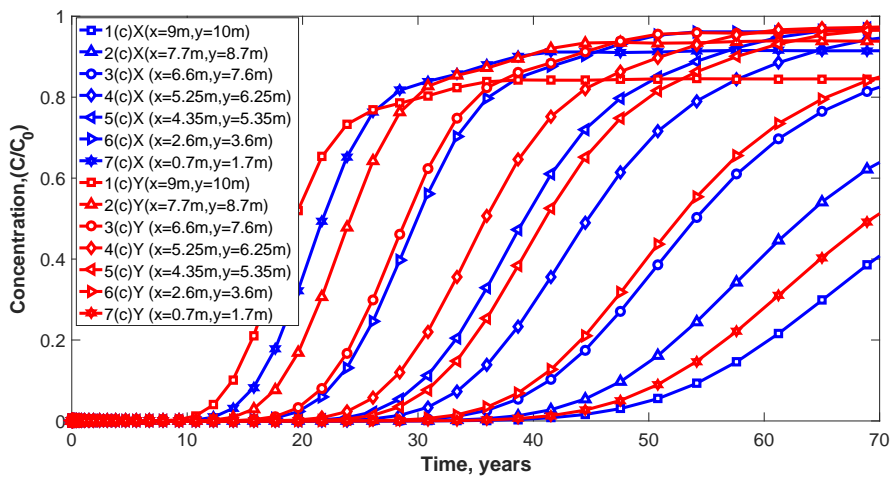
(iii) Concentration versus time for points along the fracture and flow in x and y direction

Figure 6.17: Concentration versus time for different cases of 45° fracture set

(i) Concentration versus time for flow along x direction

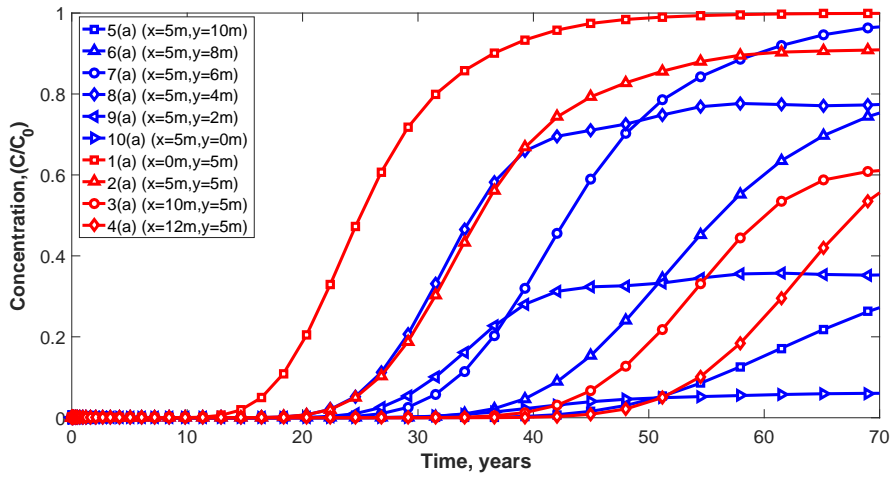(ii) Concentration versus time for flow along y direction

(iii) Concentration versus time for points along the fracture and flow in x and y direction

Figure 6.18: Concentration versus time for different cases of 135° fracture set

The reason for similar results is mainly because, in both the cases, contaminant is

flowing at an angle of 45 $^\circ$ into the system. Also, the distribution of fractures in the domain is uniform leading to a same trend of contaminant flow. This resembles a contaminant flow through homogeneous system, where the results become directionally independent. From visual inspection, it can be noticed that the contaminant plume also seems to be spread out in both the cases. For 45° fracture set, an additional set of observation points along the fracture inclination are considered as given in 6.13 (c) and the results are shown in 6.17 (iii). The results in 6.17 (iii) show that the contaminant enters from the observation point closest to the direction of flow achieves the highest concentration and it gradually moves along the fracture reaches the other end. In the case of flow in x-direction 7(c) is the closest point and in the case of flow in y-direction 1(c) is the closest point. Overall, these results help in understanding the preferential path of flow along a fracture.

In the case of 135 $^\circ$ fracture set also, Figure 6.18 (i) and (ii) show similar results. The same analogy as mentioned for 45° fracture set can be attributed to this case as well. It suggests that the fracture network behaves as a homogeneous system with directionally independent results. For 135° fracture set, an additional set of observation points along the fracture inclination are considered as given in 6.13 (d) and the results are shown in 6.18 (iii). The results show that the movement of contaminant is gradual and in the direction of fracture inclination. In the case of flow in x-direction 7(d) is the closest point and in the case of flow in y-direction 1(d) is the closest point. So contaminant moves from the closest point towards the other end of the fracture. The time of arrival of maximum concentration at closest point is very less (around 30 years) whereas, the time of arrival of maximum concentration at farthest point is very high (>70 years). The same analogy as mentioned for 45° can be attributed to 135° fracture set. However, a small discrepancy is observed in the case of flow along x-direction (indicated by blue trend lines in Figure

6.18(iii)). The reason for this might be because of the interjection of flow with the adjacent fracture, there is an offset from the actual trend. Overall, the single set fracture orientation cases demonstrate the influence of direction of flow and the fracture orientation on the contaminant movement.

6.6.4.1.2 Multiple fracture sets

In the case of single fracture sets, the fractures are long and parallel. As, there is no other fracture orientation obstructing the flow of contaminant, it becomes less complex to predict the pathway of contaminant. Nonetheless, as the number of fracture sets increase, the pattern of contaminant spread across the domain becomes unpredictable. Also, the interplay of different transport mechanisms (advection and diffusion) at fracture intersections makes it a complex system. The multiple fracture set combinations used for the present study are presented in Figures 6.19 and 6.23.

| (i) 0° - 90° | (ii) 0° - 45° | (iii) 90°- 135° |
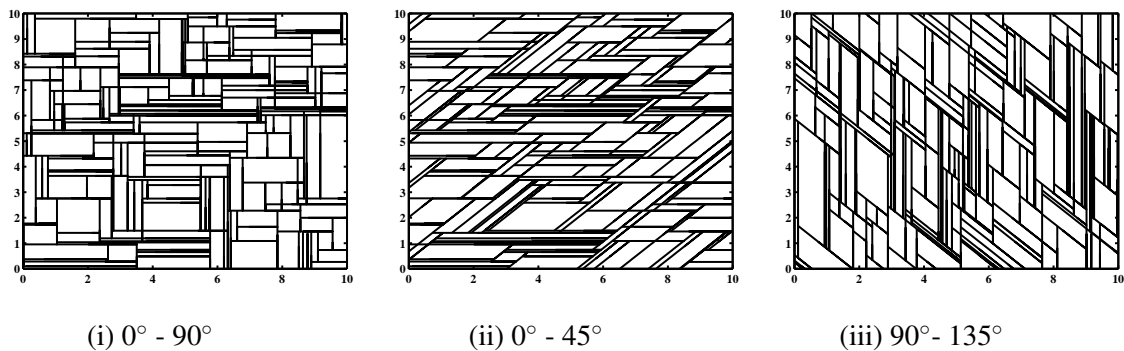
Figure 6.19: Fracture pattens with two fracture orientations

Figure 6.19 shows two fracture set combinations considered for the study which include 0° - 90°, 0° - 45° and 90° - 135°. From the fracture generation algorithm, 200 fractures are generated in each case. The results of concentration trends for the fracture set 0° - 90° along and across the flow directions are given below.
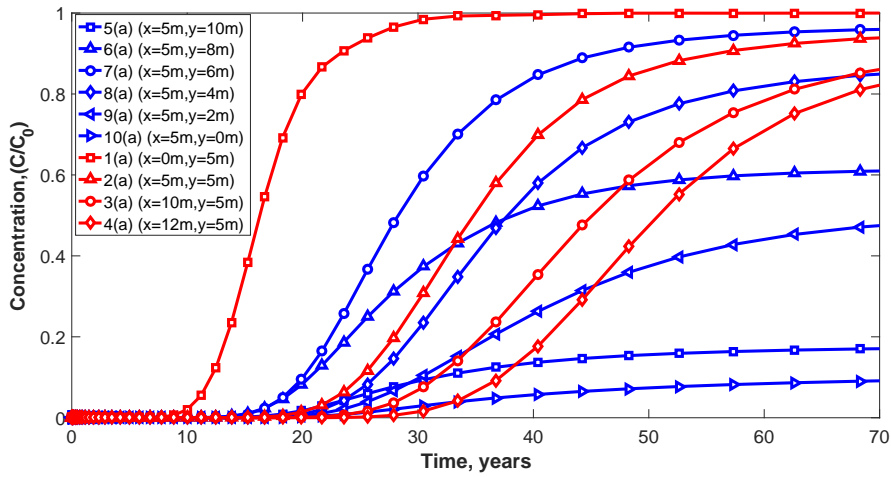
(i) Concentration versus time for flow along x direction
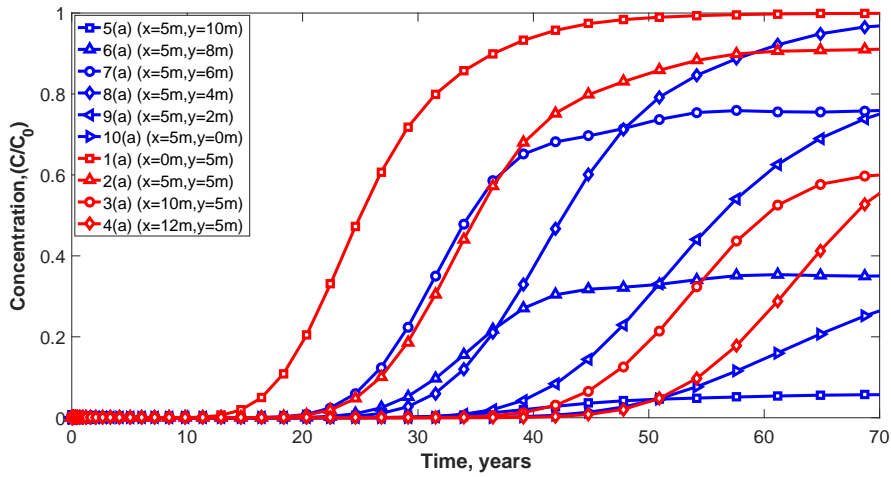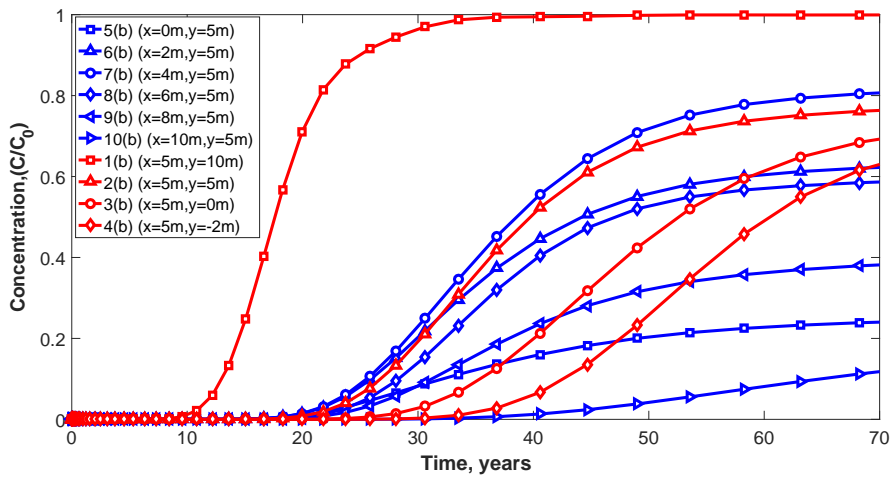

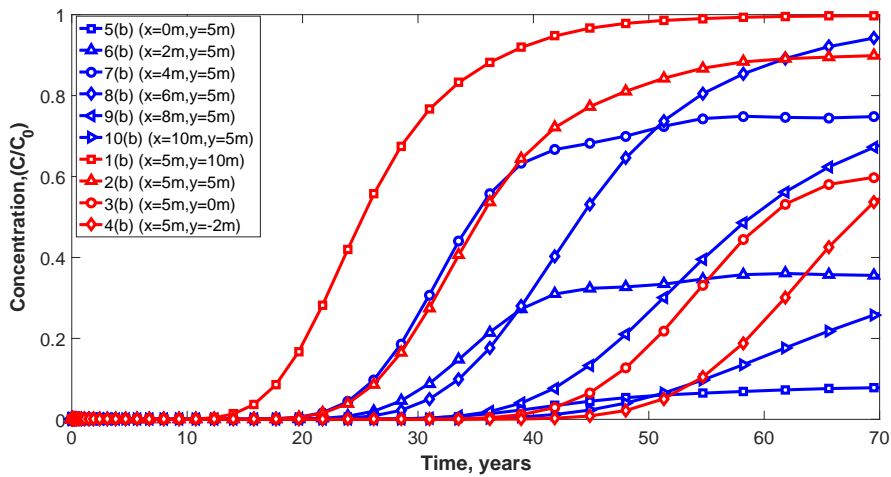(ii) Concentration versus time for flow along y direction
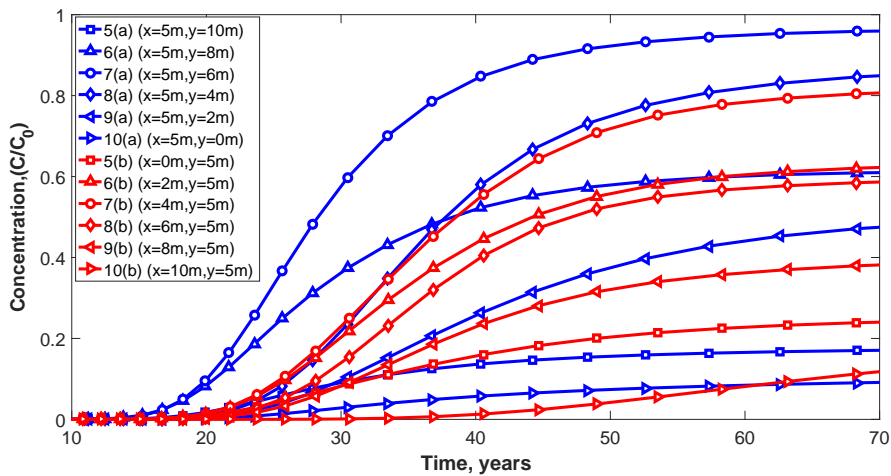
(iii) Concentration versus time for at points transverse to flow direction

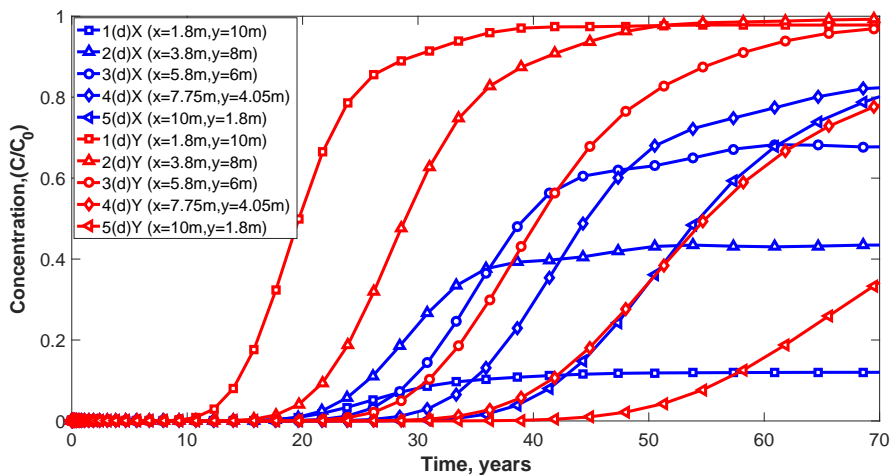(iv) Concentration versus time at points along flow direction

Figure 6.20: Concentration versus time for different cases of $0°$ - $90°$ fracture set

Figure 6.20 presents the results of concentration trends observed at different points when the contaminant travelled through $0°$ - $90°$ fracture set. Among the 200 fractures generated from the fracture generation model, 100 of them are oriented at $0°$ and 100 of them at $90°$. Figure 6.20 (i) and 6.20 (ii) present the cases when the contaminant flow is along x and y directions respectively. From these plots it can be observed that the contaminant is spead out along and across the domain. But to understand the extent of heterogeneity in the system, Figure 6.20 (iii) and Figure 6.20 (iv) are plotted. In Figure 6.20 (iii), the results for observation points orthogonal to the flow direction are plotted (i.e., blue trend lines for observation points 5(a) - 10(a); red trend lines are for observation points 5(b) - 10(b)). These observation points are orthogonal to the flow direction. From the results it is evident that there is heterogeneity in the system and the time take for the arrival of maximum concentration is faster when the flow of contaminant is in x-direction. Similarly, Figure 6.20 (iv) presents the results for observation points along to the flow direction (i.e., blue trend lines for observation points 1(a) - 4(a); red trend lines are for observation points 1(b) - 4(b)). This plot also demonstrates the difference in the

308

concentration values from both the cases. Further, the results for fracture sets $0° - 45°$ and $90° - 135°$ are presented below.

(i) Concentration versus time for flow along x direction

(ii) Concentration versus time for flow along y direction
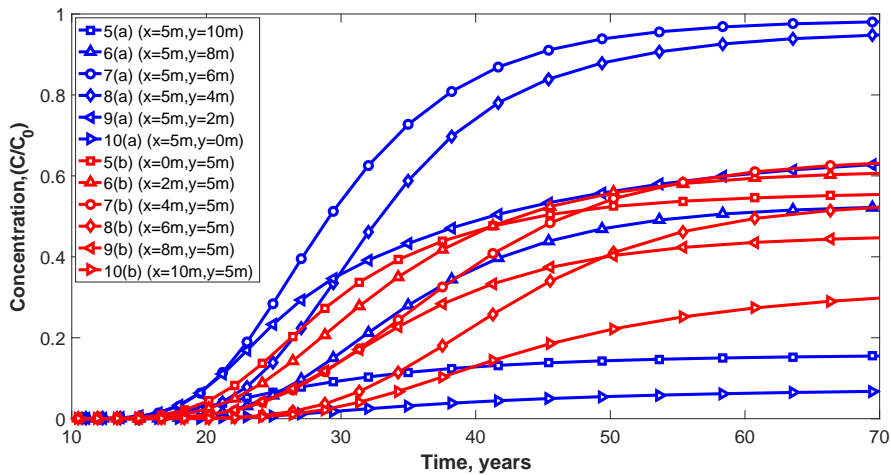
(iii) Concentration versus time for at points transverse to flow direction
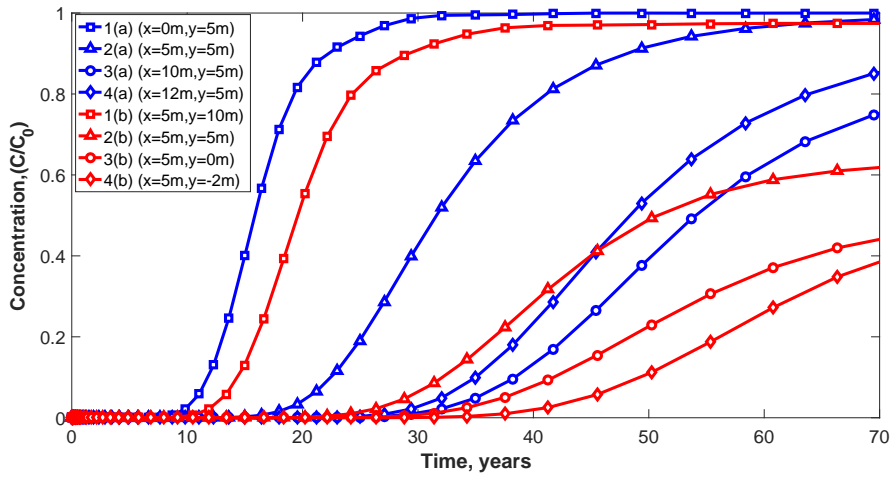
(iv) Concentration versus time for at points along flow direction

Figure 6.21: Concentration versus time for different cases 0° - 45°
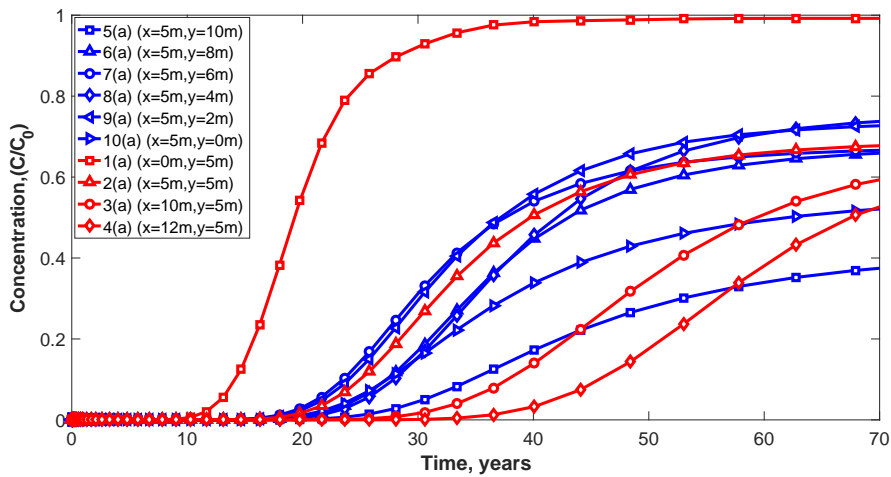
(i) Concentration versus time for flow along x direction
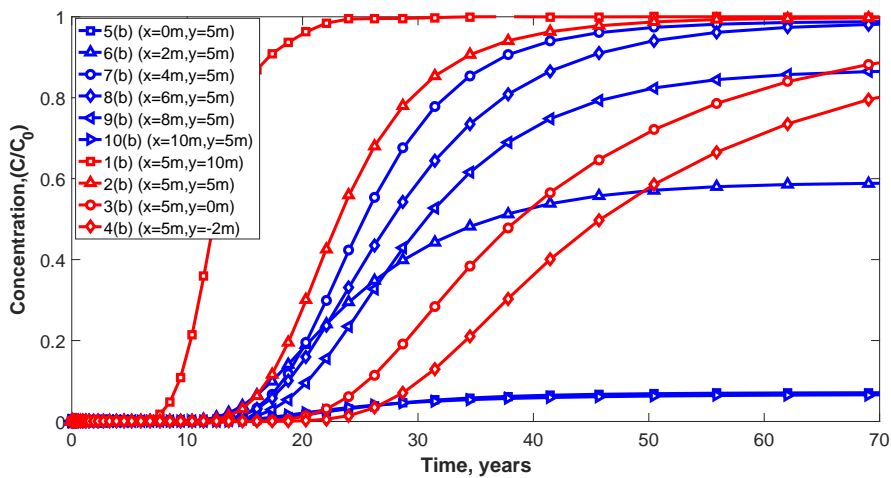
(ii) Concentration versus time for flow along y direction
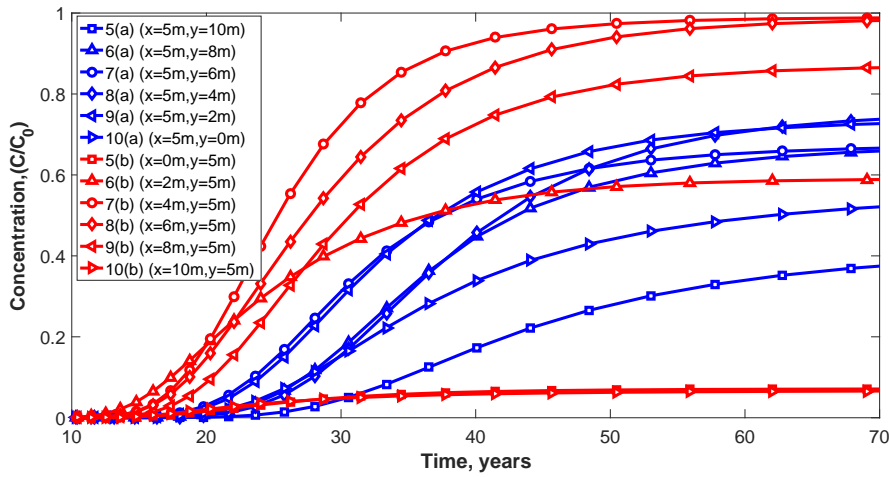
(iii) Concentration versus time for at points transverse to flow direction
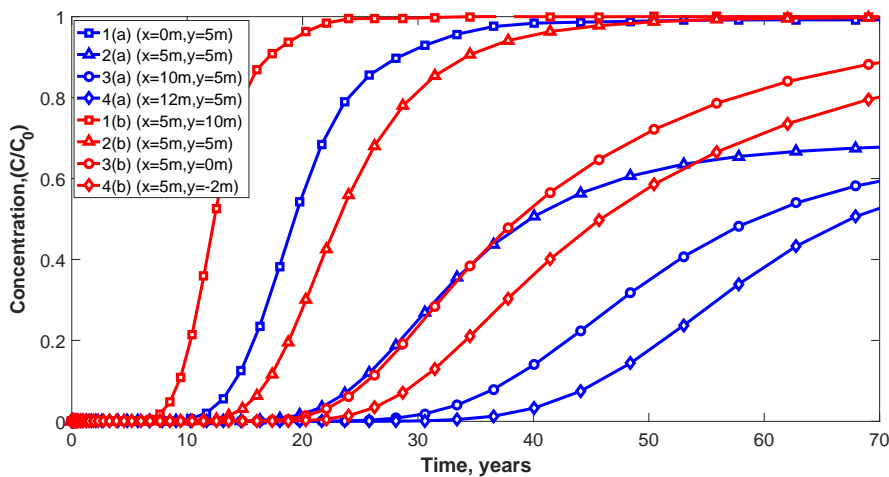
(iv) Concentration versus time for at points along flow direction

Figure 6.22: Concentration versus time for different cases of $90°$ - $135°$ fracture set

The results of the fracture set $0°$ - $45°$; $90°$ - $135°$ are presented in Figure 6.21 and Figure 6.22 respectively. The results from these sets are slightly different from $0°$ - $90°$ set, because the presence of orientations $45°$, $135°$. These fracture orientations induce more heterogeneity into the system. The same can be noticed just through visual inspection of the results. In the case of $0°$ - $45°$, Figure 6.21 (i) and 6.21(ii) show that concentration plume when the contaminant flow is along x- direction and y- direction respectively. The concentration plume in Figure 6.21 (i) is more spread out, whereas, in 6.21(ii) the concentration plume is smaller and a concentration value of $0.6\,C_0$ is observed

at almost all the observation points. The extent of heterogeneity in the system can be evidently seen from Figure 6.21 (iii) and 6.21 (iv). In the case of 90° - 135°, Figure 6.22 (i) and 6.22 (ii) shows the extent of contaminant spread across the domain. In this case also there is a strong influence of heterogeneity on the contaminant movement. So, the presence of inclined fractures alters the path of contaminant flow to a certain extent. From these results it is evident that the increase in the number of fracture sets increases the heterogeneity in the system.

The complexity in fracture network increases further when the number of fracture sets increases from two sets to three sets.

(i) 0°-45° - 90°   (ii) 0° - 45° - 135°
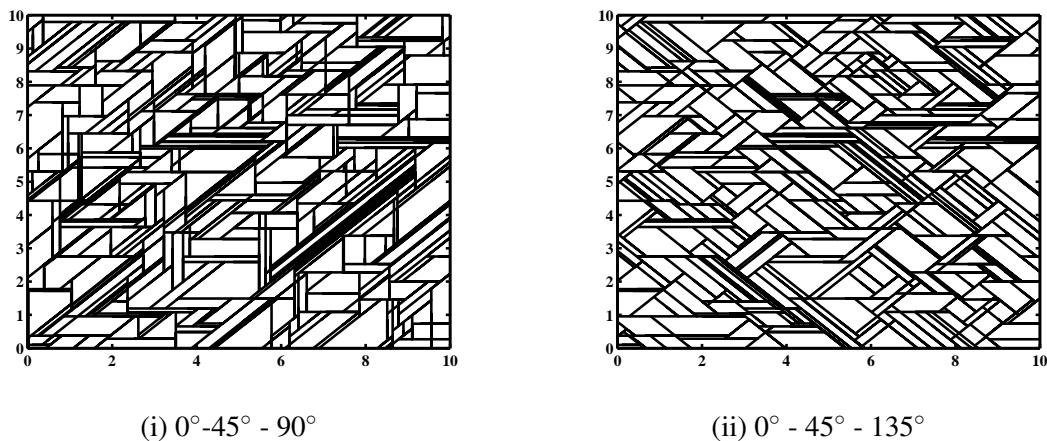
Figure 6.23: Fracture pattens with three orientations

A total number of 400 fractures are generated from the fracture generation algorithm. Two typical fracture set combinations are chosen for the analysis to investigate the spreading pattern of contaminant through the system are given in Figure 6.23. The results of concentration trends for 0° - 45° - 90° and 0° - 45° - 135° fracture sets are presented in Figure 6.24 and Figure 6.25. The direction of contaminant flow is considered both in x and y directions.
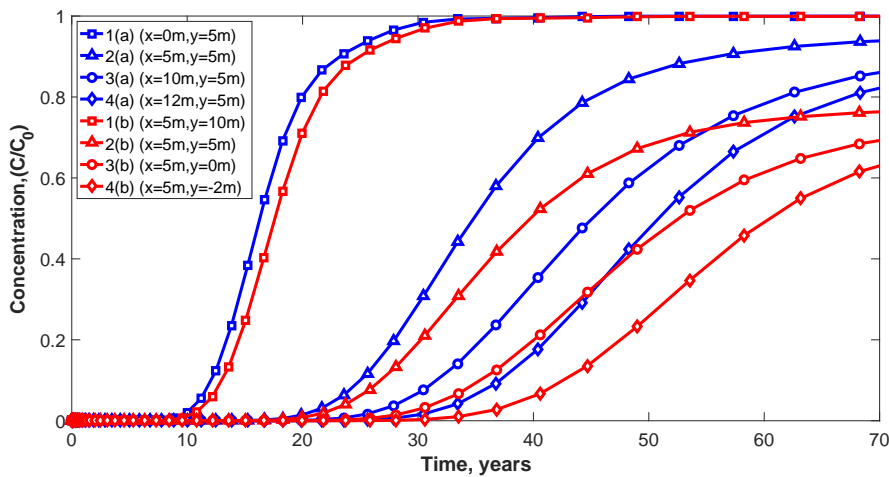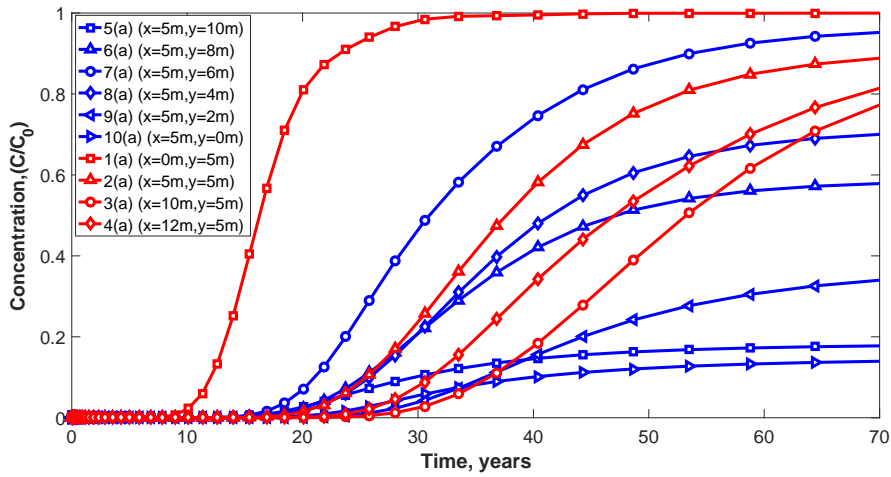
(i) Concentration versus time for flow along x direction
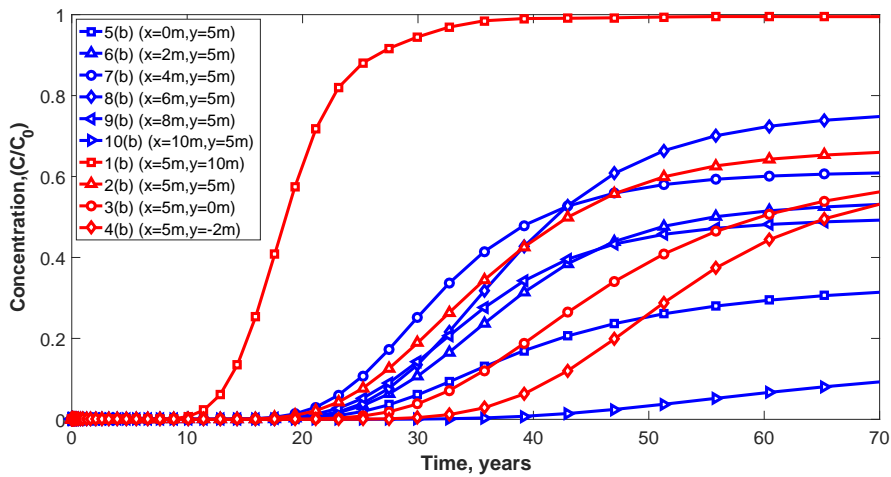
(ii) Concentration versus time for flow along y direction
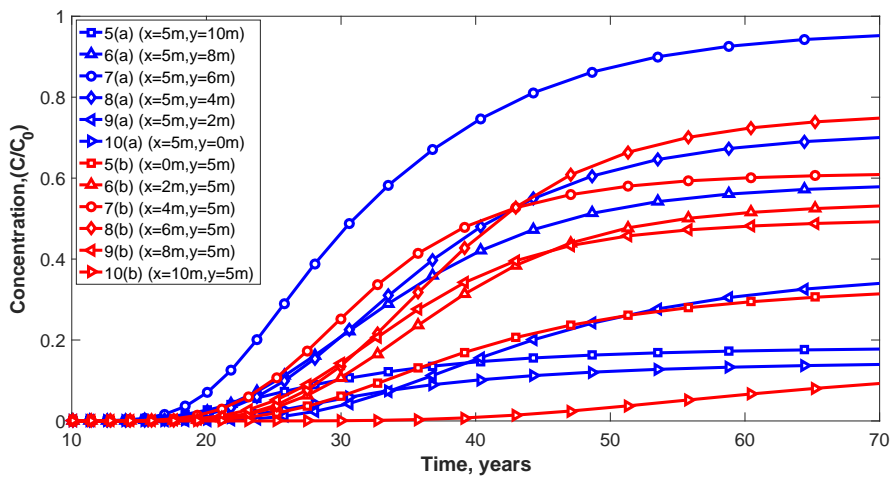
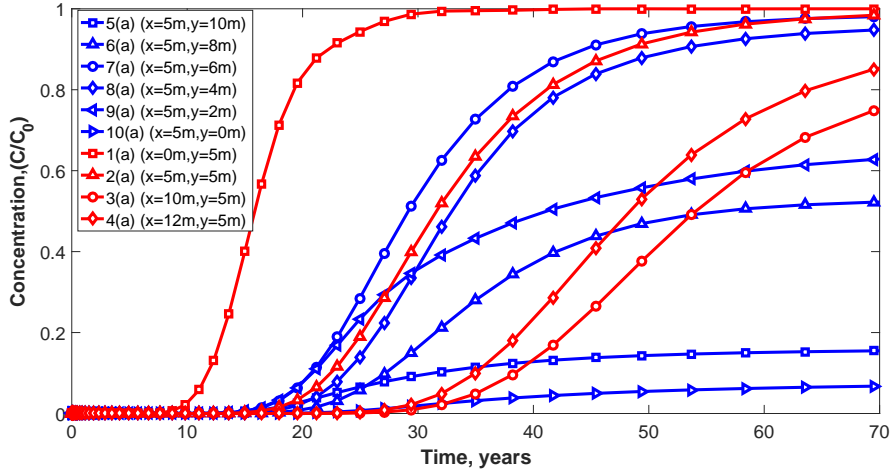(iii) Concentration versus time for flow across flow direction
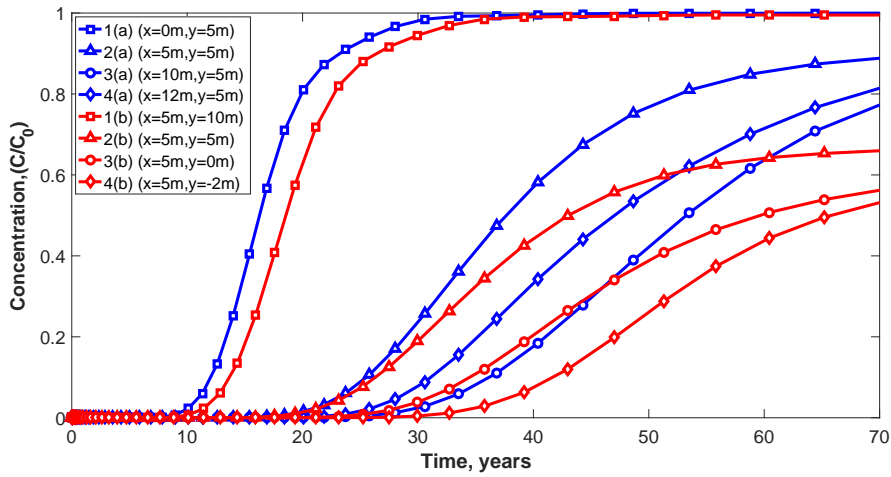
(iv) Concentration versus time for flow along flow direction

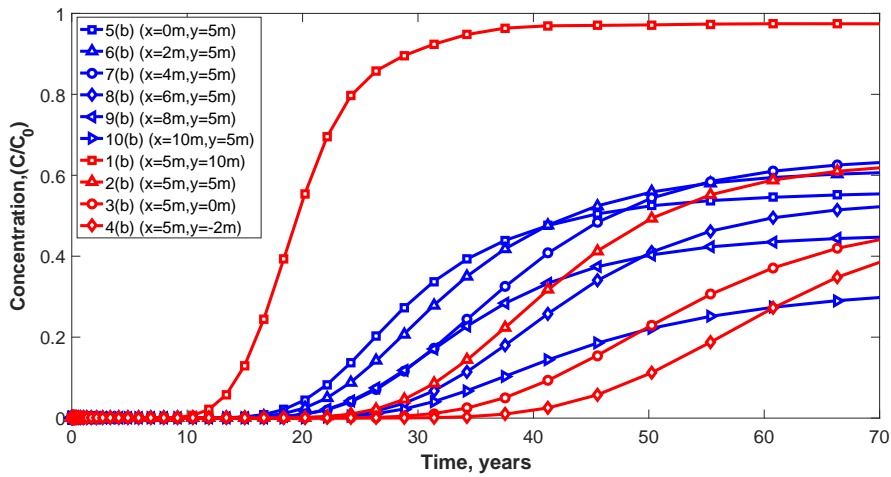Figure 6.24: Concentration versus time for different cases of $0°$ - $45°$ - $135°$ fracture set
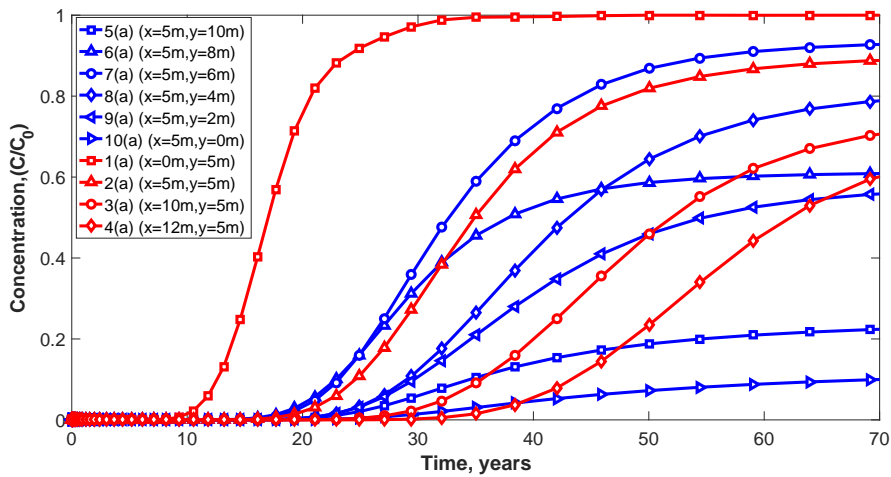
(i) Concentration versus time for flow along x direction
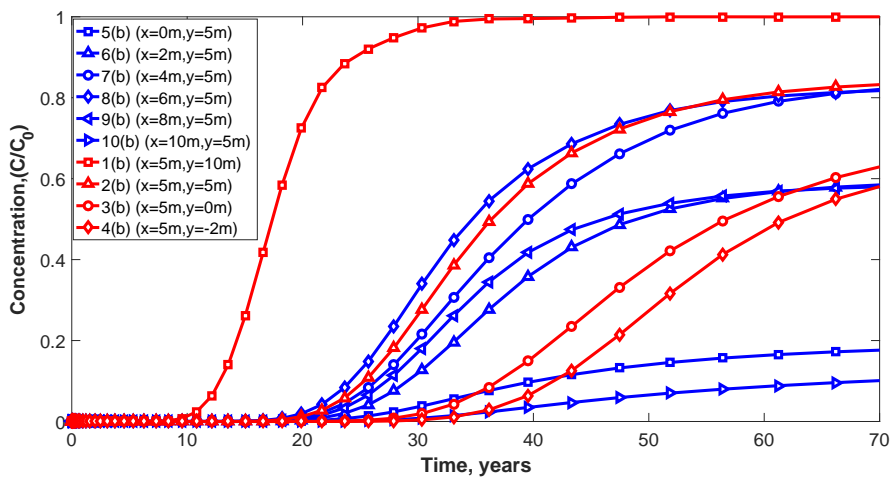
(ii) Concentration versus time for flow along y direction
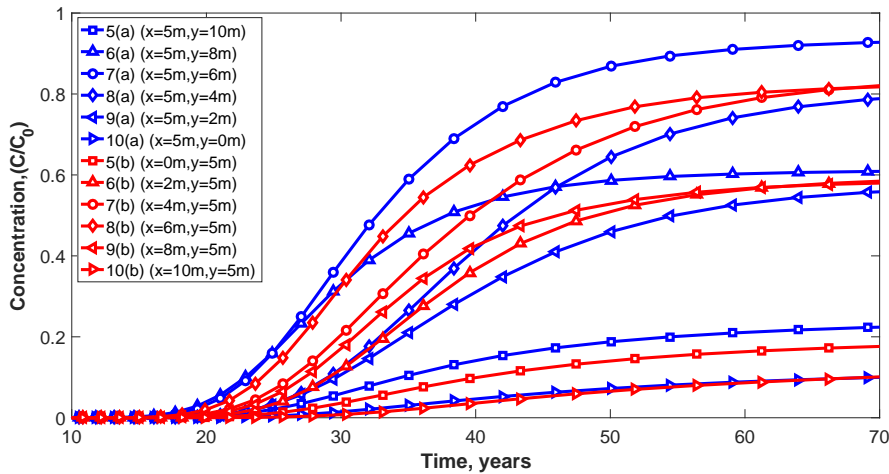
(iii) Concentration versus time for flow across flow direction

(iv) Concentration versus time for flow along flow direction

Figure 6.25: Concentration versus time for different cases of $0°$ - $45°$ - $90°$ fracture set

The results of $0°$ - $45°$-$135°$ fracture set which are given by Figure 6.24 (i) and 6.24 (ii) show that there is variation in the trend of contaminant concentration along x and y directions. The same is demonstrated in Figures 6.24 (iii) and 6.24 (iv). However, in the case of $0°$ - $45°$ - $90°$ fracture set, the pathway of contaminant movement is almost similar when the flow is along x- direction and y-direction. In a fracture network with multiple fracture sets, there will be regions within the network where the local connectivity of fractures is low (due to obstructions from other fracture orientations), which leads to low flux while it is vice-versa for local regions that are well connected. For $0°$, $45°$and $135°$

fracture set (Figure 6.24(ii)), we can observe that the same scenario, leading to lower concentration when the flow is along y-direction. In the case of $0°$ - $45°$ - $90°$ fracture set (Figure 6.25(ii)), the fractures are well connected, leading to smoother movement of contaminant both in x and y directions.

From this analysis the common observation in all the cases is that, when the contaminant tries to move through the fracture intersections, over a period of time the velocity at these points becomes lesser and the effect of diffusion becomes more prominent. But it is important to note that in a fracture network, the movement encompasses the mixing ratios of the fluid velocities throughout the system which is observed from this analysis. The results of concentration trends for different fracture set combinations are presented so far. Using these results, the time taken to reach 50% and 90% of its maximum value are examined. This analysis helps us in determining the critical of fracture set combinations and orientations that deliver the highest concentration in least amount of time. Those points needs immediate attention to avoid subsurface pollution and also these predictions gives an estimate of the time frames for remediation techniques.

For the analysis different observation points were chosen (from Figure 6.13) and bar charts of time taken to reach $0.5\ C_0$ and $0.9\ C_0$ are presented. For the purpose of discussion, observation point 3(a) which is the end-point of interest is considered. In Figure 6.26, it can be observed that, for $0°$ fracture set, it takes almost 40 years to reach $0.5\ C_0$ and around 55 years to reach $0.9\ C_0$ when the flow is along x -direction. Similar trend is observed for $90°$ fracture set, when the flow is along y-direction. In the case of $45°$ fracture set and $135°$ fracture set, the time taken to reach $0.9\ C_0$ is around 60 years which is longer than the time period observed in previous cases.
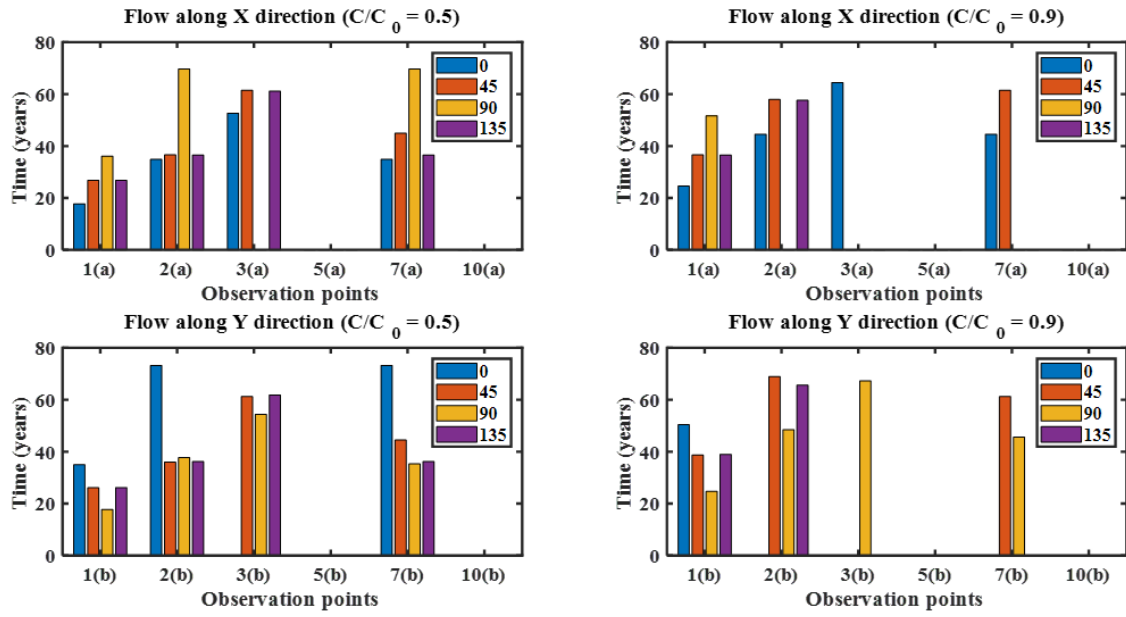
Figure 6.26: Single set
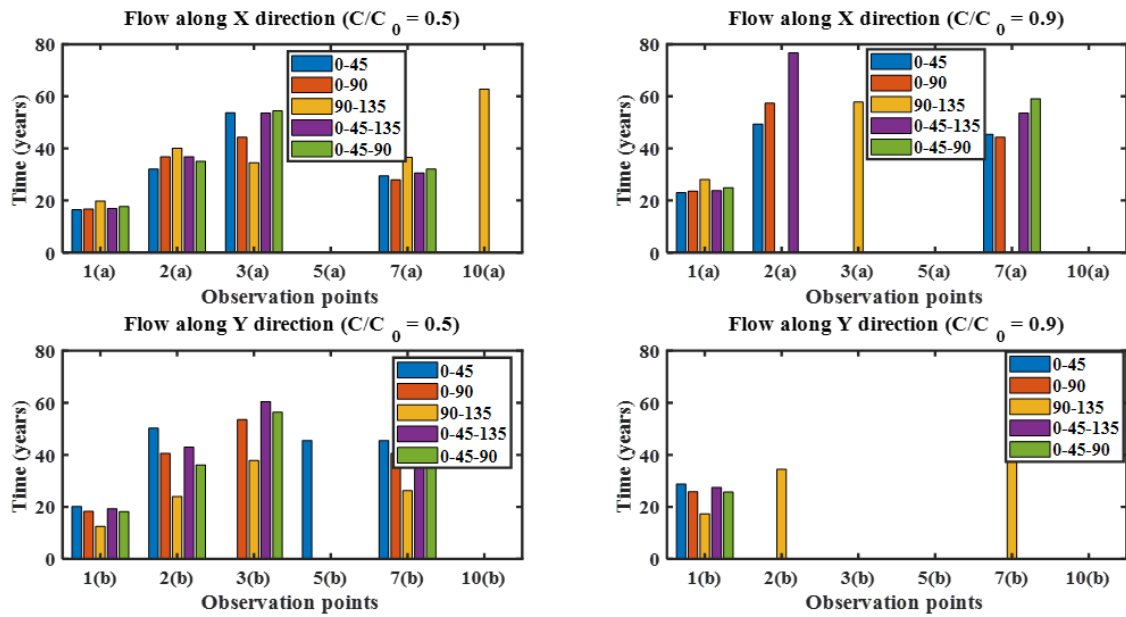
Figure 6.27: Multiple sets

So, for single fracture sets, the results are predictable due to the simple fracture network. But, the results become uncertain with the increase in number of fracture sets. From Figure 6.27, it can be noticed that, among the multiple sets containing two and three fracture sets, 90° and 135° fracture set is the only set with contaminant front spread

throughout the domain (the yellow line is seen at all the observation points). The least amount of time taken to reach 0.9 C_0 is also for 90° - 135° fracture set. The other fracture sets including three fracture combinations reached maximum values beyond 60 years. So, it is one of the critical fracture sets that has the contaminant spread throughout the domain. In such a heterogeneous network, the time required for the first 50% of the concentration to leave the system is significantly lower than that of the time taken for the rest of the 50% shown by long tails in the concentration versus time plots.

6.6.4.1.3 Concentration front for different fracture combinations from the numerical model

The snippets of concentration front at different time instants are captured from the numerical model and presented. Figure 6.28 and 6.29 are the results from contaminant transport modelling through 0° - 90° fracture set for flow along x-direction and y-direction respectively. Similarly, Figure 6.30 and 6.31 are the results from contaminant transport modelling through 0° - 45° - 90° fracture set for flow along x-direction and y-direction respectively. By inspecting Figures 6.28 and 6.29 visually, it can be observed that the fracture connectivity decides the movement of contaminant through the fracture network. The fracture zones provide almost all the yield through them. In the figures, a colorbar of contaminant concentration spread throughout the fractured domain is shown. It shows that the front moves faster in the mid-region of the fractured network due to active flow paths in that direction. In the case of contaminant flow in x-direction, the concentration front reaches the end of the domain by 50,000 days (nearly 136 years). For contaminant flow in y-direction, the concentration front reaches the mid-region and stagnates there due to an interference of horizontal fractures blocking the flow path.
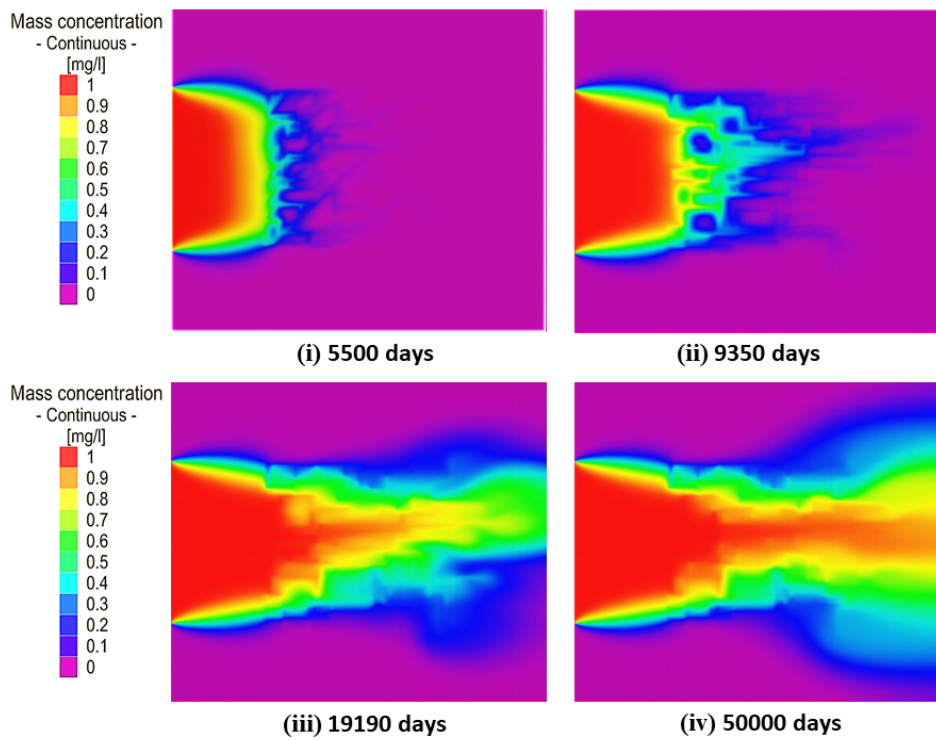
Figure 6.28: Concentration front with time for 0° - 90° fracture set - Horizontal flow (i) 5500 days; (ii) 9350 days; (iii) 19190 days; (iv) 50000 days
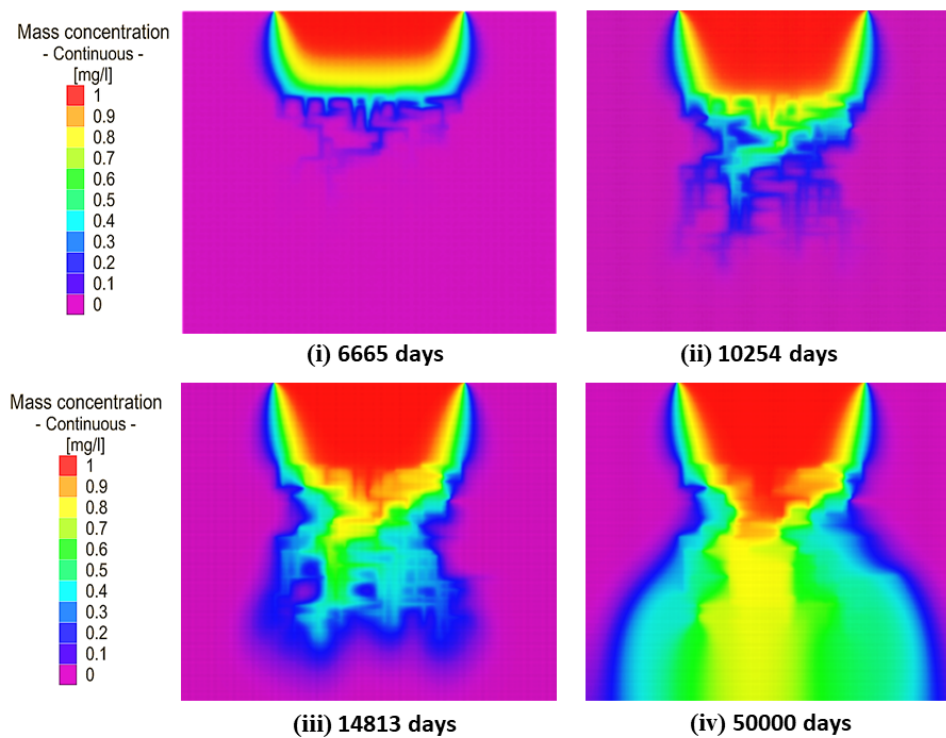
Figure 6.29: Concentration front with time for 0° and 90°- Vertical flow (i) 6665 days; (ii) 10254 days; (iii) 14813 days; (iv) 50000 days

319
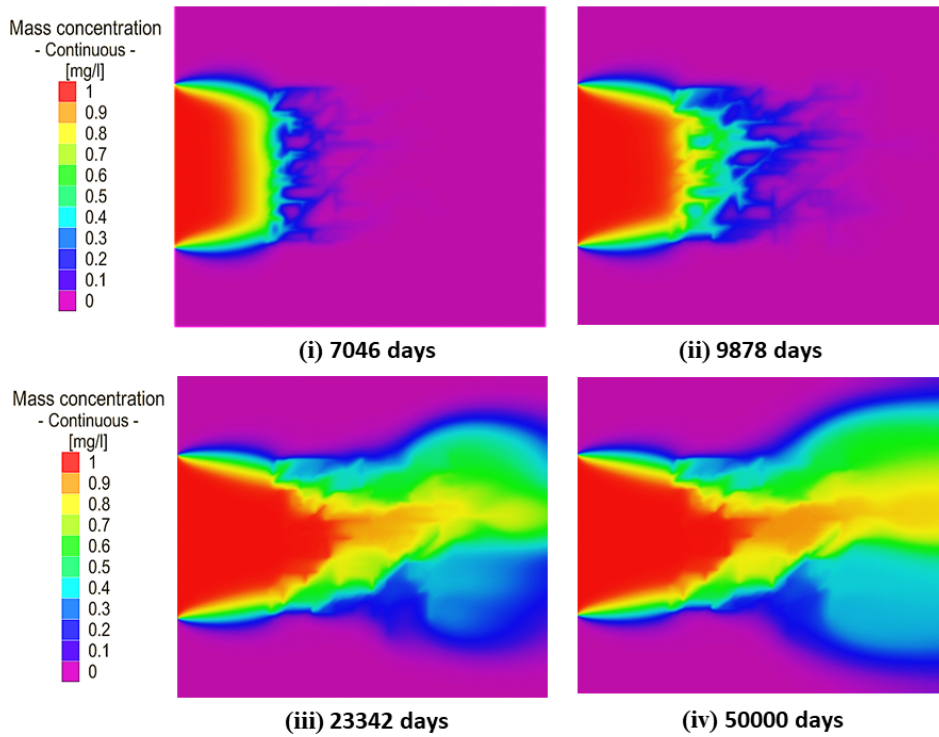
Figure 6.30: Concentration versus time for 0° , 45° and 90°- Horizontal flow (i) 7046 days; (ii) 9878 days; (iii) 23342 days; (iv) 50000 days
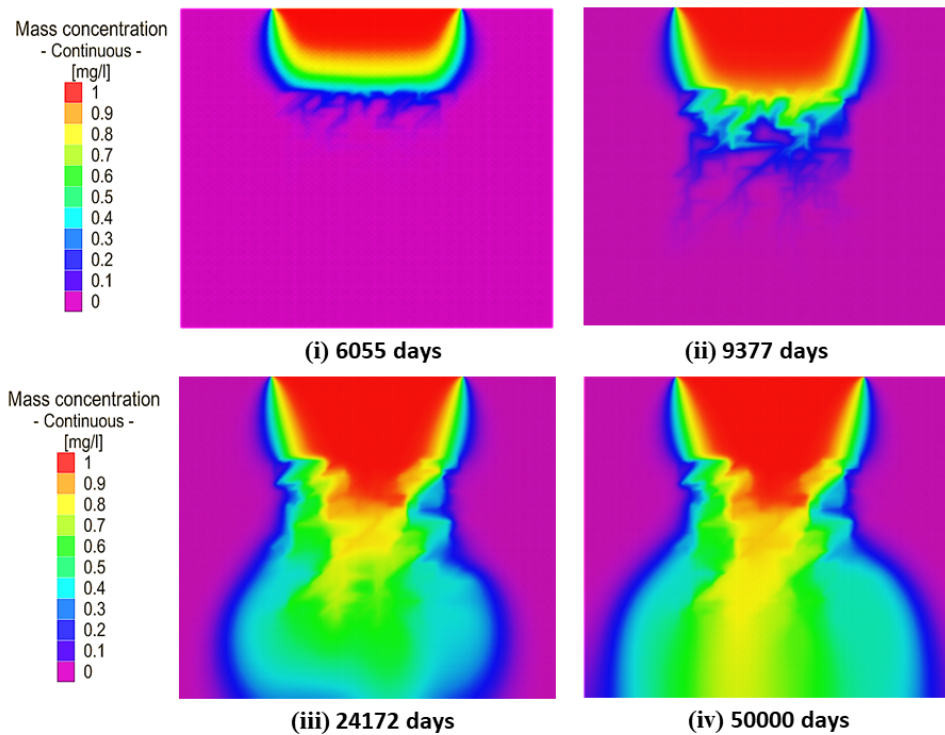
Figure 6.31: Concentration front with time for 0° , 45° and 90°- Vertical flow (i) 6055 days; (ii) 9377 days; (iii) 24172 days; (iv) 50000 days

In Figures 6.30 and 6.31, the contaminant front in a fractured domain with three fractured sets (0° - 45° - 135°) are presented. The main factors influencing the contaminant front along the system are still through the same fractures. Similar observations (as in Figures 6.28 and 6.29) can be made in this case also. Unlike the previous case, the shape of the plume is slightly smaller due to the slower movement of contaminant. This can be attributed to a more complex and intricate fracture network due to three fracture sets.

6.6.4.2 Effect of matrix diffusion and dispersion

As mentioned earlier, the contaminant transport model consists of two interacting subsystems namely, fractures and intact rock matrix. As fractures are highly conductive, the mechanism of transport through fractures is mainly by advection. Besides advection, mechanical dispersion and diffusion are the two other important transport mechanisms in contaminant transport process. In the case of mechanical dispersion, the contaminant spreads through the medium mainly due to different velocities at different points across the channel, drag exerted on the fluid by the roughness of the pore surfaces and difference in pore sizes along the flow paths. On the other hand, diffusion is the process of contaminant movement due of a concentration gradient. A combination of both these mechanical processes is called hydro-dynamic dispersion. These mechanisms are dominant in the systems with very low permeability at very low velocities and high concentration gradients. As the intact rock matrix is impervious, the main source of contaminant movement in this subsystem is through diffusion and dispersion.

Since fractures are predominant sources of contaminant movement in discrete network model, the influence of various features of fractures on the overall transport have been studied so far. In this section, a parametric study on the influence of matrix diffusion,

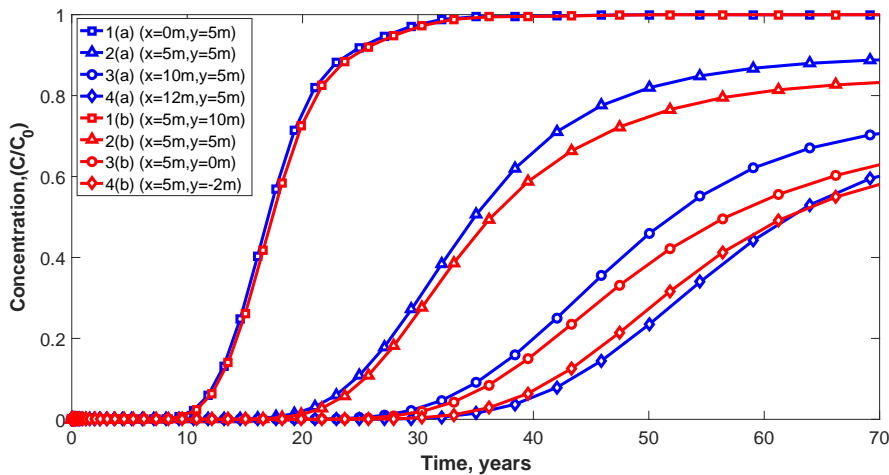matrix dispersion and fracture diffusion is carried out.
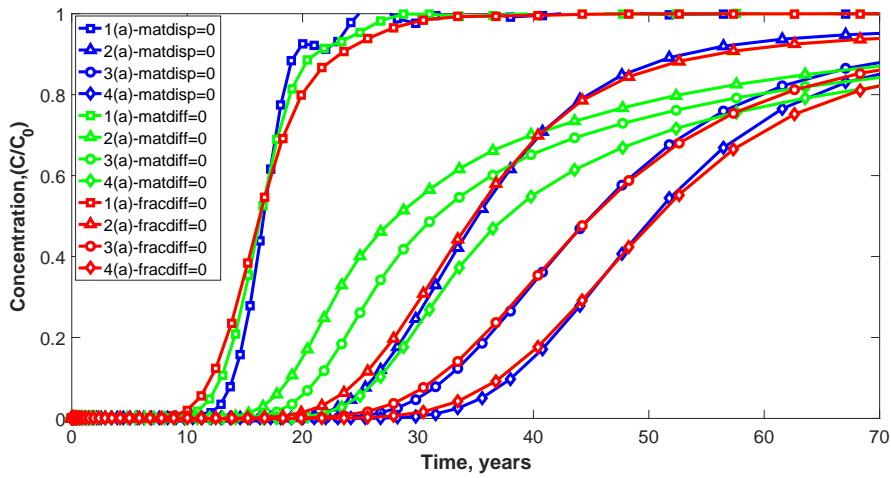
(i) Concentration versus time for flow along x direction
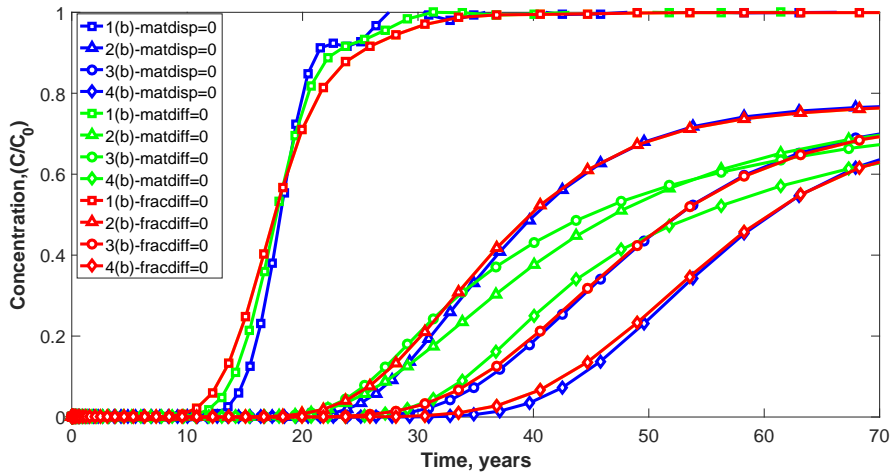
(ii) Concentration versus time for flow along y direction
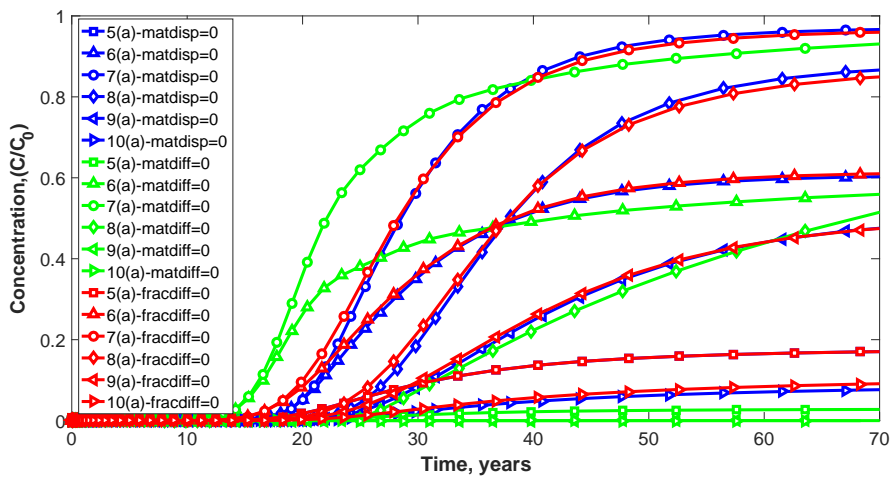
(iii) Concentration versus time for flow across flow direction
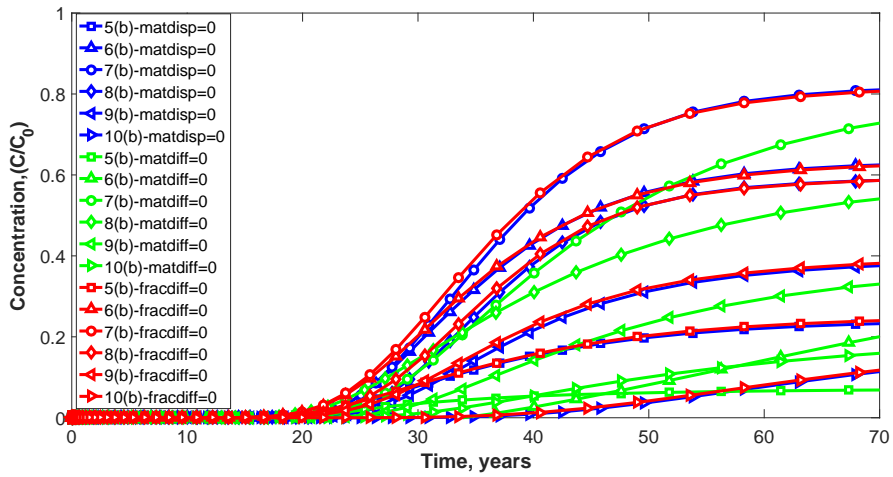
(iv) Concentration versus time for flow along flow direction

Figure 6.32: Concentration versus time for 0° - 90° fracture set
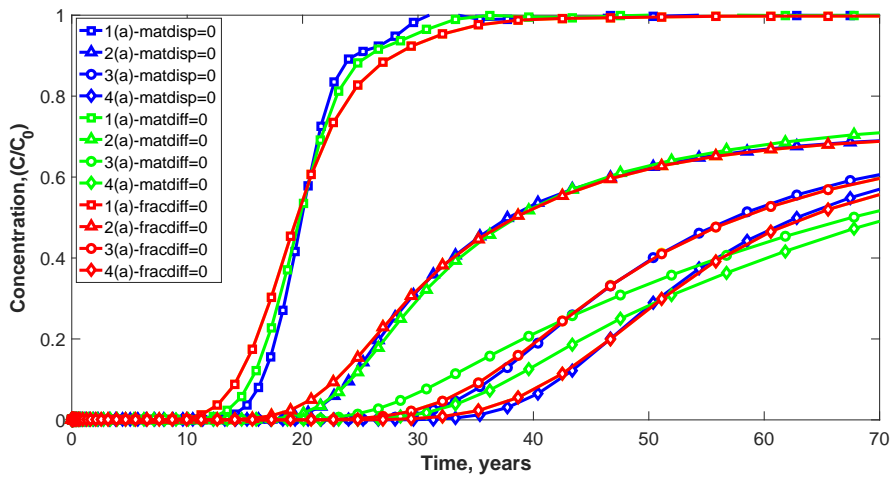
(i) Concentration versus time for flow along x direction
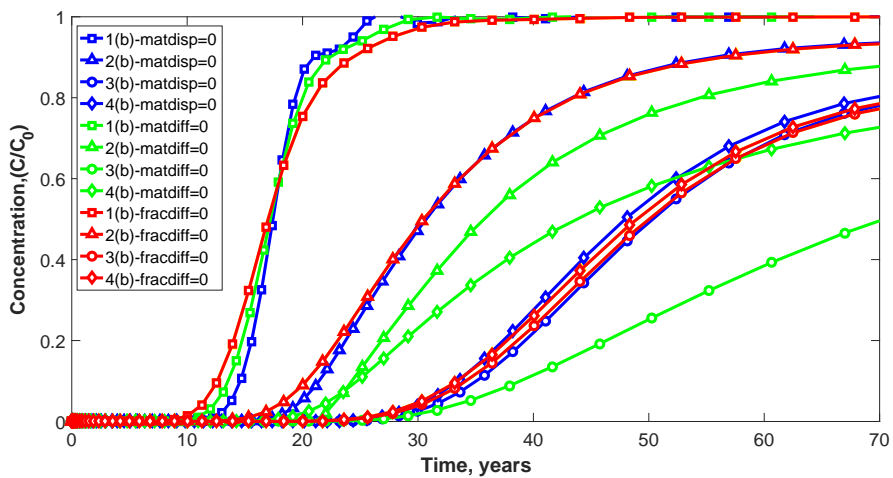
(ii) Concentration versus time for flow along y direction
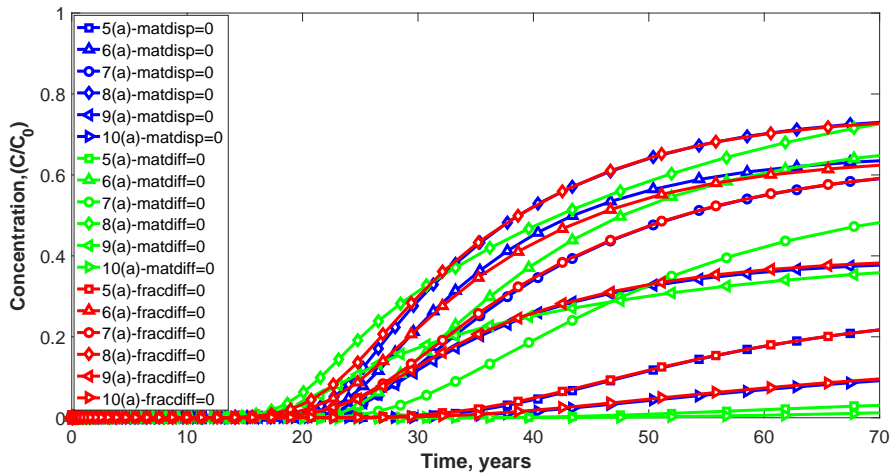
(iii) Concentration versus time at points transverse across flow direction
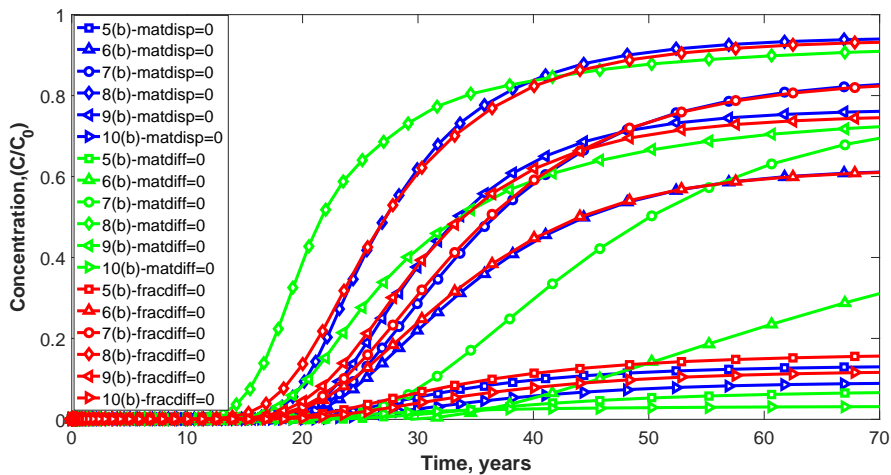
(iv) Concentration versus time at points along flow direction

Figure 6.33: Concentration versus time for $45°$-$90°$ fracture set

This study helps in understanding other important processes of transport that can influence the movement of contaminant. $0°$ - $90°$ and $45°$ - $90°$ fracture set combinations are considered for the analysis. In each case, one of the parameters is set to zero, to inspect if there is an impact of that parameter on the overall response. The results are presented in Figure 6.32 and Figure 6.33.

These figures shows concentration versus time trends for fracture sets $0°$ - $90°$ and $45°$ - $90°$ respectively. The results are examined for contaminant flow along x-direction and y-direction. In all the figures, the blue trend lines correspond to matrix dispersion

(set to zero), red trend lines correspond to fracture diffusion (set to zero), and, green trend lines correspond to matrix diffusion (set to zero). In all the cases, only green trend lines exhibit maximum deviation from the actual trend. This indicates that matrix diffusion is another important transport process that affects the transport of contaminant. They bring a sorption like effect where the solute that is stored in the pores of the matrix will be transported by diffusion into the fracture. Similar observations was made by Grisak and Pickens (1980) in their work on solute transport through fractured media. So, the other transport mechanism that controls the transport of contaminant in fractured rock mass is matrix diffusion.

6.6.4.3 Effect of variation in aperture size along the fracture

In section 6.5.3, a model that incorporates the effect of variation in aperture size along the fracture has been developed. So, to demonstrate the influence of variation in aperture size along the fracture, a parametric study is carried out. Here, the number of segments (m) within each fracture are varied from one (segment) to five (segments). By increasing the number of segments further, the complexity of the model increases, leading to computational constraints. So the number of segments are limited to five in the analysis. The typical range of aperture values considered in the literature (1×10^{-5} m to 5×10^{-5} m) have been used (Wendland and Himmelsbach, 2002; Graf and Therrien, 2005; Diersch, 2014). A random combination of aperture sizes are considered for the analysis and presented in Table 6.7.

Table 6.7: Hydraulic aperture sizes considered in the analysis

Number of parts	Value
One part (m)	5×10^{-5}
Two parts (m)	$5 \times 10^{-5}, 1 \times 10^{-5}$
Three parts (m)	$5 \times 10^{-5}, 1 \times 10^{-5}, 2 \times 10^{-5}$
Four parts (m)	$5 \times 10^{-5}, 1 \times 10^{-5}, 2 \times 10^{-5}, 4 \times 10^{-5}$
Five parts (m)	$5 \times 10^{-5}, 1 \times 10^{-5}, 2 \times 10^{-5}, 4 \times 10^{-5}, 3 \times 10^{-5}$

Figure 6.34 shows typical aperture size variations when the fracture is divided into five segments. The transport properties of fracture are also taken from the literature (Graf and Therrien, 2002; Diersch, 2014). By assigning the above aperture variations to all fractures in the fracture network, simulations are run to evaluate the contaminant concentration. The results obtained after running the model for a time period of 35000 days (around 96 years) are presented in Figure 6.35 and Figure 6.36.
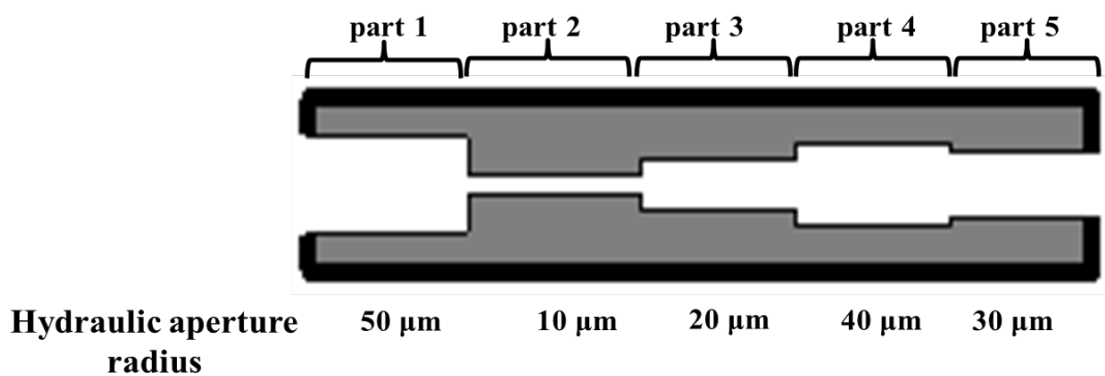
Figure 6.34: Schematic of aperture variation along the fracture

Figure 6.35 presents the results of concentration versus time when flow direction of the contaminant is along x-direction. Figure 6.35 (i) shows the result for 0°- 90° fracture set, and Figure 6.35 (ii) shows the result for 45° - 90° fracture set. The concentration values are estimated at three observation points (2(a), 4(a) and 10(a) from Figure 6.13(a)).
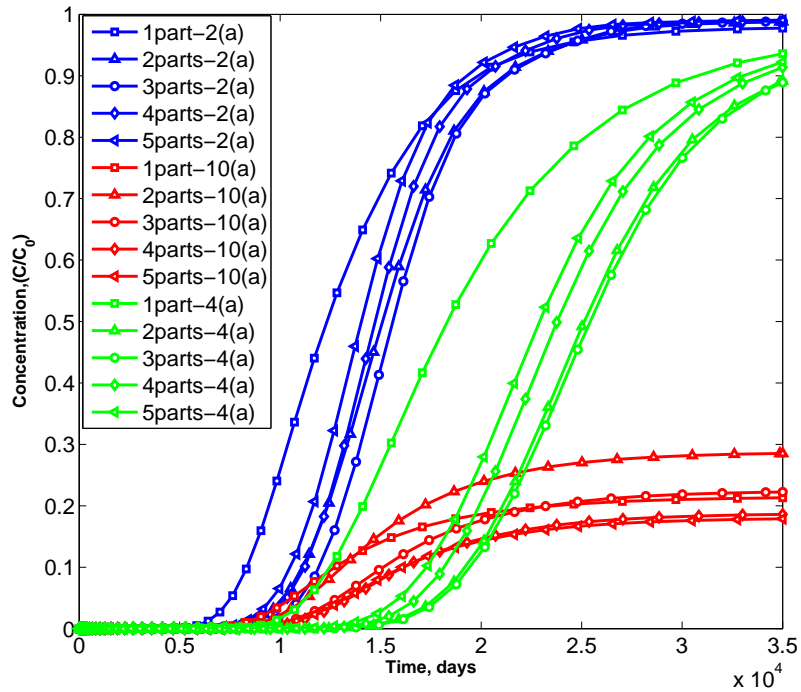
(i) $0°$ - $90°$
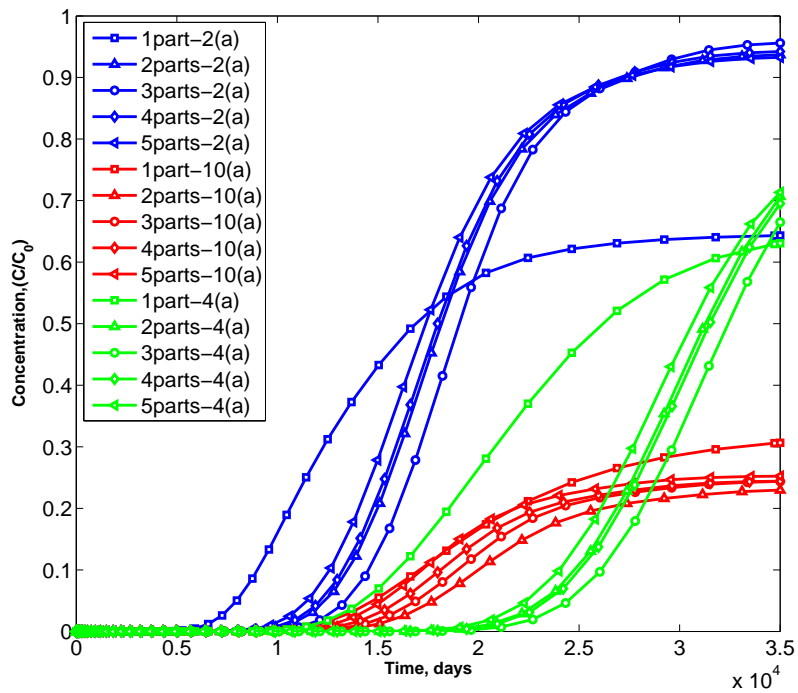
(ii) $45°$ - $90°$

Figure 6.35: Concentration trends for different cases of aperture variations along the fracture - Horizontal flow direction
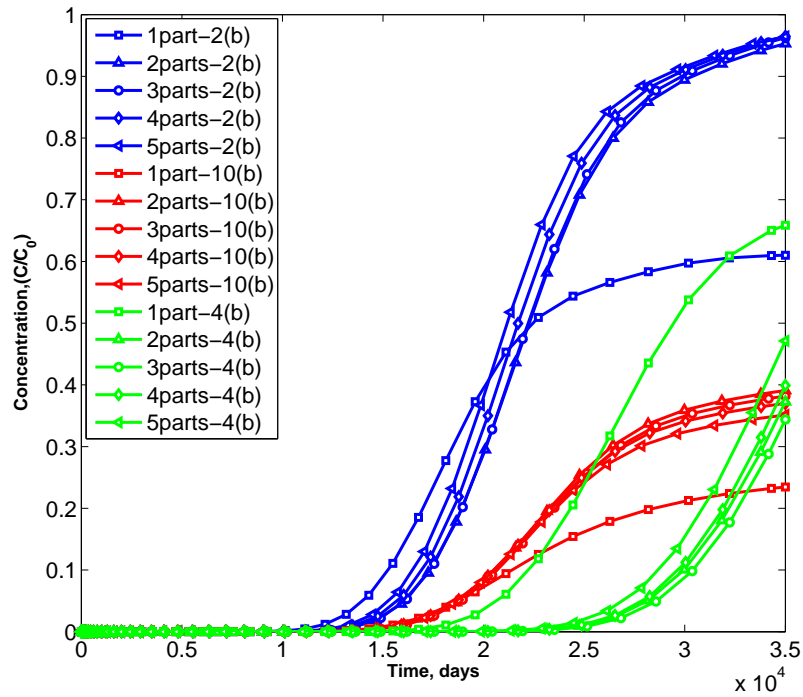
(i) $0°$ - $90°$
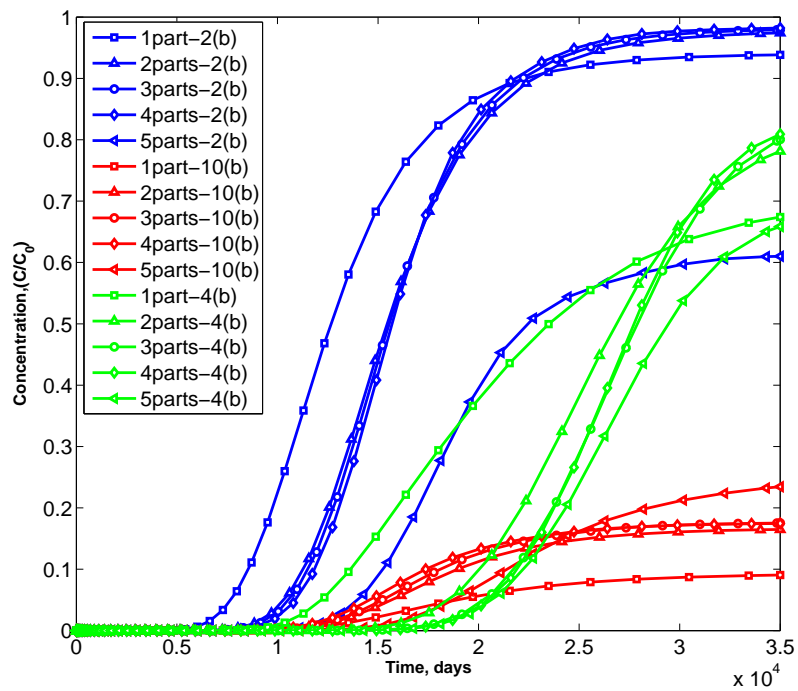
(ii) $45°$ - $90°$

Figure 6.36: Concentration trends for different cases of aperture variations along the fracture - Vertical flow direction

A prominent effect of this factor on the contaminant concentration values is observed

from these plots. The results do not follow a particular trend with respect to increasing aperture size variations. Also, the number of transitions in the fracture leading to maximum concentration is different at each observation point. This can be due to the influence of randomly arranged aperture size combinations considered in the study which indirectly affects the flow rate of the contaminant moving through the fracture. The concentration trends for Figure 6.35 (i) and 6.35 (ii) are different indicating the effect of the fracture orientations and their combinations. Figure 6.36 presents the results of concentration versus time for 0° - 90° (Figure 6.36(i)), and 45° - 90° (Figure 6.36 (ii)) fracture sets with the flow along y-direction. The concentration is estimated at three observation points (2(b), 4(b) and 10(b) from Figure 6.13 (b)). These results also confirm the effect of variation of aperture along the fracture and the angle of fracture orientation (Figure 6.37 (i) and 6.37 (ii)) on the contaminant transport.

Overall, the concentration value is affected at least by 0.5% to almost 30% of its initial value due local variation in aperture size indicating their influence on the concentration front. The results also show that the arrangement of aperture variations along the fracture plays an important role in predicting the concentration of contaminant. For a fracture having a highly variable distribution of aperture, the variation in transport times may be even larger. Since the fracture patterns are heterogeneous, the flow rate along x-direction and y-direction are varied. The influence of flow direction was also observed by comparing results Figure 6.35 and Figure 6.36. This study highlights that neglecting the effect of variation in aperture size along the fracture leads to an incorrect estimation of contaminant migration through fractured media.

6.6.4.4 Comparison of contaminant migration through a fractured medium by modelling fractures and by equivalent porous medium model

The study carried out in this section demonstrates the effect of replacing a fractured domain by an equivalent porous medium. So, the 10 m $\times$ 10 m fractured section is replaced by an equivalent porous medium that emulates a homogeneous rock mass. The porosity and hydraulic conductivity of homogeneous rock mass are 0.3 and 0.01 m/day (Šperl and Trčková, 2008; Diersch, 2014). The remaining transport properties are considered the same as that of the intact rock (Piscopo et. al., 2017). The results from the analysis are presented in Figure 6.37 and Figure 6.38.

Figure 6.37 presents the concentration versus time plots when both the properties of the equivalent medium are changed. The plots show the concentration at different points across and along the flow direction. From the figure, it can be noticed that the concentration reaches its maximum value in 50000 days. The concentration trend across the flow direction shows that the mid-region of the concentration front has the maximum value in comparison to the other points across the domain. These results are similar to that of concentration versus time plots of series of fractures from 0° fracture set (Figures 6.15 and 6.16). Figure 6.38 presents the concentration versus time across and along the flow directions in a medium where only the porosity of the equivalent rock mass is changed. The other properties are the same as that of the intact rock. In this case, the concentration front across the flow direction does not reach the peak value and along the flow direction, the concentration front is very slow-moving. This is because of the lower conductivity leading to slower movement of the front through the rock mass.
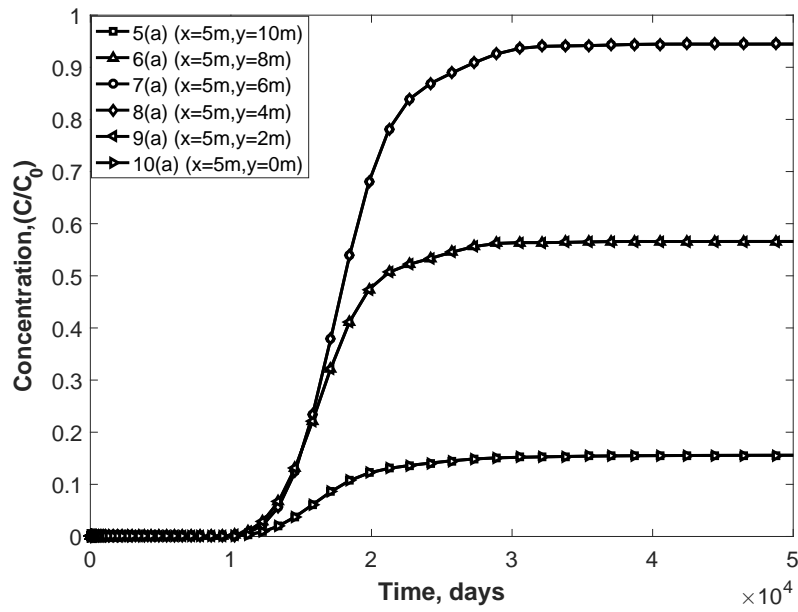
(i) Across the flow direction
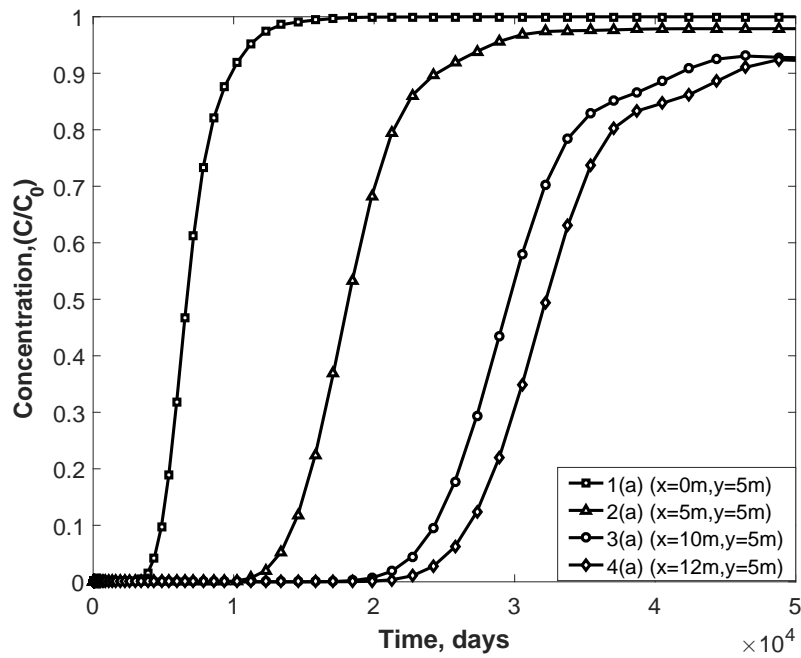
(ii) Along the flow direction

Figure 6.37: Concentration versus time when the contaminant flow is along x-direction(both hydraulic conductivity and porosity of the medium are changed)
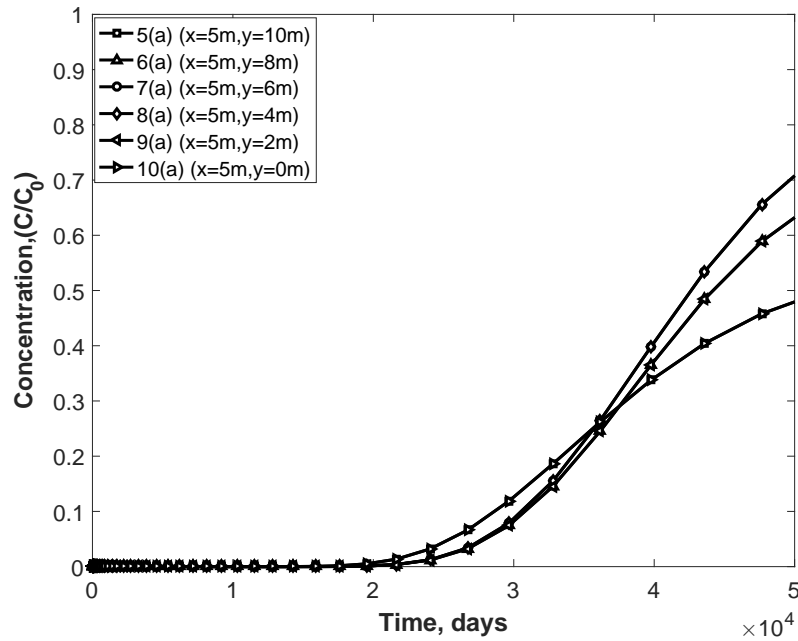
(i) Across the flow direction
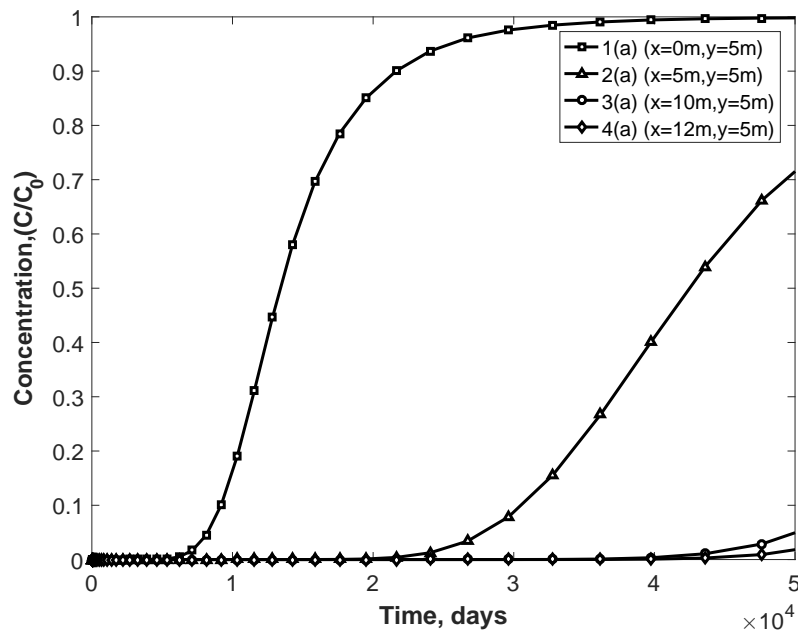
(ii) Along the flow direction

Figure 6.38: Concentration versus time when the contaminant flow is along x-direction (only porosity of the medium is are changed)

As equivalent porous medium is homogeneous, same results can be observed for cases of contaminant flow along horizontal and vertical directions. This indicates that the assumption of an equivalent porous medium either underestimates or overestimates

the movement of contaminant. However, in a fractured medium, the flow in each direction (x or y) gives a different concentration front due to the heterogeneity in the fracture patterns which has been discussed in section 6.6.4.1.

So far, different studies have been carried out using new geosphere transport model for fractured rock. They included examining the impact of fracture geometry, the transport properties of contaminant in both fractures and rock matrix, and the local aperture variations on contaminant transport. The computational efficiency of the model in predicting various aspects of contaminant transport modelling has been demonstrated from these studies.

6.6.5 Probabilistic analysis

The deterministic performance assessment model results showed that the concentration of contaminant at the end-point of interest (i.e., 10 m from the source) was less than permissible limit (i.e., $C_0 = 1$ mg/l). But there is a need to account for stochastic nature of fractures and the rock matrix leading to uncertainties in the prediction of contaminant concentrations. Also, in the fracture generation algorithm, location of seed points, the velocity of crack propagation and fracture orientations are modelled as random variables to account for randomness in fracture generation. So, it is imperative to characterize these uncertainties and quantitatively estimate the probability of concentration exceeding its permissible limit by employing efficient probabilistic techniques. The mean values (underlying normal distribution) of the input parameters, the probabilistic distribution and COV have been assumed from literature and shown in Table 6.8. So, the probability

of concentration exceeding its permissible value is estimated from the equation

$$P_f = P(g(X) < 0) \qquad where \qquad g(X) = C_0 - max(C(X,t)) \qquad (6.12)$$

$X - X_1, X_2 ... X_9$ - set of random variables considered, $g(X)$ - limit state function, C_0 - permissible concentration and $C(X)$ - maximum concentration within the time period t computed from the numerical model.

By using subset simulation method (Au and Beck, 2001), P_f is estimated. In this method, the small failure (rare events) probabilities as a product of large failure (frequent events) probabilities. The detailed procedure followed in subset simulation method is mentioned in Section 3.6.1.2 (chapter 3). If the stochasticity in fracture generation algorithm and the parameter uncertainty in the fractured system are considered simultaneously, then the entire system becomes extremely complex and computationally expensive. So, the study is conducted by choosing one of the stochastic realizations from fracture generation algorithm and perform probabilistic analysis on that system. Three cases are considered to inspect the effect of each factor on P_f.

1. Effect of fracture set realizations

2. Effect of coefficient of variation (COV)

3. Effect of different fracture sets

When the fracture pattern in generated stochastically, each realization has a unique arrangement of fractures (also a function of fracture orientation distribution and their density). The transport through such system leads to distinct channelling flow paths in each simulation that can alter the contaminant path. This analysis helps quantifying the extent

of pollution caused under the influence of there uncertainties.

Table 6.8: Statistical properties of parameters considered for the study

S.No	Property	Non-reactive contaminant		Distribution
		Mean	COV	
Rock matrix				
1	Hydraulic conductivity (m/d)	10^{-4}	0.15	Lognormal
		10^{-4}	0.30	
		10^{-4}	0.40	
2	Porosity	0.13	0.15	Lognormal
		0.13	0.30	
		0.13	0.40	
Fracture				
3	Fracture aperture (part 1) (μm)	50	0.15	Lognormal
		50	0.30	
		50	0.40	
4	Fracture aperture (part 2) (μm)	10	0.15	Lognormal
		10	0.30	
		10	0.40	
5	Fracture aperture (part 3) (μm)	20	0.15	Lognormal
		20	0.30	
		20	0.40	
6	Fracture aperture (part 4) (μm)	40	0.15	Lognormal
		40	0.30	
		40	0.40	
7	Fracture aperture (part 5) (μm)	30	0.15	Lognormal
		30	0.30	
		30	0.40	
8	Diffusion coefficient (m²/s)	5×10^{-9}	0.15	Lognormal
		5×10^{-9}	0.30	
		5×10^{-9}	0.40	
9	Longitudinal Dispersivity (m)	0.1	0.15	Lognormal
		0.1	0.30	
		0.1	0.40	

6.6.5.1 Results and Discussion

To investigate the effect of fracture pattern on the probability of failure, fracture set $45°$-$90°$ is considered. The randomness associated with the location of seed points is considered in this study. Three simulations are run to obtain three unique fracture pattern realizations. They are presented in Figure 6.39. In the analysis, nine random variables are considered.
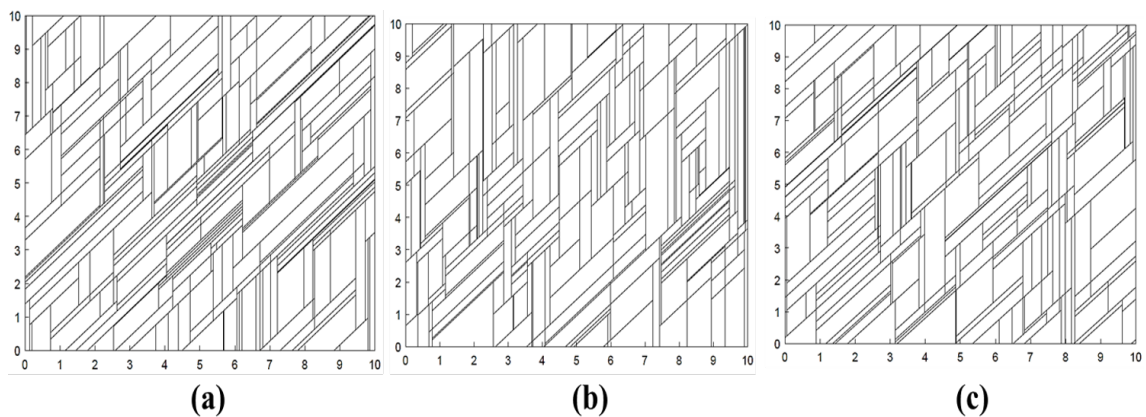
Figure 6.39: Fracture patterns obtained from three random simulations (a) First realization (b) Secon realization (c) Third realization

From the figure, it can be noticed that the patterns generated from the algorithm are different in 6.39 (a) , (b) and (c). For each realization, the probability of failure is estimated with respect to different COVs. By running the automated python programming module which has the subset simulation algorithm, P_f is estimated. The results are presented in Figure 6.40. In the Figure 6.40, each line corresponds to the results from each realization (generated using fracture generation algorithm). The range of P_f varied from 10^{-13} - 10^{-2}. Also, the results show that with the increase in COV, the probability of failure increased. For a given COV, there are three values of P_f corresponding to each fracture pattern realization. This indicates the influence of fracture pattern on the probability of failure.
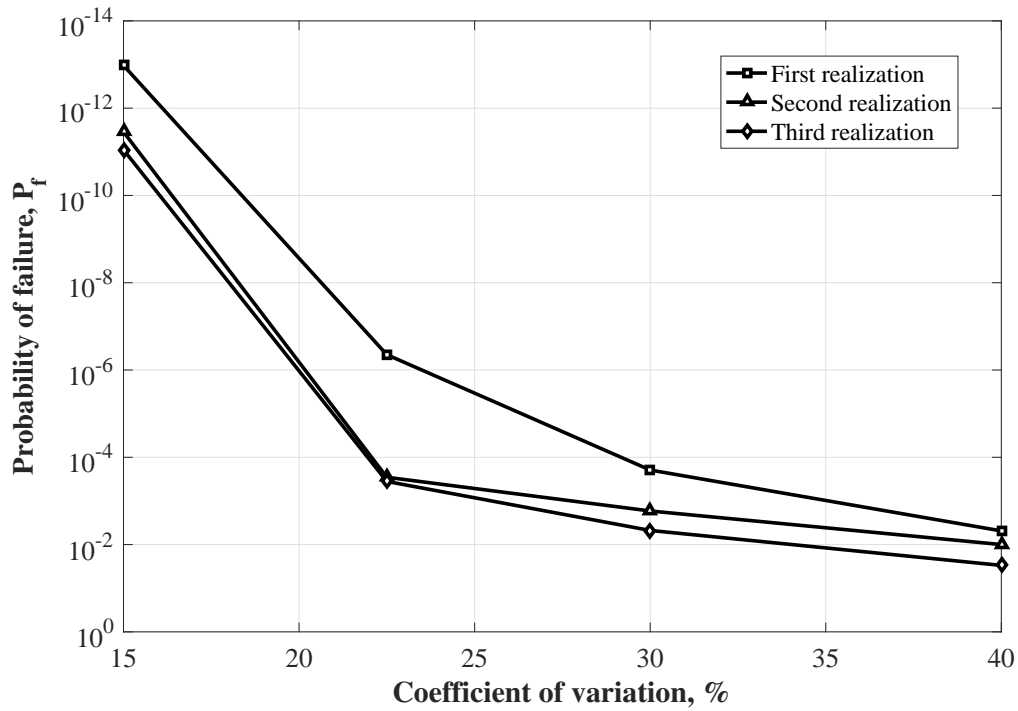
Figure 6.40: Results from subset simulation

The sample COV of failure probability over 25 independent subset simulation runs are plotted to observe the variability in P_f. To ensure the convergence of subset simulation results, a comparison is made between the coefficient of variation and number of samples per subset and the results are presented in Figure 6.41. Also the effect of number of samples per subset and probability of failure are presented in Figure 6.42. The number of samples per subset, N_{ss} were varied from 500 to 20000 for the parameter COV of 15% to 40% to obtain a convergent solution (with around 35% COV). The COV of P_f can be reduced further by increasing the size of sample. The influence of different fracture sets on the probability of failure are also estimated.

(i) COV Vs N_{ss} (ii) P_f Vs N_{ss}
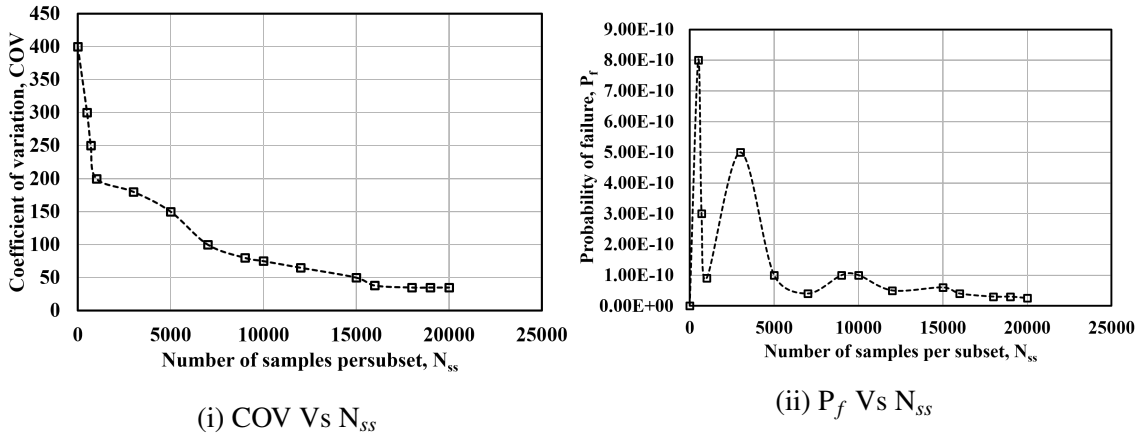
Figure 6.41: Trends of coefficient of variation and probability of failure for different number of samples per subset (15% COV)

(i) COV Vs N_{ss} (ii) P_f Vs N_{ss}
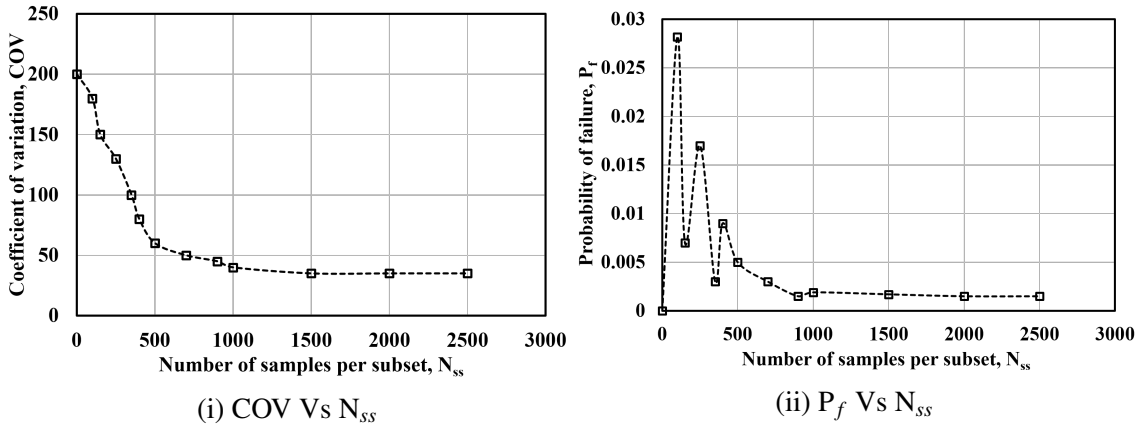
Figure 6.42: Trends of coefficient of variation and probability of failure for different number of samples per subset (15 % and 30% COV)

(i) COV Vs N_{ss} (ii) P_f Vs N_{ss}
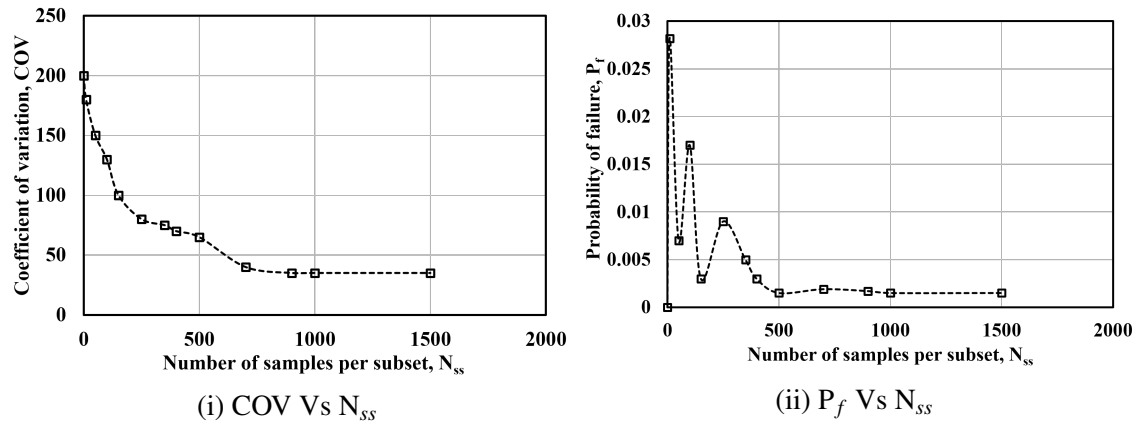
Figure 6.43: Trends of coefficient of variation and probability of failure for different number of samples per subset(30% COV)

(i) COV Vs N$_{ss}$

(ii) P$_f$ Vs N$_{ss}$
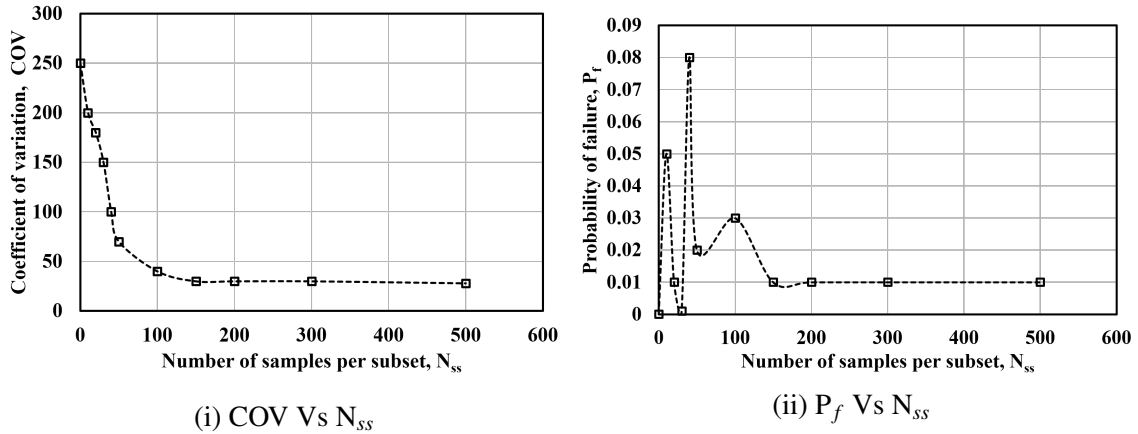
Figure 6.44: Trends of coefficient of variation and probability of failure for different number of samples per subset (40% COV)

Table 6.9: Results from subset simulation for 40% COV

Fracture set	45°	45°- 90°	0°- 90°	0°- 45°- 90°	0°- 45°- 135°
Probability of failure	0.6	0.00486	4.6×10^{-4}	0.00132	1.3×10^{-5}

The results from Table 6.9 shows that, for 45° fracture set, the P_f is very high. This is because, the presence of series of long, parallel fractures conducts the flow of contaminant towards the end-point resulting in high probability of contamination. In the case of two and three fracture sets, the range of P_f values are quite low. However, for three fracture set scenario (0°- 45°- 90°), the P_f value is more than that of two fracture set. This non-trivial result re-iterates the need to perform reliability analysis. The probabilistic analysis results quantify the extent of pollution possible due contaminant migration under the influence of various uncertainties through different fracture sets which cannot be possible through deterministic approach. The above results provide a rationale for the uncertainty analysis of contaminant transport behaviour through a fractured network. But the contribution of each parameter on the underlying performance of the system is difficult to estimate, as each parameter has a distinct effect on overall response. It is important to estimate the

critical parameters affecting the system response. This is carried out using sensitivity
analysis which is presented in the next section.

6.6.5.2 Sensitivity analysis

The sensitivity analysis is carried out by post processing the results obtained during subset
simulation. The empirical distributions at each conditional level are compared with the
actual distribution and the results are presented in Figures- 6.45 to 6.53.

(i) 1st conditional level   (ii) 2nd conditional level
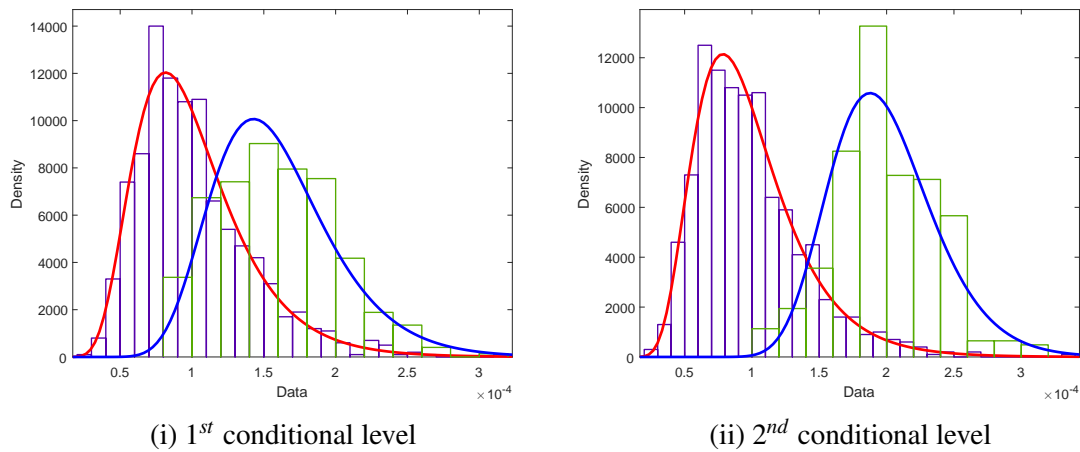
Figure 6.45: Shift in the distribution over two conditional levels for matrix hydraulic
conductivity

(i) 1st conditional level   (ii) 2nd conditional level
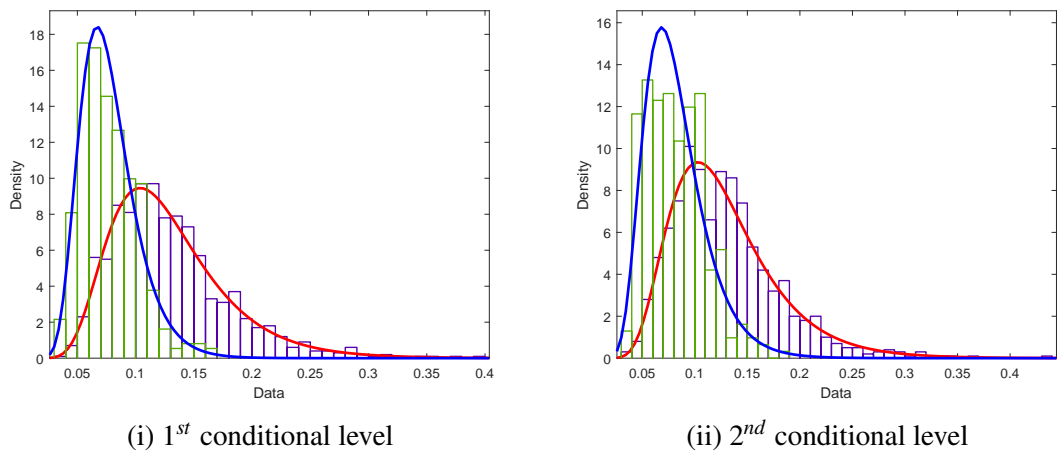
Figure 6.46: Shift in the distribution over two conditional levels for matrix porosity

(i) 1st conditional level

(ii) 2nd conditional level
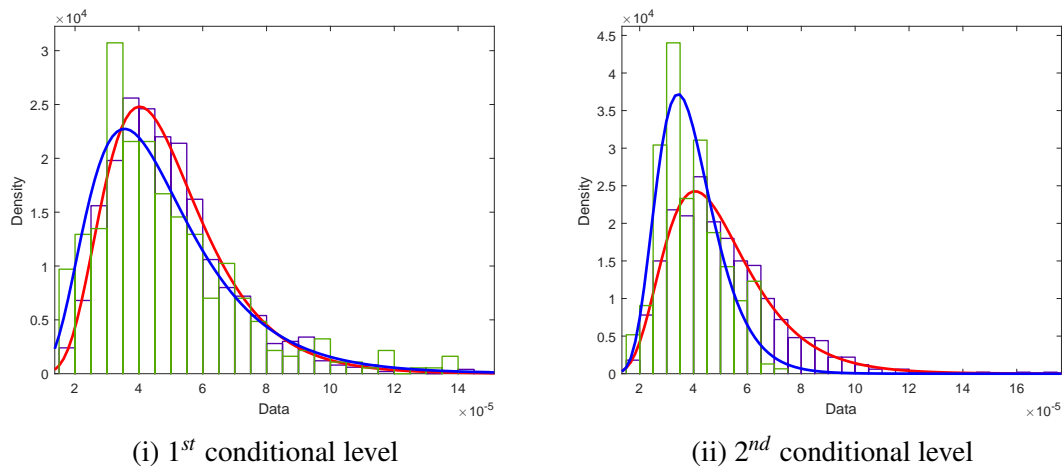
Figure 6.47: Shift in the distribution over two conditional levels for aperture part 1

(i) 1st conditional level

(ii) 2nd conditional level
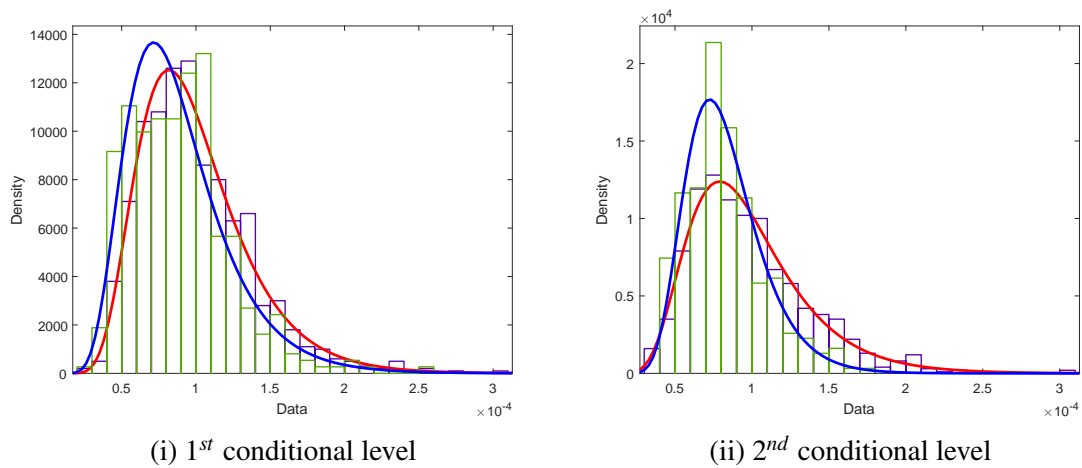
Figure 6.48: Shift in the distribution over two conditional levels for aperture part 2

(i) 1st conditional level

(ii) 2nd conditional level
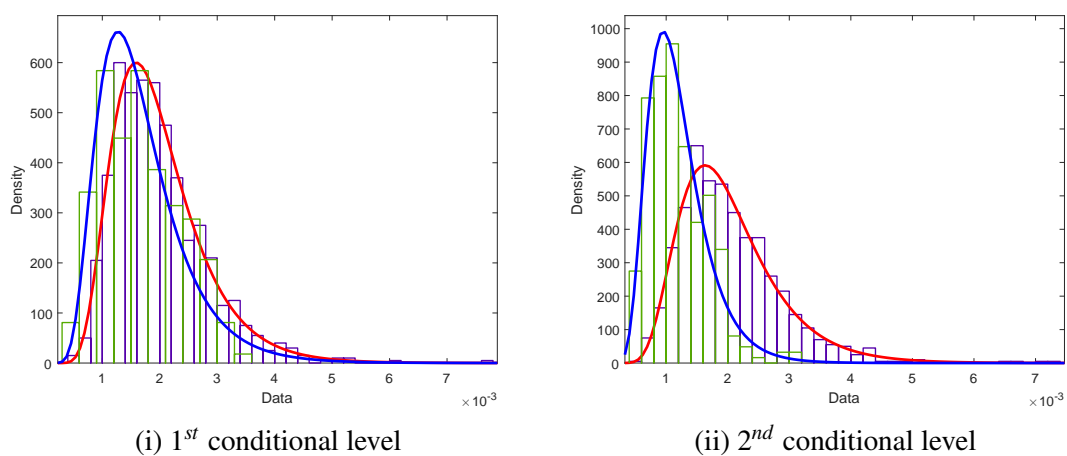
Figure 6.49: Shift in the distribution over two conditional levels for aperture part 3

(i) 1st conditional level

(ii) 2nd conditional level
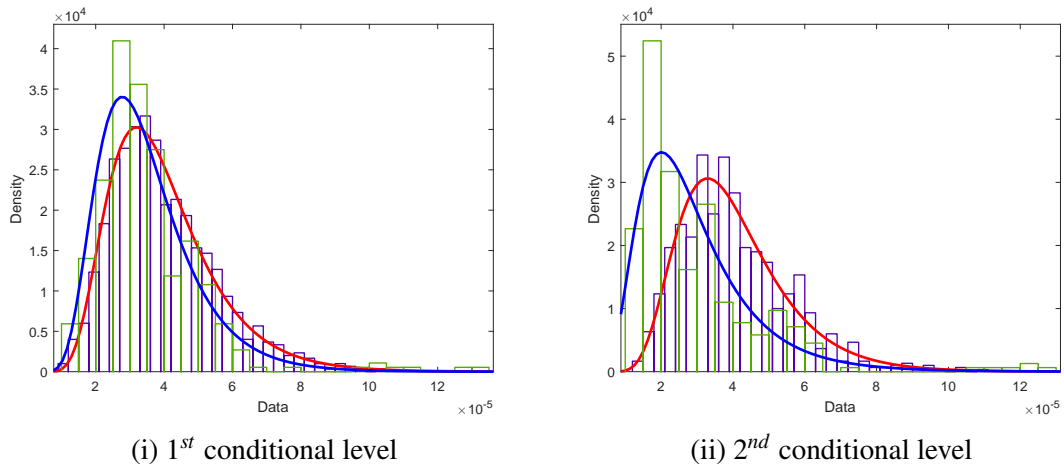
Figure 6.50: Shift in the distribution over two conditional levels for aperture part 4

(i) 1st conditional level

(ii) 2nd conditional level
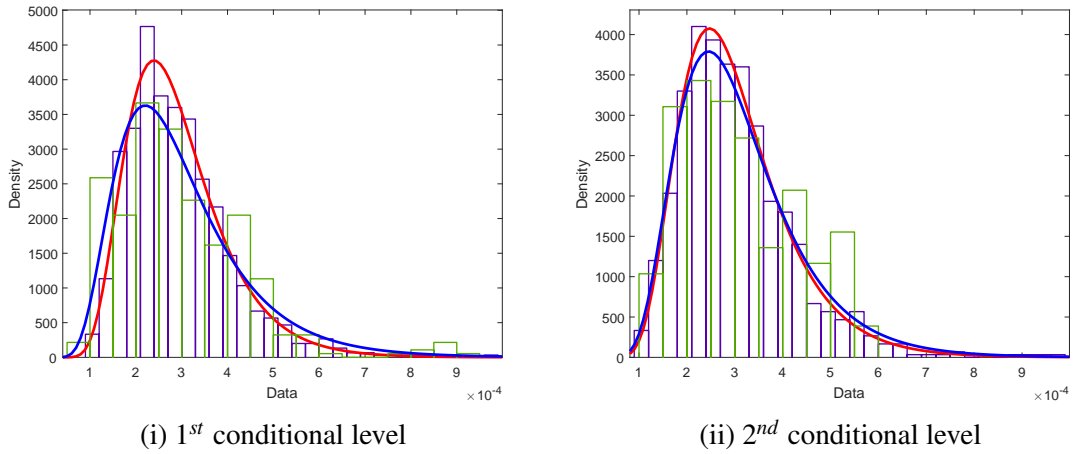
Figure 6.51: Shift in the distribution over two conditional levels for aperture part 5

(i) 1st conditional level

(ii) 2nd conditional level
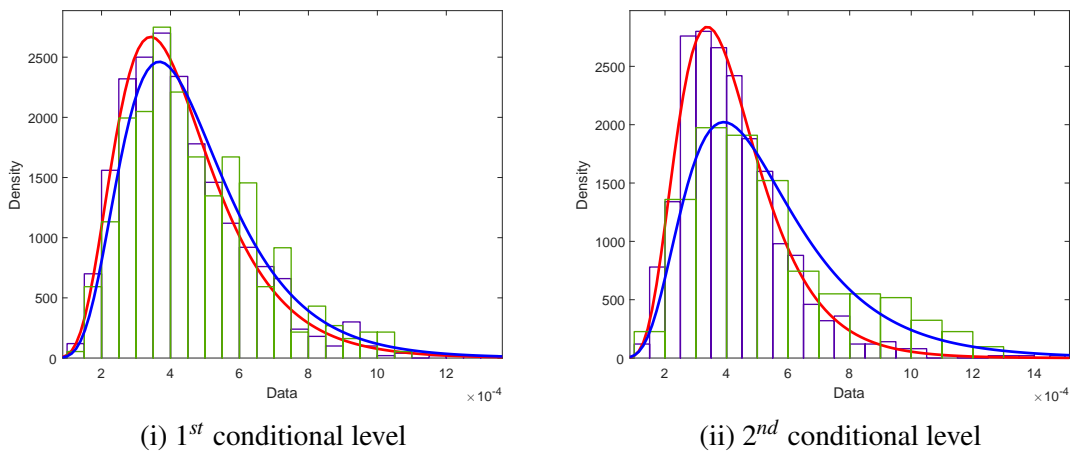
Figure 6.52: Shift in the distribution over two conditional levels for fracture diffusion

(i) 1st conditional level   (ii) 2nd conditional level
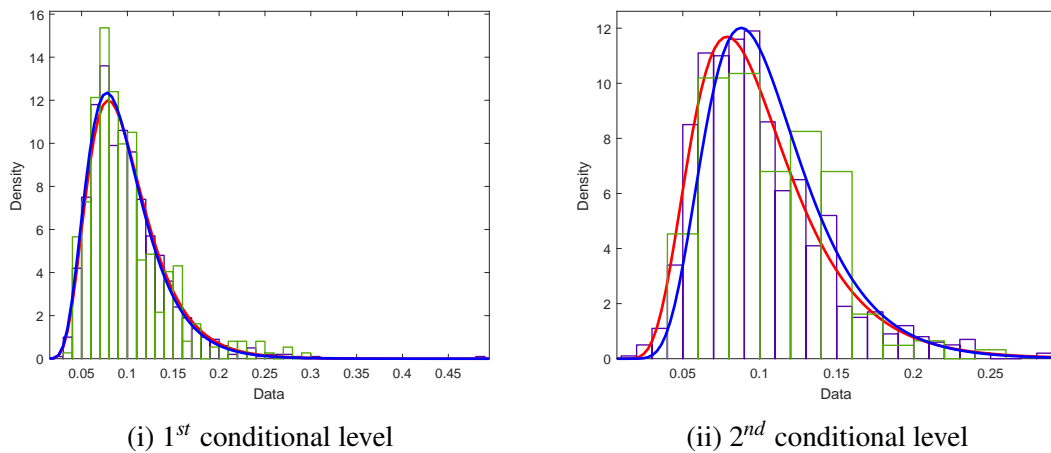
Figure 6.53: Shift in the distribution over two conditional levels for fracture dispersivity

By visual inspection, the shift between empirical pdf and actual pdf over the two conditional levels in Figures 6.46 - 6.54, it can be noted that matrix hydraulic conductivity and fracture aperture part 3 and part 4 show maximum shift from their actual pdf. So, the performance of disposal system (which is associated with the contaminant transport at the end-point) is strongly sensitive to these parameters. Hydraulic conductivity exhibits high sensitivity because, increase in the conductivity in the rock matrix leads to increase in the movement of contaminant from the matrix to the surrounding media. This impedes the storage of solute (lesser residence time) in matrix (Darcy's law). These results are in congruence with the observations made from the sensitivity analyses problems in the previous literature (Toran et. al., 1995). From the sensitivity analysis it is observed that among the five aperture variations along the length aperture sizes part 3 and part 4 exhibits maximum shift from the actual distribution. The underlying reason is that, the shift in these aperture pdfs (probability density function) lead to a fracture aperture configuration that allows maximum contaminant flow leading to failure.

To demonstrate the effect of fracture aperture configuration on contaminant flow a small illustration is made. The conductivity of a fracture with different aperture sizes

343

can be evaluated by estimating its equivalent aperture size. The equivalent aperture sizes are determined from equation developed by Sarkar et. al., 2004 for an aperture system connected in series. So, the equivalent aperture size of fracture is computed by using the mean values of five aperture sizes used in the study. The value is around 1.6156 μm. This aperture value corresponds to actual pdf case. Again, the five aperture values at the 2nd conditional level (close to failure region) are used to compute the equivalent aperture size. The equivalent aperture value increased to around 1.8μm. This value corresponds to empirical (or conditional) pdf. There is an increase in the equivalent aperture size by 0.2μm. When the equivalent aperture size is higher, then more contaminant flows through the fractures and reaches the end-point. These results show that equivalent aperture size is maximum when the fracture aperture parts 3 and 4 obtained the critical configuration (i.e, the values at $2nd$ conditional level). Another interesting observation is the transition in aperture sizes became gradual at the critical region, when compared to the abrupt variations in the actual configuration. So, a smoother path of transport indicates faster and higher amount of solute migration. These results indicate that these two values influence the contaminant transport thereby influencing the P_f of the system. Overall, this illustration shows that the fracture aperture part 3 and part 4 are critical in estimating the performance of disposal system near fractured rock.

The results suggest that field characterization in fractured media should not only emphasize on fracture geometry, which strongly influences directions of contaminant transport, but also matrix properties, which have a major influence on contaminant residence times and breakthrough concentrations. So far, the components of probabilistic safety assessment model for a disposal system near fractured sedimentary rock are developed and the one that handles geosphere transport is discussed in detail. However, the influence of

geochemical reactions between the contaminant and the geological medium on the overall concentration profile has not been explored. In the following section this aspect is studied.

6.7 Probabilistic safety assessment model for disposal system with reactive contaminant

The repositories designed for radioactive waste disposal aim for isolation of waste from surrounding environment over an indefinitely long period of time. Typically rocks possess properties like low-permeability, low groundwater velocity and, molecular diffusion is the primary solute migration process. Hence, rocky subsurface formations are considered as potential sites that can contain waste for such large time scales. However, fractures, the natural discontinuities within the rock can form pathways for the migration of radioactive waste that is emplaced in or released to the subsurface environment. So, there is an increased attention to ensure their long-term safety by developing probabilistic performance assessment models. As noted earlier, the geosphere transport is the critical component of performance assessment model. Many radionuclide transport models were developed to predict the flow and transport process in fractured media (Rasmuson and Neretnieks, 1986; Neretnieks, 1990; Krishnamoorthy et. al., 1992; Cvetkovic et. al., 2004; Mahmoudzadeh, 2014; Wei et. al., 2017). The type of host rock through which the contaminant migrates is also an important factor that affects the movement of contaminant through the medium. The geological rock formations that have been considered for the analysis include igneous rocks (like basalt, granite, tuff etc) and sedimentary rocks (like shale, limestone etc). Nonetheless, most of the investigations are carried near crystalline igneous rock deposits (Neretnieks, 1990; Krishnamoorthy et. al., 1992; Cvetkovic

et. al., 2004) due to their inert properties over sedimentary deposits. Some investigations near sedimentary deposits include (NRC, 1983; Rasmuson and Neretnieks, 1985; Jakimavičiūte-Maseliene et. al.,, 2006). It is important to model the behaviour in sedimentary rocks due to higher density of fractures and the reactive nature of these formations. Moreover, in India, there are some sites planned for radioactive waste disposal near sedimentary rock deposits. These sites include Kudankulam (Chennai), Gogi (Karnataka) and Tummalapalle area (Andhra Pradesh) (Makolil and Nagar, 2015). So, the present work focusses on understanding the behaviour of radionuclides near sedimentary rock formations using the new hybrid model that accounts for fracture geometry and aperture variations along the fractures. Further, the geosphere transport model is used to predict the extent of risk caused by the failure of these systems by taking into account various scenarios of release and pathways of intrusion.

6.7.1 Source term model

The process of performance assessment typically involves description of the system, specification of scenarios leading to failure of the system and predicting the consequences of failure in the form of radionuclide transport to biosphere through drinking water pathway (i.e, radiation dose and risk). It also involves evaluation of uncertainties in the estimations and determination of acceptability based on safety criteria. The failure of disposal system is assumed to occur due to infiltration of water into the system resulting in the transport of radionuclides to human habitat. Here, a simple source term model as given in section 5.3.11 of chapter 5 is considered to calculate the inventory of radionuclide. This source term is assigned as a decaying mass boundary condition to the numerical model.

6.7.2   Input parameters considered in the model

Among the different radionuclides considered for disposal, the analysis is carried out for

Iodine due to high ingestion dose (high risk to human health and environment). The input

data and the equation used for solving the source term are given in chapter 5 (see section

5.3.1.1). The input parameters to solve the source term are also the same as considered

in chapter 5 (see Table 5.2 and 5.3). The source term trend varying with time is shown in

Figure 6.54.
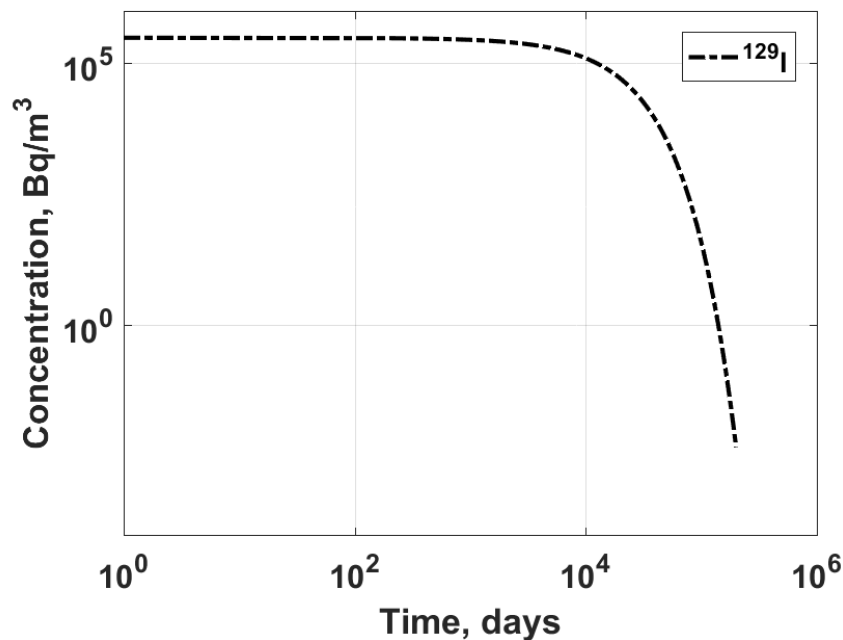
Figure 6.54: Source concentration versus time

The details of domain considered for the study are discussed elaborately in the pre-

ceding section (see section 6.6.2). An intact rock of size $20\,\text{m} \times 20\,\text{m}$ with a $10\,\text{m} \times 10\,\text{m}$

fractured network within the rock is modelled in numerical model and presented in Figure

6.11. Since radionuclide is reactive in nature, the contaminant transport due tosorption

and radioactive decay are also modelled along with advection and hydrodynamic dis-

persion processes. The fluid flow boundary conditions are same as given in Table 6.6.

However, the mass boundary condition is assigned to the section EF (see Figure 6.11) as a line source. The distribution coefficient in the fracture is assumed to be 2.6 m1/g from the literature (Jakimavičiūte-Maseliene et. al.,, 2006). The distribution coefficient in the intact rock matrix is calculated using empirical equation given by Krishnamoorthy et. al (1992).

$$K_r = \frac{K_f' \rho_s r}{3} \tag{6.13}$$

where K_f - distribution coefficient in fracture (m1/g); ρ_s - specific density (g/cm^3); r - particle radius (cm). The values for specific density and particle radius are assumed to be 2.62 g/cm^3 and 2.5×10^{-4} cm (Krishnamoorthy et. al., 1992). The geological and transport parameters used for the analysis remains the same as summarized in Table 6.3.

6.7.3   Geosphere transport model

It is important to have a rational understanding of the fundamental mechanisms that govern radionuclide transport in fractured media to develop models for performance (or safety) assessment of radioactive waste disposal systems. So, the model developed in section 6.5 is used for the estimation of risk and radiation dose of radionuclide near human habitat.

6.7.4   Deterministic analysis

The movement of radionuclide in the fractured medium is ambiguous due to an interconnected system of randomly oriented fractures. They choose preferential flow paths in the process of movement which depends on various factors. To study the influence of features of fractures and rock matrix on contaminant transport, parametric studies are carried out.

They are :

1. Effect of fracture orientation and number of fracture sets

2. Effect of aperture variation along the length of fracture

3. Comparison of contaminant migration through a fractured medium by modelling fractures and by equivalent porous medium model

6.7.4.1   Effect of fracture orientation and number of fracture sets

The results of contaminant concentrations are evaluated at different observation points spread along and across the network. The points shown in Figure 6.13 (a) are considered when the flow is along x-direction, while, the points in Figure 6.13 (b) are considered when the flow is along y-direction. The concentration trends for one, two and three fracture sets are presented below. Although, the analysis has been carried out for all the fracture combinations (as considered in the case of non-reactive contaminant), the concentration versus time plots are presented for three fracture set combinations.

6.7.4.1.1   Single set - $45°$

For a single fracture set, a total of 100 fractures inclined at $45°$ are generated from the algorithm. The results of radionuclide concentration varying over time is shown in Figure 6.55. The trends in Figure 6.55 (i) and 6.55 (ii) present the concentration trends when the flow is considered along x and y directions respectively. By visual inspection, one of the major difference in the concentration trends for a radionuclide is, the presence of a concentration peak and decline to zero post-peak, while a non-reactive contaminant trend always remains at the peak beyond its first arrival. This observation suggests the influence of the reactive nature of the contaminant (due to sorption and radioactive decay).
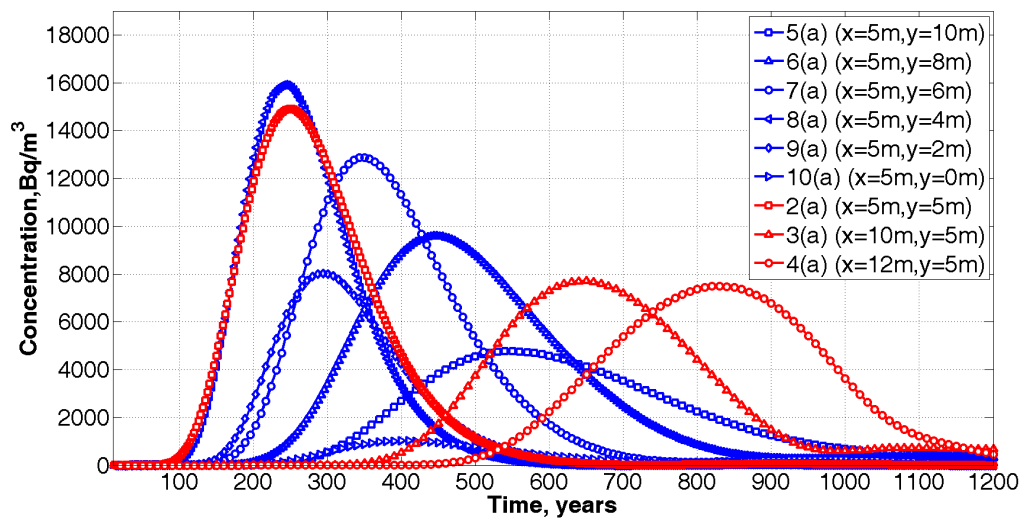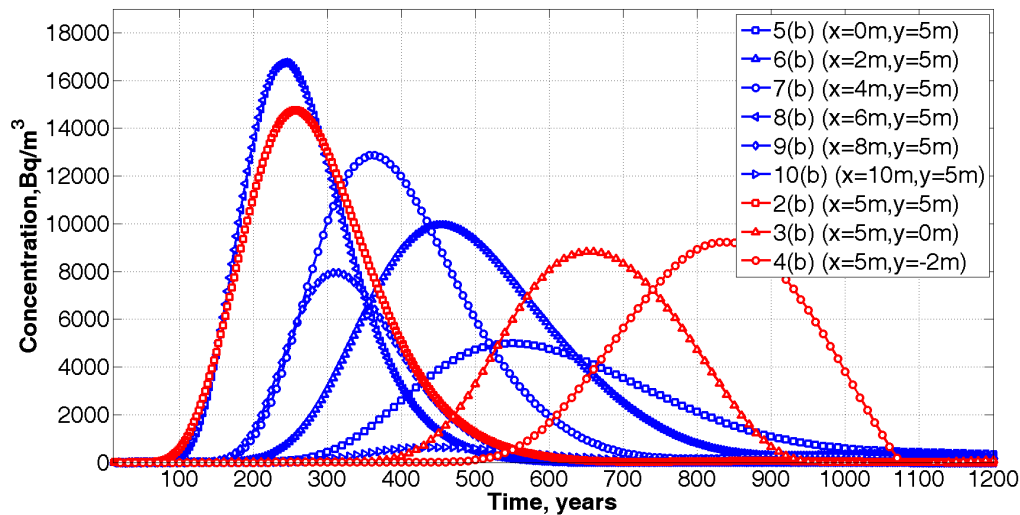
(i) Along x direction

(ii) Along y direction

Figure 6.55: Concentration versus time for $45°$ fracture set

The blue trend lines refer to the observation points transverse to the flow direction and the red trend lines refer to the observation points along the flow direction. From Figure 6.55, it can be noted that, it takes almost 250 years for the contaminant to reach maximum concentration and increases further to almost 900 years (at points farthest from the source). The concentration value at the closest observation point is 16000 Bq/m^3 and reduces by almost half of 8000 Bq/m^{3}at end-point of interest. Overall, the concentration

trends are similar in Figure 6.55 (i) and 6.55 (ii). This is because a uniform distribution of long parallel fractures that are inclined at 45° with respect to the flow direction (both x and y directions).

6.7.4.1.2 Two fracture sets - 45°-90°

When two fracture sets are considered a total of 200 fractures are generated from the algorithm. The results of concentration trends for flow along x and y directions are presented in Figure 6.56. Unlike the previous case, the concentration patterns for flow along x-direction (Figure 6.56 (i)) and y-direction (Figure 6.56 (ii)) are different. This observation hints the effect of heterogeneity due to an additional fracture set of different orientation. The peak concentration was around 16000 Bq/m^3 in the previous case (from Figure 6.55), while it reduced to around 8000 Bq/m^3(Figure 6.56 (i)) in this case. The time of arrival of maximum concentration has reduced in this case to 150 years at the closest observation point (1(a) in Figure 6.13 (a)) when compared to single fracture set case. The rate of movement of radionuclide slows down and due to the effect of retardation and decay, the peak concentration value reduces further.
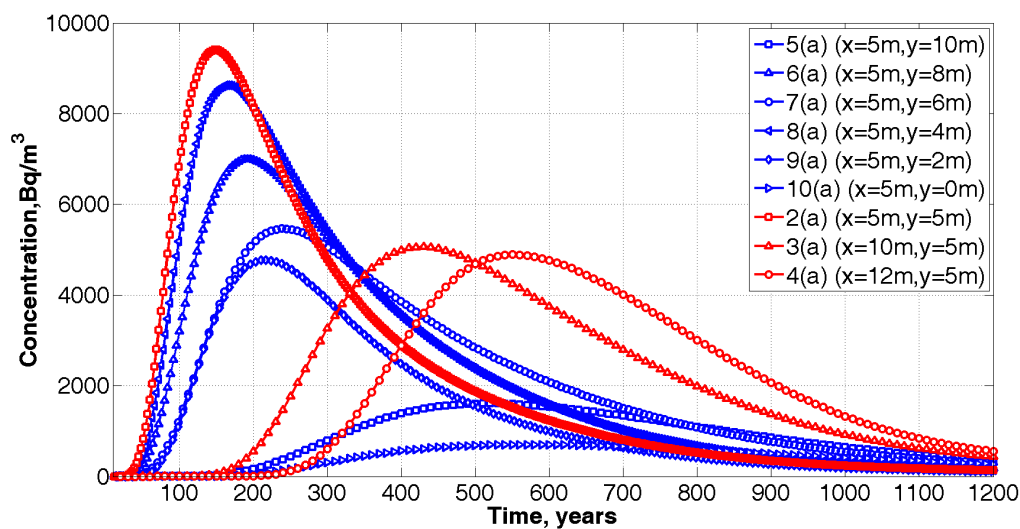
(i) Along x direction
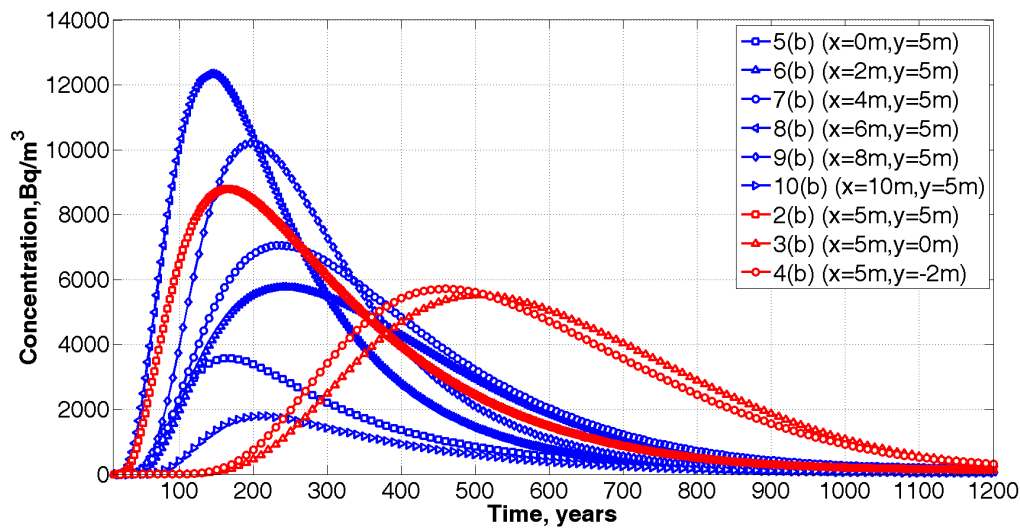
(ii) Along y direction

Figure 6.56: Concentration versus time for $45°$-$90°$ fracture set

6.7.4.1.3 Three fracture sets - $0°$-$45°$-$90°$

In the case of three fracture sets, a total number of 400 fractures are generated. The length of fractures are smaller in comparison to the previous cases. Also, it insinuates the effect of heterogeneity in the fractured network with three fracture sets of different orientations.

Figure 6.57 (i) and (ii), present the concentration trends for a three fracture set combination with the flow along x and y directions respectively. The concentration trends are not similar indicating the effect of heterogeneity in the system. The peak concentration in 6.57 (i) is around 10000 Bq/m^3 which is slightly higher than the peak concentration in 6.57 (ii) is around 9700 Bq/m^3. However the time of arrival of maximum concentration fall in the same range for both the cases. There is a small discrepancy is both the cases at the observation points falling in the mid-region of the fracture network. This can also be attributed to heterogeneity in the system. Also, the effect of fracture sets as discussed in previous sections also contribute to this behaviour. The results presented so far gives an idea of the concentration profiles for different fracture set combinations. However, there

is a need to quantify the effect of other fracture set combinations given in (Figure 6.14, Figure 6.19 and Figure 6.23). So, the same analysis is carried out for all the eleven cases fractured networks.
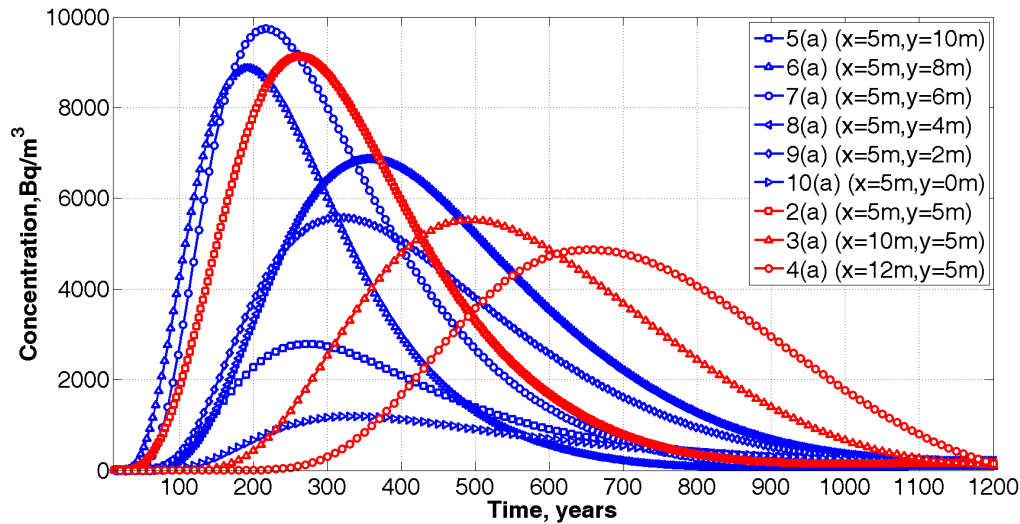
(i) Along x direction
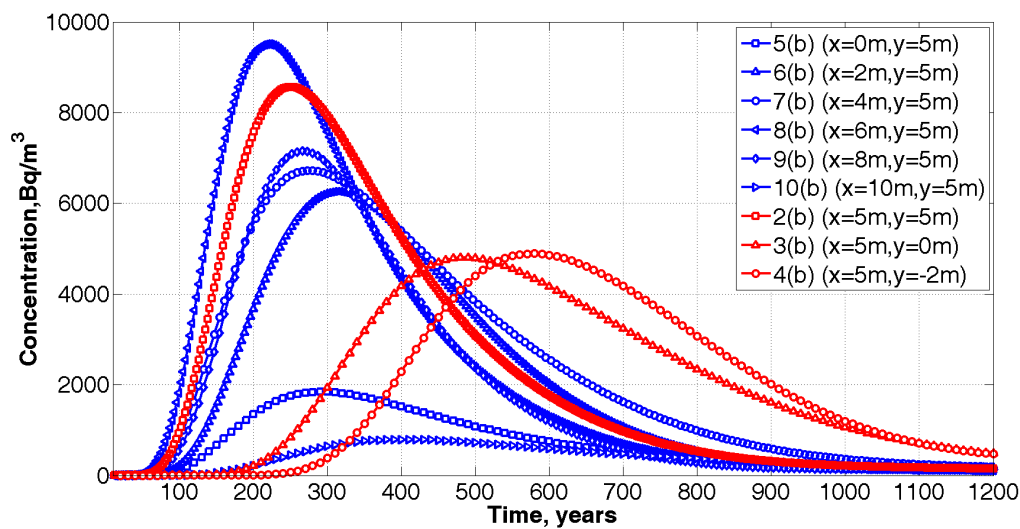
(ii) Along y direction

Figure 6.57: Concentration versus time for $0°$-$45°$-$90°$ fracture set

In the case of radionuclide transport modelling, peak radionuclide concentration values and the time of arrival of peak concentration have been evaluated. Further, radiological model is used to evaluate radiation dose to a member of the critical group due

to the consumption of groundwater for drinking and the corresponding risk values are also estimated. All these results are organized and presented in Table 6.10 for the cases corresponding to flow along x-direction.

Table 6.10: Maximum concentration, Maximum dose and Risk computed for different fracture sets when the flow is along X-direction

SNo	Fracture set	Point of interest	Maximum concentration (Bq/m^3)		Maximum dose (mSv/yr)		Risk (yr^{-1})		Time of arrival of maximum concentration (yr)	
	Division along fracture	One part*	Five parts*	One part	Five parts	One part	Five parts	One part	Five parts	
Single set										
1	0°	Center *	14197.04	13790.53	1.254	1.218	9.154E-05	8.892E-05	306	293
		End*	9733.732	8817.7372	0.860	0.779	6.276E-05	5.686E-05	614	618
2	45°	Center	14897.29	13838.63	1.316	1.222	9.606E-05	8.923E-05	250	279
		End	7588.599	7245.765	0.670	0.640	4.893E-05	4.672E-05	620	724
3	135°	Center	15736.47	16214.5	1.39	1.432	1.01E-04	1.046E-04	250	297
		End	7596.842	7572.983	0.671	0.669	4.898E-05	4.883E-05	620	706
Two sets										
4	0°-45°	Center	9297.944	11304.3	0.821	0.999	5.995E-05	7.289E-05	239	243
		End	5266.65	6828.39	0.465	0.603	3.396E-05	4.403E-05	520	548
5	0°-90°	Center	8829.2	9846.02	0.779	0.870	5.693E-05	6.349E-05	293	293
		End	6035.775	5311.148	0.533	0.509	3.892E-05	3.713E-05	441	498
6	45°-90°	Center	9403.893	9411.91	0.831	0.831	6.069E-05	6.069E-05	149	354
		End	5061.766	5366.75	0.447	0.472	3.264E-05	3.461E-05	428	651
7	45°-135°	Center	6105.842	9435.27	0.539	0.833	3.937E-05	6.084E-05	368	321
		End	4612.126	5819.66	0.407	0.514	2.974E-05	3.753E-05	527	788
8	90°-135°	Center	8001.591	6691.4	0.707	0.591	5.159E-05	4.315E-05	185	318
		End	4496.676	3800.32	0.397	0.336	2.899E-05	2.45E-05	475	676
Three sets										
9	0°-45°-90°	Center	9131.428	7730.67	0.806	0.683	5.888E-05	4.985E-05	262	332
		End	5527.92	6122.5	0.488	0.485	3.564E-05	3.948E-05	494	548
10	0°-45°-135°	Center	7061.105	8407.75	0.624	0.743	4.553E-05	5.421E-05	306	332
		End	4733.956	5495.8	0.418	0.485	3.052E-05	3.5440E-05	548	788

*center - Observation point at the center of the domain (5 m from the source)
*end - Observation point at the end of the domain (10 m from the source)
*One part - No local aperture variation along the length of fracture
*Five parts - Five aperture variations along the length of fracture

The results for maximum concentration, radiation dose and risk corresponding to case where the contaminant flow is along y-direction are presented in Table 6.11. The influence of various factors affecting the transport is also illustrated.

Table 6.11: Maximum concentration, Maximum dose and Risk computed for different fracture sets when the flow is along Y-direction

SNo	Fracture set	Point of interest	Maximum concentration (Bq/m^3)		Maximum dose (mSv/yr)		Risk (yr^{-1})		Time of arrival of maximum concentration (yr)	
	Division along fracture		One part	Five parts	One part	Five parts	One part	Five parts	One part	Five parts
			Single set							
1	90°	Center	11855	8596.851	1.047	0.759	7.644E-05	5.543E-05	329	454
		End	8395.122	7751.744	0.742	0.685	5.413E-05	5.00E-05	618	1064
2	45°	Center	14752.81	14236.16	1.303	1.257	9.513E-05	9.180E-05	257	295
		End	8417.738	8420.55	0.744	0.744	5.428E-05	5.43E-05	614	706
3	135°	Center	14726.94	14778.17	1.301	1.305	9.496E-05	9.529E-05	245	306
		End	8735.463	8930.958	0.772	0.789	5.633E-05	5.76E-05	614	697
			Two sets							
4	0°-45°	Center	5702.733	8508.25	0.504	0.752	3.68E-05	5.486E-05	367	505
		End	3279.378	4711.52	0.290	0.416	2.11E-05	3.04E-05	520	905
5	0°-90°	Center	7169.475	8481.92	0.633	0.749	4.623E-05	5.469E-05	295	224
		End	5311.148	5174.64	0.469	0.457	3.425E-05	3.34E-05	477	515
6	45°-90°	Center	8787.953	7838.02	0.776	0.696	5.667E-05	5.08E-05	166	264
		End	5520.051	5606.82	0.488	0.495	3.559E-05	4.05E-05	324	548
7	45°-135°	Center	8913.176	9381.09	0.787	0.829	5.7473E-05	6.049E-05	178	338
		End	5428.474	5828.69	0.479	0.515	3.500E-05	3.76E-05	298	173
8	90°-135°	Center	13510	8748.21	1.193	0.773	8.711E-05	5.641E-05	183	218
		End	5909.716	6494.92	0.522	0.574	3.811E-05	4.19E-05	361	270
			Three sets							
9	0°-45°-90°	Center	8565.887	9965.73	0.757	0.880	5.523E-05	6.426E-05	251	319
		End	4802.847	4648.52	0.424	0.411	3.097E-05	3.00E-05	485	652
10	0°-45°-135°	Center	6053.319	8575.59	0.535	0.757	3.903E-05	5.528E-05	239	455
		End	4420.036	5939.75	0.390	0.525	2.850E-05	3.83E-05	392	770

*center - Observation point at the center of the domain (5 m from the source)
*end - Observation point at the end of the domain (10 m from the source)
*One part - No local aperture variation along the length of fracture
*Five parts - Five aperture variations along the length of fracture

In Table 6.10, the results are computed at observation points which are 5 m from the source (i.e., 2(a) in Figure 6.13 (a)) and 10 m from the source (i.e., 3(a) in Figure 6.13 (a)). In Table 6.11, the results are computed at observation points which are 5 m from the source (i.e., 2(b) in Figure 6.13 (b)) and 10 m from the source (i.e., 3(b) in Figure 6.13 (b)). It can be observed that the results in each case are unique and manifest the complexity of the domain and, the extent of influence of various parameters on the radionuclide transport. The new component that incorporates the effect of variation in aperture sizes (section 6.5.3) along the fracture is considered for the analysis. From these results we can observe the effect of number of fracture sets, variation in aperture sizes along the fracture and direction of flow on the migration of radionuclide. With the increase in the number of fracture sets, the results become more unpredictable due to the influence of fracture combinations and also the direction of flow. There is not definite trend observed in the presence of local aperture variation as well. However, there is certainly an effect of this factor on the overall concentration values. Also, the time of arrival of maximum concentration is increased by around 10 - 30% due to local aperture variation, indicating a delay in contaminant movement in the presence of local aperture variation. For example, in Table 6.10, consider fracture set 45° - 90°. Here, the time of arrival of maximum concentration is 428 years without local aperture variation while, it is almost 650 years with local aperture variation. Amongst all the fracture sets, the maximum concentration is observed in 0° (in Table 6.10) and 90° (in Table 6.11). As the direction of fracture orientation and the direction of contaminant flow coincide in these cases, maximum concentration is observed. The risk estimated for different fractures sets falls in the range of 10^{-4} to 10^{-5} y^{-1} which is low in comparison to the risk due to natural catastrophes that lies between 10^{-3} - 10^{-4} y^{-1}. The average annual dose due to natural background radiation is estimated

to be 2.4 mSv world-wide. The corresponding risk due to natural background radiation can be estimated using the ICRP total risk factor (7.3×10^{-5} mSv^{-1}) as 1.8×10^{-4} y^{-1}. The estimated risk from numerical model falls below the risk due to natural background radiation as well. Hence, the risk values evaluated for deterministic analysis fall within the safe limits indicating the safety of disposal system.

6.7.4.2 Influence of fracture properties on the overall transport

To investigate the effect of some of the critical fracture and rock properties, a comparative study is performed. The $45°$-$90°$ fracture set combination is considered for the study. The fracture pattern is shown in Figure 6.39 (a). Four cases are considered for the analysis and they are:

1. **case (a)** - The concentration versus time trends for the given fracture set (default case)

2. **case (b)** - As the algorithm for fracture generation is stochastic in nature, the influence of this factor is examined. A new fracture pattern is generated which shown in in Figure 6.39(b). The concentration versus time trends are plotted for this case.

3. **case (c)** - The influence of aperture variation along the fracture is examined. So, each fracture is assumed to be segmented into five parts and different aperture sizes are assigned to each segment. The transition in aperture sizes along a fracture makes the fractured rock more heterogeneous. By taking this factor into account, concentration versus time trends are plotted.

4. **case (d)** - The fractured rock portion is replaced with a homogeneous equivalent porous medium. The concentration versus time trends are plotted for this case

The results are estimated at the center (i.e., 5 m from the source- 8(a)) and, at the end of fractured rock (i.e.,10 m from the source-9(a)). Each case is modelled numerically by assigning the respective conditions are simulated to obtain the results. They are presented in Figures 6.58 and 6.59. The results in Figure 6.58 corresponds to flow along x-direction and Figure 6.59 corresponds to flow along y-direction. The results from case(b), case(c) and case (d) are compared with results with respect to case (a) (i.e., default case).
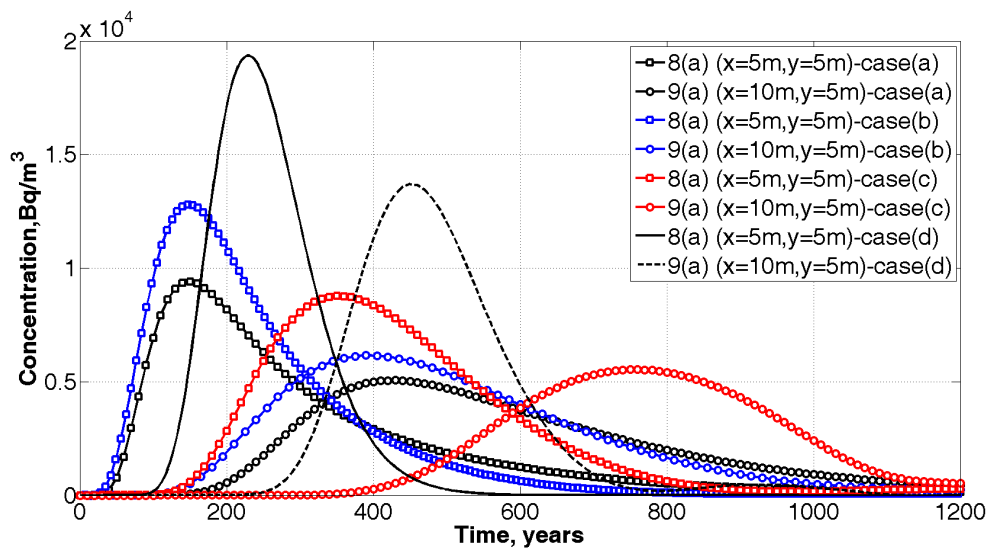
Figure 6.58: Concentration versus time for various cases (Flow in X-direction)
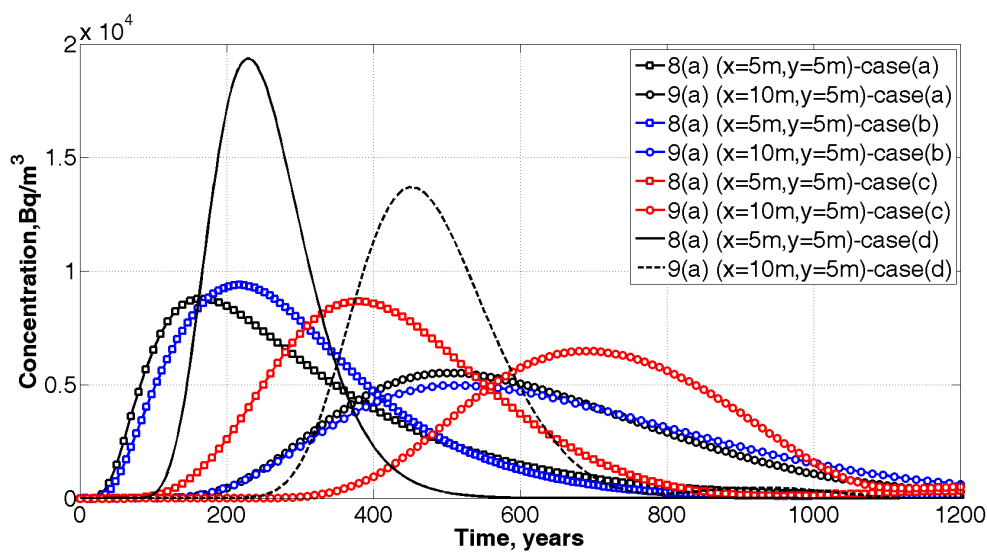
Figure 6.59: Concentration versus time for various cases (Flow in Y-direction)

1. The concentration trends in case (b) and case (a) are similar. A slight variation is observed in the concentration pattern and peak values. Also the time of arrival of maximum concentration is almost same. In the case of flow along x-direction i.e, Figure 6.58, it is around 180 years (corresponding to point 8(a)) and in the case of flow along x-direction i.e, Figure 6.59, it is around 200 years (corresponding to point 8(a)). This shows that stochastic fracture pattern generation does have an influence on the contaminant transport.

2. By comparing the case (c) plots with case (a), it can be observed that, modelling the transition along the fractures creates a more complex fracture network leading to slower movement of radionuclides. Thus we can observe that case (c) takes double the time to reach the peak concentration than case (a). In Figure 6.58, the time of arrival of peak concentration in case (c) is 400 years (corresponding to point 8(a)), while it is 200 years (corresponding to point 8(a)) in the default case.

3. The concentration trends in case (d) shows almost double the concentration and faster arrival of peak concentration in comparison with case (a). This implies that the results are highly overestimated than the actual case. This observation emphasizes the need to model fractures for in the rock for realistic prediction. Also the effect of heterogenity in the system is masked due to the assumption of equivalent porous medium.

From this analysis, it is evident that the new components developed in this chapter have a significant effect on the model predictions. So, the new model with the integrated components (that account for fracture geometry and local aperture variations) helps in simulating the geological medium better and generate more realistic results.

6.7.5 Probabilistic analysis

The main objective of this analysis is to develop a performance assessment model that can predict the radiation dose due to migration of radionuclide from barrier system, into the fractured medium and finally reach the biosphere. The results computed from deterministic analysis are within the safety limits. However, the design of barrier systems that handle hazardous waste like radioactive materials, requires probabilistic analysis. This analysis helps in improving our understanding on the factors that contribute to the maximum risk in the system. Moreover, performance assessment model entails uncertainty quantification due to variabilities in the input characteristics of the model. In this study, geological properties of fracture and intact rock matrix; and, transport properties of Iodine (^{129}I) in fracture and rock matrix are considered as random variables. The mean values (underlying normal distribution) of the input parameters, the probabilistic distribution and COV have been assumed from literature. They are presented in Table 6.12. To capture the influence of the number of uncertain parameters on the probability of failure, two scenarios are considered. They are:

1. Consider porosity, distribution coefficient of the intact rock and the transport properties of Iodine through fracture to be uncertain (i.e., fracture aperture, diffusion and dispersivity). So a total of five parameters are considered to be random variables.

2. Consider porosity, distribution coefficient of the intact rock and the transport properties of Iodine through fracture to be uncertain(i.e., fracture aperture, diffusion and dispersivity). Additionally, the aperture variations along the fracture are also considered as random variables. Since each fracture is divides into five segments, each segment of the fracture is assumed as random variable. So, a total of nine

parameters are considered to be random variables.

Table 6.12: Statistical properties of parameters considered for the study

| S.No | Property | Iodine | | Distribution |
		Mean	COV	
		Rock matrix		
1	Distribution coefficient (ml/g)	2.6	0.15	Lognormal
		2.6	0.20	
		2.6	0.30	
2	Porosity	0.13	0.15	Lognormal
		0.13	0.20	
		0.13	0.30	
		Fracture		
3	Fracture aperture (part 1) (μm)	50	0.15	Lognormal
		50	0.20	
		50	0.30	
4	Fracture aperture (part 2) (μm)	10	0.15	Lognormal
		10	0.20	
		10	0.30	
5	Fracture aperture (part 3) (μm)	20	0.15	Lognormal
		20	0.20	
		20	0.30	
6	Fracture aperture (part 4) (μm)	40	0.15	Lognormal
		40	0.20	
		40	0.30	
7	Fracture aperture (part 5) (μm)	30	0.15	Lognormal
		30	0.20	
		30	0.30	
8	Diffusion coefficient (m^2/s)	5×10^{-9}	0.15	Lognormal
		5×10^{-9}	0.20	
		5×10^{-9}	0.30	
9	Longitudinal Dispersivity (m)	0.1	0.15	Lognormal
		0.1	0.20	
		0.1	0.30	

To determine the reliability of the system, the probability of radiation dose exceeding the permissible limit (P_f) which is given in equation (6.12) needs to be evaluated. Subset simulation method is used to estimate the probability of failure (P_f).

6.7.5.1 Results and discussion

The probability of failure is estimated for both the cases and presented in Table 6.13. Also, the results are estimated by varying COV values from 15% to 30%.

Table 6.13: Result of P_f for different scenarios considered in th study

S.No	Fracture set	Number of parts along fracture	Number of random variables	Probability of failure		
				15% COV	20% COV	30% COV
1	45°-90°	1 part	5	2.63E-06	0.00167	0.0457
2	45°-90°	5 parts	9	6.73E-06	0.0043	0.06

From Table 6.13, it can be observed that, the probability of failure increased with the increase in coefficient of variation (COV). The P_f values corresponding to 1st row of Table 6.13 presents the results when five uncertain parameters are considered and P_f values corresponding to 2nd row of Table 6.13 presents the results when nine uncertain parameters are considered. The difference in both the cases is with respect to aperture variations. So, one part in Table 6.13 refers to no aperture variation and five parts refers to local aperture variation (five segments within a fracture with each segment modelled as random variable). The P_f values in first row are slightly lower than the P_f values in second row. Lower probability of failure indicates that, the samples or simulations that resulted in radiation dose above permissible values are lesser. In deterministic analysis,

a slightly opposing observation was made where the presence of local aperture variation lead to slower movement of contaminant and lower concentrations (indicating the effect of heterogeneity due to aperture variations). Unlike this observation, the probability of failure is higher in the case corresponding to variation in aperture sizes than the latter. The main reason for this trend might be because, as the aperture sizes along the fracture are treated as random variables, more uncertainty is induced into the system leading to higher possibility of reaching failure than the case with only one random value along the length of the fracture. Also, as mentioned in Section 6.6.4.1, the presence of a fracture set, its fracture orientation combination and direction of flow of contaminant affects its concentration. Since the fracture set considered for the analysis leads to a complex network, the transport through the system becomes more challenging and unpredictable as there is no particular trend for radionuclide concentration with the increasing aperture size. So, the interplay of various aspects leads to an increased P_f in the case with local aperture variation over the one without aperture variation.

The sample COV of failure probability over 25 independent subset simulation runs are plotted to observe the variability in P_f. Also, coefficient of variation versus number of samples per subset tested to check the convergence of the simulation. The results presented are for the case with aperture variation along the fracture (i.e., five parts). However, since almost same trends are observed for the case without aperture variation along the fracture (i.e., one part), they are not presented. The effect of COV versus number of samples per subset are presented in Figure 6.60 (i) - 6.62 (i). The effect of probability of failure versus number of samples per subset are presented in Figure Figure 6.60 (ii) - 6.62 (ii).

(i) COV Vs N_{ss}

(ii) P_f Vs N_{ss}
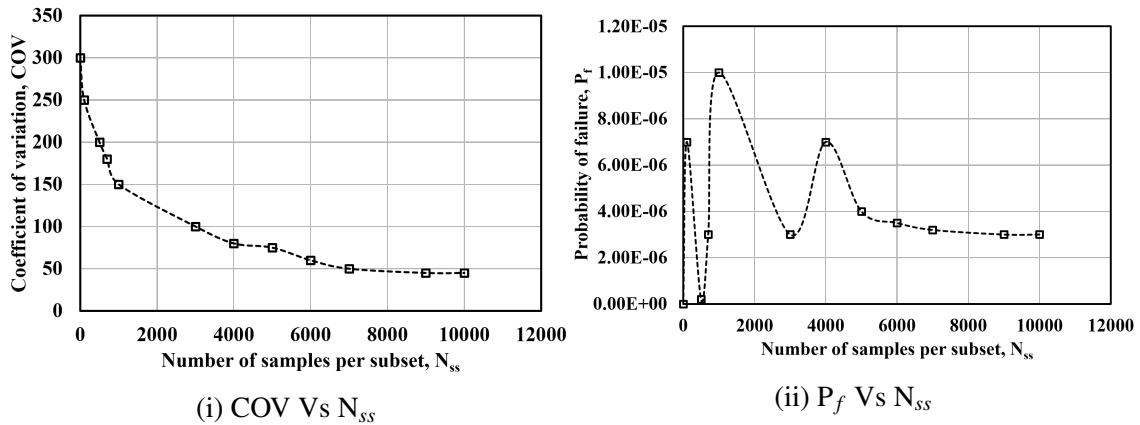
Figure 6.60: Trends of coefficient of variation and probability of failure for different number of samples per subset (15% COV)

(i) COV Vs N_{ss}

(ii) P_f Vs N_{ss}
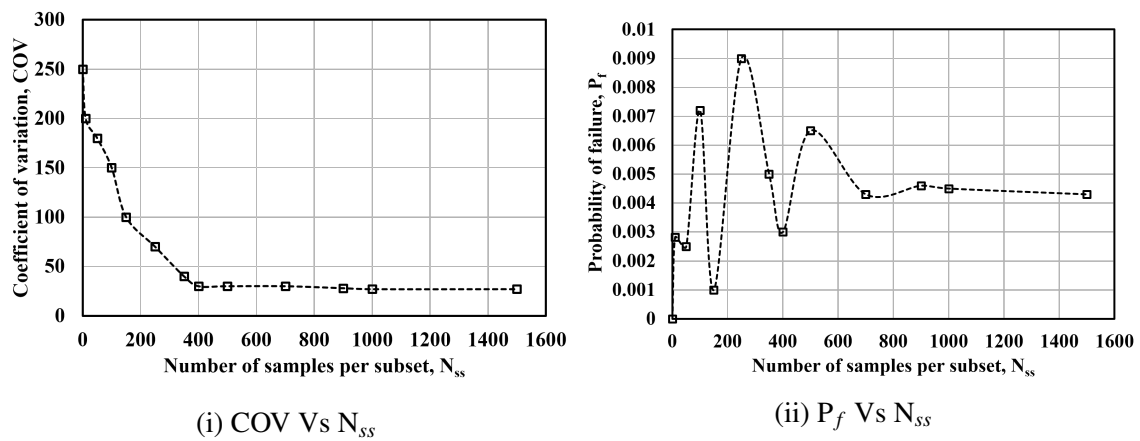
Figure 6.61: Trends of coefficient of variation and probability of failure for different number of samples per subset (20% COV)

(i) COV Vs N_{ss}

(ii) P_f Vs N_{ss}
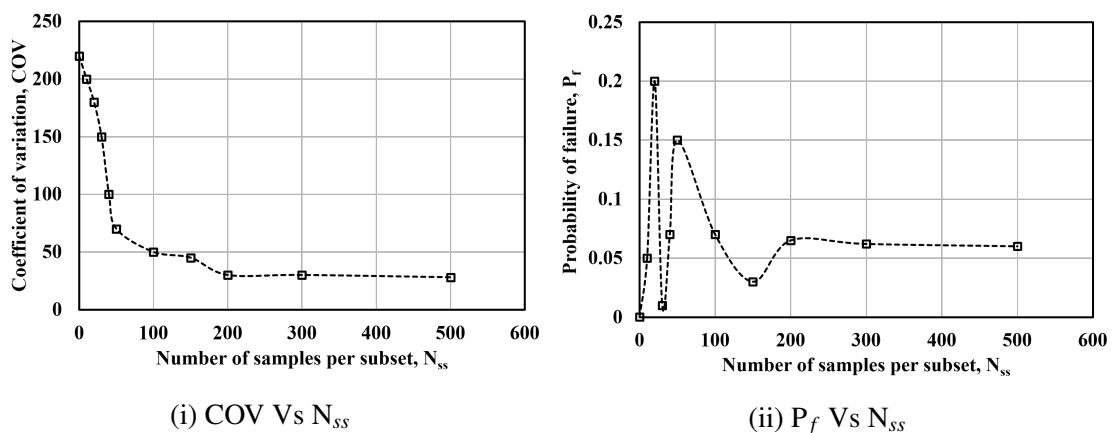
Figure 6.62: Trends of coefficient of variation and probability of failure for different number of samples per subset(30% COV)

So, amongst the cases simulated in the study, the results with high P_f values project

highest risk and need immediate attention to stop intrusion of radiation further to the environment. Further, it is crucial to know the main parameters contributing to failure of the system (i.e., high radiation dose values). This is done by carrying out sensitivity analysis using the the pdfs of intermediate conditional levels during subset simulations. The results are presented below.

6.7.5.2 Sensitivity analysis

Sensitivity analysis is performed by post-processing the results of subset simulation for the case with five uncertain parameters (without aperture variation along the fracture) and for the case with nine uncertain parameters (with aperture variation along the fracture). The results for each case are presented below.

6.7.5.2.1 For five parameters

The empirical distributions from two conditional levels are compared with the actual distribution and results are presented in Figures 6.63 - 6.67.

(i) 1st conditional level (ii) 2nd conditional level
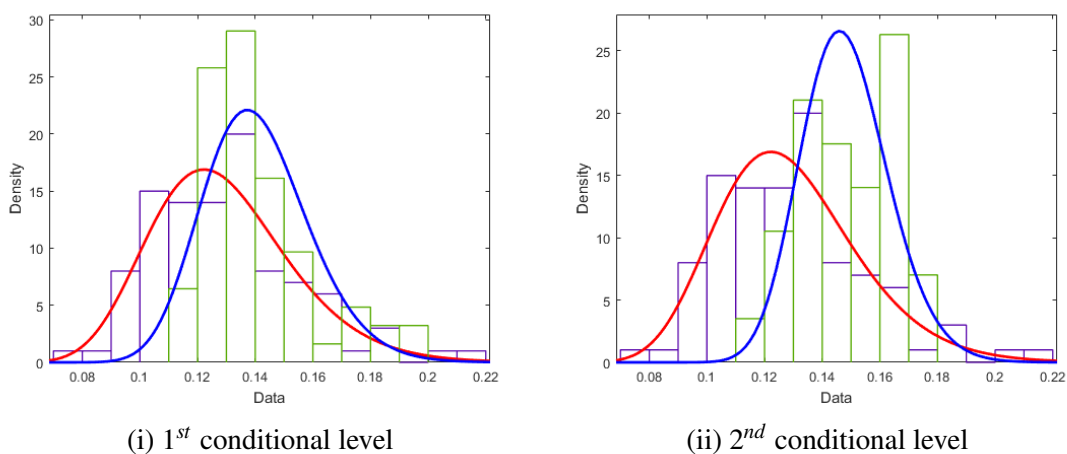
Figure 6.63: Shift in the distribution over two conditional levels for porosity

(i) 1st conditional level

(ii) 2nd conditional level
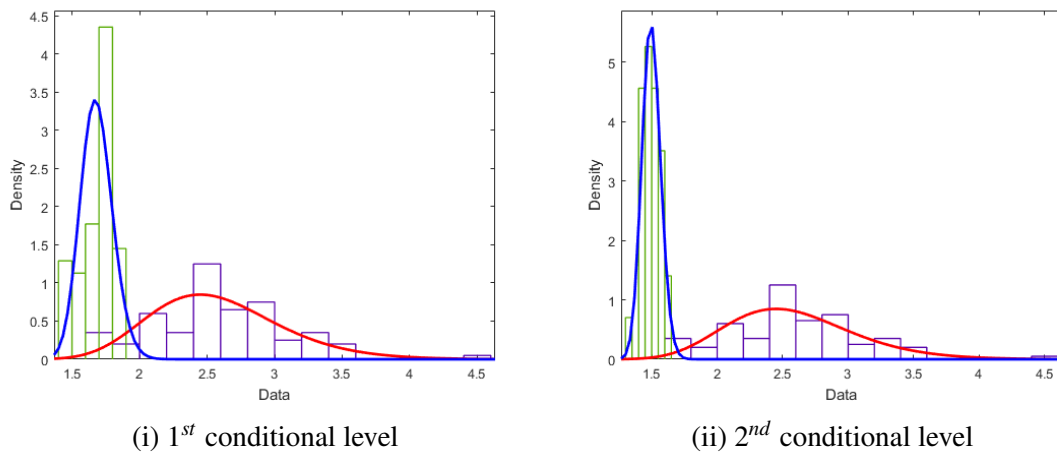
Figure 6.64: Shift in the distribution over two conditional levels for distribution coefficient

(i) 1st conditional level

(ii) 2nd conditional level
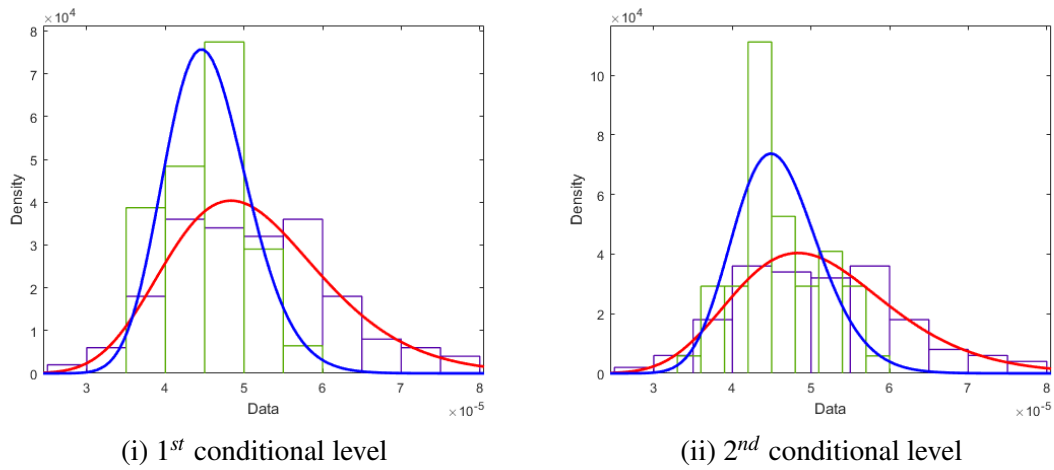
Figure 6.65: Shift in the distribution over two conditional levels for fracture aperture

(i) 1st conditional level

(ii) 2nd conditional level
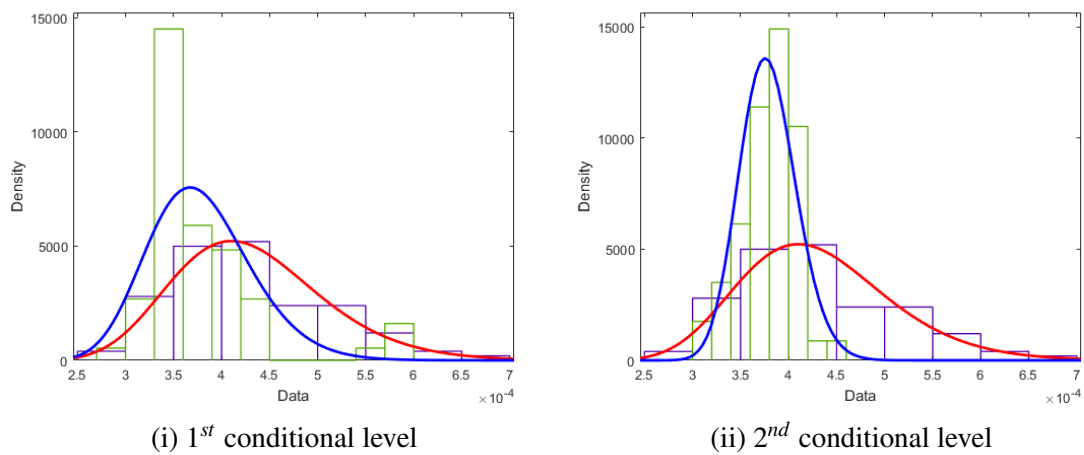
Figure 6.66: Shift in the distribution over two conditional levels for fracture diffusion

(i) 1st conditional level

(ii) 2nd conditional level
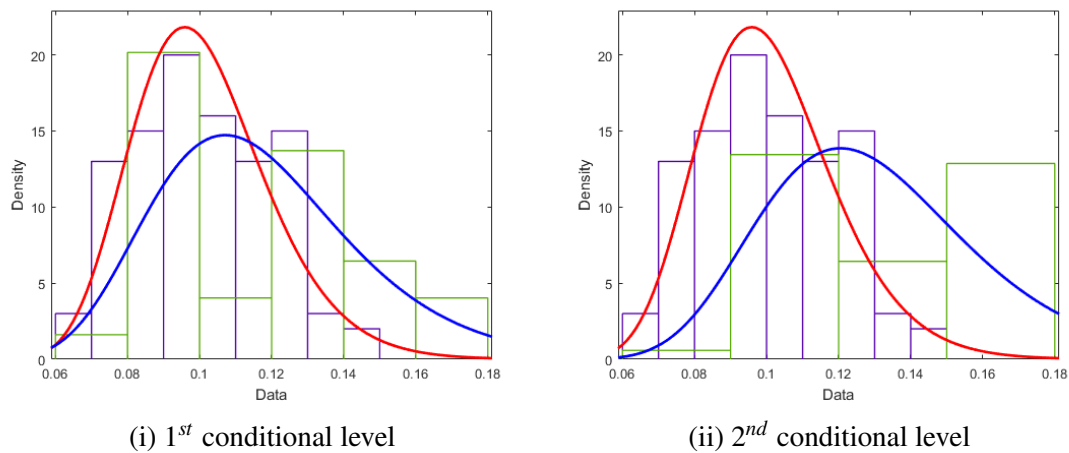
Figure 6.67: Shift in the distribution over two conditional levels for fracture dispersivity

From the Figures (6.63 - 6.67), we can observe that amongst the five uncertain parameters, distribution coefficient shows the maximum shift from the actual distribution. So, adsorption is one of the critical processes that exhibits maximum sensitivity towards the transport behaviour of radionuclide in fractured medium. These results are consistent with the observations made by previous researchers (Krishnamoorthy et. al., 1992; Toran et. al., 1995).

6.7.5.2.2 For nine parameters

By taking into account local aperture variations, the total number of uncertain parameters become nine. The sensitivity analysis results are presented in Figures 6.68 - 6.76. From Figures 6.68 - 6.76, it can observed that the three most critical parameters affecting the system response are distribution coefficient, fracture aperture (part 4) and fracture aperture (part 5). Distribution coefficient is the most sensitive parameter.

(i) 1st conditional level

(ii) 2nd conditional level

Figure 6.68: Shift in the distribution over two conditional levels for porosity

(i) 1st conditional level

(ii) 2nd conditional level
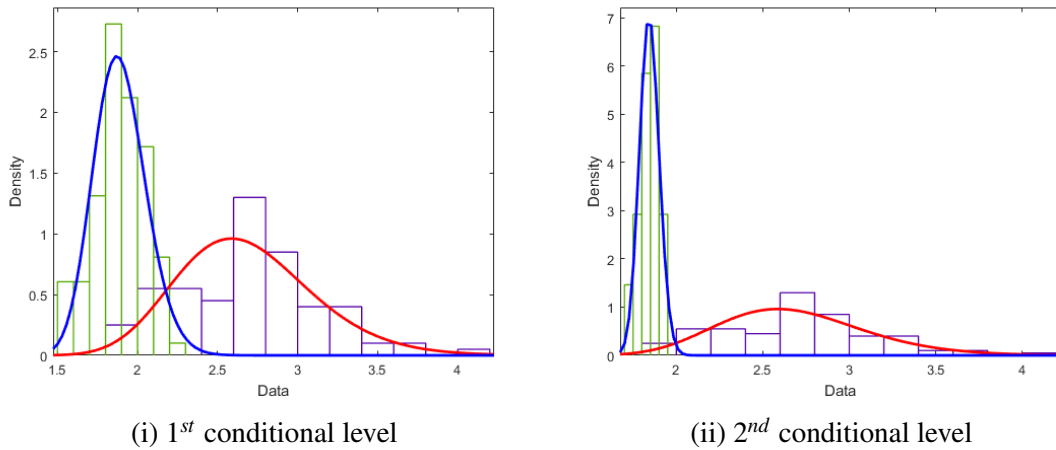
Figure 6.69: Shift in the distribution over two conditional levels for distribution coefficient

(i) 1st conditional level

(ii) 2nd conditional level
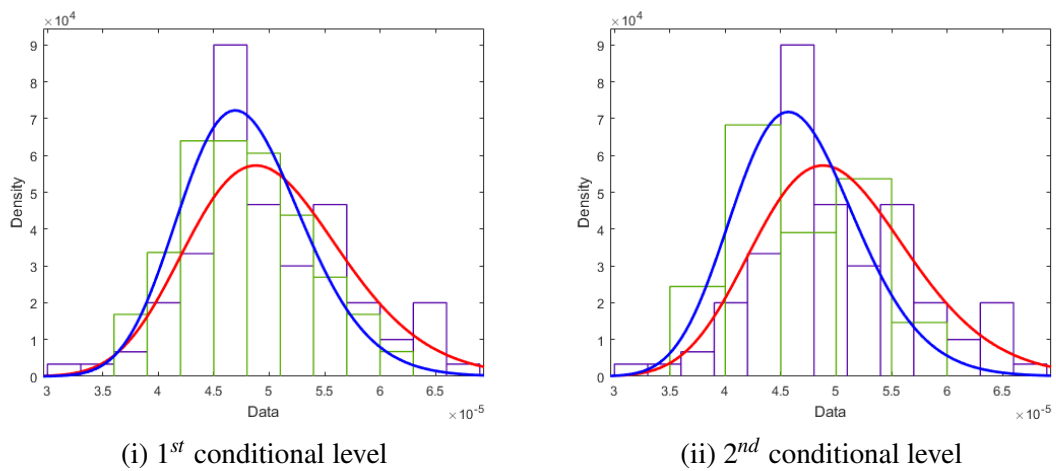
Figure 6.70: Shift in the distribution over two conditional levels for aperture part 1

(i) 1st conditional level

(ii) 2nd conditional level
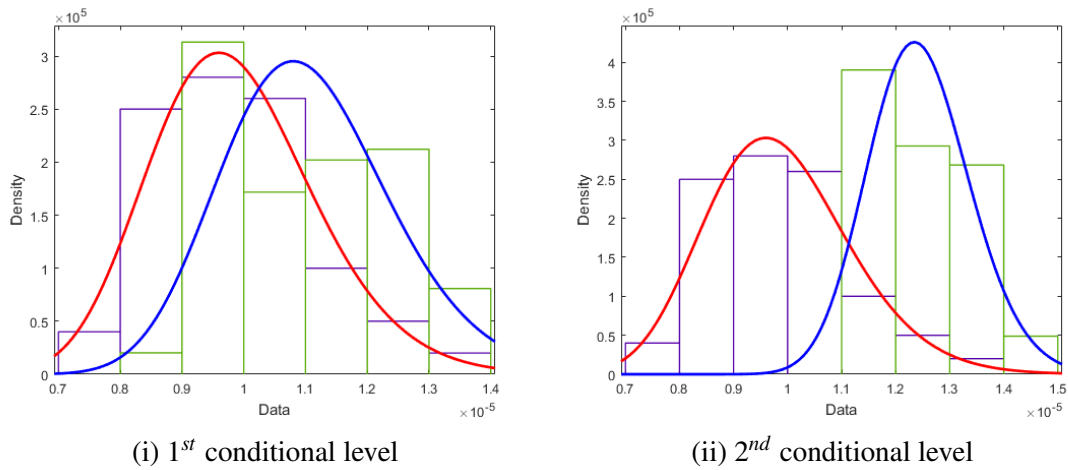
Figure 6.71: Shift in the distribution over two conditional levels for aperture part 2

(i) 1st conditional level

(ii) 2nd conditional level
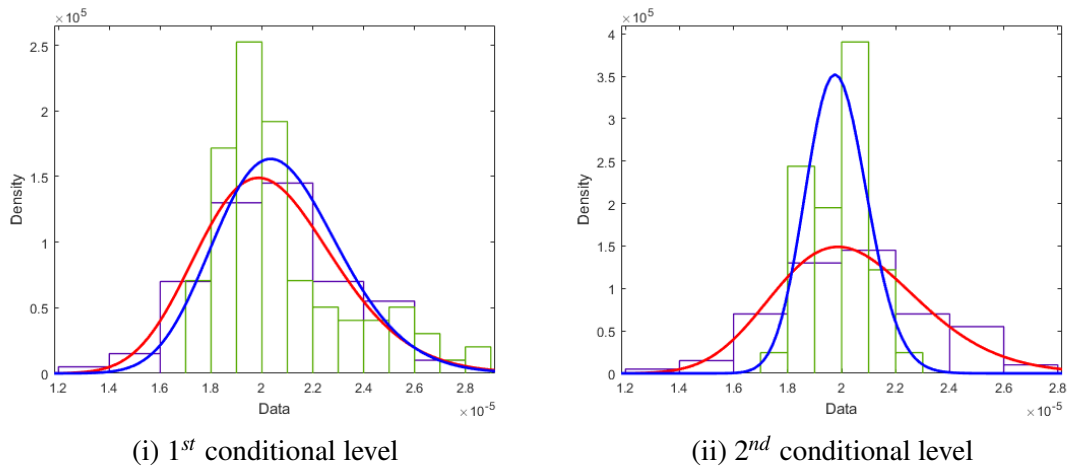
Figure 6.72: Shift in the distribution over two conditional levels for aperture part 3

(i) 1st conditional level

(ii) 2nd conditional level
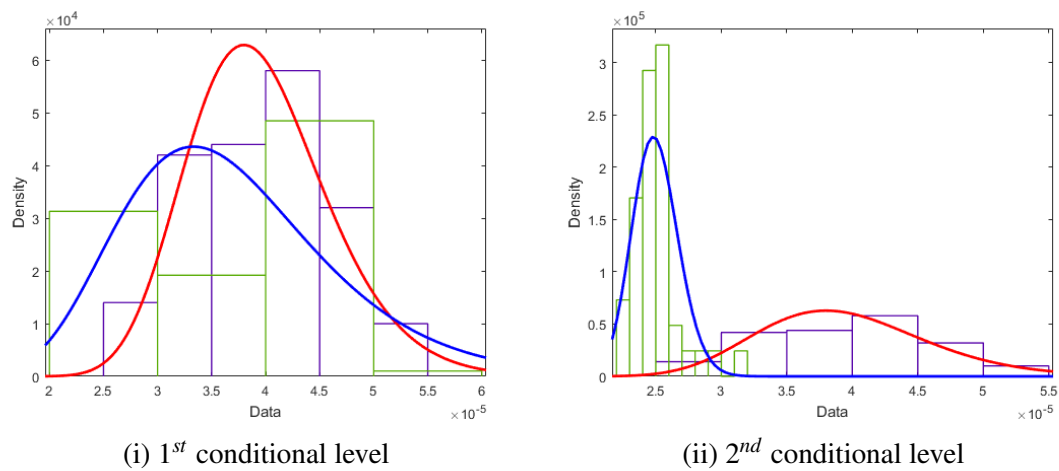
Figure 6.73: Shift in the distribution over two conditional levels for aperture part 4

(i) 1st conditional level

(ii) 2nd conditional level

Figure 6.74: Shift in the distribution over two conditional levels for aperture part 5

(i) 1st conditional level

(ii) 2nd conditional level
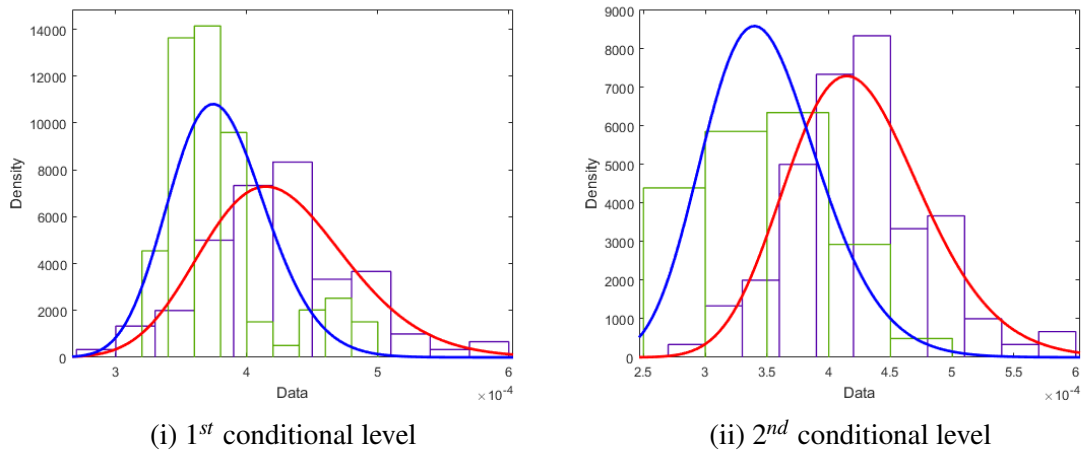
Figure 6.75: Shift in the distribution over two conditional levels for fracture diffusion

(i) 1st conditional level

(ii) 2nd conditional level

Figure 6.76: Shift in the distribution over two conditional levels for fracture dispersivity

The sensitivity of fracture aperture parts is noticed in the case of non-reactive contaminant also. During the simulation, the aperture values are varied until they attain a configuration leading to maximum radionuclide transport. Also, as mentioned in Section 6.6.5.2, the equivalent hydraulic aperture is higher for the failure case (g(X)<0). So, from the sensitivity analysis, it can be concluded that the chemical reactions during the contaminant transport (i.e., sorption) has a substantial effect on the radionuclide transport. By employing probabilistic analysis, the effect of uncertainties have been quantified and the results show that the failure probabilities are quite low and the disposal system is safe.

6.8 Concluding remarks

In this chapter, probabilistic performance assessment model has been developed for disposal systems close to fractured rock mass. Modelling geosphere transport (a component of performance assessment) through sophisticated system of fractures and intact rock matrix is an arduous task. An attempt has been made to address this issue by developing a framework for modelling the flow and transport behaviour of a contaminant in fractured rock mass. This model simulates the fracture patterns from a stochastic algorithm, models the flow and transport of contaminant (through fractures and rock) and, quantifies the contaminant migration through the system. The flow and transport processes of contaminant through fracture networks have been studied for a long time, however, this model is one of the first works that captures the features of fracture geometry, variation in aperture sizes along the fracture and their influence on contaminant migration including the radionuclide transport and systematically investigate their effect. Further, the uncertainties in the input parameters affecting the system response have been quantified by employing

efficient probabilistic techniques. The chapter is divided into two major sub-divisions that presents analysis of non-reactive and reactive contaminants.

The main conclusions from the first subdivision (for non-reactive contaminant) are as follows:

1. By numerical modelling studies, the extent of influence fractured rock network (with horizontal fractures) can impart on the contaminant migration is demonstrated. The results for contaminant migration through an intact rock and fractured rock are compared. They showed that the time taken to travel through the domain in fractured rock reduced by almost half when compared to intact rock.

2. To quantify the effect of fracture geometry (i.e., the number of fractures sets and their orientations) on contaminant migration, the fractures are modelled using a fracture generation algorithm for each case and the results are computed. With the increase in the number of fracture sets, it was observed that the transport process becomes complex and results become non-trivial. Also the influence of direction of fracture flow is analysed. The main observations are:

    (a) In the case of single fracture sets, the maximum contaminant migration is observed in $0°$ and $90°$ fracture sets when the flow is along x-direction and y-direction respectively. This is because of the presence of long parallel fractures that are along the flow direction. Since there is no obstruction, they act as conduits allowing the contaminant to flow through them.

    (b) In the case of multiple fracture sets, there are preferential flow paths that leads to channelling of contaminants. The presence of a complex fracture network results in slower movement of contaminant.

372

(c) To understand the contaminant spread in the entire fracture network, the contaminant concentrations are evaluated at different points spread along and across the domain. The presence of heterogeneity in the system and its influence on the contaminant plume is estimated from this analysis.

(d) The fracture set combination $0°$ - $90°$ and $0°$ - $45°$ - $90°$ did not exhibit the influence of heterogeneity inspite of the fracture combinations. The contaminant concentration values were same for flow in both the directions. All the other fracture set combinations had the effect of heterogeneity.

(e) The concentration at end-point of interest (i.e., 10 m from the source) is always less than the peak concentration (i.e., permissible concentration) which implies that it is within safe limits.

(f) As the fracture network is heterogeneous, the contaminant movement throughout the network become non-intuitive. So, the time taken for the concentration to reach $0.5 \, C_0$ and $0.9 \, C_0$ is plotted for different fracture sets. The critical combination of fracture sets and orientations that deliver the highest concentration in least time is determined from this analysis. It was observed that amongst all the fracture set combinations considered, $90°$ - $135°$ fracture set has concentration plume spread through the domain and reaches $0.9 \, C_0$ within 70 years. This fracture set was found to be critical from the analysis.

3. The results presented from these analyses helps in providing an insight on the areas that need immediate attention to avoid subsurface pollution and also these predictions gives an estimate of the time frames for remediation techniques.

4. To understand the influence of local aperture variations along the fracture on the

contaminant transport, a new component that can integrate the aperture variations along the fracture is developed.

(a) Although, no particular pattern was observed with increase in the variation of aperture size along the fracture with respect to the concentration of contaminant, there is a notable effect of this factor. The arrangement of aperture variations along the fracture plays an important role in predicting the concentration of contaminant.

(b) Due to local variation in aperture sizes, the concentration value is affected at least by 0.5% to almost 30% of its initial value. This implies that the local variations in aperture size has an overall influence on the concentration front.

5. The effect of modelling by simulating the fracture patterns over replacing the fractures with an equivalent porous medium is illustrated. It emphasizes the need to model the fracture network in rocks for a more realistic prediction of the flow and transport behaviour.

6. To quantify the effect of uncertainties in the input parameters and also the stochastic nature of fracture generation model, probabilistic analysis is carried out.

(a) Among the various fracture set combinations, single fracture set exhibited maximum P_f of 0.6.

(b) For the same fracture set, there was a variation in P_f due to the influence of stochastic nature of fracture pattern. This illustration is made for 45° - 90° fracture set.

(c) The value of P_f for a 45° - 90° fracture network varies from 10^{-13} to 10^{-2}.

It was observed that with the increase in coefficient of variation (COV) the probability of failure increased (where 10^{-13} corresponds to 15% COV and 10^{-2} corresponds to 40% COV.

(d) By post processing the results from subset simulation, the sensitive parameters that affect the performance of disposal systems are estimated. They are matrix hydraulic conductivity (Increase in the conductivity in the matrix leads to lesser storage of solute in matrix leading to more concentration (Darcy's law)), fracture aperture part 3 and part 4 (the aperture size achieve a configuration that leads to highest conductance). It indicates that both the interacting subsystems i.e., the conductive nature of fracture and rock matrix have an important role in contaminant transport modelling.

The main conclusions from the second subdivision (for reactive contaminant) are as follows:

1. This part of the chapter mainly focussed on modelling transport of radionuclide (a reactive contaminant) through fractured rock.

2. To examine the influence of number of fracture sets, a parametric study is carried out. The concentration profiles were different from that of the trends observed for non-reactive contaminant. The influence of sorption and radioactive decay led to post-peak decay of concentration trends. With the increase in the number of fracture sets, the heterogeneity of system increased leading to fluctuations in concentration trends.

3. The effect of local aperture variations along the fracture on the radionuclide concentration is also estimated. It was observed that the time taken for the arrival of peak

concentration is almost double in the presence of local aperture variations when compared to the default case (without any aperture variations).

4. From the deterministic analysis, the risk due to radiation of iodine through drinking water pathway is estimated and the computed values fell below the range of risk experienced due to natural catastrophes and background radiation.

5. A parametric study that compares the effect of local aperture variation, stochastic fracture pattern and effect of equivalent porous medium is conducted. The results showed that there is an influence of all these factors on radionuclide transport. This study proves that the new model with the integrated components (that accounts for fracture geometry and local aperture variations) helps in simulating the geological medium better and generate more realistic results.

6. Probabilistic analysis has been performed for two scenarios (i) without the effect of local aperture variation (five parameters) (ii) with the effect of local aperture variation (nine parameters). The results are:

   (a) Probability of failure values increased with the increase in COV of the parameters which indicates that the system becomes riskier with the increase in COV.

   (b) The P_f values are slightly lower for scenario (i) when compared to scenario (ii) which implies that as the each aperture size along the fracture are treated as random variables (in scenario (ii)), more uncertainty is induced into the system leading to higher possibility of reaching failure than the case with only one random variable along the length of the fracture (scenario (i)). Also, the interplay of fracture set, its fracture orientation combination and direction of

flow of contaminant affects its concentration leading to an increased P_f in the case with local aperture variation over the one without aperture variation.

(c) Sensitivity analysis is performed and the results showed that, for scenario (i) distribution coefficient is the most sensitive parameter indicating that the reactive nature of contaminant has a primary role in influencing the contaminant transport. In the case of scenario (ii), the critical parameters are distribution coefficient, fracture aperture part 4 and part 5 (as mentioned earlier, the equivalent aperture size achieves a configuration that leads to maximum flow of contaminant)

Overall, an efficient performance assessment model has been developed to quantitatively assess the safety of a disposal system near sedimentary rock formation.The components associated with fracture generation and variation in aperture sizes along the fracture are developed as python programs. These programs facilitate the automation of simulations for deterministic and probabilistic analysis. For the scale of the domain considered in this chapter, this study demonstrates the need to model the fracture network and then estimate the concentration of the contaminant rather than approximating the system to homogeneous equivalent porous medium and modelling it for contaminant transport.

Chapter 7

Summary and Conclusions

7.1 Introduction

The disposal of radioactive waste in a proper containment facility and, its isolation from the surrounding environment is an issue of national and international interest. However, long-term safety of the disposal systems cannot be ascertained due to unwarranted risks in the form of accidents, natural catastrophes etc leading to release of wastes from these systems to the biosphere. So, predictive models that can quantitatively assess the risk due to failure of the disposal facilities over large temporal scales provide a technical basis to evaluate the performance of these facilities. In the presence of a complex heterogeneous geological environment, the uncertainties in the geological properties and transport properties of the medium and radionuclides becomes inevitable. Therefore, estimation of risk and radiation dose under probabilistic framework provides a reasonable assurance of the performance of disposal facilities. The work carried out in the thesis is mainly focussed on developing performance assessment models that treat the uncertainties due to inability in characterizing the stochasticity in geosphere (soil and fractured rocks) and also due to inherent randomness in the geological medium. A comprehensive analysis of performance assessment models in different geological media (soil and fractured rocks) are

also described. The important conclusions from the thesis are presented in the following sections.

7.2 Important conclusions from the thesis

In Chapter 1, a general introduction on radioactive waste management is presented, highlighting the necessity to develop performance assessment models that can predict the safety of radioactive waste disposal facilities during the development, operation and closure phases of design. The need to consider the impact of the uncertainties on performance of near surface disposal facilities to ensure safe design of disposal system is also emphasized. The chapter also outlines the need for the present thesis and enumerates the major objectives of chapters in the thesis in sequential order for clarity of presentation. The specific conclusions from Chapter 2, 4, 5 and 6 are summarised in the following sections.

7.2.1 Literature review

From the review of literature on radioactive waste management it is evident that, significant research has been carried out on developing predictive models to assess the long-term performance of radioactive waste disposal facilities. The framework formulated by regulatory bodies (AERB, 2006; IAEA, 2014) for safe management of low and intermediate level wastes have been implemented nationally and globally to achieve the safety objective. However, modelling the geosphere transport, a component of performance assessment is trivialized in most of the studies to reduce the computational complexities involved in the model. So, they lack in capturing the realism in geological medium especially in the case of fractured rocks. In the framework of performance assessment, the

safety is set out over large temporal and spatial scales. So, it is imperative to incorporate the effect of uncertainties on performance assessment. The evolution of geological environment over these scales and the uncertainties in the input parameters of the model need to be taken into account in the uncertainty analysis. Although, uncertainty and sensitivity analyses have been carried out in the previous studies, the computational issues involved in quantifying the uncertainties were not handled efficiently. So, there is need to to adopt computationally efficient probabilistic techniques for uncertainty propagation and quantification. The main conclusions from this chapter are:

1. The geosphere transport models need to incorporate more features that can simulate the geological medium better such as dimensionality of transport, complex boundary conditions and heterogeneity in the medium. In the case of fractured medium, not many studies have explored the effect of encompassing the local and global properties of the fractures and intact rock matrix their impact on the performance of disposal systems.

2. There is also need to address the computational issues involved in propagating and quantifying the uncertainties through complex geosphere transport models (analytical or numerical), by adopting effective meta-modelling techniques.

3. While the existence of aleatory and epistemic uncertainties has been established in literature, the modelling of random fields in a stochastic analysis has not been well exploited; and the number of studies that capture the effect of these uncertainties on the design reliability of disposal facilities is limited. So, simulation based techniques that can efficiently estimate rare event probabilities (probability of radiation dose exceeding the permissible value) needs to be adopted.

7.2.2 Risk and Reliability analysis for Near surface disposal facilities

In Chapter 4, a framework for an efficient probabilistic performance assessment model that evaluates the risk and radiological impact from near surface disposal facilities is developed. For the analysis, an analytical formulation is considered to estimate the risk due to release of radionuclides from the near surface disposal facility to a biosphere (human habitat) is based on. The results from the deterministic analysis predicted that the risk and radiation dose values for all the radionuclides are within permissible limits. As an integral part of performance assessment, it is necessary to quantify the effect of uncertainties associated with the radionuclide transport process in complex geological medium. So, the probable measure of radiation dose exceeding its permissible value at the end-point was evaluated using Monte Carlo simulation. However, the simulations were computationally expensive and this impelled the need to develop a computationally efficient model . So, a meta-modelling technique called collocation-based response surface method (CSRSM) is adopted to propagate the uncertainties through the system. When the analytical model was replaced with the new meta-model, the computational time reduced from forty minutes to a second. An added incentive of using CSRSM is that it allows the computation of global sensitivity measures (sobol indices) by post-processing the coefficients of the meta-model. Some more interesting observations drawn from the analysis are presented below.

1. The analytical formulations considered for the analysis captured the effect of different modes of disposal (single dump, multiple dump)) and also the dimensionality of the groundwater radionuclide transport model (one-dimensional, two-dimensional).

So, a total of four scenarios are considered for the performance assessment that include: single dump - 1D transport model, single dump - 2D transport model, multiple dump - 1D transport model and multiple dump - 2D transport model.

(a) An algorithm is developed and coded in MATLAB to estimate the annual release rate, radiation dose and risk due to infiltration of water into the disposal facility, leading to sequential failure of barrier system and further transport to a human habitat through drinking water pathway. The results were evaluated for seven radionuclides (^{3}H, ^{14}C, ^{59}Ni, ^{99}Tc, ^{129}I, ^{237}Np and ^{239}Pu).

(b) Amongst the seven radionuclides, the maximum concentration is delivered by carbon (^{14}C) and the maximum dose is delivered by Iodine (^{129}I). These values are observed for the above radionuclides due to low sorption values and high half-lives.

(c) When the dimensionality of radionuclide-dispersion model in groundwater varied from 1D to 2D, a slight reduction maximum concentration values is observed. The slight difference in these values can be attributed to discrepancy in the evaluation of the cross sectional area of aquifer and also the assumption of uniform lateral mixing (in 1D model).

(d) By comparing the results for different modes of disposal, it was observed that the maximum concentration are almost same for both the dump modes. Slight variations are observed only for short-lived radionuclides.

(e) In the deterministic analysis, the maximum risk value estimated at the endpoint is lower than the risk due to industrial failures/catastrophes and also, natural background radiation.

2. CSRSM is employed to propagate the uncertainty in the input parameters and develop a surrogate model at the time of arrival of peak concentration. From the results it was found that, third order polynomial gave the best approximation to deterministic model with a coefficient of determination (R^2) of 0.99. The computational efficiency of the meta-models is demonstrated in this chapter for all the four scenarios.

3. The probability of failure P_f (radiation dose exceeding the permissible value) estimated from the Monte Carlo simulations is very low (in the range of 10^{-3}) suggesting that the risk due to migration of radionuclide (^{14}C) through drinking water pathway is negligible and also the barrier system is designed efficiently.

4. The sobol indices are obtained from global sensitivity analysis and, it is observed that the distribution coefficient is the most sensitive parameter that can have an impact on system's performance.

7.2.3 Probabilistic analysis of radionuclide transport for radioactive waste disposal facilities in soil

In chapter 4, a two-dimensional radionuclide transport model was used to predict the behaviour of radionuclides through the soil medium. But, as the dimensionality of the problem and the complexity of domain increases, developing analytical solutions becomes challenging. To overcome the above limitations and build a realistic model with complex boundary conditions, a three-dimensional numerical model is developed to predict the radionuclide transport patterns through soils in chapter 5. Also, the influence of epistemic (i.e., input parameter and model uncertainties) and aleatory uncertainties (inherent ran-

domness in soil properties) on the results (risk and radiation dose values) are investigated in this chapter. These studies help in gaining a thorough understanding on the significance of geological medium (soil) on probabilistic performance assessment models. By implementing various probabilistic methods in this study, a technical basis is created for the decision makers in gaining a level of confidence in the model results. The main conclusions from this chapter are presented below.

1. A three-dimensional groundwater radionuclide transport model with a decaying source is modelled numerically to determine the radiation dose at different points of interest for short-lived (Strontium (^{90}Sr), Caesium (137Cs)) and long-lived radionuclides (Carbon(^{14}C) and Iodine(^{129}I)).

2. The concentration and radiation dose of the radionuclides are computed upto a distance of 50 m (for short-lived radionuclides) and 200 m (for long-lived radionuclides) from the source as they become negligible (innocuous levels) beyond these points. The results from the deterministic analysis demonstrated the effect of inventory value, distribution coefficient and half-life of radionuclides on the radiation dose values.

3. It is observed that the maximum values of risk computed from the model are lower than the risk observed from industrial accidents and natural catastrophes.

4. The parameter uncertainty and the model uncertainty (for abstracting the real response of the system) are propagated through the system using CSRSM. The results showed that a second order polynomial approximated the response of the system (i.e., peak concentration) accurately with an R^2 value of 0.99 for all the radionuclides. The deterministic (FEM model) and probabilistic parts of the analysis are

bridged using PYTHON programming interface.

5. The P_f is estimated for Caesium and Iodine by performing reliability analysis using subset simulation method. The range of probability of failure is estimated as 10^{-8} - 10^{-9}. These P_f values indicates a safely designed disposal system. As the simulations using numerical model were computationally expensive, it was replaced with the surrogate model. By doing so, the computation time reduced drastically from 3 days to ≈ 10 seconds. The advantage of Method 1 (using CSRSM) and Method 2 (using numerical model) are demonstrated.

6. Further, global sensitivity analysis is carried out using polynomial chaos based approach and sobol indices are obtained. The Sobol indices for both short-lived and long-lived radionuclides showed that, the critical parameters affecting radiation dose values are mainly distribution coefficient and groundwater velocity (slightly). It indicates that, amongst the uncertain input parameters considered in the analysis, these parameters exhibit maximum influence on the performance of NSDFs.

7. To explore the effect of spatial variability in soil on radionuclide transport process, a two-dimensional numerical model is developed. The spatial variability in hydraulic conductivity of soil medium is modelled as a random field and discretized using Karhunen-Loeve series expansion.

8. The results from the deterministic analysis showed that the risk values computed for spatially varying medium are lower than the risk due to industrial failures /catastrophes and also, natural background radiation.

9. The rate of movement of radionuclide is slower in spatially varying medium when

compared to homogeneous medium. The reason being, for small auto-correlation lengths (i.e., rough field), the scale of fluctuation in the conductivity values along the length of the domain becomes more frequent. So, the flow path for radionuclide movement becomes erratic leading to slower movement. However, for large auto-correlation lengths (i.e., smooth field), the medium becomes less heterogeneous and, allows the radionuclide to move faster.

10. The influence of auto-correlation length and the coefficient of variation (COV) on the probability of failure are investigated. The P_f values for different cases ranged between 10^{-9} to 10^{-1}. The results are evaluated by using subset simulation (for low P_f) and Monte Carlo simulation (for higher P_f). The results showed that:

   (a) P_f value increased with the increase in COV of random field. At low auto-correlation lengths, there is a significant influence of COV on P_f and vicev-ersa. P_f value increased with the increase in auto-correlation length of random field. This is because, in a highly heterogeneous system, the rate of contami-nant movement is slower leading to lower P_f, whereas, in less heterogeneous case, the rate of contaminant movement is faster leading to higher P_f.

11. From the design point of view, radionuclide transport through homogeneous medium results in high P_f. But in reality, the medium is heterogeneous and the estimated P_f values are quite low indicating that the performance of system is underestimated by assuming the medium to be homogeneous. This study illustrates the need to model a spatially varying medium to predict the probabilistic performance of NSDFs ac-curately.

7.2.4 Probabilistic analysis of contaminant transport in fractured rocks

One of the important components considered in evaluating the performance of radioactive waste disposal facilities is the geosphere transport model as it has an impact on their long-term performance. This model essentially predicts the movement of radionuclides in geosphere. In chapter 6, the influence of rocky geological environment (fractured sedimentary rock) on the radionuclide transport and the performance of radioactive disposal facilities is explored. The work is mainly focussed on developing a discrete fracture network model that captures the effect of the features of fracture geometry, variation in aperture sizes along the fracture and their influence on contaminant migration. Also, the uncertainties in the input parameters affecting the system response have been quantified by employing efficient probabilistic techniques. A probabilistic performance assessment model is developed for a disposal facility designed near fractured sedimentary rock formation. To gain an overall understanding of the transport behaviour in a complex fractured medium, geosphere transport modelling is carried out for a non-reactive contaminant (case I) and a reactive contaminant (case II). The main conclusions from this chapter are

1. A new hybrid model that integrates a stochastic fracture pattern generation algorithm, and, a numerical contaminant transport model is proposed. Also, a new feature that handles the effect of local aperture variation along the fracture is developed and integrated into the hybrid model.

2. In both the cases, a parametric study is carried out to study the effect of number of fracture sets, fracture orientation and transport properties in fracture and rock matrix on the contaminant transport.

3. The main conclusions from the analysis for non-reactive contaminant (salt solution) are:

   (a) Amongst the single fracture sets considered for the analysis ($0°$, $45°$, $90°$, $135°$), the $0°$ and $90°$ fracture sets are critical as the active flow paths are along the flow direction. In the case of multiple fracture sets, the presence of a complex heterogeneous fracture network leading to slower movement of contaminant is reflected in the results.

   (b) In the case of multiple fracture sets, the critical combination of fracture sets and orientations that deliver the highest concentration in least time is observed in $90°$ - $135°$ fracture set which makes it one of the critical sets in the analysis.

   (c) Due local variation in aperture sizes, the concentration value is affected at least by 0.5% to almost 30% of its initial value suggesting the influence of local variations in aperture size on the concentration front.

   (d) The probabilistic analysis results quantify the extent of pollution possible due contaminant migration under the influence of uncertainties. The random variables considered for the analysis are matrix conductivity, matrix porosity, fracture aperture size (local aperture variation into five parts), fracture dispersion and fracture diffusion. The probability of failure (P_f) i.e., the probability of concentration exceeding the permissible concentration are estimated for various fracture networks using subset simulation. The results showed that P_f is maximum for single fracture set network. In the case of fracture set combinations, the P_f values ranged in 10^{-3} to 10^{-5}.

   (e) The influence of stochastically generated fracture pattern on P_f is also exam-

ined. For 45° - 90° fracture network, three fracture patterns are generated stochastically and the P_f value is evaluated from each fracture pattern. Each fracture pattern corresponds to a unique arrangement of fractures. The results showed that the P_f (30% COV) value estimated for each fracture pattern are 10^{-2}, 10^{-4} and 10^{-3} indicating the arrangement of fractures are has an impact on P_f.

(f) The effect of COV of uncertain input parameters on P_f showed that with the increase in COV, P_f value also increased.

(g) The critical parameters from sensitivity analysis are estimated by post-processing the results from subset simulation. They are matrix conductivity and size of the aperture segments (part 3 and part 4) along the fracture. These results indicate that both the interacting subsystems i.e., the conductive nature of fracture and rock matrix have an important role in contaminant transport modelling.

4. So, the results presented from these analyses helps in providing an insight on the areas that need immediate attention to avoid subsurface pollution and also these predictions gives an estimate of the time frames for remediation techniques.

5. The main conclusions from the analysis for reactive contaminant (radioactive Iodine ^{129}I) are:

(a) With the increase in the number of fracture sets, the concentration value reduced indicating this effect is due to the increase in heterogeneity of system (increasing number of fractures). The increase in the number of fractures sets creates a more complex fracture network leading to slower movement of radionuclides.

(b) A parametric study on the influence on number of fracture sets suggested that with the increase in the number of fracture sets, the heterogeneity of system increased leading to fluctuations in concentration trends.

(c) Th influence local aperture variations in the fracture network on the radionuclide transport is investigated. The results show that, local aperture variations in fractures create a more complex fracture network leading to slower movement of radionuclides.

(d) The risk estimated from the deterministic analysis for all the cases is compared with the risk due to natural catastrophes and natural background radiation. The values are found to be within the safe limits.

(e) The probabilistic analysis is carried for a typical fracture set (45° - 90°) using subset simulation. The random variables considered are matrix porosity, matrix distribution coefficient, fracture aperture (five parts), fracture diffusion, fracture dispersivity. The results showed that the P_f with the increase in COV.

(f) By post-processing the subset simulation results, the sensitive parameters are observed to be distribution coefficient and size of the aperture segments (part 4 and part 5) along the fracture. This suggests that the process of sorption and the conductivity of fractures play a critical role in radionuclide transport modelling.

6. Overall, a comprehensive analysis on long-term performance of radioactive waste disposal facility designed near fractured sedimentary rock is presented. The influence of fracture geometry, geological and transport properties of fractures and rock matrix are investigated. The impact of uncertainties on system performance is

quantified by performing reliability and sensitivity analyses.

In complex systems like radioactive waste repositories, the relative success in modelling the system depends on how well it is understood. So, this thesis attempted to develop probabilistic performance assessment models for radioactive waste disposal systems designed in different geological media. The significance of geosphere transport on the performance assessment is highlighted in the thesis. So, models developed for the analysis have addressed the challenges involved in simulating different geological media over large spatial and temporal scales. New radionuclide transport models are proposed to capture the complexities in dimensionality of the problem, boundary conditions, geological and transport properties of soil, fractures and rock. The models also considered the natural variations (aleatory uncertainty) in the geological properties, uncertainties in the input parameters of the model (epistemic uncertainty) in evaluating the performance of radioactive waste repositories. These uncertainties are characterized, propagated and quantified by employing effective probabilistic techniques that include Karhunen-Loeve (K-L) series expansion method, Collocation based stochastic response surface method (CSRSM) and subset simulation (SS) method. The efficiency of these methods is illustrated by comparing computational time taken in estimating the results with respect to traditional Monte Carlo simulation. The algorithms that integrate the deterministic and probabilistic parts of analysis are programmed in MATLAB and PYTHON to automate the simulations. Further, the critical parameters (amongst the uncertain input parameters) that influence the model response the most are estimated from sensitivity methods including global sensitivity analysis.

Appendix A

A.1 Multivariate Hermite polynomials

The Hermite polynomials $H(x)$ are defined in the following formula as indicated in Abramowitz and Stegan (1948). A multivariate Hermite polynomial is stated as the product of several univariate Hermite polynomials of different variables. The one-dimensional hermite polynomials are given by :

$$H_0(\delta) = 1$$

$$H_1(\delta) = \delta$$

$$H_2(\delta) = \delta^2 - 1$$

$$H_3(\delta) = \delta^3 - 3\delta$$

$$H_4(\delta) = \delta^4 - 6\delta^2 + 3 \tag{A.1}$$

$$H_5(\delta) = \delta^5 - 10\delta^3 + 15\delta$$

$$H_6(\delta) = \delta^6 - 14\delta^4 + 45\delta^2 - 15$$

$$\vdots$$

$$H_n(\delta) = \delta H_{n-2}(\delta) - H_{n-1}(\delta)$$

A.2   Development of polynomial chaos equations

A PCE of order M=3 using only R=2 random variables (δ_1 and δ_2) is considered as an illustrative example to estimate the surrogate equation using polynomial chaos expansion (PCE) (Al-Bittar, 2012).

Table A.1: Details of polynomial chaos expansion of two variables

κ	Order of the term Ψ_κ	$\Psi_\kappa = \prod\limits_{i=1}^{R} H_{\alpha_i}(\delta_i)$	$\mathbf{E}[\Psi_\kappa^2] = \prod\limits_{i=1}^{R} \alpha_i!$
0	p = 0	$\Psi_0 = H_0(\delta_1) \times H_0(\delta_2) = 1$	$\alpha_1! \times \alpha_2! = 0! \times 0! = 1$
1		$\Psi_1 = H_1(\delta_1) \times H_0(\delta_2) = \delta_1$	$\alpha_1! \times \alpha_2! = 1! \times 0! = 1$
2	p = 1	$\Psi_2 = H_0(\delta_1) \times H_1(\delta_2) = \delta_2$	$\alpha_1! \times \alpha_2! = 0! \times 1! = 1$
3		$\Psi_3 = H_1(\delta_1) \times H_1(\delta_2) = \delta_1\delta_2$	$\alpha_1! \times \alpha_2! = 1! \times 1! = 1$
4	p = 1	$\Psi_4 = H_2(\delta_1) \times H_0(\delta_2) = \delta_1^2 - 1$	$\alpha_1! \times \alpha_2! = 2! \times 0! = 2$
5		$\Psi_5 = H_0(\delta_1) \times H_2(\delta_2) = \delta_2^2 - 1$	$\alpha_1! \times \alpha_2! = 0! \times 2! = 2$
6		$\Psi_0 = H_2(\delta_1) \times H_1(\delta_2) = (\delta_1^2 - 1)\delta_2$	$\alpha_1! \times \alpha_2! = 2! \times 1! = 2$
7		$\Psi_1 = H_1(\delta_1) \times H_2(\delta_2) = \delta_1(\delta_2^2 - 1)$	$\alpha_1! \times \alpha_2! = 1! \times 2! = 2$
8	p = 3	$\Psi_2 = H_3(\delta_1) \times H_0(\delta_2) = \delta_1^3 - 3\delta_1$	$\alpha_1! \times \alpha_2! = 3! \times 0! = 6$
9		$\Psi_2 = H_0(\delta_1) \times H_3(\delta_2) = \delta_2^3 - 3\delta_2$	$\alpha_1! \times \alpha_2! = 0! \times 3! = 6$

In Table A.1, the α_i represents the highest order of the corresponding variable in the polynomial term Ψ_κ. As, two random variables have been considered in the problem, the multi-index α, takes values α_1 and α_2. Further, the important set of inputs and the polynomial equations for two random variable and different orders of polynomial expansion are presented below (Huber et. al., 2011).

Table A.2: Details of polynomial chaos expansion of two variables

M	Roots of Hermite polynomials for an order M+1	Expression PCEs for different orders	PCE_n	m
2	$\{0; \pm\sqrt{3}\}$	$P_2 = a_0 + a_{1,0}\Gamma_{1,0}(\delta_1) + a_{0,1}\Gamma_{0,1}(\delta_2)$ $+ a_{2,0}\Gamma_{2,0}(\delta_1) + a_{1,1}\Gamma_{1,1}(\delta_1,\delta_2) + a_{0,2}\Gamma_{0,2}(\delta_2)$	6	9
3	$\pm\sqrt{3 \pm \sqrt{6}}$	$P_3 = a_0 + a_{1,0}\Gamma_{1,0}(\delta_1) + a_{0,1}\Gamma_{0,1}(\delta_2)$ $+ a_{2,0}\Gamma_{2,0}(\delta_1) + a_{1,1}\Gamma_{1,1}(\delta_1,\delta_2) + a_{0,2}\Gamma_{0,2}(\delta_2)$ $+ a_{3,0}\Gamma_{3,0}(\delta_1) + a_{2,1}\Gamma_{2,1}(\delta_1,\delta_2) + a_{1,2}\Gamma_{1,2}(\delta_1,\delta_2) + a_{0,3}\Gamma_{0,3}(\delta_2)$	10	16
4	$\left\{0; \pm\sqrt{5 \pm \sqrt{10}}\right\}$	$P_4 = a_0 + a_{1,0}\Gamma_{1,0}(\delta_1) + a_{0,1}\Gamma_{0,1}(\delta_2) + a_{2,0}\Gamma_{2,0}(\delta_1)$ $+ a_{1,1}\Gamma_{1,1}(\delta_1,\delta_2) + a_{0,2}\Gamma_{0,2}(\delta_2) + a_{3,0}\Gamma_{3,0}(\delta_1) + a_{2,1}\Gamma_{2,1}(\delta_1,\delta_2)$ $+ a_{1,2}\Gamma_{1,2}(\delta_1,\delta_2) + a_{0,3}\Gamma_{0,3}(\delta_2) + a_{4,0}\Gamma_{4,0}(\delta_1) + a_{3,1}\Gamma_{3,1}(\delta_1,\delta_2)$ $+ a_{2,2}\Gamma_{2,2}(\delta_1,\delta_2) + a_{1,3}\Gamma_{1,3}(\delta_1,\delta_2) + a_{0,4}\Gamma_{0,4}(\delta_2)$	15	25

In Table A.2, PCE_n represents the number of the unknown PCE coefficients; m is the number of the available collocation points, δ_1 and δ_2 - input random variables; $\Gamma_{.,.}$ - is multivariate Hermite polynomial.

Using Table A.1 and Table A.2, the PCE (for M=3 using only R=2) as function of the input random variables is given by equation:

$$F(\delta) = u_0 + u_1(\delta_1) + u_2(\delta_2) + u_3(\delta_1\delta_2) + u_4(\delta_1^2 - 1) + u_5(\delta_2^2 - 1)$$
$$+ u_6(\delta_1^2 - 1)\delta_2 + u_7(\delta_2^2 - 1)\delta_1 + u_8(\delta_1^3 - 3\delta_1) + u_9(\delta_2^3 - 3\delta_2) \tag{A.2}$$

These results are post-processed to estimate the Sobol indices.

A.3 Estimating the sobol indices

The Sobol index as a function of the different terms of the PCE (Sudret 2008; Al-Bittar, 2012):

$$S(\delta_i) = \frac{\sum\limits_{\kappa \varepsilon I_i} \alpha_\kappa^2 E(\Gamma_\beta^2)}{\sum\limits_{j=0}^{p-1} E[\Gamma_j^2(\delta)]} \tag{A.3}$$

where I_i denotes the set of indices κ for which the corresponding terms, Γ_β are only functions of the random variable δ_i and $E(\Gamma_\beta^2) = \prod\limits_{i=1}^{n} \alpha_i!$. Thus the expressions of the first order Sobol indices for the two random variables of the above problem can be written as

$$S(\delta) = \frac{u1^2 + 2u_4^2 + 6u_8^2}{u_1^2 + u_2^2 + u_3^2 + 2u_4^2 + 2u_5^2 + 2u_6^2 + 2u_7^2 + 6u_8^2 + 6u_9^2} \tag{A.4}$$

$$S(\delta) = \frac{u2^2 + 2u_5^2 + 6u_9^2}{u_1^2 + u_2^2 + u_3^2 + 2u_4^2 + 2u_5^2 + 2u_6^2 + 2u_7^2 + 6u_8^2 + 6u_9^2} \tag{A.5}$$

where I_1=(1,4,8) and I_2=(2,5,9)

Appendix B

The sequence of steps followed to generate a Finite Element mesh for a fractured rock in FEFLOW is demonstrated by a simple example.

B.1 Generation of Finite Element mesh for a fractured medium

A two-dimensional domain of 32 m $\times$ 32 m is considered for the study and solute transport through horizontal, vertical and inclined fractures are modelled.
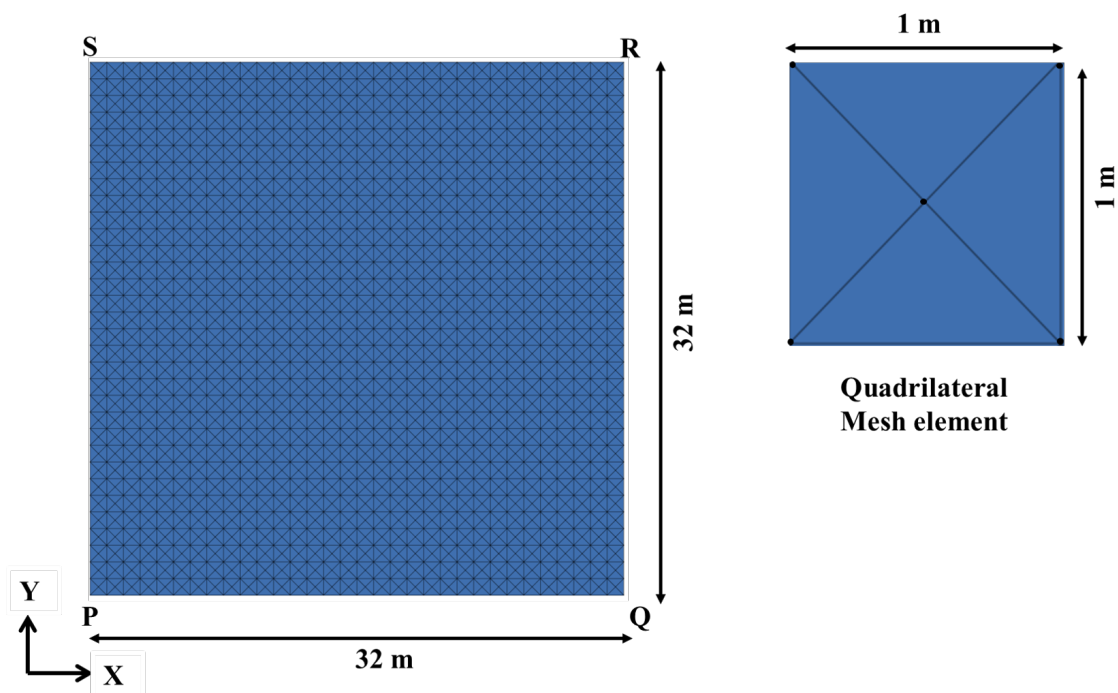
Figure B.1: FE mesh

To simulate the mesh, a quadrilateral mode of mesh generation is considered (Note: The shape functions of quadrilateral elements provide a better basis for solving the problem). This quadrilateral mesh is refined further such that a new node is introduced at the center of each quadrilateral mesh element. Due to this refinement, inclined fractures could also be generated. So, a mesh with 1089 nodes as shown in Figure B.1 is created. By using this mesh model, fractures of $0°$, $45°$, $90°$ and $135°$ orientations could be created.

B.2 Adding discrete features to the existing mesh

The fractures are introduced into the system as discrete elements. In the case of a two-dimensional medium, the fractures are one-dimensional elements. The fracture element can be generated either by 'slice edge' or 'arbitrary nodal path'. In the thesis, the latter method has been adopted for fracture generation. They are generated based on 'node-to-node' connectivity. Suppose we considered a small section 'ABCD' (for ease of visualizing the fracture) as shown in Figure B.2, to create a fracture of around 4 to 5 m length in this section the following steps are followed.

1. Initially, a discrete element is created by connecting node H1 to node H2 (Note: In python interface, IfmCreateFracElement is used to create the fracture element. See Figure B.2 (i). This command is a function of two nodes adjacent to each other). So, a horizontal fracture of 1 m is created. Further the same command is used to connect the nodes H2-H3, H3-H4, H4-H5 to create a 4 m fracture. In simple terms it means that the concentration moves along the fracture from node-to-node. Same procedure is followed for vertical fracture also.
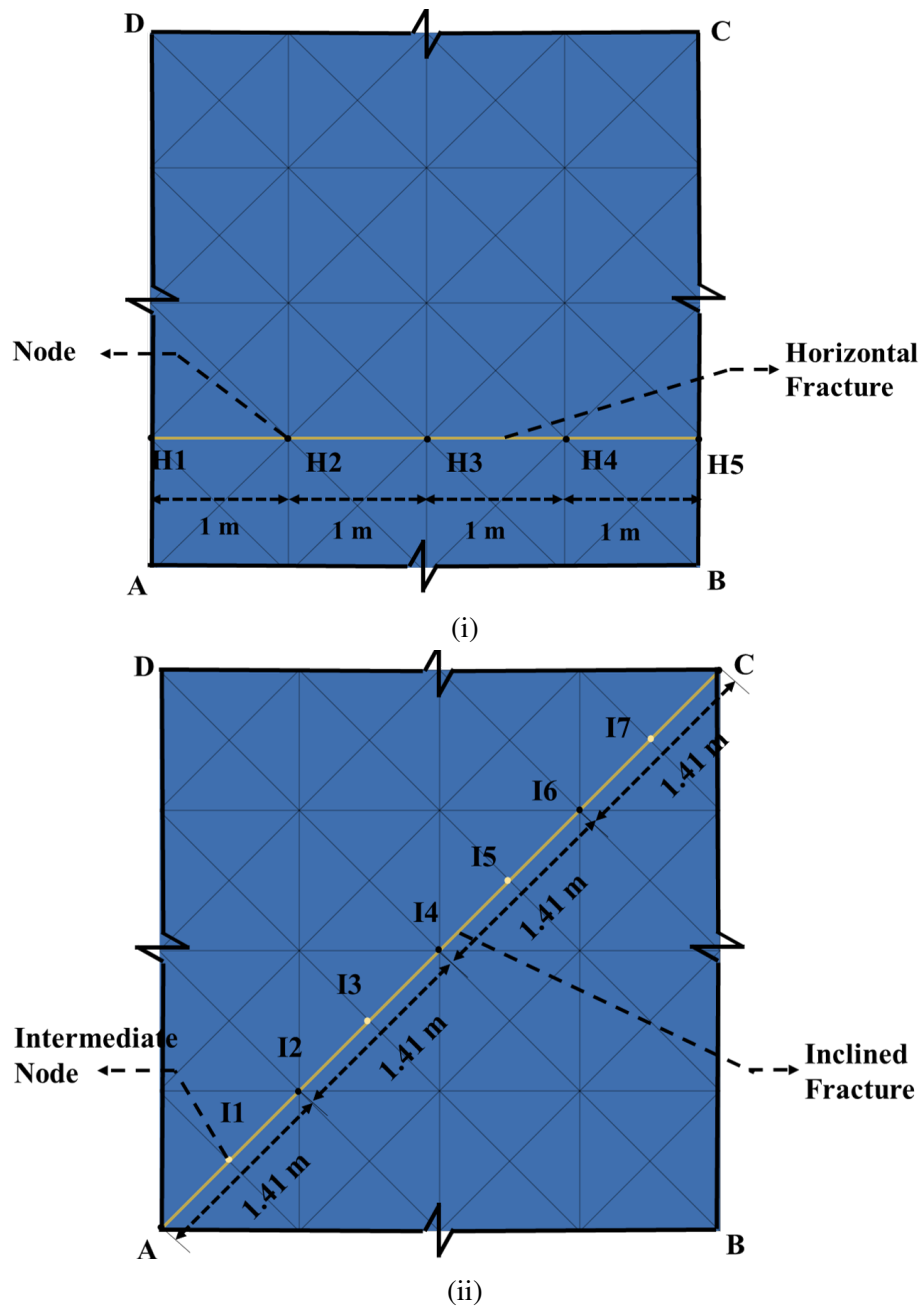
Figure B.2: (i) Horizontal fracture (ii) Inclined fracture

(a) It is important to note the fracture of any length needs to be divided into sections depending on the length of single mesh element. (Here since each element is 1 m long, the 4 m fracture is divided into four sections).

2. For the case of inclined fracture, the intermediate nodes (I1, I3, I5, I7) play an important role in node-to-node connectivity. See Figure B.2 (ii). This is because,

398

without connectivity between these nodes, a fracture element cannot be created. So by connecting nodes A to I1 a fracture element of 0.41 m is created. This process is repeated from node I1 to C (I1-I2, I2-I3, I3-I4,....I7-C). From Fgure B.2 (ii), we can observe that by connecting all these nodes a fracture of length around 5.6 m and 45° orientation is created. The same process can be adopted for 135° fracture.

3. After creating the fracture of required length and orientation, the properties of fracture like its aperture size, area, dispersivity, sorption and diffusion properties are assigned. (Note: In python interface, IfmsetFracArea, IfmsetFracFlowConductivity, IfmsetFracMassLongDispersivity,Ifm setFracMassSorptionCoeff and IfmsetFracMassDiffusion commands are used to set the properties)

To demonstrate accuracy of results from 'slice edge' option and 'arbitrary node path' option, a 4 m fracture in all the four fracture orientations is considered. The initial ad boundary conditions are as mentioned in Table 6.1 and an initial concentration of 1 mg/l are considered for the analysis. The concentration of contaminant versus time trends at every 1m within the fracture are compared for both the methods.

(a) For 0° inclination   (b) For 90° inclination
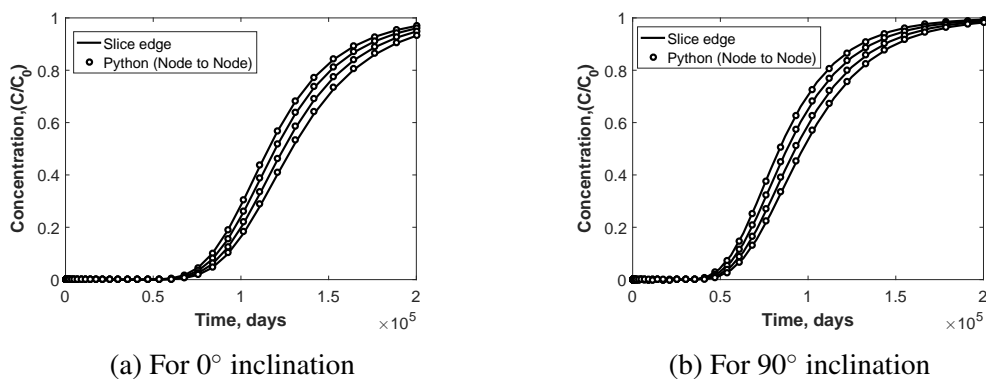
Figure B.3: Comparison of two methods of fracture modelling for horizontal and vertical fractures

(a) 45° inclination

(b) 135° inclination
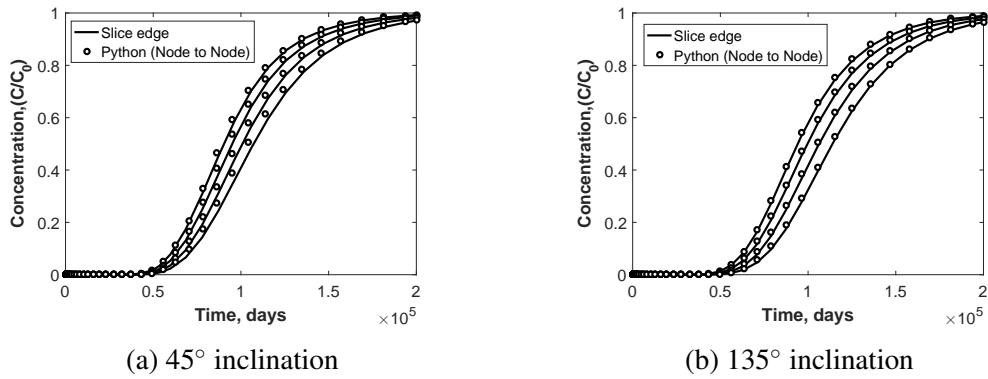
Figure B.4: Comparison of two methods of fracture modelling for inclined fractures

Figure B.3, B.4 shows that the contaminant movement along the fracture created using both the methods match well. So, the fractures are created using arbitrary node path option (i.e., by coding in python interface) for the rest of the analysis in Chapter 6.

B.2.1 Single fracture

By assigning boundary conditions for flow and transport (as mentioned in Table 6.4) along PS and QR sections of the domain, the solute transport through a horizontal fracture is simulated. An initial concentration of 10 mg/l is assigned at the boundary (PS). The results of concentration front movement over time is presented below.

(i) 12000 days

(ii) 28000 days

(iii) 54750 days
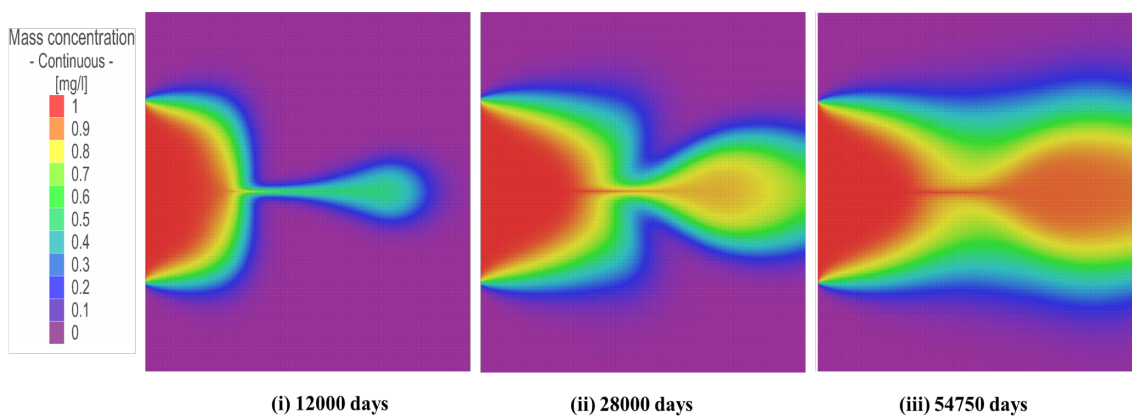
Figure B.5: Contaminant movement through a single horizontal fracture

The concentration versus time at different observation points (1, 2, 3, 4, 5, 6) of a rock

with single horizontal and inclined fracture when the flow is along *x* direction are shown

in the figure below.
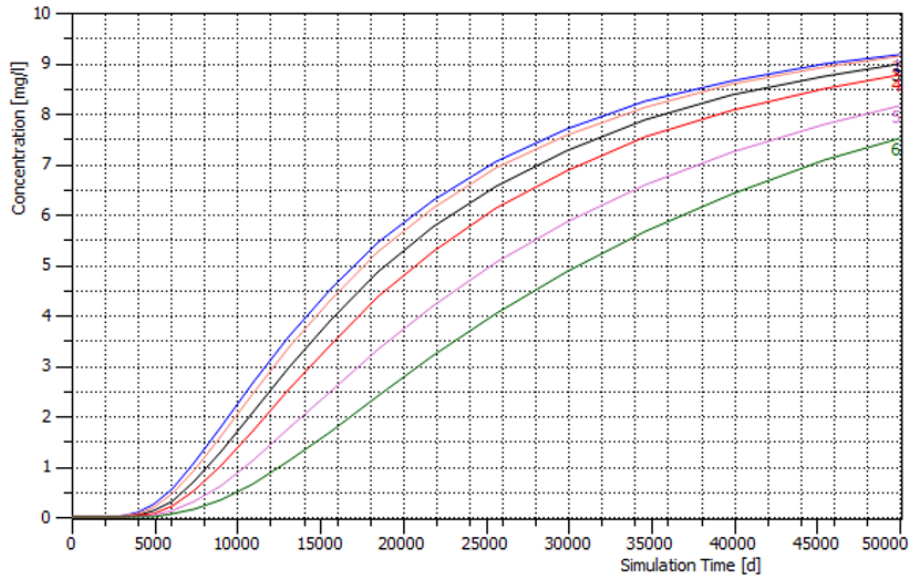
(i)
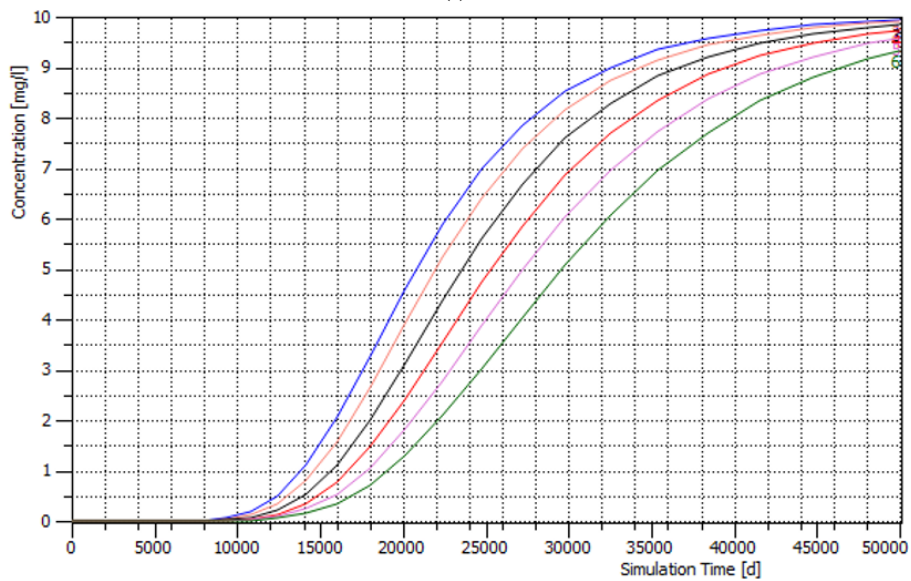
(ii)

Figure B.6: (i) Horizontal fracture (ii) Inclined fracture

The trend line at '1' in Figure B.6 (i) corresponds to node H1, trend line '2' in Figure

B.6 (i) corresponds to node H2 and so on. Similarly, in Figure B.6 (ii), the trend line '1'

correspond to node A, the trend line '2' correspond to node I2 (observation points were

not on intermediate nodes) and so on. This shows that the concentration along the fracture

is moving from node to node.

B.2.2 Multiple fractures

Unlike the previous case where only one or two fractures were considered, in the thesis, a fracture network with more than 100 fractures need to be generated. So, a routine has been developed such that the code automatically detects the fracture orientation from the output of fracture pattern generation algorithm. This helps in automatically importing the fractures onto the FE mesh. The steps followed are:

1. The (x, y) coordinates of the fractures belonging to different orientations and different fracture sets are generated from the pattern generation algorithm.

2. These coordinate values are matched with the corresponding co-ordinates of FE mesh.

3. Then, depending on the length of each fracture, using the 'node-to-node' connectivity feature explained earlier, the 1D fracture elements are imported onto FE mesh.

The results for multiple fractures and the contaminant plume movement over time are discussed in detail in Chapter 6.

References

1. Abramowitz, M., & Stegun, I. A. (1948). *Handbook of mathematical functions with formulas, graphs, and mathematical tables* (Vol. 55). US Government printing office.

2. Abu-Khader, M. M. (2009). Recent advances in nuclear power: A review. *Progress in Nuclear Energy*, *51*(2), 225–235.

3. Ackerer, P., Younes, A., & Mose, R. (1999). Modeling variable density flow and solute transport in porous medium: 1. numerical model and verification. *Transport in Porous Media*, *35*(3), 345–373.

4. Adinarayana, K., Ali, S. M., & Balasubramaniyan, V. (2017). Numerical modelling of radionuclide migration in a nsdf using porflow. In *Ishmt digital library.*

5. Adler, R. J. (1981). *The geometry of random fields*. SIAM.

6. AERB. (2007). *Management of radioactive waste* (Tech. Rep.). Atomic Energy Regulatory Board.

7. AERB. (2011). *Classification of radioactive waste* (Tech. Rep.). Atomic Energy Regulatory Board.

8. Ahmed, A., & Soubra, A.-h. (2012). Extension of subset simulation approach for uncertainty propagation and global sensitivity analysis. *Georisk : Assessment and Management of Risk for Engineered Systems and Geohazards*, *6*(3), 37–41. doi: 10.1080/17499518.2012.656296

9. Ahmed, A., & Soubra, A.-H. (2018). Application of the subset simulation approach to spatially varying soils. In *Risk and Reliability in Geotechnical Engineering* (pp. 591–625). CRC Press.

10. Aladejare, A. E., & Wang, Y. (2017). Evaluation of rock property variability. *Georisk: Assessment and Management of Risk for Engineered Systems and Geohazards*, *11*(1), 22–41.

11. Aladejare, A. E., & Wang, Y. (2018). Influence of rock property correlation on reliability analysis of rock slope stability: from property characterization to reliability analysis. *Geoscience Frontiers*, *9*(6), 1639–1648.

12. Al-Bittar, T. (2012). *Probabilistic analysis of shallow foundations resting on spatially varying soils* (Doctoral dissertation, Nantes). Retrieved from file:///C:/Users/User/Downloads/Thesis_Tamara_Al_Bittar

`_correction_6_12_finale.pdf`

13. Alexander, W. R., Smith, P. A., & McKinley, I. G. (2003). Modelling radionuclide transport in the geological environment: a case study from the field of radioactive waste disposal. In *Radioactivity in the Environment* (Vol. 4, pp. 109–145). Elsevier.

14. Allan R. Cherry, J. A. F. (1979). *Groundwater*. Prentice Hall, Englewood Cliffs, NJ.

15. Ang H-S, A., & Tang, H. W. (1975). *Probability concepts in engineering planning and design. vol. 1, basic principles* (No. BOOK).

16. Apostolakis, G. (1990). The concept of probability in safety assessments of technological systems. *Science*, *250*(4986), 1359–1364.

17. Ashraf, A., & Ahmad, Z. (2008). Regional groundwater flow modelling of upper chaj doab of indus basin, pakistan using finite element model (feflow) and geoinformatics. *Geophysical Journal International*, *173*(1), 17–24.

18. Asif, M. (2004). Experimental study of the transport of pollutants in groundwater. In *International Conference on Water Resources & Arid Environment.*

19. Atomic Energy Regulatory Board Safety Guide. (2006). *Near surface disposal of radioactive solid waste (NO. AERB/NRF/SG/RW-4)* (Tech. Rep.).

20. Au, S. K., & Beck, J. L. (2001). Estimation of small failure probabilities in high dimensions by subset simulation. *Probabilistic Engineering Mechanics*, *16*(4), 263–277. doi: 10.1016/S0266-8920(01)00019-4

21. Baalousha, H., & Köngeter, J. (2006). Stochastic modelling and risk analysis of groundwater pollution using form coupled with automatic differentiation. *Advances in Water Resources*, *29*(12), 1815–1832.

22. Baalousha, H. M. (2003). *Risk assessment and uncertainty analysis in groundwater modelling* (Doctoral dissertation, Bibliothek der RWTH Aachen). Retrieved from `https://www.researchgate.net/publication/34930190_Risk _assessment_and_uncertainty_analysis_in_ground_water_modeling`

23. Baecher, G. B., & Christian, J. T. (2003). *Reliability and statistics in geotechnical engineering*. John Wiley & Sons.

24. Bai, T., & Pollard, D. D. (2000). Fracture spacing in layered rocks: A new explanation based on the stress transition. *Journal of Structural Geology*, *22*(1), 43–57. doi: 10.1016/S0191-8141(99)00137-6

25. Barenblatt, G., Zheltov, I., & Kochina, I. (1960). Basic concepts in the theory of seepage of homogeneous liquids in fissured rocks [strata]. *Journal of Applied Mathematics and Mechanics*, *24*(5), 1286–1303. Retrieved from `http:// linkinghub.elsevier.com/retrieve/pii/0021892860901076` doi: 10.1016/ 0021-8928(60)90107-6

26. Barker, J. (1982). Laplace transform solutions for solute transport in fissured aquifers. *Advances in Water Resources*, *5*(2), 98–104.

27. Barton, R. R. (1992). Metamodels for simulation input-output relations. In *Proceedings of the 24th conference on winter simulation* (pp. 289–299).

28. Bear, J., Tsang, C.-F., & De Marsily, G. (1993). *Flow and contaminant transport in fractured rock.* Academic Press.

29. Benaafi, M., Hariri, M., Bertotti, G., Al-Shaibani, A., Abdullatif, O., & Makkawi, M. (2019). Natural fracture system of the cambro-permian wajid group, wadi al-dawasir, sw saudi arabia. *Journal of Petroleum Science and Engineering, 175*, 140–158.

30. Berkowitz, B. (2002). Characterizing flow and transport in fractured geological media: A review. *Advances in Water Resources, 25*(8-12), 861–884.

31. Berkowitz, B., Bear, J., & Braester, C. (1988). Continuum models for contaminant transport in fractured porous formations. *Water Resources Research, 24*(8), 1225–1236. doi: 10.1029/WR024i008p01225

32. Berkowitz, B., & Scher, H. (1997). Anomalous transport in random fracture networks. *Physical review letters, 79*(20), 4038.

33. Bibby, R. (1981). Mass transport of solutes in dual-porosity media. *Water Resources Research, 17*(4), 1075–1081.

34. Blatman, G., & Sudret, B. (2010). An adaptive algorithm to build up sparse polynomial chaos expansions for stochastic finite element analysis. *Probabilistic Engineering Mechanics, 25*(2), 183–197.

35. Blum, P., Mackay, R., Riley, M., & Knight, J. (2005). Performance assessment of a nuclear waste repository: upscaling coupled hydro-mechanical properties for far-field transport analysis. *International Journal of Rock Mechanics and Mining Sciences, 42*(5-6), 781–792.

36. Bonano, E. J., & Cranwell, R. M. (1988). Treatment of uncertainties in the performance assessment of geologic high-level radioactive waste repositories. *Mathematical Geology, 20*(5), 543–565.

37. Bonnet, E., Bour, O., Odling, N. E., Davy, P., Main, I., Cowie, P., & Berkowitz, B. (2001). Scaling of fracture systems in geological media. *Reviews of Geophysics, 39*(3), 347–383.

38. Booker, A. J., Dennis, J. E., Frank, P. D., Serafini, D. B., Torczon, V., & Trosset, M. W. (1999). A rigorous framework for optimization of expensive functions by surrogates. *Structural optimization, 17*(1), 1–13.

39. Bossew, P., & Kirchner, G. (2004). Modelling the vertical distribution of radionuclides in soil. part 1: the convection–dispersion equation revisited. *Journal of environmental radioactivity, 73*(2), 127–150.

40. Box, G. E., & Draper, N. R. (1987). *Empirical model-building and response surfaces.* John Wiley & Sons.

41. Briggs, S., Karney, B. W., & Sleep, B. E. (2017). Numerical modeling of the effects of roughness on flow and eddy formation in fractures. *Journal of Rock Mechanics*

and Geotechnical Engineering, *9*(1), 105–115. doi: 10.1016/j.jrmge.2016.08.004

42. Burg, J.-P. (2012). *Brittle faulting - lecture notes* (No. 1).

43. Butler, A., Chen, J., Aguero, A., Edlund, O., Elert, M., Kirchner, G., . . . Sheppard, M. (1999). Performance assessment studies of models for water flow and radionuclide transport in vegetated soils using lysimeter data. *Journal of environmental radioactivity*, *42*(2-3), 271–288.

44. Cacuci, D. (2003). *Sensitivity and uncertainty analysis: theory, sensitivity and uncertainty analysis.* CRC Press.

45. Cadini, F., Avram, D., Pedroni, N., & Zio, E. (2012). Subset simulation of a reliability model for radioactive waste repository performance assessment. *Reliability Engineering & System Safety*, *100*, 75–83.

46. Cadini, F., Gioletta, A., & Zio, E. (2015). Improved metamodel-based importance sampling for the performance assessment of radioactive waste repositories. *Reliability Engineering & System Safety*, *134*, 188–197.

47. Campbell, J. E., & Cranwell, R. M. (1988). Performance assessment of radioactive waste repositories. *Science*, *239*(4846), 1389–1392.

48. Cawlfield, J. D., & Wu, M.-C. (1993). Probabilistic sensitivity analysis for one-dimensional reactive transport in porous media. *Water Resources Research*, *29*(3), 661. doi: 10.1029/92WR01948

49. Cherubini, C. (2008). A modeling approach for the study of contamination in a fractured aquifer. *Geotechnical and Geological Engineering*, *26*(5), 519–533. doi: 10.1007/s10706-008-9186-3

50. Cho, S. E. (2012). Probabilistic analysis of seepage that considers the spatial variability of permeability for an embankment on soil foundation. *Engineering Geology*, *133*, 30–39.

51. Cho, S. E. (2014). Probabilistic stability analysis of rainfall-induced landslides considering spatial variability of permeability. *Engineering Geology*, *171*, 11–20.

52. Cho, W.-J., Chang, S.-H., & Park, H.-H. (1992). Uncertainty analysis of safety assessment for high-level radioactive waste repository. *Waste Management*, *12*(1), 45–54.

53. Cho, Y.-H., McCullough, B. F., & Weissmann, J. (1996). Considerations on finite-element method application in pavement structural analysis. *Transportation Research Record*, *1539*(1), 96–101.

54. Chopra, M., Rastogi, R., Kumar, A. V., Sunny, F., & Nair, R. (2013). Response surface method coupled with first-order reliability method based methodology for groundwater flow and contaminant transport model for the uranium tailings pond site. *Environmental Modeling & Assessment*, *18*(4), 439–450.

55. Ciriello, V., Di Federico, V., Riva, M., Cadini, F., De Sanctis, J., Zio, E., & Guadagnini, A. (2013). Polynomial chaos expansion for global sensitivity analysis applied to a model of radionuclide migration in a randomly heterogeneous aquifer.

Stochastic Environmental Research and Risk Assessment, 27(4), 945–954.

56. Crow, J. M. (2007). *Safer storage of nuclear waste.*

57. Crowe, B., Yucel, V., Rawlinson, S., Black, P., Carilli, J., & DiSanza, F. (2002). *Application of probabilistic performance assessment modeling for optimization of maintenance studies for low-level radioactive waste disposal sites at the nevada test site* (Tech. Rep.). Environmental Restoration Project Office, Los Alamos National Laboratory Las.

58. Cvetkovic, V., Painter, S., Outters, N., & Selroos, J. (2004). Stochastic simulation of radionuclide migration in discretely fractured rock near the äspö hard rock laboratory. *Water Resources Research*, 40(2).

59. DAE. (2014). *Government of India Department of Atomic Energy Lok Sabha unstarred question no. 2841.* Retrieved from http://www.dae.nic.in/writereaddata/parl/budget2014/Isus2841.pdf

60. Das, P. K., & Zheng, Y. (2000). Cumulative formation of response surface and its use in reliability analysis. *Probabilistic Engineering Mechanics*, 15(4), 309–315. doi: 10.1016/S0266-8920(99)00030-2

61. Das Gupta, S., Mohanty, B. P., & Köhne, J. M. (2006). Soil hydraulic conductivities and their spatial and temporal variations in a vertisol. *Soil Science Society of America Journal*, 70(6), 1872–1881.

62. Datta, D., & Kushwaha, H. (2011). Uncertainty Quantification Using Stochastic Response Surface Method Case Study–Transport of Chemical Contaminants through Groundwater. *International Journal of Energy, Information and Communications*, 2(3), 49–58.

63. Davy, P., Le Goc, R., & Darcel, C. (2013). A model of fracture nucleation, growth and arrest, and consequences for fracture density and scaling. *Journal of Geophysical Research: Solid Earth*, 118(4), 1393–1407.

64. Deb, S. K., & Shukla, M. K. (2012). Variability of hydraulic conductivity due to multiple factors. *American Journal of Environmental Sciences*, 8(5), 489.

65. Deering, L., & Kozak, M. W. (1990). *A performance assessment methodology for low-level radioactive waste disposal* (Tech. Rep.). Sandia National Labs., Albuquerque, NM (USA).

66. Der Kiureghian, A., & Ditlevsen, O. (2009). Aleatory or epistemic? does it matter? *Structural Safety*, 31(2), 105–112.

67. Der Kiureghian, A., & Ke, J.-B. (1987). The stochastic finite element method in structural reliability. In *Stochastic structural mechanics* (pp. 84–109). Springer.

68. Diersch, H.-J. G. (2014). *Feflow: finite element modeling of flow, mass and heat transport in porous and fractured media.* Springer Science & Business Media.

69. Dietrich, P; ·Helmig, R;Sauter, M; Hötzl, H;Köngeter, J;Teutsch, G. (2010). *Flow and Transport in Fractured Porous Media.* Retrieved from http://www.amazon.com/exec/obidos/redirect?tag=citeulike07

`-20{\&}path=ASIN/3642062318`

70. Dong, C. (2011). *Numerical Modeling of Contaminant Transport in Fractured Porous Media Using Mixed Finite-Element and Finite-Volume Methods* (Master's thesis). doi: 10.1615/JPorMedia.v14.i3.30

71. Dubourg, V., Sudret, B., & Deheeger, F. (2013). Metamodel-based importance sampling for structural reliability analysis. *Probabilistic Engineering Mechanics*, *33*, 47–57. doi: 10.1016/j.probengmech.2013.02.002

72. Duncan, I. (2003). What to do with nuclear waste. *Nuclear Energy*, *42*(03), 145–148.

73. Elango, L., Brindha, K., Kalpana, L., Sunny, F., Nair, R., & Murugan, R. (2012). Groundwater flow and radionuclide decay-chain transport modelling around a proposed uranium tailings pond in india. *Hydrogeology Journal*, *20*(4), 797–812.

74. El-Ghonemy, H., Watts, L., & Fowler, L. (2005). Treatment of uncertainty and developing conceptual models for environmental risk assessments and radioactive waste disposal safety cases. *Environment international*, *31*(1), 89–97.

75. Engelund, S., & Rackwitz, R. (1993). A benchmark study on importance sampling techniques in structural reliability. *Structural safety*, *12*(4), 255–276.

76. Faravelli, L. (1989). Response-surface approach for reliability analysis. *Journal of Engineering Mechanics*, *115*(12), 2763–2781.

77. Faybishenko, B., Witherspoon, P. A., Bodvarsson, G. S., & Gale, J. (2005). Emerging issues in fractured-rock flow and transport investigations: introduction and overview. In *Dynamics of fluids and transport in fractured rock, Washington, D.C* (Vol. 162, p. 1). American Geophysical Union.

78. Fenton, G. (2014). *Random Fields: Modeling Soil Properties in Stochastic Analysis and Inverse Modeling.*

79. Fenton, G. A. (1997). Data analysis/geostatistics. *Probabilistic Methods in Geotechnical Engineering, ASCE GeoLogan*, *97*, 51–73.

80. Fenton, G. A. (1999). Random field modeling of cpt data. *Journal of Geotechnical and Geoenvironmental Engineering*, *125*(6), 486–498.

81. Fernàndez-Garcia, D., Illangasekare, T. H., & Rajaram, H. (2005). Differences in the scale dependence of dispersivity and retardation factors estimated from forced-gradient and uniform flow tracer tests in three-dimensional physically and chemically heterogeneous porous media. *Water Resources Research*, *41*(3).

82. Gallegos, D. P., & Bonano, E. J. (1993). Consideration of uncertainty in the performance assessment of radioactive waste disposal from an international regulatory perspective. *Reliability Engineering & System Safety*, *42*(2-3), 111–123.

83. Garcia-Cabrejo, O., & Valocchi, A. (2014). Global Sensitivity Analysis for multivariate output using Polynomial Chaos Expansion. *Reliability Engineering & System Safety*, *126*, 25–36. doi: 10.1016/j.ress.2014.01.005

84. Geiger, S., Cortis, A., & Birkholzer, J. (2010). Upscaling solute transport in naturally fractured porous media with the continuous time random walk method. *Water Resources Research*, *46*(12).

85. Geiser, J. (2001). Numerical simulation of a model for transport and reaction of radionuclides. In *International conference on large-scale scientific computing* (pp. 487–496).

86. Ghanem, R., & Dham, S. (1998). Stochastic finite element analysis for multiphase flow in heterogeneous porous media. *Transport in Porous Media*, *32*(3), 239–262.

87. Ghanem, R. G., & Spanos, P. D. (1991). *Stochastic Finite Elements: A Spectral Approach*. doi: 10.1007/978-1-4612-3094-6

88. Graf, T., & Simmons, C. (2009). Variable-density groundwater flow and solute transport in fractured rock: Applicability of the tang et al.[1981] analytical solution. *Water Resources Research*, *45*(2).

89. Graf, T., & Therrien, R. (2005). Variable-density groundwater flow and solute transport in porous media containing nonuniform discrete fractures. *Advances in Water Resources*, *28*(12), 1351–1367.

90. Griffiths, D., Huang, J., & Fenton, G. (2015). Probabilistic slope stability analysis using rfem with non-stationary random fields. *Risk V, Schweckendiek T, van Tol AF, Pereboom D et al (eds) Geotechnical Safety*, 704–709.

91. Griffiths, D. V., & Fenton, G. A. (2006). Probabilistic methods in geotechnical engineering. *Cism Courses and Lectures*, *491*, 346.

92. Grill, K. (2005). Safety, justice, and transparency in nuclear waste management. *Atw. Internationale Zeitschrift fuer Kernenergie*, *50*(7), 452–453.

93. Gringarten, E. (1996). 3-D Geometric Description of Fractured Reservoirs. *Mathematical Geology*, *28*(January), 881–893.

94. Gringarten, E. (1998). Fracnet: Stochastic simulation of fractures in layered systems. *Computers and Geosciences*, *24*(8), 729–736. doi: 10.1016/S0098-3004(98)00071-5

95. Grisak, G., & Pickens, J.-F. (1980). Solute transport through fractured media: 1. the effect of matrix diffusion. *Water Resources Research*, *16*(4), 719–730.

96. Guedes Filho, O., Vieira, S. R., Chiba, M. K., Nagumo, C. H., & Dechen, S. C. F. (2010). Spatial and temporal variability of crop yield and some rhodic hapludox properties under no-tillage. *Revista Brasileira de Ciência do Solo*, *34*(1), 1–14.

97. Gupta, R., Rudra, R., Dickinson, W., Patni, N., & Wall, G. (1993). Comparison of saturated hydraulic conductivity measured by various field methods. *Transactions of the ASAE*, *36*(1), 51–55.

98. Gutierrez, M., & Youn, D.-J. (2015). Effects of fracture distribution and length scale on the equivalent continuum elastic compliance of fractured rock masses. *Journal of Rock Mechanics and Geotechnical Engineering*, *7*(6), 626–637.

99. Gutjahr, A. L., & Bras, R. L. (1993). Spatial variability in subsurface flow and transport: a review. *Reliability Engineering & System Safety*, *42*(2-3), 293–316.

100. Hakami, E. (1995). *Aperture distribution of rock fractures* (Doctoral dissertation, Royal Institute of Technology, Sweden). Retrieved from `https://inis.iaea.org/search/search.aspx?orig_q=RN:27020199`

101. Haldar, S., & Babu, G. S. (2008). Effect of soil spatial variability on the response of laterally loaded pile in undrained clay. *Computers and Geotechnics*, *35*(4), 537–547.

102. Hamed, M. M. (1996). *Reliability-based uncertainty analysis of groundwater contaminant transport and remediation* (Doctoral dissertation, Rice University). Retrieved from `https://scholarship.rice.edu/handle/1911/19110`

103. Harter, T. (2000). Application of stochastic theory in groundwater contamination risk analysis: Suggestions for the consulting geologist and/or engineer. *Geological Society of Ameica*, 43–52.

104. Hasofer, A. M., & Lind, N. C. (1974). Exact and invariant second-moment code format. *Journal of the Engineering Mechanics division*, *100*(1), 111–121.

105. Hassan, A. E., Cushman, J. H., & Delleur, J. W. (1998). Significance of porosity variability to transport in heterogeneous porous media. *Water Resources Research*, *34*(9), 2249–2259.

106. Helton, J. C. (1993). Uncertainty and sensitivity analysis techniques for use in performance assessment for radioactive waste disposal. *Reliability Engineering & System Safety*, *42*(2-3), 327–367.

107. Helton, J. C. (2003). Mathematical and numerical approaches in performance assessment for radioactive waste disposal: dealing with uncertainty. In *Radioactivity in the Environment* (Vol. 4, pp. 353–390). Elsevier.

108. Helton, J. C., Johnson, J. D., & Sallaberry, C. J. (2011). Quantification of margins and uncertainties: example analyses from reactor safety and radioactive waste disposal involving the separation of aleatory and epistemic uncertainty. *Reliability Engineering & System Safety*, *96*(9), 1014–1033.

109. Herbert, A. (1996). Modelling approaches for discrete fracture network flow analysis. In *Coupled thermo-hydro-mechanical processes of fractured media* (Vol. 79, pp. 213–229). Elsevier.

110. Higashi, K., & Pigford, T. H. (1980). Analytical models for migration of radionuclides in geologic sorbing media. *Journal of Nuclear Science and Technology*, *17*(9), 700–709.

111. Hoffman, E., & Stacey, W. (2004). Nuclear design and analysis of the fusion transmutation of waste reactor. *Fusion Science and Technology*, *45*(1), 51–54.

112. Hoffman, F. O., & Miller, C. W. (1983). *Uncertainties in environmental radiological assessment models and their implications* (Tech. Rep.). Oak Ridge National Lab.

113. Homma, T., & Saltelli, A. (1996). Importance measures in global sensitivity analysis of nonlinear models. *Reliability Engineering & System Safety*, *52*(1), 1–17. doi: 10.1016/0951-8320(96)00002-6

114. Huang, S., & Kou, X. (2007). An extended stochastic response surface method for random field problems. *Acta Mechanica Sinica*, *23*(4), 445–450.

115. Huang, S., Liang, B., & Phoon, K. (2009). Geotechnical probabilistic analysis by collocation-based stochastic response surface method: An Excel add-in implementation. *Georisk: Assessment and Management of Risk for Engineered Systems and Geohazards*, *3*(2), 75–86. doi: 10.1080/17499510802571844

116. Huang, S., Mahadevan, S., & Rebba, R. (2007). Collocation-based stochastic finite element analysis for random field problems. *Probabilistic Engineering Mechanics*, *22*(2), 194–205. doi: 10.1016/j.probengmech.2006.11.004

117. Huber, M., Westrich, B., Vermeer, P. A., & Moormann, C. (2011). Response surface method in advanced reliability based design. In *Budelmann, holst & proske: Proceedings of the 9th international probabilistic workshop.*

118. Hudson, J., & Priest, S. (1983). Discontinuity frequency in rock masses. In *International journal of rock mechanics and mining sciences & geomechanics abstracts* (Vol. 20, pp. 73–89).

119. Huenges, E., & Zimmermann, G. (1999). Rock permeability and fluid pressure at the ktb. implications from laboratory-and drill hole-measurements. *Oil & Gas Science and Technology*, *54*(6), 689–694.

120. Huysmans, M., & Dassargues, A. (2006). Stochastic analysis of the effect of spatial variability of diffusion parameters on radionuclide transport in a low permeability clay layer. *Hydrogeology Journal*, *14*(7), 1094–1106.

121. IAEA. (1995a). The principles of radioactive waste management. *Safety Series*(111-F).

122. IAEA. (1995b). Safety assessment of near surface radioactive waste disposal facilities: Model intercomparison using simple hypothetical data (test case 1).

123. IAEA. (1999). Safety Assessment for Near Surface Disposal of Radioactive Waste (No. WS-G-1.1).

124. IAEA. (2003). Scientific and Technical Basis for the Geological Disposal of Radioactive Wastes. *Technical Reports Series No. 413*(4), 90.

125. IAEA. (2004). Long term behaviour of low and intermediate level waste packages under repository conditions. (June).

126. IAEA. (2007). Operation and maintenance of spent fuel storage and transportation casks/containers - IAEA-TECDOC-1532.

127. IAEA. (2011). Safety of radiation sources: International basic safety standards, general safety requirements - interim edition, iaea safety standards series no. gsr part 3. *International Atomic Energy Agency (IAEA), Vienna.*

128. IAEA. (2014). Near Surface Disposal Facilities for Radioactive Waste - IAEA SAFETY STANDARDS SERIES (No. GS-R-3)., 124.

129. IAEA. (2018). *IAEA Power Reactor Information System, India.* Retrieved from `https://pris.iaea.org/pris/CountryStatistics/CountryDetails.aspx?current=IN`

130. ICRP. (1990). *Recommendations of the international commission on radiological protection. publication 60* (Tech. Rep.). International Commission on Radiological Protection (ICRP).

131. Isukapalli, S., Roy, A., & Georgopoulos, P. (1998). Stochastic response surface methods (srsms) for uncertainty propagation: application to environmental and biological systems. *Risk Analysis: An International Journal*, *18*(3), 351–363.

132. Isukapalli, S. S. (1999). *Uncertainty Analysis of Transport-Transformation Models* (Doctoral dissertation, Rutgers, The State University of New Jersy). Retrieved from `http://citeseerx.ist.psu.edu/viewdoc/download?doi=10.1.1.473.402&rep=rep1&type=pdf`

133. ITRC. (2011). *Diffusion and Dispersion.* Retrieved from `https://www.enviro.wiki/index.php?title=Dispersion_and_Diffusion`

134. Jakimavičiūtė-Mas'elienė, V., Mažeika, J., & Motiejūnas, S. (2016). Application of vadose zone approach for prediction of radionuclide transfer from near-surface disposal facility. *Progress in Nuclear Energy*, *88*, 53–57.

135. Jakimavičiūte-Maseliene, V., Mažeika, J., & Petrošius, R. (2006). Modelling of coupled groundwater flow and radionuclide transport in crystalline basement using feflow 5.0. *Journal of Environmental Engineering and Landscape Management*, *14*(2), 101–112.

136. Jang, Y.-S., Sitar, N., & Der Kiureghian, A. (1994). Reliability analysis of contaminant transport in saturated porous media. *Water Resources Research*, *30*(8), 2435–2448.

137. Jayarajan, K. (2017). Regulatory measures and practices for radioactive waste management in barc facilities.

138. Jiang, S. H., Li, D. Q., Cao, Z. J., Zhou, C. B., & Phoon, K. K. (2014). Efficient System Reliability Analysis of Slope Stability in Spatially Variable Soils Using Monte Carlo Simulation. *Journal of Geotechnical and Geoenvironmental Engineering*, *141*(2), 1–13. doi: 10.1061/(ASCE)GT.1943-5606.0001227.

139. Jiang, S.-H., Li, D.-Q., Zhou, C.-B., & Zhang, L.-M. (2014). Capabilities of stochastic response surface method and response surface method in reliability analysis. *Struct. Eng. Mech*, *49*(1), 111–128.

140. Johari, A., & Amjadi, A. (n.d.). Stochastic analysis of settlement rate in unsaturated soils. In *Geo-risk 2017* (pp. 631–639).

141. Josnin, J. Y., Jourde, H., Fénart, P., & Bidaux, P. (2002). A three-dimensional model to simulate joint networks in layered rocks. *Canadian Journal of Earth Sciences*,

39(10), 1443–1455. doi: 10.1139/e02-043

142. Karanki, D. R., Kushwaha, H. S., Verma, A. K., & Ajit, S. (2009). Uncertainty analysis based on probability bounds (p-box) approach in probabilistic safety assessment. *Risk Analysis: An International Journal*, *29*(5), 662–675.

143. Karniadakis, G. E. (2002). The Wiener–Askey Polynomial Chaos for Stochastic Differential Equations. (February 2017). doi: 10.1137/S1064827501387826

144. Kautsky, U., Saetre, P., Berglund, S., Jaeschke, B., Nordén, S., Brandefelt, J., . . . Andersson, E. (2016). The impact of low and intermediate-level radioactive waste on humans and the environment over the next one hundred thousand years. *Journal of Environmental Radioactivity*, *151*, 395–403.

145. Kim, S.-H., & Na, S.-W. (1997). Response surface method using vector projected sampling points. *Structural Safety*, *19*(1), 3–19. doi: 10.1016/S0167-4730(96) 00037-9

146. Kim, Y. N., Kim, J. K., & Kim, T. W. (1993). Risk assessment for shallow land burial of low level radioactive waste. *Waste Management*, *13*(8), 589–598.

147. Krishnamoorthy, T., Nair, R., & Nambi, K. (1997). Evaluation of disposal limits for shallow land burial facilities: Application to the back end of nuclear fuel cycle. *Applied Radiation and Isotopes*, *48*(9), 1203–1209.

148. Krishnamoorthy, T., Nair, R., & Sarma, T. (1992). Migration of radionuclides from a granite repository. *Water Resources Research*, *28*(7), 1927–1934.

149. Krupka, K. M., Kaplan, D., Whelan, G., Serne, R., & Mattigod, S. (1999). Understanding variation in partition coefficient, kd, values. *Volume II: Review of Geochemistry and Available Kd Values, for Cadmium, Cesium, Chromium, Lead, Plutonium, Radon, Strontium, Thorium, Tritium (3H), and Uranium. EPA*.

150. Kumar, G. S., & Sekhar, M. (2005a). Solutes in Fracture-Matrix System. *Journal of Hydrologic Engineering*, *10*(3), 192–199.

151. Kumar, G. S., & Sekhar, M. (2005b). Spatial moment analysis for transport of nonreactive solutes in fracture-matrix system. *Journal of Hydrologic Engineering*, *10*(3), 192–199.

152. Kumar, G. S., Sekhar, M., & Misra, D. (2006). Time dependent dispersivity behavior of non-reactive solutes in a system of parallel fractures. *Hydrology and Earth System Sciences Discussions*, *3*(3), 895–923.

153. Kumar, S., Ali, S., Chander, M., Bansal, N., & Balu, K. (2001). *Integrated radioactive waste management from npp, research reactor and back end of nuclear fuel cycle-an indian experience* (Tech. Rep.).

154. Lee, C.-J., & Lee, K. J. (2006). Application of bayesian network to the probabilistic risk assessment of nuclear waste disposal. *Reliability Engineering & System Safety*, *91*(5), 515–532.

155. Lei, Q., Latham, J.-P., & Tsang, C.-F. (2017). The use of discrete fracture networks for modelling coupled geomechanical and hydrological behaviour of frac-

tured rocks. *Computers and Geotechnics*, *85*, 151–176.

156. Lei, Q., & Wang, X. (2016). Tectonic interpretation of the connectivity of a multiscale fracture system in limestone. *Geophysical Research Letters*, *43*(4), 1551–1558.

157. Lei, Qinghua; Lantham, John-Paul; Tsang, C.-F. (2017). The use of discrete fracture networks for modelling coupled geomechanical and hydrological behaviour of fractured rocks. *Computers and Geotechnics*, *85*, 151–176.

158. Li, D., Chen, Y., Lu, W., & Zhou, C. (2011). Stochastic response surface method for reliability analysis of rock slopes involving correlated non-normal variables. *Computers and Geotechnics*, *38*(1), 58–68.

159. Li, D.-Q., Jiang, S.-H., Cheng, Y.-G., & Zhou, C.-B. (2013). A comparative study of three collocation point methods for odd order stochastic response surface method. *Struct. Eng. Mech*, *45*(5), 595–611.

160. Linkov, I., & Burmistrov, D. (2003). Model uncertainty and choices made by modelers: Lessons learned from the international atomic energy agency model intercomparisons. *Risk Analysis: An International Journal*, *23*(6), 1297–1308.

161. Liu, Y. (2013). *Non-intrusive Methods for Probabilistic Uncertainty Quantification and Global Sensitivity Analysis in Nonlinear Stochastic Phenomena* (Doctoral dissertation, Florida State University, USA). Retrieved from `https://pdfs.semanticscholar.org/1b01/27d4dc6fd203639ee34e1bf6a1c267738e0a.pdf`

162. Long, J., Hestir, K., Karasaki, K., Davey, A., Peterson, J., Kemeny, J., & Landsfeld, M. (1991). Fluid flow in fractured rock: Theory and application. In *Transport Processes in Porous Media* (pp. 203–241). Springer.

163. Long, J.C.S; Hestir, K; Karasaki, K; Davey, A; Peterson, J; Kemeny, J ; Landsfeld, M. (1989). *Fluid flow in Fractured Rock : Theory and Application* (Tech. Rep.).

164. Lowell, R. P. (1987). *Some Analytical Models for Contaminant Transport in Fractured Rock* (Tech. Rep. No. 701).

165. MacQuarrie, Kerry T. B; Mayer, K. Ulrich. (2005). Reactive transport modeling in fractured rock: A state-of-the-science review. *Earth-Science Reviews*, *72*, 189–227.

166. Mahmoudzadeh, B., Liu, L., Moreno, L., & Neretnieks, I. (2014). Solute transport in a single fracture involving an arbitrary length decay chain with rock matrix comprising different geological layers. *Journal of Contaminant Hydrology*, *164*, 59–71.

167. Makolil, J., & Nagar, C. (2015). *India ' s Underground Radioactive Waste Disposal site at Gogi in Karnataka ?* (Tech. Rep. No. August).

168. Mao, N., Al-Bittar, T., & Soubra, A. H. (2012). Probabilistic analysis and design of strip foundations resting on rocks obeying Hoek-Brown failure criterion. *International Journal of Rock Mechanics and Mining Sciences*, *49*, 45–58. doi:

10.1016/j.ijrmms.2011.11.005

169. Mayya, Y. (2015). *Analytical methods for solving advection-dispersion equation.*

170. McKay, M. D., Beckman, R. J., & Conover, W. J. (1979). Comparison of three methods for selecting values of input variables in the analysis of output from a computer code. *Technometrics*, *21*(2), 239–245.

171. Melchers, R. E., & Beck, A. T. (1999). *Structural reliability analysis and prediction*. John Wiley & Sons.

172. Miller, A. W., Rodriguez, D. R., & Honeyman, B. D. (2010). Upscaling sorption/desorption processes in reactive transport models to describe metal/radionuclide transport: A critical review. *Environmental Science & Technology*, *44*(21), 7996–8007.

173. Miranda, T., Santos, R., Barbosa, J., Gomes, I., Alencar, M., Correia, O., . . . Neumann, V. (2018). Quantifying aperture, spacing and fracture intensity in a carbonate reservoir analogue: Crato formation, ne brazil. *Marine and Petroleum Geology*, *97*, 556–567.

174. Montgomery, D. C., & Myers, R. H. (1995). Response surface methodology. *Design and Analysis of Experiments*, 445–474.

175. Mountford, P., & Temperton, D. (1992). Recommendations of the international commission on radiological protection (icrp) 1990. *European Journal of Nuclear Medicine and Molecular Imaging*, *19*(2), 77–79.

176. Myers, R. H., Montgomery, D. C., & Anderson-cook, C. M. (2009). Response Surface Methodology. *Wiley*(3), 1–1247. doi: 10.1007/s13398-014-0173-7.2

177. Nair, R., & Krishnamoorthy, T. (1997). *Slbm-a fortran code for shallow land burial of low level radioactive waste* (Tech. Rep.). Bhabha Atomic Research Centre.

178. Nair, R., & Krishnamoorthy, T. (1999). Probabilistic safety assessment model for near surface radioactive waste disposal facilities. *Environmental Modelling & Software*, *14*(5), 447–460.

179. Nair, R., Mayya, Y., & Puranik, V. (2006). A generic method to evaluate the reasonable upper-bound dose from near-surface radioactive waste disposal facilities through drinking water pathway. *Nuclear technology*, *153*(1), 53–69.

180. Nair, R. N., Sunny, F., & Manikandan, S. T. (2010). Modelling of decay chain transport in groundwater from uranium tailings ponds. *Applied Mathematical Modelling*. doi: 10.1016/j.apm.2009.10.038

181. Narr, W., & Suppe, J. (1991). Joint spacing in sedimenlary rocks. *Journal of Structural Geology*, *11*(9), 1037–1048. doi: 10.1016/0191-8141(91)90055-N

182. Nataf, A. (1962). Determination des distribution dont les marges sont donnees. *Comptes Rendus del Academie des Sciences*, *225*, 42–43.

183. Neretnieks, I. (1990). *Solute transport in fractured rock-applications to radionuclide waste repositories* (Tech. Rep.). Swedish Nuclear Fuel and Waste Manage-

ment Co.

184. Neretnieks, I. (2002). A stochastic multi-channel model for solute transport-analysis of tracer tests in fractured rock. *Journal of Contaminant Hydrology*, *55*(3-4), 175–211. doi: 10.1016/S0169-7722(01)00195-4

185. Neuman, S. P. (2005). Trends, prospects and challenges in quantifying flow and transport through fractured rocks. *Hydrogeology Journal*, *13*(1), 124–147.

186. Norbert, W. (1938). The Homogeneous Chaos. *American Journal of Mathematics*, *60*(4), 897–936.

187. Nordqvist, A. W., Tsang, Y., Tsang, C., Dverstorp, B., & Andersson, J. (1992). A variable aperture fracture network model for flow and transport in fractured rocks. *Water Resources Research*, *28*(6), 1703–1713.

188. NRC. (1996). *Rock fractures and fluid flow: contemporary understanding and applications*. National Academies Press.

189. NRC. (2000). *A Performance Assessment Methodology for Low-Level Radioactive Waste Disposal Facilities*. NUREG-1573.

190. Odling, N. E., & Roden, J. E. (1997). Contaminant transport in fractured rocks with significant matrix permeability, using natural fracture geometries. *Journal of Contaminant Hydrology*, *27*(3-4), 263–283.

191. Ogata, A. (1970). *Theory of dispersion in a granular medium*. US Government Printing Office.

192. Ogata, A., & Banks, R. (1961). A solution of the differential equation of longitudinal dispersion in porous media, prof. paper 411-a. *US Geological Survey*.

193. Oron, A. P., & Berkowitz, B. (1998). Flow in rock fractures: The local cubic law assumption reexamined. *Water Resources Research*, *34*(11), 2811–2825.

194. Paluszny, A., & Matthäi, S. K. (2009). Numerical modeling of discrete multi-crack growth applied to pattern formation in geological brittle media. *International Journal of Solids and Structures*, *46*(18-19), 3383–3397.

195. Paluszny, A., & Zimmerman, R. W. (2013). Numerical fracture growth modeling using smooth surface geometric deformation. *Engineering Fracture Mechanics*, *108*, 19–36.

196. Pankow, J. F; Johnson, R. L; Hewetson, J. P; Cherry J. A. (1986). An Evaluation of Contaminant Migration Patterns At Two Waste Disposal Sites on Fractured Porous Media in terms of the Equivalent Porous Medium (EPM) Model. *Journal of Contaminant Hydrology*, *1*, 65–76.

197. Papaioannou, I., Betz, W., Zwirglmaier, K., & Straub, D. (2014). MCMC algorithms for subset simulation. *Probabilistic Engineering Mechanics*, *41*, 89–103.

198. Papaioannou, I., & Straub, D. (2012). Reliability updating in geotechnical engineering including spatial variability of soil. *Computers and Geotechnics*, *42*, 44–51.

199. Park, E., & Zhan, H. (2001). Analytical solutions of contaminant transport from fi-

nite one-, two-, and three-dimensional sources in a finite-thickness aquifer. *Journal of Contaminant Hydrology*, *53*(1-2), 41–61.

200. Park, E., & Zhan, H. (2002, 01). Analytical solutions of contaminant transport from finite one-, two-, and three-dimensional sources in a finite-thickness aquifer. *Journal of Contaminant Hydrology*, *53*, 41-61. doi: 10.1016/S0169-7722(01)00136 -X

201. Parker, B. L., Cherry, J. A., & Chapman, S. W. (2012). Discrete fracture network approach for studying contamination in fractured rock. *AQUA mundi*, *3*(2), 101–116.

202. Peter, E. N., Madhav, M., & Reddy, E. S. (2009). One-dimensional non-reactive contaminant transport with scale-dependent dispersion. *Indian Geotechnical Journal*, *39*(1), 64–80.

203. Phoon, K.-K., & Ching, J. (2014). *Risk and reliability in geotechnical engineering*. CRC Press.

204. Phoon, K. K., & Kulhawy, F. H. (1999). Characterization of geotechnical variability. *Canadian Geotechnical Journal*, *36*(4), 612–624. doi: 10.1139/t99-038

205. Pierre M.Adler, Thovert J., F. (1999). *Fractures and Fracture Networks*. Springer science.

206. Piqué, À., Arcos, D., Grandia, F., Molinero, J., Duro, L., & Berglund, S. (2013). Conceptual and numerical modeling of radionuclide transport and retention in near-surface systems. *Ambio*, *42*(4), 476–487.

207. Piscopo, V., Baiocchi, A., Lotti, F., Ayan, E. A., Biler, A. R., Ceyhan, A. H., ... Taşkın, M. (2017). Estimation of rock mass permeability using variation in hydraulic conductivity with depth: experiences in hard rocks of western Turkey. *Bulletin of Engineering Geology and the Environment*, 1–9. doi: 10.1007/s10064-017-1058-8

208. Pollard, D. D. (1987). Theoretical displacements and stresses near fractures in rock: with applications to faults, joints, veins, dikes, and solution surfaces. *Fracture Mechanics of Rock*, 277–349.

209. Poteri, A., & Laitinen, M. (1997). *Fracture network model of the groundwater flow in the romuvaara site* (Tech. Rep.). Posiva Oy.

210. Pugliesi, D. (2012). *Sorption.* Retrieved from `https://en.wikipedia.org/wiki/Sorption`

211. Raj, K., Prasad, K., & Bansal, N. (2006). Radioactive waste management practices in india. *Nuclear Engineering and Design*, *236*(7-8), 914–930.

212. Rakesh, R., Yadav, D., Narayan, P., & Nair, R. (2005). *Post Closure Safety Assessment of Radioactive Waste Storage and Management Site, Trombay* (Tech. Rep.). Bhabha Atomic Research Centre, India.

213. Ramsøy, T., Christensen, G., & Varskog, P. (2004). Long term behaviour of low and intermediate level waste packages under repository conditions. *Long term be-*

haviour of low and intermediate level waste packages under repository conditions, 131.

214. Ranade, A., Pandey, M., & Datta, D. (2010). Stochastic response surface based simulation of ground water modeling. In *AIP Conference Proceedings* (Vol. 1298, pp. 213–218).

215. Rasmuson, A., & Neretnieks, I. (1986). Radionuclide transport in fast channels in crystalline rock. *Water Resources Research*, *22*(8), 1247–1256.

216. Renshaw, C. E., & Pollard, D. D. (1994). Numerical simulation of fracture set formation: a fracture mechanics model consistent with experimental observations. *Journal of Geophysical Research*, *99*(B5), 9359–9372. doi: 10.1029/94JB00139

217. Rice, E., Denning, R., Friedlander, A., & Priest, C. (1982). Preliminary risk benefit assessment for nuclear waste disposal in space.

218. Riley, M. S. (2004). An algorithm for generating rock fracture patterns: Mathematical analysis. *Mathematical Geology*, *36*(6), 683–702. doi: 10.1023/B: MATG.0000039541.36356.61

219. Robinson, B. A., Houseworth, J. E., & Chu, S. (2012). Radionuclide transport in the unsaturated zone at Yucca Mountain, Nevada. *Vadose Zone Journal*, *11*(4).

220. Robinson, M., Gallagher, D., & Reay, W. (1998). Field observations of tidal and seasonal variations in ground water discharge to tidal estuarine surface water. *Groundwater Monitoring & Remediation*, *18*(1), 83–92.

221. Rohit. (2017). *Diffusion*. Retrieved from `https://www.knowswhy.com/similarities-between-diffusion-and-osmosis/`

222. Rosenblatt, M. (1952, 09). Remarks on a multivariate transformation. *Ann. Math. Statist.*, *23*(3), 470–472. doi: 10.1214/aoms/1177729394

223. Rowe, R. K., & Booker, J. R. (1985). 1-d pollutant migration in soils of finite depth. *Journal of Geotechnical Engineering*, *111*(4), 479–499.

224. Sacks, J., Welch, W. J., Mitchell, T. J., & Wynn, H. P. (1989). Design and analysis of computer experiments. *Statistical Science*, 409–423.

225. Sahimi, M. (2011). *Flow and transport in porous media and fractured rock: from classical methods to modern approaches*. John Wiley & Sons.

226. Saltelli, A. (2000). Making best use of model evaluations to compute sensitivity indices. *Computer Physics Communications*, *145*(2), 280–297. doi: 10.1016/S0010-4655(02)00280-1

227. Saltelli, A., Tarantola, S., Campolongo, F., et al. (2000). Sensitivity anaysis as an ingredient of modeling. *Statistical Science*, *15*(4), 377–395.

228. Sanjaydas. (2018). *Radioactive Decay*. Retrieved from `https://www.sarthaks.com/57552/state-the-law-radioactive-decay-plot-graph-showing-the-number-undecayed-nuclei-function`

229. Sarkar, S., Toksoz, M. N., & Burns, D. R. (2004). *Fluid flow modeling in fractures*

(Tech. Rep.). Massachusetts Institute of Technology. Earth Resources Laboratory.

230. Schmelling, S., & Ross, R. (1989). *Contaminant transport in fractured media: Models for decision makers, us epa ground water issue paper* (Tech. Rep.). EPA/540/4-89/004, US EPA, ORD, RS Kerr Environmental Research Laboratory.

231. Schoniger, M., Sommerhauser, M & Herrmann, A. (1997). Modelling flow and transport processes in fractured rock groundwater systems on a small basin scale. In *Proceedings of rabat symposium s2*.

232. Shahkarami, P., Liu, L., Moreno, L., & Neretnieks, I. (2015). Radionuclide migration through fractured rock for arbitrary-length decay chain: analytical solution and global sensitivity analysis. *Journal of Hydrology*, *520*, 448–460.

233. Sharma, P. K., Joshi, N., & Ojha, C. (2013). Stochastic numerical method for analysis of solute transport in fractured porous media. *Journal of Hydro-environment Research*, *7*(1), 61–71.

234. Shikaze, S. G., Sudicky, E., & Schwartz, F. (1998). Density-dependent solute transport in discretely-fractured geologic media: is prediction possible? *Journal of Contaminant Hydrology*, *34*(3), 273–291.

235. Simmons, C. T. (2005). Variable density groundwater flow: From current challenges to future possibilities. *Hydrogeology Journal*, *13*(1), 116–119.

236. Simmons, C. T., Fenstemaker, T. R., & Sharp Jr, J. M. (2001). Variable-density groundwater flow and solute transport in heterogeneous porous media: approaches, resolutions and future challenges. *Journal of Contaminant Hydrology*, *52*(1-4), 245–275.

237. Simunek, J., Jacques, D., Langergraber, G., Bradford, S. A., Šejna, M., & Van Genuchten, M. T. (2013). Numerical modeling of contaminant transport using hydrus and its specialized modules. *Journal of the Indian Institute of Science*, *93*(2), 265–284.

238. Singh, K. K., Singh, D. N., & Ranjith, P. G. (2015). Laboratory Simulation of Flow through Single Fractured Granite. *Rock Mechanics and Rock Engineering*, *48*(3), 987–1000. doi: 10.1007/s00603-014-0630-9

239. Smith, L., & Schwartz, F. W. (1981). Mass transport: 3. role of hydraulic conductivity data in prediction. *Water Resources Research*, *17*(5), 1463–1479.

240. Smith, L., & Schwartz, F. W. (1984). An analysis of the influence of fracture geometry on mass transport in fractured media. *Water Resources Research*, *20*(9), 1241–1252.

241. Snow, D. T. (1970). The frequency and apertures of fractures in rock. In *International journal of rock mechanics and mining sciences & geomechanics abstracts* (Vol. 7, pp. 23–40).

242. Sobol, I. M. (2001). Global sensitivity indices for nonlinear mathematical models and their monte carlo estimates. *Mathematics and Computers in Simulation*, *55*(1-3), 271–280.

243. Sobolev, I., Dmitriev, S., Lifanov, F., Kobelev, A., Stefanovsky, S., & Ojovan, M. (2005). Vitrification processes for low, intermediate radioactive and mixed wastes. *Glass Technology*, *46*(1), 28–35.

244. Song, J. S., & Lee, K. J. (1992). System performance assessment of final repository for radioactive wastes using first-order reliability method. *Waste Management*, *12*(4), 323–335.

245. Spanos, P. D., & Ghanem, R. (1989). Stochastic finite element expansion for random media. *Journal of Engineering Mechanics*, *115*(5), 1035–1053.

246. Šperl, J., & Trčková, J. (2008). Permeability and porosity of rocks and their relationship based on laboratory testing. *Acta Geodynamica et Geomaterialia*, *5*(1), 41–47.

247. Srivastava, A., Babu, G. S., & Haldar, S. (2010). Influence of spatial variability of permeability property on steady state seepage flow and slope stability analysis. *Engineering Geology*, *110*(3-4), 93–101.

248. Stuedlein, A. W., Kramer, S. L., Arduino, P., & Holtz, R. D. (2012). Geotechnical characterization and random field modeling of desiccated clay. *Journal of Geotechnical and Geoenvironmental Engineering*, *138*(11), 1301–1313.

249. Sudicky, E., & Frind, E. (1982). Contaminant transport in fractured porous media: Analytical solutions for a system of parallel fractures. *Water Resources Research*, *18*(6), 1634–1642.

250. Sudicky, E. A. (1986). A natural gradient experiment on solute transport in a sand aquifer: Spatial variability of hydraulic conductivity and its role in the dispersion process. *Water Resources Research*, *22*(13), 2069–2082.

251. Sudret, B., & Berveiller, M. (2008). Stochastic finite element methods in geotechnical engineering. *Reliability-based design in geotechnical engineering: computations and applications*.

252. Sudret, B., & Der Kiureghian, A. (2000). *Stochastic finite element methods and reliability: a state-of-the-art report*. Department of Civil and Environmental Engineering, University of California.

253. Sujitha, S., & Babu, G. S. (2017). System reliability analysis for near-surface radioactive waste disposal facilities. *Georisk: Assessment and Management of Risk for Engineered Systems and Geohazards*, *11*(4), 315–322.

254. Suresh Kumar, G. (2014). Mathematical modeling of groundwater flow and solute transport in saturated fractured rock using a dual-porosity approach. *Journal of Hydrologic Engineering*, *19*(12), 04014033.

255. Suresh Kumar, G., Sekhar, M., & Misra, D. (2008). Time-dependent dispersivity of linearly sorbing solutes in a single fracture with matrix diffusion. *Journal of Hydrologic Engineering*, *13*(4), 250–257.

256. Tang, D., Frind, E., & Sudicky, E. A. (1981). Contaminant transport in fractured porous media: Analytical solution for a single fracture. *Water Resources Research*,

17(3), 555–564.

257. Tang, D. H., Frind, E. O., & Sudicky, E. A. (1981). Contaminant transport in fractured porous media: Analytical solution for a single fracture. *Water Resources Research*, *17*(3), 555–564.

258. Tatang, M. A. (1995). *Direct Incorporation of uncertainty in chemical and environmental engineering systems* (Doctoral dissertation, Massachusetts Institute of Technology). Retrieved from `http://hdl.handle.net/1721.1/11760`

259. Tatang, M. A., Pan, W., Prinn, R. G., & McRae, G. J. (1997). An efficient method for parametric uncertainty analysis of numerical geophysical models. *Journal of Geophysical Research: Atmospheres*, *102*(D18), 21925–21932.

260. Thiessen, K., Thorne, M., Maul, P., Pröhl, G., & Wheater, H. (1999). Modelling radionuclide distribution and transport in the environment. *Environmental Pollution*, *100*(1-3), 151–177.

261. Toran, L., Sjoreen, A., & Morris, M. (1995). Sensitivity analysis of solute transport in fractured porous media. *Geophysical Research Letters*, *22*(11), 1433–1436.

262. Trefry, M. G., & Muffels, C. (2007). Feflow: A finite-element ground water flow and transport modeling tool. *Groundwater*, *45*(5), 525–528.

263. Tsang, C.-F., Neretnieks, I., & Tsang, Y. (2015). Hydrologic issues associated with nuclear waste repositories. *Water Resources Research*, *51*(9), 6923–6972.

264. Tsang, Y. W., Tsang, C. F., Neretnieks, I., & Moreno, L. (1988). Flow and tracer transport in fractured media: A variable aperture channel model and its properties. *Water Resources Research*, *24*(12), 2049–2060. doi: 10.1029/WR024i012p02049

265. Tsang, Y. W., & Witherspoon, P. a. (1983). Bedding planes in slightl grained sandstone. *Journal of Geophysical Research*, *88*(2), 2359–2366.

266. Van Genuchten, M. T., & Wierenga, P. (1976). Mass transfer studies in sorbing porous media i. analytical solutions 1. *Soil Science Society of America Journal*, *40*(4), 473–480.

267. Vanmarcke, E. (1983). Random fields. *Random Fields, by Erik Vanmarcke, pp. 372. ISBN 0-262-72045-0. Cambridge, Massachusetts, USA: The MIT Press, March 1983.(Paper)*, 372.

268. Vanmarcke, E. (2010). *Random fields: analysis and synthesis*. World Scientific.

269. Vanmarcke, E. H. (1977). Reliability of earth slopes. *Journal of the Geotechnical Engineering Division*, *103*(11), 1247–1265.

270. Volkova, E., Iooss, B., & Van Dorpe, F. (2008). Global sensitivity analysis for a numerical model of radionuclide migration from the rrc "kurchatov institute" radwaste disposal site. *Stochastic Environmental Research and Risk Assessment*, *22*(1), 17–31.

271. Vrankar, L., Turk, G., & Runovc, F. (2004). Modelling of radionuclide migration through the geosphere with radial basis function method and geostatistics. *Journal*

of the Chinese Institute of Engineers, *27*(4), 455–462.

272. Vrankar, L., Turk, G., & Runovc, F. (2005, 06). A comparison of the effectiveness of using the meshless method and the finite difference method in geostatistical analysis of transport modeling. *International Journal of Computational Methods*, *2*. doi: 10.1142/S0219876205000405

273. Wainwright, H. M., Finsterle, S., Jung, Y., Zhou, Q., & Birkholzer, J. T. (2014). Making sense of global sensitivity analyses. *Computers and Geosciences*, *65*, 94–94. doi: 10.1016/j.cageo.2013.06.006

274. Wang, L. (2015). *Flow and Transport Through and Deformation of Rough Fractures : Analytical and Numerical* (Doctoral dissertation). Retrieved from `http://hdl.handle.net/2152/32611`

275. Wattal, P. (2013). Indian programme on radioactive waste management. *Sadhana*, *38*(5), 849–857.

276. Webster, M. D., Tatang, M. A., & McRae, G. J. (1996). *Application of the probabilistic collocation method for an uncertainty analysis of a simple ocean model* (Tech. Rep.). Massachusetts Institute of Technology MIT.

277. Wei, Y., Dong, Y., Yeh, T.-C. J., Li, X., Wang, L., & Zha, Y. (2017). Assessment of uncertainty in discrete fracture network modeling using probabilistic distribution method. *Water Science and Technology*, *76*(10), 2802–2815.

278. Wendland, E., & Himmelsbach, T. (2002). Transport simulation with stochastic aperture for a single fracture–comparison with a laboratory experiment. *Advances in Water Resources*, *25*(1), 19–32.

279. Wilson, C. R., & Witherspoon, P. A. (1974). Steady state flow in rigid networks of fractures. *Water Resources Research*, *10*(2), 328–335.

280. Winkler, R. L. (1996). Uncertainty in probabilistic risk assessment. *Reliability Engineering & System Safety*, *54*(2-3), 127–132.

281. WNA. (2015). *Nuclear Power in theWorld Today, World Nuclear Association.* Retrieved from `https://www.world-nuclear.org/information-library/current-and-future-generation/nuclear-power-in-the-world-today.aspx`

282. WNA. (2019). *Nuclear Power in India, World Nuclear Association.* Retrieved from `https://www.world-nuclear.org/information-library/country-profiles/countries-g-n/india.aspx`

283. Wörman, A., Geier, J., & Xu, S. (2003). *Modelling of Radionuclide Transport by Groundwater Motion in Fractured Bedrock for Performance Assessment Purposes* (Tech. Rep.).

284. Xiu, D., & Karniadakis, G. E. (2002). The wiener–askey polynomial chaos for stochastic differential equations. *SIAM journal on scientific computing*, *24*(2), 619–644.

285. Yao, C., Jiang, Q., & Shao, J.-F. (2015). A numerical analysis of permeability

evolution in rocks with multiple fractures. *Transport in Porous Media*, *108*(2), 289–311.

286. Yim, M.-S., & Simonson, S. A. (2000). Performance assessment models for low level radioactive waste disposal facilities: a review. *Progress in Nuclear Energy*, *36*(1), 1–38.

287. Yue, L., Sun, S., Liu, J., Wei, J., & Wu, J. (2017). Research on crack initiation mechanism and fracture criterion of rock-type materials under compression−shear stress. *Advances in Mechanical Engineering*, *9*(10), 1–13. doi: 10.1177/ 1687814017720087

288. Zhao, J. (1998). Rock mass hydraulic conductivity of the bukit timah granite, singapore. *Engineering Geology*, *50*(1-2), 211–216.

289. Zhao, Z., Jing, L., Neretnieks, I., & Moreno, L. (2011). Numerical modeling of stress effects on solute transport in fractured rocks. *Computers and Geotechnics*, *38*(2), 113–126.

290. Zheng, Q., Dickson, S., & Guo, Y. (2009). Influence of aperture field heterogeneity and anisotropy on dispersion regimes and dispersivity in single fractures. *Journal of Geophysical Research: Solid Earth*, *114*(B3).

291. Zhou, Q., Liu, H.-H., Molz, F. J., Zhang, Y., & Bodvarsson, G. S. (2007). Field-scale effective matrix diffusion coefficient for fractured rock: Results from literature survey. *Journal of Contaminant Hydrology*, *93*(1-4), 161–187.

292. Zhou, W., Wheater, H., Kovar, K., & Krasny, J. (1995). Effect of aperture variation on two-phase flow in fractures. *IAHS Publications-Series of Proceedings and Reports-Intern Assoc Hydrological Sciences*, *225*, 173–184.

293. Zimmerman, R., & Main, I. (2004). Hydromechanical behavior of fractured rocks. *International Geophysics Series*, *89*, 363–422.

294. Zio, E., & Apostolakis, G. (1996). Two methods for the structured assessment of model uncertainty by experts in performance assessments of radioactive waste repositories. *Reliability Engineering & System Safety*, *54*(2-3), 225–241.

295. Zuev, K. M. (2015). Subset simulation method for rare event estimation: an introduction. *Encyclopedia of Earthquake Engineering*, 1–25.

Publications

International journals

1. Geetha Manjari, K., & Sivakumar Babu, G. L. (2018). Probabilistic analysis of groundwater and radionuclide transport model from near surface disposal facilities. Georisk: Assessment and Management of Risk for Engineered Systems and Geo-hazards, 12(1), 60-73.

   https://doi.org/10.1080/17499518.2017.1329538

2. Sujitha, S., Manjari, K. G., Datta, S., & Babu, G. S. (2015). Risk and Reliability Analysis of Multibarrier System for Near-Surface Disposal Facilities. ASCE, Journal of Hazardous, Toxic, and Radioactive Waste, 20(2), 04015014.

   https://doi.org/10.1061/(ASCE)HZ.2153-5515.0000284

Papers under review

1. Geetha Manjari. K., and Sivakumar Babu G. L. (2020). Probabilistic analysis of radionuclide transport for radioactive waste disposal facilities in fractured sedimentary rocks. Georisk: Assessment and Management of Risk for Engineered Systems and Geohazards

2. Geetha Manjari. K., and Sivakumar Babu G. L. (2020). Probabilistic analysis of radionuclide transport for near surface disposal facilities in spatially variable soils. ASCE, Journal of Hazardous, Toxic, and Radioactive Waste.

International conferences

1. Manjari, K. G., & Sivakumar Babu, G. L (2017). Global Sensitivity Analysis of Groundwater-Radionuclide Transport Model from Near Surface Disposal Facilities. In Geo-Risk (pp. 539-548).

2. Manjari, K. G., Sujitha, S., Datta, S., & Babu, G. L. (2015). Reliability Analysis of Near Surface Disposal Facilities Using Collocation Based Stochastic Response Surface Method. Geotechnical Safety and Risk V, (pp 306 - 312).

3. Geetha Manjari. K., and Sivakumar Babu G. L. (2020). Probabilistic analysis of contaminant transport in fractured sedimentary rocks. 3rd International Symposium on Coupled Phenomena in Environmental Geotechnics, Kyoto, Japan. (abstract accepted)

National conferences

1. Sujitha,S., & Manjari, K. G. (2014). An approach for the risk assessment of a liner system, Proceedings of the Indian Geotechnical Conference (IGC), Kakinada, India. pp 2103-2108.

Award

Received Wesley-Horner Award from American Society of Civil Engineers (ASCE) for the paper "Risk and Reliability Analysis of Multibarrier System for Near-Surface Disposal Facilities."

Scope for future work

In this thesis, probabilistic performance assessment models have been developed to quantitatively estimate the safety of radioactive waste disposal facilities. New hybrid radionuclide transport models are proposed that can handle complexities in modelling geological medium and also, uncertainties in the properties that affect the concentration of the radionuclides reaching biosphere. The two important aspects that the thesis focussed on are modelling radionuclide transport through a complex geological environment i.e., soil and fractured rock and also characterize, propagate and quantify different types of uncertainties that can affect the process of radionuclide migration through this complex medium. There are some more ideas that can be implemented in future and they are mentioned below.

1. When the fractured rock was modelled numerically using FEM, only four fracture orientations and their combinations could be accommodated due to mesh generation constraints. But, this feature can to be extended to creating fracture network of any fracture orientation. To achieve this, the fracture pattern should be imported as a fracture map and this map needs to be digitized in the FE mesh. However, it becomes computationally expensive to perform probabilistic analysis by integrating stochastic fracture generation algorithm and FE mesh (which needs preprocessing).

2. The radionuclide transport through fractured rock is modelled as a two-dimensional medium with one-dimensional fracture elements. This model can be extended to a three-dimensional (3D) medium where the intact rock is modelled in 3D and the fracture elements in 2D.

3. Radionuclides are reactive contaminants that could possibly interact chemically with the adjacent geological medium (especially when the medium is also chemically active like clays or rocks made of limestone, shale etc). The only geochemical component considered in the entire analysis is the distribution coefficient (due to adsorption). But, other geochemical process like dissolution, chemical reactions with the surrounding matrix which are ignored of this thesis. These effects can also be included in the numerical model.

4. The effect of inherent spatial variability is not studied for fractured rock. Studies can be carried out by modelling a random field in fractured medium and investigating its effect on radionuclide transport.

5. Although, a two-dimensional geological medium is considered to model radionuclide transport in spatial variable soil, the spatial variability is modelled as a simple one-dimensional random field. This is because, spatial variability is assumed only along the direction of maximum radionuclide migration. But, owing to the process of spreading, the direction of radionuclide flow becomes two-dimensional. Therefore, the spatial randomness can be extended to a two-dimensional (2D) medium and modelled as a 2D random field to capture its transport behaviour.